The role of endothelial adhesins in leukocyte adhesion in response to pharmaceutical agents that induce pulmonary fibrosis.

James Denis Williamson (BSc)

PhD by Thesis

The University of Hull and the University of York

Hull York Medical School

July 2015

Abstract

Bleomycin (BLM) is an antineoplastic agent known to cause pulmonary fibrosis as a side-effect, and is often used to model fibrotic disease in rodents. Although human BLM-induced pulmonary fibrosis (BPF) results from intravenous BLM delivery, rodent modelling today primarily uses the intratracheal delivery method. However, BPF following both dosing routes is characterised by inflammatory cell influx into the lung. Though it is thought that intratracheal dosing causes intrapulmonary injury, cytokine release, and resultant immune cell recruitment, the mechanism by which intravenous dosing causes immune cell influx is less clear.

Endothelial cells are critically involved in immune cell extravasation to the site of injury, through adhesion molecule expression and cytokine release. This work assessed whether BLM induces endothelial adhesion molecule expression and cytokine release. It was found that the treatment of HUVECs and PMVECs with pharmacologically-relevant concentrations of BLM resulted in increased ICAM-1, VCAM-1, and (in HUVECs) E-selectin expression, and increased MCP-1 and IL-8 release. Endothelin-1 release was decreased by treatment. These alterations were regulated at a mRNA transcriptional level. Endothelial cell treatment with BLM also supported increased neutrophil tethering and adhesion to endothelial monolayers, although this appeared unrelated to increased ICAM-1 or E-selectin expression.

This work reports the novel finding that pharmacologically-relevant concentrations of BLM increase adhesion molecule expression in both HUVECs and PMVECs, and compares the expression of adhesion molecules and cytokines in these cell types in response to BLM. This thesis also reports the unique discovery that BLM treatment increases leukocyte adhesion to endothelial monolayers under flow *in vitro*. Finally, the finding that endothelial adhesion molecule expression and cytokine release is increased in response to treatment with etoposide, another agent which causes lung fibrosis, is presented. This work suggests a potential mechanism which may contribute to the development of human BPF via immune cell recruitment to the lung.

Table of Contents

List of Figures

List of Tables

List of Accompanying Material

Disc A: Neutrophil Flow Adhesion Movies (Isotype versus Untreated).

Abbreviations

°C - degrees celcius

µg - micrograms

µm - micrometers

µM - micromoles

ABLM - activated bleomycin

ACD - acid citrate dextrose

AECI - type I alveolar epithelial cells

AECII - type II alveolar epithelial cell

AECs - alveolar epithelial cells

AM - alveolar macrophages

ANGEN - angiotensinogen

ANOVA - analysis of variance

AP-1 - activator protein 1

a-SMA - alpha smooth muscle actin

ATII - angiotensin II

ATP5B - adenosine triphosphate synthase

AUC - area under the curve

B2M - beta-2-macroglobulin

BAL - bronchoalveolar lavage

BALF - bronchoalveolar lavage fluid

Bax - BCL-2-associated protein

Bcl-Xl - B-cell lymphoma extra large protein

BH - bleomycin hydrolase

BLM - bleomycin

bp - base pairs

BPF - bleomycin-induced pulmonary fibrosis

BSA - bovine serum albumin

C'4 - DNA base carbon 4

Ca+ - calcium

CCL2 - C-C motif ligand 2

CCR2 - chemokine receptor type 2

CD106 - cluster of differentiation 106

CD11 - cluster of differentiation 11

CD16 - cluster of differentiation 16

CD162 - cluster of differentiation 162

CD18 - cluster of differentiation 18

CD31 - cluster of differentiation 31

CD32 - cluster of differentiation 32

CD36 - cluster of differentiation 36

CD43 - cluster of differentiation 43

CD44 - cluster of differentiation 44

CD50 - cluster of differentiation 50

CD54 - cluster of differentiation 54

CD62E - cluster of differentiation 62E

CD62P - cluster of differentiation 62P

CD64 - cluster of differentiation 64

CD99 - cluster of differentiation 99

cDNA - complementary DNA

cm - centimetres

Cmax - maximum plasma concentration

CMT-93 - mouse rectum carcinoma cells

CO2 - carbon dioxide

COLIA2 - collagen alpha-2(I) chain

Cq - quantification cycle

CS - cleavage site

Css - steady-state plasma concentration

CTGF - connective tissue growth factor

CXCR1 - IL-8 receptor alpha

CXCR2 - IL-8 receptor beta

DAG - diacylglycerol

DAS - diallyl sulphide

DEPC - diethylpyrocarbonate

DMSO - dimethyl sulfoxide

DNA - deoxyribonucleic acid

dNTP - doexynucleotide

DOX - doxorubicin

DSB - double strand break

dyn/cm2 - dynes per centimeter squared

ECs - endothelial cells

ECM - extracellular matrix

EDTA - ethylenediaminetetraacetic acid

EGF - epidermal growth factor

ELISA - enzyme linked immunosorbent assay

EMSA - electrophoretic mobility shift assay

EMT - epithelial mesenchymal transition

EpC - epithelial cell

ERK1/2 - extracellular signal related kinase 1 and 2

ESL-1 - E-Selectin Ligand 1

ET-1 - endothelin 1

F(ab')2- fragment antigen binding

FACS - fluorescence activated cell sorting

Fas - Fas receptor

Fas-L - Fas ligand

Fc - fragment crystallisable

Fe - iron

Fig. - figure

FITC - fluorescin isothiocyanate

FSC-H - forward scatter

G2-M - G2 metaphase checkpoint

GAGs - glycoaminoglycans

GAPDH - glyceraldehyde 3-phosphate dehydrogenase

GC - guanine cytosine

gDNA - genomic DNA

GlyCAM-1 - glycosylation-dependent cell adhesion molecule 1

GPCRs - G protein coupled receptors

G-pyr - guanine-pyrimidine bond

H+ - hydrogen

H2O2 - hydrogen peroxide

hCT2 - human carnitine transporter 2

HEK - human embryonic kidney cells

hPMVECs - human pulmonary microvascular endothelial cells

HUVECs - human umbilical cord endothelial cells

I.M. - intramuscular

I.P.-	intraperitoneal
I.T. -	intratracheal
I.V. -	intravenous
ICAM-1 -	intercellular adhesion molecule 1
ICAM-2 -	intercellular adhesion molecule 2
ICAM-3 -	intercellular adhesion molecule 3
IFN-g -	interferon gamma
IGF -	insulin like growth factor
IgG1 -	immunoglobulin G1
IIP -	idiopathic interstitial pneumonia
IL-10 -	interleukin 10
IL-1B -	interleukin 1 beta
IL-1R -	interleukin 1 receptor
IL-4 -	interleukin 4
IL-6 -	interleukin 6
IL-6 -	interleukin 6
IL-8 -	interleukin 8
IP3 -	inositol triphosphate
IPF -	idiopathic pulmonary fibrosis
JAM-A -	junctional Adhesion Molecule A
JNK -	c-JUN N-terminal kinase
Kb -	kilobase
l -	litres
LAP -	latency associated peptide
LFA-1 -	lymphocyte function associated antigen 1
LPAM-1 -	leukocyte beta7 integrin

LPS - lipopolysaccharide

mAb - monoclonal antibody

Mac-1 - macrophage antigen 1

MaDCAM-1 - mucosal addressing cell adhesion molecule 1

MAPK - mitogen activated protein kinase

MCP-1 - monocyte chemoattractant protein 1

Mg - magnesium

mg - milligrams

MIP-1a - macrophage inflammatory protein 1 alpha

ml - millilitres

mM - millimolar

MMP - matrix metalloproteinase

MMP2 - maxtrix metalloproteinase 2

MMP9 - maxtrix metalloproteinase 9

mRNA - messenger ribonucleic acid

MTS - (3-(4,5-dimethylthiazol-2-yl)-5-(3-carboxymethoxyphenyl)-2-(4-sulfophenyl)-2H-tetrazolium),

mU - milliunits

n - number

NF-kB - nuclear factor kappa B

ng - nanograms

NKT - natural killer T cells

nm - nanometers

nM - nanomoles

No RT - no reverse transcriptase

NSIP - non-specific interstitial pneumonia

O2 - oxygen

OH- hydroxide

p53 - tumour protein p53

PAECs - pulmonary artery endothelial cells

PBS - phosphate buffered saline

PCR - polymerase chain reaction

PDGF - platelet derived growth factor

PDGF-BB - platelet derived growth factor BB

PDGFR - platelet derived growth factor receptor

PECAM-1 - platelet endothelial cell adhesion molecule 1

pH - per hydrogen

PI - propidium iodide

PI3K - phosphoinositol 3 kinase

PLC - phospholipase C

PLCgamma - phospholipase C gamma

PMNs - polymorphonucleocytes

PMVECs - pulmonary microvascular endothelial cells

PSGL-1 - P-Selectin glycoprotein ligand 1

qPCR - quantitative polymerase chain reaction

RLP13A - ribosomal protein L13a

RNA - ribonucleic acid

ROS - reactive oxygen species

RT - reverse transcriptase

S.C. - subcutaneous

Smad - mothers against decapentaplegic

SPECT/CT - single positron emission computed tomography/computed tomography

SRB - sulphorhodamine B

SSB - single strand break

SSC-H - side scatter

Syk - spleen tyrosine kinase

t1/2b - terminal half-life

TC - transmigratory cup

TEM - transendothelial migration

TGF-b - transforming growth factor beta

Th1 - T helper 1

TNF-a - tumour necrosis factor alpha

TSP-1 - thrombospondin 1

U/ml - units per millilitre

UBC - ubiquitin C

UIP - usual interstitial pneumonia

v. - version

v/w - volume per mass

VCAM-1 - vascular cell adhesion molecule 1

VEC - vascular endothelial cells

VLA-4 - very late antigen 4

w/v - mass per volume

WPB - Wiebel Palade Body

YWHAZ - tyrosine 3-monooxygenase/tryptophan 5-monooxygenase activation protein, zeta

α4β1 - alpha 4 beta 1 integrin

αVβ3 - alpha v beta 3 integrin

αvβ6 - alpha v beta 6 integrin

ΔΔCq - delta delta quantification cycle

Acknowledgements

I would like to thank everybody in Respiratory Medicine and in the Daisy Building for their continued support over the last three years. To Dr Simon Hart and Professor John Greenman, thank you for all your assistance and support over the last three years, for helping me identify the next steps in my research and advising me on which experiments to carry out to make sure I was getting the results I needed, and for reading the sections of this thesis as they have been sent to you; to Dr Laura Sadofsky, Dr Kevin Morgan, and Dr Vicky Green, thank you for your ongoing expert technical advice, for showing me how to carry out experiments I'd never done before, for helping me develop the best methods for my experiments and for helping me work out why they went wrong; and to Chris Crow, for making sure that I always had the equipment I needed, and for helping me out when I got stuck trying to use equipment and for making sure I didn't break everything I touched!

Thank you to the Platelet Research Group (Kochar, Casey, Rob, Ahmed, Zaher, Katie, Siân Miriayi, and everyone else) for providing the blood I needed for the neutrophil adhesion experiments, and a big thank you to Dr Camille Ettelaie, Dr Yu Pei Xiao, and Sophie Featherby for allowing me to use their laboratory space and equipment for this work, and for giving me excellent advice on how to optimise these experiments to get the results I needed. The sixth chapter wouldn't have happened without all your help!

I would also like to thank Dr Sam Xu, for being so involved and committed to my work as my TAPS chair, and for advising me on the best way to present my research; Elaine Brookes, for guiding me through the administrative side of my PhD and the PGTS; Dr Anne-Marie Seymour and Dr Miranda van Rossum, for being so supportive and helpful while taking my PGTS modules in Practical Demonstration and Dutch; and George Ashley and Rebecca Gover at PrimerDesign for not only supplying the equipment and reagents required to carry out the qPCR work, but also offering expert technical advice and assistance in conducting qPCR.

Finally, a massive thank you to my family, my partner, and my friends for allowing me to talk endlessly about work (and nothing else) and for giving me the time to throw myself

into my PhD (while understanding that I might not be around very often and, when I am around, that I will be too tired to be very entertaining!). And of course, thank you to my colleagues from over the years, particularly Anna, Yvette, Liz, Laura, Sam, Simon, and Alison for making the Daisy Building a place I looked forward to coming to! It's proving weird turning up to work without you guys being there!

Author's Declaration

I confirm that this work is original and that if any passage(s) or diagram(s) have been copied from academic papers, books, the internet, or any other sources these are clearly identified by the use of quotations marks and the reference(s) is fully cited. I certify that, other than where indicated, this is my own work and does not breach the regulations of HYMS, the University of Hull or the University of York regarding plagiarism or academic conduct in examinations. I have read the HYMS Code of Practice on Academic Misconduct, and state that this piece of work is my own and does not contains any unacknowledged work from any other sources. I confirm that any patient information obtained in the production of this piece of work has been appropriately anonymised.

1 General Introduction

1.1 Pulmonary Fibrosis Pathology and Incidence

Pulmonary fibrosis, considered the end-stage of many heterogenous lung conditions, is a devastating condition and a key characteristic of a range of interstitial lung diseases (Datta, et al., 2011; Meltzer and Noble, 2008). Though pathological features vary by disease, recent reviews outline common features including excessive ECM protein deposition in the interstitium and parenchyma (Datta, et al., 2011; Chua, et al., 2005), fibrotic lesion formation (Wilson and Wynn, 2009; Chua, et al., 2005) alveolar destruction, and respiratory failure (Datta, et al., 2011), often leading to a swift death.

The aetiology of fibrosis varies; a review by Wilson and Wynn (2009) discussed potential causes, including irradiation, exposure to silica and asbestos, sarcoidosis, and asthma. Generally, pulmonary fibrosis is considered to occur in response to lung injury, resulting in inflammatory and coagulation cascade activation, inflammatory mediator release, inflammatory cell infiltration, fibroblast proliferation and differentiation, and ECM synthesis and deposition. Excess ECM deposition due to dysregulation at any stage of wound healing, or in response to a persistent injurious stimulus, may lead to fibrosis (Wynn, 2011; Chua, et al., 2005). However, while inflammation occurs in sarcoidosis-, drug-, radiation, and asthma-associated fibrosis (Wilson and Wynn, 2009; Selman and Pardo, 2002), broad heterogeneity is seen in fibrotic lung conditions, and often, the aetiology remains unclear. In such cases, the disease is referred to as an idiopathic interstitial pneumonia, or IIP.

The most common IIP is idiopathic pulmonary fibrosis (IPF) (Garantziotis, et al., 2004). IPF is mainly a disease of older adults (Nalysnyk, et al., 2012) and an estimated 15,000 people in the UK suffer the disease, with around 5,000 new cases diagnosed each year and an overall incidence rate of around 7.5 cases per 100,000 person-years (Navaratnam, et al., 2011), although this is increasing (Raghu, et al., 2011). As IPF is untreatable, with a mean survival time of 3-5 years following diagnosis (Datta, et al., 2011), worse than many cancers, this is becoming an increasing problem.

IPF is characterised by usual interstitial pneumonia (UIP) (Nalysnyk, et al., 2012), patchy areas of established fibrosis and others of ongoing fibroblastic proliferation and collagenation (fibroblastic foci) (Dempsey, et al., 2006; Nicholson, et al., 2002). Symptoms

include abnormal pulmonary function and restriction (Dempsey, et al., 2006), dyspnoea, cough, and respiratory failure (Nalysknyk, et al., 2010: Raghu, et al., 2011). Subpleural and basilar abnormalities may be seen , and as disease progresses, alveolar fusion and matrix deposition result in pulmonary honeycombing (Dempsey, et al., 2006).

As an IIP, the causes of IPF are poorly defined. Within the lung, type I alveolar epithelial cells (AECI) are the thin alveolar "lining" cells which provide the gas exchange surface of, while type II alveolar epithelial cells (AECII) proliferate and differentiate to repair damage to the delicate AECI (Ward and Nicholas, 1984; Barkauskas, et al., 2013). In IPF, AECI necrosis and AECII reactive hyperplasia are common, and it is thought that this may lead to disease development via aberrant wound repair – as AECII fail to repair AECI injury – and dysregulated epithelial-mesenchymal "cross-talk" as abnormal AECII express profibrotic factors, leading to excess ECM deposition (Horowitz and Thannickal, 2008; Selman and Pardo, 2002). If inflammation plays a role remains controversial, with this hypothesis having fallen out of favour due to reports in the mid-2000s discussing a lack of an obvious role of immune cells in IPF (Selman and Pardo, 2002), though immune cell infiltration of the lung has been reported in the disease over the years, as discussed in a recent review by Williamson, et al. (2015).

While the cause of IPF remains unknown, pulmonary fibrosis is a recognised side-effect of several drugs, including amiodarone (Fan, et al., 1987) and methotrexate (Bedrossian, et al., 1979), but the most studied agent is bleomycin (BLM). BLM is known to cause pulmonary fibrosis in both rodents and in patients given the drug, and is often used to model fibrotic lung disease, e.g. IPF, non-specific interstitial pneumonia (NSIP) and bleomycin-induced pulmonary fibrosis (BPF), though these types of study have mainly been carried out using rodent models. Human BPF is under-researched, and how it develops is unresolved. Though rare, the condition has limited the use of the a efficacious chemotherapeutic agent, and so a greater understanding of the disease is desirable.

1.2 The Chemistry and Mechanisms of Action of BLM

The BLMs are anti-neoplastic antibiotics designated BLM $A_{1\text{-}6,}$ A_2, and $B_{1\text{-}6}$ (Alberts, et al., 1978) isolated from *Streptomyces verticillus* (Umezawa, et al., 1966; Umezawa, 1971; Umezawa, et al., 1967), used to treat head and neck cancer and lymphoma (Suzuki, et al., 1969; Schein, et al., 1976) as well as testicular cancer, for which it is still used today (Samuels, et al., 1975; Aouida, et al., 2010). However, while the drug is still used, how it induces cell death remains uncertain. At the most basic level, BLM binds DNA (Suzuki, et al., 1970; Chien, et al., 1977) and induces cell death via DNA scission, as the drug induces single (SSB) and double-stranded breaks (DSB), with the latter responsible for toxicity (Huang, et al., 1981; Tounekti, et al., 2001), though even how these are formed remains a topic of debate.

1.2.1 DNA Scission by BLM – An ROS-Independent Mechanism?

BLM requires metals and divalent oxygen as cofactors for DNA cleavage (Burger, et al., 1998). While early work suggested (BLM)-Fe^{II} oxidation produced DNA-damaging oxygen radicals (Sugiura and Kikuchi, 1978; Sausville, et al., 1978) - electron spin resonance spectra suggestive of OH^- formation were reported when analysing the reaction of (BLM)-Fe^{II} with O_2 (Sugiura and Kikuchi, 1978) - the lack of specificty that this would show is incompatible with BLM (Decker, et al., 2006), which cleaves preferentially at G-pyr'3 sites (d' Andrea and Haseltine, 1978; Takeshita, et al., 1978), and so the role of reactive oxygen species (ROS) in this particular process seems unlikely.

Indeed, neither Burger et al. (1979) nor Kuramochi, et al. (1981) observed ROS production by (BLM)-Fe^{II} undergoing oxidation; Kuramochi, et al. (1981) proposed that binding of the BLM metal-binding domain to Fe^{II}, reaction with O_2, and reduction produced the active intermediate (BLM)-Fe^{III}-OOH (ABLM). ABLM is the final intermediate seen prior to scission (Decker, et al., 2006) and by abstracting the C'4 H^+ of a DNA deoxyribose sugar (primarily pyrimidine), induces SSBs (Liu, et al., 2010, Chow, et al., 2008, Decker, et al., 2006). H^+ abstraction results in a radical centred on the deoxyribose C'4, and (BLM)-Fe^{IV}=O (able to induce DSBs by further abstraction) (Decker, et al., 2006) . DNA cleavage

may then occur via oxidation, reduction, and substitution reactions (*Fig 1.1).*This is the favoured theory of how BLM induces DNA cleavage today (Decker, et al., 2006).

However, how BLM binds DNA remains debated, though the BLM biathiazole domain may be involved in this process. It has been posited that the bithiazole may bind to the DNA minor groove (Manderville, et al., 1994), or intercalate between bases at specific sites 3' of the cleavage site (CS) (with or without binding to a guanine residue 5' of the CS) (Vanderwall, et al., 1997; Goodwin, et al., 2008). This binding would position the reactive metallo-BLM-OOH in an area in which it is capable of abstracting the pyr-C'4 H^+. While this seems feasible, all studies investigating this potential phenomenon have used ABLM analogues (such as BLM with cobalt, or zinc, rather than iron), and so no firm conclusions can be drawn.

Moreover, while it is thought that a single molecule causes DSBs, it is also uncertain how this occurs; some suggest ABLM is regenerated by a secondary reaction with the generated C'4 radical – possibly peroxidation or reduction – without unbinding from DNA (Steighner and Povirk, 1990), while others than an intermediate form of ABLM generated by the first H^+ abstraction - (BLM) $Fe^{(IV)}$ =O – is able to abstract a second H^+ while BLM remains bound via rearrangement of the metal binding region (Decker, et al., 2006), a theory similarly echoed by Vanderwall, et al. (2007) who instead suggested bithiazole rearrangement. Further, others suggest BLM may abstract two H^+ concurrently via placing of the reactive centre near a CS on one strand (specific cleavage), and an adenine nucleotide on the second (non-specific cleavage) (Keck, et al., 2001). That none of these critical features of BLM and its mode of action are well-defined, and that almost all attempts to determine such mechanisms use either BLM analogues or artificial modeling, leave a gap in our understanding of how BLM works. All that is agreed upoin is that the generation of DSB appears a "single-hit" reaction (Keck, et al., 2001; Steighner and Povirk, 1990).

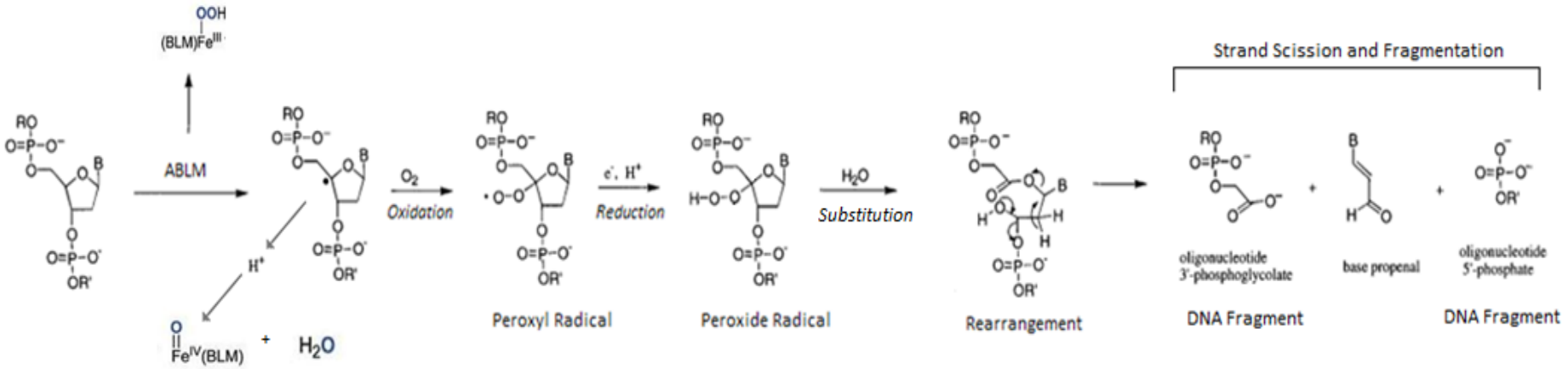

Figure 1.1: DNA Strand Scission by BLM

A schematic diagram of the generation of strand scission by ABLM following the abstraction of a deoxyribose sugar hydrogen from the C'4 position under aerobic conditions (adapted from van den Berg (2008), Hecht (2000), Pogozelski and Tullius (1998), and Burger (1998). Reaction of the C'4 radical with O_2 forms a peroxyl radical which is reduced, reacts with water, and rearranges, leading to DNA fragmentation. Only under aerobic conditions may double strand scission take place (van den Berg, 2008).

1.2.2 Other Mechanisms of BLM-Induced Cell Damage – A Role for ROS?

While DNA scission by BLM does not appear linked to the generation of ROS and free radicals, BLM may induce cell damage via ROS-dependent processes such as lipid peroxidation (Ekimoto, et al., 1985). Sato, et al. (2008) reported lipid-derived free radical adduct production in lung lipid extracts from mice treated with intratracheal BLM, and suggested that this resulted from iron-mediated peroxidation, causing cellular injury via protein damage. Lipid peroxidation via ROS may feasibly represent a mechanism of cell death seperate from DNA scission, as cell membranes degrade, destroying the cell (Kalayarasan, et al., 2008). That the iron chelator deferoxamine decreased both airway inflammation and free radical formation implies a role for ROS in BLM-induced cell toxicity (Sato, et al., 2008).

Interesestingly, Kalayarasan, et al. (2008) also reported decreased lipid peroxidation in lung tissue from mice treated with both BLM and the antioxidant diallyl sulphide (DAS) which correlated with decreased fbirosis. DAS also diminished BLM-induced NF-κB activation in the lung, the activation of which may be an result of ROS generation via nitric oxide synthetase upregulation. Asai, et al. (2007), meanwhile, reported decreased BPF in rabbits co-treated with edarovone, a hydroxyl scavanger, but no mechanism of action was suggested. However, fewer apoptotic lung cells were seen.

It is feasible that ROS generation may also induce cell death via apoptotic processes. Wallach-Dayan, et al. (2005) reported increased ROS levels in BLM-treated cells, followed by caspase-8 activation, mitochondrial leakage, and apoptosis *in vitro*; this was attenuated by the antioxidant glutathione. Therefore, while the cleavage of DNA may not require ROS, other cell damaging processes may do.

1.2.3 BLM-Induced Cell Death – Mechanimsm of Cytotoxicity

It may be expected that cells undergoing high levels of DNA damage would die by undergoing intrinsic apoptosis, involving p53 activation, cytochrome C release, and the sequential activation of caspases 3 and 9. However, much like many of the aspects of BLM

and its mechanisms, the mode of cell death induced remains uncertain; pseudoapoptosis (like apoptosis, with very rapid DNA fragmentation) and mitotic cell death (cells arrest in the G_2-M stage of the cell cycle, divide aberrantly and die within 3 doubling times, potentially via caspase-mediated apoptosis) have been suggested, depending on whether high or medium levels of the drug enter the cell, respectively, and intracellular drug availability (Tounekti, et al., 2001; Tounekti, et al., 1993; Mekid, et al., 2003).

More recently, true apoptosis has been suggested as a method by which BLM may induce cytotoxicity, but in a counter-intuitive form: extrinsic apoptosis. Both Wallach-Dayan, et al. (2007) and Mungunsukh, et al. (2010) reported the activation of caspase 8 – a marker of extrinsic apoptosis - occurring prior to the activation of caspase 9 – a marker of intrinstic apoptosis – suggesting that, while proteins involved in intrinsic apoptosis are activated by BLM, extrinsic apoptosis processes occur primarily. How this is triggered is unknown – while Wallach-Dayan, et al. (2007) suggested ROS-induced caspase-3 activation may lead to caspase-8 activation and further capsase 3 activation – a complex interplay between caspases that extends beyond the typical linear models of intrinsic and extrinsic apoptosis - Mungunsukh, et al. (2010) suggested true extrinsic apoptosis initiation, whereby caspase 8 activation leads to caspase 3 activation (noted in this study at around the same time-points as caspase 8 activation) and cell death, overlooking caspase 9. It is becoming clear that apoptotic pathways are not distinct, particularly those induced by chemotherapeutic drugs (Lin, et al., 2004; Tang, et al., 2000), although much more work is required to fully define the mechanism by which BLM induces cell death – be it by apoptosis, pseudoapoptosis, or mitotic cell death.

To induce DNA damage through the mechanisms described above, BLM must presumably enter the cell, but how this happens is unknown. That electropermeablisation, which increases the entry of BLM to the cell, greatly potentiates cytotoxicity (Tounekti, et al., 1993), however, implies that BLM entry to the cell is important in its mechanism of action. BLM is unable to cross the plasma membrane efficiently via passive diffusion (Pron, et al., 1999), though possible BLM receptors were identified on hamster lung fibroblasts and human head and neck cancer cell lines (Pron, et al., 1993; Pron, et al., 1999), which may specifically bind to, and endocytose, BLM. Further, Aouida, et al. (2010) noted high hCT2 (a carnitine transporter) expression on testicular cancer cells; this

correlated with increased BLM-A_5 uptake and toxicity, implying this receptor may internalise BLM A_5. hTC2 was also seen at high levels in a BLM A_5-hypersensitive non-Hodgkin's lymphoma cell line, further suggesting BLM is internalised by hTC2, that toxicity is related to this internalisation, and that susceptibility may be receptor-dependent, but more work is needed to determine how BLM is internalised.

However, cell entry is only the first step. Within the cell, BLM may be neutralised by BLM hydrolase (BH), a cysteine protease that deamidates the BLM β-aminoalanine moiety, producing less toxic metabolites (Lefterov, et al., 1998; Lazo and Humphreys, 1983), which, though widely conserved, has no known natural function (Schwartz, et al., 1999). The susceptibility of lungs has been associated with low levels of BH (Burger, 1998); indeed, low levels of BLM inactivation were seen in lungs of BLM-treated mice by Umezawa, et al (1972), and Lazo and Humphreys (1983) noted the lack of BH in lungs from BPF-susceptible mice, and proposed a lack of BLM inactivation as a cause of toxicity. Further, BLM-susceptible Hodgkin's lymphoma cells express less BH than BLM-resistant Burkitt's lymphoma cells (Ferrando, et al., 1996), and human lungs have only low-to-moderate levels of BH mRNA (Brömme, et al., 1996), so perhaps BH levels determine human cell BLM susceptibility.

Taking all the evidence together, it is clear that little is known about how BLM induces cell death; it appears to bind DNA, but exactly how is poorly defined. It does induce cell death, but the mechanisms causing this are unknown. Even how BLM gains access to the DNA target is uncertain. However, BLM remains an effective anti-cancer therapy modality, though a better understanding of its mechanisms of action may be needed before the mechanisms behind its unfortunate side-effects are delineated.

1.3 Bleomycin Pulmonary Fibrosis in Man – Symptoms and Risk Factors

Early links between BLM and fibrosis were made by the Clinical Screening Co-operative Group of the European Organization for Research on the Treatment of Cancer (1970) and Halnan, et al. (1972) who noted BLM-treated patients developed fatal lung fibrosis. Statistics regarding occurrence vary; O' Sullivan, et al. (2003) saw BPT incidence rates of 6.8% in treated patients, with 14% of those dying, although Sleijfer (2001) stated the incidence of BLM-induced pneumonitis to be 0-46%, with a 3% mortality rate. Moveover, it has been recorded that BPF may develop up to 2 years post-BLM (Uzel, et al., 2005), though this is an isolated report.

The characteristics of human BPF are not widely reported, however. BPF is a predominantly fibrotic condition (O' Sullivan, et al., 2003; Simpson, et al., 1998; Jones, et al., 1978; Bedrossian, et al., 1973), in which patients develop pulmonary distress, dyspnoea, and a non productive cough (Bedrossian, et al., 1973; Blum, et al., 1973). Such restrictive syndromes may gradually worsen, resulting in hypoxia prior to patient death (Simpson, et al., 1998). Post-mortem analyses of patient lungs notes AECI loss with AECII hyperplasia, with concurrent mild vascular endothelial cell (VEC) oedema and injury and alveolar collapse. The location of fibrosis is sub-pleural, may be interstitial and intra-alveolar, and is notably diffuse, with fibrosis being non-uniform, (Jones, 1978; Bedrossian, et al., 1973; Hoshino, et al., 2009; Borzone, et al., 2001; Karam, et al., 1998; Sleijfer, et al., 2001; Chua, et al., 2005; Blum, et al., 1973). Though not well characterised, it seems immune cell infiltration also occurs in man (Hoshino, et al., 2009).

Much like with IPF, there is no "golden bullet" treatment available for patients with BPF, and no known way of preventing the condition developing (Reinert, et al., 2013). Corticosteroids are most often used when patients present with the condition, though no controlled trials have been conducted in patients with confirmed BPF (Sleijfer, et al., 2000; Reinert, et al., 2013), a success rate of only around 50% has been reported, and patients are also known to relapse (White and Stover, 1984). Often, decreasing the dose of BLM, or ceasing dosing, and then allowing the condition to run its course is the only way forward (Sleijfer, et al., 2000; Reinert, et al., 2013).

It is worth noting that not all patients given BLM as part of a chemotherapeutic regimen develop BPF. Of the many risk factors for BPF development, including total dose and exposure to therapeutic oxygen, poor renal function is the most strongly associated one (O'Sullivan, et al., 2004). As BLM is renally metabolised, with around 70% of the total dose cleared in 24 hours (Azambuja, et al., 2005; Hall et al., 1982) impaired drug clearance due to renal insufficiency may increase lung exposure, increasing the likelihood of BPF (O' Sullivan, et al., 2003; Simpson, et al., 1989). Indeed, poor renal function increases the terminal half-life of the drug, which is usually ~2-5 hours (Alberts, et al., 1978) but can be up to 33 hours in patients with renal failure (Broughton, et al., 1977), dramatically prolonging the time over which BLM remains in circulation.

Further, dosing route may also be a risk factor, possibly due to increased drug plasma concentrations achieved immediately after dosing. After an I.V. bolus dose, concentrations may be as high as 6µg/ml (Alberts, et al., 1978), while I.V. infusion achieves a low steady-state plasma concentration of up to 180ng/ml (Broughton, et al., 1977) (Table 1.1). It has been stated that I.V. infusion is "less dangerous" than I.V. bolus, and I.V. bolus less dangerous than intramuscular dosing (Samuels, et al., 1976; Haas, et al., 1976), and that I.V. bolus delivery of the drug is a risk factor for BPF development (O'Sullivan, et al., 2003). That this is the case suggests that the the higher the plasma concentrations of the drug, the greater the risk of fibrosis development; bolus delivery results in increased plasma concentrations (see Table 1.1), though there have been very few studies directly observing BLM pharmacokinetics over long time periods and comparing the dosing routes. Table 1.1 shows all of those available. Moreover,while it is known that renally insufficient patients clear BLM at a much slower rate (Broughton, et al., 1977), and that patients with renal insufficiency are at a higher risk of developing BPF, there have been no studies into the clearance of the drug following different dosing types in such patients. It is possible that BLM concentrations high enough to trigger fibrosis (though these levels remain undefined) persist for hours in patients with poor renal function.

Dosing Route	Terminal half-life ($t_{1/2}\beta$)	Plasma concentration (C_{max}) in renally sufficient patients				Plasma concentration (C_{max}) in renally insufficient patients			
		Immediately after dose	**6H After Dose**	**12H After Dose**	**24H After Dose**	**Immediately after dose**	**6H After Dose**	**12H After Dose**	**24H After Dose**
15U/m^2 I.V. bolus dose (Alberts, et al., 1978)	Mean $t_{1/2}\beta$ 4.0 hours.	1 -10mU/ml (0.56µg/ml–6.6µg/ml) determined by radioimmunoassay (RIA)	0.3 - 0.8mU/ml (200-500ng/ml)	0.08-0.2mU/ml (0.50-130ng/ml)	0.05-0.5mU/ml (3-30ng /ml)	Not determined	Not determined	Not determined	Not determined
15U I.V. bolus total dose (Hall, et al., 1982)	Mean $t_{1/2}\beta$ 2.3 hours	Mean (*n=6)* peak plasma concentration of 1.5mU/ml (0.84 µg/ml).	80µU/ml (50ng/ml)	Not determined	Not determined	Not determined	Not determined	Not determined	Not determined
30U S.C. dose (Hall, et al., 1982)	Mean $t_{1/2}\beta$ 4.3 hours	1mU/ml (0.6 µg/ml) peak plasma concentration determined by RIA	50-400µU/ml (30-260ng/ml)	Not determined	Not determined	Not determined	Not determined	Not determined	Not determined
30U/day I.V. infusion (10 - 20U/m^2/day) (Broughton, et al., 1977)	Mean $t_{1/2}\beta$ 8.93 hours in renally sufficient patients.	Not done; average steady-state plasma concentration (Css) 148.5ng/ml (range 80-180ng/ml) (*n=8).*	After cessation of dosing, 30-80ng/ml	After cessation of dosing, 12-30ng/ml	After cessation of dosing, 5-8ng/ml	Not done; average steady-state plasma concentration (Css) 600ng/ml.	After cessation of dosing, 350ng/ml	After cessation of dosing, 250ng/ml	After cessation of dosing, 210ng/ml

Table 1.1: BLM Pharmacokinetics in Man

The terminal half life of BLM, and peak plasma concentrations of BLM, delivered via various routes after various times, as determined by pharmacokinetic studies. Note the wide range of concentrations present in renally sufficient patients and the disparate results obtained from renally insufficient patients.

Despite the condition being long-recognised, there are few reported studies assessing the pathology of BPF in man and little is known about how the disease develops. There are, however, a wealth of studies investigating the development of BPF in rodents, though even in rodents, the pathogenesis remains incompletely delineated. These may be of limited use, however, due to one main factor – the route of BLM delivery.

When BLM is used to model fibrotic lung disease in rodents, intratracheal (I.T.) dosing is most commonly used, as this induces the rapid development of BPF, but intramuscular (I.M.) or subcutaneous (S.C.) delivery may also be used (Sleijfer, 2001). Intravenous delivery, favoured by earlier researchers, is rarely used now, but comes with one distinct advantage; BLM given to humans is most often delivered I.V. (O'Sullivan, et al., 2003), and so represents a more physiologically relevant model of human disease. Furthermore, it has been suggested that rodent BPF, stemming from I.T. delivery, does not wholly mimic human BPF (Borzone, et al., 2001).

A comparison of the disease caused by I.T. dosing and I.V. dosing is shown in Table 1.2. As can be seen, many features are very similar, potentially suggesting similar pathogenic processes in rodents and in man. The primary differences between BPF resulting from I.T. delivery and I.V. delivery are the localisation of BPF and the primary injury to the endothelial cells.

Similarities and Differences between I.T. and I.V. Dosing in Animals		
I.T. Dosing Features	**I.V. Dosing: Similarities**	**I.V. Dosing: Differences**
No explicit reports of endothelial cell (EC) damage in works using I.T. dosing.		Endothelial blebbing and basement membrane denudation the initial injury in mice (Adamson and Bowden, 1977; Adamson and Bowden, 1974). No injury beyond VEC in some mice (Adamson, 1984).
Perivascular oedema reported in rats (Thrall, et al., 1979; Karmouty-Quintana, et al., 2007), with interstitial oedema also reported (Azuma, et al., 1998; Cortijo, et al., 2001)	Interstitial oedema is also reported in mice and dogs (Adamson and Bowden, 1974; Fleischman, et al., 1971).	Endothelial oedema appears to occur prior to interstitial oedema, and may relate to the perivascular oedema seen (Adamson and Bowden, 1977; Adamson and Bowden, 1974; Adamson, 1976)
Lymphocyte and polymorphonucleocyte influx into the lung interstitum, parenchyma, and perivascular regions, as determined by bronchoalveolar lavage (BAL) and histology (Kumar, et al., 1985; Izbicki, et al., 2002; Giri, et al., 1986; Thrall, et al., 1979; Karmouty-Quintana, et al.,2007; Saito, et al., 2008; Sato, et al., 1999) .	Alveolar, interstitial, and intrapulmonary immune cell infiltration by lymphocytes and polymorphonucleocytes in dogs and mice, as determined by BAL and histology; perivascular cellular infiltrates have also been reported (Fleischman, et al., 1971; Hagiwara, et al., 2000; Adamson, 1976).	
AECI damage and death with associated AECII/epithelial hyperplasia (Kumar, et al., 1985; Izbicki, et al., 2002)., which may be the initial injury in this manifestation (Moore and Hogaboam, 2008)	AECI death in mice with reactive AECII proliferation and hyperplasia has also been reported following BLM dosing (Adamson and Bowden, 1979; Adamson and Bowden, 1977; Adamson, 1976)	
Alveolar septal thickening (Kumar, et al., 1985; Izbicki, et al., 2002).	Alveolar thickening has also been reported in mice (Hagiwara, et al., 2000).	
Patchy/diffuse, dense subpleural, intraalveolar and interstitial fibrosis noted (Izbicki, et al., 2002; Serrano-Mollar, et al., 2007; Hagiwara, et al., 2007; Peng, et al., 2013; Kumar, et al., 1985; Adamson, et al., 1984) but fibrosis may be more bronchiolocentric (Borzone, et al., 2001).	Extensive, sub-pleural fibrosis noted, with fibrosis in the parenchyma and alveoli, in perivascular locations, and the interstitium in dogs and mice. Fibrosis is diffuse. (Fleischman, et al., 1979; Hagiwara, et al., 2000; Adamson, 1976; Adamson and Bowden, 1977; Adamson and Bowden, 1974)	

Table 1.2: Characteristics of BPF Following I.V. and I.T. BLM Dosing

Reported characteristics of BPF in models that have used intratracheal and intravenous dosing routes of BLM. The similarities and differences are highlighted.

While BPF due to I.T. delivery of BLM initially appears to feature similar histological characteristics to that of I.V.-induced BPF and human BPF, such as interstitial and intra-alveolar fibrosis with parenchymal involvement and a sub-pleural localisation, this may not be the case. In the only current study to assess long-term fibrotic changes and the localisation of fibrosis in rodents, Borzone, et al. (2001) saw initial bronchiolocentric injury following I.T. dosing, which became more widespread, involving coalescent areas of parenchyma. Fibrosis developed only in inflamed areas, and 120 days post-BLM, focal inflammation and peribronchial focal fibrosis were noted. That this has not been previously observed was attributed to the initial wide-spread nature of early-stage pulmonary fibrosis caused by BLM, while later stage disease was far more focussed in localisation. That the disease caused by I.T. delivery may focus around bronchioles is becoming a popular theory, and if this is the case, then I.T.-BLM induced BPF may not mimic human BPF as described above, or human IPF/UIP (Borzone, et al., 2001), which are diffuse and/or patchy. It could be said human disease may be more closely mimicked by I.V. BLM dosing in animals.

Moreover, single doses, as often used when rodents are given I.T. BLM, often result in resolving disease (Brown, et al., 1988), less common in man, though BPF may be reversible before fibrosis begins definitely (Sleijfer, et al., 2001). Further, while human BPF is restrictive, characterised by increasing dyspnoea and lung failure, this is not a feature of rodent BPF (Borzone, et al., 2001).

The seemingly unique feature of BPF induced by I.V. BLM is damage to the vascular endothelium, and this is likely to be the most important difference between the two conditions. This is the primary injury, and in some animals given I.V. BLM, the only injury seen is here. This is not observed in mice given I.T. BLM, a delivery route which bypasses the endothelium altogether.

As endothelial damage is the first injury seen in animals given BLM via the same delivery route as humans, it is feasible that it may also be the initial injury in man, and that the effect of BLM on pulmonary VECs impacts the pattern of disease observed, though there are very few reports of endothelial damage in human BPF. However, the endothelium may play a strong role in features of the pathogenesis of BPF – for example, in immune

cell recruitment. Immune cell recruitment is seen in rodent BPF and human BPF, and while movement into the lung in I.T.-induced BPF may be due to intra-pulmonary injury, in I.V.-induced BPF in humans and rodents, the endothelium may also play a role. Moreover, endothelial injury may well play a role in the oedema seen arounds the lung in I.V.-dosing-induced disease, and has been postulated to allow BLM and immune cells access to the lung itself (Moore and Hogaboam, 2008).

To better understand the potential pathogenic processes involved in human BPF development, what is currently known about the mechanisms of BPF development in rodents given I.T. BLM, and how this may apply to human disease, must be considered. From here, potential roles for the endothelium in the pathogenic processes of human BPF may be determined.

1.4 The Development of Bleomycin Pulmonary Fibrosis in Rodents

Iyer, et al. (2000) suggested rodent BPF development to be a multi-stage process. This begins with the "acute stage", characterised by AEC damage, inflammatory cell recruitment to the lung, and proinflammatory mediator release, with oedema and increased vascular permeability potential features. This is followed by the "sub-acute stage", in which profibrotic cytokine release predominates, AECII proliferate and differentiate to repair AECI injury, and fibroblasts proliferate and differentiate at the injury site. This then leads to the final stage, characterised by increased collagen and ECM protein deposition in damaged areas of the lung, which leads to fibrosis (*Fig 1.3*).

When BPF is modelled in rodents, these multiple steps and stages can be broadly broken down into two distinct phases – the inflammatory phase (in which AEC injury, proinflammatory cytokine expression, and immune cell influx occur) and the fibrotic phase (in which aberrant AECII proliferation peaks, fibroblasts transdifferente and proliferate, and fibrosis develops).

When I.T. dosing is used, AEC injury, cytokine release, and immune cell recruitment to the lung and associated inflammation occurs rapidly, within 7 days (the inflammatory phase). After around 14 days, the inflammatory stage recedes, and gives way to the fibrotic phase of BPF development, in which fibroblast transdifferentiation in response to lung cell-expressed profibrotic cytokines, increased collagen deposition, and associated fibrosis development begins, with a maximal fibrotic response noted by 28 days post-dosing. Thereafter, the fibrotic disease induced by BLM may resolve (Thrall, et al., 1979; Rydell-Törmanen, et al., 2012; Williamson, et al., 2015). This bi-phasic model of fibrosis development in response to I.T. BLM dosing is highlighted in Figure 1.2.

Using other dosing routes, the timescale of fibrotic development, and the shift from inflammatory to fibrotic development phases differs, though the processes remain largely analogous. Subcutaneous dosing results in a far longer development time of up to 1-2 weeks for the peak of the inflammatory disease phase, after which time the fibrotic phase occurs and fibrosis persists for up to six weeks after dosing ceases (Rydell-Törmänen, et al., 2012). Repeated intraperitoneal (I.P.) dosing, meanwhile, results in endothelial injury

after 14 days, inflammatory cell infiltration after 28 days, with the switch from inflammation to fibrosis occuring at 8 weeks (Adamson, 1974).

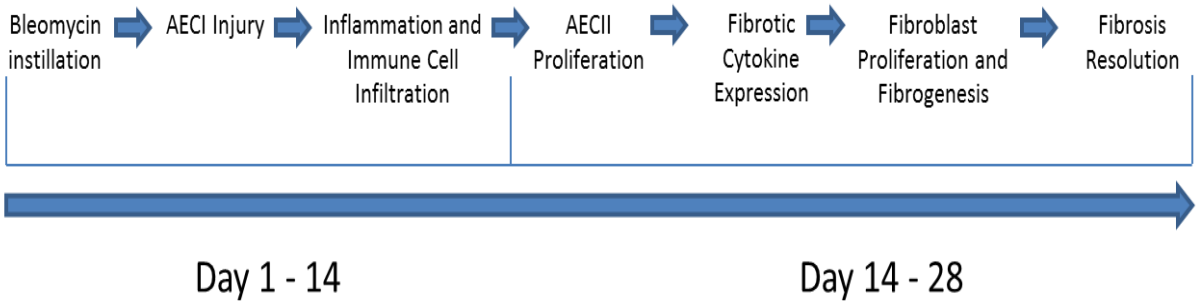

Figure 1.2: The bi-phasic development of BPF following I.T. BLM dosing.

The process and time-scales of pulmonary fibrosis development in rodents following I.T. BLM dosing are highlighted. Other routes, such as I.V. dosing, follow a similar progression to this, though the initial injury is to the endothelium and not directly to AECI.

I.V. dosing, while taking a similar time to cause fibrosis as I.T. dosing, follows the I.P. pattern; endothelial injury occurs after 2-5 days, followed by inflammation at 7 days and peak AECI injury by 14 days. Hereafter, AECII proliferation and fibrotic development begin to take hold. However, inflammation may persist throughout disease development (Adamson and Bowden, 1977; Adamson and Bowden, 1979; Hagiwara, et al., 2000).

Thus, while the various dosing routes generate disease processes which demonstrate different time-scales for fibrosis development, and I.V. dosing may be seen to be the most clinically relevant, inducing disease which more closely resembles human BPF with extensive, diffuse, and sub-pleural fibrosis (while I.T. dosing causes bronchiolocentric disease) (Adamson and Bowden, 1977; Adamson and Bowden, 1979; Hagiwara, et al., 2000; Chua, et al., 2005; Borzone, et al., 2001), it is notable that BPF caused by any BLM dosing route is characterised by an inflammatory stage of development. This also appears to be the case in the development of BPF in man (Hoshino, et al., 2009).

Figure 1.3: The Development of BPF in Rodents

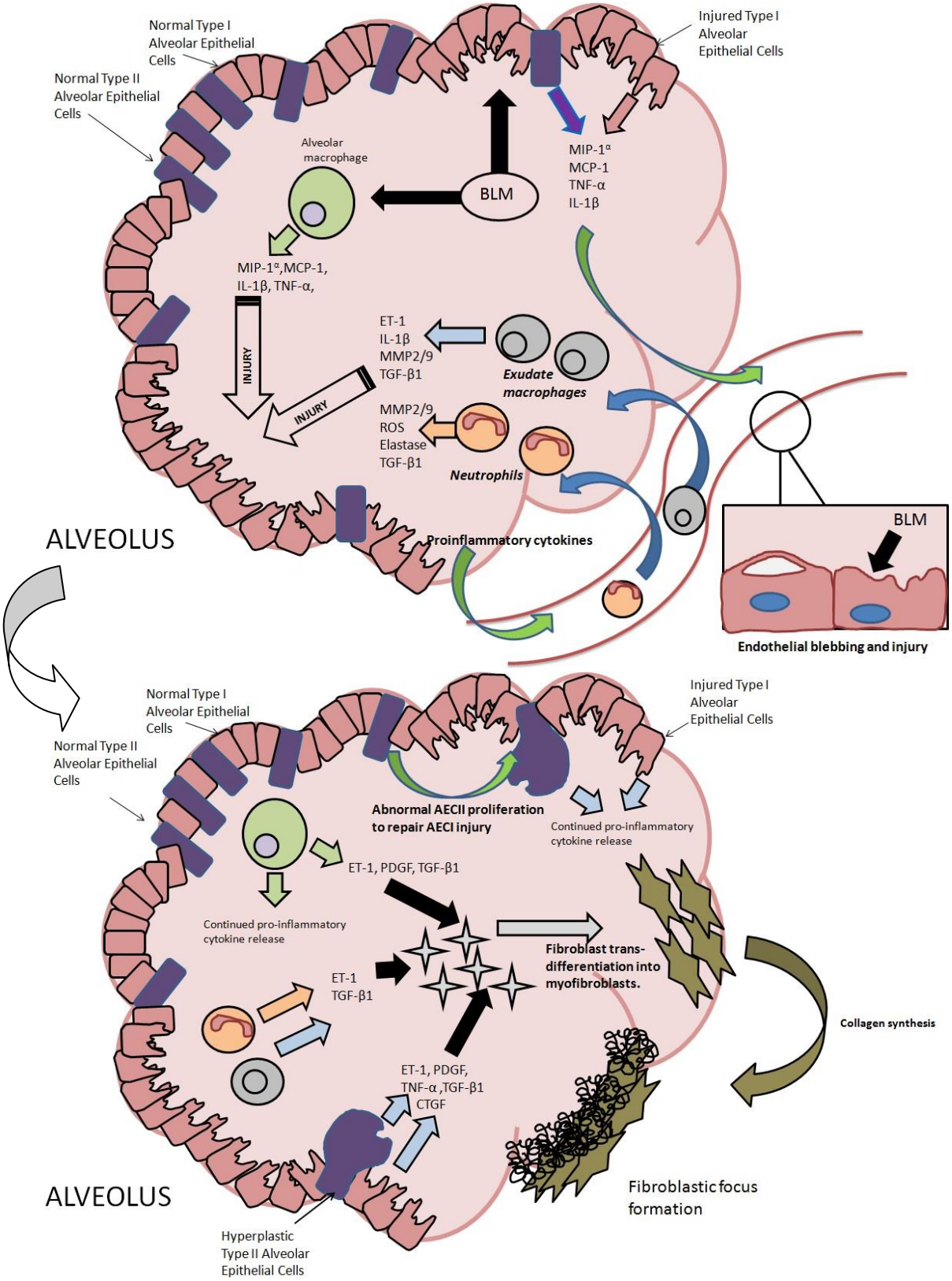

The introduction of BLM to the lung induces AEC damage and injury, leading to proinflammatory mediator release. Immune cells are recruited to the site of injury and may perpetuate AEC injury and express further proinflammatory and pro-fibrotic cytokines. AECII cells proliferate incorrectly, and add to the cytokine milieu. Profibrotic cytokines induce fibroblast transdifferentiation to myofibroblasts, leading to increased collagen synthesis and the formation of fibroblastic foci.

1.4.1 Alveolar Epithelial Cell Injury in Bleomycin Pulmonary Fibrosis

The notion that AECI and II injury may be one of the initial injuries in BPF stems from the current paradigm that states that this is the case in IPF (Degryse, et al., 2011; Wang, et al., 2000). This notion was initially proposed by Selman and Pardo (2002), who stated fibrosis resulted from inappropriate epithelial-mesenchymal cross-talk, and was due to epithelial injury and incorrect wound healing. This may be the case in BPF: AECI injury and AECII derangement appears early in BPF (Kumar, et al., 1985), and AECI death is noted as the initial injury post I.T. BLM. This has been deemed "the most critical cellular event", and BLM appears particularly toxic to AECI (Adamson, 1984). Moreover, the degree of AEC damage correlates with fibrosis severity (Wang, et al., 2000; Adamson, et al., 1984). AECI death is normally followed by the proliferation of AECII, which differentiate into AECI to repair injury, although in BPF this may be abnormal (Moore and Hogaboam, 2008; Kumar, et al., 1985; Adamson, 1984; Adamson and Bowden, 1979) or inadequate (Serrano-Mollar, et al., 2007; Aoshiba, et al., 2003), with fibrosis perhaps due to incorrect re-epithelialisation.

This has proven an attractive theory for some; Wang, et al. (2000) suggested inappropriate AEC apoptosis eliminates anti-fibrotic epithelial functions allowing profibrotic environment development, fibroblast proliferation and transdifferentiation, and accordingly, the group noted an AEC apoptosis inhibitor reduced BPF. Indeed, several groups over the years have suggested that deranged interactions of epithelial and mesenchymal cells may contribute to excess ECM protein deposition, and a story of impaired repair and association intrapulmonary derangement has gradually been built.

This theory – that AEC injury induces fibrotic development - probably began with the work of Adamson (1984), who proposed that AECI death and AECII meta- and hyperplasia result in disordered repair, perhaps due to the effects of BLM on AECII (Adamson and Bowden, 1979). Aberrant and abnormal repair may not restore normal antifibrotic epithelial-mesenchymal mechanisms in which epithelial cell factor expression prevents fibroblast growth, and fibroblast-expressed factors promote epithelial cell growth. Indeed, abnormal epithelial cells isolated from animals 6 weeks post-BLM lacked fibroblast growth inhibitory activity, and fibroblasts prevented epithelial cell growth in co-

culture, but induced differentiation when cell-cell contact occured, suggesting fibroblasts induce aberrant epithelial cell proliferation or block the re-epithelialisation of the lung in BPF (Young and Adamson, 1993), and so this theory may have some merit.

Further, Kawamoto and Fukuda (1990) noted low AECII proliferation post-BLM dosing which may prevent re -epithelialisation, and this may induce fibrosis, as fibroblast migration through damaged epithelium or epithelial-mesenchymal interaction is disrupted (Serrano-Mollar, et al., 2007; Kawamoto and Fukuda, 1990). The cause of impaired repair is unknown, though it has been reported that BLM-exposed AECII show signs of senescence that may limit proliferation (Aoshiba, et al., 2003), and that AECII transplantation into rats reversed BPF and reversed injury, potentially due to epithelial repair, or antifibrotic factor expression (Serrano-Mollar, et al., 2007) implies AECII abarrance plays a role in BPF.

Though BLM-mediated DNA damage is a known cause of cell death, particularly when BLM is introduced intratracheally, several other pathways resulting in AEC apoptosis have been explored (Table 1.3). However, there is no agreed mechanism of AECI death in the lungs of BLM treated rodents, though it appears certain that it happens. Further, that AEC death directly contributes to fibrosis development has also not been exhaustively researched, though works which have induced AECII apoptosis (in this case, using Fas antibodies) report this injury results in fibrosis (Hagimoto, et al., 1997b), while the administration of a soluble Fas antigen or anti-Fas ligand antibody was seen to prevent both AEC apoptosis and BPF development in BLM-treated mice (Kuwano, et al., 1999).

While this mechanism may indeed be important, and AEC death is certainly seen in BPF, more research explicitly investigating the role of AEC death in this pathogenic process is required. It is expected that AEC death follows insult with BLM, but this may not be the first step in the process and may not be the whole story. There are indeed many other cells in the lung which may contribute to the deposition of collagen and eventual fibrosis.

Authors	Method of AEC apoptosis in response to BLM.	Supporting Evidence	Contradicting Evidence
Hagimoto, et al. (1997)	AEC Fas mRNA and lymphocyte Fas-L mRNA overexpression, seen in response to BLM, was associated with AEC apoptosis. Corticosteroids decreased Fas /Fas-L expression, apoptosis, and fibrosis. It was suggested Fas-/Fas-L mediated apoptosis may contribute to BPF.	Inhalation of anti-Fas antibody, simulating Fas/Fas-L interaction, induced AEC apoptosis in rats (Hagimoto, et al., 1997b). Blockade of Fas-FasL interaction prevented apoptosis and BPF (Kuwano, et al., 1999).	Epithelial cell apoptosis still occurred in BLM-treated Fas/FasL deficient mice (Aoshiba, et al., 2000). Fas-L inhibitors did not prevent apoptosis (Wallach-Dayan, et al., 2005)
Li, et al, (2003),	ANGEN mRNA upregulation in AECII in response to BLM, conversion of ANGEN to ATII and autocrine ATII signalling may induce apoptosis. Blocking ATII signalling at any point prevented apoptosis.	Myofibroblast-derived angiotensin seen to induce AEC apoptosis (Wang, et al., 1999). Angiotensin induces AEC apoptosis *in vitro* (Wang, et al., 1999b).	None available.
Lee, et al. (2005)	JNK-mediated Bax activation by BLM resulted in epithelial cell mitochondrial apoptosis. Cells overexpressing Bcl-X_L, which prevents Bax activation, were resistant to apoptosis.	None available.	None available.
Fridlender, et al. (2007)	BLM initially increases, but then decreases, telomerase activity, resulting in epithelial cell apoptosis, potentially due to factors expressed by neigh-bouring mesenchymal cells.	None available.	None available.
Wallach-Dayan, et al. (2005)	BLM induces increased ROS production, causing caspase 8/9 activation, mitochondrial leakage, and intrinsic apoptosis. This was blocked by antioxidants but not Fas-L inhibitors.	None available.	None available.

Table 1.3: BLM Mechanisms of AEC Injury

A definitive summary of the theories of the occurence of alveolar epithelial cell damage and apoptosis in BPF.

It is interesting that some have reported an overlap between angiotensin and Fas-Fas-L mediated apoptosis; Wang, et al. (2000), noted that the angiotensinogen-convering enzyme inhibitor captopril prevented AEC apoptosis via inihibition of Fas-mediated apoptosis. It was suggested that angiotensin peptides are required for Fas-mediated apoptosis (Wang, et al., 1999c), and so perhaps these two aspects overlap and both contribute to BLM-induced AEC apoptosis.

1.4.2 Pulmonary Cell Cytokine Expression in Bleomycin Pulmonary Fibrosis

Following BLM stimulation, AEC and other alveolar cells (notably alveolar macrophages (AM)) express proinflammatory cytokines and chemokines , which may contribute to fibrosis. A wide range of cytokines and chemokines have been implicated in the pathogenesis of the condition, and while many of these may be expressed by infiltrating immune cells, as will be discussed, several are also expressed by resident lung cells. Table 1.4 shows the inflammatory mediators expressed at increased levels in the lungs of BLM treated rodents *in vivo*, only where an intrapulmonary cellular source of cytokines has been identified.

Proinflammatory Mediators Expressed by Alveolar Epithelial Cells	Proinflammatory Mediators Expressed by Alveolar Macrophages
TNF-α **–** proinflammatory mediator expressed at elevated levels following BLM dosing (Song, et al., 1998; Cavarra, et al., 2004).	***MIP-1α*** – proinflammatory cytokine expressed at by alveolar macrophages during rodent BPT/BPF (Smith, et al., 1994)
IL-6 – repeatedly observed at increased levels in BLM-treated rodent BALF. AECII reported to be a source (Aumiller, et al., 2013).	***MCP-1*** – chemotactic factor and activating chemokine expressed during early stages of BLM-induced injury (Sakanashi, et al., 1994).
IL-1β **–** expressed by AECII explanted from BLM-treated rodents; increased BALF IL-1β levels also reported (Aumiller, et al., 2013).	***TNF-α*** – elevated levels are expressed by AM post BLM dosing in rodents (Cavarra, et al., 2004; Chen, et al., 1996; Everson and Chandler, 1992). AM are the primary source (Ortiz, et al., 1998b).
	IL-1β – seen at increased levels in rodent lungs post BLM (Gasse, et al., 2009; Cavarra, et al., 2004) and in rodent BPF (Gasse, et al., 2007).

Table 1.4: Proinflammatory Cytokine Expressed in BPF

Proinflammatory cytokines expressed by AECs and AMs post-BLM in the lungs of rodents.

TNF-α is a multi-functional cytokine with a number of functions which may contribute to BPF. TNF-α in the lung may induce fibroblast collagen synthesis and proliferation (Piguet, et al. (1989) – though this has been debated by some (Tufvesson and Westergren-Thorsson, 2000; Solis-Heruzo, et al., 1988), and also induce TGF-β expression (Sullivan, et al., 2009) while also inducing significant AEC necrosis (Piguet, et al., 1989) and AEC apoptosis, reportedly via angiotensinogen (ANGEN) synthesis (Wang, et al., 2000b), potentially leading to the aberrant epithelialisation seen in the lung. Moreover, TNF-α induces the expression MIP-1α (Smith, et al., 1998) which may contribute to the immune cell influx associated with BPF. Several studies have suggested that TNF-α is important to the pathogenesis of BPF; the administration of soluble TNF-α receptors to BLM treated rodents prevented BPF (Piguet and Vesin, 1994), while TNF-receptor knockout mice were impervious to BLM (Ortiz, et al., 1998; Ortiz, et al., 1999). Moreover, the administration of recombinant TNF-α was seen to result in fibrosis in rodent lungs, associated with immune cell influx (Sime, et al., 1998).

IL-1β may be a key mediator in inflammation leading to BPF (Gasse, et al., 2007), and, like TNF-α, there is a wealth of evidence to support this. It was reported that the direct application of IL-1β to the murine lung induces the expression of PDGF, TGF-β, and TNF-α (Kolb, et al., 2001), resulting in severe fibrosis; indeed, Lappalainen, et al. (2005) noted transgenic mice expressing human IL-1β in the lung epithelium experienced lung neutrophil influx and developed subpleural and alveolar fibrosis. It has also been noted that IL-1R antagonists prevent or revert fibrosis in BLM-treated mice (Piguet, et al., 1993), and mice dosed with BLM or IL-1β experienced pulmonary neutrophil infiltration and fibrosis. Administration of an IL-1β neutralising antibody attenuated this, while IL-1R knockout mice saw less neutrophil influx and fibrosis, indicating a role for IL-1 and signalling in BPF (Gasse, et al., 2007). Moreover, both TNF-α and IL-1β may induce EC adhesion molecule expression required for immune cell diapedesis (Male, et al., 2006; Madan, et al., 2000; Rahman, et al., 1998), e.g., into the lung.

Unlike TNF-α and IL-1β, MCP-1 and MIP-1α act primarily as chemoattractants for monocytes and macrophages, and lymphocytes, respectively (Sakanashi, et al., 1994; Deshmane, et al., 2009; Smith, et al., 1994), with the former implicated in the influx of macrophages to the lung following BLM dosing (Sakanashi, et al., 1994; Okuma, et al.,

2004). While the roles of MIP-1α in BPF are poorly delineated, more is known about MCP-1. In addition to leukocyte recruitment, MCP-1 has a suspected profibrotic role; MCP-1 was identified as a mitogen for fibroblast collagen production via signalling effects on fibroblasts and autocrine TGF-β upregulation by Gharaee-Kermani, et al. (1996). Later work showed that knockout mice demonstrate decreased fibrosis following BLM, and that MCP-1 may suppress the synthesis of prostaglandin E2, an inhibitor of fibroblast collagenation and proliferation, by AECs. Thus, increased MCP-1 permits fibrosis (Moore, et al., 2003). MCP-1 may also induce fibroblast IL-6 production, which may act in an autocrine fashion and prevent apoptosis (Liu, et al., 2007). Lastly, MCP-1 plays a role in monocyte-endothelium adhesion, which will be discussed.

Finally, increased IL-6 levels have been noted in BLM-treated rodent lungs by several groups (Smith, et al., 1998; Aumiller, et al., 2013). IL-6 induces MIP-1α expression (Smith, et al., 1998), and it was found that IL-6 knockout mice experience decreased immune cell infiltration and lung collagenation in response to BLM than wild-type animals (Saito, et al., 2007). IL-6 may also activate neutrophils, potentially important in BPF development (Borish, et al., 1989), and, as suggested above, may prevent lung fibroblast apoptosis in BPF (Moodley, et al., 2003). Lastly, IL-6 upregulates endothelial ICAM-1 expression (Wung, et al., 2004), which may contribute to increased immune cell recruitment.

While these works are suggestive of a strong role for these cytokines in the development of BPF, the studies in the table above used I.T. and intranasal administration of BLM to induce fibrosis. When exposing lung cells to such an immediate insult, one would expect an inflammatory response. It is also uncertain whether this cytokine expression is a direct result of BLM, or whether the cells would react similarly and express cytokine as "distress signals" if another stimulus were used (though in this case, whether such a response was BLM-mediated may be irrelevant).

Regardless, the expression of these cytokines within the lung may induce immune cell recruitment, either by their chemoattractant properties or their effects on other cell types, and this is an important part of the pathogenic processes of both human and rodent BPF

1.4.3 Immune Cell Infiltration of the Lung in Bleomycin Pulmonary Fibrosis

Pulmonary immune cell infiltration is widely reported in rodent BPF*;* neutrophils, macrophages, eosinophils, and lymphocytes have been seen to infiltrate the lung (Giri, et al., 1986; Helene, et al., 1999; Sakanashi, et al., 1994; Zhu, et al., 1996). Though the order, and duration, of infiltration by each cell type is debated (Giri, et al., 1986; Thrall et al., 1982), neutrophils represent the majority of immune cells in bronchoalveolar lavage fluid – fluid extracted from the lung - 2 days post-BLM, with macrophage and lymphocyte counts increasing up to 21 days post-BLM (Giri, et al., 1986). Indeed, Izumo, et al (2009) noted sequential infiltration, beginning with neutrophils (as noted by Izbicki, et al., 2002), then macrophages, and lymphocytes. However, the full contribution of immune cell infiltration to BPF is undefined. Neutrophils and macrophages, though, have been the subject of several compelling works, and seem likely to contribute to the development of fibrosis due to BLM. The potential contribution of each cell type will therefore be reviewed.

1.4.3.1 Neutrophils

Work directly studying the role of neutrophils in BPF gives conflicting results, with some reporting that inhibition of neutrophil and macrophage infiltration prevents BPF development (Li, et al., 2002), and others that reduced neutrophil infiltration does not ameliorate BPF (Matsuse, et al., 1999), suggesting pathogenesis may be neutrophil-independent. Indeed, it has been stated that while neutrophils enter the lung first, their transient presence suggests no direct contribution to fibro-genesis, but a neutrophil-mediated inflammatory cascade leading to fibrosis (Izbicki, et al., 2002).

This seems likely; neutrophilic ROS and elastase may induce further AEC injury (Serrano - Mollar, et al., 2002; Taooka, et al., 1997) and activate TGF-β, adding to the profibrotic milieu (Chua, et al., 2007). Neutrophil expressed IL-18, which is associated with BPF, may also be involved, as IL-18 knockout mice appear protected from BPF (Hoshino, et al., 2009). In addition, neutrophils also express high levels of TGF-β1 and MMP9 in BPF (Izumo, et al., 2009; Kim, et al., 2009), the latter of which is a gelatinase which may activate TGF-β (Yu and Stamenkovic, 2001) and also degrade the basement membrane,

allowing the migration of immune cells and fibroblasts into the lung, though this is controversial (Fattman, et al., 2008).

1.4.3.2 Exudate Macrophages

In contrast to neutrophils, the role of macrophages is more well understood. Studies assessing their contribution to BPF have reported increased exudate macrophage numbers in the lung post-BLM, with MCP-1 deemed to have induced recruitment (Sakanashi, et al., 1994), and that macrophage influx inhibition may attenuate the development of the condition (Li, et al., 2002). As MCP-1 knock-out decreased macrophage recruitment, MMP2 and 9 expression, and fibrosis (Okuma, et al., 2004), it may be suggested that MCP-1 is involved in BPF. Macrophages are also rich sources of proinflammatory and profibrotic factors.

The increased levels of MMP2/9 observed in BPF may be macrophage-derived (Okuma, et al., 2004), while both ET-1 (Mutsaers, et al., 1998) and TGF-β1 (Izumo, et al., 2009), potent inducers of collagen synthesis and fibroblast proliferation and transdifferentiation, have been identified as macrophage-derived in rodent BPF. Moreover, IL-4, which may regulate fibroblast collagen synthesis, has been seen to be expressed in higher levels in the lungs of rodents treated with BLM (Gharaee-Kermani, et al., 2001) may also be macrophage-derived. Further, while not directly assessed in BPF, activated macrophages are a ready source of IL-1β (Gasse, et al., 2007), and express TNF-α (Baer, et al., 1998). Therefore, the argument for macrophages playing a role in BPF appears strong.

1.4.3.3 Lymphocytes and Eosinophils

Lymphocytes and eosinophils, though also reported to infiltrate the lung, have been the focus of far less work. While eosinophils infiltrate the lung, release cytotoxic mediators and oxygen radicals exacerbating injury, and express factors implicated in BPF, e.g. MCP-1 (Zhang, et al., 1994), their role is unresolved; some show that eosinophil depletion attenuates BPF (Gharaee-Kermani, et al., 1998), while others report that it had no effect

(Hao, et al., 2000). Roles for lymphocytes in BPF are also uncertain. While infiltration is seen and factors expressed by lymphocytes, e.g. TNF-α (Huaux, et al., 2003), and IL-4 may be T-cell-derived in BPF (Gharaee-Kermani, et al., 2001), these factors are also expressed by macrophages and AM. Moreover, though Schrier, et al. (1983) stated athymic, T-cell deficient, mice were protected against BPF, other work using nude mice noted BPF development in the absence of T-cells (Helene et al., 1999). Thus, the contribution of lymphocytes and eosinophils remains obscure.

The cascade of damage incurred by the death of AECs, the expression of cytokines by pulmonary cells, and the entry of immune cells to the lung, invariably results in a cytokine storm. This may then lead to the defining feature of fibrotic disease, the aberrant expression of collagen by mesenchymal cells.

1.5 The Myofibroblast in Bleomycin Pulmonary Fibrosis

As with all fibrotic diseases, collagen deposition is a defining feature of BPF, and the primary cell involved is the myofibroblast. These cells are the main source of procollagen-I mRNA expression in rodent lungs post-BLM, (Zhang, et al., 1994b), and are deemed "responsible for the increased collagen gene expression" in BPF, present as they are in greater numbers in BPF lungs than control lungs (Zhang, et al., 1996) and in BPF lesions, becoming more numerous as BPF progresses (Zhang, et al., 1996; Zhang, et al., 1994).

Though the origin of myofibroblasts in pulmonary fibrosis has been questioned, and both endothelial-mesenchymal transition and fibroblastic pre-cursor cell migration into the lung have been suggested (Tanjore, et al., 2009; Hashimoto, et al., 2004), there is no compelling evidence for the existence of pre-cursor cells, and there is evidence to suggest EMT does not contribute (Yamada, et al., 2008; Rock, et al., 2011), and so it appears resident fibroblasts are the primary source of myofibroblasts in the fibrotic lung. The switch from fibroblast to myofibroblast (transdifferentiation) may be initiated by a host of pro-fibrotic cytokines, which may be expressed by pulmonary cells (Table 1.5). This expression can result in increased numbers of α-smooth muscle actin (α-SMA) and vimentin positive myofibroblasts that synthesise excess collagen and ECM proteins (Phan, 2002).

Profibrotic Mediators Expressed by Alveolar Epithelial Cells	Profibrotic Mediators Expressed by Alveolar Macrophages
TGF-β1 – expressed following BLM exposure (Azuma, et al., 2005). However, AEC expression of TGF-β post-BLM was questioned by Kumar, et al. (1996).	***TGF-β1*** – expressed during periods of ongoing disease (Khalil, et al., 1989), AM deemed a key source in BPT/BPF (Nakagome, et al., 2006).
PDGF – profibrotic mediator expressed by AECII at elevated levels following BLM exposure (Song, et al., 1998)	***PDGF –*** elevated mRNA expression by AM seen post-BLM dosing (Gurujeyalakshmi, et al., 1999).
Endothelin 1 – expressed by AECII following BLM exposure, also implicated in human BPF/BPT development (Mutsaers, et al., 1998; Park, et al., 1997).	
CTGF – expressed by AECII in mice treated with bleomycin; potentially due to autocrine TGF-β signalling (Yang, et al., 2014).	

Table 1.5: Profibrotic Cytokines Expressed in BPF

Profibrotic factors expressed by AECs and AMs following exposure to BLM.

Interestingly, fibroblasts and myofibroblasts may also be a source of profibrotic cytokines. TGF-β expression by myofibroblasts has been reported following BLM dosing (Zhang, et al., 1995), and this may stimulate the synthesis of connective tissue growth factor (CTGF) from mesenchymal cells, as suggested in Fig. 1.4; there have been reports of increase CTGF expression in fibroblastic cells isolated from the BLM-treated murine lung (Ponticos, et al., 2009), so this is a possibility. The autocrine signalling that could potentially result from this may lead to further fibroblastic activation and collagen synthesis.

It is also known that human lung fibroblasts express basal ET-1 levels (Ahmedat, et al., 2012) and it has been demonstrated that TGF-β induces the expression of ET-1 by human lung fibroblasts (Ahmedat, et al., 2012). These fibroblasts also express ET-1 receptors, permitting an autocrine system of fibroblast ET-1 expression and subsequent fibroblast collagen synthesis in response to ET-1 receptor binding (Ahmedat, et al., 2012), which may lead to furtherfibrosis. Though fibroblast endothelin-1 expression, or increase expression in response to TGF-β, has not yet been demonstrated in BPF, it is a feasible that this process occurs in this environment. The expression of other profibrotic cytokines, such as PDGF by fibroblasts is yet to be described in the BPF model, however.

1.5.1 TGF-β in the Bleomycin-Treated Lung

The most widely implicated factor is TGF-β, reported at increased levels in the lungs of BLM-treated rodents, with TGF-β1 being the predominant isotype (Coker, et al., 1997). A role for this cytokine in BPF and excess collagenation has long been suspected, with early reports noting increased numbers of myofibroblasts at 24h post-BLM located in areas of excess collagen. These cells increased in number over time, and the phenotypic alteration was associated with TGF-β expression and signalling (Vyalov, et al., 1993). With regard to studies that have focussed on the expression of the cytokine itself, it was reported that TGF-β1 is expressed at increased levels in the lungs at a gene expression level following BLM insult (Coker, et al., 1997), at mRNA and protein level in both the inflammatory and the reparative stages of BPF, particularly by alveolar macrophages and bronchial epithelia, respectively (Santana, et al., 1995; Khalil, et al., 1989). This, together with reports of temporal and spatial concordance between maximum TGF-β expression in the

lung and maximum collagen production, and of TGF-β localisation in areas of fibrotic repair (Khalil, et al., 1989), suggests TGF-β has an important role in rodent BPF.

TGF-β induces fibroblast α-SMA expression and modulates transdifferentiation and collagen expression via multiple signalling pathways (Fine and Goldstein, 1987; Desmoulière, et al., 1993). These include the complex Smad signalling pathways, which induce increased collagen expression via stimulation of COLIA2 gene transcription (Cutroneo, et al., 2007), and α-SMA gene expression via Smad3 (Hu, et al., 2007). TGF-β receptor binding causes Smad3 phosphorylation and complexing with Smad 4, which translocates to the nucleus and binds Smad-binding elements, inducing gene transcription (Ponticos, et al., 2009).

TGF-β may also act by inducing synthesis of, and responsiveness to, CTGF by fibroblasts via autocrine CTGF signalling (*Fig.* 1.4) (Grotendorst and Duncan, 2005; Grotendorst, et al., 2004; Duncan, et al., 1999; Kothapalli, et al., 1997). CTGF mRNA upregulation and protein expression have been reported in murine lungs post-BLM dosing and prior to fibrosis, potentially mediated by TGF-β stimulation (Lasky, et al., 1998) and are associated with increased fibroblast collagen synthesis in BLM-treated mice (Ponticos, et al., 2009). Moreover, application of CTGF to mice can itself induce pulmonary fibrosis (Bonniaud, et al., 2003), so CTGF may play a role in the colleagenation of the lung post-BLM. Indeed, CTGF blockade was found to reduce BPF in rodents (Yang, et al., 2014) Interestingly, AECII are known to express CTGF in IPF patients (Pan, et al., 2001).

Interestingly, increased active TGF-β levels in the lung post-BLM have been reported (Russo, et al., 2009; Atzori, et al., 2004). TGF-β requires activation - conversion to a biologically active form - to exert activity, and latent TGF-β is secreted with the latency-associated peptide (LAP) or the latent TGF-β-binding protein (LTBP) (Annes, et al., 2004). Latent TGF-β may be activated by MMP 2/9 (Yu and Stamenkovic, 2000), present in the lungs and increased levels in BPF (Okuma, et al., 2004; Kim, et al., 2009); and thrombospondin-1 (TSP-1) (Schultz-Cherry and Murphy-Ullrich, 1993), expressed by AM post-BLM (Yehualaeshet, et al., 2009). In BPF, these proteins may interact, with MMP2/9-mediated activation, dependent on interaction with AM CD36-bound TSP-1 (Yehualaeshet, et al., 1999), activating TGF-β, potentially explaining the increase in

alveolar macrophage active TGF-β expression (Khalil, et al., 1996; Khalil, et al., 1993). Activation may also be isoform-dependent; when secreted with LTBP-1, latent TGF-β is activated by interaction with αvβ6 and fibronectin (Annes, et al., 2004; Fontana, et al., 2005; Zhou, et al., 2009), the former expressed at increased levels by epithelial cells post-BLM (Nakagome, et al., 2006).

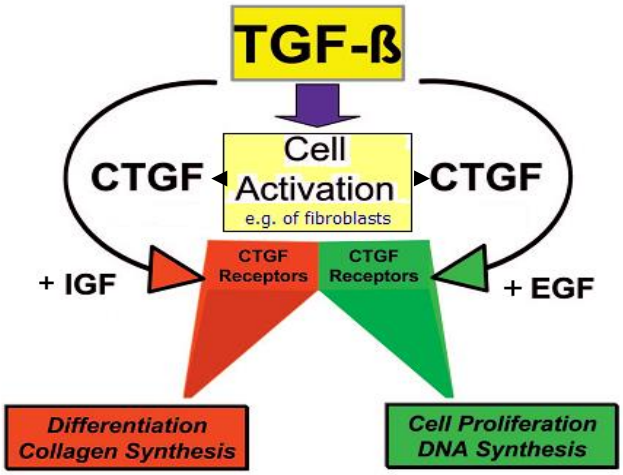

Figure 1.4: CTGF Induction in Mesenchymal Cells

Adapted from Grotendorst and Duncan (2004). Activation of rodent fibroblasts by TGF-β induces fibroblast proliferation via induction of CTGF production and priming of cells to become responsive to CTGF. CTGF is a downstream mediator of TGF-β functions. Presence or absence of other growth factors, e.g. epidermal growth factor (EGF) and insulin -like growth factor (IGF) mediates the biological response. Notably, ICF and ECF alone do not mediate proliferation or transdifferentiation.

Considering its potential importance, there is surprisingly little direct research into the contribution of TGF-β to the development of BPF. Wang, et al. (1999d) and Arribillaga, et al. (2010) saw decreased collagenation post-BLM in hamsters treated with soluble TGF-β receptors, and fewer myofibroblasts and fibrosis post-BLM in mice treated with TGF-β1 peptide inhibitor, respectively, appearing to confirm earlier suspicions of a role of TGF-β in fibrogenesis. Meanwhile, TGF-β signalling blockade was reported to decrease fibroblast transdifferentiation and BPF (Kurotani, et al., 2011), as was inhibition of the activation and synthesis of the cytokine using IL-10 gene delivery (Nakagome, et al., 2006),

suggesting a strong role for this cytokine in the generation of fibrotic disease. Of course, these are not the only effects of TGF-β. In addition to fiboblast proliferation, TGF-β is a chemoattractant for monocytes (Reibman, et al., 1991), and may act upon lung epithelial cells, preventing the proliferation of AECII (Khalil, et al., 1994; Zhang, et al., 2004; Yue and Mulder, 2001), and inducing the apoptosis of lung epithelial cells via caspase-3 activation (Hagimoto, et al., 2002). This may precipitate the AEC death that so characterises fibrotic diseases such as BPF, and TGF-β may therefore contribute to the pathogenesis of the disease in many ways.

1.5.2 Other Profibrotic Cytokines in the Bleomycin-Treated Lung

Though their direct effects have not been investigated, ET-1 and PDGF may contribute to BPF. Park, et al. (1997) noted increased ET-1 expression in airway epithelia, AECII and immune cells in BLM-treated rats, and the inhibitor bosentan reduced fibrosis. Meanwhile Gurujeyalakshmi, et al. (1999) noted increased PDGF-A and –B mRNA levels in BLM-treated hamster AM; BALF from BLM-treated hamsters co-treated with the inhibitor pirfenidone showed decreased mitogenic activity on fibroblasts, possibly due to decreased PDGF protein expression via decreased mRNA translation.

PDGF is a potent fibroblastic mitogen, inducing the survival and proliferation of myofibroblasts, and may also induce myofibroblast collagen expression via interaction with PDGFRα and β receptors and the associated signalling cascades, reviewed by Bonner, et al. (2004). PDGF, particularly the B isoform, has been implicated in non-BLM lung fibrosis (Lo Re, et al., 2011; Hoyle, et al., 1999), and the overexpression of PDGF-B mRNA by AM has been seen in IPF and interstitial lung disease patients (Antoniades, et al., 1990; Nagaoka, et al., 1990; Martinet, et al., 1987). Moreover, the concomitant expression of PDGF and TGF-β is associated with fibrosis in rodents (Yoshida, et al., 1995) and man (Bergmann, et al., 1998), suggesting that this cytokine may play a role in the development of fibrotic disease.

Also profibrotic, ET-1 is expressed by many cells including AECII (Giaid, et al., 1993), AMs (though this has not necessarily been observed in rodent BPF) (Fagan, et al., 2001), and

endothelial cells (ECs) (Yanagisawa, et al., 1988), and its release is induced by factors such as TGF-β (Fonseca, et al., 2009). ET-1 mediates fibroblast chemotaxis, proliferation (Peacock, et al., 1992) and transdifferentiation (Shi-Wen, et al., 2004; Ross, et al., 2009), potentially via NF-κB and CTGF induction (Ross, et al., 2009), and promotes increased collagen production by mesenchymal cells (Fonseca, et al., 2009). Further, TGF-β and ET-1 together may induce myofibroblast apoptosis resistance (Kulasekaran, et al., 2009), prolonging collagen deposition. Roles for ET-1 in fibrosis are poorly defined, though lung and BALF samples from IPF patients contain increased levels of ET-1 (Saleh, et al., 1997; Reichenberger, et al., 2001), with neutrophils, macrophages, and AMs potential sources in fibrotic disease (Saleh, et al., 1997; Shahar, et al., 1999), suggesting many sources for ET-1 in fibrosis, one of which may be ECs, that could potentially contribute to fibrosis.

Interestingly, BLM itself may result in increased collagen expression by fibroblasts. Koslowski, et al. (2004) saw increased collagen production in rat fibroblasts cultured with BLM, while Lu, et al. (2009) and Moseley, et al. (1986) noted human fibrolast proliferation in response to BLM alone and in combination with PDGF. In addition, it has been reported that treatment of fibroblasts with BLM may induce pro-collagen-I and –III expression, as well as that of TGF-β (Breen, et al., 1992), suggesting that in BPF, BLM itself may induce the expression of collagen and cytokines.

1.6 The Potential Role for Vascular Endothelial Cells in Bleomycin Pulmonary Fibrosis

Of course, when I.T. BLM dosing is used, as it so often is in rodent modelling studies, the primary site of injury would be expected to be to the AECs, and no damage would be expected to vascular endothelial cells (VECs), as this cell type is bypassed by I.T. drug delivery. However, the disease caused by this delivery route may not mimic that seen in humans (Borzone, et al., 2001), and though the pathogenesis of the disease caused by I.T. BLM is better defined, it may be missing a vital step.

When BLM is delivered intravenously, as it is in humans, VECs (notably pulmonary VECs) may be the first cell type of the lung to come into contact with the drug. It has indeed

been reported that, when I.V. BLM is used in animal works, the vascular endothelium is the site of initial, and in some cases, sole injury. As I.V. dosing is rarely used in experimental modelling, many aspects of the potential model of BPF development either bypass or ignore the potential role of VECs in these processes. However, some current research suggests that the vascular endothelium is more than a passive bystander in the development of BPF.

1.6.1 Endothelial Cell Junction Permeability

It has been reported that I.T. BLM delivery in the rat results in endothelial tight junctions being held in an open state following dosing (Yin, et al., 2012). This was suggested to potentially increase immune cell influx into the lung, as open cell-cell junctions permit easier passage through the endothelium, but it is also possible that this increased vascular permeability accounts for the oedema reported in BPF, and may also allow the movement of systemic cytokines or blood-borne BLM into the lung, which may precipitate the AEC injury and damage that so characterises the disease.

1.6.2 Endothelial Cell Profibrotic Cytokine Expression

Interestingly, BLM appears to induce the expression of profibrotic cytokines in rodent endothelia. It was reported that TGF-β expression is induced *in vitro* by rodent endothelial cells exposed to BLM (Phan, et al., 1991), while Yin, et al. (2011) reported TGF-β1 and CTGF synthesis and expression by PMVECs isolated from I.T. BLM-treated rats 7 days post-BLM. This correlated with the development of interstitial fibrosis in BLM-dosed rodents, and with interstitial fibroblast transdifferentiation as determined by fibroblast α-SMA and collagen synthesis. PMVECs isolated from BLM-treated rats also promoted fibroblast transdifferentiation and collagen I protein expression when co-cultured *in vitro*.

Of course, it is difficult to assign a role for BLM in this process; profibrotic cytokine expression may have been induced by AEC and AM-expressed cytokines acting on VECs.

Moreover, as I.T. BLM administration results in a cytokine storm within the lung, then AEC or AM expressed cytokines may have induced interstitial fibroblast transdifferentiation. Work assessing this phenomenon using I.V. BLM dosing would be required to delineate whether BLM is directly causing these effects.

However, if such cytokine expression is BLM-mediated, it is possible that VEC-expressed cytokines, as diffusible mediators, may translocate into the lung and interstitium, though no current research has directly tracked endothelial cytokine movement into these areas. The increased endothelial permeability caused by BLM (Yin, et al., 2011), may feasibly assist this, allowing fibroblast transdifferentiation to occur and fibrosis to develop in these regions.

If such profibrotic cytokine release also occurs in man, then this may be a contributing factor to the development of BPF. Human endothelial cells express a broad range of such factors. Endothelin-1 is expressed by endothelial cells of various types including HUVECs and pulmonary VECs in response to various stimuli (Golden, et al., 1998; Wang, et al., 1993; Kurihara, et al., 1989; Bilsel, et al., 2000; Stow, et al., 2011), while PDGF may also be expressed by endothelial cells from the umbilical vein and lung microvasculature (Collins, et al., 1987; Kourembanas and Faller, 1989; Albelda, et al., 1989; Harlan, et al., 1986). TGF-β is also synthesised and expressed by HUVECs and human intestinal endothelia (Nilsen, et al., 1998; Pintervorn and Ballerman, 1997) and PAECs in rodents (Phan, et al., 1992) and potentially in response to BLM (Yin, et al., 2012), and the diffusion of these mediators into the lung or their effects on the fibroblasts in the interstitium may result in fibrosis development leading to BPF.

1.6.3 Endothelial Cell Adhesion Molecule and Proinflammatory Cytokine Expression

Immune cell infiltration is clearly a major feature of rodent BPF development to which VECs may contribute, and VECs are also a ready source of proinflammatory cytokines, such as MCP-1 and IL-8 which may recruit and activate immune cells which may then migrate into the lung, increasing pulmonary cellularity. Further, endothelial cells likely play a large role in the recruitment of immune cells to the lung by expression adhesion

molecules which are vital in the anchoring of immune cells to the luminal surface of vessels, the first step of diapedesis. Interestingly, both proinflammatory cytokine release and adhesion molecule expression have beeenreported in the literature in human and rodent endothelial cells.

In rodents, the amount of research is relatively low. However, there have been reports of cytokine expression by VECs explosed to BLM *in vitro*, such as those of increased expression of IL-6 (Karmiol, et al., 1993;), while in *in vivo* studies, strong E-selectin mRNA induction in response to intravenous BLM in pulmonary vasculature of rodents was reported by Azuma, et al. (2000), with increased lung myeloperoxidase levels suggesting neutrophil infiltration in I.V. BLM dosed mice. At a functional level, Li, et al (2002) and Matsuse, et al (1999), both having used I.V. dosing, noted significant lung infiltration by neutrophils, lymphocytes, and macrophages in BLM-treated rodents which was decreased when ICAM-1 and VCAM-1 were blocked with antibodies and macrolides, respectively. This suggests that adhesion molecules are expressed, and function in immune cell recruitment in this model, though while the blockade of ICAM-1 expression by Matsuse, et al. (1999) did not ameliorate BPF, the blockade of VCAM-1 by Li, et al. (2002) did, and so the roles of these molecules in rodent BPF remain unclear.

Interestingly, there are reports of endothelial cell adhesion molecule expression stemming from I.T. BLM dosing, and these are more numerous. Perhaps the most relevant is the work of Weiner, et al. (1998), which using an indium-labelled anti-ICAM-1 antibody, noted ICAM-1 upregulation in the lung within 4 hours of dosing, though increased P-selectin expression post-I.T. BLM dosing in rodents has also been reported (Serrano-Mollar, et al., 2002), as has ICAM-1 upregulation by pulmonary VECs isolated from rats post-I.T. BLM dosing by Sato, et al. (2000). This increased ICAM-1 expression was seen to have a functional relevance, resulting in increased leukocyte rolling and entrapment in venules and capillaries. More recently, Wang, et al. (2011) noted leukocyte migration across pulmonary venules to the perivascular space, associating with ICAM-1 and VCAM-1 in areas of transmigration, which also signifies a functional relevance of adhesion molecules in the lung post-BLM. Further, Hamaguchi, et al. (2002) noted decreased collagen deposition, leukocyte infiltration, and cytokine production in the lungs of I.T. BLM-treated, ICAM-1 knock-out mice, compared to treated wild-type mice,

suggesting ICAM-1 may be particularly relevant; thus, it appears adhesion molecules may be expressed by VECs when I.T. dosing is used, and this may contribute to BPF.

The importance of the Weiner, et al. (1998) work extends beyond the identification of ICAM-1 upregulation in the lung post-BLM. Other organs assessed, the liver and spleen, did not show such upregulation until 24-hours post-dose, and even then, this was less significant. It was also reported that LFA-1, a CD18-bearing ligand for ICAM-1, was upregulated on polymorphonucleocytes (PMNs), potentially "priming" these cells for interaction with ICAM-1. This is the only study to assess adhesion molecule upregulation in various organs of the BLM-treated mouse, and not only suggests that ICAM-1 is upregulated in the lung, but that this is an organ specific effect, and may be why the lung is the most affected organ following dosing. However, this work only examined ICAM-1 expression in three organs, and so a blanket statement cannot be made about ICAM-1 upregulation in non-assessed organs. However, this work provides a valuable framework on which to build other studies. It would surely be very interesting to assess where and when adhesion molecules are upregulated in response to BLM in a wider variety of organs.

However, in rodents, the role of these adhesion molecules is uncertain, as shown above with the work of Li, et al., and Matususe, et al., whereby adhesion molecule blockade did and did not ameliorate BPF, respectively. Furthermore, Horikawa, et al. (2006), reported that E-selectin knock-out mice treated with anti-P-selectin monoclonal antibody endured increased fibrosis and mortality, and demonstrated decreased numbers of IFNγ-expressing natural killer T-cells (NKT) in BALF compared with wild-type mice. The lack of IFN-γ expressing NKT cells may have been deleterious, as IFN-γ inhibits collagen production (Rosenbloom et al., 1984), and downregulates TGF-β expression (Gurujeyalakshmi and Giri, 1995). Thus, the role of the adhesion molecules in rodent BPF requires more study, though they appear to induce the recruitment of immune cells. In addition, none of these works assessed whether adhesion molecule and cytokine expression was mediated by BLM directly, or by the action of AEC/AM-expressed factors. For once, *in vitro* work may be preferable, as this would allow researchers to determine whether such upregulation is indeed BLM-related. Of course, research into adhesion molecule expression by BLM-treated human cells has been just that.

Work assessing adhesion molecule expression in BLM treated human cells has revealed E-selectin and ICAM-3 mRNA and protein expression, and IL-8 and MCP-1 secretion by HUVECs stimulated with BLM (Miyamoto, et al., 2002), though the protein expression of IL-8 and MCP-1 was only induced to high levels when cells were incubated with BLM over 48 hours, not a typical exposure time in BLM-treated patients. In other work, Ishii and Takada (2002) observed increased E-selectin expression by HUVECs treated with between 1 and 7μg/ml BLM *in vitro*, potentially mediated by direct activation of the E-selectin promoter, so it appears that BLM may also upregulate the expression of this particular adhesion molecule. While ICAM-1 expression in HUVECs was not noted by Miyamoto, et al. (2002), this is in contrast to the only other published work in this field, the work of Fichtner, et al. (2004), who noted BLM-induced increased ICAM-1 protein and IL-8 expression by human pulmonary microvascular ECs (PMVECs), though again, at supra-pharmacological concentrations of around 50μg/ml. Therefore, there is no real agreement observed in these studies, other than that E-selectin is upregulated in BLM-treated HUVECs, that IL-8 is expressed by VECs exposed to high-dose or long-duration BLM treatment, and that the expression of these proteins is most likely BLM-related.

A further question is how stimulation by BLM *in vitro* mediates cytokine and adhesion molecule expression. Ishii and Takada (2002) suggested NF-κB/Rel activation by BLM-associated ROS induces NF-κB/Rel nuclear translocation and transcriptional activation of the E-selectin gene, as NF-κB/Rel, but not AP-1, inhibition attenuated E-selectin expression, but no ROS source was suggested. E-selectin expression requires NF-κB activation and NF-κB binding to the promoter (Montgomery, et al., 1991; Read, et al., 1994; Schindler and Baichwal, 1994), along with high-mobility-group protein I(Y) binding (Lewis, et al., 1994; Whitley, et al., 1994) and JNK/p38 activation, (Read, et al., 1997; Min and Pober, 1997), so this seems feasible. Moreover, ICAM-1 induction following VEC stimulation depends on NF-κB signalling (Ledebur and Parks, 1995; Rahman, et al., 1999; Guo, et al., 2012), as does VCAM-1 expression in response to TNF-α, IL-1β, and LPS (Ahmad, et al., 1998; Iademarco, et al., 1992; Marui, et al., 1993) though PI3K and MAPK have also been implicated (Binion, et al., 2009). Thus, if BLM initiates NF-κB activation, then this may result in the expression of several molecules.

The expression of IL-8 and MCP-1 may also depend on NF-κB activation (Tanner, 2004; Brasier, 2010; Molestina, et al., 2000), though Fichtner, et al. (2004), noted that BLM induced P38 MAPK phosphorylation and activation, the inhibition of which decreased IL-8 expression. IL-8 expression by BLM-treated VEC may be MAPK-mediated, though the authors conceded the involvement of P38 MAPK in IL-8 expression was cell type- and stimulus-dependent. Both, or either, pathway may induce expression. Currently, no literature exists clarifying the mechanisms of factor or adhesion molecule upregulation and expression by BLM-stimulated VECs, so no inferences can be made regarding how or if BLM stimulation induces this expression. However, this would be an interesting avenue for future research into this field.

Currently, publications by Miyamoto, et al. (2000), Fichtner, et al. (2004), and Ishii and Takada (2002) are the only works assessing adhesion molecule and cytokine expression by human endothelial cells exposed to BLM. As immune cell recruitment is a feature of the disease in man as well as mouse, and VECs are known to express many cytokines which may contribute to immune cell recruitment and fibrosis, then this is an area desperate for new research. Of particular interest would be studies using pharmacologically-relevant concentrations of the drug over relevant time points, and further investigation into which adhesion molecules and cytokines are upregulated in response to BLM.

Previous work in into this field is limited, much concerns rodents, and some is at supra-pharmacologically-relevant BLM concentrations. Of the three studies studies assessing the response of human cells to BLM, one used concentrations of BLM that would not be encountered in the circulation of patients receiving the drug (Fichtner, et al., 2004), and another, a narrow range (Ishii and Takada, 2000). One would expect the adhesion molecule expression and cytokine release in response to supra-pharmacological concentrations to be higher than when cells were subject to pharmacologically-relevant BLM concentrations.Therefore, the findings of these works, while interesting, may not be totally relevant. Work assessing endothelial adhesion molecule expression and cytokine release using a range of pharmacologically-relevant concentrations, outlined in Table 1.1, would be more applicable to the true environment initiated by BLM treatment in man, and may give results that more accurately mirror the endothelial response to BLM.

Further, work assessing the response of the most relevant cell type, PMVECs, to pharmacologically-relevant BLM concentrations, would be of particular use. By doing this, a better picture of the processes ongoing in the human lung following BLM dosing may be built, and how the effect of the drug on the pulmonary endothelium may contribute to the inflammation which precedes BPF development may be better elucidated. The expression of profibrotic cytokines in this environment will also be invaluable, to determine whether this is another role for VECs in BPF onset.

As all of the adhesion molecules and pro-inflammatory cytokines mentioned above are involved in the diapedesis cascade - whereby immune cells are recruited to, adhere to, and traverse through, the endothelium, the role of these proteins - and others - in this process must be discussed. From this, appropriate adhesion molecules and cytokines to assess in future works may be determined.

1.7 The Process of Diapedesis and the Adhesion Molecules and Cytokines Involved

The diapedesis cascade, by which immune cells enter the site of injury, is a multi-step process, as shown in Fig. 1.5. First, immune cells may be recruited to the endothelium by chemoattractant cytokines such as IL-8 and MCP-1, in the case of the relevant cell types in this work (monocytes and neutrophils) and from here, cells may tether to the endothelium. This tethering is mediated by a wide range of adhesion molecules and ligands. ICAM-1, E-selectin, P-selectin, PECAM-1, PSGL-1, and a many other molecules are involved in immune cell-endothelial interaction, adhesion and diapedesis (Ley, et al., 2007), and each stage of the multi-step process of transmigration involves different molecules, ligands, and chemokines, summarised briefly in Table 1.6.

Adhesion molecule expression profiles determine the immune cells that tether to the endothelium, as each binds specific ligands (*Table 1.6)*. VEC E-selectin (Rahman, et al. 1999) VEC/platelet P-selectin, and potentially PSGL-1 on VEC and leukocytes (da Costa Martins, et al., 2007) mediate tethering by binding leukocyte ligands. Such interactions slow cells, inducing rolling on the endothelial surface, and slowed cells may subsequently

be triggered by selectin ligation (Ley, et al., 2007) or by chemokines at the endothelial surface - bound to glycosaminoglycans (GAGs), VEC-released, or tissue-expressed and transported across the endothelium - which bind specific G-protein coupled receptors (GPCRs) on tethered cells (van Gils, et al., 2009; Male, 2006).

Adhesion Molecule	Function/Cell Type	Functional Ligands
E-selectin	Mediates rolling and tethering of neutrophils, monocytes, and subsets of T-cells.	• Binds CD44, ESL-1, and Mac-1 ($\alpha_M\beta_2$) on neutrophils (Zarbock, et al., 2009; Zen et al., 2007) • Binds monocyte PSGL-1 and CD44 (Ley, 2007), PSGL-1 on previously activated "memory" T-cells (Borges, et al., 1997) • Binds ESL-1 and CD43 on T_H1 and T-lymphocytes, respectively (Zarbock, et al., 2011)
Endothelial P-selectin	Mediates rolling and tethering of neutrophils, monocytes, and T lymphocytes.	• Binds PSGL-1 on neutrophils and monocytes (Zimmerman, 2001), memory T-cells (Borges, et al., 1997), and eosinophils (Woltmann, et al., 2000).
ICAM-1	Mediates adhesion of lymphocytes, neutrophils, monocytes, and eosinophils.	• Binds LFA-1 ($\alpha_L\beta_2$) expressed on lymphocytes, Mac-1 and LFA-1 expressed on neutrophils (Hopkins, et al., 2004; Lefort and Ley, 2012; Hertzen, et al., 2000) • Binds monocytes and eosinophil LFA-1 and Mac-1 (van Gils, et al., 2009; Jia, et al., 1999). LFA-1 also binds to ICAM-2, inducing adhesion (Yusuf-Makagiansar, et al., 2002).
VCAM-1	Mediates adhesion of monocytes, eosinophils, and neutrophils. Mediates rolling and tethering of lymphocytes.	• Binds VLA4 on monocytes, eosinophils, (Yusuf-Makagiansar, et al., 2002), and may mediate rolling and tethering of lymphocytes via VLA-4 interaction (Alon, et al., 1995) • VLA4 may also be expressed by neutrophils (Lomakina and Waugh, 2009), while this had not previously been supposed (Yusuf-Makagiansar, et al., 2009). • May also bind to lymphocyte LPAM-1 (Yang, et al., 1998).
Endothelial PSGL-1	Mediates leu-kocyte rolling, tethering, and adhesion.	• Binds P-selectin expressed on platelets and L-selectin expressed on monocytes and neutrophils (da Costa Martins, et al., 2007; Sperandio, et al., 2003; Spertini, et al., 1996).

Table 1.6: Endothelial Cell Adhesion Molecules

Molecules involved in the rolling, tethering, and adhesion of immune cells to the endothelium in man.

Chemokine triggering induces integrin activation, resulting in conformational changes to immune cell integrins (van Gils, et al., 2009; Ley, et al., 2007) such as LFA-1 and VLA-4, inducing increased-affinity binding of these ligands to adhesion molecules. Outside-in signalling by bound integrins stabilises adhesion (Ley, et al., 2007). VEC ICAM-1/2 and leukocyte Mac-1/LFA-1 dependent crawling (Phillipson, et al., 2006; Schenkel, et al., 2004) may then deliver leukocytes to migration locations.

Junction molecules - those located in the endothelial cell-cell junctions - are also involved in extravasation, including PECAM-1, CD99, and possibly JAM-A; homophilic interaction between VEC and leukocyte PECAM-1 and CD99 occur during diapedesis (Ley, et al., 2007) while JAM-A may undergo heterophilic interactions with LFA-1 (Ostermann, et al., 2002). Both are important in diapesesis, and may guide leukocytes through the junction and, in the case of BPF, potentially into the lung.

Many of these adhesion molecules are involved is several steps of diapedesis, and their expression is controlled in many different ways within the endothelial cell. Therefore, each of these molecules will be discussed independently, and their role in the process of immune cell transmigration considered. Further, MCP-1 and IL-8, both involved in the recruitment of immune cells to the site of adhesion molecule expression prior to adhesion molecule tethering, and also involved in the activation of immune cells prior to their adhesion to the endothelium, must also be investigated.

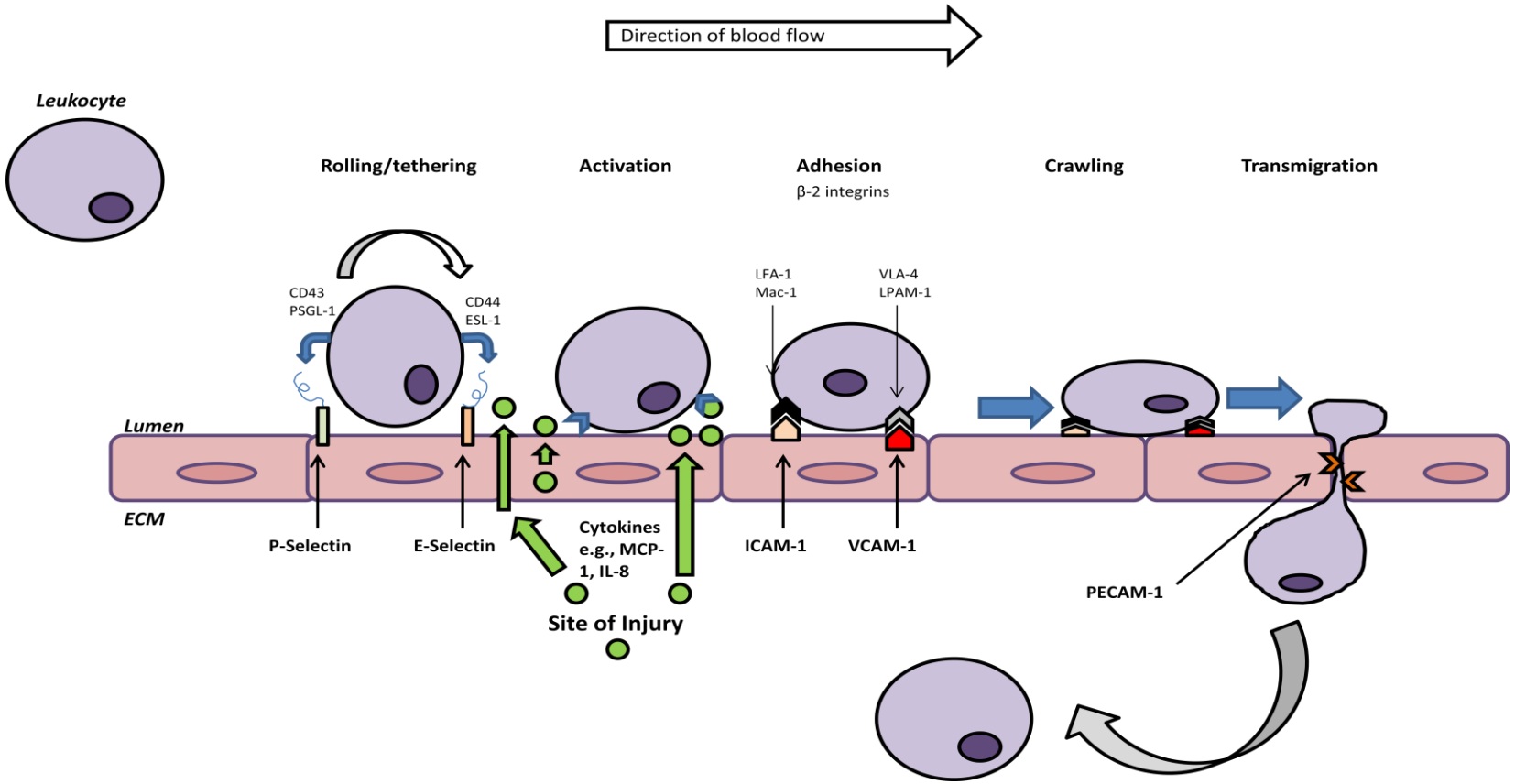

Figure 1.5: The Transendothelial Migration Cascade

The process of diapedesis. Selectins, e.g. P- and E-selectin, mediate leukocyte rolling and tethering as bonds are formed and broken rapidly, slowing the cell. Slowed cells are activated by cytokines, e.g. IL-8 and MCP-1. Activated cells then bind to ICAM-1 and VCAM-1 via β-2 integrin ligation to adhesion molecules. Leukocytes may then crawl along the endothelium to the site of transmigration (usually cell-cell junctions), through which leukocytes move via interactions between leukocyte and junctional ligands such as PECAM-1, expressed on both cell types. As described in *Table 1.6,* the immune cells recruited depend on the adhesion molecules expressed.

1.7.1 Rolling and Tethering – The Initial Step in Transendothelial Migration (TEM)

The initial step in transendothelial migration (as shown in Fig. 1.5) is the rolling of immune cells captured from circulation and the tethering of these cells to the vascular endothelium. This may be mediated by molecules including E-selectin and P-selectin, but may also be mediated by molecules such as PSGL-1.

1.7.1.1 E-selectin (CD62E)

E-selectin, exclusively expressed by ECs, is involved in the initial capture and tethering of circulating immune cells (Ley, et al., 2007; Rahman, et al., 1998). E-selectin expression occurs in response to cytokine stimulation, for example, by TNF-α, IL-1, and LPS (Bevilacqua, et al., 1987; Carlos, et al., 1991; Haraldsen, et al., 1996), and peaks rapidly, within around four hours, before expression tapers off after 24-30 hours (Male, et al., 2006).

E-selectin binds fucose-rich glycoproteins containing sialylated Lewis^X oligosaccharides as a minimal recognition motif, mainly PSGL-1 and CD44 in humans (Ley, et al., 2007; Rahman, et al., 1998; Foxall, et al., 1992), and upon tethering, induces the rolling of leukocytes, allowing chemokine-mediated ligand activation. E-selectin binds ligands with rapid on/off rates – meaning that bonds form quickly but also break quickly (McEver and Zhu, 2010) - allowing leukocyte capture, slowing the cell, while dissociation allows rolling. This appears to be a triphasic binding system involving both slip (rapid transient binding) and catch (more enduring, stable binding) bonds (Wayman, et al., 2010), though neutrophil adhesion to E-selectin may also occur under static conditions (Simon, et al., 2000), and so the nature of E-selectin mediated binding is uncertain. Regardless, binding of E-selectin by its ligands may induce signalling leading to TEM.

It appears binding of leukocyte PSGL-1 to E-selectin may induce integrin affinity modulation allowing the adhesion of leukocytes to the endothelium, though this is not well resolved. Simon, et al. (2000) reported that human neutrophils adhered stably to E-selectin-transfected L-cells in a β2 integrin-mediated fashion, and that E-selectin-PSGL-1

interaction-mediated affinity modulation of β2 integrins was caused by MAPK and p38 signalling, as blockade of either prevented stable adhesion. The affinity modulation of β2 integrins allowed the adhesion of the neutrophils to other adhesion molecules. Later, Kuwano, et al. (2010) suggested the binding of neutrophil PSGL-1 to VEC E-selectin, via Syk activation, leads to LFA-1 activation. This led to decreased neutrophil rolling velocity and firm adhesion, potentially to ICAM-1, which was expressed concurrently with E-selectin. E-selectin binding to CD44 may also induce inside-out signalling - Green, et al. (2004) noted neutrophil ligation to E-selectin resulted in the focal redistribution and clustering of L-selectin, PSGL-1, and β2 integrins in human neutrophils – though the functions of this are unknown. However, it does appear that E-selectin binding may not only slow the cell and allow rolling, but alter the affinity of other ligands on the rolling immune cell, allowing these cells to tether to other adhesion molecules.

Finally, E-selectin ligation may lead to VEC junction opening. Lorenzon, et al. (1998) observed ligation of E-selectin with mAb induced intracellular Ca^{2+} increases and stress fibre formation. E-selectin associates with cytoskeletal components, and its ligation may result in PLCγ recruitment and tyrosine phosphorylation, thus Ca^{2+} mobilisation and cytoskeletal rearrangement, which may contribute to TEM, potentially via junctional remodelling (Kiely, et al., 2003).

1.7.1.2 P-Selectin (CD62P)

P-selectin, expressed by endothelial cells and platelets, (Ley, 2003), is also involved in the tethering of immune cells, via interaction with leukocyte PSGL-1(Borges, et al., 2004; Zimmerman, et al., 2001; Woltmann, et al., 2000). Unlike E-selectin, P-selectin is constitutively synthesised (Liu, et al., 2010b) and is stored in Wiebel-Palade Bodies (WPB), rod-shaped cytoplasmic components that contain many proteins (Weibel and Palade, 1964; Metcalf, et al., 2008; McEver, et al., 1989). Expression by HUVECs occurs rapidly in response to thrombin and histamine and peaks around 10 minutes post-stimulation, with the molecule beinginternalised again within 30-60 minutes (Hattori, et al., 1989; Sugama, et al., 1992; Vestweber and Blanks, 1999), though it may also be expressed constitutively by low-passage HUVECs *in vitro* (Melrose, et al., 1998).

Like that of E-selectin, P-selectin tethering occurs with high on-off rates, and binding requires the expression of sialylated Lewis^X oligosaccharides in the ligand (McEver and Zhu, 2010), though the binding of P-selectin is impacted by shear force. Increases in shear increase the mean time of tethering, mediated by catch-bonding. As shear increases further, the duration of tethering decreases, representing a shift to slip-bonding (Marshall, et al., 2003b), and the rolling cell slows.

Compared to other adhesion molecules, the role of P-selectin appears to be restricted. However, there is evidence that the binding of P-selectin to neutrophil PSGL-1 may give a higher affinity conformation of neutrophil Mac-1, increasing neutrophil adhesiveness to the substrate (in this case, fibrinogen) (Ma, et al., 2004), though other reports have stated that this does not augment adhesiveness of neutrophils to physiological adhesion molecules such as ICAM-1 in humans (Blanks, et al., 1998). Further, an overlapping function for P-and E-selectin has been reported in mice, where blockade of one did not prevent TEM, but blockade of both did (Subramaniam, et al., 1997) and in work where genetic knockout of both E- and P-selectin was required to prevent neutrophil TEM (Homeister, et al., 1998). Whether this is the case in man is uncertain, but as P-selectin is known to be involved in the initial tethering of immune cells to VECs, and therefore must be considered here.

1.7.1.3 P-selectin glycoprotein ligand (PSGL-1; CD162)

P-selectin glycoprotein ligand 1 (PSGL-1) is expressed by many cell types including leukocytes, and also ECs, on which it is constitutively expressed, and not impacted by treatment with TNF-α, IL-1β, or other secretagogues (da Costa-Martins, et al., 2006). EC PSGL-1 may bind monocyte L-selectin (da Costa-Martins, et al., 2006), and this may induce rolling, though it has been reported that this only occurs on TNF-α-treated HUVECs, and this was suggested to be due to alterations in glycosylation of EC PSGL-1 by TNF-α treatment. Blocking EC PSGL-1 or monocyte L-selectin also decreased monocyte rolling, so it seems that this adhesion molecule may also have a role in the tethering of monocytes to the endothelium. However, the aforementioned study is the only one available in the literature.

1.7.2 Immune Cell Activation – The Second Step in TEM

Once slowed on the endothelium and tethered, recruited immune cells may be activated, or "triggered", by a wide range of cytokines which may bind to cellular receptors. Two cytokines involved in this process are MCP-1 and IL-8, both of which may also be implicated in the directional migration of immune cells towards the endothelium and through the endothelium after triggering.

1.7.2.1 Monocyte Chemoattractant Protein 1 (MCP-1)

MCP-1 has a strong role in inflammation. It is a potent monocyte and macrophage chemoattractant, and induces directional migration to the site of expression (Mukaida, et al., 1998; Matsushima, et al., 1989). EC consititutively synthesise MCP-1, which is stored in granule 2 in the cell (Øynebråten, et al., 2005), from where it may be expressed in response to secretagogues such as histamine and forskolin. MCP-1 is soluble or bound to glycosaminoglycans (GAGs) (Lau, et al., 2004), though it is uncertain whether soluble or GAG-bound MCP-1 induces directional migration (Weber, et al., 1996; Weber, et al., 1999; Kuschert, et al., 1999; Hardy, et al., 2004).

As with many chemokines, MCP-1 activates cells via receptor binding, and is involved in monocyte and macrophage activation (Mukaida, et al., 1998; Matsushima, et al., 1989). Upon tethering of monocytes by E-selectin, MCP-1 triggers adhesion to molecules such as ICAM-1 and VCAM-1 via α_4 and β_2 integrin affinity modulation (Gerszten, et al., 1999), or VLA-4 and -5 activation, which may also induce monocyte shape change and TEM (Weber, et al., 1996). Further, the binding of MCP-1 to monocyte CCR2 initiates multiple pathways such as GPCR signalling, leading to phospholipase C activation, Ca^{2+} release, and protein kinase C and NF-κB activation, causing directional motion of the monocyte (Melgarejo, et al, 2009), while MAPK activation and p38 MAPK signalling may also induce chemotaxis (Yen, et al., 1997; Ashida, et al., 2001). Thus, MCP-1 may induce monocyte influx to the lung, and could be an important factor involved in diapedesis following BLM insult.

1.7.2.2 Interleukin 8 (IL-8)

IL-8, also expressed by endothelial cells exposed to BLM, is a strong neutrophil chemoattractant (Huber, et al., 1991). When expressed, IL-8 may bind GAGs, such as heparan sulphate (Webb., et al., 1993) forming chemotactic gradients along which neutrophils migrate (Marshall, et al., 2003; Rot, et al., 1996; Tanaka, et al., 1993).

IL-8 is synthesised by VECs and stored in granules or WPB in many endothelial cell types, though it may also be stored in the Golgi apparatus. However, its appearance in WPB often only occurs after stimulation of the cell with inflammatory cytokines (Metcalfe, et al., 2007). Its expression is stimulated by cytokines or secretagogues, and it has been suggested that the cellular source of IL-8 may be determined by the type of secretory stimulus or cell (Harada, et al., 1994; Utgaard, et al., 1998; Wolff, et al., 1998; Hol, et al., 2012); in HUVECs, stimulation with mediators such as IL-1β causes release from the Golgi apparatus, while stimulation with IL-1β followed by withdrawal and the addition of histamine releases IL-8 from WPB (Wolff, et al., 1998)

Similar to MCP-1 acting on monocytes, IL-8 activates neutrophils (Kuijpers, et al., 1992; Daniels, et al., 1992). Neutrophils express two IL-8 receptors, CXCR1 and -2 (Godaly, et al., 2000), and binding of IL-8 to these may activate or modulate the affinity of LFA-1 and Mac-1, and in fact increase Mac-1 expression, inducing neutrophil arrest on adhesion-molecule expressing VECs (Takami, et al., 2002; Seo, et al., 2001; Detmers, et al., 1990) via binding of integrins to appropriate molecules including ICAM-1. As well as modulating integrin affinity, IL-8 receptor binding may also mediate neutrophil exocytosis and degranulation, mediated by Ca^{2+} flux, a result of PLC, IP_3 and DAG activation (Zeilhofer and Schorr, 2000). Such Ca^{2+} flux may also polarise cells, inducing the formation of a psudopod at the head of the cell, allowing directional migration (Schaff, et al., 2008). Therefore, IL-8-mediated neutrophil activation may be vital for neutrophil transendothelial migration.

1.7.3 Adhesion to the Endothelium – The Third Step in TEM

Following the activation of recruited immune cells, adhesion to the endothelium occurs via interaction between immune cell integrins and VEC-expressed adhesion molecules such as ICAM-1 and VCAM-1. This step is vital prior to the movement of recruited immune cells through the endothelium to the site of injury.

1.7.3.1 Intercellular Adhesion Molecule 1 (ICAM-1; CD54)

ICAM-1 is expressed constitutively by VECs (Hopkins, et al., 2004) and is induced by TNF-α, IFN-γ, IL-1β, and LPS (Pober, et al., 1986; Swerlick, et al., 1991; Haraldsen, et al., 1996), with protein expression increasing over time and reaching peak levels between 24-48 hours after stimulation (Haraldsen, et al., 1996).

ICAM-1 mediates immune cell tethering via binding to LFA-1 and Mac-1 integrins on leukocytes, and these integrins may then undergo integrin affinity and valency changes as VEC-bound chemokines interact with leukocyte G-coupled protein receptors (GCPR). PLC-dependent inside-out signalling may then induce integrin conformation changes, causing high and intermediate-affinity binding of leukocytes to ICAM-1, as outside-in signalling stabilises this adherence (Ley, et al., 2007). ICAM-1-to-integrin binding may also alter ICAM-1 expression and localisation, and may result in VCAM-1 and IL-8, synthesis, inducing further immune cell recruitment (Rahman and Fazal, 2009).

ICAM-1 has many roles in diapedesis. ICAM-1 localises to EC microvilli and cell-cell junctions (Millán, et al., 2006; Thompson, et al., 2002), and upon ligation, clusters. Ligation by monocytes resulted in ICAM-1 clustering around the cell, promoting adhesion and spreading (Wójciak-Stothard, et al., 1999). ICAM-1 is also present in the intercellular junctions, and interaction with LFA-1 or Mac-1 at this stage may aid the transmigration of leukocytes (Ley, et al., 2007), while the ligation of ICAM-1 increases intracellular Ca^{2+}, activating myosin light chain kinase, promoting VEC contraction and junction opening, allowing increased leukocyte transmigration (Huang, et al., 1993; Su, et al., 2000; Etienne-Manneville, et al., 2000).

Interestingly, ICAM-1-LFA-1 ligation may induce the formation of cup-shaped projections rich in ICAM-1, which engulf adhered leukocytes (Carman, et al., 2003). Both para- and transcellular TEM of leukocytes have been associated with the formation of this "transmigratory cup" (TC) (Carman and Springer, 2004), as leukocytes migrating via both mechanisms were engulfed by the TC prior to transmigration. This has also been observed when assessing lymphocyte migration (Millán, et al., 2006). Therefore, it appears ICAM-1 has many roles in the diapedesis cascade after adhesion.

1.7.3.2 Vascular Cell Adhesion Molecule 1 (VCAM-1; CD106)

VCAM-1 is also involved in the adhesion of leukocytes to the endothelium, and binds the leukocyte integrin $\alpha_4\beta_1$ (Cook-Mills, 2002), or very late antigen (VLA) 4 following the tethering and triggering of circulating immune cells and subsequent VLA-4 activation via GPCR and PLC activation resulting in intracellular Ca^{2+} flux (Cook-Mills, 2002; Weber and Springer, et al., 1998; Hyduk, et al., 2007), permitting the firm adhesion of VLA-4 to VCAM-1. VCAM-1 is not constitutively expressed, but appears on endothelial cells in response to TNF-α, IL-1β, and LPS (Chuluyan, et al., 1995; Osborn, et al., 1989; Carlos, et al., 1990; Swerlick, et al., 1991; Haraldsen, et al., 1996).

Like ICAM-1, VCAM-1 plays many roles in TEM. Barreiro, et al. (2002) reported that a similar docking structure to the TC is formed by the ligation of VCAM-1 with VLA-4; VCAM-1 clustered around T lymphoblasts upon adhesion to, and spreading on, the EC. Carman and Springer (2004) also noted that both ICAM-1 and VCAM -1 were expressed in TCs that surrounded adherent leukocytes prior to transmigration, thus this may be a further contribution of VCAM-1 to TEM. Further, van Buul, et al. (2010) saw VCAM-1 clustering with ICAM-1 following ICAM -1 engagement, augmenting adhesion. Thus VCAM-1 appears to contribute to adhesion; furthermore, VCAM-1 may assist leukocyte crawling. Weber and Springer (1998) stated VCAM-1-VLA4 interactions were required for adherent monocyte migration along the endothelium, while Ronald, et al. (2001) noted that VCAM-1 induced morphological alterations associated with leukocyte spreading such as pseudopodia and lamellipodia formation; when VCAM-1 was blocked, there was no

shape change, a 30% decrease in migration and a decreased migration distance. Thus, VCAM-1 mediates both adhesion and transit.

Lastly, VCAM-1 ligation may open endothelial junctions. VCAM-1 ligation by VLA-4 induced signalling pathways which stimulate NADPH oxidase, which enters cells and generates ROS which activate cell-surface MMPs, altering VEC shape. In addition, H_2O_2 generated from superoxide may diffuse into the cell altering actin structure, inducing junction separation (Cook-Mills, 2002; Matheny, et al., 2000). This may result from VCAM-1 cross-linking; van Wetering, et al. (2003) reported VCAM-1 crosslinking resulted in ROS generation with stress fibre formation and junction opening, dependent on Rac and p38 MAPK signalling.

1.7.4 Migration Through the Endothelium – The Final Step in TEM

Following the tethering, activation, and adhesion of immune cells to the endothelium, and the migration to sites of transendothelial migration, the final step of this process is the movement of immune cells through the endothelial barrier to the site of injury. This in itself involves adhesion molecules, with perhaps the primary molecule being PECAM-1.

1.7.4.1 PECAM-1 (CD31)

PECAM-1 is constitutively expressed by ECs, at cell-cell junctions (Newman, 1994; Thompson, et al., 2001) where it mediates cell-cell adhesion (Albelda, et al., 1991), and by monocytes and neutrophils (Privratsky, et al., 2010; Newman and Newman, 2003), and though not upregulated by inflammatory mediators, PECAM-1 expression may be decreased (Stewart, et al., 1996) or the distribution altered (Romer, et al., 1995) by IFN-γ and TNF-α.

PECAM -1 mediates paracellular leukocyte transmigration via homophilic intereactions between EC and leukocyte PECAM-1 (Liao, et al., 1995), and it has been widely reported that PECAM-1 blockade prevents TEM (Privratsky, et al., 2010; Ley, et al., 2007; Muller, et al., 1993; Lou, et al., 2007) while leukocytes that lack PECAM-1 are less capable of

diapedesis (Duncan, et al., 1999; Thompson, et al., 2001), though the extent of the role of these interactions depends on the stimulus inducing TEM (Thompson, et al., 2001; Wakelin, et al., 1996).

PECAM-1 may be internalised and targeted to areas of the junction in which diapedesis is occuring (Mamdouh, et al., 2003), potentially dependent on interaction between leukocyte and EC PECAM-1. This may facilitate leukocyte TEM either by increasing junctional surface area, or providing a pool of PECAM-1, unencumbered by ligation to adjacent ECs (Mamdouh, et al., 2003). Further, the direct cycling of PECAM-1 to areas of transcellular migration may create a channel through which leukocytes migrate, while PECAM-1 blockade may prevent this (Mamdouh, et al., 2009). Moreover, ligation of EC PECAM-1 with monoclonal antibody or soluble PECAM-1 induces a prolonged Ca^{2+} transient (O'Brien, et al., 2001), which assists in EC-EC junction opening (Huang, et al., 1993). Therefore, PECAM-1 may be heavily involved in the movement of leukocytes through the endothelium.

Though the primary role of PECAM-1 in TEM appears to be in the movement of leukocytes through the endothelium, PECAM-1 binding to neutrophils may activate Mac-1, allowing stronger binding in a Mac-1-dependent manner (Berman and Muller, 1995), while homophilic interactions of neutrophil and EC PECAM-1 induced increased expression of the neutrophil integrin $\alpha_6\beta_1$, involved in neutrophil migration at the basal lamina (Dangerfield, et al., 2002).

Based on the wide range of known roles of these adhesion molecules in the diapedesis cascase, these are obvious choices to assess the expression of by BLM-treated HUVECs. However, the relevance of some of these molecules in the transendothelial cascase in the lung may be questioned due to the heterogeneity demonstrated by pulmonary VECs, and the mechanisms of immune cell recruitment to the lung.

1.8 The role of Lung Endothelium in BPF Development

Endothelial cells demonstrate a degree of heterogeneity, dependent on their location within the body, and even within a series of vessels. While the information above

pertains largely to the systemic circulation, many organs including the lungs are somewhat different. Not only must immune cells exiting the lung vasculature cross two barriers, the vessel and the alveolar epithellium (Aird, et al., 2007), but some lung vessels utilise very different immune cell recruitment mechanisms.

The primary site of immune cell sequestration and migration in the lung is the pulmonary micro-vasculature (Doerschuk, 2001). However, these vessels express few endothelial adhesion molecules; the selectins are absent, although as transit through pulmonary microvessels is slow and requires immune cell deformation, the velocity-dependent adhesion achieved by selectins is precluded (Doerschuk, 2001). Only ICAM-1 appears to be induced in lung capillary VECs by inflammatory stimuli (Doerschuk, 2000; Aird, 2007; Segel, et al., 2011), and even then, this depends on the stimulus; for example, *E. coli* LPS increases ICAM-1 expression, but *S. pneumonia* infection does not (Doerschuk, 2000; Doerschuk, 2001). Therefore, immune cell recruitment through capillaries may be said to be either CD18 (therefore ICAM-1) dependent or independent, based on the stilumus.

This suggests that the role of adhesion molecules in immune cell recruitment in the pulmonary capillaries may be minor, with only ICAM-1 involved. Of course, if pharmacologically-relevant concentrations of BLM induce ICAM-1 upregulation – as supra-pharmacological ones do in pulmonary vessel VECs (Fichtner, et al., 2004), then this may contribute to the increased numbers of neutrophils and monocytes – the CD18-harbouring immune cells – in the lung, though no other adhesion molecules would be considered to be involved, so perhaps do not need to be investigated?

However, while the main site of leukocyte migration is the pulmonary capillary bed, immune cell migration may also occur through post-capillary venules (Gane and Stockley, 2011; Wang, et al., 2011), which utilise the more typical adhesion cascade seen in the systemic circulation (Doerschuk, et al., 2001; Aird, 2007; Feuerhake, et al., 1998). VECs in these vessels express a range of adhesion molecules including ICAM-1, VCAM-1, and E-selectin under inflammatory conditions (Doerschuk, et al., 2000). While little literature assesses which lung VECs express adhesion molecules in response to BLM, the two studies that have suggest increased adhesion molecule expression may occur in both lung venules and capillaries, offering multiple sites of immune cell recruitment.

Wang, et al. (2011) reported neutrophil infiltration of the perivascular interstitium in BLM-treated rodents via venules; groups of sequestered neutrophils were noted along the luminal surface and moved through the endothelium at sites of notable ICAM-1/VCAM-1 expression. Sequestration, infiltration, and adhesion molecule expression at sites of trans-migration occurred concurrently, suggesting that ICAM-1 expression was related to the movement of leukocytes into the perivascular interstitium from the venules. Meanwhile, Sato, et al. (2000) reported both increased pulmonary capillary and venule ICAM-1 expression in response to BLM treatment, resulting in increased leukocyte slow rolling in the venules and increased sustained entrapment in the capillaries, both of which could be blocked by anti-ICAM-1 antibodies. This concurrent ICAM-1 expression and leukocyte rolling and entrapment also mirrored the times at which perivascular and peribronchiolar leukocyte infiltration were observed.

Therefore, at least in rodents, BLM induces increased expression of ICAM-1 and VCAM-1 in the lung venules and capillaries, resulting in immune cell sequestration and infiltration of the lung and surrounding areas. This may also occur in man, and the potential relevance of this is high – if , as in rodents and *in vitro*, BLM induces the increased expression of adhesion molecules in human pulmonary venule and capillary endothelial cells, and this has functional relevance, then this may contribute to the inflammation seen in BPF and we may be a step closer to elucidating the pathogenesis of human BPF.

As a wider range of adhesion molecules are expressed by pulmonary venule VECs than capillary VECs, then molecules other than ICAM-1 also require investigation, to determine whether they may contribute to immune cell recruitment into the lung in human BPF as they do in rodents.

1.9 Aims of the Work

Pulmonary fibrosis is a devastating condition which has often been modelled in rodents using the chemotherapy agent BLM , which is known to cause pulmonary fibrosis as a side effect when given to human patients as part of therapy regimens. While a considerable amount is known about BLM-induced fibrosis when induced in rodents using BLM delivered by intratracheal dosing routes - the primary injury appears to be alveolar epithelial cell death followed by intense inflammation and a period of cytokine release within the lung, leading to fibroblast proliferation, profibrotic cytokine release, and lung scarring - little is known about the processes involved in the development of the human equivalent of the disease, which is similar in that AEC death, subsequent inflammation, and fibrosis are noted, but has some differences from the rodent version of BPF.

In patients who develop BPF, the drug is delivered intravenously. This method was originally used to model the disease in rodents, but was superseded by intratracheal delivery which was faster and cheaper, and delivered BLM directly to the lung. Of course, in doing this, researchers are ensuring the initial injury is to alveolar epithelial cells, which then leads to fibrosis. In humans with BPF, this is unlikely to be the initial injury; in rodents given BLM intravenously, the first injury is often seen to be to the endothelium of the vessels surrounding the lung, and this may also be the case in humans who develop BPF.

The endothelium has many roles that may contribute to the development of lung fibrosis. Most notably, it is a rich source of both proinflammatory and profibrotic cytokines, and expresses adhesion molecules vital for immune cell recruitment. A handful of *in vitro* and *in vivo* studies in rodents have characterised cytokine and adhesion molecule expression patterns in endothelial cells, and even assessed the functional relevance of these molecules, though little such research has been conducted using human cells, and to our knowledge, there is no functional research in publication. The intimate positioning of pulmonary vasculature and alveoli suggests that such expression by endothelial cells could potentially contribute - either via inflammatory cell recruitment or cytokine release - to the development of this condition in human patients.

Therefore, based on previous research in man and mouse and the known functions of the endothelium in inflammation, it is hypothesised that the effect of BLM on human endothelial cells may contribute to the development of BPF via cytokine release and adhesion molecule expression which may lead to inflammation and fibrosis in and around the lung.

In this work, the expression of a panel of adhesion molecules - some of which have known roles in the adhesion of immune cells to the endothelium, and others of which do not - will be assessed by flow cytometry on HUVECs treated with concentrations of BLM which may feasible be encountered in the human body following dosing. To our knowledge, this is the first work to assess the panel of adhesion molecules chosen, and to use pharmacologically-relevant concentrations of BLM. Whether the expression of the adhesion molecules seen to be upregulated is regulated at an mRNA level will be assessed by qPCR. Again, to our knowledge, this has not previously been attempted.

Concurrently, the release levels of the pro-inflammatory cytokines IL-8 and MCP-1 will be assessed by ELISA in BLM-treated HUVECs, while the release of three profibrotic cytokines - TGF-β, PDGF-BB, and Endothelin-1 - by BLM-treated HUVECs will also be determined. To our knowledge, the expression of PDGF-BB and Endothelin-1 by BLM-treated HUVECs has not been previously assessed. This will also be confirmed by qPCR.

As endothelial cells within different regions of the same vascular bed - and most definitely between different sites of origin - demonstrate substantial heterogeneity, the expression of the aforementioned panel of adhesion molecules by PMVECs - pulmonary microvascular endothelial cells, a mixture of cells from vessels surrounding the lung including venules, arterioles, and capillaries - will be assessed by flow cytometry. In addition, the release of IL-8, MCP-1, and Endothelin-1 by BLM-treated PMVECs will be assessed be ELISA. To our knowledge, this represents the first time that the expression of many of the adhesion molecules chosen to be in the panel, and Endothelin-1 release, have been assessed in PMVECs. These results will then be compared to those obtained from HUVECs to determine whether HUVECs may represent an adequate model for the behaviour of BLM-treated PMVECs in future experiments, and whether endothelial cell heterogeneity extends to the responses seen when cells are treated with BLM.

The functional relevance of any increased adhesion molecule expression will then be assessed using flow chamber systems, in which isolated human neutrophils from healthy donors adhere more or less strongly to BLM-treated endothelial cells when flowed over the monolayer. This will represent the first instance of a functional study investigating what relevance any increased endothelial cell adhesion molecule expression in response to BLM has to the development of the disease. Increased neutrophil adhesion may suggest that the response of endothelial cells to BLM is at least in part responsible for the inflammation that is seen to precede the development of fibrosis in man as well as in mouse models. To determine which, if any, adhesion molecules are responsible for any increased adhesion observed, blocking studies will be carried out to assess which molecule is responsible for any increased neutrophil adhesion to the BLM-treated monolayer.

Finally, to assess whether any observed increases in adhesion molecule and cytokine expression are of particular relevance to the development of BPF in man, the response of HUVECs to other chemotherapeutic agents which operate in a similar fashion to BLM, but are not associated with the development of pulmonary fibrosis, will be assessed by flow cytometry and ELISA.

By attempting to generate a more complete picture of the response of endothelial cells to BLM – with a focus on adhesion molecule expression and cytokine release by various endothelial cells in response to BLM – and by assessing the functional relevance of such expression, it is hoped that a slightly better or broader understanding of the pathogenic process of human BPF, particularly with regards to the role of endothelial cells in the pathogenesis of the disease, will be obtained.

Should this work allow the development of a greater understanding of the pathogenesis of BPF – or, indeed, contribute in any way to our current understanding - then perhaps this work will represent a stepping stone towards developing better therapies or preventative treatments, to supercede the “watch and wait” and decreased-dosing methods used to treat BPF when it occurs today.

This work may also proffer some advice for other researchers on how to model such reactions to BLM – if endothelial cells do react to BLM, then perhaps utilising a dosing

method which avoids the endothelium is counter-productive, and should be retired or replaced in future works.

In addition, by comparing the expression of adhesion molecules and the release of cytokines by multiple endothelial cell types, this work will draw conclusions regarding which cell types are suitable for use when modelling the reponse of pulmonary microvascular endothelial cells to drugs *in vitro*.

In an attempt to begin to confirm any conclusions that are drawn regarding the involvement of endothelial cells and their reaction to BLM in the development of BPF, it will be determined whether the response of endothelial cells to BLM is unique, or whether it is a general response to the application of cytotoxic drugs. If the latter is the case, then perhaps the effect of BLM on endothelial cells is not necessarily the reason that fibrosis is such a common side-effect of BLM, and this may act as a "warning bell" to other researchers to proceed in this line of research with caution, and to not infer any adhesion molecule or cytokine upregulation as a sign that the action of BLM on the endothelium is a sign that such reactions induce the stark inflammation seen in BPF.

Of course, negative results obtained from the functional assays carried out in this work would provide a similar caveat; if adhesion molecules are seen to be upregulated, but do not increase immune cell adhesion to the endothelium, then caution must be exercised in making any such inferences. If the former is the case, and not all chemotherapy agents induce adhesion molecule and cytokine expression, then it is hoped that the results obtained in this work will act as a further gentle suggestion to encourage future researchers to re-adopt the intravenous method of BLM administration in rodents, despite the additional time and costs incurred; if a probable role for the endothelium in BPF can be inferred from this work, then perhaps a method of BLM delivery that essentially bypasses the endothelium altogether will no longer appear the logical choice when attempting to model fibrotic diseases such as BPF in rodents.

2 General Materials and Methods

2.1 Human Umbilical Vein Endothelial Cell Culture

Three batches of human umbilical vein endothelial cells were purchased from from TCS Cellworks, Buckingham, United Kingdom and Promocell GmbH, Heidelberg, Germany. Cells were cultured to passage 3-5 in 75cm^2 Corning flasks (Gibco) with 10ml media and incubated in an atmosphere containing 5% CO_2 at 37°C. The medium used was endothelial cell basal medium (Promocell GmbH) containing foetal calf serum (2%), endothelial cell growth supplement (0.4%), recombinant human epidermal growth factor (0.1ng/ml), recombinant human fibroblast growth factor (1ng/ml), hydrocortisone (1µg/ml) (Promocell GmbH) penicillin (100µg/ml)-streptomycin (100U/ml) (PAA, Pasching, Austria), and L-glutamine (2nM) (Lonza, Basel, Swtizerland) Cells were not cultured beyond passage 5.

2.2 Pulmonary Microvascular Endothelial Cell (PMVEC) Culture

PMVECs were purchased from Promocell and stored in liquid nitrogen until use. When seeded, PMVECs were thawed at room temperature and seeded into 25cm^2 flasks (Gibco) or 75cm^2 flasks at a concentration of 10,000 cells per cm^2 in 10 ml endothelial cell media MV (Promocell) supplemented with fetal calf serum (5%), endothelial cell growth supplement (0.4%), recombinant human epidermal growth factor (10 ng/ml), heparin (90 µg/ml) and hydrocortisone (1 µg/ml) supplements (Promocell); penicillin (100µg/ml)-streptomycin (100U/ml) (PAA, Pasching, Austria); and L-glutamine (2nM) (Lonza, Basel, Swtizerland). Cells were then incubated in an atmosphere containing 5% CO_2 at 37°C until confluent. Cells were not cultured beyond passage 5.

2.3 Cell Dissociation from Culture Flasks

When confluent, the cells were washed with Dulbecco's PBS (PAA) (5ml), aspirated, rinsed with TrypLE ™ Express (Gibco, Paisley, United Kingdom) (2ml), aspirated, and incubated with TrypLE™ Express (3ml). For HUVECs, the incubation lasted for 1 minute in an atmosphere containing 5% CO_2 at 37°C. If cells remained adherent, a further 1 minute

incubation took place. This continued until the cells were no longer adherent, to a maximum time of 3 minutes. Endothelial cell medium (5ml) as described above was added to each flask to quench the activity of TrypLE ™ Express. PMVECS required longer incubation time with TrypLE^{TM} to dissociate from the flask. Therefore, cells were allowed to incubate with TrypLE^{TM} for three minutes before being aspirated from the flask. Endothelial cell media MV (as described above) (5ml) was added to quench the activity of the TrypLE and cells were centrifuged as HUVECs.

The cell-containing media was centrifuged at 205 x *g* for 5 minutes. The supernatant was discarded and the pellet re-suspended in either endothelial basal cell medium (1ml) or endothelial cell medium MV (1ml) and cell number was determined by haemocytometry (section 2.4).

2.4 Cell Viability Determination and Cell Counting

Cell suspension (10µl) was added to Trypan Blue (0.4% v/w) (10µl) (Sigma Aldrich) and applied to a Neubauer haemocytometer. Viable cells were visualised by microscopy. Cells staining blue were considered unviable as dead cells cannot extrude the Trypan Blue dye (Strober, et al., 2001). The number of viable cells was determined by counting cells in the 1mm x 1mm x 0.1mm central square. To determine cells/ml, this number was multiplied by 1 x 10^4, and multiplied by 2 to account for dilution with Trypan Blue. The suspension was diluted in endothelial basal cell medium or endothelial cell medium MV to the required concentration of viable cells for either cell passage or assays.

2.5 Flow Cytometric Analysis of Surface Adhesion Molecule Expression

Cell suspension (100µl) contaning a pre-defined number of cells was pipetted into each well of a 96-well multi-plate (Costar, Sigma Aldrich) inlaid with a round-bottomed cell insert (Costar, Sigma Aldrich) to prevent cells adhering to the flat bottom of the 96-well plate. The cells were centrifuged for three minutes at 250 x *g* in a plate centrifuge cooled to 4°C, and the PBS aspirated. To each well, PBS 0.1% w/v BSA (50µl) was added, and the

cells centifuged again, to wash away any media. The cells were then incubated with a range of primary antibodies at a final concentration of 20µg/ml (40µl):

- Purified mouse IgG1 negative control (Serotec, Oxford, United Kingdom)
- Purified mouse anti-human CD31 (clone WM59) isotype IgG1 (κ) (Biolegend, San Diego, California, USA)
- Purified mouse anti-human CD50 (clone MEM-17) isotype IgG1 (κ) (Biolegend)
- Purified mouse anti-human CD51/61 (clone 23C6) isotype IgG1 (κ) (Biolegend)
- Purified mouse anti-human CD54 (clone HA58) isotype IgG1 (κ) (Biolegend)
- Purified mouse anti-human CD62E (clone HAE-1f) isotype IgG1 (κ) (Biolegend)
- Purified mouse anti-human CD62P (clone AK4) isotype IgG1 (κ) (Biolegend)
- Purified mouse anti-human CD106 (clone STA) isotype IgG1 (κ) (Biolegend)
- Purified mouse anti-human CD162 (clone KPL-1) isotype IgG1 (κ) (Biolegend)
- Rabbit F(ab')2 anti-mouse IgG:FITC (Serotec).

The cells were incubated with the primary antibody for 30 minutes on ice, in darkness. Following incubation, cells were washed. 50µl PBS 0.1% w/v BSA was added to each well, and the cells were centrifuged for three minutes at 250 x *g* in a plate centrifuge (Thermo Scientific, Waltham, Massachusetts, USA) cooled to 4°C, and the PBS aspirated. To each well, 80µl PBS 0.1% BSA was added, and the cells centrifuged again, as above, for three minutes. To each well containing cells treated with primary antibody, anti-mouse FITC secondary antibody (polyclonal rabbit F(ab)'2 anti-mouse IgG:FITC, (Serotec)) at a concentration of 20µg/ml (40µl) was added. Cells were then incubated on ice for 20 minutes in darkness.

Following incubation, 50µl PBS 0.1% BSA was added to each well, and the cells were washed again, as outlined above. The cells were resuspended in 50 µl PBS 0.1% BSA, and 25µl of this suspension was added to Leukogate tubes containing PBS 0.1% BSA (300µl). The cells were then analysed using the FACSCalibur (Beckton Dickinson and Company, New Jersey, USA) flow cytometer on the CellQuest programme. Ten thousand cell events were counted in this analysis unless otherwise indicated. During analysis, a gate (G2) was applied to the live cell population based on side and forward scatter characteristics, to ensure the expression of adhesion molecules only by live cells was counted.

The data were presented as average geometric mean without correcting using a gating method whereby expression is determined as a difference in fluorescence from the isotype control, as this may augment apparent expression by over-emphasising the contribution of events occuring within a “tail” (small number of events with very high or very low fluorescence) (personal communication, Dr S. Hart). This is demonstrated in Fig. 2.1, where the application of a gate ignores the antigen expression of 56% of cells in the analysis, and provides an overestimation of the fluorescence intensity in this sample. Using the non-gating method, marker expression the same as that of the binding of the control antibody may be therefore regarded as no expression. The geometric mean of the control antibody (secondary antibody only) was included on all graphs unless otherwise stated, to highlight the lack of expression of markers in particular experiment sets. The reason for using the secondary antibody alone as the negative control is discussed in Section 4.3.2. In brief, this is related to the impact of treatment with BLM, TNF-α, and other mediators on the binding of the negative control antibody to endothelial cells, while the binding of the secondary antibody only to endothelial cells was not impaced by the treatment of cells with chemotherapuetic agents or inflammatory mediators. This is demonstrated in a tabular format in Table A.1.

The geometric mean was obtained from readouts generated by CellQuest. The geometric mean represents the central tendency of a series of values by determining the mean from the product, rather than the sum, and is better suited to calculating means when determined on a logarithmic scale, as outliers do not skew the mean so dramatically. The geometric mean of each sample was recorded and plotted onto bar graphs. This includes samples treated with the target antibody (“test” samples) and seconday antibody only (“control”) samples. To denote “no expression” or expression due to non-specific binding alone, the seconday antibody only-treated “control” geometric mean results were plotted alongside the target antibody-treated “test” sample geometric mean results on all graphs, unless otherwise stated. Fluorescence above the “no expression” level (the geometric mean of secondary antibody-treated “control” samples) was regarded as “positive expression”, or specific binding to the target antigen suggestive of the expression of the target antigen or protein. Statistical analysis on all generated bar charts was carried out using the Mann-Whitney-U test in SPSS v. 19 statistical analysis software.

In Figures 2.1, 3.5, 4.3, 4.5, 5.1, and 5.2, raw data is shown with gating applied. This was generated by applying a gate to the control (secondary antibody) peak and incorporating as close to 1% of the events in this read-out within the gate, as is standard practice. Note that this method was NOT used for determining expression (expression was determined using uncorrected data and plotted on graphs as outlined above). Gates are only applied to these images to show the peak-shift and increase in positive cells when cells were treated as stated in the figures.

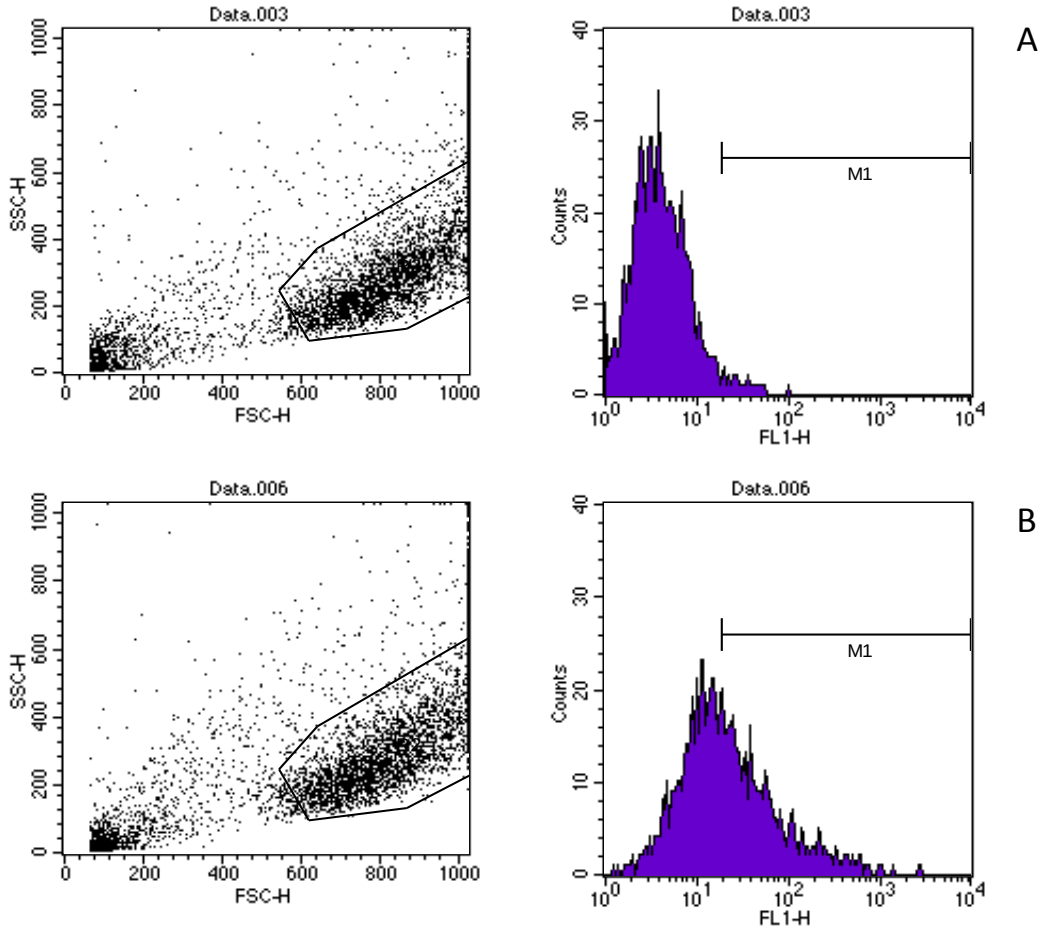

Figure 2.1: Representative raw data from flow cytometry experiments

Representative raw data from flow cytometry experiments to determine surface marker expression on PMVECs. Using the control (secondary antibody only) sample (A), gate M1 was drawn. This gate was drawn to incorporate as close to 1% of the control peak as possible. M1 was then applied to other geometric mean read-outs, to demonstrate the peak-shift only and show that cells were positive for the antigen tested. While there is a definite peak shift when ICAM-1 expression was assessed in untreated cells (B), 44% of cells fall within gate M1. Assessing the geometric mean of the cells in gate M1 in B, the average geometric mean in 48.02, compared to 19.66 when all cells are taken into account. However, this does not take into account the 56% of cells which are outside of gate M1, thus biases the calculated geometric mean by giving more weight to the fluorescence values recorded for events which fall within the "tail" of B, generating unrepresentatively high results values.

2.6 BLM Treatment of Endothelial Cells

Cells were cultured as outlined in 2.1 and 2.2. When confluent, cells were incubated in serum-contaning culture medium containing BLM sulphate, purchased from Carbosynth (Carbosynth, Compton, United Kingdom) (at concentrations of 0.1µg/ml, 1µg/ml, and 10µg/ml) for 6 and/or 24 hours and incubated as outlined in 2.1. The volume of BLM-containing medium used was dependent on the experimental protocol being undertaken. BLM was weighed and dissolved in endothelial cell culture medium (endothelial cell basal media or endothelial cell media MV) to a concentration of 1mg/ml. This was vortexed to ensure dissolution and stored for up to 24 hours in a refrigerator. Dilution of this stock concentration was carried out to ensure correct final concentrations.

2.7 Supernatant Collection for Cytokine ELISAs

Cells were cultured to confluence as outlined in 2.1 and 2.2. Cells were split and re-seeded at a concentration of 2 x 10^6 cells per T75 flask in 10ml serum-containing media (endothelial cells basal or endothelial cell media MV) dependent on cell type for at least 24 hours to ensure adhesion to the flask. When adherent, cells were treated as appropriate for each experiment. The required drugs were dissolved in serum contaning media (3ml), used to ensure high levels of cell viability. Cells were then incubated as described in 2.1 for the appropriate amount of time

Negative control cells were incubated in serum-containing media (3ml) for 6 and 24 hours to show baseline cytokine expression. 3ml of media was used as this was sufficient to cover the base of the flask and ensure cell viability over time, while also producing suitable concentrated supernatants.

Positive control supernatants were generated as required for each experiment. Cells were incubated with medium containing TNF-α (10ng/ml) for 6 and 24 hours to act as a positive control for IL-8 and MCP-1 expression (Hu, et al., 2009; Choe, et al., 2009; Hashimoto, et al., 2001; Yang, et al., 2004; Ahmed, et al., 2009; Murao, et al., 1999; Park, et al., 2004); human plasma thrombin (henceforth referred to simply as thrombin) (Calbiochem, MerckMillipore, Feltham, UK) (4U/ml) for 6 and 24 hours to act as a positive control for

endothelin-1 expression (Bilsel, et al., 2000; Marsen, et al., 1995); and thrombin (3U/ml) for 6 and 24 hours to act as a positive control for PDGF-B expression (Bowen-Pope, et al., 1989; Harlan, et al., 1986; Starksen, et al., 1987; Kavanaugh, et al., 1988). No reliable positive control treatment condition could be found for TGF-β.

Following incubation, the media was aspirated and centrifuged at 205 x *g* for 5 minutes. The supernatant was then aliquoted into 0.5ml eppendorf tubes and stored until required in a -80^{o}C freezer. Supernatants were not subjected to repeated freeze-thaw cycles to ensure no loss of protein.

2.8 ELISAs for Proinflammatory and Profibrotic Cytokine Expression

ELISA kits for a range of cytokines were purchased. ELISA kits for interleukin-8 (IL-8), monocyte chemoattractant protein-1 (MCP-1), and latent transforming growth factor β (TGF-β) were purchased from Biolegend. An ELISA kit for platelet-dervied growth factor dimer BB (PDGF-BB) was purchased from Sigma Aldrich. An ELISA kit for endothelin-1 (ET-1) was purchased from R&D Systems (Abingdon, UK). All ELISA were conducted in accordance with the instructions provided.

Prior to running the ELISA, supernatants were removed from the freezer and thawed at room temperature. Initial ELISA experiments sought to determine the ideal concentrations of supernatant to use with the ELISA kits, and a range of dilutions were tested. All test plates were run with the standards present in duplicate. Ideal concentrations of supernatant (those detectable by the plate reader which did not result in optical density readings too high or low to be detected by the plate reader) were determined for all sets of supernatants. Plates were read using a plate-reader (Thermo Multiskan FC, Thermo Scientific) at the wavelengths instructed by the manufacturers. Due to the low number of replicates and that the data were not expected to be normally distributed, data were analysed using Mann-Whitney-U tests in SPSS v. 19 statistical analysis software.

A standard curve for each ELISA conducted was carried out using the absorbance readings obtained from the plate-reader and the Graphpad data analysis software (GraphPad

Prism v. 5.04). Standard curves were used to determine the realibility of the standards and to ensure the reliability of the concentrations of protein per well as determined by the plate reading software. Standard curves can be found in the appendix (section A.2).

2.9 RNA Extraction, Reverse Transcription, and cDNA Synthesis

Cells were cultured as outlined in 2.1 and treated with BLM (as outlined in 2.7) or positive control cytokines. In these experiments, cells were either treated with BLM (at concentrations of 0.1µg/ml, 1µg/ml, and 10µg/ml) for 6 and 24 hours, TNF-α (10ng/ml) for 6 and 24 hours to act as a positive control for ICAM-1, VCAM-1, and E-selectin, or as outlined in 2.8 to act as a positive control for IL-8, MCP-1, Endothelin-1, and PDGF-BB. No reliable positive control for TGF-β was found.

Cells were dissociated from culture flasks as outlined in 2.3. Cells were washed in ice-cold PBS (5ml) and centrifuged at 205 x *g* for 5 minutes. RNA extraction was conducted in line with the instructions of the ReliaPrep™ RNA Cell Miniprep System (Promega, Madison, Wisconsin, United States of America). Extracted RNA was stored at -80^{o}C until such time that RNA could trascribed to cDNA for use with quantitative PCR. Samples were thawed at room temperature and the RNA content of the sample quanitifed using the Qubit quantification kit, as per manufacturer's instructions. The total RNA in each sample was determined.

The amount of sample containing 1µg total RNA was determined. This was transferred to a sterile, RNAse-free tube. To this, Oligo(DT) (1 µl) (Thermo Scientific) and 10mM dNTP mix (1µl) (Thermo Scientific) was added. The solution was made up to 14.5µl using diethylpyrocarbonate (DEPC)-treated water (produced in-house). To this, 5X RT buffer (4µl) (Thermo Scientific), Ribolock RNAse inhibitor (0.5µl) (Thermo Scientific) and Revertaid Premium Reverse Transcriptase (1µl) (Thermo Scientific) was added, to a total volume of 20µl, giving a total RNA content of the sample of 1µg RNA per 20µl (50ng/µl). The sample was mixed gently and vortexed.

In addition, No RT samples were generated. These samples contain no reverse transcriptase and therefore the conversion of RNA to cDNA is prevented. The amount of

sample containing 1µg total RNA was determined. This was transferred to a sterile, RNAse-free tube. To this, Oligo(DT) (1 µl) (Thermo Scientific, Waltham, Massachusetts, USA) and 10mM dNTP mix (1µl) (Thermo Scientific) was added. The solution was made up to 15.5µl using DEPC-treated water (produced in-house). To this, 5X RT buffer (4µl) (Thermo Scientific) and Ribolock RNAse inhibitor (0.5µl) (Thermo Scientific) was added, to a total volume of 20µl, giving a total RNA content of the sample of 1µg RNA per 20µl.

The samples were then subject to reverse transcription. The Techne TC-3000 thermal cylinder (Bibby Scientific, Stone, Staffordshire, UK) was used. The reverse transcription was carried out according to manufacturer's instructions; in brief, as an oligo(dT) primer was used, the sample was incubated at 50^{o}C for 30 minutes, and the reaction was terminated by heating the samples to 85^{o}C for 5 minutes. The samples were stored at -80^{o}C, until used.

2.10 Primer design and acquisition for qPCR and optimisation

All primers used in both optimisation and qPCR experiments were designed by PrimerDesign Ltd (Southampton, United Kingdom). All Mastermix used in qPCR experiments and optimisation was also provided by PrimerDesign. Primers for human ICAM-1 (CD54), E-selectin (CD62E), VCAM-1 (CD106), TGF-β, PDGF-BB, Endothelin-1, MCP-1 (CCL2), and IL-8 were obtained and all followed the sequences and product lengths shown below. . In addition, primers for reference genes were generously gifted to the group by PrimerDesign. Only the details (accession number, product size) for UBC (ubiquitin C), the reference gene used for this work, is shown below. Accesion numbers for the other reference genes used are shown in Table 3.2.

2.11 Generation of Graphs

All graphs were generated using the GraphPad Prism software (V 5.04) unless otherwise explicity stated.

Table 2.1: Primers used in optimisation and qPCR experiments and their sequences

Primer	Sense/Antisense Primer	Product Length
ICAM-1 (Homo sapiens intercellular adhesion molecule, CD54)	Sense: CCTATGGCAACGACTCCTTC Antisense: TCTCCTGGCTCTGGTTCC	**111bp**
VCAM1_24444 (Homo sapiens vascular cell adhesion molecule VCAM1, transcript variant 1)	Sense: TGTGAATCCCCATCTTTCTCCT Antisense: CTCAGGGTCAGCGTGGAAT	**95bp**
IL-8 (Homo sapiens interleukin 8).	Sense: CAGAGACAGCAGAGCACAC Antisense: AGCTTGGAAGTCATGTTTACAC	**95bp**
MCP-1 (Homo sapiens chemokine (C-C motif) ligand 2 (CCL2)).	Sense: ACCGAGAGGCTGAGACTAAC Antisense: AATGAAGGTGGCTGCTATGAG	**122bp**
E-selectin (Homo sapiens selectin E (endothelial adhesion molecule 1 (SELE)).	Sense: TTCTTGCCTACTATGCCAGATG Antisense: AGGAAAGGGAACACTGAGTCT	**123bp**
PDGF-BB (Homo sapiens platelet-derived growth factor beta polypeptide (simian sarcoma viral (v-sis) oncogene homolog) (PDGFB), transcript variant 1)	Sense: AGCACACGCATGACAAGAC Antisense: GGGGCAATACAGCAAATACCA	**108bp**
ET-1 (Homo sapiens endothelin 1 (EDN1), mRNA.)	Sense: TGAGAATAGATGCCAATGTGCTA Antisense: GAACAGTCTTTTCCTTTCTTATGATT	**132bp**
TGF-β1 (Homo sapiens transfroming growth factor, beta 1 (Camurati-Engelmann disease (TGFB1) mRNA)	Sense: CACTCCCACTCCCTCTCTC Antisense: GTCCCCTGTGCCTTGATG	**83bp**
UBC (Homo sapiens ubiquitin C)	Not available: Accession number: NM_021009 Anchor nucleotide: 452	**192bp**

A list of the primers used in both qPCR optimisation and final qPCR experiments, and their respective sequences as provided by PrimerDesign.

2.12 Statistical Analysis

Statistical analyses were carried out using SPSS statistical software (version 19) unless otherwise stated. The test used was the Mann-Whitney-U test, unless otherwise stated. This non-parametric test was used due to the low number of repeats conducted in experiments, meaning Gaussian distribution could not be guaranteed, but data was presented using a parametric format (bar charts).

In all cases, error bars on graphs are representative of the standard error of the mean (SEM) calculated and overlaid on the charts using GraphPad software (GraphPad Prism version 5.04). Statistical significance ($p=\leq 0.05$) was determined using the results obtained from statistical analysis using SPSS unless otherwise stated.

In all cases, where statistical significance ($p=\leq 0.05$) is denoted by an asterisk on bar charts, this refers to a statistically significant difference in the observed value in the test sample compared to the observed value of baseline (untreated) sample in each experiment, unless otherwise stated. For example, an asterisk above a bar denoting a sample treated with 10µg/ml BLM demonstrates a statistically significant difference in the expression of the protein assessed, compared to the expression of this protein in the baseline (untreated) sample.

3 Optimisation of Methods for Flow Cytometry and qPCR

3.1 Introduction

Prior to the assessment of adhesion molecule expression and cytokine release by BLM-treated HUVECs, optimisation is required. Firstly, suitable concentrations of BLM to be used throughout this work required determination. Such concentrations would be pharmacologically-relevant (as outlined in table 1.1), and fall within and around the range of around 10ng/ml to 6.6µg/ml as observed in renally competent patients immediately after, and 24 hours after dosing, respectively (Broughton, et al., 1977; Alberts, et al., 1978) - though, as renally impaired patients experience impaired BLM clearance, higher concentrations will also be assessed. Ideal concentrations would also not cause high levels of endothelial cell death, as this is not reported in BPF (Adamson and Bowden, 1974; Jones, et al., 1978; Bedrossian, et al., 1973; Adamson, 1984).

As BLM does not efficiently enter cells (Pron, et al., 2003) incubation time may impact cytotoxicity. While the terminal half-life of BLM is 2-6 hours in healthy patients (Alberts, et al., 1978), in renally impaired patients, this may be up to 33 hours (Broughton, et al., 1977), so some patients may be exposed to cytotoxic concentrations of BLM for extended periods. Therefore, to assess how viability is impacted by incubation time would also be of value. Assessment of cell viability can be conducted in a variety of ways, though here, the sulphorhodamine B (SRB) and MTS assays have been selected, as both are widely used and well-validated assays for determining cell viability and proliferation.

The MTS assay determines the number of living cells by measuring formazan, produced by enzymatic degradation of MTS by dehydrogenases in metabolically active cells. The amount of formazan, measured by the absorbance of the sample at 490 nm, is proportional to the number of living cells. This assay assumes dead cells cannot reduce the MTS tetrazolium component (Rinne, et al., 2004) and so the colour and absorbance change reported reflect the number of live cells. Described by Skehan, et al (1990), the SRB assay determines cell number by binding to basic amino acid residues in trichloroacetic acid-fixed cells, providing a cellular protein content value relative to the cell number. The optical density of the SRB stain read at between 490nm and 564nm is an accurate representation of the total amount of protein in the sample, and a total cell count can be inferred, though this method cannot distinguish between living and dead

cells, and relies on dead cells being removed by washing. The results may therefore offer a conservative estimate of the number of viable cells present (Rinne, et al., 2004).

In this thesis, flow cytometry will be used to assess adhesion molecule expression, and so optimisation is required to determine the correct population of cells upon which to gate. For this, a propidium iodide assay will be carried out to ensure that only the live population of cells is gated. Furthermore, as adhesion molecule expression is to be determined, several methods of cell dissociation were trialled, to ensure adhesion molecules were not cleaved during dissociation. Dissociation using 0.05% w/v Trypsin 0.02% w/v EDTA is the standard method (Mutin, et al., 1996), though in this laboratory, cells are dissociated using TrypLE ™ Express, a synthetic protease-like reagent, which may cleave adhesion molecules, resulting in inaccurate molecule quantification.

Finally, optimisation of the positive control will be carried out; a single adhesion molecule upregulated by a particular treatment, e.g., ICAM-1, would be ideal, though there appears to be no consensus as to which mediators induce the highest expression of endothelial adhesion molecules. Three that are often used are TNF-α, IFN-γ, and lipopolysaccharide (LPS). TNF-α induces ICAM-1, VCAM-1, and E-Selectin expression (Zhang and Issekutz, et al., 2001; Asimakopolous, et al., 2001; Haraldsen, et al., 1996), while IFN-γ increases the expression of ICAM-1, E-Selectin, VCAM-1, and PECAM-1 (Lou, et al., 1997;Weber, et al., 1995; Zhang and Issekutz, 2001; Konstantopoulos, et al., 1997; Romer, et al., 1995) and LPS , the upregulation of E-Selectin, ICAM-1, and VCAM-1 (Yan, et al., 2002; Schumann, et al., 1996; Biffl, et al., 1996; Haraldsen, et al., 1996; Carlos, et al., 1991). However, there are no publications directly comparing the efficacy of these mediators save that of Haraldsen, et al. (2006), which used only a limited panel of adhesion molecules. As a broad range of concentrations of all of the aforementioned mediators has been used, the ideal mediator and mediator concentration to use as a positive control will be assessed.

Furthermore, optimisation is required to allow the development of the qPCR component of this work in line with the MIQE guidelines (Bustin, et al., 2009). The selection of an appropriate reference gene is an important component of qPCR. Though GAPDH is often used as a reference gene for PCR experiments, the stability of this gene as a reference gene in qPCR may be questionable (Kozera and Rapacz, 2013). Moreover, it is required

that genomic DNA (gDNA) has not contaminated any samples prepared for experiments, as this may provide erroneous results as incorrect (gDNA) transcripts, rather than (or as well as) the target mRNA transcripts are amplified in the qPCR reaction. The use of No RT samples in qPCR experiments (samples which contain no cDNA as reverse transcriptase is omitted when conducting reverse transcription) is the primary method of determining the presence of gDNA contamination (Laurell, et al., 2012), as the presence of DNA in No RT samples is suggestive of gDNA contamination which may also affect the other samples being used. No RT samples will therefore be used in all qPCR experiments. Agarose gels will also be used to ensure that gDNA contamination has not occurred, while ensuring that the primer is specific for the target transcripts.

Finally, primer efficiency will be determined. Efficiencies between 90-110% will be regarded as comparable and the standard $\Delta\Delta C_q$ or Livak method will be used to analyse results. In instance where this is not the case, the Pfaffl method will be used to normalise the results (Pfaffl, 2001).

3.2 Materials and Methods

3.2.1 MTS and SRB Concentration-Effect/Time-Effect Assay

Cells were cultured as outlined in 2.1, dissociated as outlined in 2.3, and counted as outlined in 2.4. Into each well of a 48-well plate, cells were seeded at a density of 10,000 cells per well in 500µl media (20,000 cells/ml). The cells were incubated for 24 hours in serum-containing media. Twenty-four hours prior to treatment with BLM, the medium was aspirated and replaced with serum-free endothelial basal cell medium containing endothelial cell growth supplement (0.4%), recombinant human epidermal growth factor (0.1ng/ml), recombinant human fibroblast growth factor (1ng/ml), hydro-cortisone (1µg/ml) (Promocell GmbH) and penicillin (100µg/ml)-streptomycin (100U/ml) (PAA). This was aspirated immediately prior to BLM treatment. BLM sulphate (Carbosynth, Compton, United Kingdom) was prepared to a concentration of 2mg/ml in serum-free media as described above. A range of dilutions (0.01, 0.05, 0.1, 0.25, 0.5, 1, 5, 10, 100µg/ml) was prepared using serial dilution. Serum-free medium was use to retard further cell growth.

Each concentration of BLM sulphate (500µl) was added to six wells of HUVECs at the appropriate time-points and was not replaced for the duration of the time-course. The plates were incubated for 6, 12, 24, 48, and 72 hours. The positive control was incubated in serum-containing media for 24 hours; serum-free media, for 24 hours; and 10mM hydrogen peroxide (Fisher Scientific, Loughborough, United Kingdom) in serum-free media, added at the same time points as BLM. The negative control was incubated in serum containing media for 24 hours, serum-free for 24 hours; and fresh serum-free media (500µl) for as long as treated cells.

The results of each triplicate were expressed as a percentage viability of the negative controls to allow the comparison of BLM cytotoxicity over each time point and at each concentration while acknowledging cell death due to time spent in unchanged media. Each assay was run in triplicate, with each positive and negative control also run in triplicate. This was carried out for the MTS assay and the SRB assay. Following incubation with the required concentrations of BLM for the required times, the media containing BLM in each well was aspirated and replaced with serum-free endothelial cell basal media

(500µl). Cells were then prepared for assay by both MTS and SRB assay, to assess the toxicity of BLM.

3.2.1.1 MTS Assay for Cell Viability

The CellTiter 96 AQ_{ueous} non-radioactive cell proliferation assay (Promega, Madison, Wisconsin, United States of America) was used to determine the number of viable cells in each well post-BLM. 3-(4,5-dimethylthiazol-2-yl)-5-(3-carboxymethoxyphenyl)-2-(4-sulfophenyl)-2H-tetrazolium was combined with phenazine methosulphate as directed, and a volume as stated in the kit (100µl) was added to the fresh medium in the cell-containing vessel, as outlined in the CellTiter 96 AQ_{ueous} protocol. The plate was incubated for two hours in an atmosphere containing 5% CO_2. MTS-media solution (100µl) was pipetted into wells of a 96 well multiplate. The absorbance at 492nm was read using the Thermo Multiskan FC plate reader. Data were analysed using Mann-Whitney-U tests in SPSS v. 19 statistical analysis software.

3.2.1.2 SRB Assay for Cell Viability

The SRB assay, as described by Skehan, et al. (1990), was also used to measure cell cytotoxicity. The SRB plates were read at at 492nm. Culture medium was removed from the cells, the cells were rinsed with PBS 0.1% w/v BSA (500µl) to remove dead cells and debris, and media (500µl) was added to each well. To this, trichloroacetic acid (Sigma Aldrich) (250µl) was added, and cells were incubated on ice for an hour to fix. Following fixation, the supernatant was aspirated and the wells washed four times with deionised water. Sulphorhodamine B solution (acetic acid (Sigma Aldrich) 0.4% w/v sulphophodamine B (Sigma Aldrich)) (50µl) was added to the wells. This was left to incubate for thirty minutes. The stain was aspirated and the wells washed four times with 1% v/v acetic acid and left to dry for 24 hours. Stained cells were then dissolved in 10mM TRIS base (Sigma Aldrich), pH10 (607.5mg TRIS base in 500ml distilled water) (100µl). Stained TRIS base was transferred into wells of a 96-well multi-plate and read at 492nm

on the plate reader. Data were analysed using Mann-Whitney-U tests in SPSS v. 19 statistical analysis software

3.2.2 Cell Dissociation Assessment

Cells were cultured to confluence as outlined in 2.1. When confluent, HUVECs were treated with TNF-α (10µl, to give a final concentration of 10ng/ml) (Sigma Aldrich). The cells were left to incubate for 24 hours. Following treatment and incubation, the cells were washed with Dulbecco's PBS (PAA) (5ml). One flask of cells not treated with TNF-α was prepared and dissociated using TrypLE ™ Express. This provided a baseline expression of adhesion molecules, by which to compare the expression of TNF-α treated cells dissociated by each method. These methods included dissociation as outlined in 2.2, but also dissociation by 1mM EDTA in PBS, 0.05% trypsin 0.02% EDTA, chilling in PBS for 30 minutes, and scraping. When dissociated, cells were counted as described in 2.4, diluted to a concentration of $1x10^6$/ml in serum-containing endothelial cell basal medium, and subjected to flow cytometric analysis as outlined in 2.5 using the same range of antibodies.

3.2.2.1 Dissociation by 1mM EDTA in PBS

Cells were rinsed with 1mM EDTA in PBS (2ml) (produced in-house), aspirated, and were then incubated with 1mM EDTA in PBS (3ml) in an atmosphere containing 5% CO_2 at 37°C. This often required prolonged incubation of between five and 30 minutes, depending on the passage number of the cells. Earlier passage cells required longer incubation times. Cells were incubtaed with EDTA for a maximum of 60 minutes. Endothelial cell medium (5ml) as described above was added to each flask to quench the activity of EDTA. The cell-containing media was centrifuged at 205 x *g* for 5 minutes. The pellet was resuspended in endothelial basal cell medium (1ml) and cell number was determined by haemocytometry as outlined in 2.4.

3.2.2.2 Dissociation by 0.05% Trypsin 0.02% EDTA

Cells were rinsed with 0.05% w/v Trypsin 0.02% w/v EDTA (Sigma-Aldrich) (2ml), aspirated, and incubated with 0.05% w/v Trypsin 0.02% w/v EDTA (3ml) for 1 minute in an atmosphere containing 5% CO_2 at 37°C; If the cells remained adherent, a further 1 minute incubation took place. This continued until the HUVECs were no longer adherent, for a maximum time of three minutes. Endothelial cell medium (5ml) as described above was added to each flask to quench the activity of 0.05% Trypsin 0.02% EDTA. The cell-containing media was centrifuged at 205 x *g* for 5 minutes. The pellet was resuspended in endothelial basal cell medium (1ml) and cell number was determined by haemocytometry as outlined in 2.4.

3.2.2.3 Dissociation by Chilling in PBS

PBS (PAA) at a temperature of 4°C was added to the flask, and the cells were incubated with the PBS in the refrigerator at a temperature of 4°C. The cells were checked every ten minutes to determine the number of cells dissociated. Cells were incubated in the refrigerator until all cells were dissociated. This incubation occurred for a maximum time of 60 minutes. The cell-containing PBS 0.1% BSA was centrifuged at 205 x *g* for 5 minutes. The pellet was resuspended in endothelial basal cell medium (1ml) and cell number was determined by haemocytometry as outlined in 2.4.

3.2.2.4 Dissociation by Scraping

Confluent cells were dissociated using a cell scraper, ensuring that all cells were dissociated from the bottom of the flask. The cell-containing media was centrifuged at 205 x *g* for 5 minutes. The pellet was resuspended in endothelial basal cell medium (1ml) and cell number was determined by haemocytometry as outlined in 2.4.

3.2.3 Propidium Iodide Assay

The propidium (PI) iodide assay was used to determine the live cell population in flow cytometric dot-plots. Apoptotic cells, or those with membrane damage, are unable to exclude PI, while live cells may exclude the dye, due to its membrane impermeability. Within the cell, PI binds to DNA, and when analysed by flow cytometry, cells containing DNA-bound PI are shown to have a greater mean fluorescence when measured by FL2 (or FL3) than live counterparts (Davies and Hughes, 2000; Frey, 1995). In this experiment, FL2 has been used. This allows the determination of populations of living and dead cells.

1ml of cell suspension was transferred into a 5ml leukogate polyurethane FACS tube. To this, 10 µl of propidium iodide (Sigma Aldrich) solution in PBS was added (at a concentration of 500µg/ml, to permit a concentration of 5µg/ml PI in each sample). Tubes were incubated on ice for five minutes before being run on a FACSCalibur flow cytometer. One stained and one unstained tube of cells was analysed for each of the three different HUVEC cell lines assessed. The viability of the cells in the gated area was determined by the average geometric mean fluorescence of cells within this gated area, and the fact that cells staining positive for PI were not present within this gate. By gating around populations of cells that showed no staining, gating around a live population of cells could be ensured.

3.2.4 Determination of an Ideal Positive Control; Adhesion Molecule and Inflammatory Mediator

Cells were cultured as outlined in 2.1. Upon reaching confluence, cells were treated with LPS, TNF-α, IFN-γ, or left untreated as a control, at final concentrations of 1 ng/ml, 3 ng/ml, 10 ng/ml, and 30 ng/ml TNF-α (Promokine GmbH, Heidelberg, Germany) 100 U/ml, 300 U/ml, 1000 U/ml, and 3000 U/ml IFN-γ (Biolegend), and 100 ng/ml, 300 ng/ml, 1 µg/ml, and 3 µg/ml LPS (Sigma Aldrich). The required amount of each was added to a flask of HUVECs containing 10ml serum-containing media. In addition, all experiments were run with a negative control. The cells were then incubated for the required amount of time in an atmosphere containing 5% CO_2 at 37°C before being dissociated as outlined

in 2.3, counted as described in 2.4, resuspended to a concentrations of 1 x 10^6 cells/ml, and prepared for flow cytometric analysis of adhesion molecule expression as outlined in 2.5, using the same panel of antibodies.

3.2.5 Agarose Gel Electrophoresis to Determine RNA Quality and Viability

To ensure the purity of the cDNA samples generated in 2.9, and to ensure the RT process occured correctly, an agarose gel was run. Prior to the running of the gel, the cDNA samples underwent a PCR reaction to amplify a target gene (GAPDH) within the samples.

The cDNA and No RT samples generated in 2.9 were prepared for PCR. A master mix was created by combining DreamTaq Green buffer (Thermo Scientific) (5µl), 2mM dNTP mix (Thermo Scientific) (5µl) GAPDH primer (1:15 dilution) (MWG Eurofin, Luxembourg) (4µl) and Taq polymerase (Thermo Scientific) (0.25µl). To this, the template cDNA sample prepared earlier (2µl) was added, and DEPC-treated water was added to make up to a final volume of 50µl. This mixture was created for all samples. The GAPDH primer specifications were as shown in Table 3.1. Sequences were obtained from Sun, et al., (2012).

Table 3.1: GAPDH primer sequence

Primer	Sense/Antisense Sequence	GC Content	Tm
GAPDH	Sense: GAGCCCGCAGCCTCCCGCTT Antisense: CCCGCGGCCATCATCACGCCACAG	Sense: 75% Antisense: 76.2%	Sense: 67.6 ^{o}C Antisense: 69.6 ^{o}C

The sequence of the GAPDH primer used for PCR experiments to determine the quality of the cDNA samples generated. Sequences were obtained from Sun, et al., (2012). GC content and melt temperature were obtained from PrimerBlast.

In addition, a No cDNA sample was generated. DreamTaq Green buffer (Thermo Scientific) (5µl), was combined with 2mM dNTP mix (Thermo Scientific) (5µl) GAPDH primer (MWG Eurofin, Luxembourg), and Taq polymerase (Thermo Scientific) (0.25µl). DEPC-treated water was added to make up to a final volume of 50µl. No cDNA was included in this sample.

PCR was run using the Techne TC-3000 thermal cylinder (Bibby Scientific, Stone, Staffordshire, UK). In brief, an initial denaturing stage of 3 minutes at 95^{o}C was followed by 35 cycles of denaturing (30 s at 95^{o}C), annealing (30 s at 58^{o}C) and Elongation (45 s at 72^{o}C), with a final elongation stage of 10 minutes at 72^{o}C. The resultant cDNA samples were then frozen at -20^{o}C until required. An agarose gel was run using these PCR products to ensure the purity and viability of the cDNA, and that the initial reverse transcription step had proceeded as required.

Agarose gel was made by combining 2.6g agarose (Fisher Scientific UK Ltd, Loughborough, UK) with 200ml 1 x TAE solution (produced in-house) and boiling until clear. Ethidium bromide (8µl) (Sigma) or Midori Green (10µl) (Nippon Genetics, Düren, Germany) was added and the gel was transferred into a mould and allowed to set for one hour. Combs were inserted to create wells.

Each sample, including the no cDNA negative control sample and the No RT sample, was pipetted onto the agarose gel (25µl). A sample of cDNA isolated from HEK-259 cells by the group previously, or cDNA isolated from HUVECs earlier in this work, was used as a positive control. The reference ladder used was the Gene Ruler 1Kb plus DNA ladder (Thermo Scientific) unless otherwise specified. The ladder was prepared by combining one part DNA ladder with one part 6x DNA Loading Dye (Thermo Scientific) and 4 parts deionized water. Ladder (25µl) was then loaded onto the gel, and the gel was run at 87 volts for 30 minutes or until the dye had reached the end of the gel. The gel was read using a UVP Lab Products EPI Chem II Darkroom and visualised using the ethidium bromide or Midori Green setting with the transilluminator control on. Results were analysed using LabWorks v4.6.0.00.

The presence of a single band corresponding to the molecular weight of GAPDH (around 700kb) suggested that the reverse transcription had been successful. In instances where

multiple bands appeared, or no band appeared, samples underwent reverse transcription and PCR again, or new samples were generated from treated cells, to ensure a pure cDNA sample was available. cDNA was stored in a -20 °C freezer for up to one month.

3.2.6 Performance of PCR to Assess Primer Specificity and Sample gDNA Contamination

Samples were generated as outlined in 2.9. For this work, positive control samples (cDNA isolated from cells treated with TNF-α and thrombin) were used for assessing ICAM-1, E-Selectin, VCAM-1, IL-8, MCP-1 (CCL2), ET-1, and PDGFB primers. cDNA samples from untreated cells were used to assess the specificity of the UBC and TGF-β primers. The quality of the cDNA samples was assessed as outlined in 3.2.6. These samples were prepared for additional polymerase chain reaction (PCR).

DreamTaq Green buffer (Thermo Scientific) (5µl) was combined with 2mM dNTP mix (Thermo Scientific) (5µl), Taq polymerase (Thermo Scientific) (0.25µl), and the required primer (6.6µl) (as outlined in 2.1). To this, cDNA or No RT sample as generated in 2.9 (2µl) was added. The cDNA contaning samples used for this work were the positive control samples generated as outlined in 2.9. For TGF-β samples, cDNA collected from untreated cells was used. DEPC-treated water was added to given a final volume of 50µl, with an overall primer concentration of 20µM. A no cDNA sample was also generated. In this case, the cDNA or No RT sample was omitted from the mixture and replaced with DEPC-treated water.

The samples were placed in the Techne TC-3000 thermal cylinder and run. An initial denaturing stage of 3 minutes at 95^{o}C was followed by 35 cycles of denaturing (30 s at 95^{o}C), annealing (30 s at 53^{o}C) and elongation (45 s at 72^{o}C). The sample was then stored at -20^{o}C until required.

An agaorse gel was made as previously described (section 3.2.6). The gel was run for 60 minutes and the banding on the gel visualised using a transilluminator (UVP Lab Products EPI Chem II Darkroom).

Primer specificity was assessed by examining band locations on the resulting gel. If single bands were seen to appear at points on the gel representative of the known size of the primer target (Table 2.1), primer specificity was assumed. The presence of gDNA contamination was also assessed using these gels. The presence of multiple bands or a smeared band is suggestive of gDNA contamination of the sample, as is presence of a band in the No RT sample. If only a single band was observed in the samples, and no band was observed in the No RT sample, gDNA contamination was considered to be absent.

In instances were visible bands were not achieved, a secondary PCR was run. Samples were exposed to 20 cycles of denaturing (30 s at 95^{o}C), annealing (30 s at 53^{o}C) and elongation (45 s at 72^{o}C). Samples were then run on an agarose gel as outlined in 3.2.6, and analysed as outlined above.

3.2.7 GeNorm Analysis to Identify a Stable Reference Gene

Prior to use with the qPCR, samples were thawed at room temperature. Samples from untreated cells and from cells treated with each concentration of BLM were diluted 1 in 100 in RNAse and DNAse free water (PrimerDesign) to give a final concentration of 0.5ng/µl. Initially, a suitable reference gene for use with the PCR was determined. Primers for several known candidate reference genes (GAPDH, B2M, UCB, ATP5BN, YWHAZ, and RPL13A) were a kind gift from PrimerDesign. Each primer was diluted with RNAse/DNAse free water (PrimerDesign) to a final concentration of 0.5ng/µl, and kept on ice during use. Reference gene primer details are shown in Table 3.2.

Table 3.2: Reference genes used in GeNorm experiment

Primer	Accession Number	Product Size
ATP5B (Homo sapiens ATP synthase, H+ transporting, mitochondrial F1 complex, beta polypeptide)	NM_001686	119bp
B2M (Homo sapiens beta-2-microglobulin)	NM_004048	114bp
GAPDH (Homo sapiens glyceraldehyde-3-phosphate dehydrogenase, transcript variant 1)	NM_002046	110bp
UBC (Homo sapiens ubiquitin C)	NM_021009	137bp
YWHAZ (Homo sapiens tyrosine 3-monooxygenase/tryptophan 5-monooxygenase activation protein, zeta, transcript variant 1)	NM_003406	120bp
RLP13A (Homo sapiens ribosomal protein L13a , transcript variant 1)	NM_012423	153bp

The putative reference gene primers used in the GeNorm experiment. Sequences for these primers were not available, however the accession numbers and product size were supplied by PrimerDesign.

Using these reference gene primers, a Mastermix was generated by combining 2 x Precision master-mix containing SYBR Green and Taq polymerase (PrimerDesign) (10µl), RNAse/DNAse free water (PrimerDesign) (4µl), and the appropriate primer (1µl). Mastermix (15µl) was then pipetted into each well of a 48-well qPCR plate (PrimerDesign). To each well, 5µl of diluted cDNA extracted from untreated cells and treated cells was added at a concentration of 0.5ng/µl, to give a total concentration of 2.5ng/well, as recommended by PrimerDesign. qPCR assays were run in triplicate (three technical replicates) to ensure reliability of results. Each reference gene was trialled, in triplicate, for each sample, and the results averaged using the GeNorm software provided. Each sample was run with each primer.

3.2.8 Standard Curve Generation to Ensure Primer Efficiency

Following the determination of a reliable reference gene for use with qPCR assays, a standard curve was carried out for each of the genes to be assessed. All primers were generated by PrimerDesign and 100% efficiency was guaranteed, although standard curves were carried out for confirmation. All standard curves were conducted in duplicate using the Mastermix described above, and five ten-fold dilutions of samples, as outlined in work by Lai, et al. (2005) and used by Rajeevan, et al. (2001), Noble, et al. (2010), and Johnson, et al. (2012). The layout used to determine the standard curve is shown in Figure 3.1. Standard curves were generated using the Eco software (version, 5.0.16.0, Illumina).

For all experiments, a concentration of 1ng/µl cDNA was generated by combining 1µl cDNA with 49µl DNAse/RNAse free water. In each well containing this dilution, 5ng cDNA would be present. Dilutions of the cDNA were prepared via serial dilution (1ng/µl, 0.1ng/µl, 0.01ng/µl, 0.001ng/µl, and 0.0001ng/µl) using RNAse and DNAse free water. In wells containing these dilutions, 5ng, 0.5ng, 0.05ng, 0.005ng, and 0.0005ng of cDNA were present. These were run in accordance with the example layout. For the PDGFB primer, concentrations of 2ng/µl, 0.2ng/µl, 0.02ng/µl, 0.002ng/µl, and 0.0002ng/µl were used for the standard curve, due to the scarcity of the target gene.

1ng/µl cDNA (ICAM1)	1 in 10 Dilution cDNA (ICAM1)	1 in 100 Dilution cDNA (ICAM1)	1 in 1000 Dilution cDNA (ICAM1)	1 in 10000 Dilution cDNA (ICAM1)
1ng/µl cDNA (ICAM1)	1 in 10 Dilution cDNA (ICAM1)	1 in 100 Dilution cDNA (ICAM1)	1 in 1000 Dilution cDNA (ICAM1)	1 in 10000 Dilution cDNA (ICAM1)

Figure 3.1: qPCR standard curve template.

The template used to generate standard curves to determine primer efficiency.

The results from duplicate standard curve experiments were plotted on linear regression graphs using GraphPad (version 5.04). The efficiency of the primer could be determined.

In some cases, wells failed as the amount of mRNA in the well was insufficient to give a C_q value and instead generated a primer-dimer. If this occured in only the lowest well, then this result was excluded and the linear regression generated using four C_q values, as this is deemed acceptable. If this occurred in more than one well, then a higher concentration of cDNA was used, until a concentration in which only the lowest, or indeed no concentrations, produced a primer dimer. In cases where the highest concentration offered potentially erroneous results, as there was overlap between the highest and the second-highest concentration due to the mRNA content exceeding the limit of detection, standard curves were run again. In instances where this exceedance occurred repeatedly, the range of dilutions used was altered.

3.2.9 Purification and Secondary Amplification of cDNA from Agarose Gel

In instances in which the target mRNA was too scarce to be able to accurately generate a standard curve, a secondary PCR experiment was run to amplify the target DNA. Samples were prepared as outlined in 3.2.7. This was placed in the Techne TC-3000 thermal cylinder and run. An initial denaturing stage of 3 minutes at 95^{o}C was followed by 35 cycles of denaturing (30 s at 95^{o}C), annealing (30 s at 55^{o}C) and elongation (60 s at 72^{o}C). The sample was then stored at -20^{o}C until required.

An agarose gel was made as previously described (3.2.6). The banding on the gel was visualised using a transilluminator (UVP Lab Products EPI Chem II Darkroom) and the bands cut from the gel using a scalpel. The excised gel was then placed in a DNAse/RNAse free eppendorf and the cDNA prepared for quantification using the Macherey-Nagel Nucleospin RNAII kit (Macherey-Nagel, Düren, Germany). This step was carried out according to manufacturer's instructions. The cDNA content was then determined using the Qubit quantification kit, as outlined in 2.13. If sufficient cDNA was present to achieve a total concentration of at least 50ng/µl, as discussed in 2.13, the cDNA was stored and used to generate standard curves. If not, the sample was again amplified as described above.

3.3 Results

3.3.1 Concentration-Effect Assay to Determine the Cytotoxic Effects of BLM on HUVECs

The cytotoxicity of BLM at a range of concentrations was assessed to determine the concentrations of BLM to be used in future assays. Fifty percent was chosen as a cut-off point, to ensure sufficient cells were viable for subsequent analysis; time points and concentrations that induced >50% cell death were discarded. Cell death is expressed as a percentage of the number of viable cells in the untreated "0 hour" group, incubated only in serum free media for the same time as treated cells. An untreated group was included for each time-point to allow the elimination of senescence-mediated death which may overestimate BLM-induced death. The concentrations and time-points were selected as being representative of pharmacologically-relevant concentrations and times at and during which BLM may be present in the blood in renally competent and impaired patients.

Generally, as incubation time and BLM concentration increased, cell death increased. Unexpectedly, however, high levels of cell death were observed when cells were treated with 250ng/ml. The reasons for this are unknown, and may represent anomalous results, though this was observed in all three repeats. There was generally good agreement in levels of cell death between the two assays, though the SRB results show decreased viability compared to the MTS results at longer times. The reasons for this are currently unknown but may be due to the differences in the method; the SRB method requires cells to be washed prior to staining, and live cells may have been lost during the washing step of this protocol.

Table 3.3: MTS assay cell viability results

Incubation Time with BLM – MTS Assay

Concentration	0 hours	6 hours	12 Hours	24 Hours	48 Hours	72 Hours
0.01µg/ml	100	101.1	98.6	**81.2 ***	**71.8 ***	**68.6 ***
0.05µg/ml	100	97.3	**95.4 ***	**82.0 ***	**78.4 ***	**61.0 ***
0.1µg/ml	100	103.6	101.4	**94.8 ***	89.4	**75.2 ***
0.25µg/ml	100	**71.3 ***	**64.6 ***	**56.4 ***	**57.5 ***	**59.1 ***
0.5µg/ml	100	83.1	**87.8**	**72.7 ***	**57.8 ***	**58.1 ***
1µg/ml	100	103	96.1	**78.7 ***	**68.6 ***	**64.1 ***
5µg/ml	100	108	**89.3 ***	**67.8 ***	**69.0 ***	**55.6 ***
10µg/ml	100	**88.3 ***	**78.8 ***	**59.6 ***	**54.9 ***	**39.1 ***
100µg/ml	100	**58.0 ***	**48.5 ***	**38.4 ***	**22.5***	**24.7 ***

>100% viability

100-75% viability

75-50% viability

<50% viability

Table 3.4: SRB cell viability results

Incubation Time with BLM – SRB Assay

Concentration	0 Hours	6 Hours	12 Hours	24 Hours	48 Hours	72 Hours
0.01µg/ml	100	**90.7 ***	**83.6 ***	**86.7 ***	**74.2 ***	**45.8 ***
0.05µg/ml	100	**85.6 ***	**78.5 ***	**76.8 ***	**64.5 ***	**44.5 ***
0.1µg/ml	100	**89.2 ***	**82.1 ***	83.4	80.9	**41.8 ***
0.25µg/ml	100	**56.1 ***	**46.6 ***	**47.3 ***	**41.3 ***	**22.8 ***
0.5µg/ml	100	**77.0 ***	**73.6 ***	**74.2 ***	**58.8 ***	**30.4 ***
1µg/ml	100	**87.3 ***	**81.8 ***	**74.6 ***	**52.5 ***	**35.1 ***
5µg/ml	100	**84.0 ***	**67.1 ***	**53.6 ***	**51.2 ***	**28.8 ***
10µg/ml	100	**67.8 ***	**54.2 ***	**47.4 ***	55.3	**27.8 ***
100µg/ml	100	**62.6 ***	**45.2 ***	**30.0 ***	**3.8 ***	**0.0***

MTS and SRB Assay Cell Viability Results. Average (*n*=3) percentage cell viability as compared to un-treated cells (0 hour time-point, negative control) in HUVECs treated with various concentrations of BLM for various times. Statistically significant decreases in cell viability from baseline are denoted by an asterisk (*p=<0.05*).

3.3.2 Identification of Population of Viable HUVECs

The identification of a viable population of HUVECs on which to gate was assessed by propidium iodide assay to ensure that only live populations of cells were assessed using flow cytometric analysis. Representative results from one assay are shown. Within the gated area, the majority of the cells were viable. Therefore, this area will be gated in all future experiments and used as the representative area of live cells (Figure 3.2, Figure 3.3). The cells in the second peak (at an FL2-H of around 10^3) were dead. Notably, the level of dead cells was almost nil in the gated area.

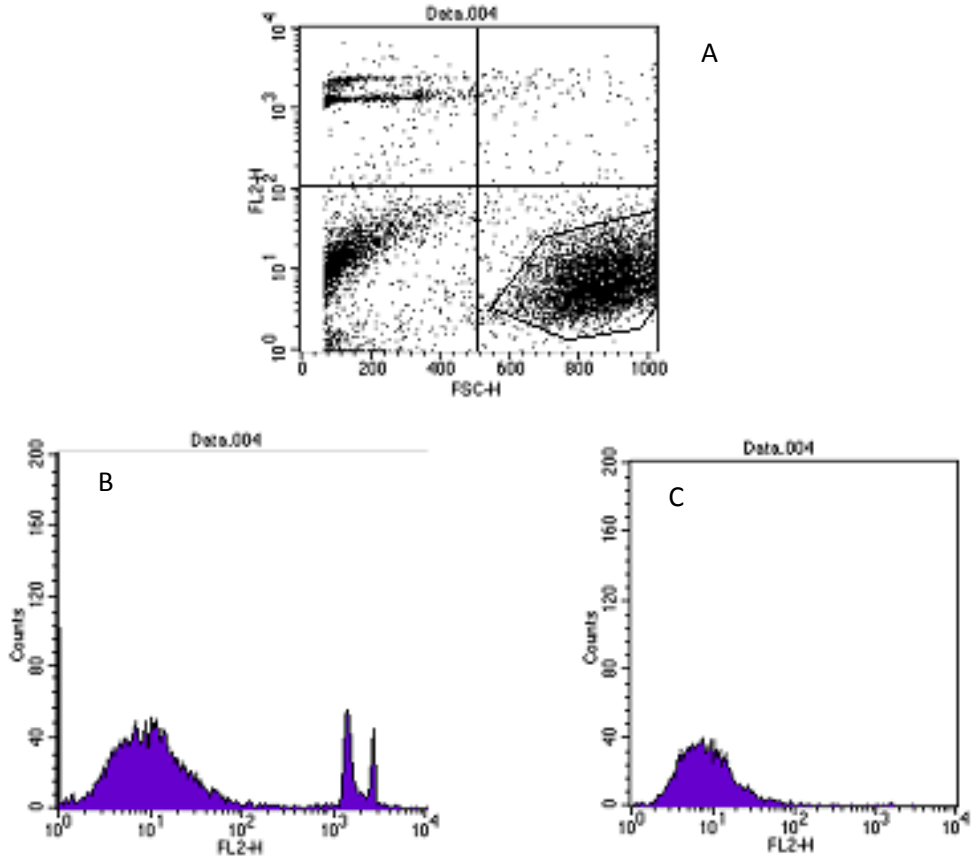

Figure 3.2: Propidium iodide experiment results (FSC-H vs. FL2-H)

A representative series of results from propidium iodide experiments to determine the viability of the gated area by flow cytometry using FSC-H vs. FL2-H. A) the dot-plot obtained. B) the histogram showing the viability of all cells in the dot-plot. C) the histogram showing the viability of cells in the gated area only. PI-positive cells (dead) are visible in the top-left quadrant of A. Results are representative of three experiments.

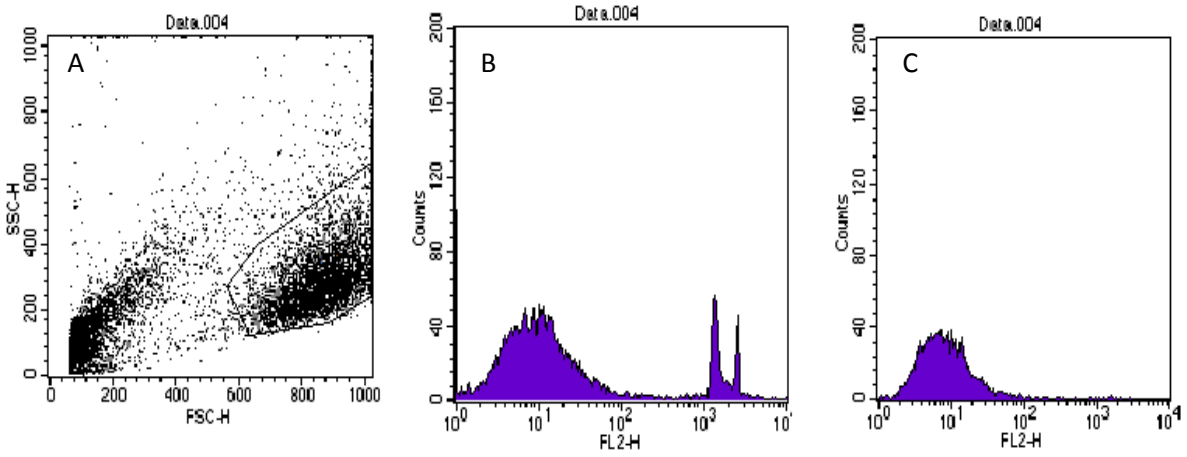

Figure 3.3: Propidium iodide experiment results (FSC-H vs. SSC-H).

The propidium iodide results obtained in 3.2, expressed as FSC-H vs. SSC-H to demonstrate the viable cell population as visualised when conducting flow cytometry using the FL-1 setting (used during all non-propidium iodide experiments in this work). A) the dot-plot obtained from this experiment. B) the histogram showing the viability of all cells in the dot-plot. C) the histogram showing the viability of cells in the gated area only. Results are representative of three experiments.

3.3.3 Cell Dissociation from Flasks

As endothelial adhesion molecule expression was being measured, a method for HUVEC dissociation which would not cleave adhesion molecules was required. Analysis of adhesion molecule expression by TNF-α-treated cells dissociated using 1mM EDTA and using a cell scraper could not be conducted, as incubation with 1mM EDTA for one minute did not dissociate cells, and incubation for 5 and 30 minutes resulted in extensive cell death. Very few live cells were detected by the flow cytometric analysis. When scraped, cells dissociated from the bottom of the flask in large sheets. It was not possible to determine the number of live cells remaining following dissociation by haemocytometry. When analysed by flow cytometry, again, very few cells were viable.

When cells were dissociated using PBS and chilling, few cells dissociated from the flask within 30 minutes. Cells were incubated in the refrigerator for another 30 minutes in PBS 0.1% w/v BSA. Still, very low number of cells dissociated from the base of the flask. Those that were dissociating were lifting in sheets. When cells were removed, centrifuged, and counted, an insufficient number of cells were present to run flow cytometric analysis.

3.3.3.1 Dissociation by TrypLE Express™ and 0.05% Trypsin 0.02% EDTA

Cells dissociated from flasks easily within 1 to 2 minutes of treatment with TrypLE Express™. Cells dissociated from culture flasks using 0.05% w/v Trypsin 0.02% w/v EDTA dissociated efficiently within the same time-scale as those treated with TrypLE Express™. In both cases, cells were found to be mostly viable by haemocytometry, and when assessed using flow cytometry, around 70% of cells fell within the gated area denoting viable cells. To determine which method is preferable, adhesion molecule expression by cells dissociated with each method was assessed (Figure 3.4). No significant difference was observed.

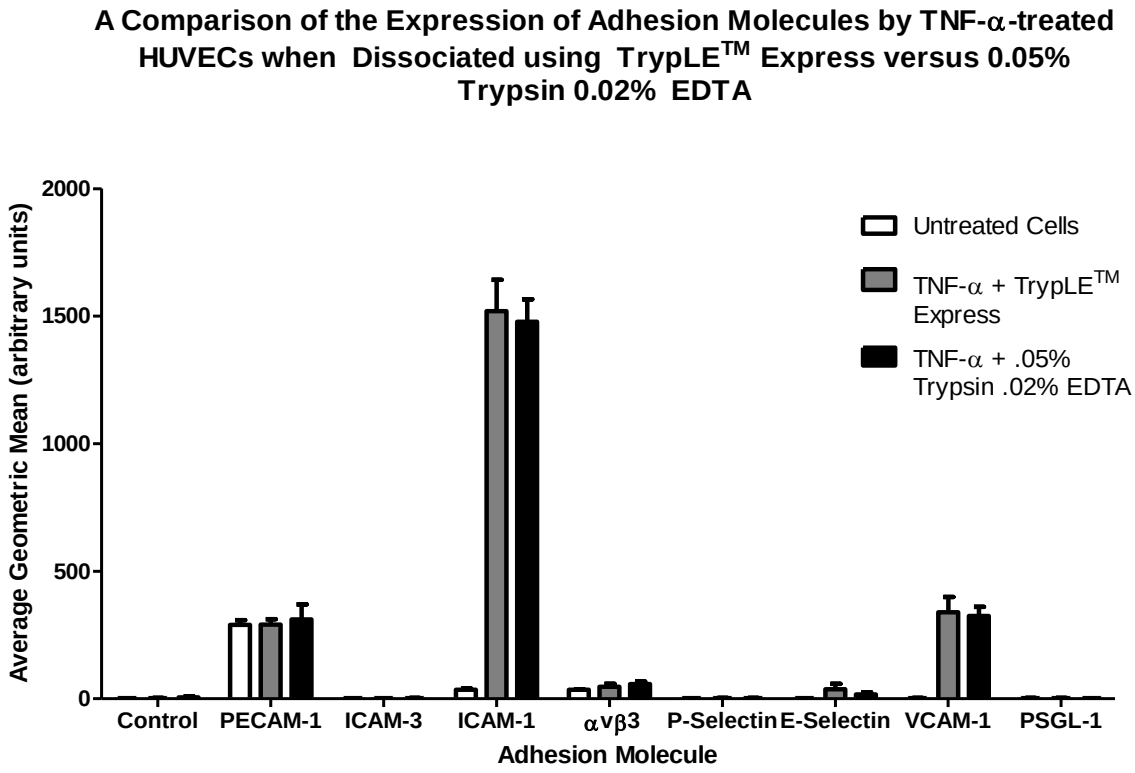

Figure 3.4: Adhesion molecule expression by HUVECs dissociated by two different methods

Adhesion molecule expression by TNF-α treated HUVECs dissociated with TrypLE™ Express and 0.05% Trypsin/ 0.02% EDTA. There was no significant difference between adhesion molecule expression by cells dissociated using TrypLE Express™ and 0.05% w/v Trypsin 0.02% w/v EDTA. *N = 3*.

3.3.4 Positive Control Determination for Adhesion Molecule Expression Experiments

In addition to a negative control, a positive control was needed. The expression of a panel of adhesion molecule in response to various concentrations of inflammatory mediators (LPS, TNF-α, and IFN-γ) was assessed. These molecules were PECAM-1, ICAM-3, ICAM-1, $\alpha_V\beta_3$ integrin, P-selectin, E-Selectin, VCAM-1, and PSGL-1. Concentration-effect experiments were conducted to determine the ideal cytokine, and the ideal concentration of this, to use to upregulate adhesion molecules for use as a positive control.

Only the expression of ICAM-1, E-Selectin, and VCAM-1 was seen to be substantially increased by treatment with inflammatory mediators. Six and 24 hour TNF-α and LPS treatment induced increased ICAM-1, E-Selectin, and VCAM-1 expression. IFN-γ treatment at all concentrations for six hours increased ICAM-1 expression, but this expression was increased by only 3000U/ ml concentrations when treated for 24 hours. In all groups, there was a significant increase in the binding of the isotype control antibody to cells treated for 6 and 24 hours (demonstrated in a tabular format in Appendix A, Table A.1). The upregulation of ICAM-1 expression was the greatest in all cases (Fig 3.6, 3.7, 3.8).

Raw data is shown in Fig 3.5. Raw data is shown with a gate applied to highlight the peak-shift and increase in ICAM-1 positive cells when cells were treated with TNF-α. Note that correction using gating was NOT used to determine expression (expression was determined using uncorrected data and plotted on graphs as outlined in section 2.5).

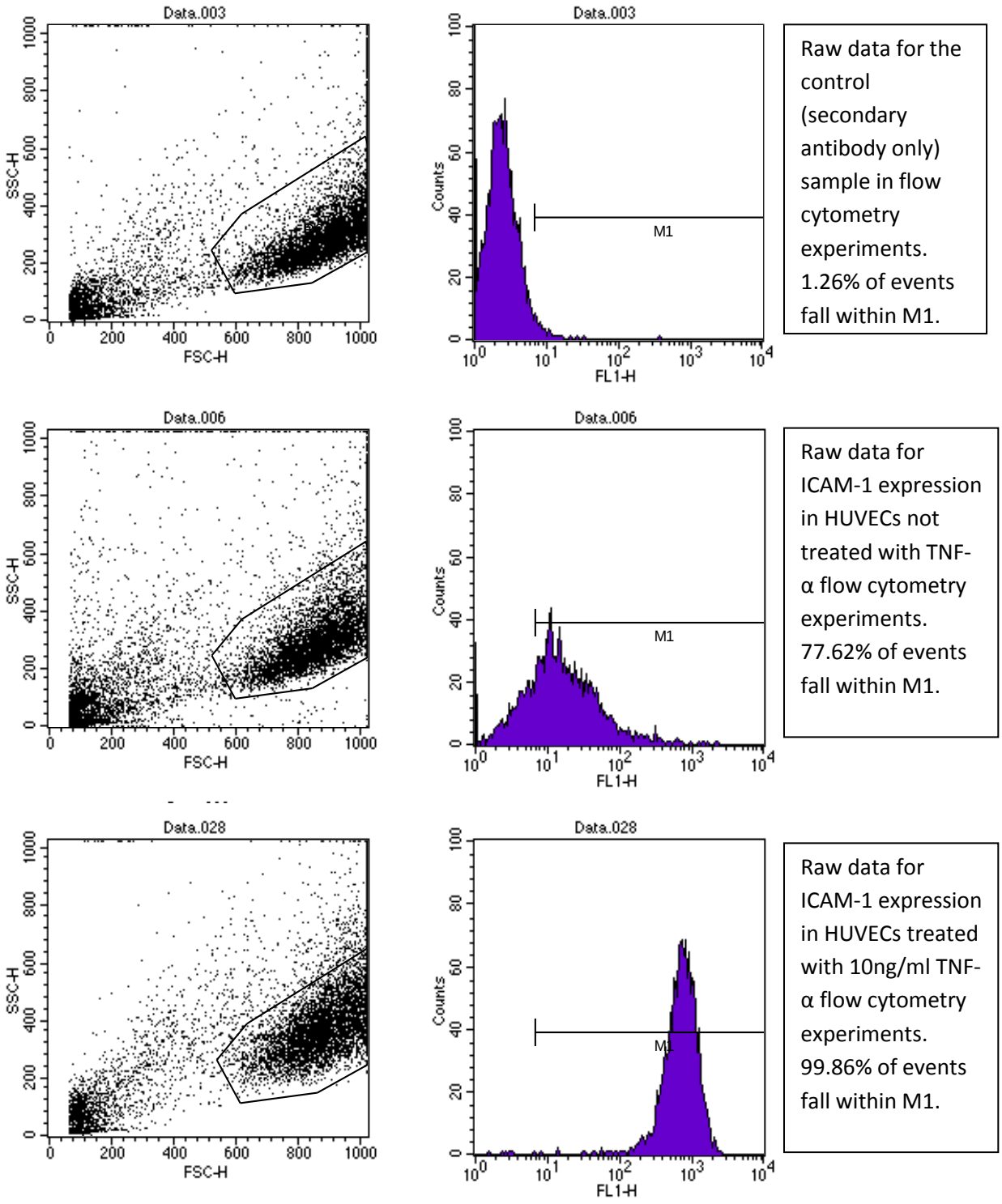

Figure 3.5: Raw data obtained for flow cytometry experiments using TNF-α

Raw data generated from flow cytometric analysis of negative control samples (top), ICAM-1 expression by untreated cells (middle) and cells treated with 10ng/ml TNF-α for 6 hours (bottom). Gate M1 was drawn to incorporate 1% of the control peak. There was a substantial peak shift from baseline ICAM-1 expression when cells were treated with TNF-α. Representative images of three experiments.

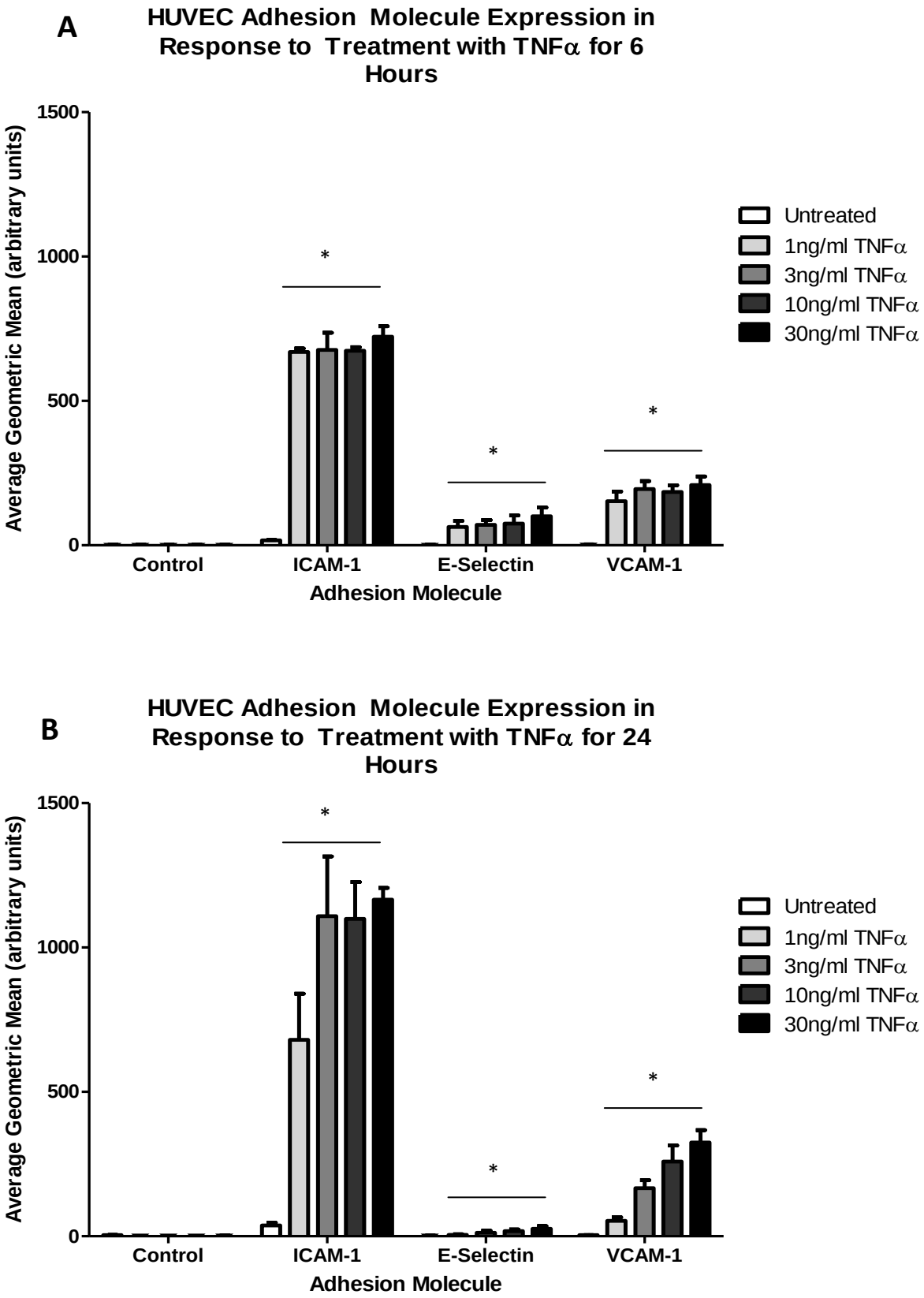

Figure 3.6: Adhesion molecule expression by TNF-α treated HUVECs

A) The expression of ICAM-1, E-Selectin, and VCAM-1 by HUVECs treated with TNF-α for 6 (A) and 24 (B) hours (*n=3*). The expression of all three adhesion molecules was significantly increased from baseline (*p=≤0.05*) by treatment with TNF-α of all concentrations.

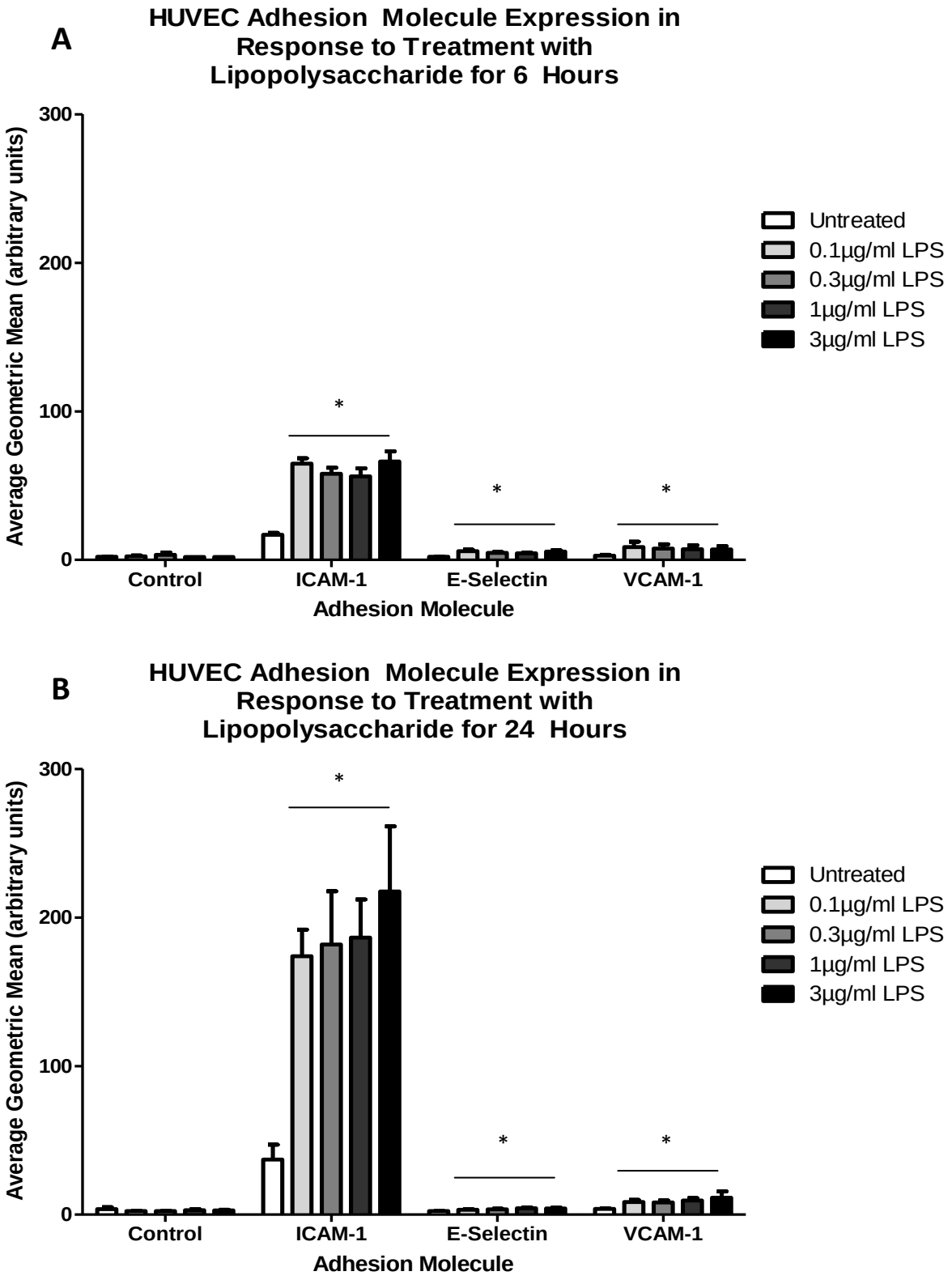

Figure 3.7: Adhesion molecule expression by LPS treated HUVECs

A) The expression of ICAM-1, E-Selectin, and VCAM-1 by HUVECs treated with LPS for 6 (A) and 24 (B) hours (*n=3*). The expression of all three adhesion molecules was significantly increased from baseline (*p=≤0.05*) by treatment with LPS of all concentrations.

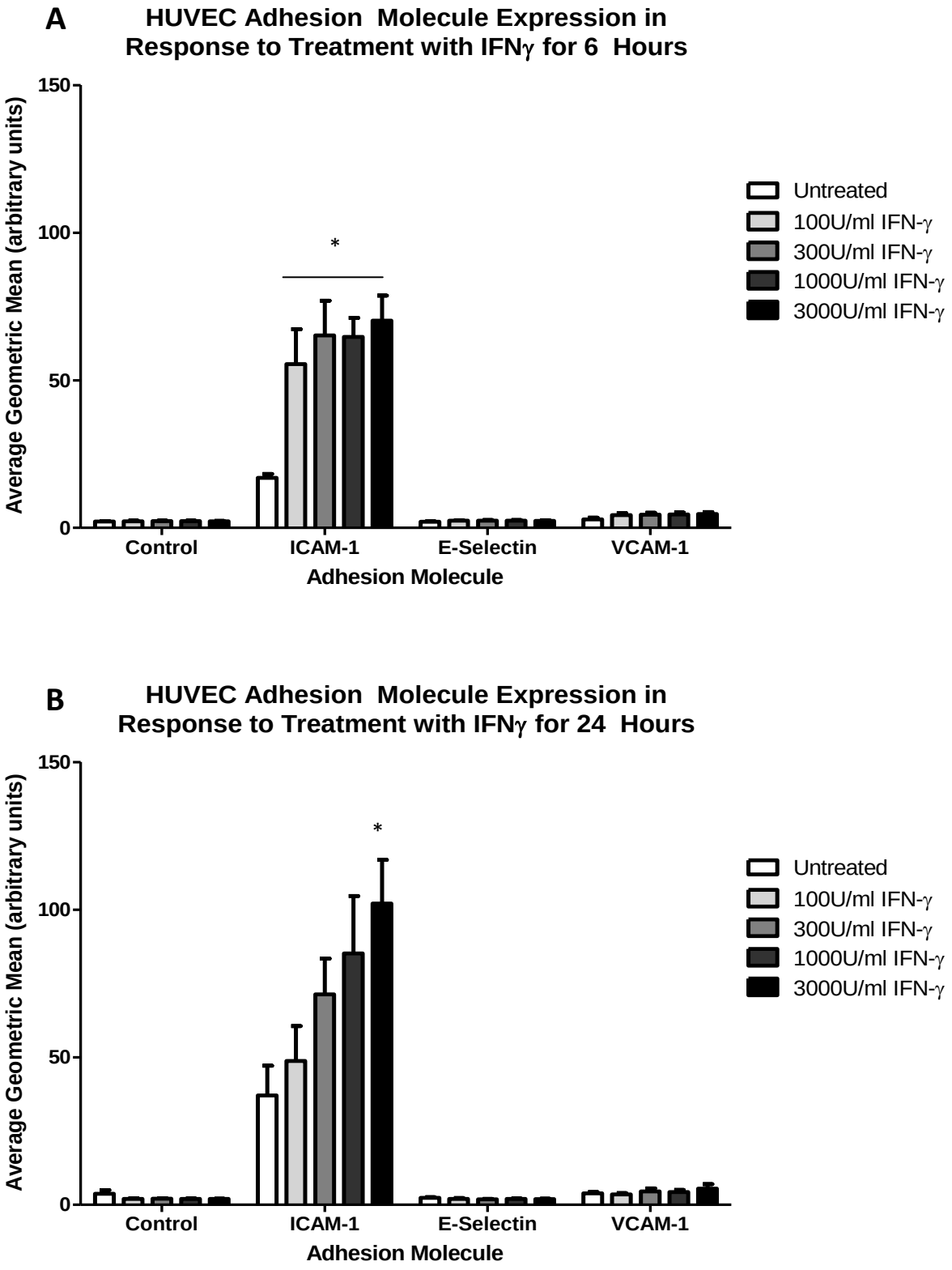

Figure 3.8: Adhesion molecule expression by IFNγ-treated HUVECs

A) The expression of ICAM-1, E-selectin, and VCAM-1 by HUVECs treated with IFN-γ for 6 (A) and 24 (B) hours (*n=3*). The expression of CD54 was significantly increased from baseline (*p=≤0.05*) by treatment with IFNγ of all concentrations when cells were treated for 6 hours, but only by 3000U/ml IFNγ when cell were treated for 24 hours.

3.3.5 Comparative Statistics - 6 and 24 Hour Incubations with Proinflammatory Mediators

ICAM-1 expression by cells treated with TNF-α at all concentrations for 6 hours was significantly greater ($p \leq 0.05$) than by cells treated with all concentrations of LPS and IFN-γ for 6 and 24 hours, as seen in Fig 3.9. ICAM-1 expression by cells treated with different concentrations of TNF-α was not significantly different when cells were treated for 6 hours, but when treated for 24 hours, there was a significant difference in ICAM-1 expression in cells treated with 1ng/ml and 3ng/ml, with this difference diminishing as concentrations increased. There is no clear concentration-dependent increase in ICAM-1 expression by cells treated with varying concentrations of TNF-α, suggesting ICAM-1 expression has achieved a plateau. While VCAM-1 and E-Selectin were also upregulated by TNF-α and LPS treatment, this upregulation was less substantial than that of ICAM-1.

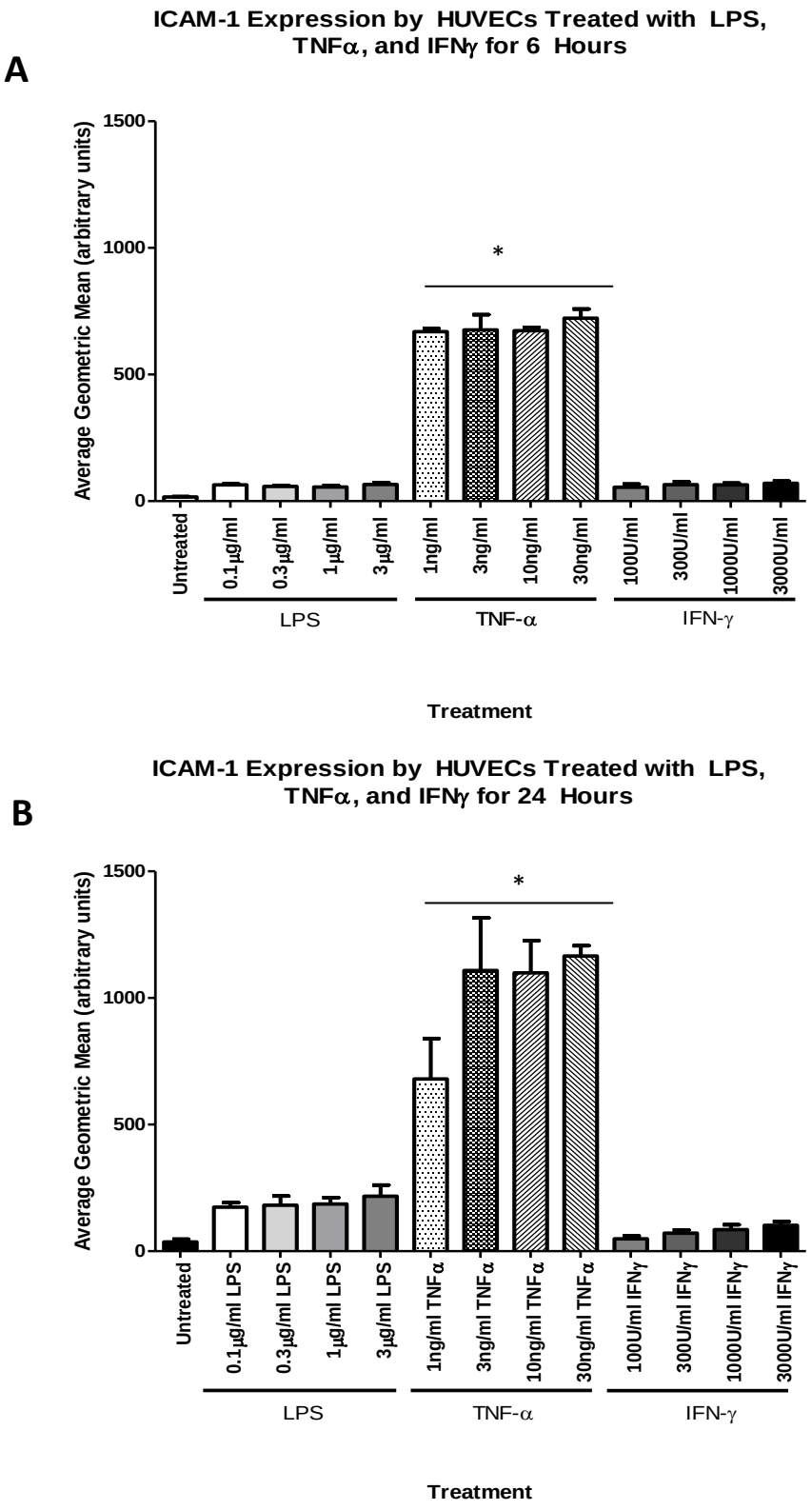

Figure 3.9: ICAM-1 expression by HUVECs treated with TNF-α , LPS, and IFNγ.

A) ICAM expression by HUVECs treated with TNF-α, LPS, and IFN-γ for 6 (A) and 24 (B) hours. Increases in ICAM-1 expression compared to baseline in response to TNF-α were significantly higher (*p=≤0.05*) than to LPS or IFNγ (*n=3*).

3.3.6 Confirmation of cDNA Purity and Quality

To confirm that the reverse transcription step of this work was conducted correctly, agarose gels were run to confirm whether cDNA was present in each sample. A representative agarose gel is shown in Fig. 3.10. As a GAPDH primer was used, bands were present at around 700bp, as expected. These samples were used to run the GeNorm experiments, to determine the preferred housekeeping gene for use with qPCR experiments.

3.3.7 Determination of an Ideal Reference Gene using GeNorm Experiments

Six reference genes were used (GAPDH, B2M, UBC, RPL13A, YWHAZ, and ATP5B, a kind gift from PrimerDesign) and the stability of these genes in each cell line (28543, 28756, and 2062502) under each treatment condition (untreated, 0.1µg/ml/ml, 1µg/ml, and 10µg/ml for 6 or 24 hours) assessed. Results from each geNorm experiment from each cell line under each treatment condition were compiled and analysed using the qBase+ programme to determine the most stable reference gene on average. In total, 12 geNorm experiments were carried out. The most stable reference gene overall was UBC, the ubiquitin C gene (Fig. 3.11), and this was used in all future experiments.

Using the GeNorm technique, the stability of the reference genes in each sample is compared and the stability assigned a value, the GeNorm M value. The qBase+ software uses a logarithm based on the work of Vandesompele, et al. (2002), whereby the relatively stability of genes to one another is determined and the least stable gene is excluded in a stepwise fashion. The M value is used as a marker of the variability of the gene expression. The lower the M value, the higher the stability of the gene (Vandesompele, et al., 2002). All graphical outputs are based on those used in this work.

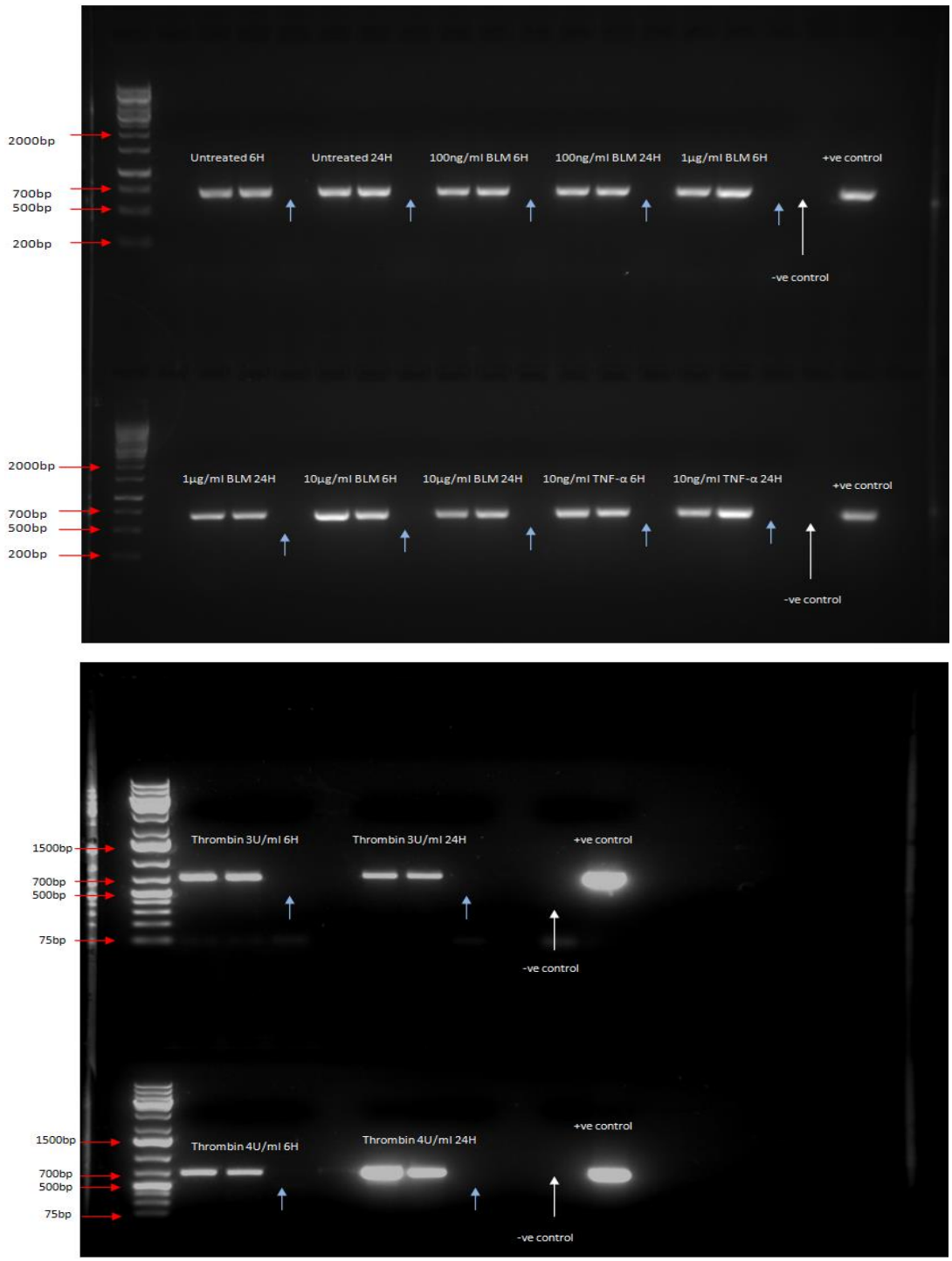

Figure 3.10: The quality of cDNA samples used for qPCR experiments as determined by PCR using a GAPDH primer.

Agarose gels showing the quality of cDNA samples following reverse transcription. Light blue arrows represent No RT controls for samples to the left of the arrow. The positive control was cDNA extracted from HEK cells. Negative control wells contained no cDNA. The ladder used in the upper gel was the 1kb ladder; in the lower gel, the 1kb plus ladder. These images are representative of three gels carried out.

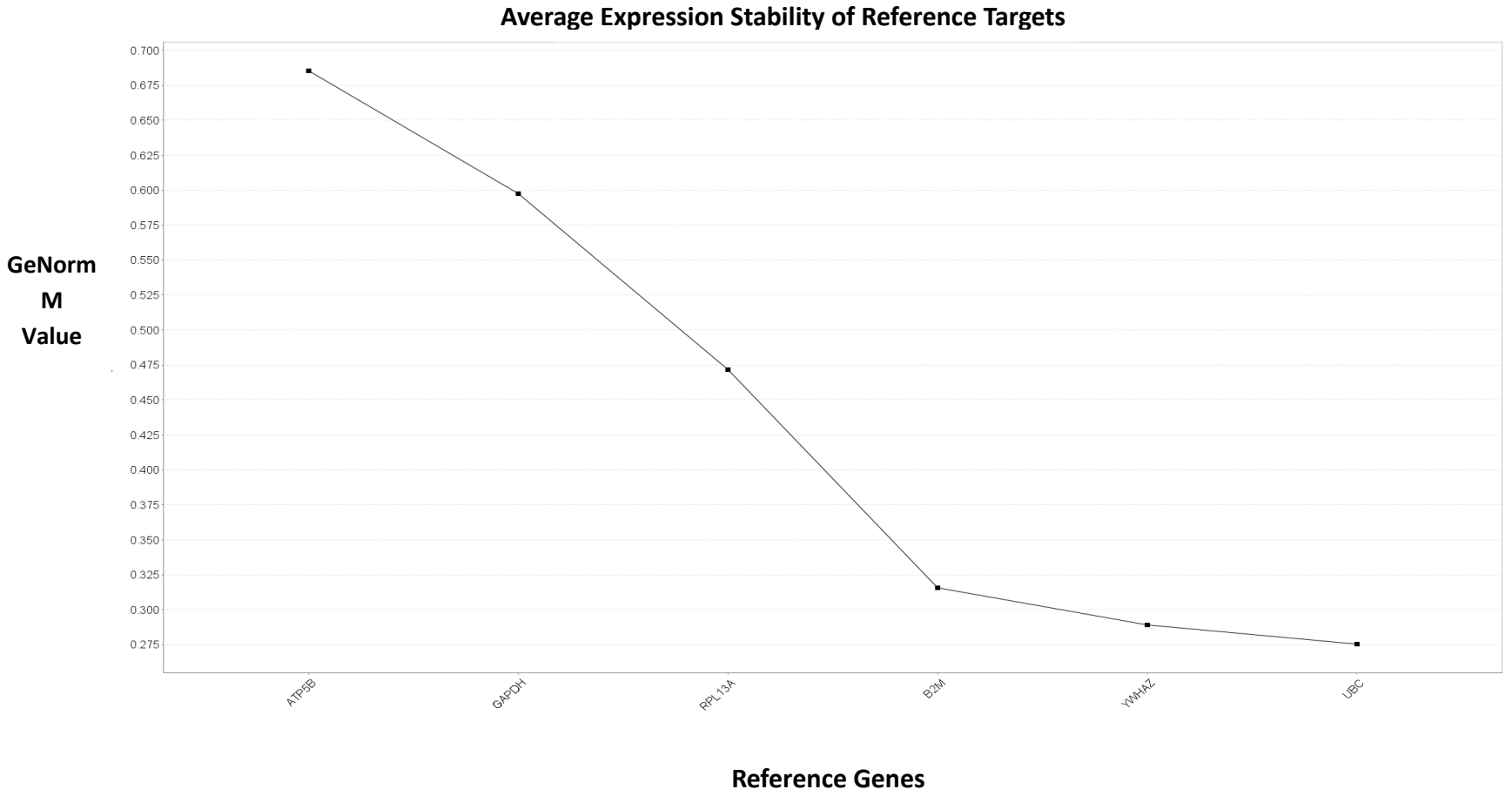

Figure 3.11: The stability of reference genes used in the GeNorm experiment.

The results of the geNorm experiment carried out on all samples of all cell lines assayed, as generated by the BioGazelle qBase+ software. The most stable reference gene across all samples assessed was UBC (ubiquitin C), and the least stable ATP5B. All samples were run in triplicate.

3.3.8 Assessment of Primer Specificity and gDNA Contamination

To ensure all primers amplified only specified target transcripts, a PCR was run using samples as outlined in 3.2.7 and the qPCR primers obtained, and the resulting PCR product was run on agarose gels. Using all primers, only a single band which correlated with the known size of the product (Table 2.1) was achieved. Representative gels are shown in Fig. 3.12 and Fig 3.13. The TGF-β band remained faint in 3 repeats, potentially due to low levels of target transcript. However, this band appeared as a band of the correct size. While faint bands were detected in the No RT and No cDNA samples for VCAM-1 and PDGF-BB, these bands were found to be smaller than that of the target transcript. It is feasible that in these samples, primer dimerisation has occurred due to a lack of target transcript. The primers were therefore used for further work.

No RT samples, which contained no cDNA due to the absence of reverse transcriptase in sample preparation, were run to assess gDNA contamination. The appearance of a band in these samples suggests gDNA contamination, as gDNA does not require reverse transcription to be present. Similarly, if banding appears in No cDNA controls, this suggests contamination of the reagents used. That no band appeared in No RT samples suggests gDNA contamination has not occurred. Moreover, that a single band was observed when cDNA-containing samples were run also suggests there is no gDNA contamination, as this would generate more than one band when samples were run.

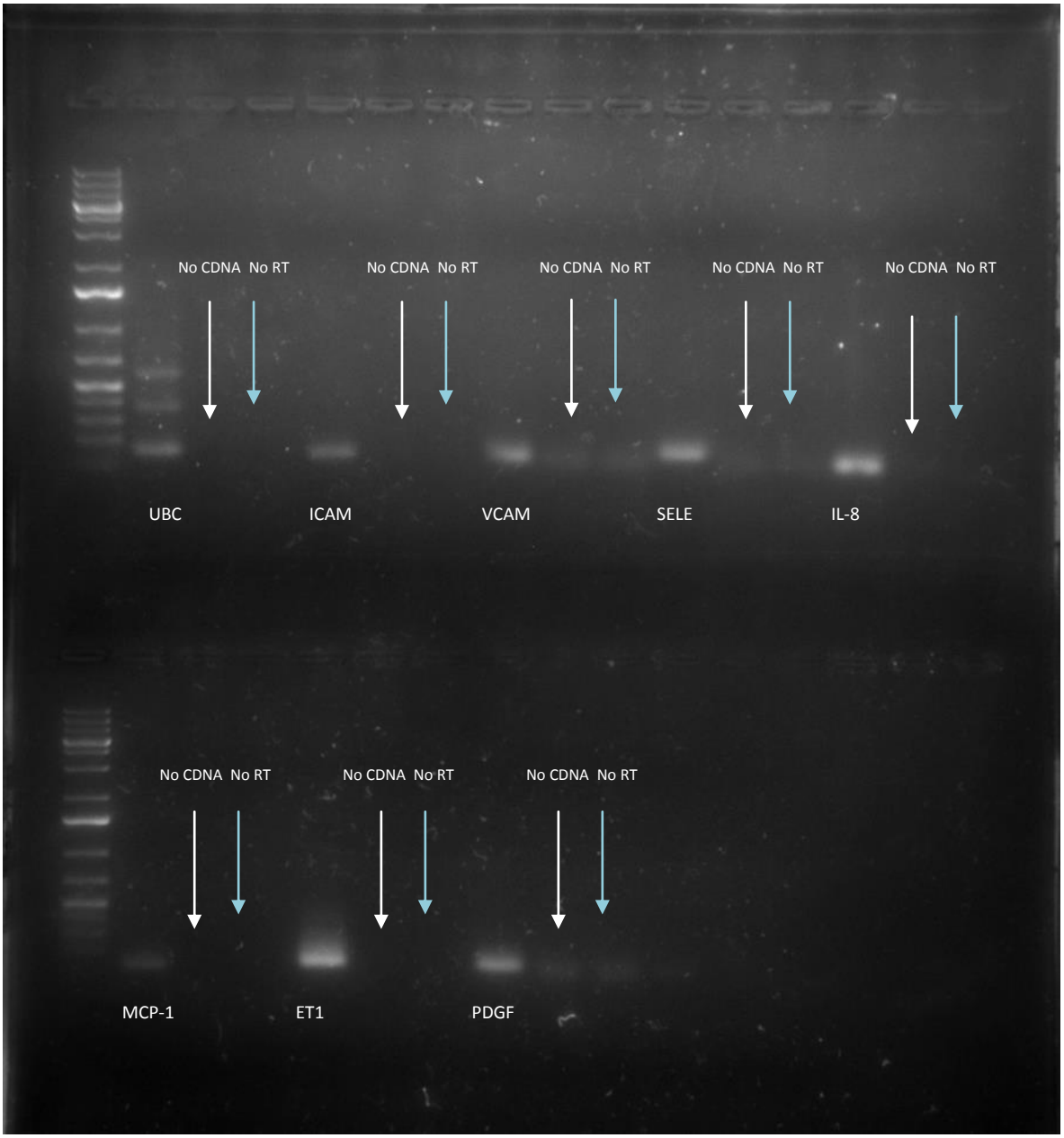

Figure 3.12: The specifity of primers used in qPCR experiments.

A representative agarose gel showing products when samples of HUVEC cDNA (positive control samples for all target transcript primers, negative control sample for UBC primer) underwent PCR. In all cases with the exception of UBC (for which a sequence was not available due to copyright), a single band of expected size (based on the known size of the products outlined in Table 2.1) was generated.

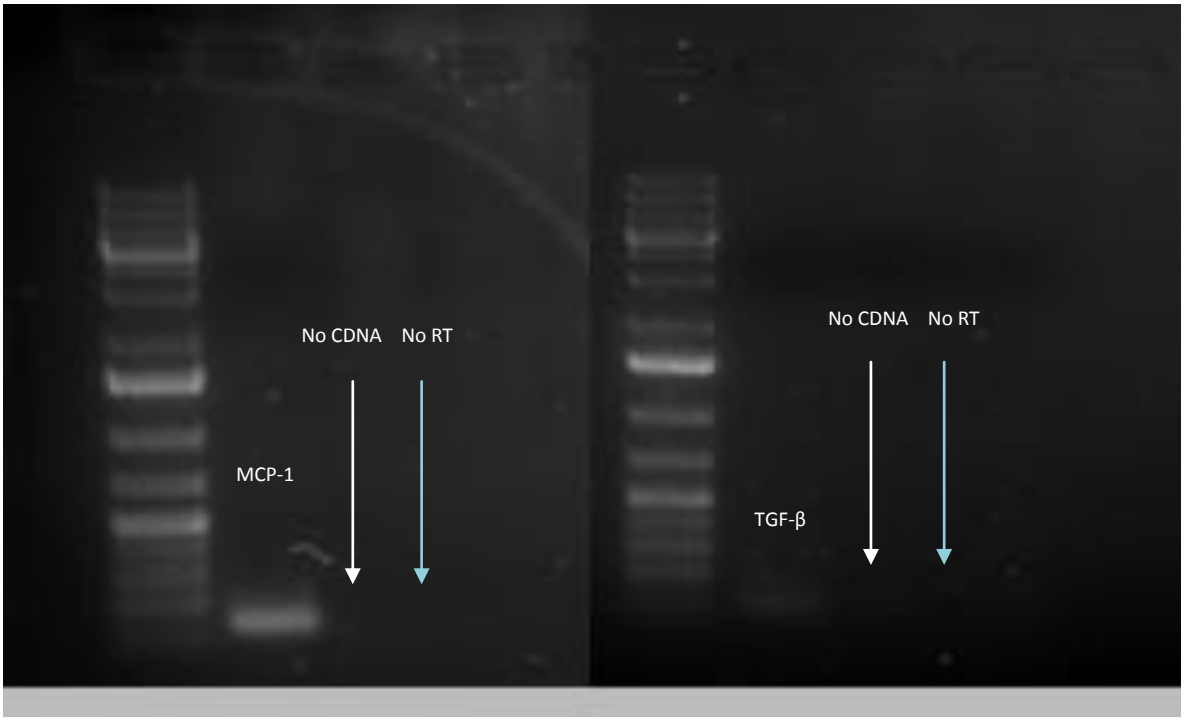

Figure 3.13: The specifity of primers used in qPCR experiments II

A representative agarose gel showing the PCR products when the MCP-1 and TGF-β primers were used in the PCR reaction. As above, the single band of expected size and a lack of No RT and No cDNA sample bands was seen.

3.3.9 Generation of Standard Curves to Determine Primer Efficiency

Standard curves were generated for all primers as, though the supplier guaranteed efficiency within the 90-110% window (denoting 100% efficiency), confirmation of this using our cDNA samples was necessary. The results of these standard curves are shown in Table 3.5. An example standard curve for the IL-8 primer is shown in Figure 3.14. Standard curves for all other primer assessed can be found in the appendix. In most cases, standard curves were generated using five points.

Tenfold dilutions of 1ng/ml cDNA (5ng – 0.0005ng per well, 1ng/µl - 0.0001ng/µl) were sufficient to generate a standard curve for VCAM-1, E-Selectin, IL-8, UBC, MCP-1, and Endothelin-1. Tenfold dilutions of 2ng/ml (10ng – 0.001ng per well; 2ng/µl-0.0002ng/µl) were required to generate a standard curve for PDGF-BB.

In cases where the lowest concentration was too low for detection, standard curves were generated using four points. Though all efforts were made to generate standard curves which did not require the exclusion of any samples, in the case of the PDGFB and SELE primer standard curves, the lowest concentration values were discarded as primer dimers had formed due to low levels of target transcript in the samples.

In the case of TGFB1, cDNA purification and amplification was required, as the target transcript was very scarce. A total concentration of 2ng/ml pure TGF-β1 cDNA was generated. This was then diluted to give concentrations of 0.01ng/µl – 0.0001ng/µl, using which a standard curve was generated.

No standard curve could be generated in-house for the ICAM-1 primer; repeated attemps generated curves in which the highest concentration overlapped, and the lowest formed primer dimers, and a suitable concentration for use could not be developed. However, a standard curve was graciously generated by PrimerDesign using lung cDNA by Rebecca Gover at concentrations of 6ng/µl-0.006ng/ µl (30ng-0.03ng/well). The ICAM-1 standard curve, as some others, contained only four points as the lowest concentration was unable to achieve readable values.

All primers tested fell within the 90-110% efficiency bracket, including the ICAM1 and TGFB primers, therefore the correction of results based on primer efficiency discordance

via the Pfaffl method (Pfaffl, 2001) is not needed in this work. Therefore, the $\Delta\Delta C_q$, or Livak method, may be used.

The concentration of 2.5ng/well (0.5ng/µl) for use in qPCR experiments, previously suggested by PrimerDesign (3.2.7), was confirmed by standard curve generation to be a suitable concentration to use; this concentration falls within the range of concentrations seen to produce results that were not the result of a primer dimer, and fell within the preferred limit of detection (>10 but <35 cycles required to exceed the threshold) in all standard curves produced. This concentration, when then used in later qPCR experiments, produced consistent results that again fell within the preferred limit of detection and were not the result of primer dimerisation.

The standard curve generated by Rebecca Gover for the ICAM-1 primer also incorporated this concentration, and test runs found this to be a concentration that contained sufficient target ICAM-1 transcript to generate results. Although the TGF-β standard curve did not incorporate this concentration, test runs again found this amount of cDNA contained sufficient target transcript to produce replicable, reliable, results.

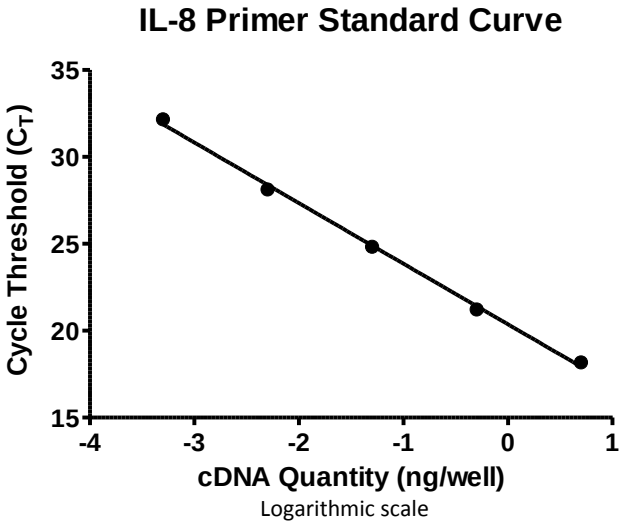

Slope	-3.486
Y Intercept	20.37
R^2 value	0.997
P value	< 0.0001
Efficiency	93.58%

Figure 3.14: The qPCR efficiency standard curve for the IL-8 primer.

An example standard curve as generated using the results of qPCR standard curve experiments. This curve shows that the efficiency of the IL-8 primer lies at 93.85%, within the 90-110% threshold for assuming 100% primer efficiency, negating the need for correction via the Pfaffl method.

Table 3.5: The efficiency of primers used in qPCR experiments as determined by standard curves.

Primer	Sense/Antisense Primer	Efficiency	Product Length	Standard Curve
ICAM-1 (Homo sapiens intercellular adhesion molecule, CD54)	Sense: CCTATGGCAACGACTCCTTC Antisense: TCTCCTGGCTCTGGTTCC	**95.75% (Four points)**	**111bp**	R^2 value: 0.996 slope value: -3.428 Y intercept: 27.49
VCAM1_24444 (Homo sapiens vascular cell adhesion molecule VCAM1, transcript variant 1)	Sense: TGTGAATCCCCATCTTTCTCCT Antisense: CTCAGGGTCAGCGTGGAAT	**105.21%**	**95bp**	R^2 value: 0.9944 Slope: -3.203 Y intercept: 23.70-24.45
IL-8 (Homo sapiens interleukin 8).	Sense: CAGAGACAGCAGAGCACAC Antisense: AGCTTGGAAGTCATGTTTACAC	**93.58%**	**95bp**	R^2 value: 0.997 Slope: -3.486 Y intercept: 20.07-20.67
MCP-1 (Homo sapiens chemokine (C-C motif) ligand 2 (CCL2)).	Sense: ACCGAGAGGCTGAGACTAAC Antisense: AATGAAGGTGGCTGCTATGAG	**99.37%**	**122bp**	R^2 value: 0.9986 Slope: -3.337 Y intercept: 20.67-21.05
E-Selectin (Homo sapiens selectin E (endothelial adhesion molecule 1 (SELE)).	Sense: TTCTTGCCTACTATGCCAGATG Antisense: AGGAAAGGGAACACTGAGTCT	**105.26% (Four points)**	**123bp**	R^2 value: 0.9952 Slope: -3.202 Y intercept: 21.56-22.18
PDGF-BB (Homo sapiens platelet-derived growth factor beta polypeptide (simian sarcoma viral (v-sis) oncogene homolog) (PDGFB), transcript variant 1)	Sense: AGCACACGCATGACAAGAC Antisense: GGGGCAATACAGCAAATACCA	**108.73% (Four points)**	**108bp**	R^2 value: 0.9941 Slope: -3.129 Y intercept: 24.59 - 25.18
ET-1 (Homo sapiens endothelin 1 (EDN1), mRNA.)	Sense: TGAGAATAGATGCCAATGTGCTA Antisense: GAACAGTCTTTTCCTTTCTTATGATT	**93.03%**	**132bp**	R^2 value: 0.9872 Slope: -3.501 Y intercept: 23.59-24.84
TGF-β1 (Homo sapiens transfroming growth factor, beta 1 (Camurati-Engelmann disease (TGFB1) mRNA)	Sense: CACTCCCACTCCCTCTCTC Antisense: GTCCCCTGTGCCTTGATG	**105.35% (Four points)**	**83bp**	R^2 value: 0.9877 Slope: -3.200 Y intercept: 0.124-2.884
UBC (Homo sapiens ubiquitin C)	Not available: Accession number: NM_021009 Anchor nucleotide: 452	**99.91%**	**192bp**	R^2 value: 0.9766 Slope: -3.324 Y intercept: 22.63-24.25

The efficiency of primers used in qPCR experiments as determined by standard curves. All primers fell within the desired 90-110% efficiency range, suggesting that the efficiency of the primers was sufficiently close to 100% to negate the need for normalisation of the results using the Pfaffl Method. The linearity of the results was also generally greater than R^2=0.98, suggesting high reproducibitility between duplicate standard curves. Though the R^2 value acheived when the UBC primer was assessed was 0.976, this was deemed sufficiently linear.

3.4 Discussion and Conclusions

3.4.1 Cytotoxicity Assay

As 72 hour and 48 hour incubations with many concentrations of BLM induced relatively high cell death, not seen *in vivo*, these time-point were disregarded from further work. However, 24, 12, and 6 hour incubations induced acceptable levels of cell toxicity, with 6 and 12 hour incubation times producing very similar levels of cell death. As 24 hours is around the terminal half-life of BLM in renally impaired patients, who are susceptible to BPF, and 6 hours represents the terminal half-life of patients who are renally competent, these time points will be used in future work.

As expected, 100µg/ml BLM induced very high cytotoxicity, though concentrations of 250ng/ml were seen to produce high toxicity also. The reasons for high cell death at 250ng/ml are unknown; this may simply represent an anomalous result, though all three cell lines incurred similar cell death when treated with 250ng/ml BLM. Neither concentration will be used further. Concentrations of 10ng/ml and 50ng/ml caused low cytotoxicity, but very similar levels of cytotoxicity as 0.1µg/ml, and so only one will be used. All other concentrations caused physiologically relevant cytotoxicity. Therefore, 0.1, 1, and 10µg/ml will be used in future work.

Though few groups have studied time and concentration dependence of BLM-mediated cytotoxicity in HUVECs, the current results are somewhat similar to those of Miyamoto, et al. (2002), who, using [H^3]-thymidine incorporation assays, noted HUVECs incubated with 50ng/ml BLM over 6, 12, and 48 hours remained around 80% viable. However, cell viability after treatment with higher BLM concentrations (0.1µg/ml - 100µg /ml) in the Miyamoto work was lower than the cell viability noted in the current work, and almost total cell death was noted immediately after HUVECs were treated with 10µg/ml and 100µg/ml BLM by Miyamoto, et al. (2002). The only similarity between the Miyamoto work and the current work at these concentrations is that 10µg/ml and 100µg/ml BLM induced substantial death after 48 hour incubation. The difference in method may explain this.

The [H^3]-thymidine incorporation assay determines cell viability by determining the amount of thymidine incorporated into replicating DNA of proliferating cells, therefore determining cell proliferation rather than viability. [H^3]-thymidine incorporation may be impacted by increased or decreased cell proliferation – in this work, cells were incubated in serum-free media to retard proliferation. The current work uses the MTS and SRB assays, which count all living cells. Todorovic, et al. (2009) used an MTS assay similar to that employed by the current study to determine the viability of murine rectum carcinoma cells (CMT-93) following exposure to BLM, and, though using a different cell line and only a single 16-hour time point, produced similar results to those from our 12 hour incubation; i.e., low levels of cell death. That the SRB assay suggested a similar, but slightly lower, percentage of viable cells than the MTS assay in the current work suggests that washing may have removed live cells, though a similar pattern was observed.

3.4.2 Cell Dissociation

It is clear that cell scraping, incubation with 1mM EDTA, and chilling in PBS were not suitable as methods of dissociation as cells were largely non-viable after removal. Dissociation by both TrypLE™ Express and 0.05% Trypsin 0.02% EDTA resulted in a sufficient number of cells for FACS analysis, and a high percentage of viable cells, and neither induced a higher level of enzymatic adhesion molecule cleavage than the other.

The method of dissociation selected is TrypLE™ Express. Although there is no precedent for this, this work has shown that there is no difference between the number of adhesion molecules present on cells dissociated by TrypLE™ Express or 0.05% Trypsin 0.02% EDTA when analysed by FACS. As this product is used to passage HUVECs in our laboratories and appears gentle to adhesion molecules, along with the consistency acheived by using the same product for passaging and dissociation prior to FACS, this product will be used in future work.

3.4.3 Positive Control Determination

The results of the control experiment clearly show that ICAM-1 was upregulated to a greater degree than all other adhesion molecules assessed, notably VCAM-1 and E-Selectin, similar to the results of previous works by Zhang and Issekutz (2001), Jägels, et al.(2000), and Choi, et al., (2009). This suggests ICAM-1 is the best adhesion molecule to use as a positive control. Moreover, that TNF-α was able to upregulate ICAM-1 to a greater degree than IFN-γ or LPS at both 6 and 24 hours suggests that TNF-α is the best treatment to upregulate adhesion molecule expression over this timeframe.

That TNF-α induced the expression of ICAM-1 at similar levels when treated with 3ng/ml, 10ng/ml, and 30ng/ml TNF-α in the 24 hour experiments and with all concentrations of TNF-α in the 6 hour incubation experiments suggests that any concentration would be suitable for inducing ICAM-1 expression in future work. Similar reports of a slight, but not obvious, concentration dependence have been published by others; Willam, et al. (1999) noted a concentration-dependent increase in ICAM-1 expression when treating HUVECs with TNF-α of varying concentrations (0.01-100ng/ml); ICAM-1 expression increased from 0.01ng/ml to 10ng/ml TNF-α, and then plateaued between 10ng/ml and 100ng/ml. Sawa, et al. (2007), noted a slight concentration-dependent increase in ICAM-1 expression as TNF-α concentration increased (5ng/ml, 10ng/ml, and 20ng/ ml), with a plateau at 10ng/ml. Therefore, the concentration of 10ng/ml, which upregulated ICAM-1 expression to high levels and a level not significantly different from that of 30ng/ml, will be used in this work as a positive control.

3.4.4 GeNorm Experiments for the Determination of a Suitable Reference Gene

This work has provided many interesting foci for discussion. Firstly, it was found that the most stable putative reference gene was UBC, and not GAPDH, which is widely used and is sometimes regarded as the classical reference gene in qPCR (de Jonge, et al., 2007). Though there is a tendency in some papers to not validate the reference genes used, or to refer back to “the qPCR gold standard”, to justify the choice of gene, the expression of GAPDH can vary on a tissue-to-tissue basis, and may be impacted by experimental

techniques, as discussed recently in a substantial review, although this is not the only putative reference gene for which this is the case (Kozera and Rapacz, 2013). Therefore, when a different cell type or tissue is used, a GeNorm experiment or equivalent must be conducted.

This work was carried out on all samples and the results pooled together to give *n=3*. It is interesting to note that UBC was not the most stable reference gene in each individual experiment (data not shown), but when all data from each line was analysed using the GeNorm software, the average stability of UBC was superior to that of other genes across lines, including GAPDH. Therefore, UBC will be used as the reference gene in all qPCR experiments.

3.4.5 Standard Curve Generation to Determine Primer Efficiency

While all primers fell within the accepted range of efficiencies (90-110%), the success of standard curve experiments to determine this depended on the abundance of the target transcript. In cases such as VCAM1_2444, CCL2, IL8, and UBC - where the transcript was abundant - such experiments were performed with ease. In cases such as E-Selectin (SELE), where the target transcript was more scarce, the lowest dilution often produced a primer dimer due to a lack of target amplification. This was also the case with PDGFB, where the lowest concentration produced primer dimers regardless of initial concentration. In both cases, a standard curve of four points was generated. However, that all primer standard curves were run in duplicate and concordance was very high suggests that the efficiencies obtained were reliable.

Although it was not possible to achieve a concentration high enough for TGFB standard curves to be generated, gel purification of the TGFB transcript proved sufficient to generate a 4-point standard curve. This, however, was not the case for ICAM1, and lung cDNA was used to generate a 4-point standard curve by Rebecca Gover at PrimerDesign. When an ICAM1 standard curve was attempted in-house, low starting concentrations yielded many primer dimers or failed wells, and high starting concentrations yielded wells with very similar C_q values - usually the two highest concentrations. A dilution range which resulted in neither C_q overlap or primer dimerisation occurred could not be

identified. It is also notable that no similar efficiencies could be generated with this primer in-house when run in duplicate, mostly due to a high number of failed wells. The issue of similar C_q values may have been due to a narrow range of detection of the ICAM1 primer, or the excedence of the limit of detection due to transcript overabundance, but this remains unknown.

While neither case is ideal, it is notable that, when running qPCR experiments using a concentration of 2.5ng/well cDNA, neither of these target transcripts proved too scarce for detection. Indeed, both universally generated C_q values below 35 - an arbitrary cut-off point - and neither were beset with problems of primer dimer formation. While the reason for the issues generating the standard curve for the TGFB primer are clear, it is unknown why the efficiency of the ICAM1 primer could not be determined in-house.

In conclusion, it was determined that all primer used fell within the required 90-110% efficiency bracket, and that obtained results would not need correction using the Pfaffl method to be directly compared.

3.4.6 Primer Specificity Assessment

In assessing the specificity of the primers, all bar UBC were seen to generate only a single band on agarose gels, suggesting primer specificity in the positive control samples used for assessing ICAM-1, E-Selectin, VCAM-1, IL-8, MCP-1, ET-1, and PDGFB primers, and in the negative control sample used to assess the TGF-β primer. These experiments were conducted as the sequences of the primers were not all intron-spanning, which may have resulted in gDNA or incorrect transcript amplification when qPCR experiments were run. The group had no control over the primers used, as this work was sponsored by PrimerDesign, and the sequence and Tm of UBC were not made available. However, assurances were made that this primer was intron-spanning, and the No RT and No cDNA samples did not provide a band, so the cause of the additional banding is unknown but appears not to be gDNA contamination and amplification. It is feasible that the melt temperature used during PCR was too low for the UBC primer, resulting in non-specific binding to non-target transcript; when higher melt temperatures (55^o versus 60^o) were

used in both preliminary and later qPCR experiments, raw data showed extremely non-variable C_q values for samples containing the UBC primer (data not shown), and so it was regarded the UBC primer was specific when this higher melt temperature was used. Thus, the UBC primer was used as the reference gene primer in future qPCR experiments.

All primers appeared specific, and this experiment suggested that gDNA contamination was minimal or absent; in all cases apart from VCAM-1 and PDGF-BB, the No RT sample did not generate a band. In these cases, however, the band was very faint, and may be due to primer dimer formation, where primers self-hybridise in the absence of target transcripts, and are amplified by the DNA polymerase. A No RT sample was still run for each sample in each qPCR experiment to further determine whether gDNA contamination was present. No RT samples in each qPCR run remain the gold standard for ensuring no gDNA contamination (Laurell, et al., 2012).

4 Human Umbilical Cord Endothelial Cell Adhesion Molecule Expression and Cytokine Release in Response to Treatment with BLM

4.1 Introduction; Adhesion Molecules in the Pathogenesis of BPF

Crucial to immune cell recruitment to the site of injury is the diapedesis cascade, which depends on the expression of endothelial adhesion molecules, described in chapter 1. As pulmonary infiltration by immune cells is a feature of BPF prior to fibrogenesis, and immune cells are so heavily implicated in the development of the disease, endothelial adhesion molecule expression may well contribute to BPF in both humans and rodents.

Previous reports suggest that BLM treatment upregulates HUVEC E-Selectin expression (Ishii and Takada, 2002; Miyamoto, et al., 2000), and PMVEC ICAM-1 expression (Fichtner, et al., 2004), though the range of adhesion molecules expressed requires better characterisation. Furthermore, Fichtner, et al. (2004) used supra-pharmacological concentrations of over 50μg/ml (100mU/ml), which may result in different adhesion molecule expression profiles to pharmacologically-relevant concentrations. The expression of adhesion molecules by HUVECs in response to BLM of pharmacologically-relevant concentrations will therefore be investigated. A panel of adhesion molecules known to be expressed by HUVECs and/or have a role in diapedesis was chosen – these were PECAM-1, ICAM-3, ICAM-1, $\alpha_V\beta_3$, P-selectin, E-Selectin, VCAM-1, and PSGL-1 – and the effect of various concentrations of BLM over various incubation durations on the expression on these molecules will be assessed.

In this work, BLM and TNF-α increased isotype control binding to HUVECs. In flow cytometry, the isotype control provides a baseline level of non-specific antigen binding so that antigen-positive and antigen-negative cell populations (the latter fluorescent due to non-specific binding) may be differentiated (Keeney, et al., 1998). It also allows the determination of the level of fluorescence on positive cells attributable to non-specific binding. Several factors may cause increased non-specific binding readings, including Fc receptor expression, or simulate increased non-specific binding, such as increased autofluorescence (Hulspas, et al., 2009). Though it has been reported that HUVECs do not express Fc receptors (Zhao, et al., 2011), Pan, et al. (1999) observed expression of CD16, CD32, and CD64 by HUVECs co-treated with TNF-α and IFNγ. Whether BLM and TNF-α induce Fc receptor expression will therefore be assessed.

Endothelial cells may also express cytokines to recruit leukocytes, such as IL-8 and MCP-1, which attract and activate neutrophils and monocytes/macrophages, respectively (Detmers, et al., 1990; Sakanashi, et al., 1994; Mukaida, et al., 1998; Matsushima, et al., 1989; Huber, et al., 1991), and induce directional and transendothelial migration (Schaff, et al., 2008; Weber, et al., 1996; Melgarejo, et al., 2009). These cytokines may be relevant to BPF development; for example, MCP-1 expression by BLM-stimulated endothelia has been associated with inflammatory cell influx in BPF (Okuma, et al., 2004). Therefore, an assessment of the expression of these protein in response to BLM in human cells is also desirable.

Although there have been previous reports of increased IL-8 and MCP-1 release by BLM treated HUVECs (Miyamoto, et al., 2002), this increased release was only noted when cells were treated with 10ng/ml and 50ng/ml BLM, for 12 hours (IL-8) and 48 hours (MCP-1). In man, the majority of BLM would have been metabolised within 48 hours. Whether higher BLM concentrations, such as those used in this work, and shorter incubation times, also affect IL-8 and MCP-1 expression is of interest.

Finally, TGF-β, PDGF, and Endothelin-1 - which induce fibroblast proliferation, transdifferentiation, and collagen synthesis - may be expressed by the endothelium, and may induce fibrogenesis in the interstitium and alveoli if such factors diffuse into the lung. Though not described in man, endothelial TGF-β and CTGF expression in BLM-treated rodents was reported, and suggested to play an important role in the differentiation of interstitial fibroblasts to a fibrotic phenotype (Yin, et al., 2012). This work will therefore also assess the expression latent TGF-β1, PDGF-BB, and Endothelin-1 by BLM-treated HUVECs .

Any alterations in cytokine release and adhesion molecule expression will then be confirmed by qPCR, a method not previously used when assessing BLM-induced cytokine and adhesion molecule upregulation. This will not only confirm previous results at the protein level, but also determine whether BLM regulates the expression and release of inducible proteins, and impacts the increased expression and release of constitutively-expressed proteins, at a transcriptional level. qPCR may also detect increases in transcript that do not correlate with increases in protein, suggesting that transcription, but perhaps

not yet translation and expression, has occurred. This may be of particular use when assessing adhesion molecules such as VCAM-1 and E-Selectin, which require NF-κB activation in response to cytokines to be expressed (Read, et al., 1994; Lewis, et al., 1994; Ahmad, et al., 1998; Iademarco, et al., 1992; Carlos, et al., 1990; Bevilacqua, et al., 1987; Carlos, et al., 1991; Osborn, et al., 1989) and may appear "delayed", and ICAM-1, the increased expression of which is also regulated by NF-κB (Guo, et al., 2012; Ledebur and Parks, 1995).

Moreover, while cytokines such as IL-8 and MCP-1 may be constitutively synthesised and expressed, they may also be synthesised *de novo* in response to NF-κB activation, and immediately expressed, e.g., from the Golgi body (in the case of IL-8) (Lakshminarayanan, et al., 1998; Ping, et al., 2000; Wolff, et al., 1998) or stored in granules for later release via exocytosis (Øynebråten, et al., 2005; Utgaard, et al., 1998; Metcalf, et al., 2008). Therefore, qPCR may also hint at the mechanism of increased cytokine release; transcriptional regulation and direct release, synthesis and storage, or solely exocytosis with BLM acting as the secretagogue, depending on whether both transcript and protein levels increased, or whether one and not the other was increased.

qPCR will be conducted for the adhesion molecules and cytokines whose expression and release was seen to alter as determined by flow cytometry and ELISA, to assess whether increased protein expression is mirrored by increase transcript levels. The transcript levels of cytokines not seen to be released at an increase level in response to BLM will also be assessed, to determine whether synthesis has occurred, but release has not.

4.2 Materials and Methods

4.2.1 HUVEC Adhesion Molecule Expression Determination Following Treatment with BLM

Cells were cultured as outlined in 2.1. To appropriate flasks, 10ml of serum-contaning endothelial cell basal medium contaning various concentrations of BLM – as outlined in 2.6 - was added. Cells were treated with BLM for 6 and 24 hours, as outlined in 2.6. The negative control used was HUVECs incubated in serum-contaning endothelial cell basal medium (10ml) without BLM. The positive control used was HUVECs incubated in endothelial cell basal medium contaning 10ng/ml TNF-α (10ml). Both negative and positive control cells were incubated for the same time as BLM-treated cells (6 or 24 hours, as required). After treatment, cells were dissociated, counted, resuspended to a concentration of 1 x 10^6 cells/ml in endothelial cell medium, and prepared for flow cytometry and analysed as described in section 2.3, 2.4, and 2.5, respectively.

4.2.2 Fc Receptor Expression by HUVECs

HUVECs were cultured as outlined in 2.1. Cells were pre-treated with TNF-α (final concentration 10ng/ml), IFNγ (final concentration 1000U/ml), or cotreated with both cytokines, or treated with various concentrations of BLM as outlined in 2.6. Cells were dissociated and counted as outlined in 2.3 and 2.4. Cells were resuspended to a concentration of 1x10^6, plated as outlined in 2.5 and washed as outlined in 2.5. Cells were then incubated with antibodies against a panel of Fc receptors: CD16, CD32A, CD32B, and CD64.

The antibodies used were as follows:

- Purified mouse IgG1 negative control (Serotec, Oxford, United Kingdom)
- Anti-CD32 antibody [AT10] - Azide free, isotype IgG1 (Abcam, Cambridge, United Kingdom)
- Purified anti-human CD32 (clone IV3), isotype unknown, produced in house.
- Purified mouse anti-human CD16 (clone LNK16), isotype IgG1 (Serotec)

- Purified mouse anti-human CD64 (clone 10.1), isotype IgG1 (Serotec)
- Rabbit F(ab')2 anti-mouse IgG:FITC (Serotec).

For a positive control, Daisy Cells were used. This is a macrophage-like cell line generated in house (Hayman, et al., unpublished data). These cells have previous been shown to be positive for CD16 (Hayman, et al., unpublished data). Daisy cells were cultured in RPMI 1650 (Lonza) supplemented with 10% v/v foetal bovine serum, penicillin (100µg/ml)-streptomycin (100U/ml) (PAA), and L-glutamine (2nM) (Lonza). Daisy cells are both adherent and non-adherent cells. Adherent cells were harvested using a cell scraper and centrifuged and counted as outlined in 2.2 and 2.2.2, respectively.

To assess the binding of immunoglobulin complexes to BLM-treated endothelial cells, HUVECs were cultured, treated with BLM, dissociated, and counted as outlined in 2.1, 2.7, 2.3, and 2.4, respectively. Cells were plated as outlined in 2.5, and coincubated with heat aggregated immunoglobulin G and BXB immunoglobulin complexes. BXB complexes were generated in line with Hart, et al. (2004). In brief, biotinylated bovine serum albumin (500µg) (Sigma Aldrich) was combined with FITC-conjugated anti-biotin monoclonal IgG1 (170µg) (Sigma Aldrich) in PBS (1ml) and incubated on ice for 30 minutes. Concentrations of 300, 100, 30, and 10µg/ml biotinylated BSA were generated by dilution in PBS/0.1% BSA. Heat-aggregated IgG was generated in line with Hart, et al. (2004) by heating FITC-conjugated human IgG (Sigma Aldrich), at concentrations of 100, 30, and 10µg/ml in PBS, for 20 minutes at 63°C. Complexes were stored at 4°C for up to two weeks until required. BLM-treated cells were incubated with these complexes on ice for 30 minutes prior to binding assessment by flow cytometry. Data were analysed using Mann-Whitney-U tests in SPSS v. 19 statistical analysis software.

4.2.3 HUVEC Cytokine Release Determination in Response to BLM Treatment

Cells were cultured as outlined in 2.1 and replated as outlined in 2.7. When adherent, 3ml of serum-containing endothelial cell basal medium containing 0.1µg/ml, 1µg/ml, or 10µg/ml BLM, was added. Cells were treated with BLM for 6 and 24 hours. Positive and negative control supernatants were generated as outlined in section 2.7. The

supernatants were then collected as outlined in 2.7 and used for cytokine ELISAs. The ELISA kits used were as outlined in 2.8. Supernatants for ELISAs were treated as outlined in 2.8. Preliminary work for each ELISA was conducted as outlined in 2.8, and all ELISA were carried out in accordance with the manufacturer's instructions

Plates were read using a plate-reader (Thermo Multiskan FC, Thermo Scientific) at the wavelengths instructed by the instructions provided with the kits. For IL-8, MCP-1, TGF-β1, and ET-1, this was an initial reading at 450nm and a subsequent reading at 570nm, the second subtracted from the first to reduce background. For the PDGF-BB ELISA, a single 450nm measurement was required. Standard curves and data analysis was carried out as outlined in 2.8.

4.2.4 Performance of qPCR Experiments and Data Handling

qPCR samples (cDNA samples and No RT samples) were prepared as outlined in (section 2.9) and Mastermix was prepared as outlined in section 3.2.7. This Mastermix contained either primers for the appropriate target gene or for the reference gene. To 24 wells of a 48-well plastic qPCR plate, Mastermix (15µl) contaning the target gene primer was added, and to 24 wells, Mastermix (15µl) contaning the reference gene primer was added. To each well, cDNA (5µl diluted cDNA at a concentration of 0.5ng/µl) from appropriate samples was added. All samples were run in triplicate for both target gene and reference gene (i.e., sample A was present in three wells containing the target gene primer, and three wells containing the reference gene primer). No cDNA samples were also run in this way. No cDNA samples used RNAse/DNAse free water (5µl) in lieu of diluted cDNA sample, and therefore contained no template. No RT samples were run for each primer-sample combination (i.e. Sample A plus target gene, Sample A plus reference gene, Sample B plus target gene, and so on). Two plates were required for one full experiment (one cell batch treated with all concentrations of BLM for 6 and 24 hours, plus No RT and No cDNA controls).

The qPCR was then run using the Illumina ECO qPCR machine (Illumina, Little Chesterton, Essex, UK). The qPCR plate was subject to 10 minutes at 95^{o}C for polymerase activation;

40 cycles of PCR comprising 15 seconds at 95^{o}C and 60 seconds at 60^{o}C, and a melt curve period for which the plate was heated to 95^{o}C for 15 seconds, 55^{o}C for 15 seconds, and again 95^{o}C for 15 seconds. The results were then exported as an Excel file.

4.2.5 qPCR Data Analysis

Initial data analysis was carried out manually. The qPCR analysis programme (Eco, version 5.0.16.0, Illumina) analysed all qPCR experiments and determined the C_q value of each sample based on a threshold of 0.02 units of fluorescence. Derviative melt curves were analysed for each reaction in a plate to identify outliers and erroneous results. Results stemming from the formation of primer dimers were identified by the low melt temperature and the broad-based peak as shown on the derivative melt plot displayed by the Eco software (Fig 4.1). These results were often higher or lower in C_q value obtained than other wells which contained the same sample (Fig. 4.2). All potential primer dimers were identified using both the derivative melt and the amplification plots. Such results were excluded from analysis.

If more than one result in each triplicate failed, or was a primer dimer, this sample was re-run in triplicate. Samples where one of the three replicates was a primer dimer or failed, but the other two represented true readings, contained sufficient relibable information from which to obtain a mean C_q value for this sample. Each set of results was also assessed for the presence of genomic DNA, denoted by a higher than expected melt temperature (>90^{o}C). This was not expected, as the agarose gel experiments showed no genomic DNA in the samples.

No RT samples and No cDNA controls were also assessed to ensure gDNA contamination had not occurred. Where values were obtained for either sample, it was determined whether this was the result of primer dimer formation. Where this was the case, these values were discarded, and the sample treated as though no value was obtained. These No RT and No cDNA results, as well as those that failed to obtain a C_q value, were regarded as zero. All no cDNA and no RT sample results were plotted on final results graphs.

Analysis of results was conducted using Microsoft Excel. A calculator was created in-house using Microsoft Excel to conduct Livak ($\Delta\Delta C_q$) calculations to determine the fold change in mRNA content in each test (treated) sample as compared to its respective calibrator (untreated) sample. Repeated-measures ANOVA statistical analyses were then carried out on the ΔC_T values obtained for each sample using the GraphPad InStat3 programme (version 3.00, GraphPad Software).

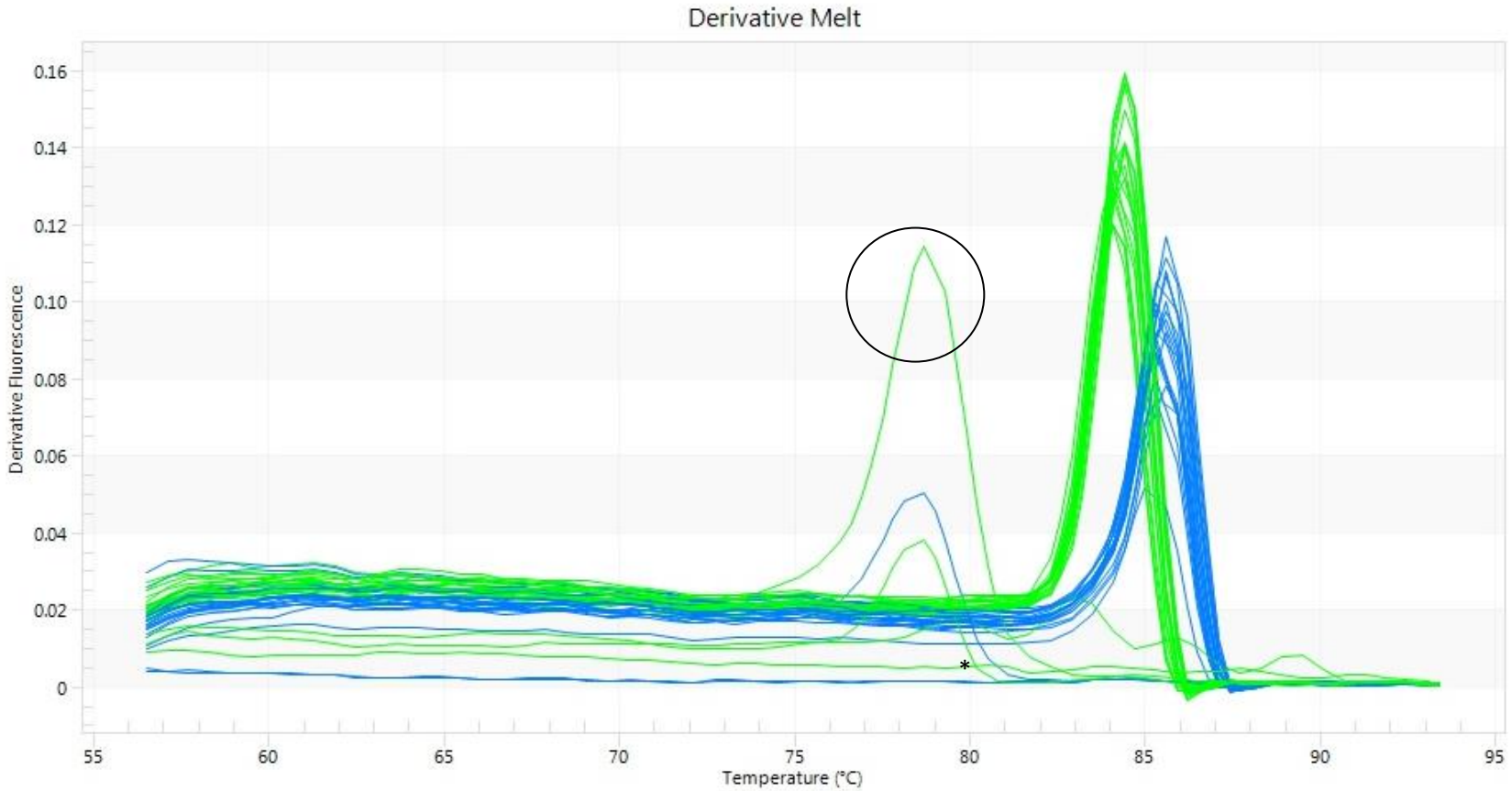

Figure 4.1: Example derivate melt curve from qPCR experiments showing primer dimer formation.

An example derivative melt curve showing the derivative melt for a primer dimer (circled). Note the lower melt temperature and a wider-based peak than genuine results (seen at melt temperature of around 81-86^{o}C). Such primer dimers will give erroneous results. No derivative melt peak (denoted by the asterisk) represents a failed reaction. These appear on derivative melt graphs as flat lines.

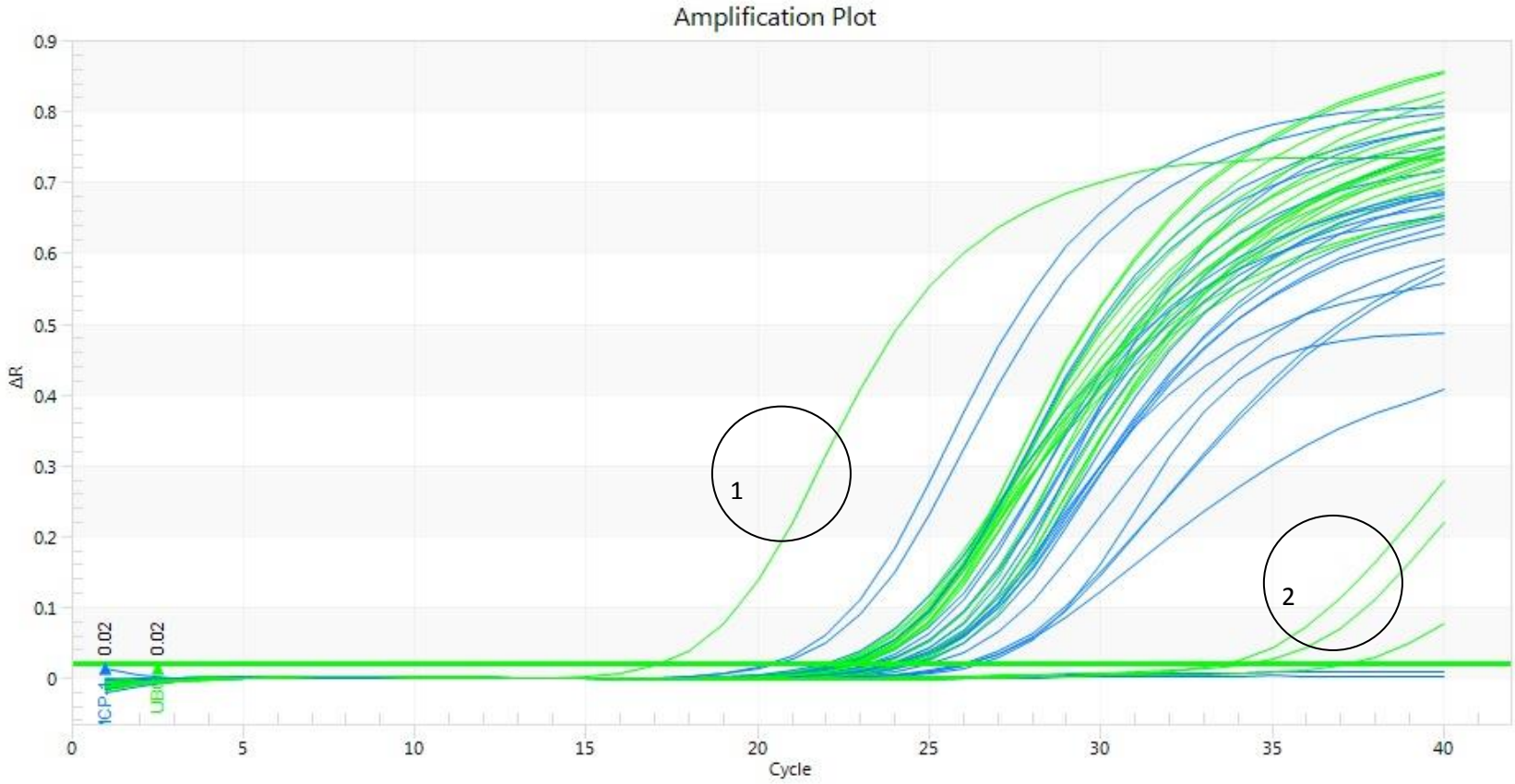

Figure 4.2: An example amplification plot from qPCR experiments showing primer dimer formation.

An amplification plot showing primer dimer formation (1, 2), characterised by a C_q value that is higher or lower than genuine results. In this graph, genuine results have a C_q value between 20 and 30 cycles. Each primer will have a different standard C_q value. Here, for UBC (green lines) this is between 22 and 24; for MCP-1 (blue lines), between 20 and 26, though this will differ based on the abundance of the target transcript. Any results that appear to have a C_q value of greater than 35 are likely to be the result of a primer dimer

4.3 Results

4.3.1 Adhesion Molecule Protein and mRNA Expression Following 6 Hour BLM Incubation

The expression of ICAM-1, E-selectin, and VCAM-1 was increased from baseline following treatment with BLM for 6 and 24 hours. Example raw data obtained for this experiment is shown in Figure 4.3.Raw data is shown with a gate applied to highlight the peak-shift and increase in ICAM-1 positive cells when cells were treated with BLM. Note that correction using gating was NOT used to determine expression (expression was determined using uncorrected data and plotted on graphs as outlined in section 2.5).

4.3.1.1 ICAM-1 Expression in Response to BLM

Though the expression of ICAM-1 protein increased in cells treated with BLM for 6 hours compared to baseline, (Figure 4.4A), this was not significant. qPCR confirmed a slight increase in ICAM-1 mRNA transcript levels in HUVECs treated with 10µg/ml BLM for 6 hours (Fig 4.4C), though again, this was not significant under any treatment condition. In this case, the fold-change observed in ICAM-1 transcript levels broadly reflected the increases in protein expression observed - a 2-fold increase in transcript and a 1.5-fold increase in protein.

The expression of ICAM-1 protein was significantly greater (*p=0.05*) in cells treated with 10µg/ml BLM for 24 hours, compared to untreated cells (Figure 4.4B). When assessed by qPCR, there was a significant increase in ICAM-1 transcript levels in samples treated with 1µg/ml, and 10µg/ml BLM (Fig 4.4D), which reflects earlier results obtained by flow cytometry, though in the flow cytometric results, only cells treated with concentrations of 10µg/ml BLM showed a significant increase in ICAM-1 expression. The fold change observed by qPCR when assessing cells treated with 1 and 10µg/ml was, however, broadly similar to the magnitude of protein expression increase observed, with a 3-fold increase in protein expression matching a 2.5-fold increase in transcript levels.

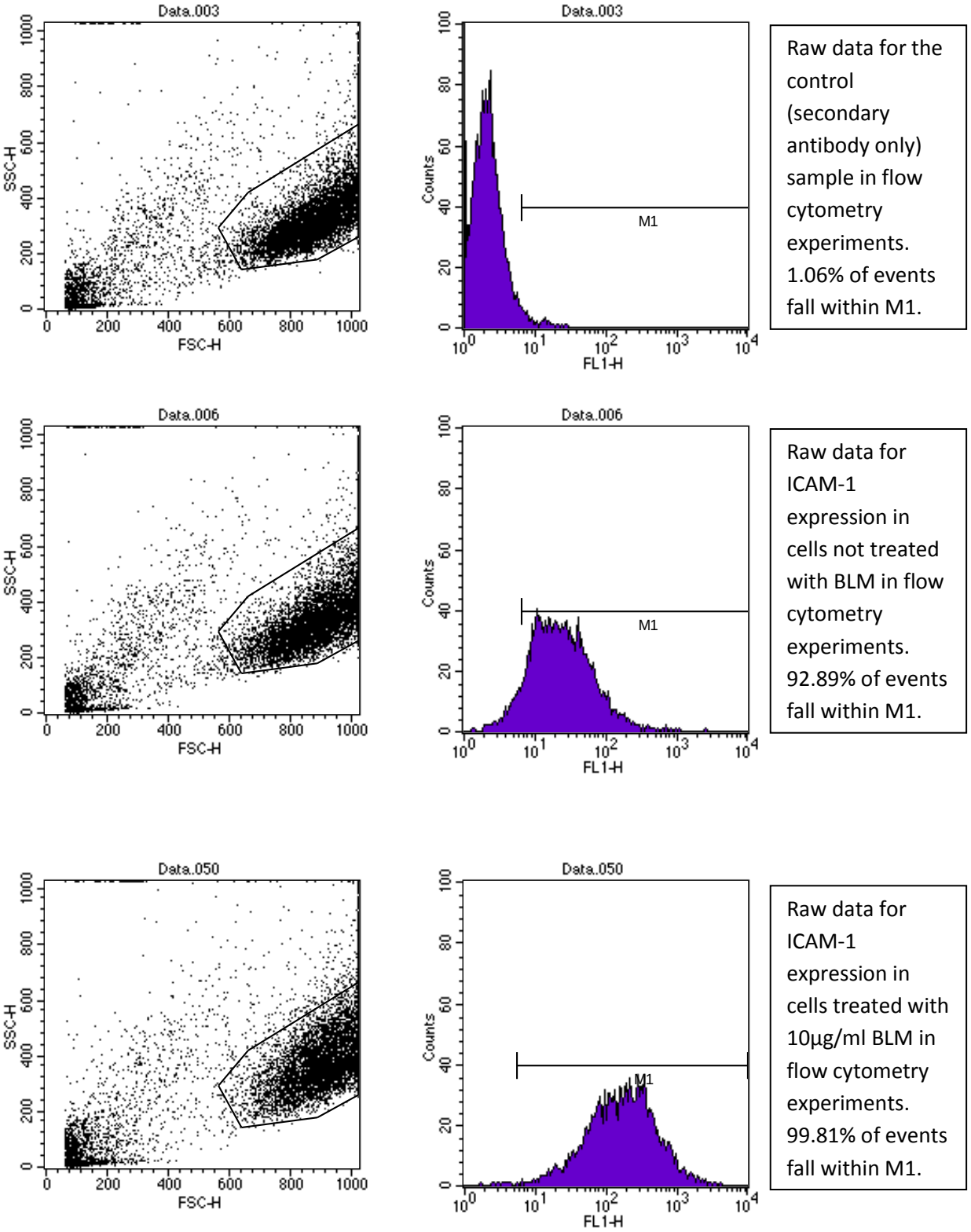

Figure 4.3: Raw data from flow cytometry experiments assessing adhesion molecule expression (ICAM-1) by BLM-treated HUVECs.

Raw data generated from flow cytometric analysis of control (secondary antibody only) samples of HUVECs (top), ICAM-1 expression by untreated HUVECs (middle) and HUVECs treated with 10µg/ml BLM for 24 hours (bottom). Gate M1 was drawn to incorporate 1% of the control peak. There was a notable peak shift from baseline ICAM-1 expression when cells were treated with BLM. Respresentative images of three experiments.

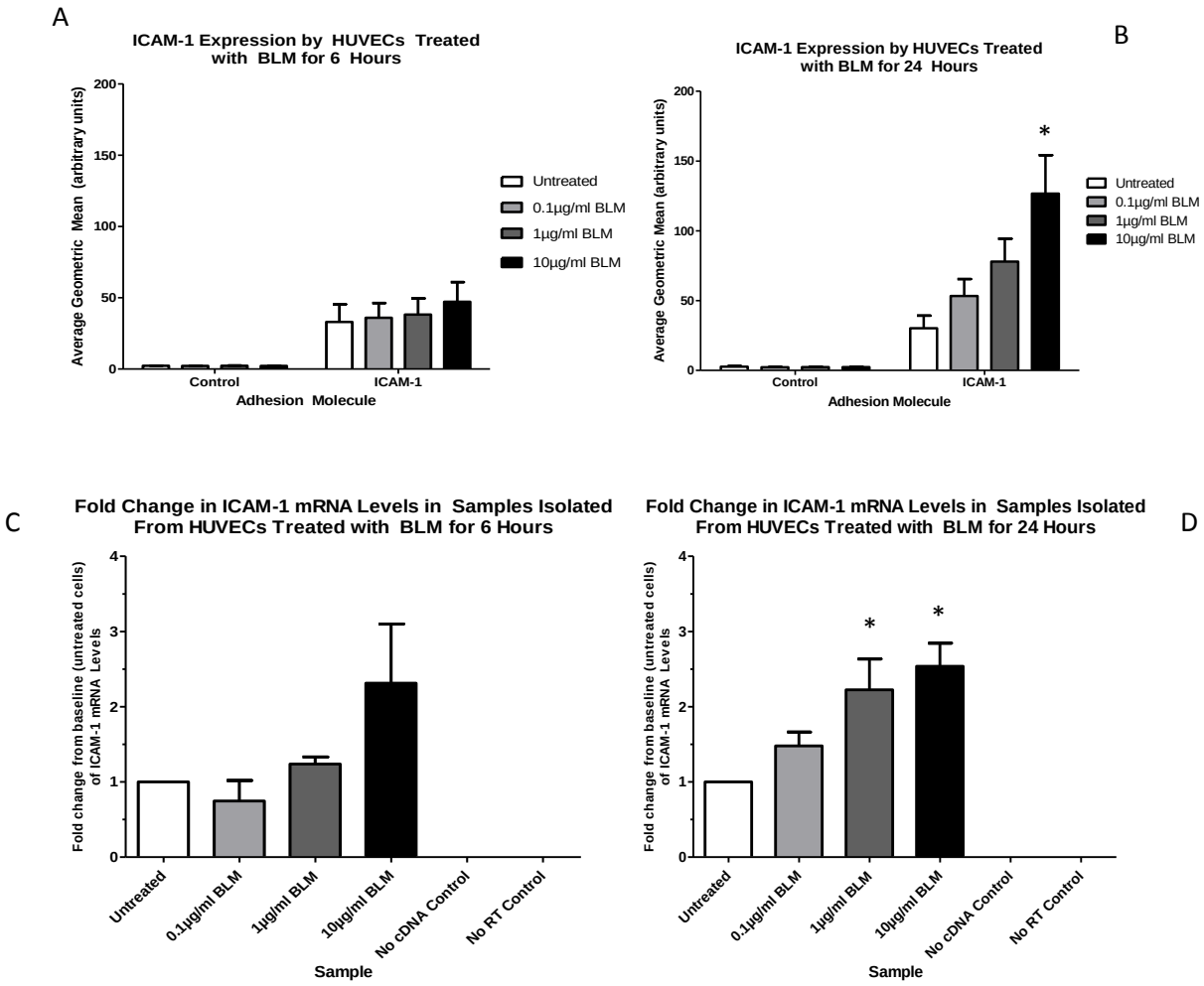

Figure 4.4: ICAM-1 expression by BLM-treated HUVECs determined by flow cytometry and qPCR.

The expression of ICAM-1 by HUVECs treated with BLM for 6 (A) and 24 (B) hours as determined by flow cytometry, and the fold-change in ICAM-1 transcript levels in cells treated with BLM for 6 (C) and 24 (D) hours as determined by qPCR. Statistical analysis of qPCR results was conducted using repeated-measures ANOVA (as outlined in section 4.2.5). Statistically significant increases in protein or transcript levels from baseline (*p=0.05*) are denoted by asterisks. *N=3.*

4.3.1.2 E-Selectin and VCAM-1 Expression in Response to BLM

The expression of E-Selectin protein was significantly different from baseline (untreated cells) in cells treated with 10µg/ ml BLM for 6 hours (Figure 4.6A). The qPCR results demonstrate a significant increase in E-Selectin mRNA levels in cells treated with 1µg/ml BLM and 10µg/ml BLM (Figure 4.6E). Though the increase in E-Selectin mRNA levels in cells treated with 10µg/ml BLM reflects the increase in E-Selectin protein expression, increased protein expression by cells treated with 1µg/ml BLM was not observed, and the magnitude of the increases in transcript levels is higher than increases in protein expression - a 17-fold increase was observed in transcript levels, but only a 2-fold increase in protein expression levels was noted.

The expression of VCAM-1 protein was significantly different from baseline in cells treated with 10µg/ ml BLM for 6 hours (Figure 4.6A). There was also a large increase in VCAM-1 transcript levels in cells treated with 10µg/ml BLM (Figure 4.6C), and again, this was of a greater magnitude than the increase in protein expression; an 8-fold increase in transcript levels was observed, compared to a 1.5-fold increase in protein expression levels. Therefore, when cells are treated with BLM for 6 hours, the fold-change in transcript levels is proportionally greater than the increase in E-Selectin and VCAM-1 protein expression levels.

The expression of E-Selectin was significantly greater ($p=0.05$) in cells treated with all concentrations of BLM for 24 hours than at baseline (Figure 4.6B). The results from qPCR experiments mirrored this. E-Selectin mRNA levels following treatment of cells with BLM for 24 hours closely resemble the increases in E-Selectin protein expression in previous experiments (Figure 4.6F). In all cases, there was a statistically significant increase in the level of mRNA in cells treated with BLM.

There was a noticeable increase in the expression of VCAM-1 also, but this was not statistically significant (Figure 4.4B). There was also a slight increase in VCAM-1 transcript levels in cells treated with all three concentrations of BLM for 24 hours (Figure 4.6D), though none of these increases were significant, much like the flow cytometric analyses, and the standard error of the mean in this case is high. This is due to one set of results from a single cell line in which the VCAM-1 mRNA levels in the cells treated with 10µg/ml

BLM was low. However, the fold changes in transcript levels in this experiment closely mirror the increases in protein expression observed.

Raw data obtained from flow cytometry experiments assessing VCAM-1 expression in cells treated with BLM is shown in Figure 4.5. Raw data is shown with a gate applied only to highlight the peak-shift and increase in VCAM-1 positive cells when cells were treated with BLM. Note that correction using gating was NOT used to determine expression (expression was determined using uncorrected data and plotted on graphs as outlined in section 2.5).

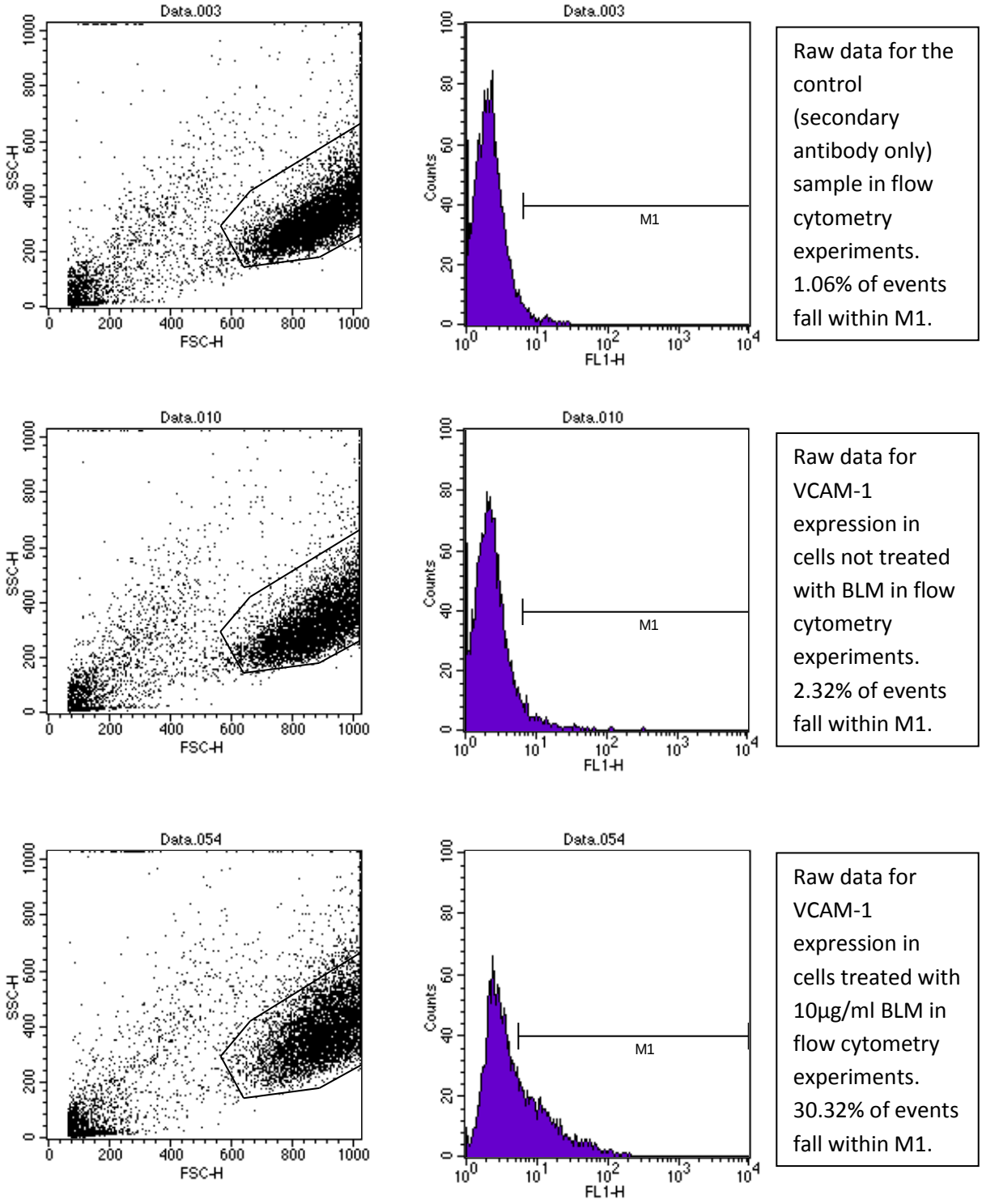

Figure 4.5: Raw data from flow cytometry experiments assessing adhesion molecule expression (VCAM-1) by BLM-treated HUVECs.

Raw data generated from flow cytometric analysis of control (secondary antibody only) samples of HUVECs (top), VCAM-1 expression by untreated HUVECs (middle) and HUVECs treated with 10 µg/ml BLM for 24 hours (bottom). Gate M1 was drawn to incorporate 1% of the control peak. There was a peak shift from baseline VCAM-1 expression when cells were treated with BLM, as around 30% of cell appeared to express VCAM-1 in response to BLM, but the majority of cells still expressed essentially zero VCAM-1, as shown by the population outside the gate (M1) on the bottom histogram. Respresentative images of 3 experiments.

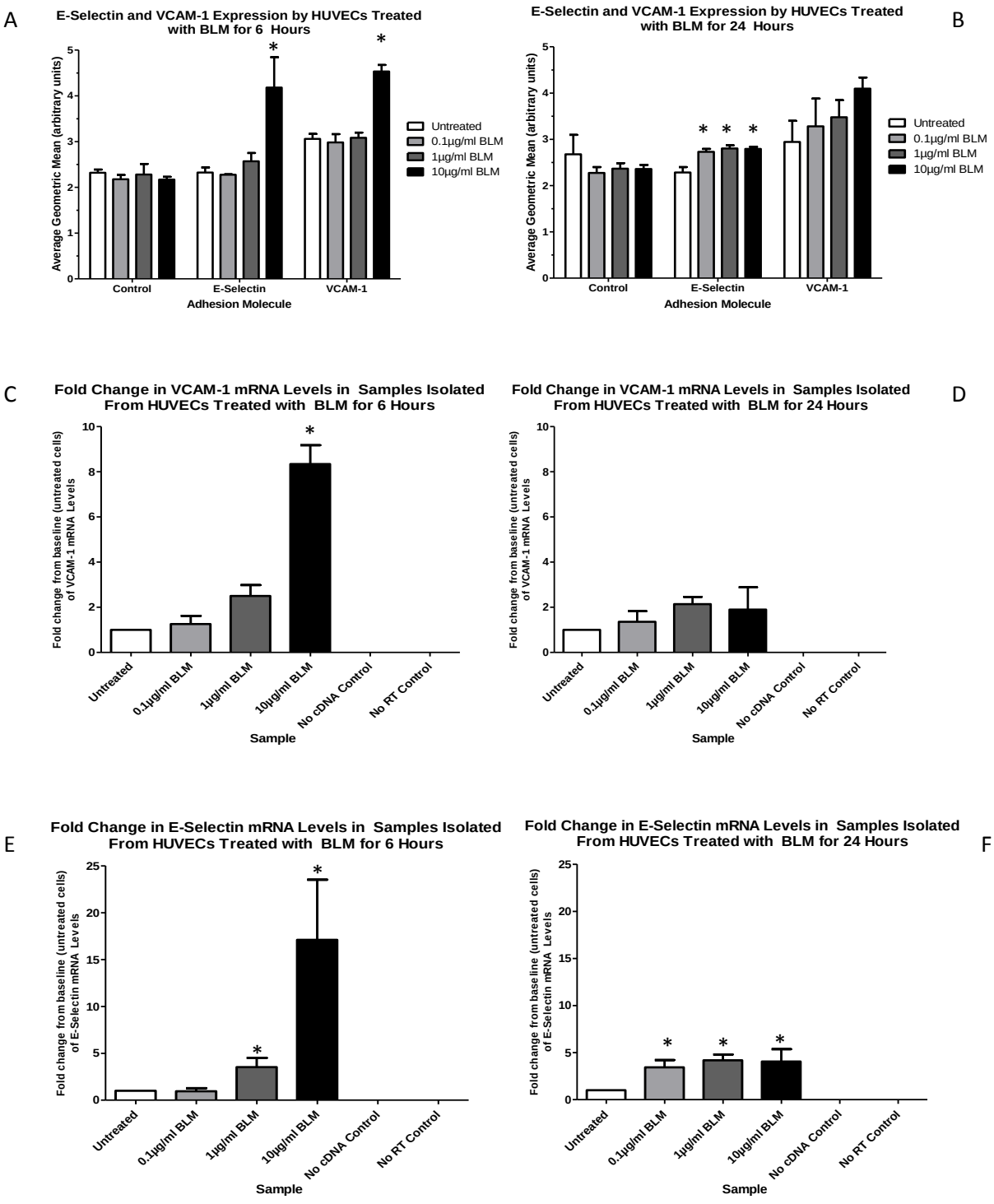

Figure 4.6: VCAM-1 and E-selectin expression by BLM-treated HUVECs as assessed by flow cytometry and qPCR.

The expression of E-Selectin and VCAM-1 by HUVECs treated with BLM for 6 (A) and 24 (B) hours as determined by flow cytometry, the fold-change in VCAM-1 transcript levels in cells treated with BLM for 6 (C) and 24 (D) hours, and the fold-change in E-selectin transcript levels in cells treated with BLM for 6 (E) and 24 (F) hours as determined by qPCR. Statistical analysis of qPCR results was conducted using repeated-measures ANOVA (as outlined in section 4.2.5). Statistically significant increases in protein and transcript levels from baseline are denoted by asterisks (*p=0.05*). *n=3.*

4.3.2 Fc Receptor Expression by HUVECs

In the first round of experiments using BLM to treat the HUVECs and TNF-α as a positive control, and experiments using TNF-α to determine the ideal positive control mediator to use, the binding of the isotype control was increased by treatment with both substances (Fig. 4.7). This was also noted when HUVECs were treated with IFN-γ and LPS in earlier work (Table A.1). As HUVECs did not demonstrate increased autofluorescence in response to TNF-α or BLM (which would simulate increase non-specific isotype control binding) (Fig. 4.7), if Fc receptor expression was occurring due to treatment was assessed.

A

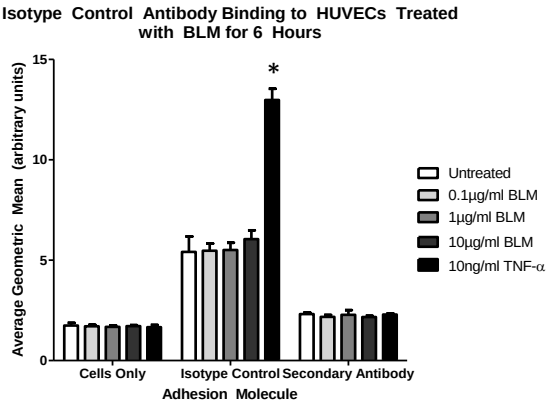

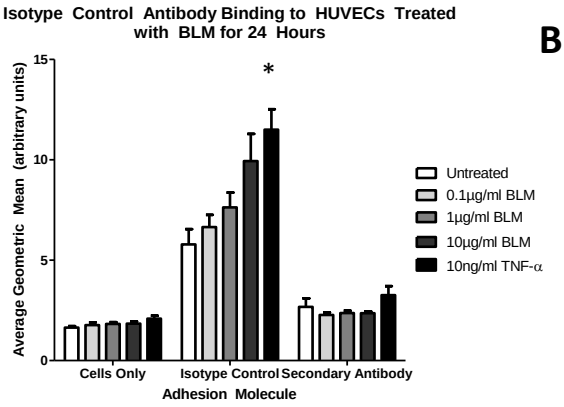

B

Figure 4.7: Isotype control binding to HUVECs treated with BLM and TNF-α.
Isotype control binding to BLM and TNF-α treated HUVECs. Treatment with increasing concentrations of BLM increased non-specific binding, as did treatment with TNF-α. Statistically significant increases in isotype control binding compared to baseline (*p=0.05*) are denoted by an asterisk. *n=3.*

It was initially assessed whether Fc receptor expression could be induced by treatment of HUVECs with 10ng/ml TNF-α, 1000U/ml IFN-γ, or co-treatment with both cytokines, as in work by Pan, et al. (1999). However, no Fc receptor expression was observed (data not shown). Similarly, treatment with BLM of various concentrations did not induce the expression of CD16, CD32, or CD64 by HUVECs over 6 hour treatment times, though this treatment did increase the non-specific binding of the isotype control to the cells. While there appeared to be statistically significant increases in the expression of Fc receptors by HUVECs treated with BLM for 24 hours, these increases mirror the slight increases in binding of the secondary antibody to the cells, and likely represent an artifact (Fig 4.8).

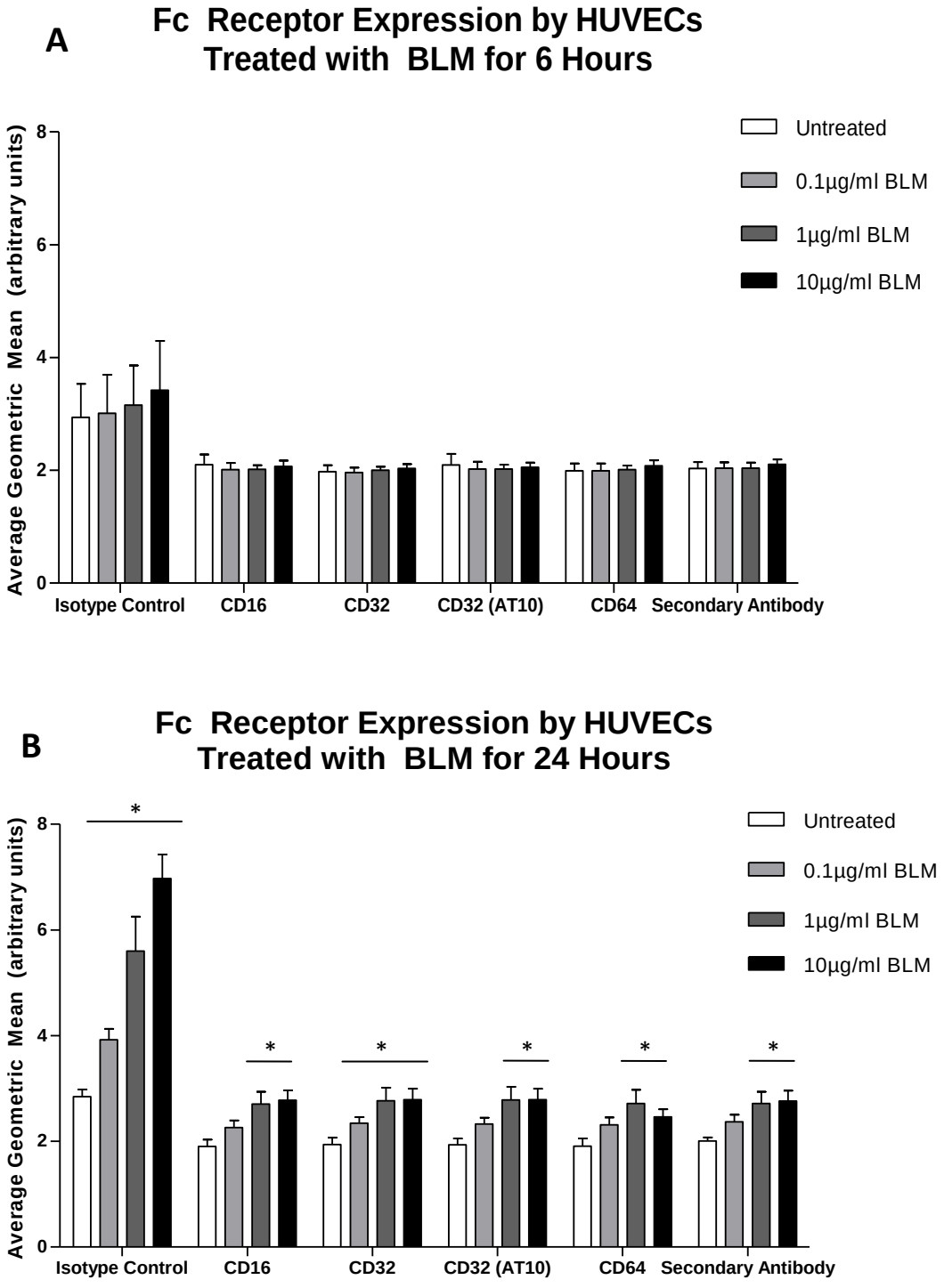

Figure 4.8: Fc receptor expression by HUVECs treated with BLM

Fc receptor expression by HUVECs treated with various concentrations of BLM for 6 (A) and 24 (B) hours. Non-specific binding of the isotype control increased with BLM treatment, and though Fc receptor expression appears to increase compared to baseline, these increases mirror the binding of the secondary antibody to cells and therefore likely represent an artefact.

To further determine whether BLM treatment was increasing Fc receptor expression, the binding of heat-aggregated IgG1, non-aggregated IgG1, and BXBs (IgG1 complexes) to BLM-treated HUVECs was also assessed. As shown in Fig. 4.9-4.11, there appeared to be a slight but significant increase in the binding of non- and heat-aggregated IgG1 and BXBs to BLM- and TNF-α-treated HUVECs, though again, this mirrored the increased binding of the isotype control antibody, and the slight increase in the autofluorescence of the cells alone. It may therefore be said that the increased binding observed when cells were treated with BLM and TNF-α was an artifact, and that Fc receptor expression was not increased by treatment with BLM of any concentration, or with TNF-α.

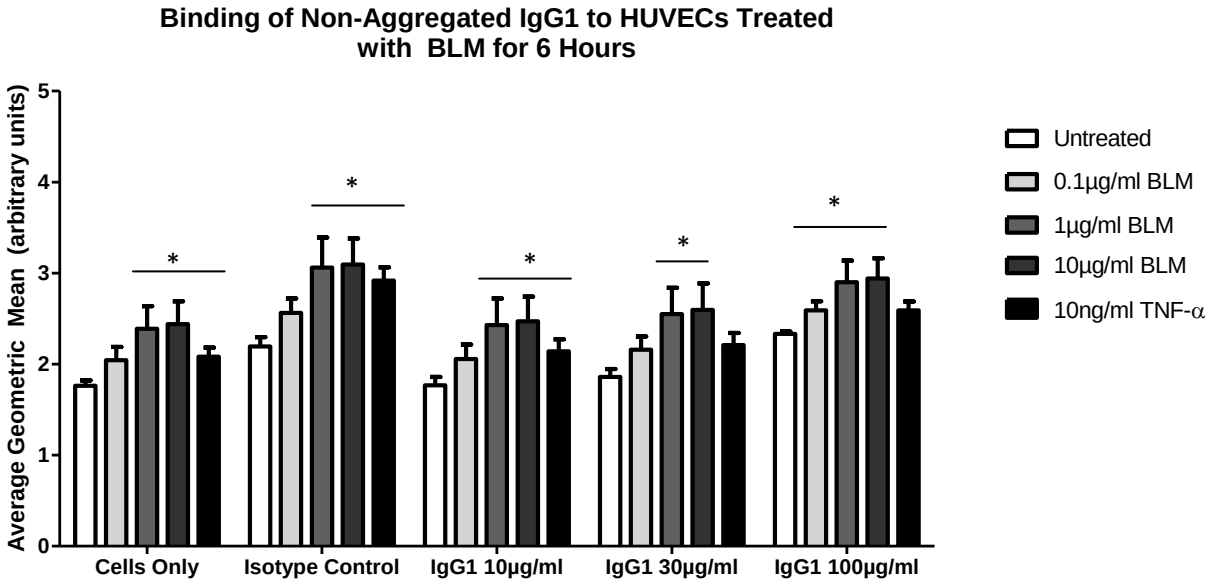

Figure 4.9: Non-aggregated IgG binding to HUVECs treated with BLM

The binding of non-aggregated IgG1 to BLM-treated HUVECs. While IgG1 binding appears to increase compared to baseline, and some of these increases are statistically significant (denoted by asterisks), these increases mirror the increases in cell autofluorescence and likely represent an artefact.

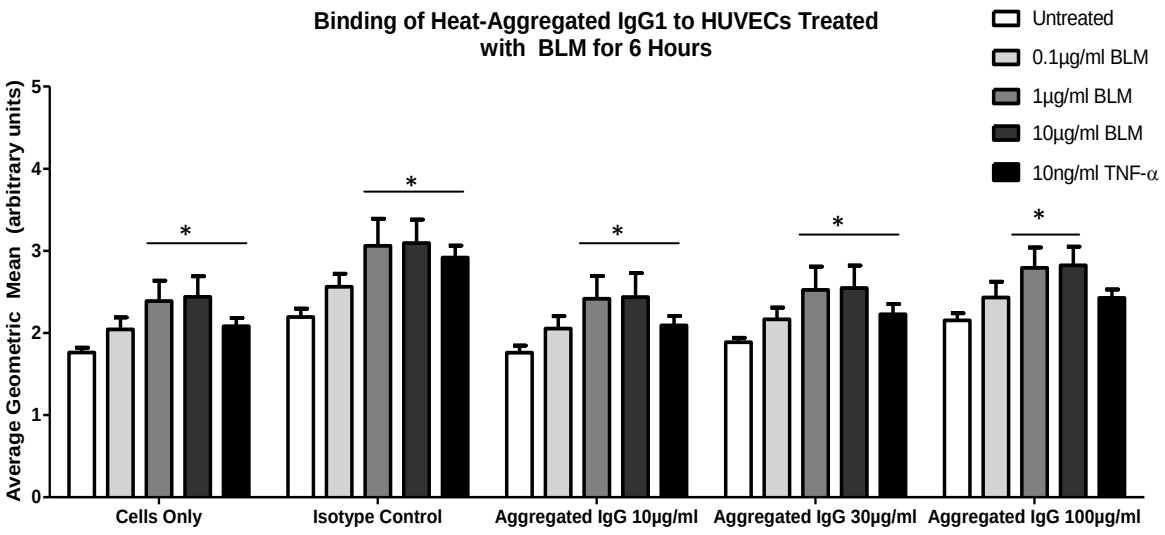

Figure 4.10: Heat-aggregated IgG binding to HUVECs treated with BLM

The binding of heat-aggregated IgG1 to BLM-treated HUVECs. While IgG1 binding appears to increase compared to baseline, and some of these increases are statistically significant (denoted by asterisks), these increases mirror the increases in cell autofluorescence and likely represent an artefact.

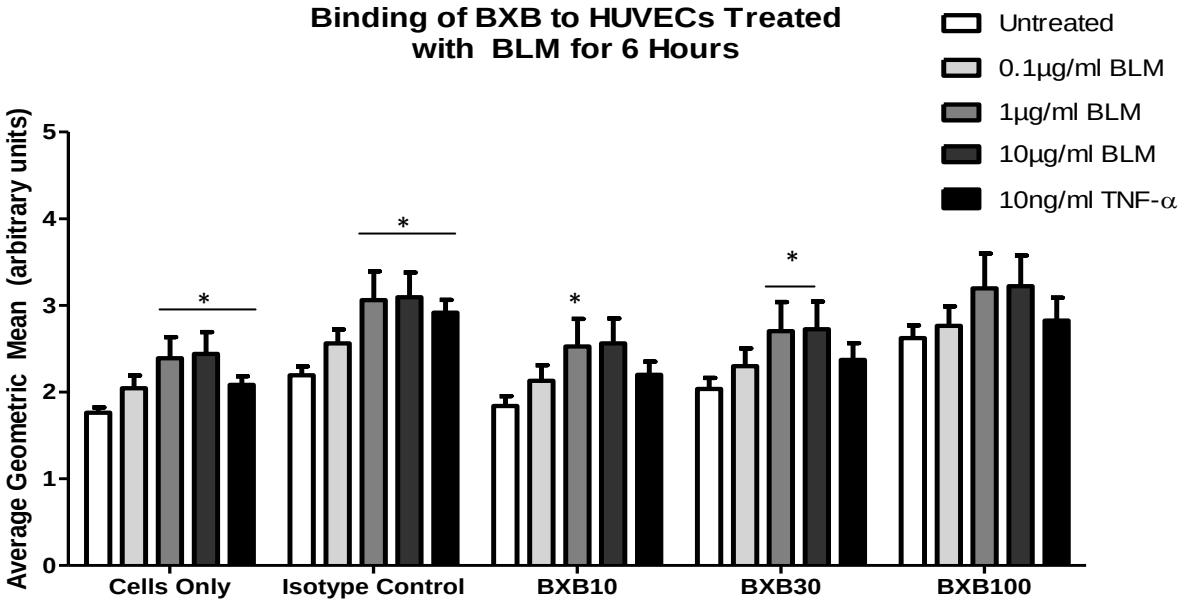

Figure 4.11: BXB binding to HUVECs treated with BLM

The binding of immune complexes (BXBs) to BLM-treated HUVECs. While IgG1 binding appears to increase compared to baseline, and some of these increases are statistically significant (denoted by asterisks), these increases mirror the increases in cell autofluorescence and likely represent an artefact.

As no reason for increased isotype control binding was evident, the batch of isotype control used was altered. However, changing the batch or type of isotype control did not appear to ameliorate the non-specific binding observed. However, when assessing the secondary antibody alone for potential use as a control antibody, is it evident that the binding of the secondary antibody to assessed cells did not appear to be impacted as dramatically by treatment of HUVECs with TNF-α or BLM, as shown in Figure 4.7. Therefore, the secondary antibody alone control sample was used as the "control" sample in all experiments.

4.3.3 Pro-Inflammatory Cytokine Release by HUVECs Treated with Bleomycin

There was an increase in the release of IL-8 by HUVECs treated with all concentrations of BLM over 24 hours, though only when cells were treated with 10µg/ml BLM was this increase significant. Increases were seen only in cells treated with 1µg/ml and 10µg/ml BLM over six hours (and only cells treated with 10µg/ml BLM exhibited a statistically significant increase). Cells treated with 0.1µg/ml BLM over six hours exhibited significantly decreased release (Figure 4.12A). When MCP-1 release by BLM-treated HUVECs was assessed (Figure 4.13A), release was noticeably increased in response to 1µg/ml and 10µg/ml BLM over six hours, though over 24 hours, only cells treated with 10µg/ml BLM showed a large increase in MCP-1 release. There were no statistically significant changes in MCP-1 expression when cells were treated with BLM compared to controls.

The qPCR results obtained for IL-8 are roughly analogous to those obtained in the previous ELISA experiments which showed a slight decrease in IL-8 protein release in cells treated with 0.1µg/ml BLM compared to baseline, and an increase in IL-8 release by cells treated with 10µg/ml BLM compared to baseline, when cells were treated with BLM for 6 hours (Figure 4.12B). However, the increases shown by qPCR were not significant, unlike those seen using ELISA. The increases in transcript levels when cells were treated with BLM for 24 hours were very similar to the increase seen in protein expression, but again, the increase in transcript levels was not significant, while the increase in IL-8 release by cells was, when cells were treated with 10µg/ml BLM (Figure 4.12C). Overall, the increases in transcript levels as determined by qPCR were similar to protein levels detected by ELISA; there was a slight concentration-dependent increase in IL-8 mRNA levels, and this is of roughly the same magnitude as the results of the ELISA would suggest.

Results from qPCR experiments assessing MCP-1 transcript levels did not correlate strongly with those obtained by ELISA. When cells were treated with BLM for 6 hours, there was a statistically significant increase in the levels of MCP-1 mRNA in cells treated with 10µg/ml BLM compared to baseline (Figure 4.13B). This was not reflective of ELISA results, in which there was a slight, but non-significant, increase in MCP-1 release when

cells were treated with BLM for 6 hours (Figure 4.13A). Moreover, when cells were treated for 24 hours, there was only a slight increase in MCP-1 transcript levels above baseline in all BLM-treated samples (Figure 4.13C), while the release of MCP-1 as determined by ELISA was far more substantial, with the increase in MCP-1 release by cells treated with 10µg/ml BLM being far higher than baseline (Figure 4.13A). The results from cells treated with BLM for 24 hours in fact more closely resemble those obtained by ELISA from cells treated with BLM for 6 hours.

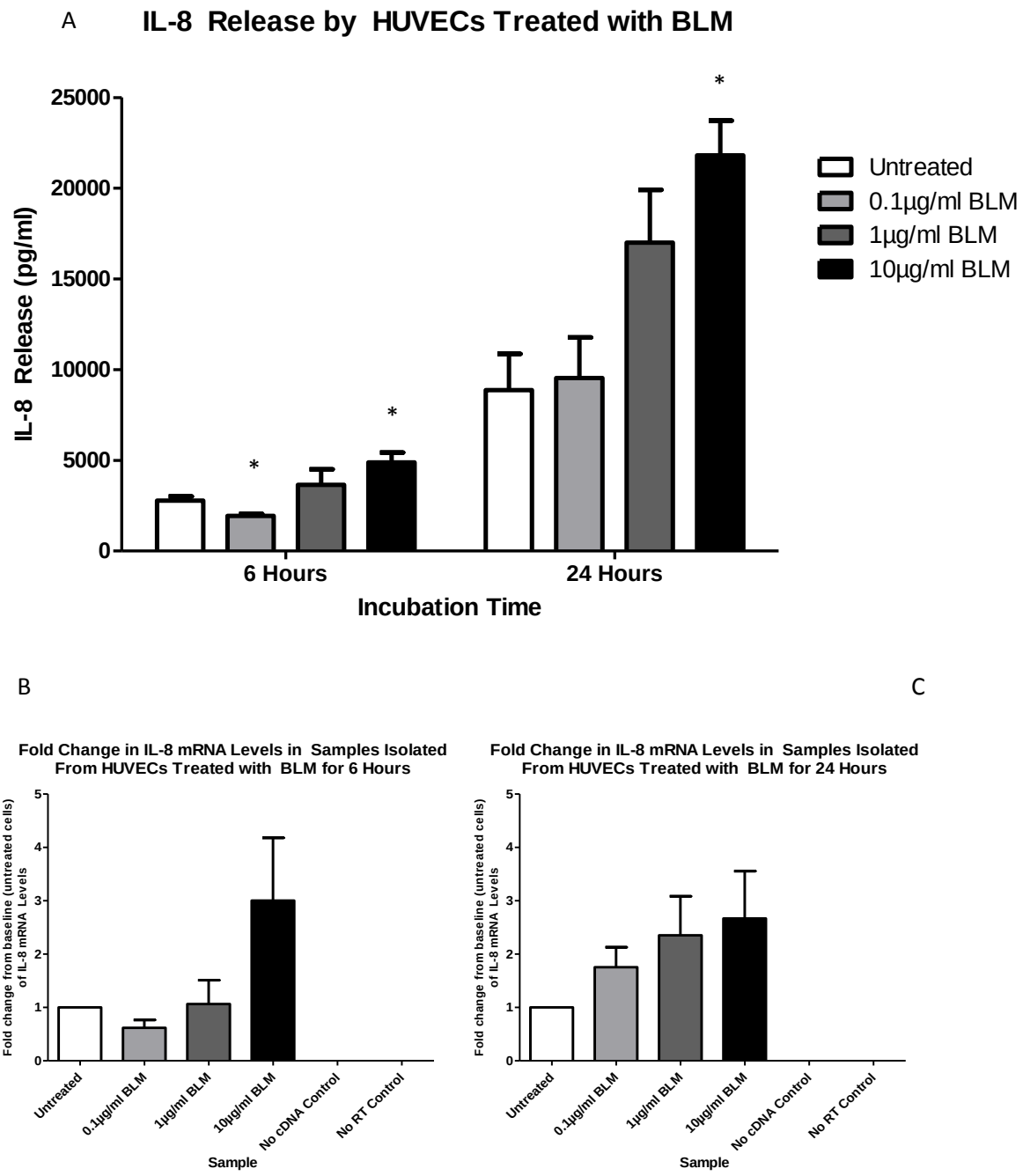

Figure 4.12: IL-8 release by BLM-treated HUVECs and IL-8 transcript expression levels in BLM-treated HUVECs assessed by ELISA and qPCR.

The release of IL-8 by HUVECs treated with BLM for 6 and 24 hours (A) as determined by ELISA and the fold-change in IL-8 transcript levels in cells treated with BLM for 6 (B) and 24 (C) hours. Statistical analysis of qPCR results was conducted using repeated-measures ANOVA (as outlined in section 4.2.5). Statistically significant increases in protein and transcript levels from baseline are denoted by asterisks (*p=0.05*). *n=3.*

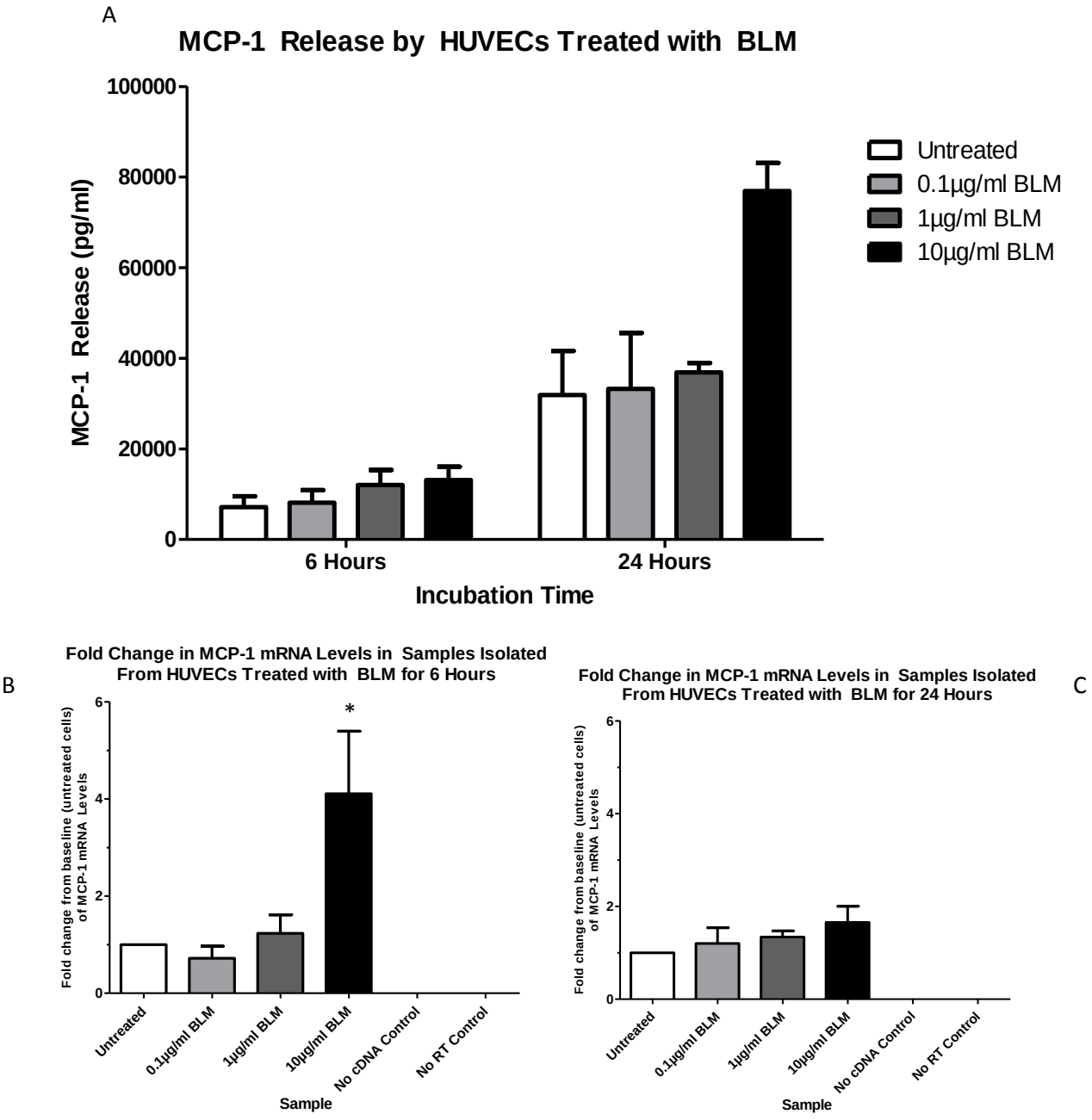

Figure 4.13: MCP-1 release by BLM-treated HUVECs and MCP-1 transcript expression by BLM-treated HUVECs as assessed by ELISA and qPCR.

The release of MCP-1 by HUVECs treated with BLM for 6 and 24 hours (A) as determined by ELISA, and the fold-change in MCP-1 transcript levels in cells treated with BLM for 6 (B) and 24 (C) hours. Statistical analysis of qPCR results was conducted using repeated-measures ANOVA (as outlined in section 4.2.5). Statistically significant increases in protein and transcript levels from baseline are denoted by asterisks (*p=0.05*). *n=3.*

4.3.4 Pro-fibrotic Cytokine Expression by HUVECs Treated with Bleomycin

Cells treated with BLM did not show any increase in the level of TGF-β released under any treatment condition (Figure 4.14A). This was mirrored by qPCR results which showed no increase in trascript levels when cells were treated with BLM for 24 hours (Figure 4.14B). The expression of PDGF-BB decreased in response to BLM treatment over 6 hours, though this was not statistically significant. PDGF-BB expression by BLM treated HUVECs was not impacted by treatment with any concentration of BLM over 24 hours (Fig. 4.14C). Again, this was mirrored by qPCR results (Figure 4.14D).

The expression of Endothelin-1, a profibrotic and potentially vasoconstrictive cytokine, was impacted by cell treatment with BLM, however. Increases in expression were noted when cells were treated with 1µg/ml and 0.1µg/ml BLM over six and 24 hours, respectively (Figure 4.15A), though neither increase was statistically significant (*p=0.05*) . However, the standard error of the mean was high as these samples showed a large difference in expression between cell lines. There does appear to be a trend towards endothelin-1 expression decreasing when exposed to high concentrations of BLM, however, though this was not significant (Figure 4.15A). However, this decrease is confirmed by qPCR results, in which treatment of HUVECs with 10µg/ml BLM for 24 hours greatly decreased the levels of ET-1 mRNA (though not significant again) (Figure 4.15B), and when cells were treated with 0.1µg/ml BLM, the increase in Endothelin-1 release at a protein level does mirror the slight increase in Endothelin-1 mRNA levels (Figure 4.15B).

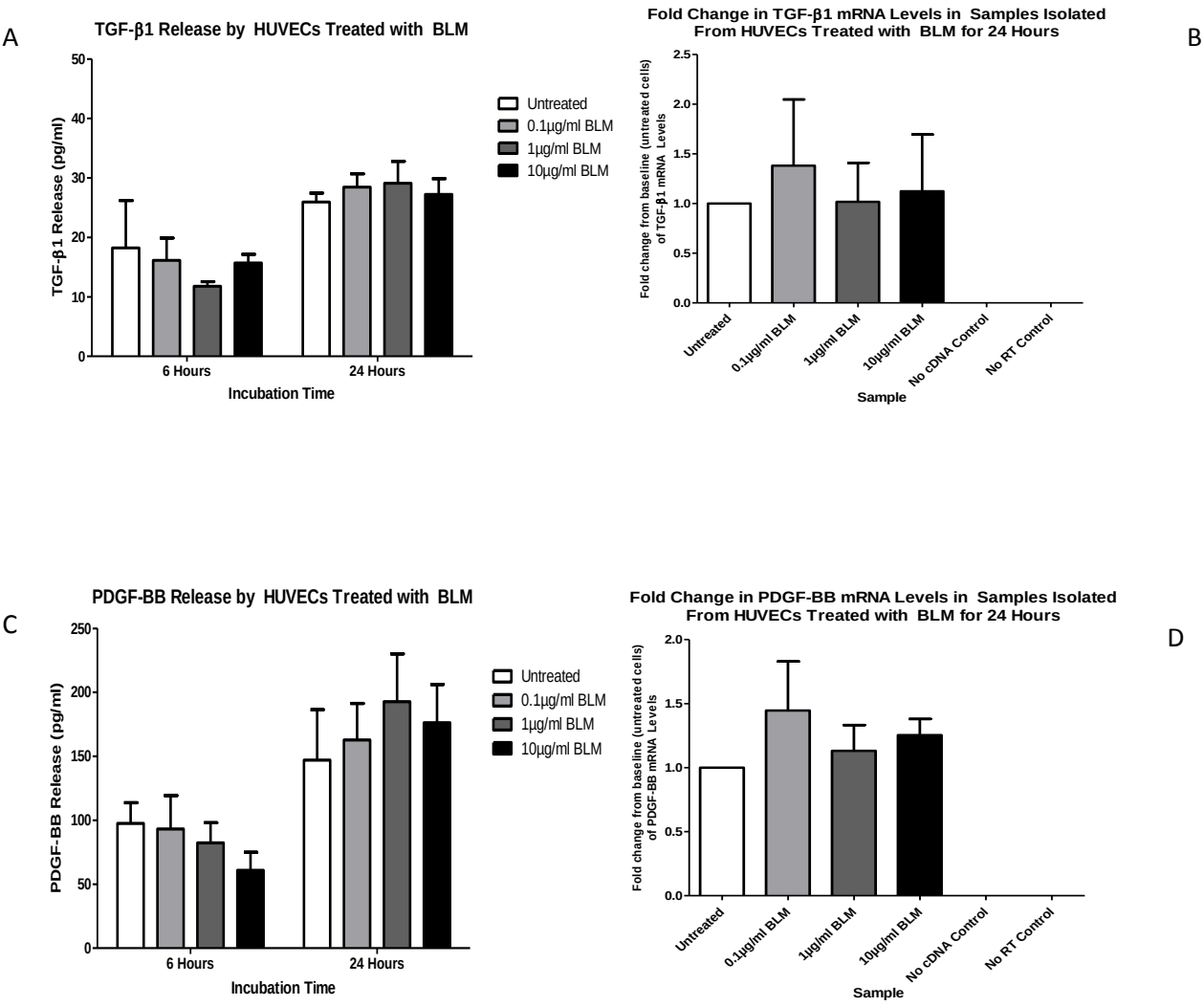

Figure 4.14: TGF-β1 and PDGF-BB release by BLM-treated HUVECs and TGF-β1 and PDGF-BB transcript expression by BLM-treated HUVECs as assessed by ELISA and qPCR.

The release of TGF-β1 by HUVECs treated with BLM for 6 and 24 hours (A) as determined by ELISA; the fold-change in TGF-β1 transcript levels in cells treated with BLM for 24 hours (B); The release of PDGF-BB by HUVECs treated with BLM for 6 and 24 hours (C) as determined by ELISA; the fold-change in PDGF-BB transcript levels in cells treated with BLM for 24 hours (D). Statistical analysis of qPCR results was conducted using repeated-measures ANOVA (as outlined in section 4.2.5). Statistically significant results are denoted by asterisks (*p=0.05*). *n=3.*

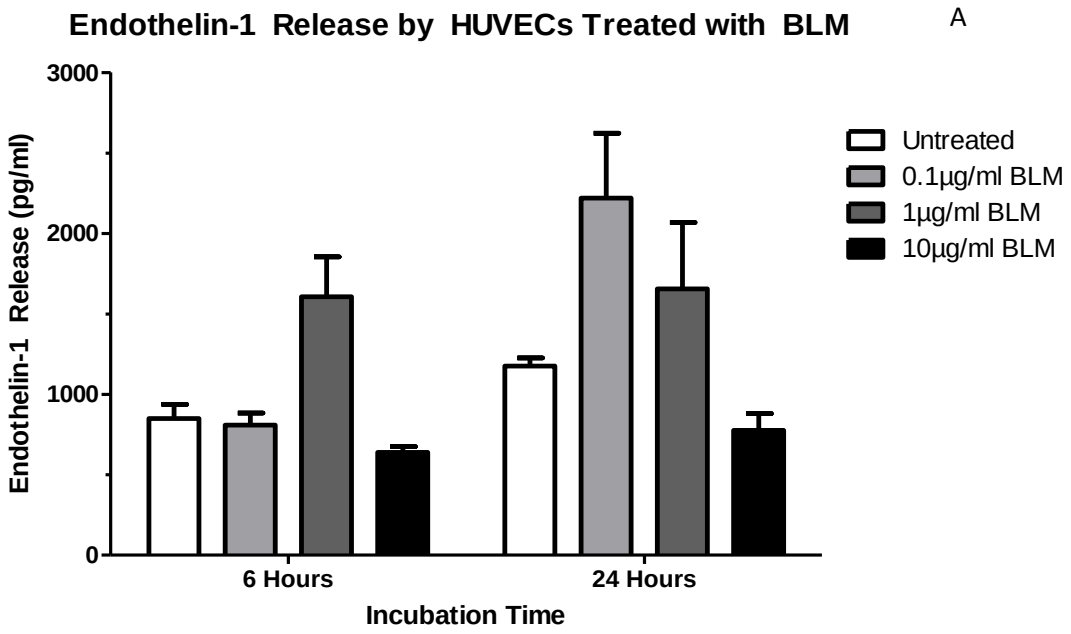

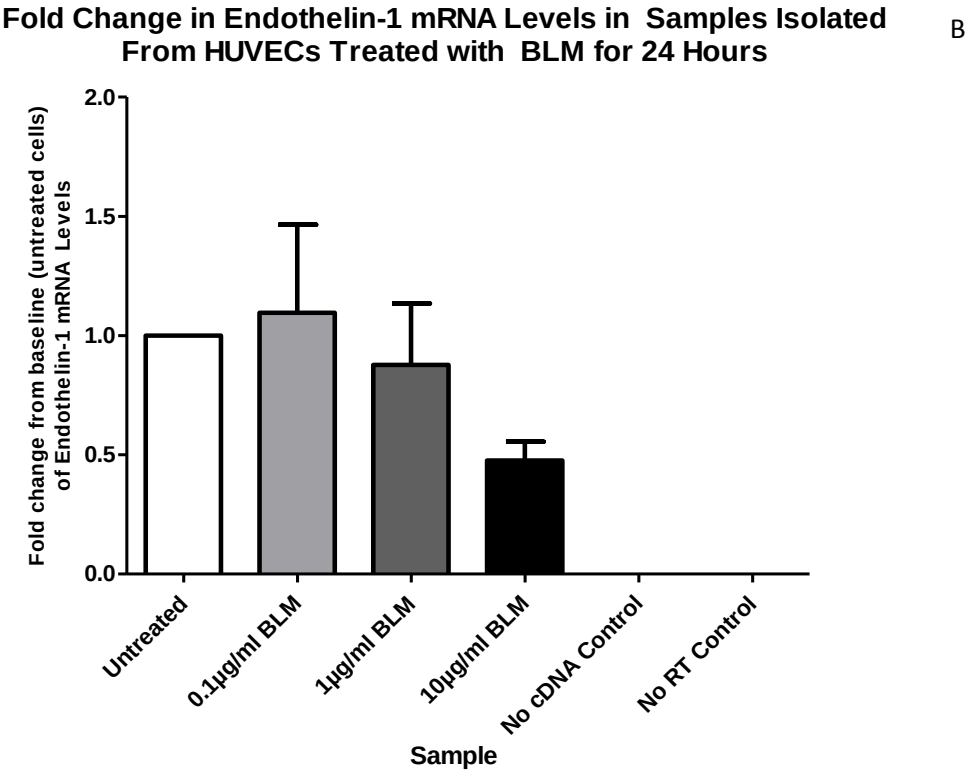

Figure 4.15: Endothelin-1 release by BLM-treated HUVECs and Endothelin-1 transcript expession by BLM-treated HUVECs assessed by ELISA and qPCR.

The release of Endothelin-1 by HUVECs treated with BLM for 6 and 24 hours (A) as determined by ELISA, and the fold-change in Endothelin-1 transcript levels in cells treated with BLM for 24 hours (B). Statistical analysis of qPCR results was conducted using repeated-measures ANOVA (as outlined in section 4.2.5). Statistically significant results are denoted by asterisks (*p=0.05*). *n=3.*

4.4 Discussion and Conclusions

These results extend our knowledge of how HUVECs respond to BLM treatment, in terms of adhesion molecule upregulation and cytokine release. These data show that, when HUVECs are incubated with BLM over a 6 hour period, there is a statistically significant increase in E-Selectin and VCAM-1 expression in cells treated 10µg/ml BLM, while over 24 hours, E-Selectin expression was significantly increased in cells treated with all concentrations of BLM, and the expression of ICAM-1 was significantly increased in cells treated with 10µg/ml BLM for 24 hours. In addition, cells treated with 1µg/ml BLM showed an almost significant increase in ICAM-1 expression; further repeats of this experiment may allow a statistically significant difference in the expression of ICAM-1 to be achieved. Thus, BLM appears to impact the expression of adhesion molecules by endothelial cells.

4.4.1 Adhesion Molecule Expression in Response to BLM

While previous literature has reported increased expression of E-Selectin, ICAM-1, and ICAM-3 following the treatment of ECs with BLM (Miyamoto, et al., 2002; Ishii and Takada, 2002; Fichtner, et al., 2004), this the first report of increased VCAM-1 expression in response to BLM, and of ICAM-1 expression by HUVECs. Miyamoto, et al. (2002) reported that treatment of HUVECs with BLM at concentrations of 250-500 ng/ml for 6 hours induced increased E-Selectin expression, while ICAM-3 expression was induced after HUVECs were treated with 100ng/ml -250ng/ml BLM for 24 and 48 hours, but no ICAM-1 expression was reported by this group, who stated that the origin of the cell type - HUVECs - was the cause of the absence of ICAM-1; indeed, ECs of different origin demonstrate heterogeneity, though in this work, strong expression of cell-surface ICAM-1 in response to BLM (10µg/ml for 24 hours) was observed. Moreover, this work reports no increased, or baseline, expression of ICAM-3, which was shown to be upregulated at a transcript level via Western Blots by Miyamoto, et al. (2002). In fact, when assessing adhesion molecules the only observed similarity between this work and that of Miyamoto in the increase in E-Selectin expression observed.

That increased E-Selectin expression was seen in the current work also tallies with the results of Ishii and Takada (2002), who noted a time- and concentration-dependent increase in E-Selectin mRNA and protein expression by BLM-treated HUVECs, with 6 hour incubations and incubations with 5μM BLM resulting in the strongest upregulation. In this respect, the current work adds further weight to the evidence that E-Selectin expression may be BLM-mediated.

There has only been one previous report of ICAM-1 expression increasing in response to BLM, and this is in the work by Fichtner, et al. (2004), who observed increased ICAM-1 protein and mRNA expression in human pulmonary microvascular ECs (hPMVECs) - a more physiologically relevant cell type, and one which will be used later in this work - treated with 100U/ml (over 50μg/ml) BLM for 24 hours. While this is a different cell type, and the heterogeneity of endothelial cells has been discussed, this suggests that ICAM-1 upregulation in response to BLM is feasible.

How such adhesion molecule upregulation occurs in response to BLM is unknown. Ishii and Takada (2002) suggested increased E-Selectin expression was mediated by activation of the promoter. The promoter has three binding sites for NF-κB (Collins, et al., 1995; Schindler and Baichwal, 1994), a heterodimer of p50 and p65 (RelA) which, under unstimulated conditions, is inactivated by association with IκBα (Anwar, et al., 2004). In response to stimulation, degradation of IκBα releases NF-κB, allowing translocation to the promoter (Rahman, et al., 2000), which mediates transcription. Ishii and Takada noted that BLM treatment resulted in NF-κB/Rel and AP-1 activation, and NF-κB translocation. Blockade of NF-κB activation and binding reduced E-Selectin expression (though whether AP-1 is necessary for E-Selectin expression is debated (Montgomery, et al.,1991; Read, et al.,1997; Min and Pober, 1997)). However, if BLM induces NF-κB activation, required for the transcription of other molecules including VCAM-1 and ICAM-1, then this may be the cause of adhesion molecule upregulation in response to BLM.

Assessing the results obtained for qPCR experiments, it is clear that for the most part, the levels of adhesion molecule protein by BLM-treated HUVEC was similar to the mRNA levels observed. This was the case for ICAM-1, where small increases in mRNA levels mirrored small increases in protein expression. Increases in mRNA levels were broadly

similar to protein expression increases, and are comparable enough to suggest that ICAM-1 protein upregulation in response to BLM is controlled at a transcriptional level, and that increased ICAM-1 expression when cells were assessed by flow cytometry was not merely a chance occurrence.

However, when the mRNA and protein expression levels of both VCAM-1 and E-Selectin were compared, discrepancies were noted in the magnitude of the increase. VCAM-1 and E-Selectin are not expressed constitutively and so their expression at a protein level requires increased transcription. As the baseline level of VCAM-1 and E-Selectin expression is almost identical to the control, which suggests no protein expression at baseline, the magnitude of increased transcript levels may in fact mirror the increase in protein expression more closely than evident at first glance, as the relative increase in protein expression may be higher than first thought. These discrepancies, however, may also be related to post-transcriptional and post-translational regulatory processes, discussed in section 4.4.5. Regardless, the trends seen in transcript level and protein expression increases for both VCAM-1 and E-Selectin were broadly similar, and these results suggest BLM regulates increased VCAM-1 and E-Selectin protein expression at a transcriptional level.

There may be other reasons for these discrepancies. Both FACS and qPCR are "snap-shots" of cellular processes; VCAM-1 is expressed in response to inflammatory stimuli, and maximal VCAM-1 protein expression occurs at 8 hours, declining after 12 hours (Scholz, et al., 1996; Haraldsen, et al., 1996), while maximal synthesis is noted at 4-6 hours (Scholz, et al., 1996). It is possible that in our results, synthesis has peaked, but expression has not, due to a time-lag in protein expression. However, ICAM-1 protein expression peaks at 24-48 hours after stimulation (Haraldsen, et al., 1996) - seen in our results – but peak gene expression occurs after 4-6 hours in response to inflammatory stimuli (Scholz, et al., 1996). In this work, ICAM -1 transcript levels correlated closely with protein expression at both time points, and both were consistently upregulated. This may be due to enduring incubation with BLM, though this is speculative. However, discrepancies in E-Selectin transcript levels and protein expression cannot be explained in this way; E-Selectin is expressed quickly following sitmulation, peaking 4-6 hours after stimulation, and decreasing at 24 hours (Khew-Goodall, et al., 1996; Haraldsen, et al.,

1996). However, gene expression peaks concurrently (Scholz, et al., 1996), and mRNA expression mirrors protein expression; both decrease simultaneously, stimulus independent (Bevilacqua, et al., 1989; McEver, 1997). Therefore, this gives no clue as to why levels of E-Selectin transcript were higher than protein levels.

Overall, the flow cytometric analyses and qPCR experiments confirm that BLM increases ICAM-1, E-Selectin, and VCAM-1 expression at both protein and transcriptional levels. These are arguably the most important three adhesion molecules in the diapedesis cascade in systemic circulation (though there are some differences in the profile of adhesion molecules expressed in the systemic circulation and in lung venules when compared to lung capillaries, as discussed in 1.8 and 5.1), and suggest that BLM may induce the increased immune cell infiltration into the lung via adhesion molecule upregulation. Though not explicitly investigated in this work, this upregulation may be NF-κB regulated; this would provide a fascinating focus for future work, to unravel the mechanisms behind how BLM induces such expression upregulation.

4.4.2 Fc Receptor Expression by BLM and TNF-α Treated HUVECs

As it was observed when initial experiments were carried out that treatment with BLM and TNF-α increased the binding of the isotype control antibody to HUVECs, and increased autofluorescence which may simulated increased non-specific binding was absent, whether these treatments induced Fc receptor expression by HUVECs was assessed. However, no expression of any of the assessed Fc receptors by HUVECs treated with BLM or TNF-α was reported. That HUVECs do not express Fc receptors in response to BLM or TNF-α was confirmed by experiments in which non-aggregated and heat-aggregated IgG1 and BXB (immune complexes) did not adhere to treated HUVECs. Therefore, it can be stated that BLM and TNF-α do not induce the expression of Fc receptors by HUVECs.

This goes against the published literature of Pan, et al. (1999), and fails to explain the increased isotype control binding observed when cells were treated with TNF-α and BLM in this work.

In light of this, the batch of isotype control antibody was replaced, to determine whether the batch of isotype control being used was contaminated. However, this made no difference to the binding of the isotype control antibody to the treated HUVECs. As the increased binding of the isotype control to TNF-α and BLM-treated HUVECs could not be explained or prevented, the decision was made to use the secondary antibody control as the baseline expression level of markers in this series of experiments and all others. The binding of this antibody to cells was not impacted by the treatment of cells with various concentrations of BLM or TNF-α, and was thus deemed a more reliable representation of non-specific binding of target antibodies to HUVECs in this, and future, series of experiments. For this reason, the secondary antibody was also used as the control antibody in series of experiments carried out using flow cytometry earlier (those to determine the best mediator to use as a positive control).

4.4.3 Cytokine Release in Response to BLM

In this work, it was observed that the release of MCP-1 and IL-8 are increased in response to BLM treatment. It is also worth mentioning that, as IL-8, MCP-1, and Endothelin-1 are constitutively released, the differences between 6 hour and 24 hour baseline expression were expected. However, only IL-8 showed statistically significant increases in release when cells were treated with BLM. It is surprising that the release of MCP-1 when cells were treated with 10µg/ml BLM was not significantly different from baseline as there is clearly an increased level of MCP-1 release. However, this was mostly likely due to the low number of replicates and the high degree of variation in MCP-1 release by untreated cells. Further experiments may generate results showing the increased release of MCP-1 when cells were treated with 10µg/ml BLM to be significantly different from MCP-1 release by untreated cells.

In this respect, the Endothelin-1 results are also curious; increased release was noted when cells were treated with 0.1 and 1µg/ml BLM, and 1µg/ml BLM for 24 and 6 hours, respectively, but these were not significant. A decrease in Endothelin-1 release was noted in cells treated with 10µg/ml BLM for 24 hours, but again, this was not significant. Further experiments generating more repeats may show that Endothelin-1 release by

HUVECs treated with these concentrations of BLM over these time points is statistically different, or that this increase is not as substantial as suggested. Lastly, there was no increase in the release of TGF-β and PDGF-BB in response to BLM.

When comparing this work to previous publications, it appears that in the current work, the release of IL-8 and MCP-1 was quite different to that reported by Miyamoto, et al. (2002). This group reported that, when cells were treated with BLM for 6 and 24 hours at various concentrations, there was no increase in IL-8 release. Instead, this group reported only significant increases in release at 12 hours, and only at concentrations of 10ng and 50ng/ml BLM. Our results instead show that there was a definite dose-dependent increase in the release of IL-8 by HUVECs treated with BLM over 24 hours, and at higher concentrations of the drug. Few other studies have assessed the release of proinflammatory cytokines by endothelial cells in response to BLM, though Fichtner, et al. (2004) reported the increased IL-8 release by PMVECs in response to concentrations of BLM of over 50µg/ml, and as such a high concentration was used, and on a different cell type, the results of Fichtner cannot be directly compared to the results obtained in this work.

With regards to MCP-1, Miyamoto and colleagues reported a slight increase in MCP-1 release in cells treated with 10ng/ml and 50ng/ml BLM for 12 and 48 hours only. However, we noticed a substantial increase in MCP-1 release was observed in this work when cells were treated with 10µg /ml BLM, which was not observed by Miyamoto and colleagues, who instead reported a cessation of release at high BLM concentrations. These differences may be due to the high levels of cell death reported at higher BLM concentrations by Miyamoto and colleagues, a phenomenon that not observed in the current work.

There are very few published works assessing pro-fibrotic expression by BLM-treated HUVECS. While Miyamoto, et al. (2002) found no significant difference in TGF-β1 release by BLM-treated HUVECs, these results were not published, and it is not clear whether active or latent TGF-β was being measured in this study, or what the baseline expression levels were. Yin, et al. (2012), however, reported increased TGF-β release by endothelial cells in I.T. BLM-treated rodents, but the group did not determine whether this increased

expression was due to the effect of BLM on endothelial cells, or whether endothelial TGF-β expression was due to the expression of cytokines in the murine lung affecting the endothelium. However, this is worth investigating.TGF-β is recognised as an important cytokine in the development of pulmonary fibrosis, and the release of TGF-β by epithelial cells in the lung is widely regarded as contributory to BPF development (as reviewed by Williamson, et al., 2015).There have been no reports investigating the expression of PDGF-BB by HUVECs exposed to BLM.

That BLM impacts Endothelin-1 release has not previously been reported. It appears that treatment with low concentration BLM increases Endothelin-1 release, and this may be of importance in future work. Endothelin-1 is a potent pro-fibrotic cytokine, inducing the transdifferentiation of fibroblasts (Shi-Wen, et al., 2004; Ross, et al., 2009) and collagen synthesis by mesenchymal cells (Fonseca, et al., 2009). Moreover, human lung fibroblasts express Endothelin-1 receptors and may produce their own Endothelin-1 in response to TGF-β and Endothelin-1 in combination (Ahmedat, et al., 2012), resulting in increased numbers of myofibroblasts - which may be apoptosis-resistant (Kulasekaran, et al., 2009) - and increased collagen synthesis. Therefore, endothelially-expressed Endothelin-1 may feasibly induce autocrine Endothelin-1 signalling loops in proximate mesenchymal cells, contributing to BPF development. However, high BLM concentrations appeared to decreased Endothelin-1 release from baseline. The relevance of this is unknown. Moreover, the apparent increase in release demonstrated a large standard error in both ELISA results, and so care must be taken in drawing strong conclusions from these results.

Like the results obtained when assessing adhesion molecule mRNA levels, the results obtained from ELISAs to determine IL-8 release by BLM-treated HUVECs and the qPCR results to assess transcription levels correlate well. In both the 6 hour and the 24 hour experiments, protein release mirrored mRNA levels, as treatment with 10µg/ml BLM induced a 2.5-fold increase in both protein and transcript levels in both. The decrease in IL-8 release induced by 0.1µg/ml BLM was also seen to correlate with mRNA levels, which was not expected. Therefore, it appears transcription regulated protein release in IL-8.

This was also the case for MCP-1, though the results were less concordant. Slight increases in transcript level were seen to mirror slight increases in protein release in both the 6 and 24 hour experiments when cells were treated with 0.1 and 1μg/ml BLM. Only the results from cell treated with 10μg/ml BLM appear discordant, though in the 24-hour experiment, a transcript fold increase of around 1.5 resulted in a tripling of the protein released into the supernatant. In the 6-hour experiment, however, a fold-increase of approximately 4 was seen in MCP-1 transcript levels in cells treated with 10μg/ml BLM; this was not reflected in protein release, though the large error bars in the qPCR results from these samples is notable.

The results from the IL-8 and MCP-1 qPCR experiments are interesting, however, as they confirm that BLM is not acting solely as a secretagogue. IL-8 can be stored in WPB and other vesicles, as well as in the Golgi body in response to inflammatory stimuli such as IL-1β (Wolff, et al., 1998; Utgaard, et al., 1998), with expression from vesicles regulated by secretagogues such as histamine (Wolff, et al., 1998). As both *de novo* synthesis of IL-8 mRNA and increased release were noted, it appears that, rather than simply inducing the release of IL-8 from granules, BLM was actively inducing IL-8 transcription, and the protein was potentially released from the Golgi, as previously observed (Wolff, et al., 1998). It is possible that IL-8 was being synthesised and stored in granules which were being exocytosed, but whether IL-8 storing granules were generated could not be assessed. It does appear, however, that the increased IL-8 release by BLM-treated HUVECs is due to increased transcription.

Similarly, MCP-1 may also be synthesised and stored in granules in response to proinflammatory stimuli, and released in response to secretagogues (Øynebråten, et al., 2005), or directly released in response to inflammatory stimuli (Makó, et al., 2010; Parry, et al., 1998), potentially from the Golgi body, where MCP-1 is present following IL-1β stimulation (Øynebråten, et al., 2005).Increased transcript levels broadly followed the trend of increased protein release. However, in this case, there appeared to be a peak in transcript synthesis at 6 hours in cells treated with 10μg/ml BLM. It is possible that MCP-1 synthesis has peaked at this time, and a time-lag in release has occurred, resulting in high release after 24 hour stimulation with BLM, or that the 6-hour results are the result of cell line variability and a low number of repeats. As with IL-8, the intracellular localisation of

MCP-1 in response to BLM treatment was not investigated, though the results suggest that MCP-1 synthesis was stimulated by BLM, and release appears direct, not simply the result of granule exocytosis, though MCP-1 storage in granules and subsequent exocytosis may also have occurred.

Neither transcript nor protein release levels of TGF-β and PDGF-BB were impacted by BLM. These experiments were unertaken to determine whether the protein synthesis was occuring although release was not, and in the case of TGF-β, where an ELISA for latent TGF-β was used, to determine whether the protein was somehow being activated upon release and therefore the ELISA was overlooking altered levels of protein. Neither appeared to be the case. However, the results from qPCR examining Endothelin-1 synthesis show that BLM does in fact appear to be regulating both transcript levels and protein release.

In line with the results of the ELISAs, the reuslts from qPCR suggest that, at low concentrations, BLM increases the transcript levels, of Endothelin-1. This results is unexpected; though the magnitude of protein release does not perfectly mirror the magnitude of transcript level increases, the two correlate reasonably well. Of course, this could be the result of low numbers of repeats – the error bars in both sets of data are large, and a greater number of repeats may redress this, reducing the impact of unusually high or low transcript or protein release levels . However, it appears that treatment with 10µg/ml BLM downregulates the synthesis of the protein and its release.

Endothelin-1 is expressed both via constitutive and regulated pathways in endothelials cells (Russell and Davenport, 1999), with the former localising the protein to constitutive secretory vesiscles, and the latter to WPB, which exocytose upon stimulation with secretagogues such as thrombin, and environmental factors such as hypoxia, which also stimulate further endothelin-1 gene expression and production (Stow, et al., 2011). Both pathways rely on mRNA transcription and protein bioavailability (Russell and Davenport, 1999; Stow, et al., 2011) to mediate Endothelin-1 release

These results suggest that, as transcript levels mirror protein release, the constitutive pathway is at work in response to BLM. This is particularly true of the results obtained from cells treated with 10µg/ml BLM. Were BLM to act as a WPB secretagogue alone,

increased levels of the protein in supernatants and increased trascript levels, compared to baseline, would be expected when cells were treated with 10μg/ml BLM, as both the constitutive and regulated pathways would be at work, and WPB exocytosis increases transcript synthesis. It is unlikely that BLM acts as a WPB secretagogue whilst also decreasing mRNA synthesis. However, were this the case, one may expect to see higher or equal levels of endothelin-1 in supernatants collected from cells treated with 10μg/ml BLM than those seen at baseline, as the constitutive pathway may be impeded, but the regulated pathway would ensure Endothelin-1 release into the supernatant. Finally, were BLM not a secretagogue, but also to have no effect on transcript production, the results from cells treated with 10μg/ml would be no different from baseline, as the constitutive pathway would continue unimpeded. This also suggests that at the lower concentrations of BLM used, where both protein release and transcript levels increased, BLM may not have been acting as a secretagogue but instead increasing protein synthesis and release via the constitutive pathways.

As the protein and transcript levels correlate well when cells were treated with BLM for 24 hours, it appears that BLM actively prevents the synthesis of Endothelin-1 and its release via the constitutive pathway at high concentrations (10μg/ml), and at low concentrations (0.1μg/ml), it is feasible that BLM increases the synthesis and release of Endothelin-1 via the constitutive pathway. While it is also possible that at lower concentrations, BLM acts as a WPB secretagogue resulting in the increased Endothelin-1 transcript synthesis, why the drug would cease to act as a secretagogue at high concentrations is now known; thus, control of the constitutive pathway seems the logical explanation .

In all, treatment with BLM increased the release of IL-8 and MCP-1, and both increased and decreased the release of Endothelin-1, by endothelial cells. It appears that BLM impacted the synthesis of IL-8, MCP-1, and Endothelin-1, thereby modulating the release of these cytokines, though it may have also acted as a secretagogue for IL-8 and MCP-1, as well as increasing their synthesis. The role of the increased synthesis and release of MCP-1 and IL-8, in particular, may be of great importance in the recruitment of immune cells to the endothelium, and their activation, prior to diapedesis and the movement of these cells into the lung, and is an important focus for future work in this field.

4.4.4 Initial Data Analysis and Issues with the qPCR Experimental Method

Initial data analysis, and the establishment of guidelines relating to this - for example, when a sample needed to be re-run, the identification of primer dimers, and identification and re-running of samples when technical replicates proved discordant in C_q value, proved vital. The reason for this, however, is the nature of the experimental technique. The appearance of failed wells - often one of three technical replicates - could only be explained by random failure. If more than two wells failed, experiments were re-run to give an average of at least 2 replicates, deemed necessary, though single unexplained failures were tolerated. Further, that no cDNA and no RT samples on occasion produced a C_q result, always the result of primer dimer formation, is merely a characteristic of the technique, as primers may hybridise and amplify due an an absence of target product, and the DNA-binding SYBRGreen dye bound to this. Rarely, this also happened to wells containing primers for target genes; in some instances, one of three C_q values proved to be a primer dimer. Visualisation of the derivative melt curve (Fig. 5.5) was sufficient to identify such primer dimers, though that this analysis had to be performed with every experiment run implies that this is a quirk of the qPCR technique. However, the formation of primer dimers was not a common occurrence, suggesting the primers used were fit for purpose, and when primer dimers did occur, they were easily identified.

Often, intra-assay variation - the acquisition of discordant results for technical replicates, which occurred rarely - was also attributed to primer dimer formation, though sometimes this was not the case. In the latter instance, samples were re-run in triplicate. In all instances, the results of re-run experiments were universally concordant with low inter-assay variability, and the incorrect result from the initial run made obvious. That is to say, when assays were re-run, there was little or no difference in C_q results deemed to be correct and concordant between assays, found to be the case in all re-runs. Again, there was no clear reason for this intra-assay variability. As this occurred infrequently, and re-running of the samples generated concordant results, this again appears to be a quirk of qPCR that must be tolerated and dealt with accordingly.

4.4.5 Considerations of the qPCR Technique and the Correlation Between mRNA and Protein Levels

While the results of these experiments generally found good correlation between protein and mRNA levels, there were of course exceptions, mostly pertaining to the magnitude of increases. However, while transcript abundance is used as a surrogate marker for protein abundance, there are many regulatory steps in between transcript generation and protein expression. This has been expertly reviewed by Vogel and Marcotte (2012). In brief, post-transcriptional regulatory processes may modify protein synthesis from transcripts, meaning that relvative transcript abundance is only somewhat correlatory with relative protein abundance. Protein abundance can not only be affected by mRNA synthesis, but also mRNA degradation, translation, and protein degradation, so protein expression may be higher than mRNA levels, or vice versa. The pair suggested that, while transcription act as a "stochiometric on-off swtich", post-transcriptional regulation fine-tunes protein expression. Therefore, perhaps mRNA and protein abundance would not be expected to correlate perfectly.

A recent publication by Schwanhäusser, et al. (2011), also expertly defines the role of translation in the correlation between mRNA transcript levels and protein levels. While 40% of correlation is accounted for by mRNA levels, 55% of protein abundance as compared to transcript levels is controlled by translational efficiency, the number of proteins generated per transcript per unit of time. Thus, a transcript rapidly synthesised but inefficiently translated would appear more abundant than its corresponding protein (and vice versa). The "snap-shot" nature of qPCR, FACS, and ELISA - and the method of comparing the results of transcriptional analyses to analyses of expression - do not account for this, and so one may appear far higher than the other. The remaining 5% of correlation is accounted for by transcript and protein stability (which impacts degradation) - thus, if one is stable and the other not, then similar discrepancies may be noted (Schwannhäusser, et al., 2012).

This may account for the results observed with IL-8 and MCP-1; IL-8 may conceivably have a far higher translational efficiency, allowing transcript and protein to be detected concurrently.

With these factors in mind, it can be concluded that the increased protein expression observed in cells treated with BLM is most likely not due to chance, and that BLM increases gene transcription of these proteins through as yet unresolved mechanisms. Notably, all proteins seen to be upregulated, save endothelin-1, are associated de novo synthesis in response to NF-κB activation. Therefore, work to assess NF-κB activation in BLM treated HUVECs would be the next logical confirmatory step, and would provide an interesting avenue for other groups to continue research into the impact of BLM on endothelial cells.

5 Pulmonary Microvascular Endothelial Cell Adhesion Molecule Expression and Cytokine Release in Response to Treatment with BLM

5.1 Introduction

In vivo, pulmonary microvascular endothelial cells (PMVECs) line the venules, arterioles, and capillaries around the alveoli, representing a barrier between the alveoli and the circulation. Previous work suggests that, at least in rodents, dysfunction of this cell type may be involved in BPF development (section 1.5). As endothelial cells from different sites, and different points within the same site, have high levels of phenotypic heterogeneity and demonstrate heterogeneous responses during inflammation (Aird, 2012; Scott, et al., 2013), the expression of adhesion molecules and cytokines by BLM-treated HUVECs may not be analogous to that of BLM-treated human PMVECs. In this chapter, the adhesion molecule expression and cytokine release profiles of BLM-treated PMVECs will be characterised, to develop an understanding of how PMVECs respond to BLM, and this will be compared to the expression profiles observed in HUVECs, to assess the differences between the responses to BLM of these two cells types.

The range of adhesion molecules expressed by human PMVECs is not well characterised. Shen, et al. (1995) reported that PMVECs are positive for ICAM-1, VCAM-1, and E-selectin – with ICAM-1 being expressed constitutively, and ICAM-1, VCAM-1, and E-selectin being inducible by TNF-α treatment. In contrast, Jiang, et al. (2005), reported a low level baseline expression of ICAM-1 and VCAM-1 in PMVECs, with the expression of ICAM-1 and E-selectin greatly increased by treatment with TNF-α. Comparing the expression profiles of HUVECs and PMVECs, Scott, et al. (2013) noted low-level baseline expression of ICAM-1 and VCAM-1 by PMVECs, increased by treatment with TNF-α. HUVECs also expressed baseline ICAM-1 levels, but expression of ICAM-1 and VCAM-1 was greater in HUVECs than PMVECs both under basal conditions and after treatment with 10ng/ml TNF-α. This mirrors the work of Krump-Konvalinkova, et al. (2001) which also found that, while E-selectin was inducible in PMVECs using TNF-α, the expression was lower than that induced in HUVECs.

However, PMVEC adhesion molecule expression is related to the site of origin, and the works cited above fail to define which vessels the PMVECs used originate from. Feuerhake, et al. (1998) stated that while ICAM-1, VCAM-1, and E-selectin were detected in alveolar non-capillary vessels, alveolar capillaries were negative for all adhesion

molecules. This is in agreement with other works which state that the adhesion molecule expression profile in pulmonary venules is more akin to those of the systemic venules (Doerschuk, et al., 2000), though capillaries may not be completely devoid of adhesion molecules, and may express ICAM-1 under inflammatory conditions (Doerschuk, et al. 2000; Aird, et al., 2007; Segel, et al., 2011). However, as venules, capillaries, and arterioles are all potential sites of leukocyte migration (Doerschuk, et al., 2000; Gane and Stockley, 2011), the adhesion molecule expression profiles of all PMVECs may be relevant to BLM induced fibrosis and shall be investigated.

As the results from previous work are often divergent, the full adhesion molecule expression profile of this cell type remains only partially resolved. Further, there is only one previous study that has assessed the expression of adhesion molecules by PMVECs treated with BLM, and this is the work of Fichtner, et al. (2004), which reported an upregulation of ICAM-1 by PMVECs stimulated with >50μg/ml BLM, and no studies have assessed the expression of adhesion molecules by HUVECs treated with this concentration of BLM, so no comparison can be conducted. It will be interesting to assess how the expression of other adhesion molecules is impacted by BLM, and how this expression compares to that of HUVECs.

The release of cytokines by PMVECs treated with BLM will also be assessed. Much like HUVECs, PMVECs exhibit endothelin-1, MCP-1, and IL-8 release (Star, et al., 2009; Brown, et al., 1994; Beck, et al., 1999). In the case of endothelin-1, release may be induced or increased by treatment with the secretagogue thrombin (Golden, et al., 1998), but there is no work directly comparing the expression of endothelin-1 by HUVECs and PMVECs in response to any factors. In the case of IL-8 and MCP-1, both may be induced via treatment with IL-1, TNF-α, and LPS in PMVECs though comparative studies show that IL-8 is released more strongly by cytokine-treated HUVECs than PMVECs (Brown, et al., 1994). However, this is also stimulus dependent, with PMVEC releasing more MCP-1 in response to IL-1 and LPS than HUVECs. Interestingly, the basal release of both cytokines was seen to be higher in PMVECs than HUVECs (Beck, et al., 1999). Thus, the expression of cytokines by PMVECs may be different to those of HUVECs in response to BLM.

Again, the only previous work that has assessed the release of any of these cytokines by PMVECs in response to BLM is Fichtner, et al. (2004), which reported increased IL-8 expression, though again, there are no studies against which this can be compared. Moreover, only IL-8 was assessed, and so whether PMVECs release other cytokines in response to BLM is of interest. By assessing PMVEC adhesion molecule expression and cytokine release in response to pharmacologically relevant concentrations of BLM, the response of these cells to BLM may be better characterised, and by comparing this expression to that of HUVECs, differences between the response of the two cell types to BLM may be highlighted. Such differences in expression have not previously been investigated. In doing so, this work will also confirm whether HUVECs represent a suitable surrogate cell type for PMVECs for use in future work.

5.2 Materials and Methods

5.2.1 PMVEC Adhesion Molecule Expression Determination Following Treatment with BLM

Cells were cultured as outlined in 2.2 in T25 flasks. To appropriate flasks, 10ml of serum-contaning endothelial cell basal medium containing BLM – as outlined in 2.6 - was added. Cells were treated with BLM for 6 and 24 hours. The negative control used was PMVECs incubated in serum-containing endothelial cell basal medium (10ml) without BLM. The positive control used was PMVECs incubated in endothelial cell basal medium containing 10ng/ml TNF-α (10ml). Both were incubated for the same time as BLM-treated cells. After treatment, cells were dissociated, counted, re-suspended to a concentration of 1 x 10^5 cells/ml in endothelial cell medium, prepared for flow cytometry using the same panel of antibodies, and analysed as outlined in 2.3., 2.4, and 2.5, respectively. The same panel of antibodies were used as outlined in 2.5. Only five thousand cell events were captured due to the low numbers of cell cultured.

5.2.2 PMVEC Cytokine Release Determination in Response to BLM Treatment

Cells were cultured as outlined in 2.2 and re-plated as outlined in 2.7. When adherent, 3ml of serum-containing endothelial cell basal medium containing 0.1µg/ml, 1µg/ml, or 10µg/ml BLM, was added. Cells were treated with BLM for 6 and 24 hours. Negative control supernatants were generated as outlined in 2.7. Positive control supernatants were generated for IL-8, MCP-1, and ET-1, as outlined previously. The supernatants were then collected as outlined in 2.7 and used for cytokine ELISAs.

ELISA kits for IL-8 and MCP-1 were purchased from Biolegend. An ELISA kit for endothelin-1 (ET-1) was purchased from R&D Systems. All ELISAs were conducted in accordance with manufacturer's instructions. Supernatants for ELISAs were treated as outlined in 2.8. Preliminary work for each ELISA was conducted as outlined in 2.8.Plates were read using a plate-reader (Thermo Multiskan FC, Thermo Scientific) at the wavelengths instructed by the instructions provided with the kits. In brief, this was an initial reading at 450nm and a

subsequent reading at 570nm, the second subtracted from the first to reduce background. Standard curves and data analysis were carried out as outlined in 2.8.

5.3 Results

5.3.1 Adhesion Molecule Expression and Cytokine Release by PMVECs

There was no statistically significant increase in ICAM-1 expression by PMVECs treated with any concentration of BLM apart from 10µg/ml when cells were treated for 6 hours (Fig 5.3A). There was a small but statistically significant increase in the expression of VCAM-1 and E-selectin when PMVECs were treated with 1 and 10µg/ml BLM, and 10µg/ml BLM, for 6 hours, respectively (Fig 5.3C), though the increase in E-Selectin expression was small. However, given that the expression as baseline was essentially zero, it is feasible that low level E-Selectin induction occurred.

When PMVECs were treated with BLM for 24 hours, there was a statistically significant increase in the expression of ICAM-1 by PMVECs treated with 1 and 10µg/ml (Fig 5.3B). This was also observed when VCAM-1 expression was assessed, although this increase was less substantial than when cells were treated for only 6 hours. When E-Selectin expression was assessed, there was no change in the baseline expression of this molecule when cells were treated for 24 hours with BLM (Fig. 5.3D). Raw data is shown in Figs. 5.1 and 5.2. Gating is applied in these images only to highlight the peak-shift and increase in ICAM-1 and VCAM-1 positive cells when cells were treated with BLM as stated in 2.5.

The expression of IL-8, MCP-1, and Endothelin-1, was also assessed, as these three cytokines had shown alterations in release due to BLM treatment in HUVECs. Both IL-8 and MCP-1 release increased in a dose and time dependent fashion in BLM-treated PMVECs (Fig. 5.4A and 5.4B), though only when PMVECs were treated with 10µg/ml BLM for 24 hours and IL-8 was measured were any of these changes significant. The standard error of the mean appeared high in both sets of results obtained. In both cases, a wide range of baseline cytokine release and release by cells stimulated with BLM was observed. There was also a dose-dependent decrease in the release of ET-1 when PMVECs were treated with BLM for 24 hours (Fig 5.4C), although this decrease did not reach statistical significance. The results obtained using supernatants from PMVECs treated with BLM for 6 hours are more erratic, but also suggest a decrease in ET-1 release.

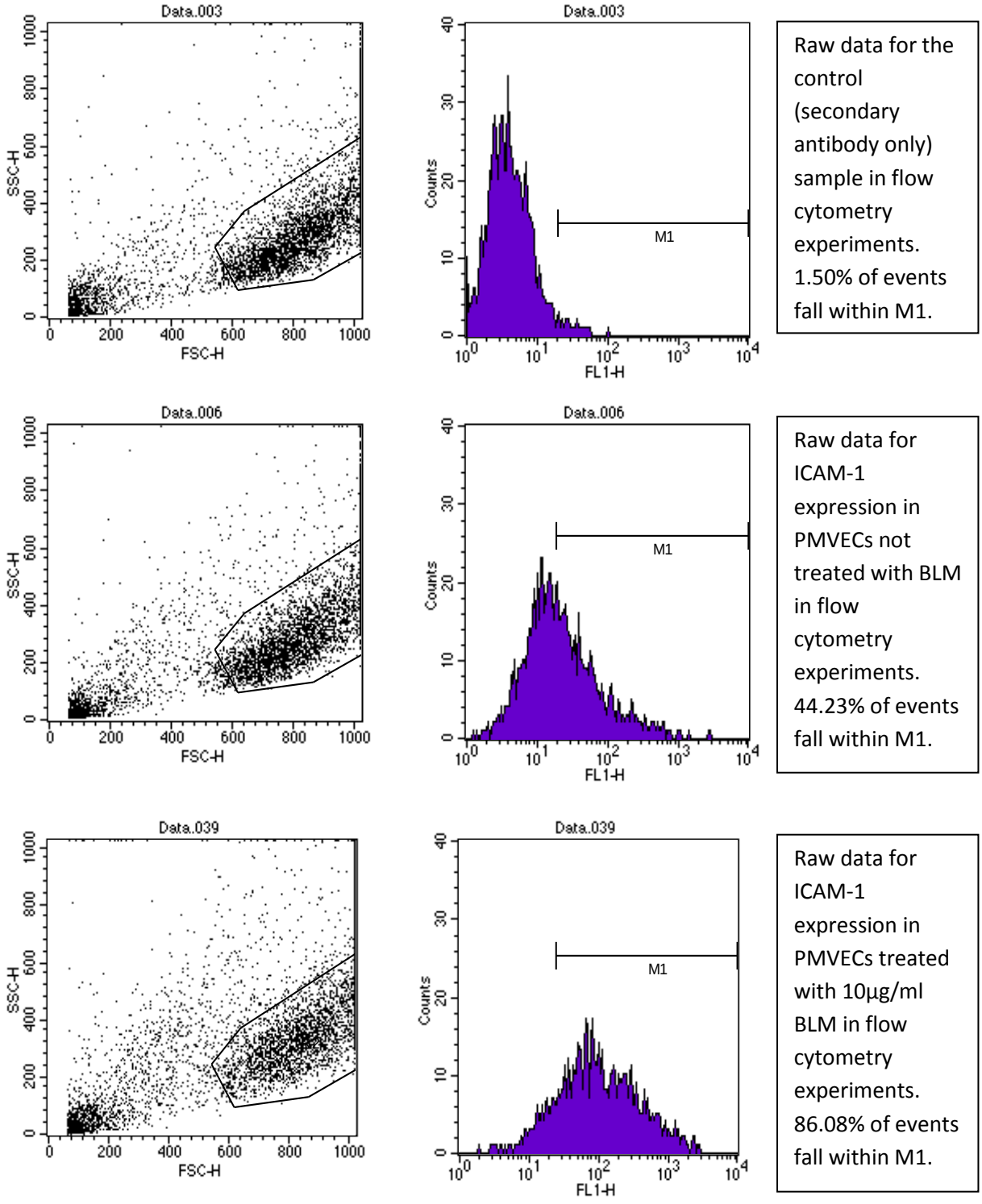

Figure 5.1: Raw data from flow cytometry experiments assessing adhesion molecule expression (ICAM-1) by BLM-treated PMVECs.

Raw data generated from flow cytometric analysis of control (secondary antibody only) samples of PMVECs (top), ICAM-1 expression by untreated PMVECs (middle) and PMVECs treated with 10µg/ml BLM for 24 hours (bottom). Gate M1 was drawn to incorporate as near to 1% of the control (secondary antibody only) peak as possible. There was a notable peak shift from baseline ICAM-1 expression when cells were treated with BLM. Respresentative images of three experiments.

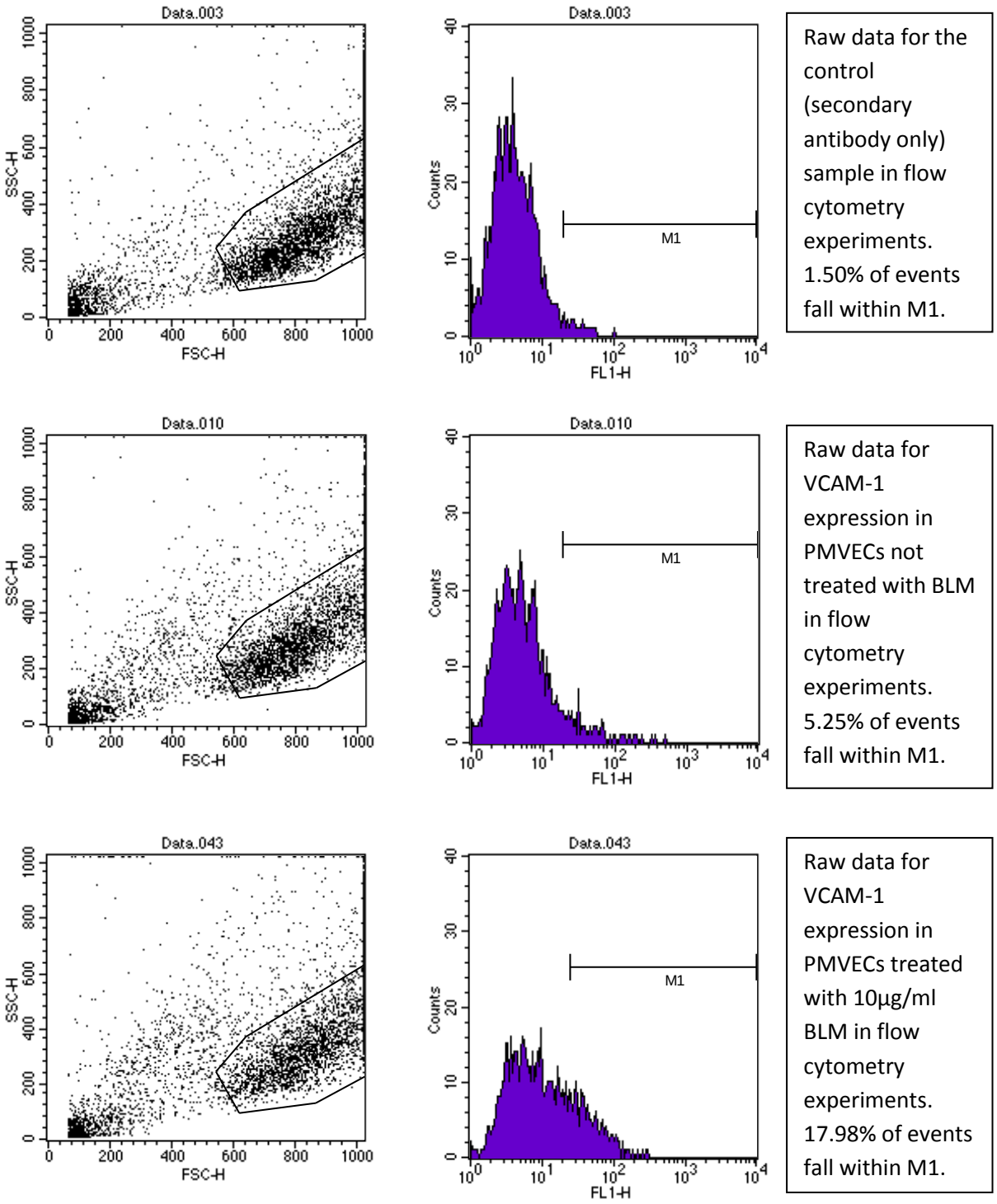

Figure 5.2: Raw data from flow cytometry experiments assessing adhesion molecule expression (VCAM-1) by BLM-treated PMVECs.

Raw data generated from flow cytometric analysis ofcontrol (secondary antibody only) samples of PMVECs (top), VCAM-1 expression by untreated PMVECs (middle) and PMVECs treated with 10µg/ml BLM for 24 hours (bottom). Gate M1 was drawn to incorporate as near to 1% of the control (secondary antibody only) peak as possible. There was a peak shift from baseline VCAM-1 expression when cells were treated with BLM, as around 18% of cells appeared to express VCAM-1 in response to BLM, but the majority of cells still expressed essentially zero VCAM-1, as shown by the population outside the gate (M1) on the bottom histogram. Respresentative images of 3 experiments.

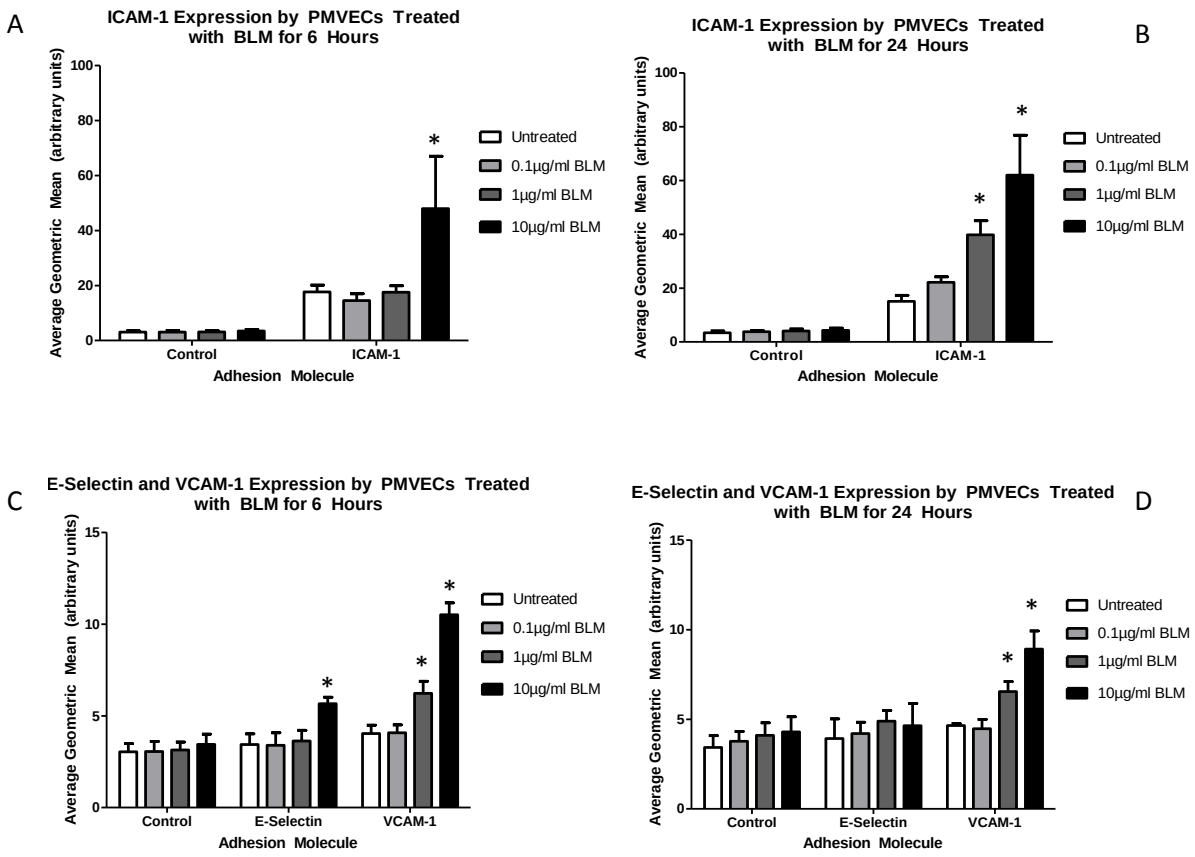

Figure 5.3: Adhesion Molecule Expression by BLM-Treated PMVECs

The expression of ICAM-1 by PMVECs treated with BLM for 6 and 24 hours (A and B) and of VCAM-1 and E-Selectin by PMVECs treated with BLM for 6 and 24 hours (C and D). Statistically significant increases in protein expression from baseline are denoted by an asterisk. Only 5,000 cell events per experiments were recorded in this series of work. *n = 3.*

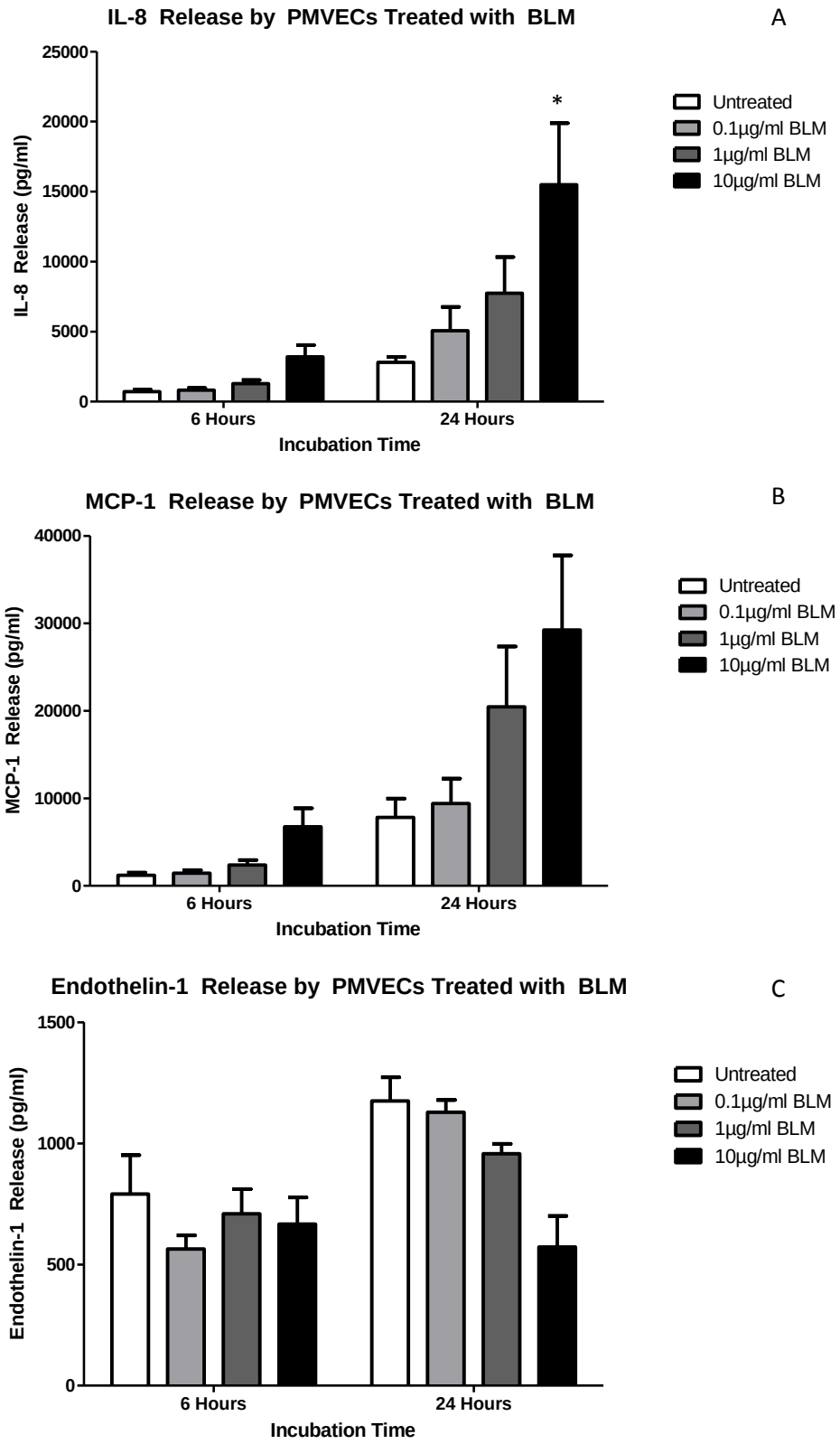

Figure 5.4: Cytokine release by BLM-treated PMVECs.

Cytokine release by PMVECs in response to BLM for IL-8 (A), MCP-1 (B), and Endothelin-1 (C). Statistically significant increases in protein release from baseline are denoted by an asterisk. 2 x 10^6 cells per flask were used to generate the supernatants used in this work. *n = 3.*

5.3.2 A Comparison of PMVEC and HUVEC Adhesion Molecule Expression

The expression of adhesion molecules and cytokines expressed and released by HUVECs and PMVECs treated with BLM was compared, and statistical analysis conducted using the Mann-Whitney-U test. This test was used due to the low number of repeats in each experiment.

Though ICAM-1 expression was higher at baseline in HUVECs than PMVECs, only ICAM-1 expression by HUVECs treated with 0.1µg/ml BLM was significantly different to that of PMVECs after 6-hour treatment (Fig 5.5A). Only untreated HUVECs and those treated with 0.1µg/ml BLM expressed significantly higher ICAM-1 levels after 24-hour treatment. In both cell types, there was a trend showing a dose-dependent increase in ICAM-1 expression when cells were treated with BLM for 24 hours (Fig 5.5B).

In both cell types treated with BLM for 6 hours, ICAM-1 expression increased 1.5-fold from baseline when cells were treated with 10µg/ml BLM. When treated for 24 hours, there was a 3-fold increase in ICAM-1 expression from baseline in both cell types. While HUVECs expressed more ICAM-1, the magnitude of increase in the two cell types was similar (Fig 5.5A and 5.5B).

PMVECs and HUVECs express similar levels of E-Selectin, when compared to the control antibody. When cells were treated with BLM, the increase in expression was more substantial in HUVECs. There was a two-fold increase in expression in HUVECs treated with 10µ/ml BLM, compared to only a 1.5-fold increase in PMVECs when cells were treated with BLM for 6 hours (Fig 5.5C). Only very minor increases in E-Selectin expression were seen when both HUVECs and PMVECS were treated with all concentrations of BLM for 24 hours (Fig 5.5D).

Assessing VCAM-1 expression, PMVECs and HUVECs express similar baseline levels when compared to the control. PMVECs appeared to express significantly higher levels of VCAM-1 than HUVECs when treated with all three concentrations of BLM for 6 hours. PMVECs treated with 10µg/ml BLM demonstrated around a 3-fold increase in VCAM-1 expression while HUVECs only a 1.5-fold change. While statistical analyses suggested a statistically significant difference in VCAM-1 expression between HUVECs and PMVECs

treated with 0.1µg/ml BLM, this may be reflective only the higher baseline VCAM-1 expression by PMVECs; neither cell type demonstrated a change in expression from baseline when cells were treated with 0.1µg/ml BLM (Fig 5.5E). In the 24 hour experiments, PMVECs also demonstrated a higher baseline expression of VCAM-1 than HUVECs (though slightly higher binding of the control antibody to untreated PMVECs than untreated HUVECs may have contributed to this observation). PMVECs treated with 1 and 10µg/ml BLM for 24 hours expressed significantly higher levels of VCAM-1 than HUVECs; PMVECs treated with 10µg/ml BLM exhibited a higher increase in VCAM-1 expression (a 2.5-fold increase) compared to that seen in HUVECs (a 1.5-fold increase) (Fig 5.5F).

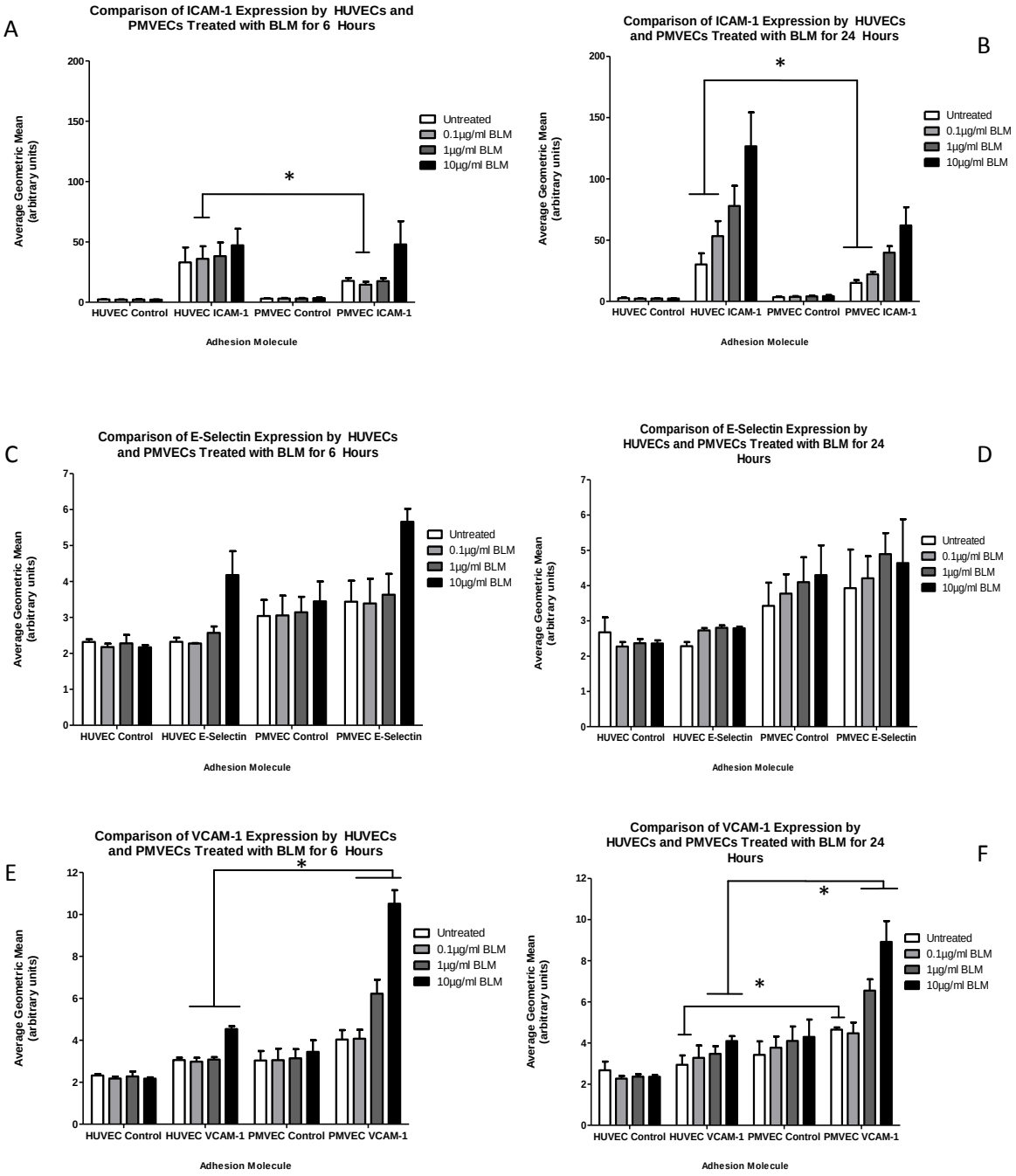

Figure 5.5: Comparisons of PMVEC and HUVEC adhesion molecule expression in response to BLM treatment.

Comparisons of the expression of endothelial cell adhesion molecules ICAM-1 (A, B), E-selectin (C,D), and VCAM-1 (E,F) in PMVECs and HUVECs treated with BLM for 6 hours (A, C, E) and 24 hours (B, D, F). Statistically significant differences in protein expression between cell samples are denoted by an asterisk and connecting bars. *n = 3.*

5.3.3 A Comparsion of PMVEC and HUVEC Cytokine Release

The total release levels of both IL-8 and MCP-1 were greater by HUVECs than PMVECs when cells were treated with BLM (Fig 5.6A and 5.6B). IL-8 and MCP-1 release by HUVECs at baseline and when cells were treated with 0.1 and 1μg/ml BLM were greater than IL-8 and MCP-1 release by PMVECs treated with these concentrations for 6 hours (Fig 5.6A and 5.6B). There was no statistically significant difference in IL-8 release between PMVECs and HUVECs when both cell types were treated for 24 hours (Fig 5.6A). Only MCP-1 release by cells treated with 10μg/ml BLM was significantly different, with HUVECs releasing greater levels of the cytokine (Fig 5.6B). However, the magnitude of the increased IL-8 and MCP-1 release by HUVECs and PMVECs was broadly similar when cells were treated with 0.1 and 1μg/ml BLM. The magnitude increase of IL-8 and MCP-1 release by PMVECs was greater than that of HUVECs in response to 10μg/ml BLM (Table 5.1).

When Endothelin-1 release was assessed, release levels were similar in PMVECs and HUVECs. Only when cells were treated with 0.1μg/ml BLM for 6 and 24 hours, and 1μg/ml BLM for 6 hours was there a significant difference (Fig 5.6C). However, in these instances, HUVEC Endothelin-1 release appeared to be increased from baseline by treatment with BLM. This was not observed under any treatment condition in PMVECs, where BLM treatment appeared to universally decrease Endothelin-1 expression. With the exception of these results, the magnitude decrease in Endothelin-1 release observed was broadly similar (Table 5.1).

Cytokine Measured	Incubation Time	Cell Type Assessed	Fold Change from Baseline		
			0.1µg/ml BLM	1µg/ml BLM	10µg/ml BLM
IL-8	6 hours	HUVEC	0.7	1.3	1.8
		PMVEC	1.1	1.8	4.5
	24 hours	HUVEC	1.1	1.9	2.5
		PMVEC	1.8	2.8	5.5
MCP-1	6 hours	HUVEC	1.1	1.7	1.8
		PMVEC	1.2	2.0	5.6
	24 hours	HUVEC	1.0	1.2	2.4
		PMVEC	1.2	2.6	3.7
Endothelin-1	6 hours	HUVEC	1.0	1.9	0.8
		PMVEC	0.7	0.9	0.8
	24 hours	HUVEC	1.9	1.4	0.7
		PMVEC	1.0	0.8	0.5

Table 5.1: Comparison between HUVEC and PMVEC cytokine release in response to BLM

The fold-change in cytokine release by HUVECs and PMVECs treated with BLM over 6 and 24 hours, assessed by ELISA.

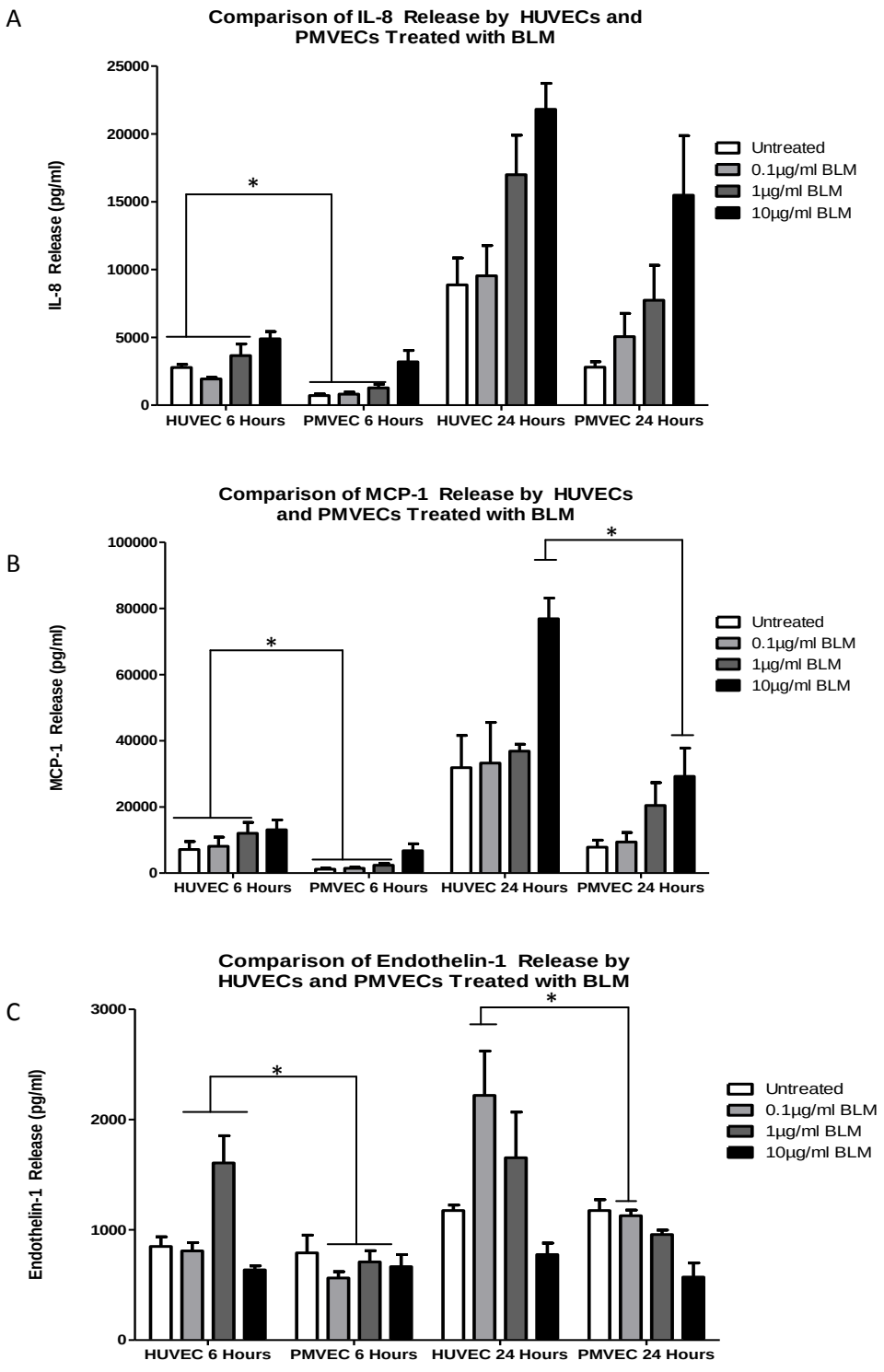

Figure 5.6: Comparisons of HUVEC and PMVEC cytokine release in response to BLM treatment

Comparisons of the release of IL-8 (A), MCP-1 (B), and Endothelin-1 (C) by PMVECs and HUVECs treated with BLM for 6 hours and 24 hours. Statistically significant differences in protein release between samples are denoted by an asterisk. *n = 3.* 2 x 10^6 cells per flask were used to generate the supernatants used in this work.

Interestingly, there were statistically significant differences in the maximum levels of E-Selectin, ICAM-1, and VCAM-1 when cells were treated with 10ng/ml TNF-α (Fig 5.7A-C). This was particularly noticeable when E-Selectin was assessed, as the maximum inducible expression was far greater in HUVECs than in PMVECs (Fig. 5.7B). Further, maximum inducible release of both IL-8 and MCP-1 was significantly greater in HUVECs treated with 10ng/ml TNF-α than in TNF-α-treated PMVECs (Fig 5.8A, 5.8B).

Note that, in these graphs, the secondary antibody alone (control antibody) value has been subtracted from the geometric mean value obtained from flow cytometric analysis. The reason for this is purely related to ensuring the clarity of the images.

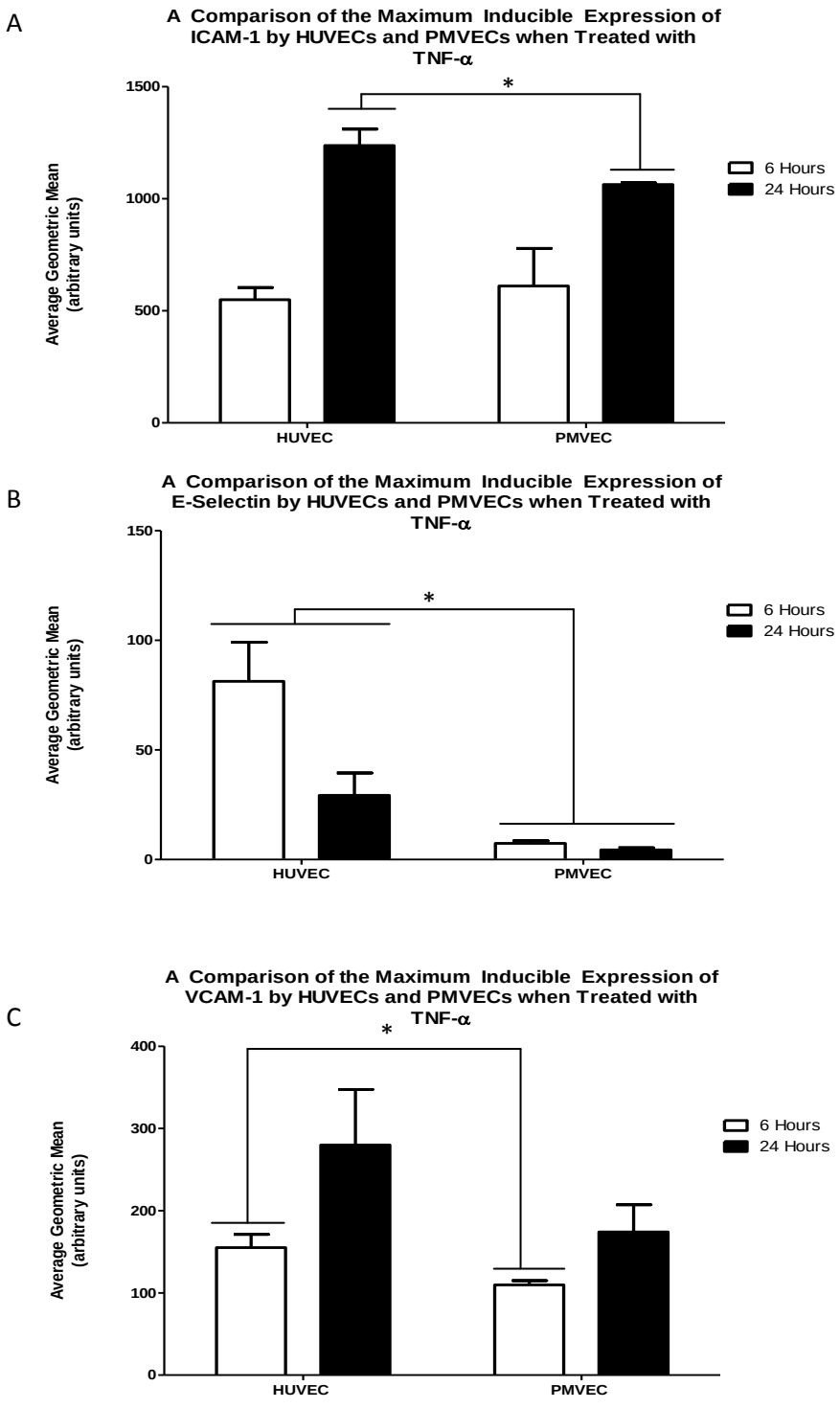

Figure 5.7: Comparisons of the maximal induction levels of adhesion molecules by TNF-α-treated HUVECs and PMVECs.

Maximal expression of ICAM-1 (A), E-selectin (B), and VCAM-1 (C) by HUVECs and PMVECs treated with TNF-α (10ng/ml). Note that the control has been subtracted from the geometric mean for clarity. Statistically significant differences in protein expression between cell types are denoted by an asterisk. *n = 3.*

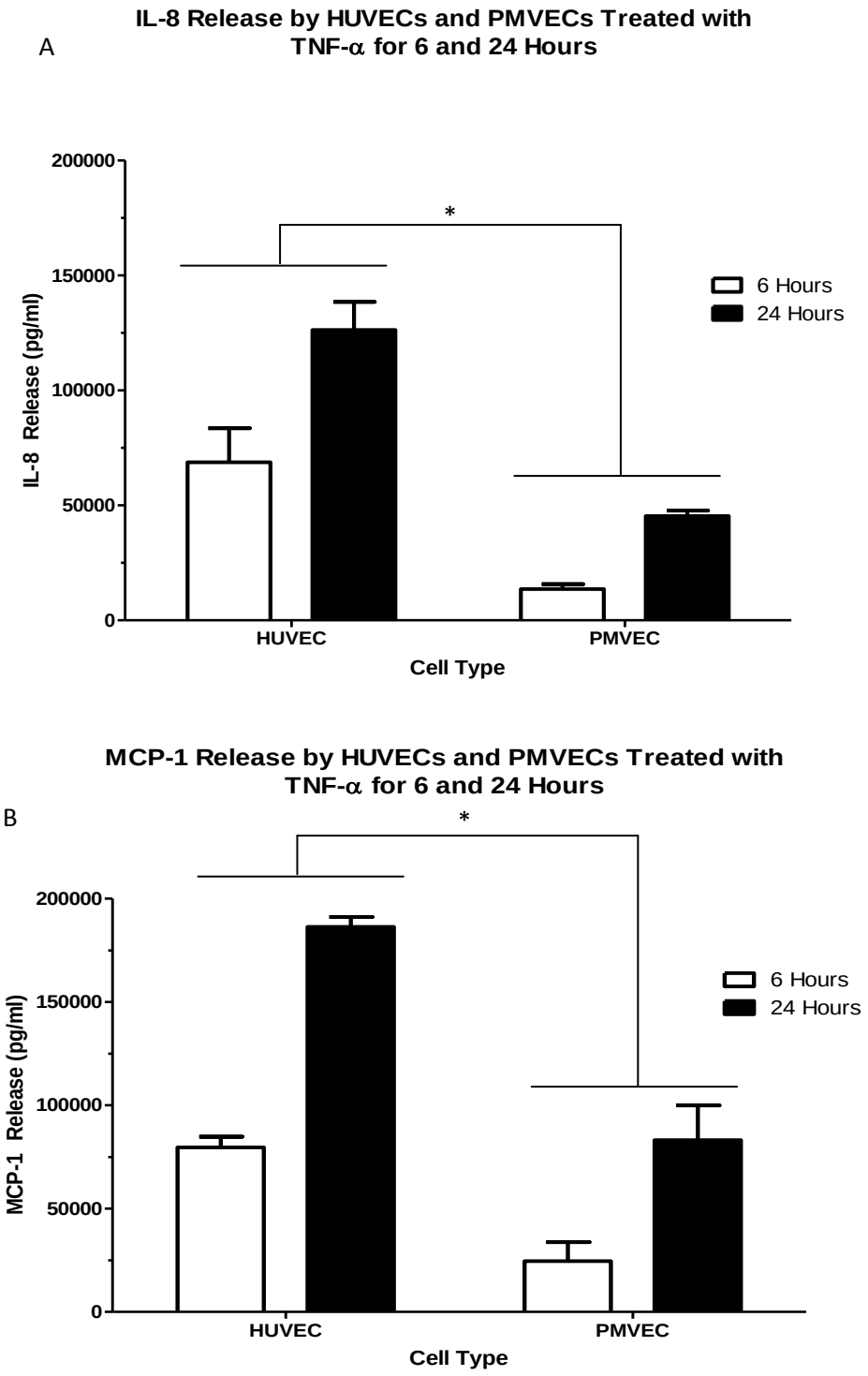

Figure 5.8: Comparisons of the maximal cytokine release levels by TNF-α-treated PMVECs and HUVECs.

The maximal IL-8 (A) and MCP-1 (B) release by PMVECs and HUVECs in response to TNF-α (10ng/ml). Statistically significant differences in protein release between cell types are denoted by an asterisk. *n = 3.* 2 x 10^6 cells per flask were used to generate the supernatants used in this work.

5.4 Discussion and Conclusions

Overall, there was an increase in the expression of adhesion molecules when PMVECs were treated with BLM. In agreement with the work of Fichtner, et al. (2004), increased ICAM-1 expression was observed in PMVECs treated with BLM. In addition, increased VCAM-1 expression and, to a small degree, increase E-selectin expression, was also noted – this has not previously been reported. Though a full panel of antibodies was assessed, including PECAM-1, ICAM-3, ICAM-1, $\alpha_V\beta_3$, P-Selectin, E-Selectin, VCAM-1, and PSGL-1, these were the only adhesion molecules upregulated. However, there were differences observed in the levels of adhesion molecule expression when comparing HUVECs and PMVECs.

Though the maximum level of ICAM-1 expression by BLM-treated PMVECs in this work was not as substantial as that noted in HUVECs, the observed magnitude of increase was similar. Higher levels of VCAM-1 expression were noted in PMVECs than were in HUVECs, with a higher level of protein and a higher magnitude of change from baseline observed. This suggests that the two cell types demonstrate different adhesion molecule expression profiles in response to BLM and suggests that BLM may impact PMVEC adhesion molecule expression in a different fashion to HUVECs. The increase in E-selectin by PMVECs when treated with BLM was broadly similar to that induced in HUVECs, though it is notable that, when comparing PMVEC and HUVEC responses to BLM, HUVECs upregulated E-Selectin expression to a higher magnitude compared to baseline than PMVECs.

In the positive control experiments run in parallel to this, there was a far lower upregulation of E-selectin expression in PMVECs treated with TNF-α than HUVECs treated with the same concentration of the mitogen. Therefore, perhaps an analogous statistically significant increase in E-Selectin expression by PMVECs compared to HUVECs was not feasible in this scenario. That treatment with TNF-α did not induce high levels of E-selectin and also induced lower levels of VCAM-1 and ICAM-1 in PMVECs than in HUVECs agrees with the work of Krump-Konvalinkova, et al. (2001) and Scott, et al. (2013). This work is the first to assess PMVEC adhesion molecule expression in response to BLM and compare this to the response observed in HUVECs.

When treated with BLM, PMVECs released increased levels of both MCP-1 and IL-8. This is similar to the results of the work carried out using HUVECs, and shows that both cell types demonstrate a concentration-dependent increase in cytokine release in response to BLM. Though total release levels of MCP-1 and IL-8 were lower in PMVECs than HUVECs, the magnitude of the increase was higher in PMVECs than in HUVECs. This highlights the difference in baseline expression. This differs from previously published work, which suggests MCP-1 expression is constitutively higher in PMVECs (Beck, et al., 1999); the reasons for this are unknown. However, the range of measured MCP-1 expression levels when PMVECs were assessed is very broad. This was also the case when IL-8 expression was measured. Therefore, unusually low results from one PMVEC line may impact the average MCP-1 and IL-8 expression observed. Further experiments with a greater number of repeats would surely give a more accurate picture of cytokine release by PMVECs.

Assessing Endothelin-1 release, a universal dose-dependent decrease in endothelin-1 expression was observed when PMVECs were treated with BLM, unlike the results observed when BLM-treated HUVECs were assessed. Significant differences were noted between HUVECs and PMVECs treated with 0.1 and 1µg/ml BLM for 6 hours, and 0.1µg/ml BLM for 24 hours, likely due to the apparent increase in endothelin-1 release by HUVECs under these conditions. However, high levels of standard error were seen when HUVECs were assessed, and additional experiments would likely give more consistent results. While both PMVECs and HUVECs released decreased Endothelin-1 levels compared to baseline when treated with 10µg/ml BLM, the increase seen when HUVECs were treated with the lower concentrations were not seen in PMVECs and therefore it may be said that these two cell types respond differently to BLM. The reasons for the apparent disparity between the two cell types is unknown.

These results suggest that PMVECs – a cell type more relevant to human patients receiving BLM – also express increased levels of adhesion molecules and release increased levels of IL-8 and MCP-1 when exposed to BLM. Though there were some differences between the expression profiles of these adhesion molecules and cytokines, mostly related to the total

levels of proteins expressed and release, both PMVECs and HUVECs demonstrated increases and total levels that were similar enough to suggest that HUVECs may be used as a surrogate for PMVECs in future work.

Further, that PMVECs treated with BLM express not only increased levels of ICAM-1, but also VCAM-1, builds on previous reports of PMVEC adhesion molecule expression in response to BLM (Fichtner, et al., 2004), and may allow a better characterisation and understanding of the impact of BLM on the human pulmonary vascular endothelium. Importantly, this increased molecule expression may have functional consequences. It seems logical that, as PMVEC adhesion molecule and cytokine expression is increased by BLM, then the impact of the drug on the pulmonary vascular endothelium may contribute to the inflammation that precedes BPF as immune cells are recruited to the lung vessels by chemoattractant cytokines, and recruited or already present leukocytes may then adhere to and move through the endothelium via the diapedesis cascade.

The notion that adhesion molecules expressed by pulmonary microvascular endothelial cells may induce leukocyte movement into the lung following BLM administration is strengthened by recent work. Wang, et al. (2011), for example, reported that the expression of ICAM-1 and VCAM-1 in the pulmonary vasculature of the rat is associated with an observed migration of leukocytes into the perivascular space and interstitium, while Sato, et al. (2000) noted an increase in the expression of ICAM-1 by the endothelium of the pulmonary venules and the capillaries following BLM administration in rats, which resulted in increased leukocyte rolling along the endothelium, increased leukocyte entrapment in the pulmonary capillaries (which was inhibited by a blocking antibody against ICAM-1) and increased leukocyte infiltration of the perivascular and alveolar spaces of the rats used.

This may feasibly occur in humans; the current work reports increased ICAM-1 and VCAM-1 expression by human PMVECs treated with BLM which, as in rodents, may lead to the increased trapping, migration, and accumulation of leukocytes in and through the pulmonary vascular endothelium and in the lung *in vivo* in man, leading to the inflammation that so characterises the early stages of BPF development. While immediate conclusions cannot be

drawn from these results – it is unwise to draw parallels between human and rodent work – the similarities between the adhesion molecules seen to be expressed in our work and that of Sato and Wang are striking, and highlight an area of interest for future work.

While this work used PMVECs isolated from pulmonary capillaries, venules, and arterioles, and work such as that by Wang, et al. (2011) and Sato, et al. (2000) has noted such adhesion molecule upregulation in these regions, it is considered that the majority of the leukocyte migration in the lung takes place in pulmonary capillaries (though recruitment may also occur through larger vessels). One must be careful when inferring roles for ICAM-1 in leukocyte recruitment via the capillary beds, as the involvement of neutrophil CD11/CD18 ligands, and therefore endothelial ICAM-1, in this region is entirely stimulus specific. ICAM-1 is considered to have a role in immune cell recruitment via the capillary beds when inflammation is induced by LPS, IL-1, or immune complexes, but no role if induced by hyperoxia or *Staphylococcus pneumoniae,* for example (Doerschuk, et al., 2001).

Whether pulmonary immune cell recruitment via the capillaries occurs in response to BLM in man, and if so, whether it is a CD18-dependent or independent process, requires elucidation, though it appears it may be dependent, at least in rodents (Sato, et al., 1999). This would be an interesting avenue for future research. Regardless, leukocyte recruitment may occur through the pulmonary venules and arterioles, and so increased adhesion molecule expression here may partially account for the increase in immune cells in the lung, and adhesion and transmigration from these regions is likely to be at least partially ICAM-1-CD18 interaction dependent, as this molecule is expressed in the pulmonary venules (Doerschuk, et al., 2000) and appears to have a role in rodent BPF (Sato, et al., 1999; Wang, et al., 2013).

While neither of the pro-inflammatory cytokines discussed here has been inferred in the recruitment of leukocytes to the lung vasculature in BPF, it is entirely feasible that the increased expression of MCP-1 and IL-8 increases the movement of neutrophils and monocytes to this area, and may contribute to the increased leukocyte transit into the lung observed in works such as that of Wang, et al. (2011) and Sato, et al. (2000). This would require further research to delineate, though it is a logical contribution of these cytokines, as

both are potent chemoattractants (as discussed in section 1.7.2.1 and 1.7.2.2). However, the relevance of the observed decrease in Endothelin-1 release by BLM-treated PMVECs is unknown.

Endothelin-1, in addition to being a pro-fibrotic cytokine, is also a potent vasoconstrictor (Stow, 2011), and it was reported by Sato, et al. (2000) that, although vessel diameter decreased in the early stages of rodent BPF, by the end of stage of condition (day 42), vessel diameter was increased compared to baseline. Decreased Endothelin-1 release may have contributed to this. To the author's knowledge, this is not an avenue of research that has previously been explored, but the relevance of decreased endothelin-1 expression to BPF may be an interesting topic to investigate.

Finally, as HUVECs demonstrate similar expression levels of all involved adhesion molecules, it may be possible to model the BLM-treated vasculature using this cell type. A flow-chamber model will be used in which leukocytes will be flowed over BLM-treated HUVEC monolayers (to mimic BLM-treated PMVECs), to assess not only if BLM treatment and the associated increase in adhesion molecule expression increase leukocyte adhesion to the human endothelium under flow, but also to assess which, if any, adhesion molecules are primarily responsible for any increases in adhesion seen.

6 The Functional Relevance of Endothelial Adhesion Molecule Expression in Response to BLM Treatment

6.1 Introduction

To determine the functional relevance of increased adhesion molecule expression, the adhesion of neutrophils to BLM-treated monolayers was investigated. Both neutrophils and monocytes – involved in the development of BPF - utilise adhesion molecules such as ICAM-1 and E-Selectin to roll on and adhere to the endothelium (Table 1.6) and so increased expression may mediate increased interactions. As neutrophils are readily activated in the experimental setting and are the first cell type to infiltrate the lung during BPF development, this cell type will be assessed.

6.1.1 Neutrophil Recruitment and Adhesion in the Systemic Circulation

In the systemic circulation, neutrophil rolling is mostly mediated by interactions between neutrophil ligands (PSGL-1, CD44) and endothelial selectins, such as E-selectin. Selectins bind with rapid on/off rates, with the rate dependent on the ligand to which the selectin is binding and the shear stress exerted on the cells (McEver and Zhu, 2010; Wayman, et al., 2010), and this allows transient leukocyte capture and rolling. In addition, selectins have an optimal shear at which tethering is frequent due to increased interaction (McEver and Zhu, 2010; Yago, et al., 2007) and E-selectin appears to use a triphasic system, at least when binding to PSGL-1. It was reported that, as shear increases from 0 dyn/cm^2, neutrophils increasingly interacted with endothelial E-selectin via easily-broken slip-bonds. At around 0.3 dyn/cm^2, catch-bonds (strong bonds) became more frequent as shear reached the optimum of 0.5 dyn/cm^2 and the duration of the bonds increased while the rolling velocity decreased (Wayman, et al., 2010). The slowing and tethering of leukocytes via interaction with selectins in this fashion allows may then be followed by stronger adhesion, via interactions between leukocyte integrins and endothelial ligands, such as ICAM-1.

The firm binding of neutrophil ligands such as Mac-1 (CD11b/CD18) and LFA-1 (CD11a/CD18) to ICAM-1 requires integrin activation, mediated by chemokines such as IL-8, which activates both integrins (Takami, et al., 2002; Seo, et al., 2001; Lum, et al., 2002), and was released by

BLM-treated endothelial cells in this work. Such cytokines interact with neutrophil receptors, activating ligands via outside-in G-coupled protein signaling. This alters integrin conformation from low to high or intermediate affinity conformations, allowing integrin-ligand binding (Lum, et al., 2002; Lomakina and Waugh, et al., 2010; Ley, et al., 2007; Lefort and Ley, 2012; Smith, et al., 1991; Zeilhofer and Schorr, 2000). Interestingly, neutrophil LFA-1 is also activated constitutively, though the binding of unstimulated neutrophils to ICAM-1 via LFA-1 is infrequent and brief (Smith, et al., 1989; Hentzen, et al., 2000; Green, et al., 2006). Alternatively, integrin activation may be induced by neutrophil interaction with E-selectin, as reported by Simon, et al. (2000). This group demonstrated that neutrophil-to-E-selectin binding under flow increased adhesion to ICAM-1, related to β2 integrin conformational changes via PSGL-1-E-selectin binding. Indeed, the binding of neutrophil PSGL-1 to E-selectin is now known to induce the intermediate affinity conformation of LFA-1 (Yago, et al., 2010; Zarbock, et al., 2008; Kuwano, et al., 2010), as well as both activating Mac-1 and inducing its movement to the cell surface, allowing further ligand binding upon Mac-1 activation (Simon, et al., 2000).

While neutrophils express Mac-1 and LFA-1 in equal amounts, and the blockade of neutrophil adhesion to ICAM-1 can only be achieved by blocking both (Seo, et al., 2001; Hentzen, et al., 2000; Takami, et al., 2002) the two are thought to have overlapping but differing functions, with LFA-1 required for adhesion to the endothelium, and Mac-1 required for the stabilisation of this adhesion and leukocyte crawling along the endothelium (Ding, et al., 1999; Hentzen, et al., 2000; Li, et al.,2013). However, LFA-1 and Mac-1 both appear involved in the initial rolling step of transmigration. Green, et al. (2006) stated neutrophil adhesion to ICAM-1 via LFA-1 was conformation dependent; intermediate affinity LFA-1 allowed rolling, and high affinity, adhesion, while, Chesnutt, et al. (2006) noted that, when activated by E-selectin interaction, LFA-1 was primary responsible for rolling adhesion on ICAM-1, but Mac-1 also contributed. This was supported by Ding, et al. (1999), who reported that while LFA-1 knockout mice exhibited far lower neutrophil adhesion to ICAM-1-only expressing cells, Mac-1 knockout neutrophils also decreased their adhesion, but less severely. Thus, both integrins appear to play a role in the tethering of neutrophils to ICAM-1.

Following integrin activation, neutrophils bind ICAM-1 in the presence of cations (Petruzzelli, et al., 1998) and this may then initiate ICAM-1 outside-in signaling events which stabilize this adhesion (Lum, et al., 2002; Ley, et al., 2007; Giagulli, et al., 2006). From here, neutrophil spreading and migration lead to the movement of neutrophils across the endothelium into the site of injury. Similar adhesion events may occur with VCAM-1; though interactions between neutrophils and VCAM-1 are less well defined, it has been reported that neutrophils are capable of binding to VCAM-1 via VLA-4 (Lomakina and Waugh, 2009), and the role of VCAM-1 is similar to that of ICAM-1, inducing firm adhesion, though this requires further investigation before any definite conclusions may be drawn.

6.1.2 Neutrophil Recruitment and Adhesion in the Pulmonary Circulation

However, the process of transmigration – in which cells roll, undergo firm adhesion and arrest, and eventually migrate through the endothelium - does not occur in all vessels. As discussed previously (1.8), the main site of pulmonary neutrophil sequestration – the process by which leukocytes "accumulate in the inflamed lung in preparation for migration" - is the capillary bed, an area devoid of selectins (Doerschuk, et al., 2001). Instead, neutrophil binding via integrins such as Mac-1 to endothelial ICAM-1 may promote leukocyte adhesion to the capillary endothelium (Doerschuk, et al., 2001; Aird, et al., 2007; Segel, et al., 2011), but while only ICAM-1 appears to be induced by inflammatory stimuli in the capillaries, the involvement of ICAM-1 is stimulus-dependent. It is unknown whether BLM induces ICAM-1 dependent or independent adhesion. Previous work by Sato, et al. (2000) reported increased ICAM-1 expression in rodent pulmonary capillaries in response to BLM, leading to increased leukocyte entrapment and sequestration in the vessels, and this suggests that BLM may induce a CD18-dependent migration pattern for neutrophils in lung capillaries. If this is the case, then increased neutrophil infiltration of the lung following BLM treatment may be related to increased ICAM-1 expression in the capillary beds, though other vessels may also be sites of leukocyte transmigration in the lung.

This may include pulmonary venules. Pulmonary venules utilise a more systemic-like adhesion cascade involving VCAM-1, ICAM-1, and E-selectin under inflammatory conditions, and may also be sites of neutrophil accumulation and migration (Gane and Sotckley, et al., 2011; Wang, et al., 2011; Doerschuk, et al., 2001; Aird, et al., 2007). Previous research suggests that this may have functional relevance; Wang, et al., (2011) reported increased ICAM-1 and VCAM-1 expression in the venules of BLM-treated rats, and neutrophils gathered around areas expressing the adhesion molecules. Neutrophil infiltration of the perivascular interstitium occurred via these vessels, and neutrophil infiltration of the lung was observed concurrently with adhesion molecule expression. This suggests venular ICAM-1 and VCAM-1 may support firm adhesion and promote transmigration. However, Sato, et al. (2000) reported increased ICAM-1 expression and concurrent leukocyte slow rolling in the pulmonary venules of BLM-treated mice, which was blocked by anti-ICAM-1 antibody, but firm adhesion to venular walls was not observed. Entrapment was only noted in the capillaries. However, as increased slow rolling in the venules and increased entrapment in the capillaries occurred simultaneously with increased ICAM-1 expression and increased peribronchiolar and perivascular leukocyte infiltration, increased adhesion molecule expression may have led to increased neutrophil movement of into the lung. Capillary entrapment may have played a larger role in neutrophil transmigration in this study, however, but it appears increased adhesion molecule expression permits increased infiltration.

Previous results from this work have demonstrated increased ICAM-1 and VCAM-1 expression by PMVECs in response to BLM. If such increased expression occurs *in vivo*, then this may contribute to the inflammation that precedes fibrosis. However, as the PMVECs used were isolated from both pulmonary venules and capillaries, no definitive conclusions can be drawn regarding the precise role of each molecule and each cell type in this process. By assessing whether treatment of the endothelium with BLM increased neutrophil rolling on and adhesion to the endothelium, a better understanding of how the impact of BLM on the human endothelium – particularly the endothelium of the pulmonary venules and capillaries - leads to the inflammation seen in BPF may be developed.

6.1.3 Experimental Design

To determine whether increased adhesion molecule expression by BLM-treated endothelial cells may contribute to neutrophil adhesion and infiltration *in vivo*, an *in vitro* model of circulation was used. An experimental system similar to that developed by the Nash group (Cooke, et al., 1993; Rainger, et al., 1995) and a protocol devised by McGettrick, et al. (2010) will be used. This will involve a flow chamber system, which mimics the conditions of the vasculature, and allows the generation of a confluent endothelial monolayer and the application of suspended cells at the shear stress (the force exerted on the endothelium by the flow of blood through the vessel) encountered *in vivo*. The shear required depends on the vessel modelled; venules have a shear stress of around 15 dyn/cm^2, large veins, around 5 dyn/cm^2 , and post-capillary venules, 1 dyn/cm^2 (Papaioannou and Stefanadis, 2005; McGettrick, et al., 2010). To mimic the shear stress in the lung microvasculature, including the venules and capillaries, the shear stress required would be around 1-5dyn/cm^2, although this value is not well defined or extensively researched (Kroll and Afshar-Khargan, 2012; Kuebler, 2009). Therefore, a physiologically relevant shear rate used previously in flow chamber studies will be assessed to model the rolling and adhesion of neutrophils to the endothelial monolayer when BLM and TNF-α treated.

It has been reported that a shear rate of over 1 dyn/cm^2, as well as being physiologically relevant, prevents integrin-ligand interactions, e.g., between LFA-1 and Mac-1 (CD11a/CD18 and CD11b/ CD18) and ICAM-1 (Li, et al., 2013; Hentzen, et al., 2000; Ding, et al., 1999) but permits those between leukocytes and selectins (Bahra, et al., 1998; Rainger, et al., 1995; Lawrence and Springer, 1991). As such, studies focussing on selectins often use this rate, however, this work is not focussed exclusively on selectins, but on all adhesion molecules which may be involved in leukocyte adhesion to, and transmigration though, the endothelium.

It has been suggested that ICAM-1 binding may be an important mode of neutrophil migration in vessels with low shear, such as in the lung (Hentzen, et al., 2000). Although it is often stated that neutrophil adhesion to ICAM-1 without initial binding by selectins does not

occur (Chesnutt, et al., 2006; Simon, et al., 2000), experimental work has shown that neutrophil adhesion to ICAM-1 may occur at shear stresss of up to 1 dyn/cm^2, though increasing shear stress decreased neutrophil adhesion to, and spreading on, the ICAM-1 substrate monolayer, and a shear rate of between 0.2 and 0.5 dyn/cm^2 resulted in a greater number of adherent neutrophils (Zhan, et al., 2012). Similarly, Lawrence and Springer (1991) reported a slight binding of neutrophils to ICAM-1 at shear stresss of up to 0.3 dyn/cm^2; this may contribute to the movement of neutrophils to sites of injury under low shear stresss.

As the shear in the pulmonary capillaries is likely to be extremely low because cells deform to traverse these vessels; neutrophils roll on ICAM-1 and VCAM-1 in pulmonary venules, at least in rodent models; the shear stress in post-capillary venules in man is around 1 dyn/cm^2; and lung capillaries (and indeed unstimulated lung venules) lack selectins, so neutrophil adhesion related to E-selectin mediated integrin activation will not occur in these vessels, using a shear of over 1 dyn/cm^2 - which precludes ICAM-1-neutrophil interactions - cannot model the effects of increased adhesion molecule expression in the lung. Therefore, a range of shears, between 0.1 dyn/cm^2 and 1 dyn/cm^2 will be trialled.

As treatment of endothelial cells with BLM appeared to increase the expression of endothelial E-selectin, ICAM-1, and VCAM-1 in both 6 and 24 hour experiments, increased neutrophil adhesion to the monolayer may be observed when neutrophils are flowed over BLM-treated endothelium. The adhesion of neutrophils to BLM-treated endothelium will therefore be assessed. As several adhesion molecules were noted to be expressed at increased levels by BLM-treated endothelial cells, and the shear stress used will not prevent adhesion mediated by any one molecule, work will be conducted to determine the adhesion molecules responsible for any observed adhesion. Blocking studies using the anti-CD18 antibody TS1/18, which blocks the CD18 component of both LFA-1 and Mac-1 will assess the contribution of ICAM-1 to neutrophil adhesion, while E-selectin function blocking antibody P2H3 will assess this molecule's contribution to neutrophil adhesion under flow.

6.2 Materials and Methods

6.2.1 Construction of the flow chamber system.

µ-Slide I 0.4 Luer flow chambers (ibiTreat, tissue culture treated, sterile), sterile silicone tubing with an internal diameter of 1.6mm and Luer elbow connectors were purchased from Thistle Scientific (Glasgow, United Kingdom). A 50ml glass syringe was purchased from Hawksley (Lancing, Sussex, United Kingdom). BD Connectas, 10ml plastic syringes, male-male, and female-female connectors were a kind gift from Dr. Rob Bennet (Perfusion, Castle Hill Hospital, Cottingham, United Kingdom). Uncoated slides were used, as typical of previous work (Y.P. Xiao, personal communication), rather than collagen-coated slides.

This equipment was combined to create an artificial flow system through which cell suspension could be flowed over an endothelial monolayer within the flow chamber according to instruction from Dr. Yu Pei Xiao (personal communication, as shown in Fig. 6.1). The 10ml plastic syringes were elevated and held in place using a clamp stand. The 50ml glass syringe was fitted to a Harvard 2000 PHD pump set to withdraw the cell suspension at a rate of 3.8ml/min initially, to generate a shear stress of 5 dyn/cm^2 within the flow chamber, as determined by the manufacturers of the flow chambers (see application note 11, ibidi). Various flow rates, and hence various shear stresss, were used throughout these experiments.

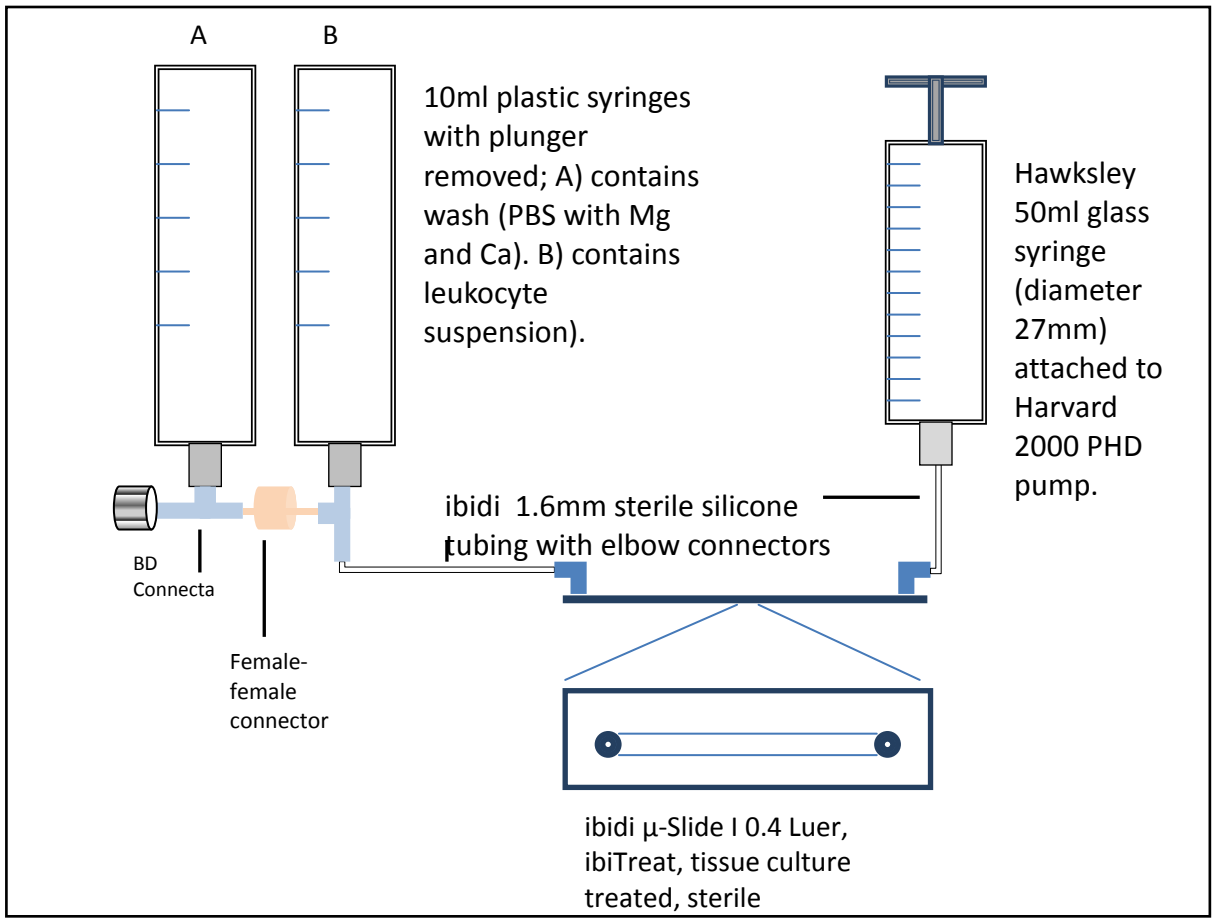

Figure 6.1: A schematic representation of the flow chamber system.

A schematic representation of the set-up used through the flow chamber experiments. The 50ml glass syringe was attached to a Harvard PHD 2000 pump while experiments were running. The 10ml syringes were suspended from a clamp stand to allow ready flow of cell suspensions.

6.2.2 Optimisation of confluent monolayer creation and exposure to shear flow.

HUVECs were cultured to near-confluence (90% confluent) in accordance with ibidi application note AN13 and were used between passage 3 and 5. Cell culture was conducted as outlined in 2.1. When around 90% confluent, cells were dissociated from culture flasks and centrifuged as outlined in 2.2 and 2.3. Cells were then counted using haemocytometry as

outlined in 2.4, and re-suspended in endothelial cell basal medium. Cell suspension (100µl) was then pipetted into the flow chambers.

Caps were then placed securely over the media reservoirs of the flow chamber and the chambers incubated for 15 minutes to allow the cell suspension to equilibriate within the chamber and to cells to begin to adhere to the flow chamber, as outlined in application note AN13, after which time, 60µl of fresh media was added to each reservoir.

To ensure humidity in an otherwise open system, flow chambers were placed within a large petri dish containing sterile padding moistened with sterile deinionised water (produced in-house). The lid was then secured on top of the petri dish and the petri dish placed inside the incubator in an atmosphere containing 5% CO_2 at 37°C . Cells were checked after four hours using a light microscope to ensure cell adherence and determine confluence. Four hours was selected as this was demonstrated to be sufficient time for seeded cells to adhere to the flow chamber and begin to form a layer in ibidi Application Note AN13.

6.2.2.1 Capture of Images of Flow Chambers

All photographs were taken using the QCapture Pro version 6 software. In brief, flow chambers were placed on the stage of a light microscope (Nikon Eclipse TS100, Nikon, Tokyo, Japan) and an attached camera (QImaging Retiga 2000R Fast1394, QImaging, Surrey, Canada) was switched on. The QCapture software was opened and the cells visualised on screen. Using the “single photograph” or “multiple photograph” setting, images were obtained and saved as .png files. These files were then converted and saved as .jpg files.

6.2.2.2 Optimisation of the Ideal Seeding Density

Once cultured, dissociated, and counted, cells were re-suspended to variety of concentrations: $2.5x10^5$, $5x10^5$, $7.5x10^5$, $1x10^6$, $1.75x10^6$, $2.5x10^6$ per ml. An aliquot (100µl) of cell suspension was pipetted into the ibidi µ-slide $I^{0.4}$ Luer flow chamber, to give a total

concentration of $1x10^4$, $2x10^4$, $3x10^4$, $4x10^4$, $7x10^4$, and $1x10^5$ cells per cm of growth area within the flow chamber (total growth area, $2.5cm^2$), thus a total per-slide cell count of $2.5x10^4$, $5x10^4$, $7.5x10^4$, $1x10^5$, $1.75x10^5$, $2.5x10^5$ per slide. The flow chambers were then placed in an incubator as outlined in 6.2.2. After four hours, the cells were removed from the incubator and visualised as outlined in 6.2.2.1. Photographs were taken, and the concentration that resulted in the best confluence was noted. All experiments were carried out in triplicate.

6.2.2.3 Impact of Incubation Time on Monolayer Confluence

It was then determined whether increased incubation time impacted confluence. Cells were seeded at the concentrations described in 6.2.2.2 and cultured for four, 12 or 24 hours as outlined in 6.2.2. The confluence and adhesion of cells incubated for each time point was then assessed as outlined above. All experiments were carried out in triplicate. Cells were then removed from the incubator and visualised as outlined in 6.2.2.1. The concentration and incubation time which resulted in the most favourable cell confluence were assessed via visualisation as described in 6.2.2.1.

6.2.2.4 Impact of a Full Media Change on Monolayer Confluence

To determine whether a full media change improved the condition of the monolayers achieved, cells were seeded into the flow chambers at the four highest concentrations as outlined in 6.2.2.2, and incubated for four hours as outlined in 6.2.2. These cells were also subjected to a full media change after four hours of incubation. A full media change was performed by carefully aspirating all media from the flow chamber using a pipette tip. Fresh endothelial cell basal medium (220µl) was then pipetted into the chamber and the chamber placed back inside the petri dish in the incubator. The confluence of the monolayer was then either immediately assessed, or the flow chambers were placed back in the incubator and allowed to incubate for a further 8 hours or 20 hours, to give a total incubation time of 12

and 24 hours as outlined in 6.2.2.3, prior to assessment via visualisation and photography, as outlined in 6.2.2.1. All experiments were carried out in triplicate.

6.2.2.5 HUVEC Monolayer Stability in Response to Shear

The stability of HUVEC adhesion to the uncoated ibidi flow chamber when seeded at $1.75x10^6$ and $2.5x10^6$ per ml ($1.75x10^5$ and $2.5x10^5$ per slide) and incubated for 24 hours was then assessed. The flow chamber was then attached to the flow system as shown in Fig. 6.1. The Harvard 2000 PHD pump was set to withdraw room temperature PBS over the cells at a shear stress of 5 dyn/cm^2 in the centre of the flow chamber channel. This was achieved by programming the Harvard 2000 PHD pump to withdraw 3.8ml/min with the diameter function set to 14.5mm, the diameter of the Hawksley 50ml glass syringe. This withdrawal rate was chosen according to the manufacturer's instructions (ibidi application note 11), which was determined by ibidi based on the equation, derived by Cornish (1928).

Cells were photographed using the QCapture Pro software, as outlined in 6.2.2.1, prior to the beginning of flow. Under conditions of flow, photographs were taken using the software at 15, 30, 60, 120, 180, and 240 seconds. The stability of adherence was determined by analysing the images and determining the number of cells lost under flow conditions. In later optimisation experiments, cells were also exposed to a shear flow rate of 1 dyn/ cm^2 by drawing PBS over the cells within the flow chamber at a rate of 0.72ml/min.

6.2.2.6 Deciding upon Incubation Time and Seeding Density

In all future experiments, cells were seeded at the density which resulted in the best confluence (1 x 10^5 cells/cm^2, $2.5x10^6$ cells per ml) and incubated for the time which resulted in the best confluence and cell viability (24 hours).

6.2.3 Ability to Withstand TNF-α and BLM Treatment.

To ensure treatment with BLM and TNF-α did not impact cell viability within the chamber, cells were cultured as outlined in 6.2.2.6, before being treated with various concentrations of BLM and TNF-α. In brief, culture medium was aspirated and replaced with culture medium containing either 0.1, 1, or 10µg/ BLM, or 10ng/ml TNF-α. Cells were allowed to incubate in either BLM or TNF-α for six or 24 hours.

In cells treated for 24 hours with all concentrations of BLM and 10ng/ml TNF-α, the initial BLM or TNF-α-containing media was removed after 4 hours and replaced with identical BLM or TNF-α-containing media, to eliminate the possibility that changes in adhesion of viability were due to senescence or cell stress due to spent culture medium.

The viability of cells and the quality of the monolayer was assessed as outlined in 6.2.2.1. In addition, the ability of TNF-α and BLM-treated cells to withstand shear stresss of 5 dyn/cm^2 was assessed as outlined in 6.2.2.4 and visualised accordingly.

6.2.4 Neutrophil isolation

Neutrophils were isolated based on a modified version of the protocol outlined in Rainger, et al. (1995) and also via single-step density gradient. Whole blood was collected by venepuncture of consenting healthy volunteers and was collected into a syringe containing sufficient anticoagulant acid citrate dextrose (ACD) to give an overall concentration of 20% ACD in whole blood. Blood collection was kindly performed by members of the Hull Platelet Research Group. Neutrophils were then isolated using either a two-step or a single-step density gradient. All gradients were conducted in polypropylene tubes to prevent granulocyte adherence to the plastic, and all reagents were used at room temperature.

A two-step density gradient consisting of 7.5ml histopaque 1119 and 7.5ml histopaque 1077 (Sigma Aldrich, Poole, UK) was overlaid with 15ml whole blood diluted 1:1 in 1x PBS without calcium and magnesium. This was centrifuged at 800 x *g* for 30 minutes at room temperature

using an Eppendorf 5207 centrifuge. The plasma layer was then removed and plasma (10ml) was filtered through a 0.45µm syringe into a falcon tube. Neutrophils were isolated and transferred into a 50ml falcon tube containing 1x PBS (without calcium and magnesium) with 5% autologous plasma (10ml). Neutrophils were then washed by centrifugation for ten minutes at 800 x *g*.

When using the single-step density gradient, 15ml diluted whole blood was layered over 15ml histopaque 1077. This was centrifuged at 400 x *g* for 30 minutes at room temperature using an Eppendorf 5207 centrifuge. The plasma and PBMC layers were removed leaving only the erythrocyte pellet containing the neutrophils. Erythrocyte lysis was carried out by adding 40ml deionised water (pH 6.8) and agitating the pellet gently. 10x PBS (3.6ml) was added to restore the isotonicity, and the cells were centrifuged for ten minutes at 800 x *g* to generate a neutrophil pellet. Lysed erythrocytes were discarded

In both cases, the neutrophil pellet was then suspended in 1x PBS with calcium and magnesium, 0.15% bovine serum albumin, and 5mM D-glucose (henceforth referred to as supplemented PBS) (5ml) and the number of cells counted using a haemocytometer as previously outlined.

To ensure the purity of the cells isolated (i.e., that neutrophils were not contaminated with lymphocytes or mononucleocytes, and that ≤50% of cells in the sample were erythrocytes), a cytospin experiment was carried out. The cell suspension was adjusted to a concentration of $1x10^6$/ml and 100µl was applied to a Polysine slide (Thermo) using a plastic funnel attachment. The slide was centrifuged in a Cytospin 3 cytocentrifuge (Shandon, Thermo Shandon, Cheshire, UK) for five minutes at 800rpm. The slide was air-dried for up to half an hour and dyed using the Rapi-Diff staining kit (Atom Scientific, Cheshire, UK). In brief, the slide was fixed using methanol (five second exposure), and stained by exposing for five seconds each to eosin and methylene blue dyes. The slide was then washed and allowed to air dry for up to 30 minutes before mounting using DPX mounting medium (Fluka Biochemika, Buchs, Switzerland) and visualisation using light microscopy. Neutrophils were identified by the multi-lobed nucleus. Cytospin slides were generated for all experiments. A

modicum of erythrocyte contamination was permitted as erythrocytes are non-adherent cells under normal conditions (see section 6.4.3).

Neutrophils were then suspended in supplemented PBS to a concentration of $5x10^5$ cells/ml and loaded into the 10ml plastic syringe shown in Fig. 6.1, ready to be used for the flow chamber experiments.

6.2.4.1 Identification and Consenting of Volunteer Blood Donors

Ethical approval was gained from Hull York Medical School for the collection of blood from healthy volunteer donors (see approval 13 09 – The Immunology of Bleomycin-Induced Pulmonary Fibrosis, Appendix B, Figure B.I). Ethical approval for all documentation associated with this work (Patient Information Sheet, Patient De-briefing Sheet, Consent Form) was obtained from Hull York Medical School.

Healthy volunteer blood donors were identified from donor lists used by the Hull Platelet Research Group. Donors were approached and consented using the consent form (v1.1). All donor information was anonymised and no donor identifiers were used to label collected data. Instead, donors were assigned a four-digit code (e.g., 0001) at the time of consent, and this code only was used to identify the data once collected. Donor identifiers were re-used if the donor gave blood on more than one occasion. Donor samples were not screened for blood-borne viruses (as outlined in the patient information sheet (v1.1).

All attempts were made to gender-match, age-match and ethnicity-match donors used in experiments. In all cases (with the exception of neutrophil flow over 6-hour treated endothelial monolayers, which contained two females and one male), each donor group contained two males and one female. In all cases (with the exception of neutrophil flow over 24-hour treated endothelial monolayers, which contained three caucasian donors), all groups contained two caucasian donors and one East Asian donor. All donors who gave blood in the experiments which were used in the final data were between the ages of 18 and 40 years.

6.2.5 Optimisation of Shear Flow Rate

HUVECs were cultured, dissociated, centrifuged, and counted, as outlined in 6.2.2. Cells were re-suspended to a concentration of $2.5x10^6$ per ml and seeded into the flow chamber as outlined in 6.2.2.2. These were allowed to incubate for 24 hours to ensure a confluent monolayer and were treated with 10ng/ml TNF-α or left untreated, for six hours, as outlined in 6.2.3. Neutrophils were isolated using the single-step density gradient as shown in 6.2.3, the re-suspended to a concentration of 5 x 10^5/ml prior to use.

The neutrophil suspension and wash buffer (supplemented PBS) was added to each empty plastic syringe as shown in Fig 6.1. Tubing was connected and wash buffer allowed to flow through the tubing for 10 seconds at 10ml/min to ensure no air bubbles were present in the tubing. The tubing was then connected to the flow chamber and the flow chamber was washed out by allowing the flow of wash buffer to pass over the monolayer for 30 seconds at 3.8ml/min (5 dyn/cm^2). This was followed by a wash-through of the neutrophil suspension for the same time at the same flow rate. The neutrophil suspension was then allowed to flow over the monolayer for 80, 160, 800, and 1600 seconds at a flow rate of 0.76 ml/min (1 dyn/cm^2), 0.38 ml/min (0.5dyn/cm^2), 0.076 ml/min (0.1 dyn/cm^2), and 0.038 ml/min (0.05 dyn/cm^2) prior to photographing, to ensure $1x10^6$ neutrophils were present in the chamber. The adhesion of neutrophils to the monolayer at each of these rates was assessed as outlined in 6.2.6 and compared.

6.2.6 Data Collection and Offline Analysis of Obtained Photographs of Cell Adhesion Under Flow

When assessing neutrophil adhesion to endothelial monolayers under flow conditions, photographs were taken at five sites along the mid-line of the flow chamber (as outlined in Fig. 6.2). At each site, one photograph was taken per second for a total of twenty seconds, giving twenty photographs. This was achieved by placing the flow chamber on the stage of the aforementioned light microscope and using the QCapture Pro 6 software. The software

was then set to take one photograph per second for a total of twenty photographs. This allowed a snap-shot of the neutrophil adhesion activity in this field to be recorded. All images were recorded moving left-to-right, i.e. the field furthest from the entrance reservoir was recorded first. Each series of 20 photographs required a time period of 20 seconds. Data assessment was carried out offline.

In brief, the .TIFF files generated by the programme were downloaded and converted into .JPEG files using Serif Photoplus 10. Photographs were then loaded into Microsoft Picture Manager and played in a loop to detect adhering and rolling cells. These photographs were also loaded into Microsoft Word to determine the distance travelled by rolling cells. Adherent, rolling, and spreading neutrophils were then identified.

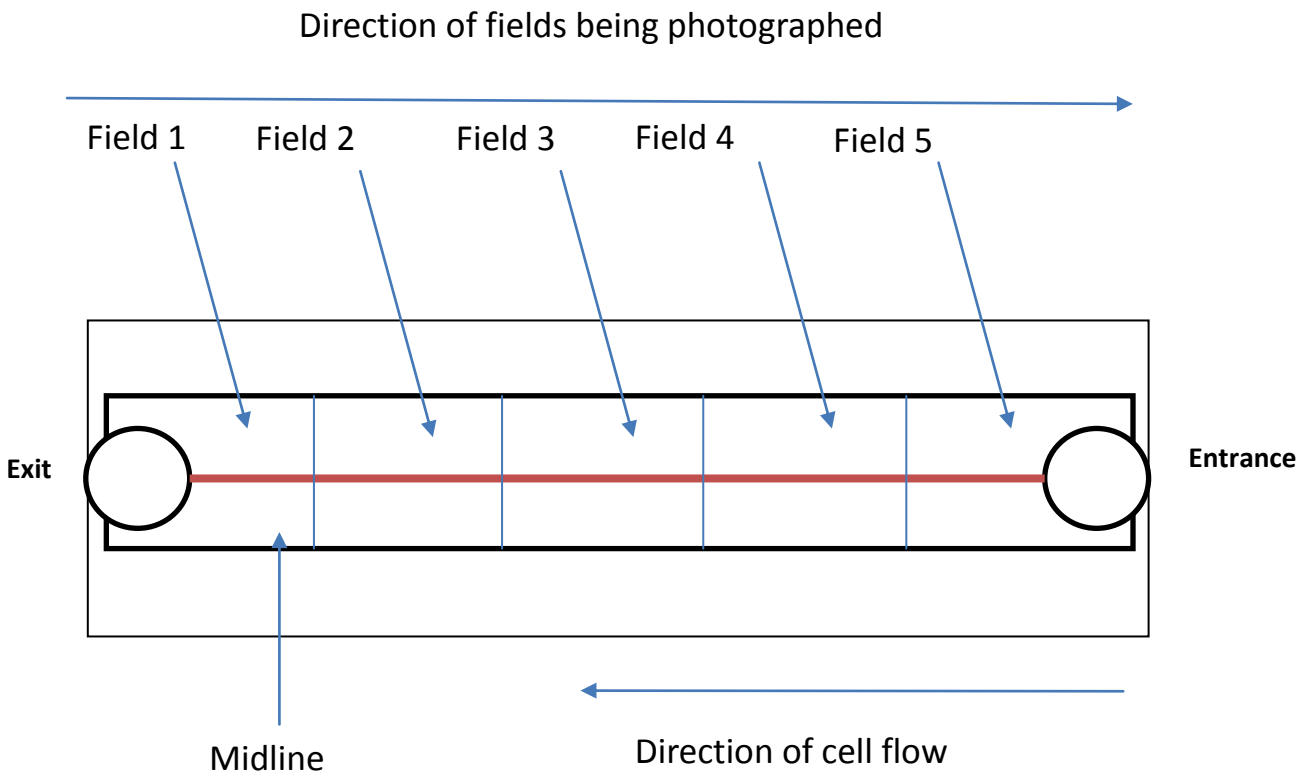

Figure 6.2: A schematic plan of image collection for flow chamber experiments.

A schematic of how fields were photographed during flow chamber experiments. 20 pictures were taken in each field, along the midline which could be easily distinguished within the flow chambers. Pictures were taken against the direction of flow due to ease of photography.

6.2.6.1 Identification of Cell Adhesion Events from Obtained Images

Cells were identified by their appearance. Identification was conducted manually as software to automatically detect neutrophils was not available. Adherent neutrophils were identified as small, round, phase-bright cells, clearly distinguisahble from endothelial cells and not moving along the endothelium (Fig 6.3A). Spreading neutrophils were identified as partially bright-phase (around the edges of the cell, but not as bright as adherent non-spreading cells), and larger but not clearly round, as outlined by Zhan, et al. (2012) (Fig 6.3B). Spreading neutrophils were also not seen to move along the endothelium. This spreading behaviour was rare compared to adherent and rolling cells; in a representative field, only one event out of 21 detected events was a spreading neutrophil, the others all being adherent or rolling. However, the spreading neutrophil events also required taking into account. Rolling neutrophils were identified as phase bright cells moving slowly along the endothelium.

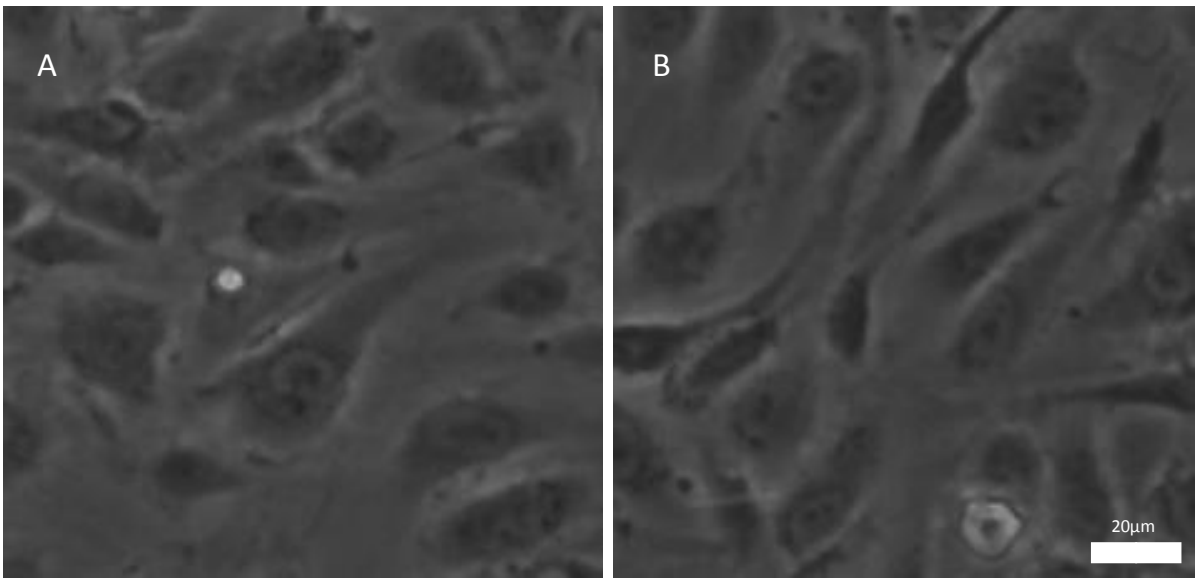

Figure 6.3: Adherent and spreading neutrophils as seen in flow chamber experiments.

An adherent (left) and a spreading neutrophil (right), as outlined by McGetterick, et al. (2010) and Zhan, et al. (2012). Both images were obtained from photographs taken in this work. More images of adherent neutrophils can be found in the appendix.

Erythrocytes were identified as small cells which did not adhere to the endothelium and, though visible under light microscopy, appeared phase-dark when viewed using the QCapture Pro 6 software. These cells were moving rapidly, appeared to "tumble" through the chamber, were therefore not as round as neutrophils, and did at no point adhere to the endothelium. Non-adherent neutrophils could be clearly identified as white, phase-bright blurs moving accross the screen when the images were played in a loop (McGettrick, et al., 2010) using Microsoft Picture Manager. Images of these cells are not shown due to the extreme difficulty of obtaining clear images when cells are flowing along the chamber. However, the supplementary videos of neutrophil suspension (marked as 9.4 in the appendix and submitted as a supplemenary disc) submitted with this thesis shows non-adherent neutrophils travelling along the flow chamber, appaearing as white streaks.

The nature of rolling neutrophils was also considered. Rolling cells were considered slow rolling if the velocity of the cells - as determined by measuring the distance travelled when images were loaded into Microsoft Word - was at a velocity of ≤10µm/sec. Phase-bright spheres moving along the endothelium (clearly visible spheres moving at a velocity of ≥10µm /sec when measures as outlined above) were regarded as rolling events. These two types of cells were combined to give the total number of rolling neutrophils. On occasion, granulocytes would appear to adhere to the endothelium in one still, but not be present on the next still. These were regarded as non-adherent and non-rolling, and their presence attributed to screen-capture timing. Such events were not included in the analysis based on the protocol of McGettrick, et al. (2010).

The number of adherent, rolling, or spreading neutrophils was counted and totalled to give the total number of adherent neutrophils in a given field. Events on photographs that did not fit any of these profiles were regarded as not being neutrophil adhesion events, and so were not counted as such.

6.2.7 Assessment of Neutrophil Adhesion to Endothelial Monolayers under Flow

Cells were cultured, removed from culture flasks, centrifuged, and counted as outlined above in 6.2.2. Cells were suspended to a concentration of $2.5x10^6$ and 100µl of cell suspension was pipetted into each flow chamber used. The flow chambers were incubated for 15 minutes, after which time, media was added to the reservoirs, and were subject to a full media change after 4 hours. Chambers were then incubated for a further 20 hours to permit monolayer formation. When confluent, cells were treated with BLM and TNF-α for 6 and 24 hours, as required, as outlined above. Cells treated with TNFα and BLM for 24 hours were subjected to a media change at 6 hours.

The flow chamber system was set-up as shown in Figure 6.1. Tubing was attached to the syringe and wash buffer flowed through at 10 ml/min to ensure no air bubbles were trapped in the tubing. Tubing was then connected to the flow chamber, which was attached to the microscope stage. Wash buffer was run through the flow chamber at a flow rate of 3.8ml/min (5 dyn/cm^2) for 30 seconds to remove any non-adherent endothelial cells and all culture medium. Following this initial wash-out step, granulocyte-containing cell suspension was run through the system at a flow rate of 3.8ml/min (5 dyn/cm^2) for 30 seconds to ensure cell suspension was present in the tubing and the flow chamber, and to remove any "dead space" in the tubing. This flow rate will allow 1 x 10^6 granulocytes to have entered the experimental set-up, but at a velocity and shear sufficient to prevent any unwanted granulocyte adhesion to the endothelial monolayer.

The flow rate was then decreased to 0.38ml/min (0.5 dyn/cm^2) for 160 seconds and neutrophils were allow to pass through the chamber. During this period, 5 x 10^5 neutrophils will have passed through the chamber at a rate slow enough to allow adhesion or rolling on the surface of the cells, and the shear rate required will have been achieved and maintained.

Photographs were then taken along the midline as outlined in figure 6.2 and section 6.2.6. Each series of 20 photographs (five series in total) required a time period of 20 seconds. A gap of 20 seconds was left between each field to allow a further $5x10^5$ cells to have entered

the chamber by the end of the experiment. By the time the final field was photographed, a total of 1 million cells had entered the flow chamber at a shear rate low enough to permit adherence (2 million cells in total when the initial perfusion at 5 dyn/cm^2 is included).

Following the recording of adhesion under flow conditions as further granulocytes entered the chamber, the valves were switched and wash buffer allowed to flow into the chamber. The wash buffer was flowed through at a 0.38 ml/min (0.5 dyn/cm^2) for 180 seconds. Fields were then recorded as outlined above to determine the levels of firm adhesion and rolling adhesion along the endothelial monolayer when further granulocytes were not being introduced into the chamber. Though this data was recorded, this was not used in final results.

Data analysis was carried out offline. Total numbers of adherent, slow-rolling, and rolling cells were recorded from each series of stills and outlined in 6.2.6. The results of each experiment were expressed as the mean number of adhesion and rolling events per field (field size 1mm^2). Five fields were photographed per slide, and three slides per treatment were assessed; therefore the mean is the average number of events determined from the assessment of 15 fields under each treatment condition. Though normalisation for the number of cells present within the chamber (correction to number of cells/mm^2/10^6 cell infused) has been carried out by other groups previously (McGettrick, et al., 2010; McGettrick, et al., 2009; Luu, et al., 2000), it was found in this work that the number of cells did not impact the number of adherent events, but that the field analysed did (with fewer adhesion events noted at the entry and exit points of the chamber). Therefore, normalisation was deemed inappropriate. Data were analysed using Mann-Whitney-U tests in SPSS v. 19 statistical analysis software.

6.2.8 Generation of neutrophil adhesion movies.

Converted TIFF files were converted into movies using the Ulead Video Studio (version 10; Corel, Ottawa, Canada). Movies of neutrophil adhesion to endothelial monolayers are found in the accompanying material (Disc A) provided with this document (described in A.IV).

6.2.9 Treatment of isolated neutrophils with anti-CD18 antibody and isotype control.

Neutrophils were isolated using a single density gradient as previously described (section 6.2.4) and counted using haemocytometry. Neutrophils were then re-suspended to a concentration of $4x10^6$ cells/ml in supplemented PBS. To differentiate between neutrophils and erythrocytes when cells were counted, cell suspension was mixed with 3 x PBS. Crennilated erythrocytes could be easily detected by haemocytometry and so were rapidly differentiated from neutrophils.

To the cell suspension, anti-CD18 antibody (clone TS1/18), isotype IgG1κ (low endotoxin, azide-free, Biolegend) or Mouse IgG1κ isotype control (low endotoxin, azide-free, Biolegend) antibody was added to a final concentration of 20μg/ml.

TS1/18 is a widely used allosteric antibody (Zhang, et al., 2012) which blocks the CD18 component of the CD11a/CD18 and CD11b/CD18 (LFA-1 and Mac-1) ligands of ICAM-1, expressed on neutrophils. TS1/18 has been demonstrated to block the adhesion of both lymphocytes and leukocytes to activated endothelial monolayers (van Epps, et al., 1989; López Farré, et al., 1993; Meerschaert and Furie, 1994; Smith, et al., 1989; Carmona, et al., 2008) and the binding of leukocytes, ligand-transfected cells, and immobilised CD18 ligands to ICAM-1 (Smith, et al., 1989; Zhang, et al., 2008; Xu, et al., 2013). Previous reports have suggested that TS1/18 is capable of preventing leukocyte adhesion to inflammatory-mediator stimulated endothelial cells by between 20-50% (van Epps, et al., 1989; Smith, et al., 1988; Meerschaert and Furie, 1993; López Farré, et al., 1993), and so whether ICAM-1 mediates the adhesion of neutrophils to BLM-treated endothelium in this model, and the efficacy of this antibody in blocking neutrophil adhesion to TNF-α-treated endothelium in this series of experiments, was assessed.

Neutrophils were incubated with the TS1/18 antibody at room temperature in the dark for 30 minutes to allow binding. The neutrophils were then washed in supplemented PBS (3 times the original volume of neutrophils) by centrifugation at 800 x g for 10 minutes. TS1/18-treated cells were re-suspended to a concentration of $5x10^5$ neutrophils/ml and used in flow

chamber experiments as described in 6.2.7. Following incubation with antibodies, cytospin slides were generated to ensure neutrophils were still present in the suspension, and had not become activated during the incubation with the antibodies use in this experiment. Neutrophils were again counted as outlined in 6.2.4, and were then used for flow chamber experiments as previously outlined (section 6.2.4). Images were captured and analysed offline as previously described (section 6.2.6). Only 6-hour experiments (incubation with BLM or TNF-α, or left untreated, for 6 hours) were conducted. Only concentrations of 1 and 10μg/ml BLM were used in this series of experiments. Data were analysed using Mann-Whitney-U tests in SPSS v. 19 statistical analysis software.

6.2.10 Optimisation of anti-CD62E Treatment of Endothelial Monolayers

Endothelial cells were cultured, dissociated from culture flasks, counted, seeded into flow chambers at a concentration of $2.5x10^6$ cells/ml, and incubated with media changes as previously outlined. After 24 hours of incubation, culture medium was removed and replaced. Images of the monolayer were obtained prior to, and after, the change of culture medium. Cells were then incubated for 30 minutes, 1 hour, 2 hours, and 4 hours. Chambers were then subjected to flow to determine the stability of the monolayer. The chamber was placed on the microscope stage and the chamber connected to the flow chamber system. Images of the monolayer was captured prior to flow beginning. Cells were then subjected to flow at a shear stress of 0.5dyn/cm^2 for one minute. Five images were obtained along the flow chamber after this period. Cells were then subject to 5 dyn/cm^2 shear for one minute. Images were again captured after this period.

6.2.11 Treatment of endothelial monolayers with anti-CD62E antibody and isotype control.

Endothelial cells were cultured, dissociated, counted, transferred to flow chambers at a concentration of $2.5x10^6$ cells/ml ($2.5x10^5$ per slide), and incubated with media changes as

outlined in 6.2.7. Cells were incubated for 24 hours. Prior to use in experiments, culture medium was aspirated and replaced by culture medium containing appropriate concentrations of BLM and anti-CD62E antibody (clone P2H3) (isotype IgG1κ) (to a final concentration of 20μg/ml) (Novus Biologicals, Cambridge, UK) or Mouse IgG1κ isotype control (as described in 6.2.9).

P2H3 is a widely used anti-CD62E antibody, and has been reported to block the adhesion of polymorphonucleocytes to LPS-treated HUVECs under flow by approximately 90% (Ploppa, et al., 2010), and the binding of metastatic tumour cells (HAL-24Luc cells) to endothelial monolayers to a similar degree (Martin-Satué, et al., 1998). The binding of leukocytes to VEGF-treated endothelial monolayers was also reduced by approximately 30% when HUVECs were treated with P2H3 (Kim, et al., 2001), and so even though there is no literature explicitly investigating the blockade of neutrophil adhesion to endothelial cells by P2H3, it may be expected that treatment with P2H3 would decrease such adhesion.

HUVECs were incubated for 6 hours in antibody plus treatment (BLM or TNF-α) containing medium to ensure the endothelial cell monolayer had stably re-adhered to the flow chamber and to mirror the time used for incubation with BLM previously. Only 6-hour experiments (incubation with BLM or TNF-α, or left untreated, for 6 hours) were conducted. Only concentrations of 1 and 10μg/ml BLM were used in this series of experiments.

Neutrophils were isolated and counted as previously described using the single-step density gradient technique (section 6.2.4). Neutrophils were then re-suspended in supplemeneted PBS to a concentration of $5x10^5$ cells/ml and used in flow chamber experiments as previously described (section 6.2.7). In this series of experiments, untreated neutrophils were flowed over isotype control and P2H3-treated endothelial monolayers to determine whether blocking endothelial adhesion molecules prevented neutrophil adhesion to the monolayers. Photographs of the endothelial monolayer as neutrophils were flowed through the flow chamber were acquired as outlined previously. Data analysis was carried out offline as previously described (section 6.2.6). Data were analysed using Mann-Whitney-U tests in SPSS v. 19 statistical analysis software.

6.3 Results

6.3.1 The Impact of Seeding Density, Incubation Times, and Media Changes on the Generation of Confluent Monolayers

Initially, optimisation experiments were carried out to determine the ideal cell-seeding concentrations for this work. Though the manufacturer suggested seeding at a concentration of 3-7x 10^5 cells/ml (3-7 x10^4 cells per slide, 1.2-2.8x10^4 cells/cm^2), only 50% confluence would be acheived after 24 hours, and in these experiments, a rapidly confluent monolayer was desirable. Therefore, several concentrations were trialled, to determine seeding concentration that would generate a monolayer able to withstand shear after 24 hours. The concentrations trialled were 2.5 x 10^4, 5 x 10^4, and 7.5 x 10^4, 1 x 10^5, 1.75 x 10^5, and 2.5 x 10^5 cells per slide (2.5 x 10^5, 5 x 10^5, 7.5 x 10^5, 1 x 10^6, 1.75 x 10^6, and 2.5 x 10^6 cells/ml). Each slide held 100µl of cell suspension.

After seeding the cells at the concentrations outlined above, slides were incubated for 4 hours and the adherence of the cells and the confluence of the monolayer was assessed. However, no concentration produced a fully confluent monolayer (Fig 6.4). Thereafter, longer incubation times (12 and 24 hours) were trialled. Increasing incubation time appeared to increase the confluence of cells seeded at highest concentrations to some degree (Fig. 6.5), though it is possible that cells merely adhered and spread more. The confluence of the monolayer generated by the two lowest concentrations (2.5 x 10^4, 5 x 10^4) did not appear to alter at all with even 24 hour incubation (Fig. 6.6). No further optimisation was carried out using these concentrations.

Although ibidi Application Note 13 (AN13) states that a media change is only required every 24 hours, it was observed that, after 12 and 24 hours with no media change, cells began to look stressed – acquiring spindle-shaped, elongated morphologies, rather than the characteristic cobblestone morphology (Fig 6.9A, 6.9B). Therefore, it was assessed whether a media change after 4 hours of incubation would improve the monolayer produced when cells were seeded at a density of 7.5 x 10^4, 1 x 10^5, 1.75 x 10^5, and 2.5 x 10^5 cells per slide. It

appeared that at the higher seeding concentrations, a media change improved the condition of the monolayer achieved (Fig 6.8) and did not wash away adherent cells (Fig. 6.7).

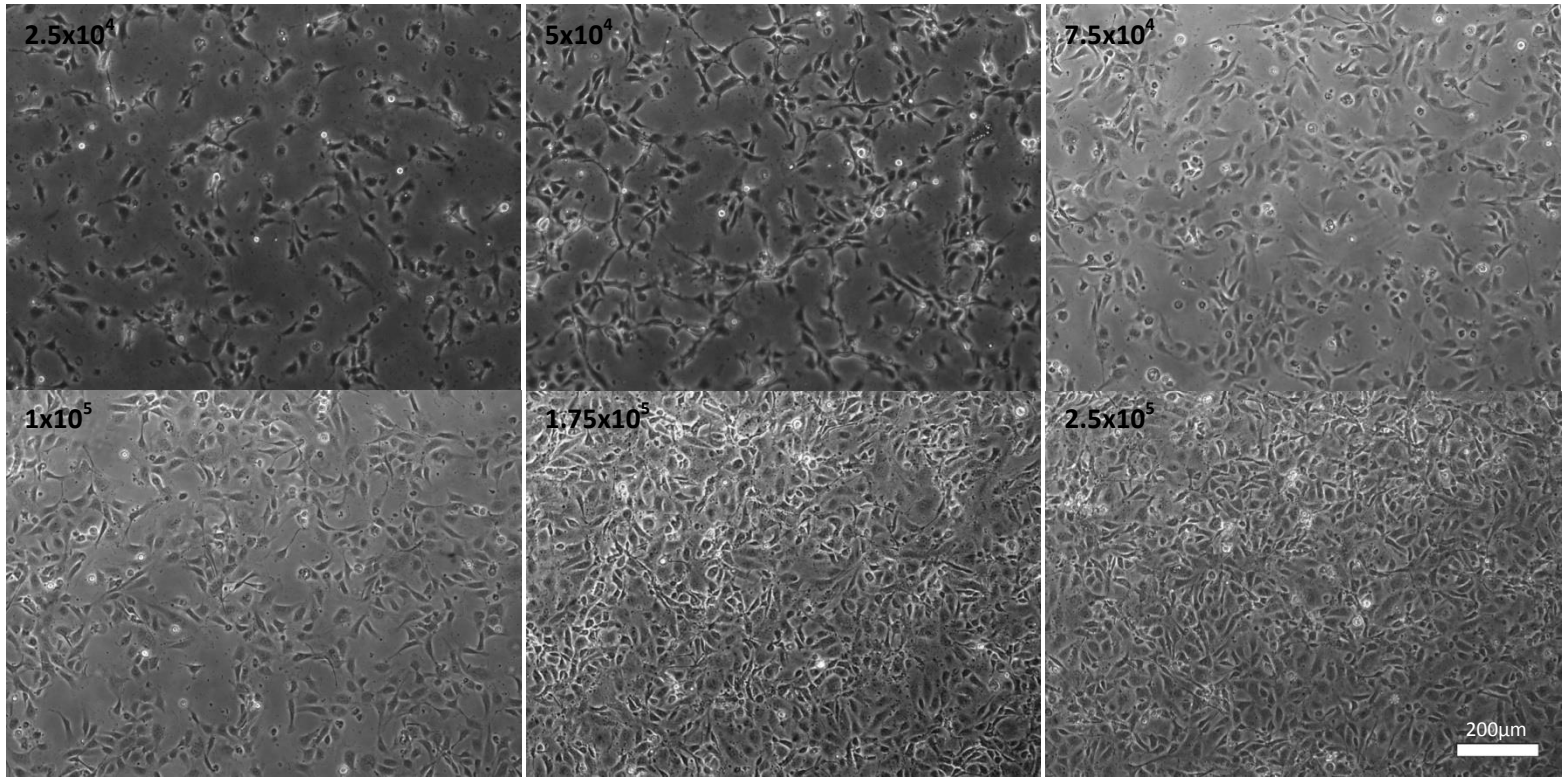

Figure 6.4: HUVEC monolayer confluence after 4 hour incubation when seeded at a variety of concentrations.

The confluence of HUVECs seeded at a variety of concentrations within a flow chamber after four hours. None of the concentrations assessed resulted in a 100% confluent monolayer after four hours, though both the $1.7x10^5$ and $2.5x10^5$ cells/slide flow chambers produced layers that were almost 100% confluent, with only small patches without cells observed. The confluence acheived was directly proportional to the seeding density. These photographs are representative images of three experiments.

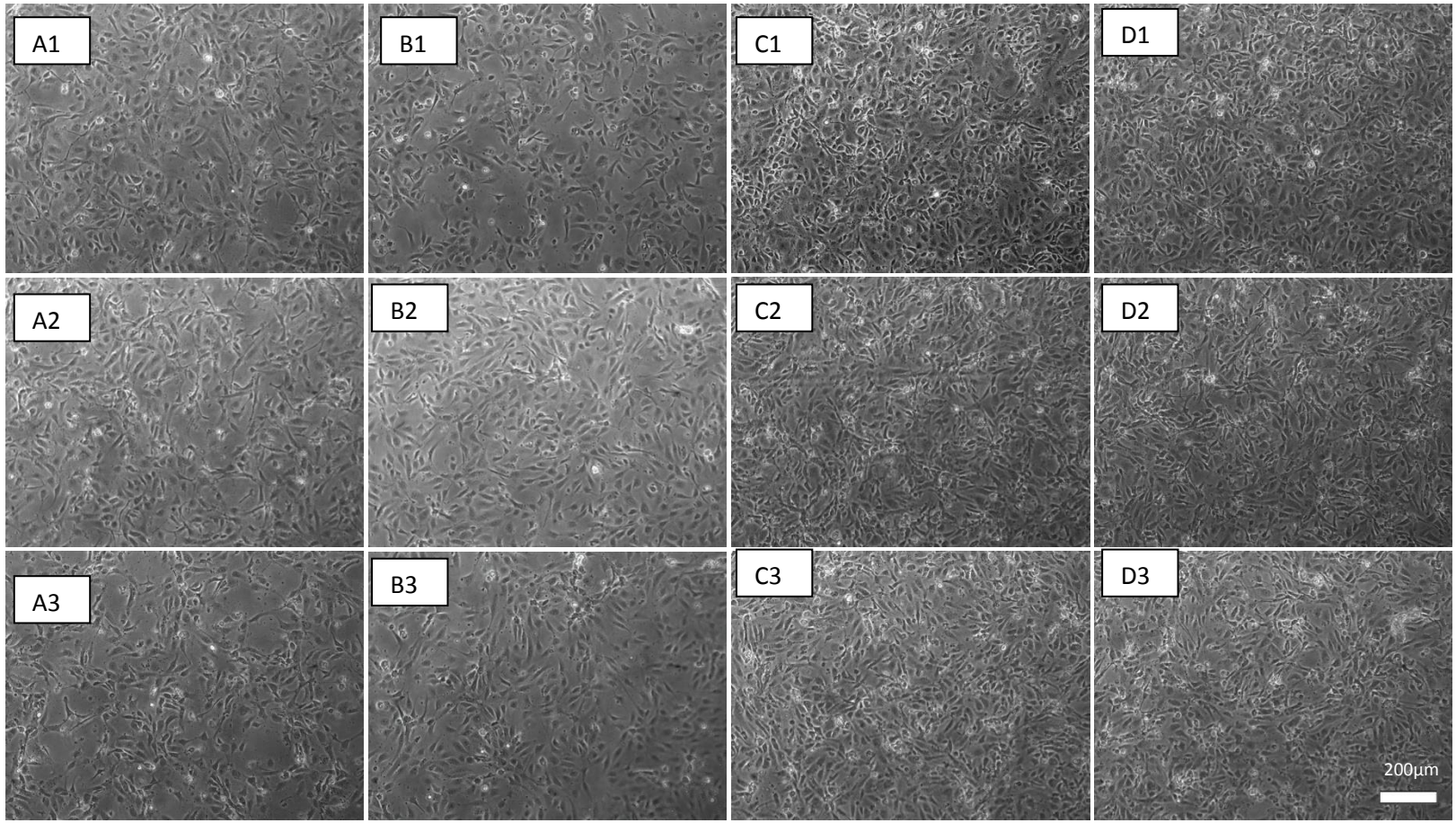

Figure 6.5: An assessment of the impact of incubation time on HUVEC monolayer confluence.

Cells seeded at different concentrations incubated for various time points. Cells were seeded at a density of $7.5x10^4$/slide (A), $1x10^5$/slide (B), $1.75x10^5$/slide (C), and $2.5x10^5$/slide (D), and allowed incubate for four (1), twelve (2), or 24 hours (3) without a media change. Both A and B failed to generate a confluent monolayer over this time. While C and D both generated a confluent monolayer, cells appeared to be slightly stressed, with some exhibiting an elongated, spindle-like morphology. Images are representative of three experiments.

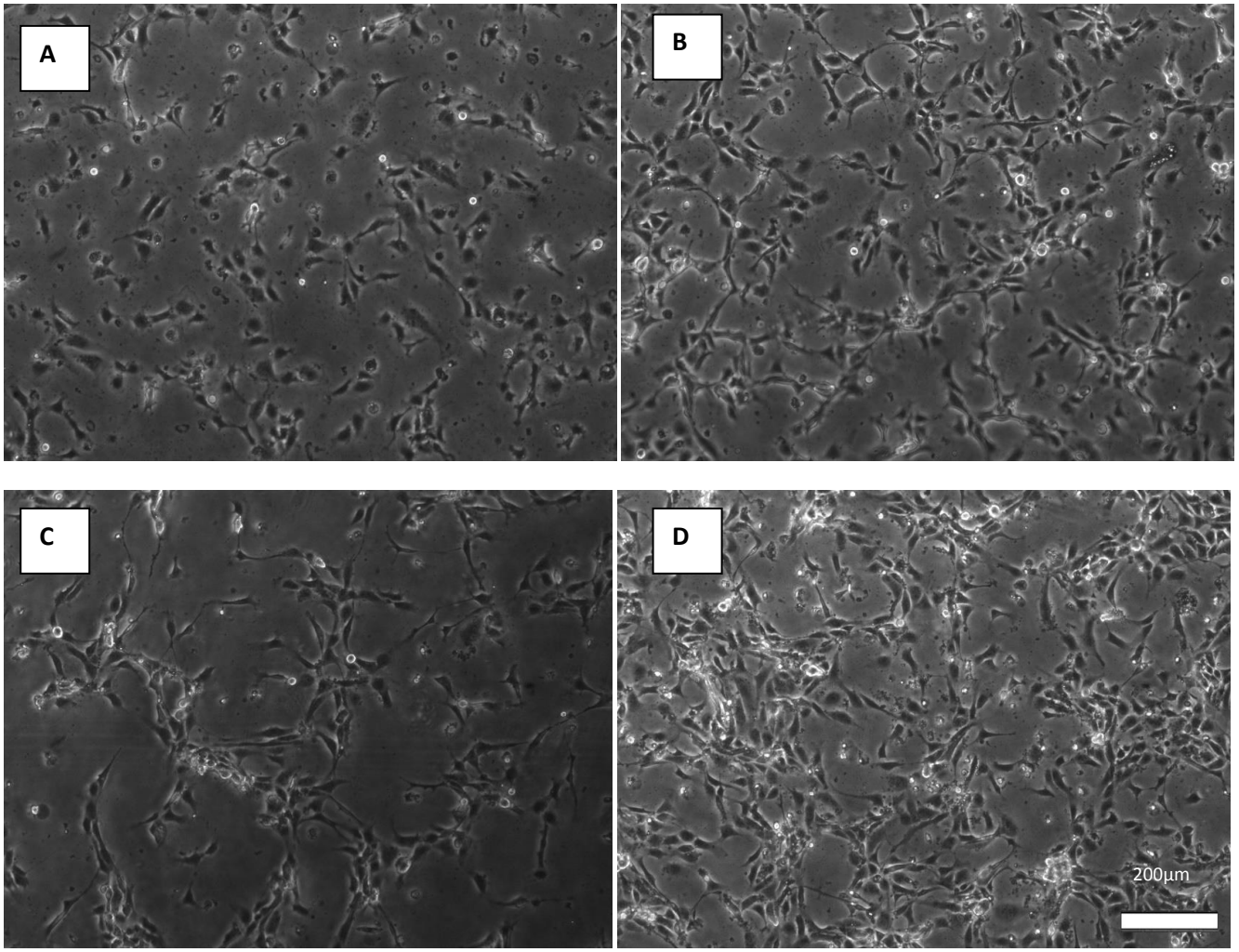

The confluence of cells seeded at concentrations of $2.5x10^4$/slide (A and C) and $5x10^4$/slide (B and D) after four (A and B) and 24 (C and D) hours. While increasing the incubation time increased the number of cells present in the slide, a confluent monolayer could not be acheived. Therefore, further optimisation work was not conducted using these concentrations. Images are representative of three experiments

Figure 6.6: An assessment of the impact of incubation time on HUVEC monolayer confluence II.

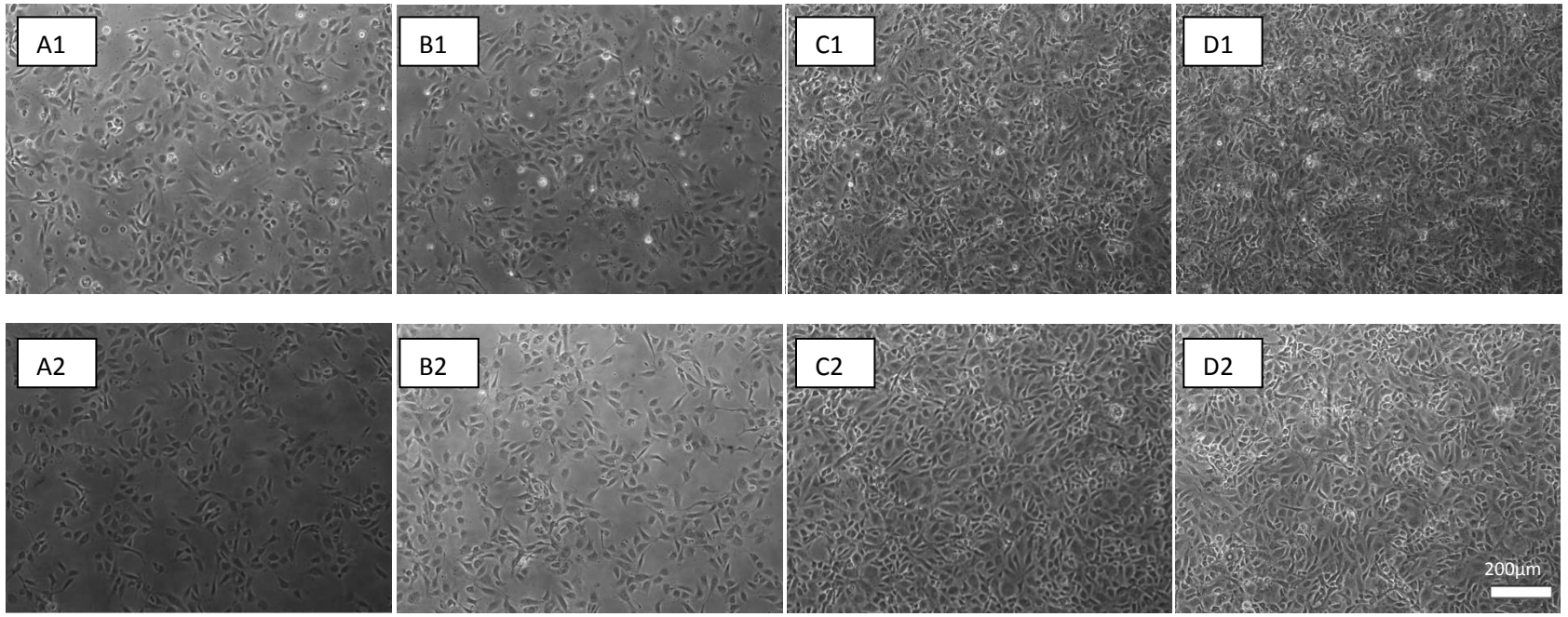

Figure 6.7: An assessment of the impact on a fourth-hour media change on monolayer stability.

Images showing cells seeded at a density of $7.5x10^4$/slide (A), $1x10^5$/slide (B), $1.75x10^5$/slide (C), and $2.5x10^5$/slide (D), before (1) and after (2) a full media change after four hours of incubation. As can be seen from these images, the full media change did not result in any large-scale or noticeable loss of cells, suggesting that all cells had adhered to the slide within four hours after initial seeding. Images are representative of three experiments.

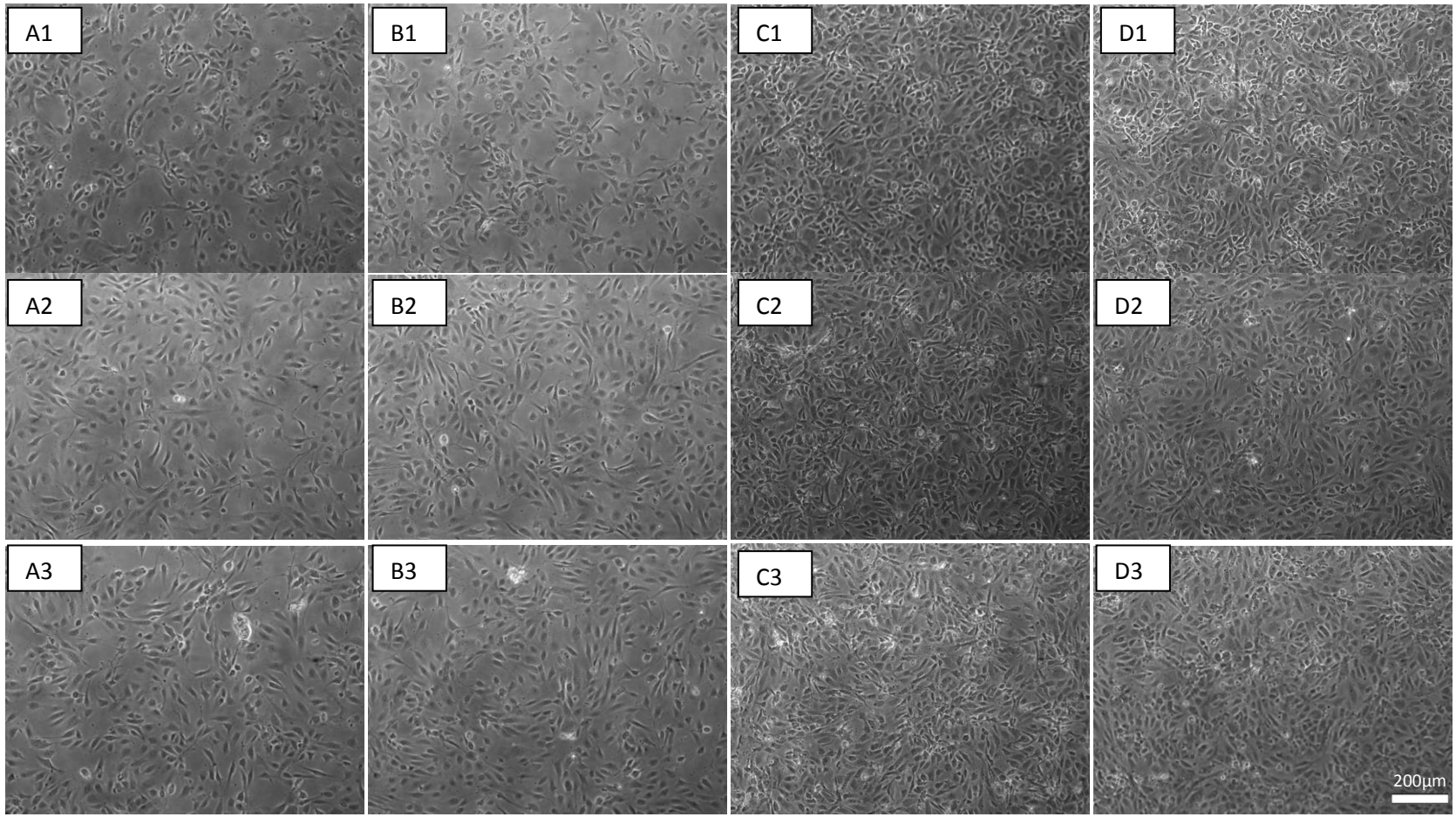

Figure 6.8: An assessment of the impact on a fourth-hour media change on monolayer confluence.

Cells seeded at different concentrations incubated for various time points following a full media change at 4 hours. Cells were seeded at a density of $7.5x10^4$/slide (A), $1x10^5$/slide (B), $1.75x10^5$/slide (C), and $2.5x10^5$/slide (D), and allowed incubate for four (1), twelve (2), or 24 hours (C). Images marked 1 show cells immediately after the 4 hour media change. While changing the media improved the condition of the monolayer over 12 and 24 hours, A and B failed to generate a confluent monolayer over this time. C and D both generated a confluent monolayer over 24 hours following a 4^{th} hour media change. Images are representative of 3 experiments.

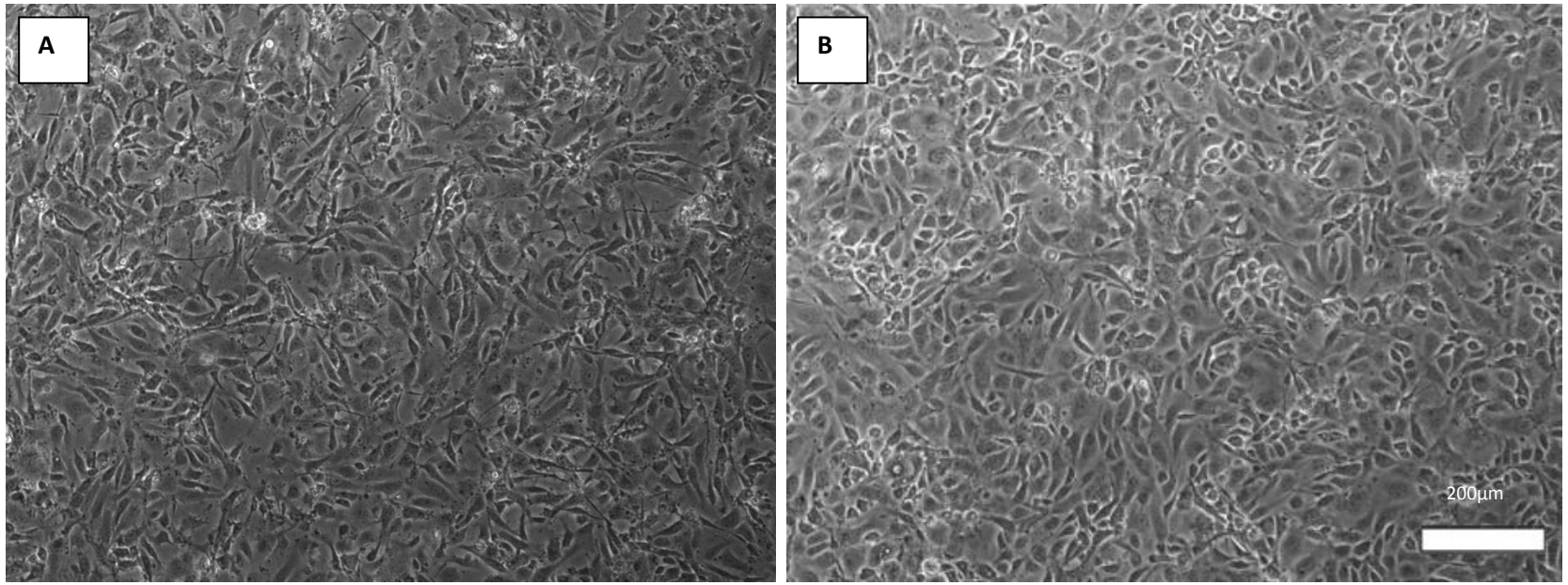

Figure 6.9: Morphology of cells incubated for 24 hours with and without a media change.

Cells seeded at a density of $2.5x10^5$/slide and allowed to incubate for 24 hours without (A) and with (B) a media change after four hours of incubation. Without a media change, cells appears stressed and have an elonganged, spindle-like morphology (A). With a media change, there are fewer elongated spindle-like cells, and the morphology is rounder, more characteristic of the cobblestone morphology typically observed with endothelial cells (B).

6.3.2 The Ability of Confluent Monolayers to Withstand Shear Stress

Seeding concentrations of $1.75x10^5$ cells/slide and $2.5x10^5$ cells/slide ($1.75x10^5$ cells/ml and $2.5x10^5$cells/ml) were both able to generate a confluent monolayer. Both seeding concentrations were therefore assessed to determine whether the integrity of the monolayer would remain during, and after, flow conditions at a shear stress of 5 dyn/cm^2. Cells seeded at both concentrations were found to withstand flow at a shear stress of 5dyn/cm^2 without any large scale loss of cells (Fig 6.10 and 6.11). Therefore, the seeding concentration of $2.5x10^5$ cells per slide was chosen, and would be used for future experiments.

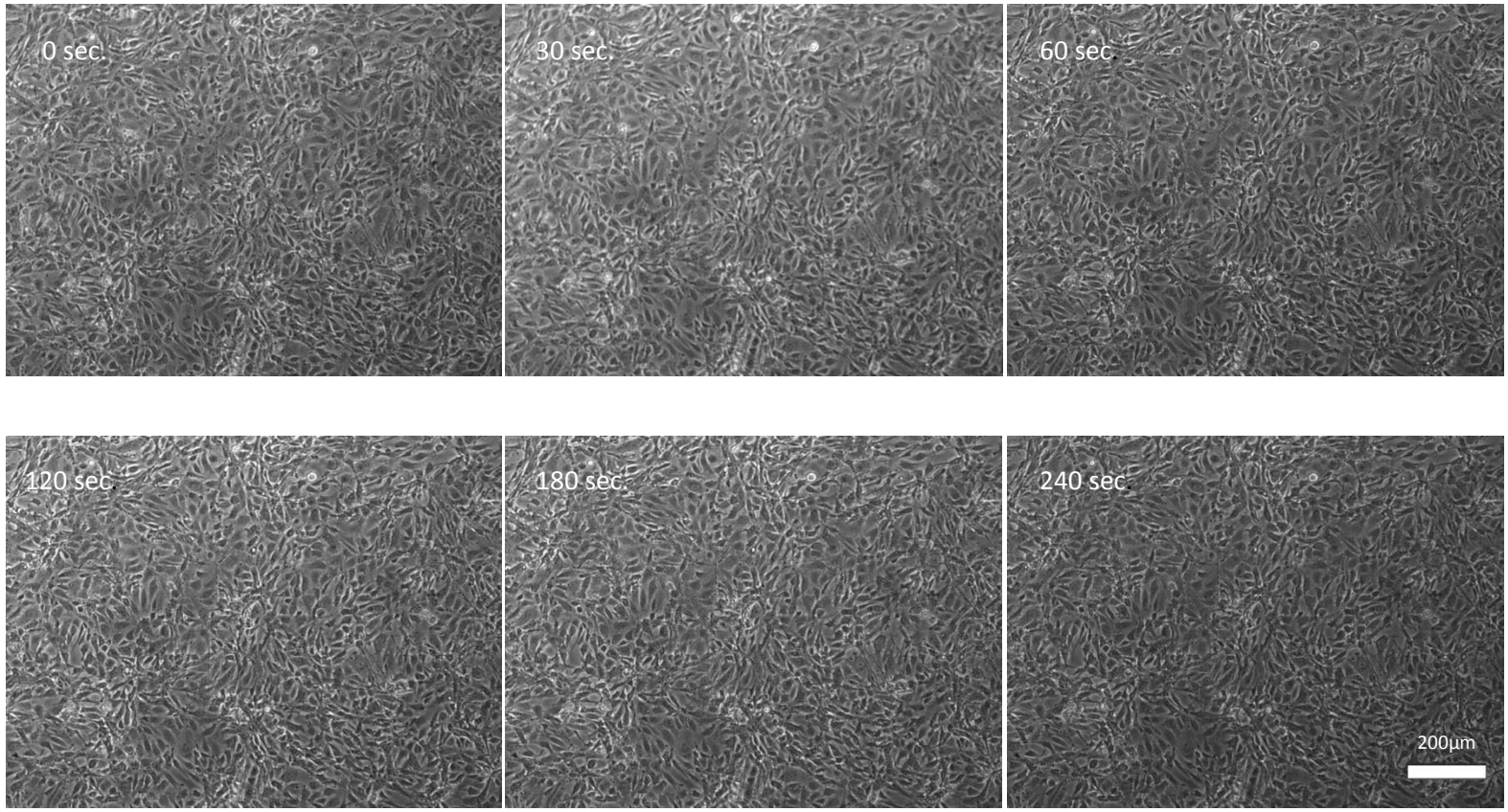

Figure 6.10: The ability of monolayers to withstand shear stress.

The endothelial cell monolayer resulting from seeding cells at a density of $1.75x10^5$ cells per slide. There was no cell loss when cells were exposed to a shear force of 5 dyn/cm^2, and the integrity of the monolayer was maintained over the full four minute flowing period. Images are representative of three experiments.

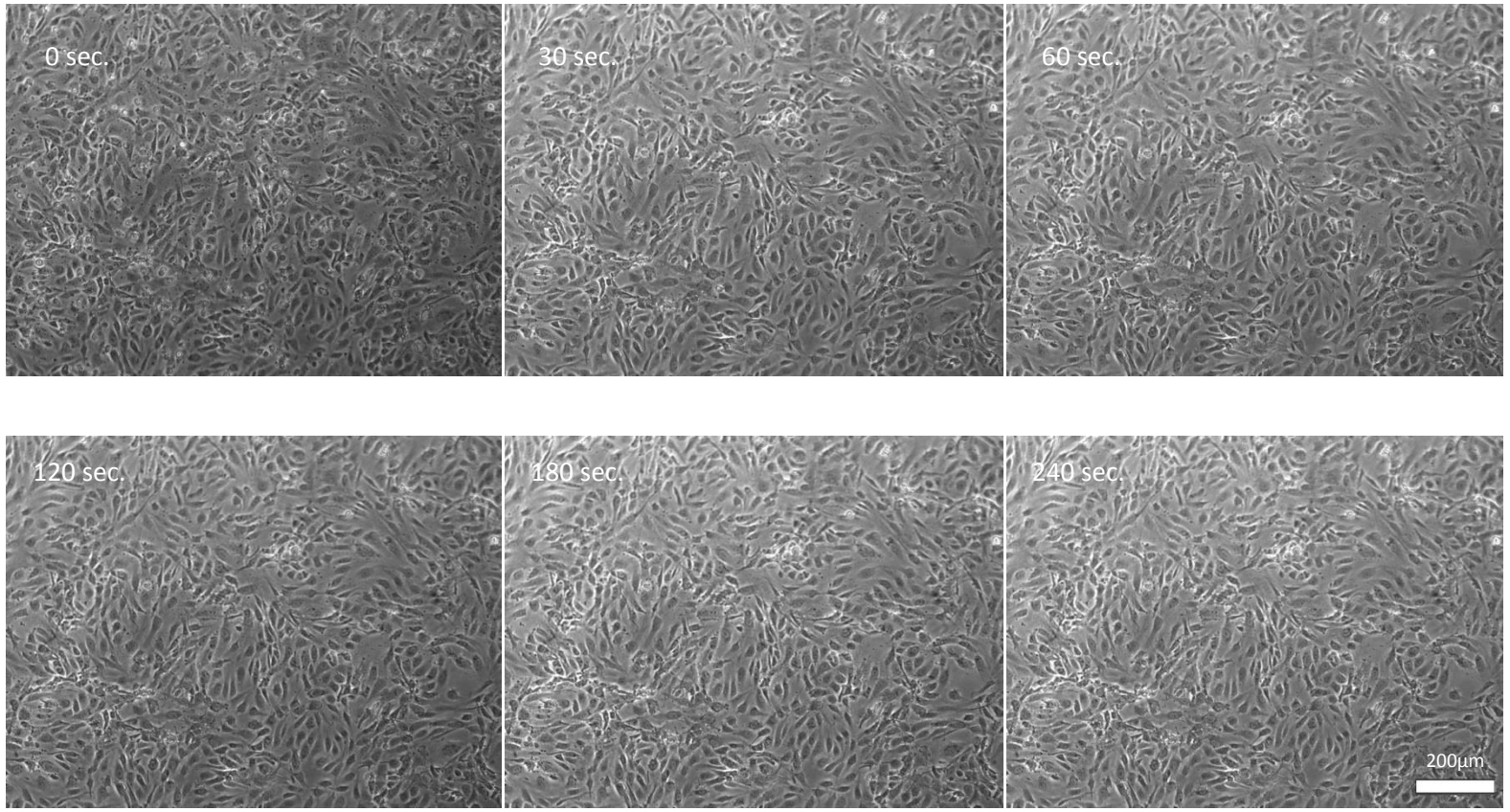

Figure 6.11: The ability of monolayers to withstand shear stress II.

The endothelial cell monolayer resulting from seeding cells at a density of $2.5x10^5$ cells per slide. There was no cell loss when cells were exposed to a shear force of 5 dyn/cm^2, and the integrity of the monolayer was maintained over the full four minute flowing period. Images are representative of three experiments.

6.3.3 The Ability of Monolayers to Withstand Treatment with BLM and TNF-α

As seen in Fig. 6.11, cells seeded at $2.5x10^5$ cells/slide generated a confluent, healthy monolayer able to withstand shear stress of 5 dyn/cm^2. Next, it was assessed whether cells seeded at a density of $2.5x10^5$ cells/slide maintained a confluent monolayer when treated with 0.1µg/ml, 1µg/ml, and 10µg/ml BLM, or 10ng/ml TNF-α for 6 and 24 hours. Both agents are cytotoxic, so the resilience of the monolayer to these agents needed determining. When cells were allowed to incubate for 24 hours with a 4th hour media change, treatment with TNF-α for 24 hours slightly altered the morphology of the monolayer. Treatment for 6 hours had no effect (Fig. 6.12). However, confluence was maintained as in Fig. 6.11.

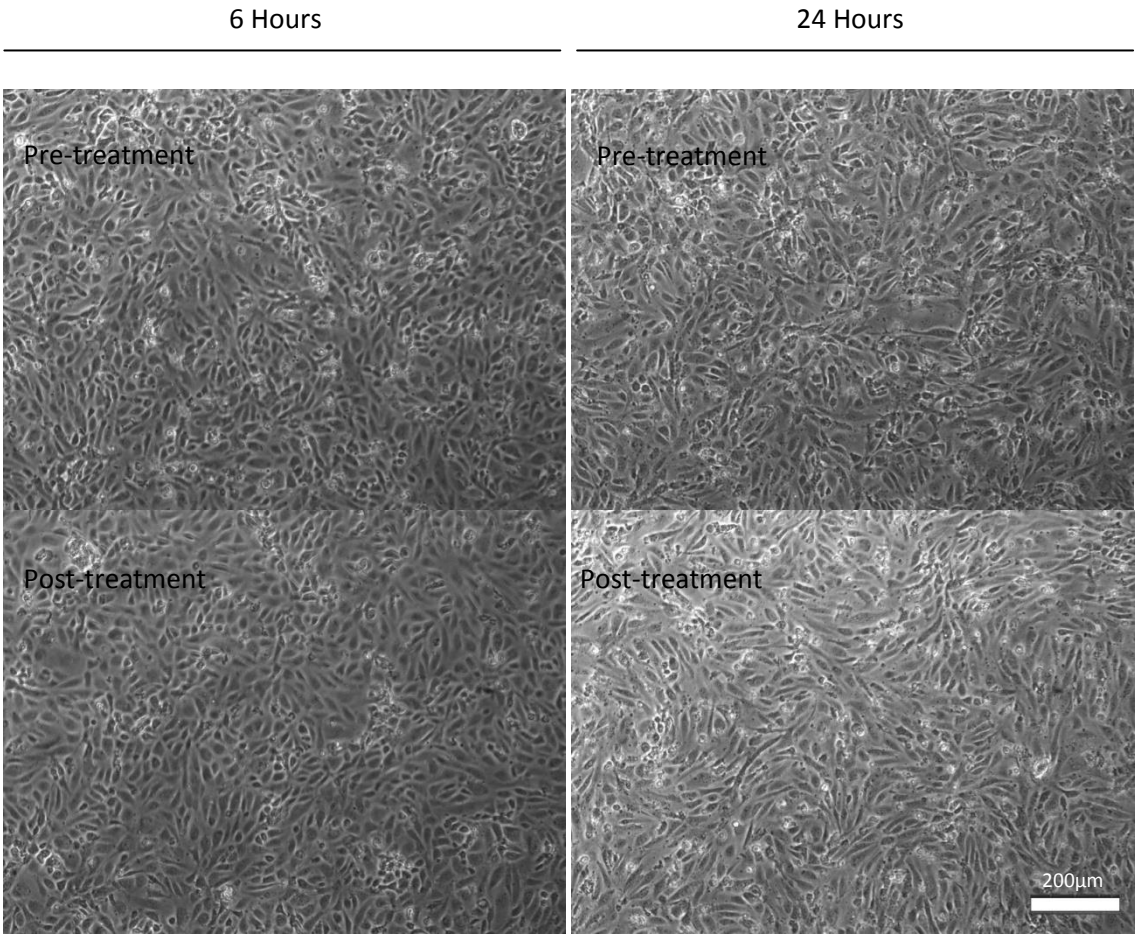

Figure 6.12: Endothelial monolayers within a flow chamber before and after treatment with TNF-α

Cells treated with TNF-α (10ng/ml) for 6 hours and 24 hours before addition of TNF-α to the monolayer, and after the full incubation period. Images are representative of 3 experiments.

Despite the slight alterations in morphology when cells were treated with TNF-α for 24 hours, cells remained adhered even under flow at 5 dyn/cm^2 for four minutes (data not shown). Therefore, these conditions were deemed viable for use as a positive control in this experiment. The integrity of the monolayer was also maintained after treatment with BLM; no large-scale cell death was observed.

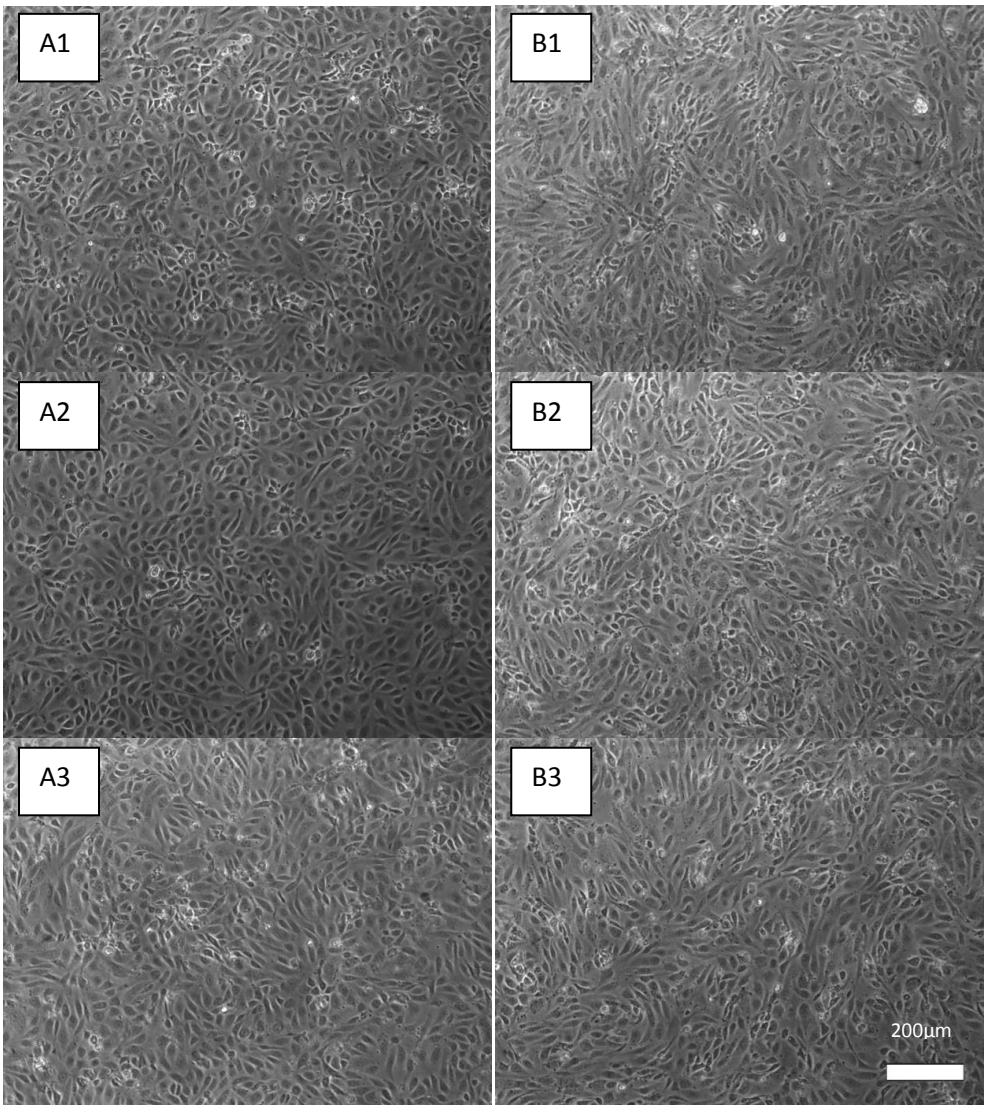

Figure 6.13: Endothelial monolayers within a flow chamber after BLM treatment.

Cells treated for 6 (A) and 24 (B) hours with 0.1µg/ml (1), 1µg/ml (2), and 10 µg/ml (3) BLM. The confluence of the monolayers when cells were seeded at a concentration of 2.5x10^5 cells/slide and allowed to incubate for 24 hours with a fourth hour media change (as shown in Fig. 7) was not diminished by treatment with BLM for 6 and 24 hours. The monolayers were also able to withstand shear (not shown). Images are representative of three experiments.

6.3.4 Optimisation of Neutrophil Isolation

Initially, a two-step gradient protocol was used for the isolation of neutrophils from whole blood (Rainger, et al., 1995; McGetterick, et al., 2010). However, it was quickly found that this technique was not reproducible or reliable, and it was not possible to generate a distinct band between the two histopaque layers. Therefore, optimisation experiments were carried out to develop a reproducible and reliable method for isolating human neutrophils. Two techniques were trialled and compared.

In the first method (Fig 16.4A), the double-density gradient technique was used. The granulocyte layer was extracted from between the two layers of histopaque, washed, and resuspended in PBS contaning calcium, magnesium, 5mM glucose, and 1.5% BSA. The neutrophils were then counted. In the second method (Fig 16.4B), only a single-step gradient was used to allow granulocytes to gather in with the erythrocyte pellet. The erythrocyte pellet was then lysed as outlined in 6.2.4, to leave only the granulocytes in this layer. Again, cells were washed and re-suspended as described above.

In both cases, small volumes of histopaque were also extracted along with the granulocyte layer/ erythrocyte pellet to ensure no granulocytes were lost. This was particularly important in method A, as it was found that no distinct granulocyte band could be obtained. This was unexpected, as distinct bands of mononucleocytes and plasma, as well as distinct erythrocyte pellets, were routinely obtained. The reasons for the lack of granulocyte layer are unknown.

The purity of the cell samples obtained using each of these methods was determined by cytospin slide generation. The results are shown in Fig. 6.15 and 6.16. Though succesful neutrophil isolation using the double-density gradient method was achieved, this was not reliable, and this method could either result in the harvest of many (Fig. 6.15A), or few neutrophils (Fig. 6.15C).

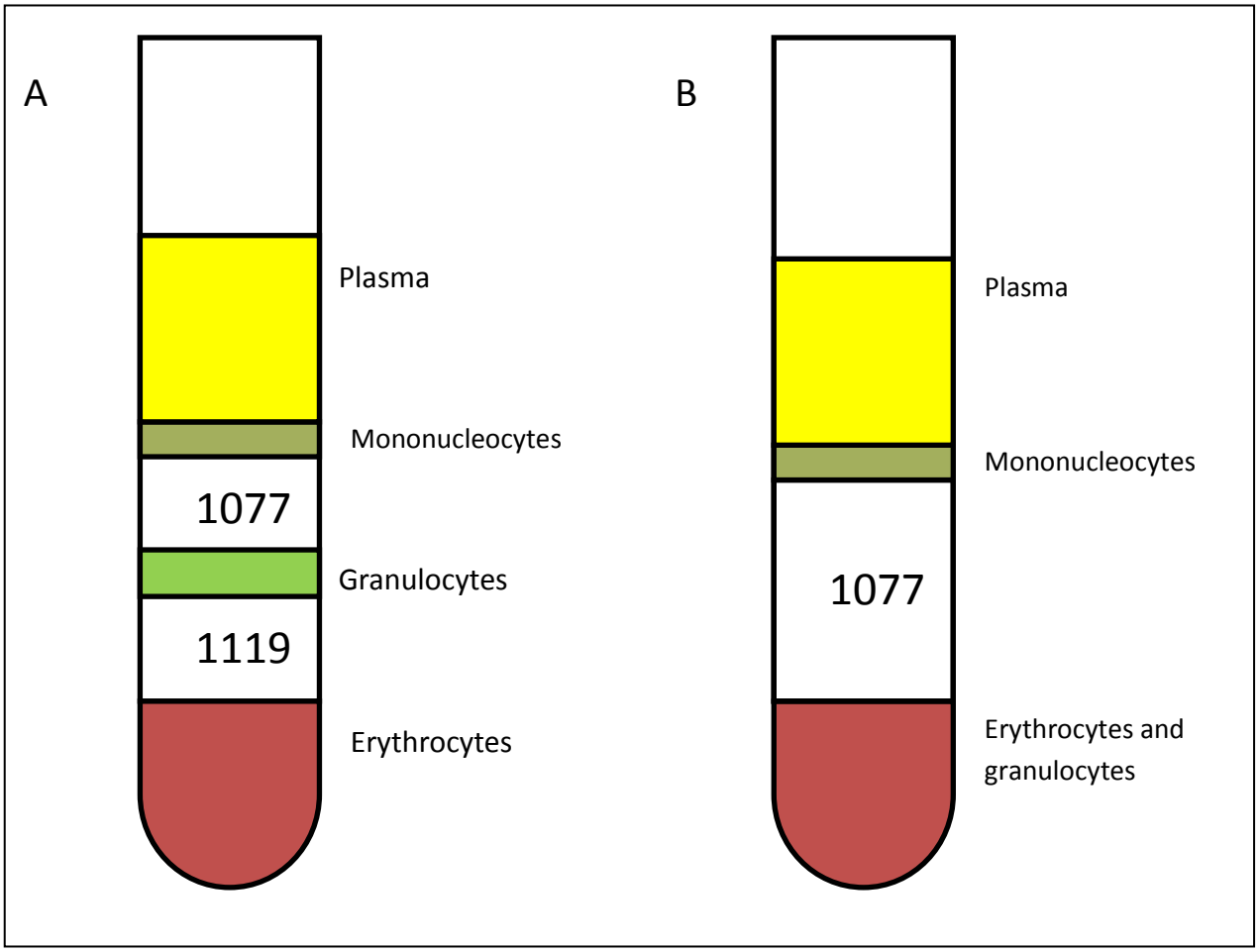

Figure 6.14: The separation of whole blood using the single and double density gradient techniques.

A diagram representing the expected results of blood separation using the two-step density gradient method (A) and the single-step density gradient method (B). 1077 and 1119 refer to the densities of the histopaque used in each layer. In this experiment, when a two-layer density gradient was used, no clear granulocyte band was acheived at any stage.

Using the single-density method, a population of pure neutrophils could be acheived providing red blood cells lysis was achieved by carrying out the lysis step only once. Multiple attempts to lyse the erythrocytes resulted in neutrophil activation. A lysis technique in which the red cell pellet (from 15ml whole blood) containing the neutrophils was re-suspended in 40ml of deionised, sterile water (to generate a hypotonic environment) and swirled for 30 seconds, prior to the addition of 3.6ml 10 x PBS (to create an isotonic environment), and

spun at 800 x g for 10 minutes, was found to lyse the vast majority of erythrocytes while leaving a substantial population of unactivated, therefore usable, neutrophils (Fig. 6.16). Some erythrocyte contamination was deemed acceptable as erythrocyte adhesion to the BLM-treated monolayer was not expected in this series of experiments, as discussed in section 6.4.3.

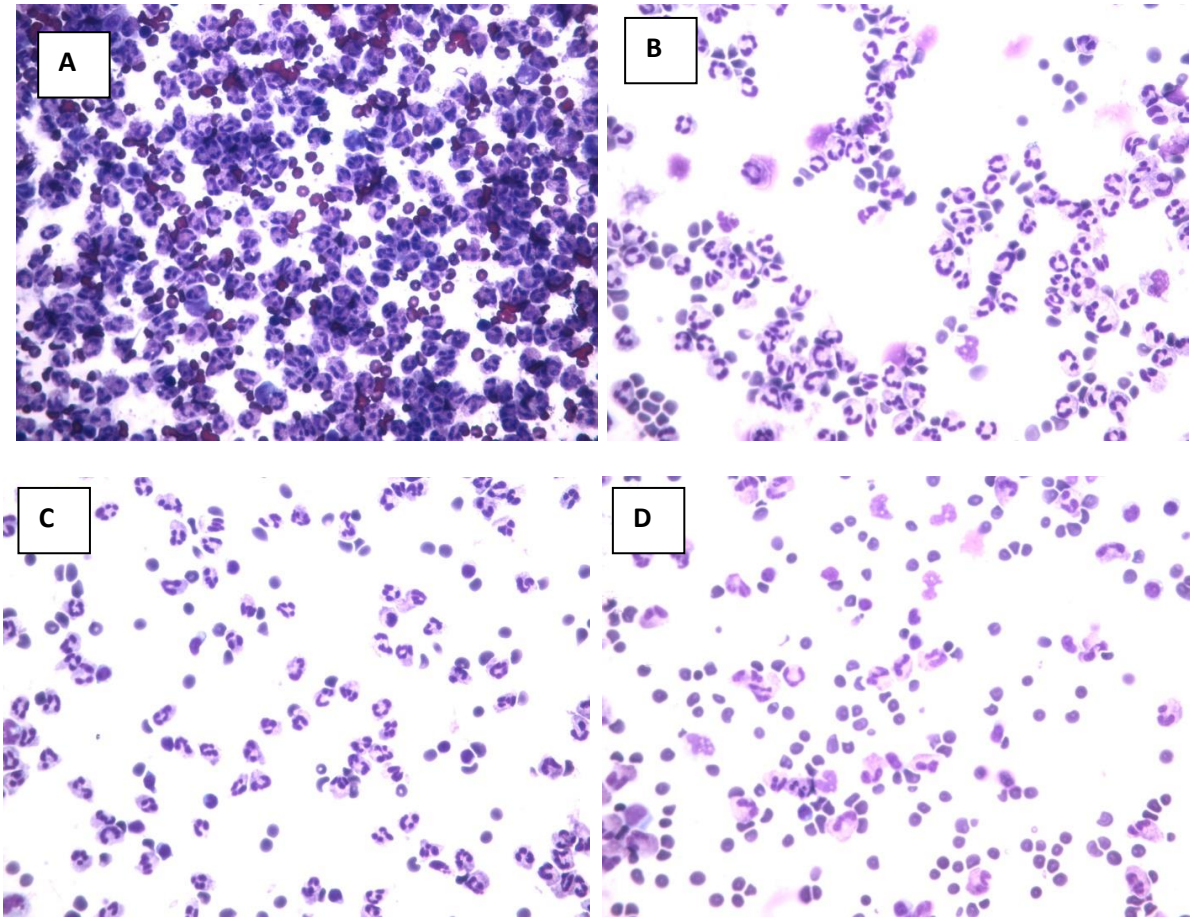

Figure 6.15: Neutrophils isolated by the double-density gradient technique.

Using a double-density gradient technique could result in a good neutrophil yield (A), but this was not always the case; the use of the same technique could also result in mediocre yields (B and C) or poor yields where most isolated cells were erythrocytes (B), though why this occurred is unknown. Shown are representative cytospin slides of five experiments (a total of 12 slides).

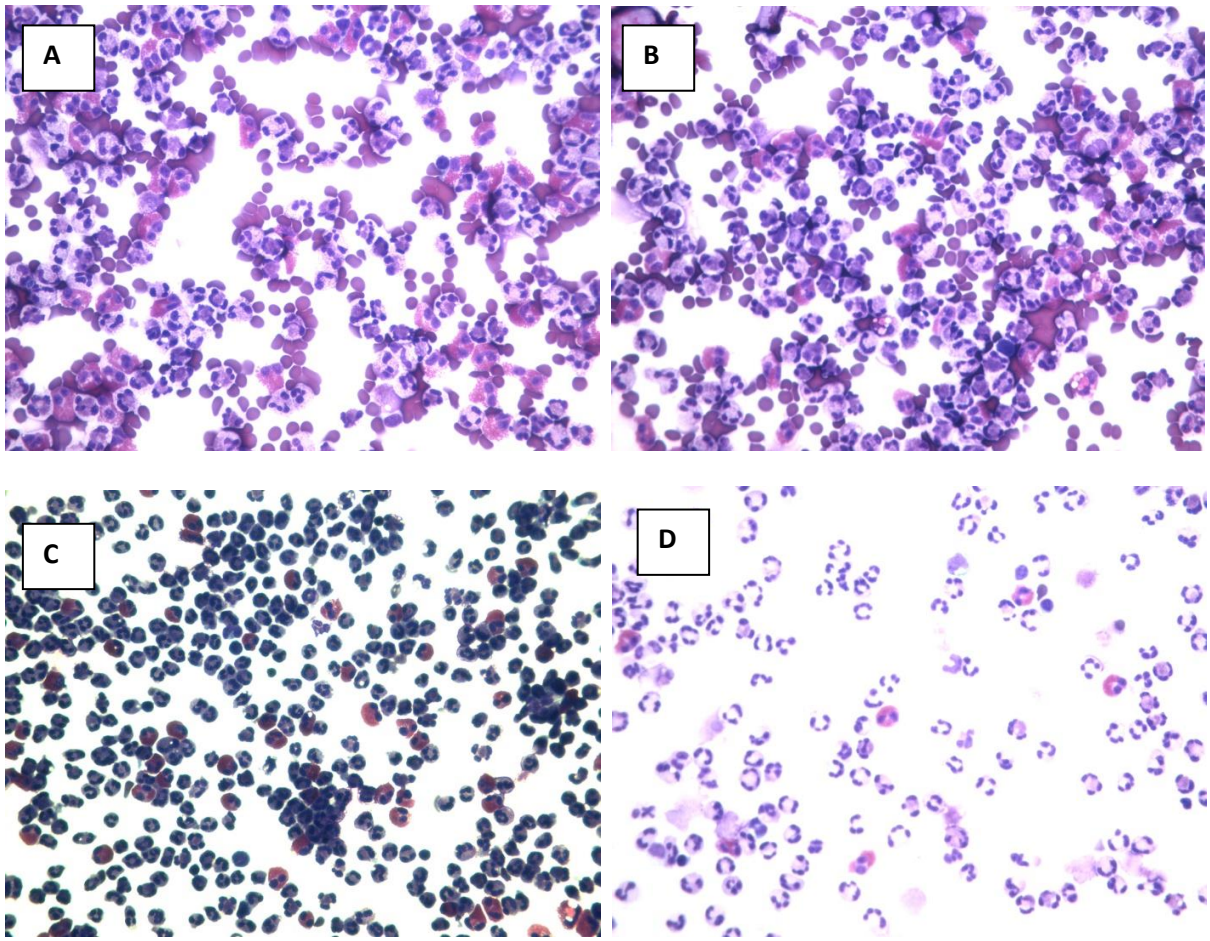

Figure 6.16: Neutrophils isolated by the single-density gradient technique.

Using a single-density gradient technique often resulted in a good neutrophil yield (A, B, C), though a pure yield of neutrophils was often difficult to acheive using this method, with many cytospin slides showing erythrocyte contamination (A, B). It was possible to yield pure neutrophil yields with multiple washes (C, D), though this often resulted in lower neutrophil yields due to neutrophil activation (d). Shown are representative cytospin slides of five experiments (a total of 12 slides) in which the single-density gradient technique was used to isolate neutrophils.

Approximately $1x10^7$ neutrophils were needed for each series of experiments (20ml of neutrophil suspension at a concentration of $5x10^5$ neutrophils/ml) to ensure sufficient cells to carry out all plates. Therefore, $1x10^7$ was regarded as the threshhold level of neutrophils

that needed to be isolated from 15ml of whole blood. A good yield is regarded as ≥1x10^7 neutrophils/ml, and a poor yield, <1x10^7 neutrophils/ml, when assessed by haemocytometry.

The results of multiple optimisation experiments showed that, using the double-step density gradient technique, poor neutrophil yields were obtained in two out of five experiments. The single-density gradient yielded very good numbers of neutrophils in four out of five experiments (therefore adequate for conducting the experiment), and a poor yield in one, though this donor was found to be neutropenic. While neutrophil purity was generally less in cells isolated using the single-step gradient compared to the double-step gradient (Fig 6.15 and 6.16), erythrocyte contamination was not deemed to be problematic, as erythrocytes do not adhere to endothelial monolayers. The single-step density gradient with a single lysis step was therefore chosen.

6.3.5 Optimisation of Shear Stress Used in Experiments to Allow Neutrophil Adhesion to the Monolayer

Following the optimisation of the seeding density and neutrophil isolation technique, monolayers were generated and treated with BLM or TNF-α as previously outlined. Neutrophils isolated from healthy donors using the single-step density gradient technique and suspended to a concentration of 5x10^5 cells/ml were then flowed over the monolayer for up to four minutes at a shear stress of 5 dyn/cm^2. However, initial results showed that, at this shear stress, neutrophils were not able to adhere to the monolayer. Monolayers treated with BLM, TNF-α, or left untreated, were unable to support tethering, rolling, or adhesion. Neutrophils were seen to move rapidly across the field and did not appear to contact the endothelium (data not shown).

Therefore, the shear stress was deemed to be too high to allow neutrophil adhesion, despite being physiologically relevant in the pulmonary microvasculature. The shear stress was therefore decreased to 1 dyn/cm^2, in line with the protocol of McGetterick. Initially, it was determined whether a shear stress of 1 dyn/cm^2 would disrupt the endothelial monolayer.

This was not found to be the case, and endothelial cell integrity at this shear stress was also maintained (Fig. 6.17). As expected, further decreases in shear stress applied to the endothelial monolayer also failed to disrupt the integrity (data not shown).

However, when assessing neutrophil adhesion at a shear stress of 1 dyn/cm^2, similar problems were encountered to when 5 dyn/cm^2 was used. Though previous works by the Nash group have found that at a shear stress of 1 dyn, neutrophils were capable of adherence to the monolayer (Rainger, et al., 1995; Sheikh, et al., 2005), a different flow chamber set-up was used in this work, and few neutrophils adhered to the central region of the chamber at a shear stress of 1 dyn/cm^2. This was deemed potentially due to laminar flow resulting from the velocity of media travelling through the chamber, calculated to be approximately 3.8cm/min. Though there is no current literature which adequately describes the flow rate of blood through human pulmonary venules and arterioles, which this experiment aims to model, it was decided that a lower shear stress rate, and therefore a lower velocity, may be required.

Lowering the shear stress used may make the model more physiologically relevant. A shear stress rate of 1 dyn/cm^2, used previously, precludes integrin-mediated adhesion. It is possible that the upregulation of adhesin expression - such as that of VCAM-1 and ICAM-1 - may contribute to the recruitment of neutrophils within the pulmonary microvasculature. Therefore, a series of experiments assessing neutrophil adhesion to monolayers at shear stress rates of 0.01, 0.1, and 0.5 dyn/cm^2 were conducted. The results of these experiments showed that, while at 0.5dyn/cm^2, neutrophils adhered to the monolayer when treated with TNF-α, but not to the untreated monolayer, using rates slower than this resulted in large-scale neutrophil adhesion to even the untreated monolayer. It was also very difficult to differentiate between slow rolling and rolling neutrophils, and non-adherent neutrophils, when these shear rates were used in this experiment. Therefore, a shear rate of 0.5dyn/cm^2 was used, as this both resulted in clear and analysable results, and also may potentially allow the adhesion of neutrophils to the monolayer initiated by integrin-mediated attachment.

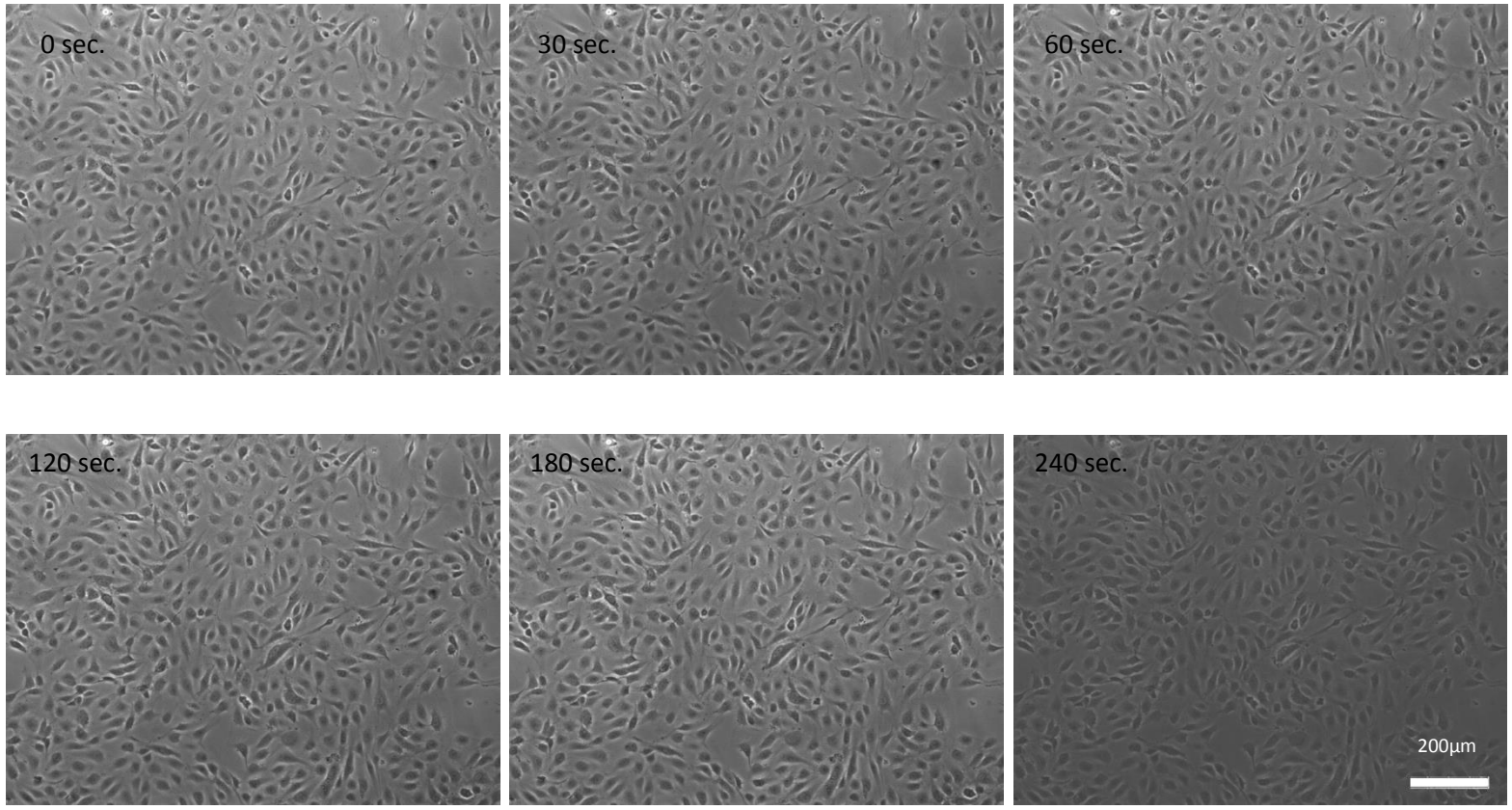

Figure 6.17: The integrity of endothelial cell monolayers exposed to a shear stress of 1dyn/cm^2

An endothelial monolayer generated by seeding HUVECs at a density of 2.5x10^5 cells per slide. There was no cell loss when cells were exposed to a shear force of 1 dyn/cm^2, and the integrity of the monolayer was maintained over the full four minute flowing period, as would be expected when comparing this to earlier results where a shear force of 5 dyn/cm^2 was used and the integrity of the monolayer was also maintained.

6.3.6 The Identification of Adherent Neutrophils under Flow

Data analysis required the assessment of the cells adherent to the monolayer, and this was conducted manually as outlined in 6.2.6. Shown in Figure 6.18 is a representative image of neutrophils adherent to the endothelium. Adherent neutrophils are shown by yellow circles. Often, neutrophils accumulated in groups. No spreading neutrophils are shown. Figure 6.19 shows a spreading neutrophil (red circle). These cells were characterised by the phase-bright ring surrounding the cell with the dark inner area (the nucleus) and the slightly less distinctive circular shape (Zhan, et al., 2012). Few examples of spreading neutrophils were observed.

As the determination of adherent neutrophils to the endothelium was dependent on the discretion of the investigator, the size and shape of adherent events were used as determinants of cell identity. The size of a human neutrophil is relatively uniform, at around 10µm in diameter (Kolaczkowska and Kubes, 2013). Though the size of HUVECs is not determined, as the shape and growth habit of HUVECs is not uniform, this work has measured a HUVEC to be between 30-50µm long, and around 10-20µm wide, compared to the scale bar. Any potential adhesion events that were far greater in size, not circular, and not identifiable as spreading neutrophils, were deemed to be raised patches of endothelium, or where endothelial cell division was occuring. These were relatively common, potentially due to the seeding density used, and were easily identified and dismissed. Such raised patches are shown in Fig 6.18, denoted by blue circles. Usually, such patches were removed by the initial washing step in the protocol, but some remained in some experiments.

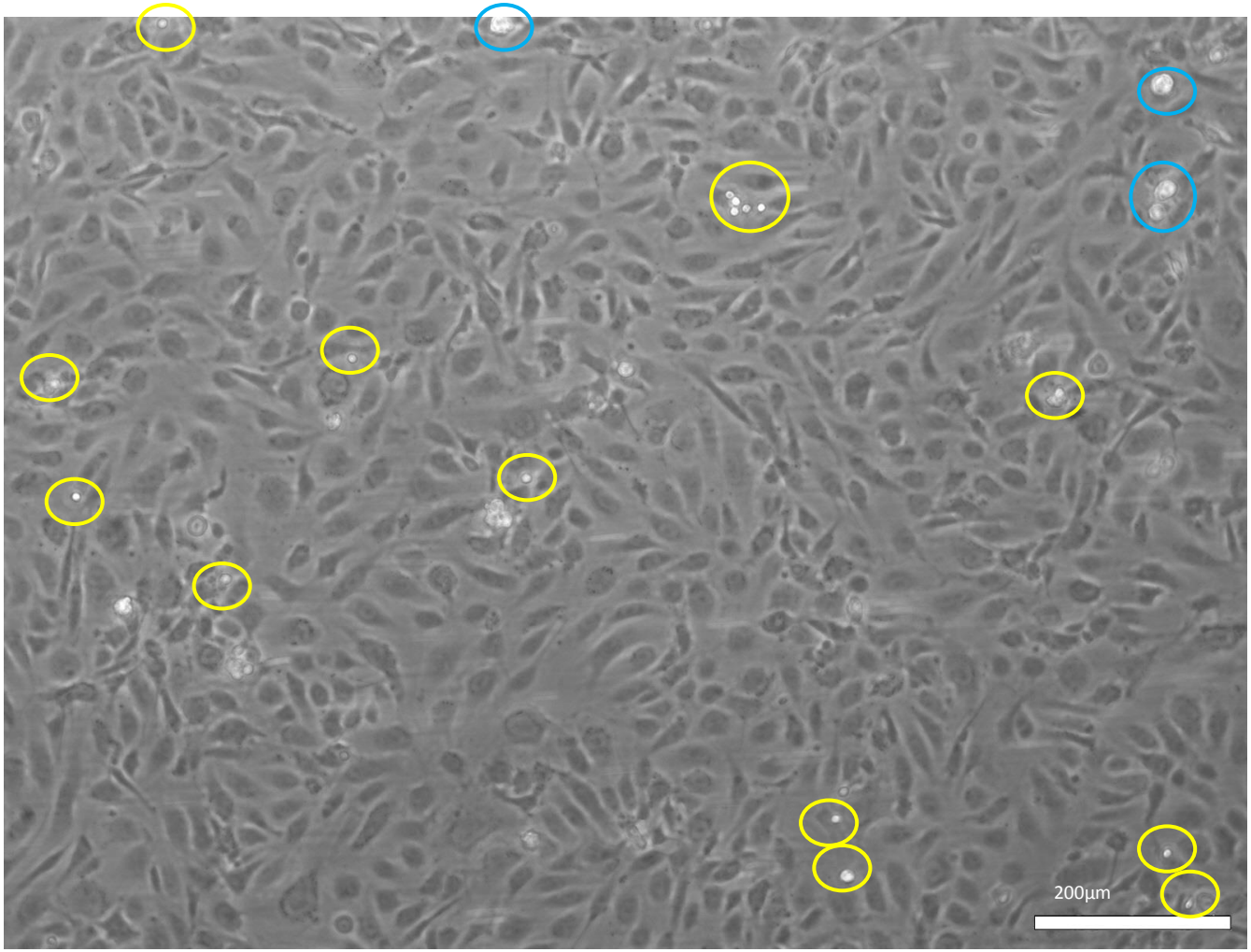

Figure 6.18: A representative image of neutrophils adherent to the endothelial monolayer under flow.

A still showing neutrophils adherent to the endothelial monolayer (yellow circles) and areas of endothelial raising (blue cirlces). Neutrophils were identified by their size and shape. The image is representative of 120 images obtained for one experiment. The total number of experiments conducted was three per treatment condition.

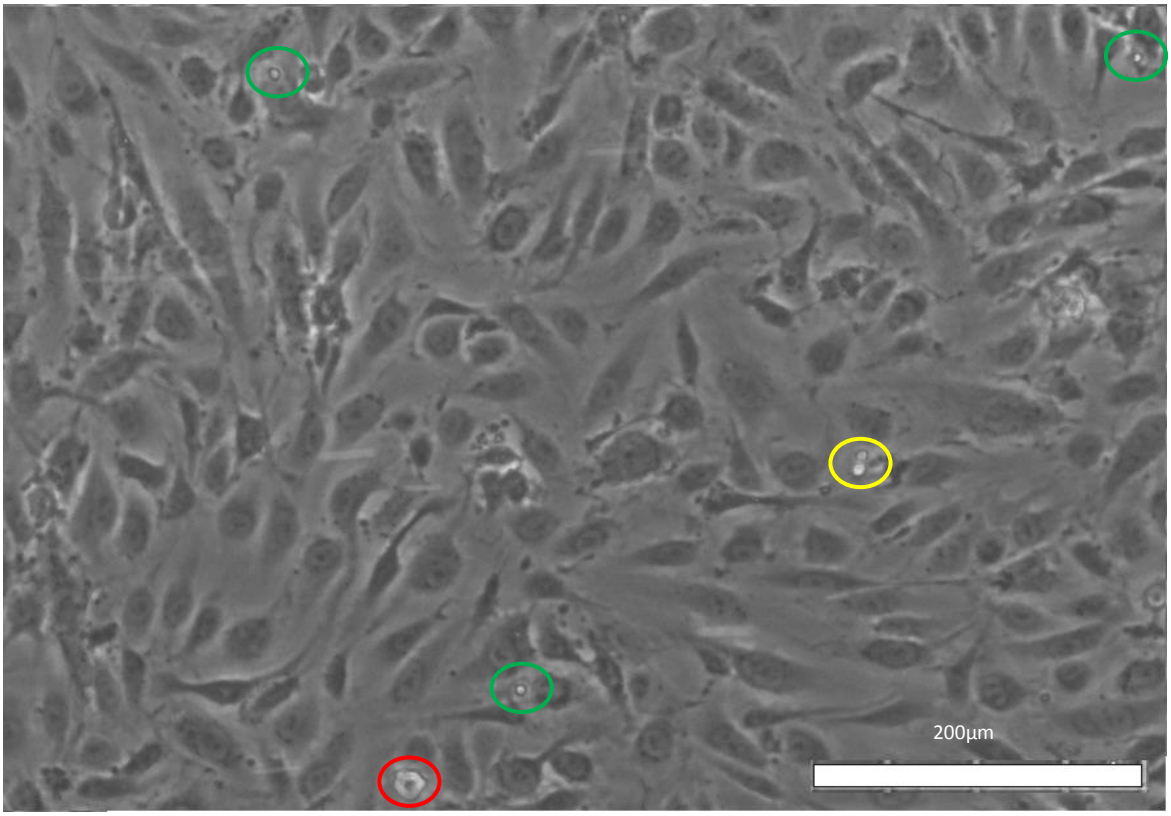

Figure 6.19: A representative image of a spreading neutrophil and debris adherent to the endothelial monolayer.

Characteristic spreading neutrophils are marked with a red circle. Adhesion events too small to be neutrophils, potential cell debris, are marked with a green circle. The image is representative of 120 images obtained for one experiment. Three experiments were conducted in total.

Occasionally, very small, non-circular, not especially phase-bright events were encountered. Adherent neutrophils have previously been determined to be broadly circular, phase bright, and of a general size (Zhan, et al., 2012). If these small events were deemed to be far smaller than one-third to one-fifth of the size of a HUVEC, smaller than a neutrophil, and non-circular, these events were regarded as cell debris and were not counted as neutrophils. Such criteria meant that non-adhesion events were not counted and the over-estimation of cell adherence was prevented. However, this phenomenon was uncommon; one such an occurence is highlighted above with a green circle. Finally, bright patches between endothelial cells were regarded to be visualisation of the

basement membrane. These were not circular and could be of any size, so were easily identified and also discounted immediately from adherent neutrophil counts.

6.3.7 Neutrophil Adhesion to BLM Treated Monolayers under Flow Conditions

There was an increase in the number of adherent neutrophils observed when cells were treated with BLM of various concentrations for 6 hours. Although there was no statistically singificant increase in the adhesion of neutrophils to the monolayer when cells were treated with the lowest concentration of BLM, the two higher concentrations appeared to increase neutrophil adhesion (Fig. 6.20A).

As expected, the greatest increase in neutrophil adhesion to the monolayers was induced by treatment with TNF-α (10ng/ml). It is also notable that the highest number of "new" adhesion events – that is, events whereby neutrophils which were not previous adhered to the endothelium in the initial image captured slow, roll, and move along the endothelium, was greatest in the TNF-α-treated monolayers. Other treatment conditions, however, had roughly similar numbers of "new" adhesion events (Table 6.1). Very few spreading events (fewer than one per field) were recorded in any of the three series of experiments outlined above, and so the frequency of these events was not recorded.

When endothelial cells were treated with BLM or TNF-α for 24 hours, similar results were observed. There was a statistically significant increase in the number of neutrophils adhering to the monolayer when endothelial cells were treated with 1μg/ml or 10μg/ml BLM, or 10ng/ml TNF-α, for 24 hours, compared to baseline (Figure 6.20B). Again, the greatest number of "new" adhesion events was seen in cells treated with TNF-α (Table 6.2), though this was of a smaller magnitude than observed when 6-hour treated endothelial monolayers were assessed. Adhesion of neutrophils to the monolayer did not increase in line with increased treatment time; both 6 hour and 24 hour treatment with BLM and TNF-α resulted in similar levels of adhesion.

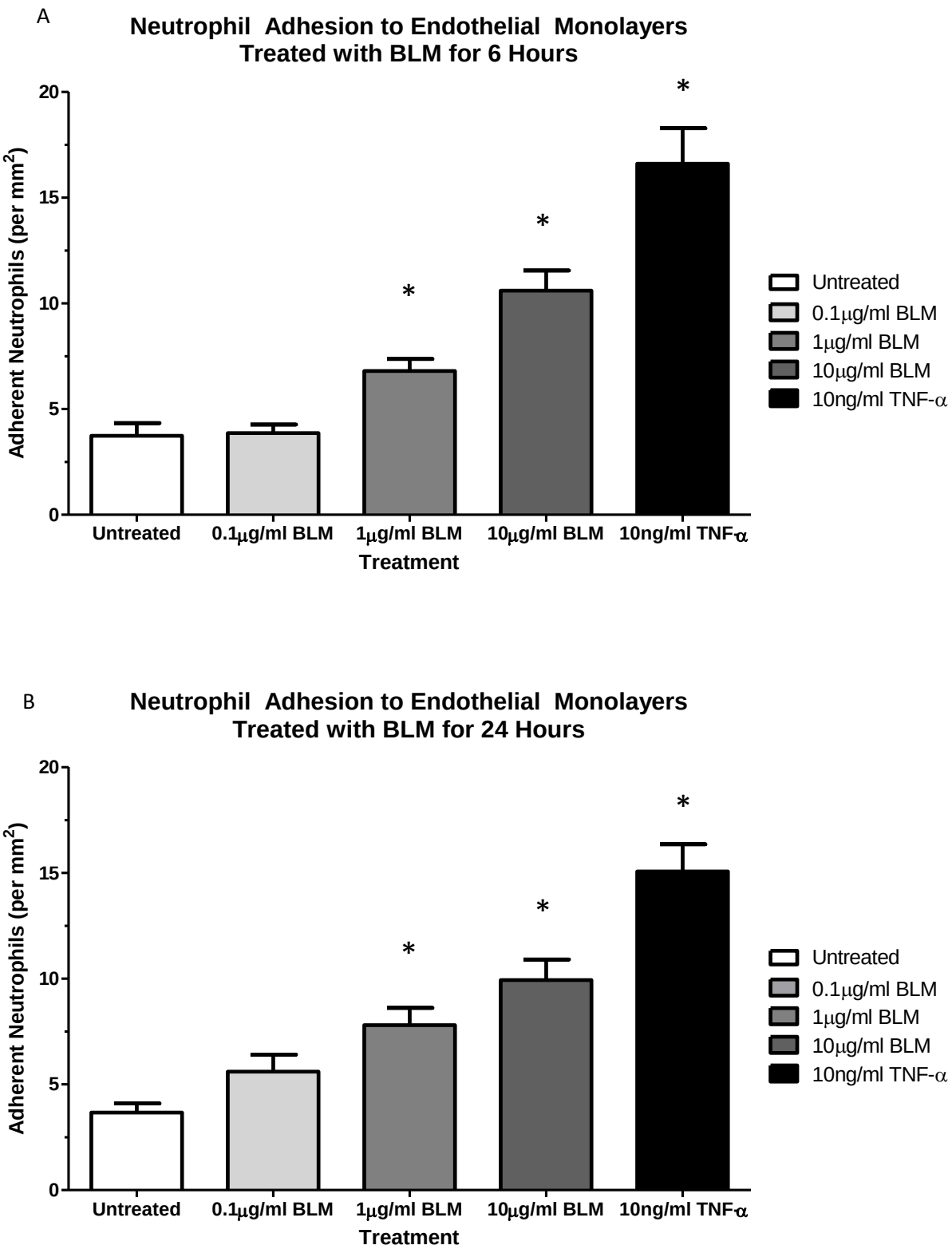

Figure 6.20: Neutrophil adhesion to endothelial monolayers treated with BLM and TNF-α for 6 and 24 hours.

Neutrophil adhesion to endothelial cell monolayers treated with 0.1, 1, and 10μg/ml BLM, 10ng/ml TNF-α, or media alone, for 6 (A) and 24 (B) hours. Statistically significant differences in neutrophil adhesion to the monolayer compared to baseline (*p=<0.05*) are denoted by an asterisk. *N=3.*

	New Neutrophil Adhesion Events					
	Average Per Field			Total in all 5 Fields		
Treatment Condition	Donor 1	Donor 2	Donor 3	Donor 1	Donor 2	Donor 3
Negative Control	0.6	0.6	0.8	3	3	4
0.1µg/ml BLM	0.8	0.8	0.8	4	4	4
1µg/ml BLM	1.4	0.6	1	7	3	5
10µg/ml BLM	0.2	0.8	1	1	4	5
10ng/ml TNF-α	6.2	5	1.2	31	25	6

Table 6.1: New adhesion events observed in 6 hour flow chamber experiments.

The total number of new adhesion events observed when neutrophils were flowed over endothelial monolayers treated with BLM or TNF-α (6 hour treatment).

	New Neutrophil Adhesion Events					
	Average Per Field			Total in all 5 Fields		
Treatment Condition	Donor 1	Donor 2	Donor 3	Donor 1	Donor 2	Donor 3
Negative Control	0.4	0	0.2	2	0	1
0.1µg/ml BLM	0.2	0	0.2	1	0	1
1µg/ml BLM	0.2	0.4	0.6	1	2	3
10µg/ml BLM	0.6	0.4	1	3	2	5
10ng/ml TNF-α	2.4	0.8	2.4	12	4	12

Table 6.2: New adhesion events observed in 24 hour flow chamber experiments.

The total number of new adhesion events observed when neutrophils were flowed over endothelial monolayers treated with BLM or TNF-α (24 hour treatment).

6.3.8 Anti-CD18 Antibody-Treated Neutrophil Adhesion to Monolayers under Flow.

To determine the adhesion molecules likely to be involved in the increased adhesion of neutrophils to the BLM-treated endothelium, flow experiments were carried out in which molecules or ligands were blocked. Initially, to assess whether ICAM-1 was involved in adhesion, CD18 was blocked using the TS1/18 antibody. This antibody was used at a concentration of 20μg/ml, deemed to be sufficient to block all CD18 molecules on neutrophils used in this experiment.

It was noted that both the isotype control antibody and the CD18 antibody resulted in activation and therefore aggregation of neutrophils in many of these experiments. Whether this was the case appeared to be a donor specific phenomenon, with neutrophils isolated from donors of generally identical profiles (age, gender, and ethnicity) demonstrating very different responses to treatment with antibody. Moreover, the additional time required to treat the isolated neutrophils with these antibodies may have contributed to the activation and aggregation seen. For this reason, while *n=3* was achieved for the experiments, eight attempts at conducting the experiments were required to achieve this. In four of these experiments, incomplete data was collected (as there were insufficient viable cells), or no viable neutrophils were present in the isolated samples. In one experiment, the endothelial monolayer had not formed correctly and the chambers were discarded. Incomplete data was discarded and only data from the three complete experiments was used.

Pre-treatment of neutrophils with TS1/18 did not prevent neutrophil adhesion to BLM treated monolayers. The level of adhesion of TS1/18-treated and isotype-treated neutrophils to the endothelium was similar, and was not statistically different. However, pre-treatment with TS1/18 appeared to decrease the adhesion of neutrophils to TNF-α-treated monolayers by around 30% (Fig 6.21).

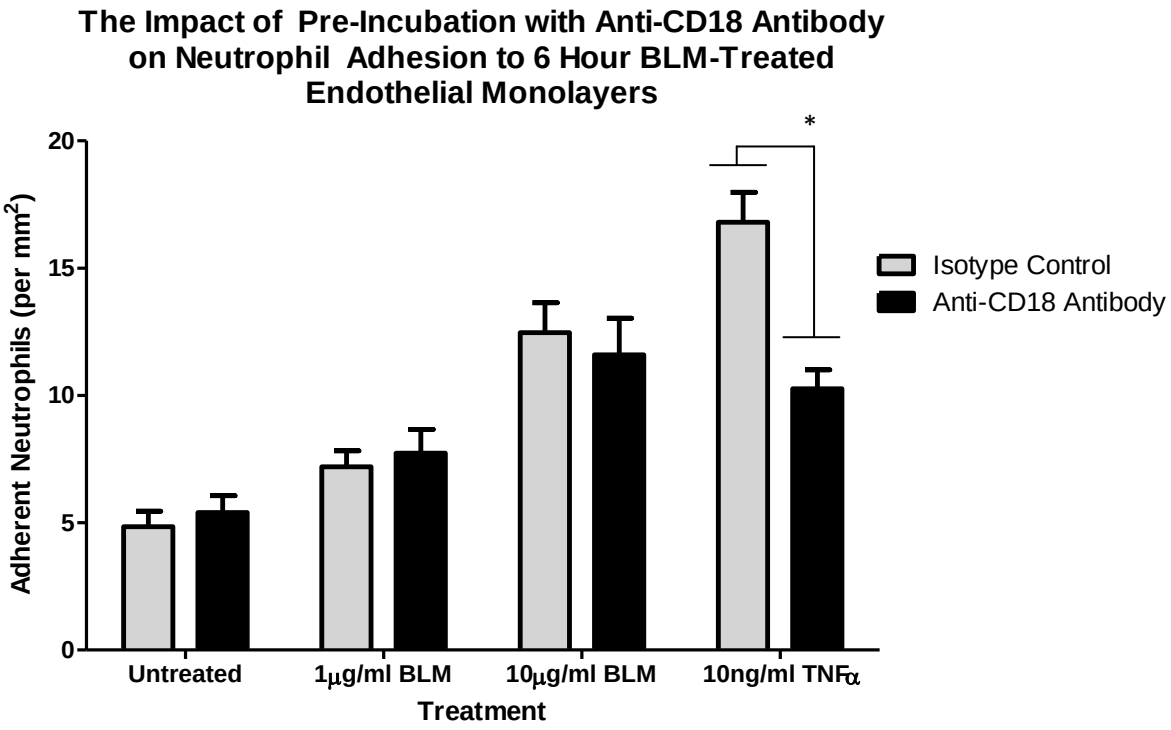

Figure 6.21: Anti-CD18 antibody and isotype control treated neutrophil adhesion to BLM and TNF-α-treated endothelial monolayers under flow.

The adhesion of isotype control treated and anti-CD18 antibody treated neutrophils to endothelial cell monolayers treated with 1μg/ml and 10μg/ml BLM, 10ng/ml TNF-α, or left untreated for 6 hours. Statistically significant differences in neutrophil adhesion to the monolayer (*p=<0.05*) are denoted by an asterisk. *N=3.*

6.3.9 Optimisation of Monolayer Treatment with Anti-E-selectin Antibody

Optimisation work carried out to determine how viable endothelial monolayers were immediately after media changes (for use with the CD62E blocking experiments) revealed that, after an initial media change, there was large scale dissociation of endothelial cells from the flow chamber base. This was not immediate; dissociation appeared to occur between five and thirty minutes after the media change. This disrupted the integrity of the monolayer. Once dissociated (but still present in the flow chamber), endothelial cells were noted to re-adhere to the chamber after around four hours, but not before (one and two hours after the media change, there were still many non-adherent endothelial cells present in the flow chambers). Therefore, the minimum incubation time that could be used with the concurrent BLM/TNF-α and anti-CD62E antibody treatment experiments was four hours. Because of this, cells were concurrently treated with the two agents for 6 hours to mirror the incubation time with BLM/TNF-α in earlier experiments. This was deemed to be unlikely to compromise the integrity of the endothelial monolayer.

6.3.10 Adhesion of Neutrophils to Anti-E-selectin Antibody-Treated Monolayers under Flow.

When endothelial monolayers were pre-treated with anti E-selectin antibody and neutrophils were rolled over the monolayer, a large decrease of around 60% in the adhesion of neutrophils to TNF-α-treated flow chambers was observed. However, once again, there was no statistically significant blockade of neutrophil adhesion to monolayers treated with BLM or untreated monolayers (Fig 6.22).

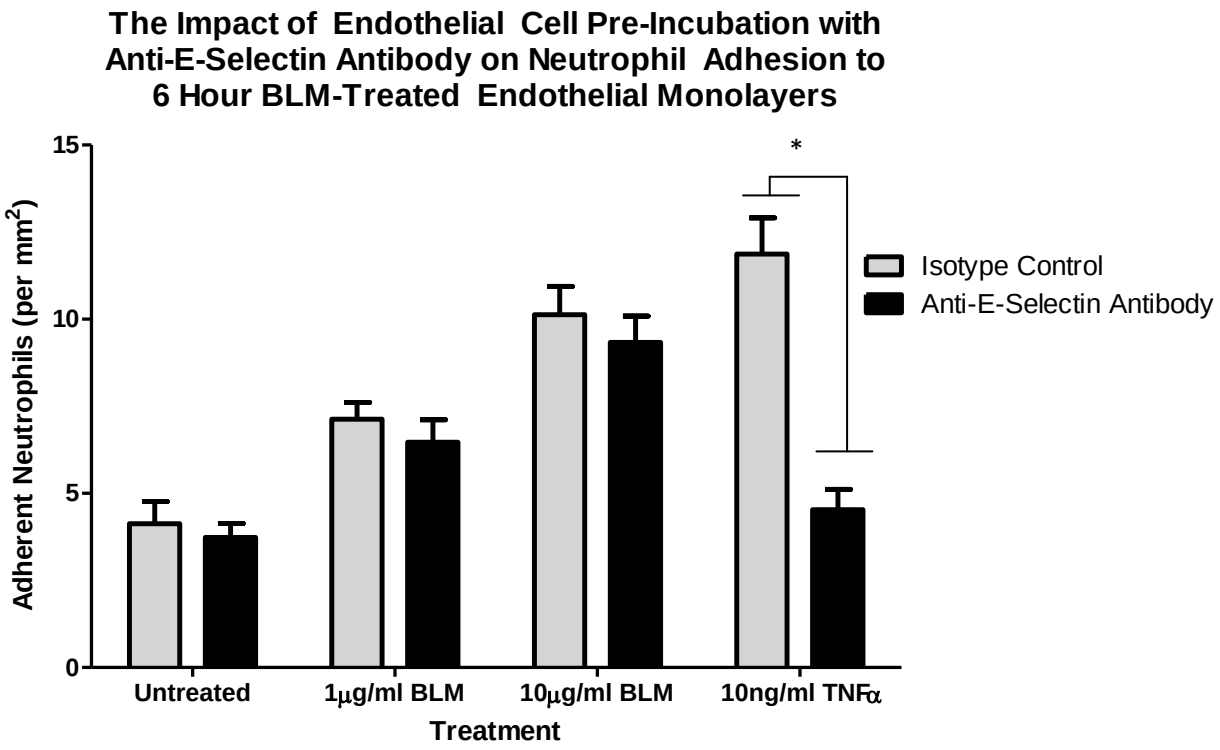

Figure 6.22: Neutrophil adhesion to anti-E-selectin and isotype control treated endothelial monolayers concurrently treated with BLM and TNF-α under flow.

The adhesion of neutrophils to endothelial cell monolayers co-treated with 1μg/ml and 10μg/ml BLM, 10ng/ml TNF-α, or media alone, with anti-CD62E antibody or isotype control antibody, for 6 hours. Statistically significant differences in neutrophil adhesion to the monolayer (*p=<0.05*) are denoted by an asterisk. *N=3.*

6.3.11 The Impact of Isotype Control Antibody Treatment of Monolayer on Neutrophil Adhesion under Flow.

In addition, the results obtained from these experiments suggest that the isotype control antibody used may have slightly decreased neutrophil adhesion to the endothelial monolayer. In all cases, neutrophil adhesion to the monolayer was slightly lower when untreated neutrophils were flowed over isotype control-treated HUVECs, than when isotype control-treated neutrophils were flowed over untreated HUVECs. However, the differences observed were not statistically significant, with the exception of endothelial monolayers treated with TNF-α (Fig 6.23). It is possible that the isotype control may have prevented the adhesion of neutrophils to the monolayer in these experiments, potentially due to the isotype control binding slightly to an adhesion molecule responsible for allowing neutrophil adhesion to the endothelial monolayer.

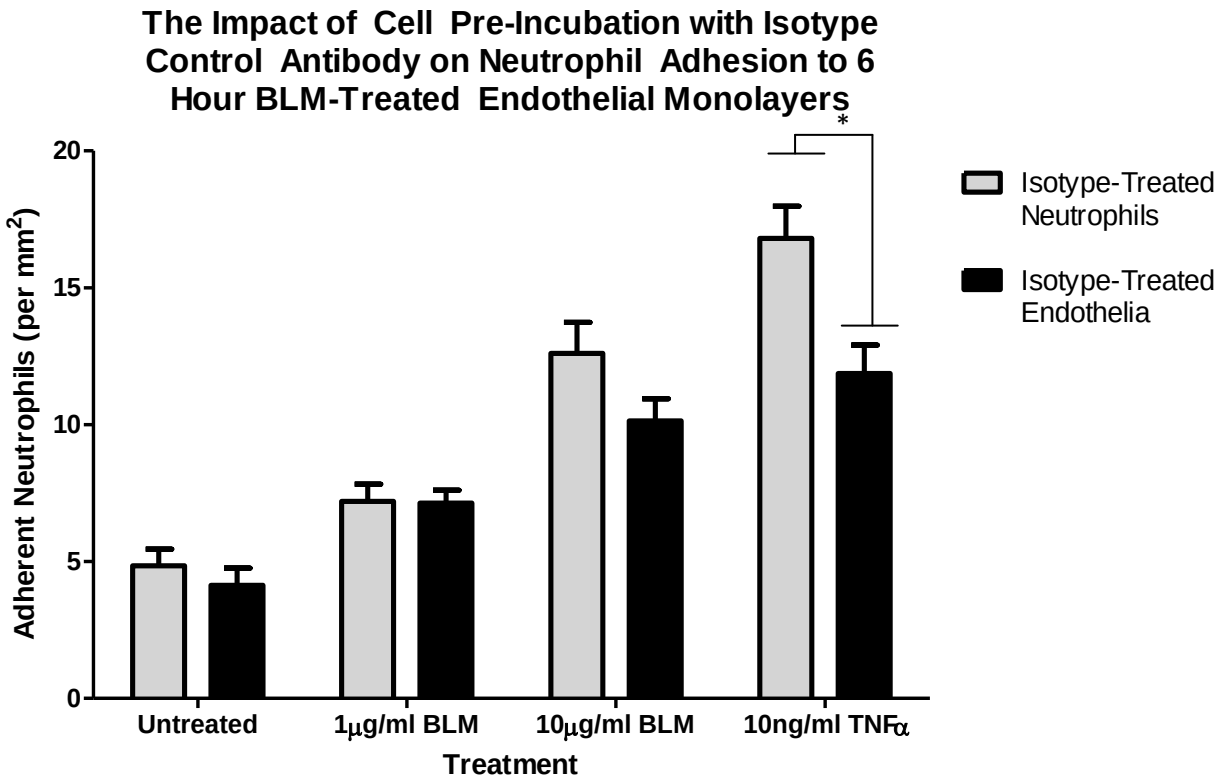

Figure 6.23: Neutrophil adhesion to BLM and TNF-α treated monolayers when neutrophils or endothelial cells were treated with isotype control antibody.

The adhesion of isotype control-treated neutrophils to endothelial cell monolayers treated with 1μg/ml and 10μg/ml BLM, 10ng/ml TNF-α, or media alone, and the adhesion of neutrophils to endothelial cell monolayers co-treated with 1μg/ml and 10μg/ml BLM, 10ng/ml TNF-α, or media alone, and isotype control , for 6 hours. Statistically significant differences in neutrophil adhesion to the monolayer compared to baseline (*p=<0.05*) are denoted by an asterisk. *N=3.*

6.4 Discussion and Conclusions

In this section of work, a flow chamber system was used to model the movement of neutrophils through the pulmonary vasculature in order to determine whether the increased adhesion molecule expression previously observed in endothelial cells treated with BLM exhibited functional relevance; that is to say, whether the adhesion molecules expressed by BLM-treated endothelial cells resulted in increased leukocyte adhesion to the monolayers. However, as this was a new system, extensive optimisation was required.

6.4.1 Optimisation of Flow Chamber Seeding and Treatment

Though the manufacturer's instructions supplied with the ibidi vessels suggested using 3-7x10^5 cells/ml (1.2-2.8x10^4 cells/cm^2) per chamber and incubating for several days to allow a confluent monolayer to develop, a more rapid method was desirable in this work. Accordingly, higher seeding concentrations were trialled, and it was noted that concentrations of 2.5x10^6 cells/ml (2.5x10^5 cells/slide) were capable of generating a confluent monolayer within 24 hours. As the seeding concentration was altered, other factors such as incubation time and time-points of media changes required optimisation; by allowing cells to adhere for 24 hours, and by changing the media 4-6 hours after seeding, complete monolayers which could be used for experimental work were generated. These monolayers withstood shear stresses $\geq$ 5 dyn/cm^2, suggesting that chambers generated using this method were suitable for use. This work has provided a reliable method by which confluent monolayers can be generated rapidly, allowing work to be carried out more efficiently, and thus represents an improvement on the suggested methods of flow chamber seeding and endothelial monolayer generation.

As the integrity of monolayers was maintained when cells were treated with BLM and TNF-α over 6 and 24 hours, this reinforces earlier observations that the concentrations of BLM used are not overtly toxic to endothelial cells over these time-points, and that the use of these concentrations is representative of *in vivo* processes, whereby large-scale endothelial death is not observed (Adamson, 1984).

6.4.2 Optimisation of Shear Stress for Use in Experimental Modelling

Though the shear stress in the post-capillary venules and larger veins is between 1-5dyn/cm^2 (Kroll and Afshar-Khargan, 2012; Kuebler, 2009), these values are not fully defined, and in this work, at 5 dyn/cm^2, neutrophils did not adhere to the monolayer. When 1 dyn/cm^2 was used, few cells adhered. Thus, it may appear that, at shear stresses of >1 dyn/cm^2, adhesion molecules expressed by BLM-treated endothelial cells do not have functional relevance. Therefore, to allow sufficient cells to adhere to the monolayers, the shear stress was decreased to 0.5 dyn/cm^2. While shear stresses ≥1 dyn/cm^2 are more frequently used (McGetterick, et al., 2010; Luu, et al., 2000), there are several reasons for using shear stresses of 0.5dyn /cm^2 in this work.

The lower shear stress used (0.5 dyn/cm^2) may have been favourable in this experimental set-up. Shear stresses over 1 dyn/cm^2 prevent integrin-ICAM-1-mediated adhesion (Bahra, et al., 1998; Rainger, et al., 1995; Lawrence and Springer, 1991), a process inferred in neutrophil tethering and recruitment in BLM-treated rodents (Wang, et al., 2011; Sato, et al., 2000). Thus, while shear of <1 dyn/cm^2 may not be completely physiologically relevant, this value is poorly defined and the prevention of integrin-ICAM-1 interactions mediating adhesion was not desirable in this work.

Moreover, the current work is not the first to report low neutrophil adhesion to monolayers at a shear stress of 1 dyn/cm^2. Lawrence and Springer (1991) reported that, as shear stress became greater than 1 dyn/cm^2, neutrophil adhesion to ICAM-1 and E-selectin harbouring bilayers decreased, with adhesion greatest at around 0.5 dyn/cm^2. This decreased adhesion at shear stresses greater than 1 dyn/cm^2 was suggested to be related to the location of the visualised fields. Laminar flow along the centreline, where the velocity is greatest, may hold neutrophils in suspension, preventing interaction with the monolayer. This may have occurred in the current work; flow chambers with deep channels were used, as these were the chambers in which the greatest range of shear stress could be achieved, and so neutrophils may have been held in suspension some distance from the monolayer.

The low leves of adhesion when shear stresses of 1 dyn/cm^2 were used in this work may also have been due to the time for which the experiments were conducted. While it was

reported that, as low numbers of neutrophils begin to adhere to the monolayer at shear >1dyn/cm^2, disruption of laminar flow may result in turbulence, allowing increased neutrophil-monolayer interaction, but this is a gradual process (Lawrence and Springer, 1991). As the number of neutrophils that could be harvested from a single donor in this work was limited, it was unfeasible to run experiments for times sufficient for this turbulence to occur; all experiments were run for 4 minutes only, as running experiments for longer time periods would have meant insufficient neutrophils to run all four or five plates in the experiment using neutrophils extracted from a single donor.

Therefore, the use of a lower shear stress in this work of 0.5 dyn/cm^2 both allowed measurable results to be obtained, and ensured that ICAM-1-neutrophil ligand interactions, which may be physiologically relevant in the adhesion of neutrophils to BLM-treated monolayers *in vivo,* were not precluded.

6.4.3 Optimisation of Neutrophil Isolation and Neutrophil Identification

Though the usual method for neutrophil isolation involves a double-density gradient, it was found that this method can be unreliable. A single-step density gradient protocol to isolate neutrophils was therefore used. While this resulted in some erythrocyte contamination of the samples, erythrocytes do not adhere to endothelial cells under normal conditions (de Oliveira and Saldanha, 2010; Chappey, et al., 1996; Yang, et al., 2010). Only in conditions such as malaria, in which parasite proteins contribute to the erythrocyte membrane ligand milieu, and sickle cell anaemia, in which reticulocytes may express VLA-4, do erythrocytes adhere to endothelial adhesion molecules (Ockenhouse, et al., 1992; Gee and Platt, 1995; Lutty, et al., 2001; Matsui, et al., 2001; McCormick, et al., 1997) do erythrocytes routinely adhere to endothelial cells; donors with these conditions were excluded. Therefore, in this work, erythrocyte contamination of samples was deemed to not be a counfounding factor in the counting of adherent neutrophils.

Neutrophils were readily identified in this work, appearing as phase-bright, circular cells which were either adherent to the endothelium, or seen to roll and stop on the endothelium. This is in line with work by Zhan, et al (2012) and the identification

guidelines offered by McGettrick, et al. (2010) and Luu, et al. (2010). Further, erythrocytes within the chamber were visualised as non-adherent blurred streaks travelling across the endothelium that appeared phase-dark when visualised using the QCapture Pro 6 software. At no point did these cells adhere to the TNF-α or BLM treated endothelium. Therefore, the chance that erythrocyte adhesion may be mistaken for neutrophil adhesion was deemed negligible. As previously stated, small, non-phase bright adherence events, which may represent cell debris, and larger, non-circular phase-bright events, which represented area of endothelium, were also discounted as they did not meet the criteria of neutrophils. Therefore, the identification of round, phase-bright adherent or rolling cells as neutrophils can be stated. Adhesion of neutrophils to the endothelium based on the appearance criteria outlined above was verified by Dr. Laura Sadofsky and an independent individual not connected to this work.

6.4.4 Neutrophil Adhesion to BLM-Treated Endothelial Monolayers

When endothelial monolayers are treated with various concentrations of BLM for 6 and 24 hours, the adhesion of neutrophils to these monolayers is increased. Of course, this is also the case when the endothelial monolayers are treated with TNF-α. Surprisingly, the degree to which neutrophil adhesion is increased in both the 6 hour and the 24 hour stimulated monolayers is very similar, with monolayers treated for 6 hours showing slightly higher degrees of neutrophil adherence. In this experiment, it was expected that increased adherence was mediated by E-selectin – upregulated quickly and reaching a peak at 4-6 hours - or ICAM-1 - upregulated slowly and reaching a peak at 24 hours - or a combination of the two. However, these results give no clear suggestions as to which molecule(s) are involved in the increased adherence. Regardless, at the flow rate used (0.5 dyn/cm^2), endothelial adhesion molecule expression in response to BLM has a functional consequence.

Interestingly, the number of adherent neutrophils was similar in monolayers treated with BLM (shown to induce a modest increase in adhesion molecule expression) and those treated with TNF-α (which induced larger increases in adhesion molecule expression). The reasons for this are unknown. It is possible that, as photographs were taken at selected

points along the chamber, as outlined in the protocol of McGetterick, et al. (2010), areas of dense adhesion may have been missed. The chambers used in this experiment have a surface area of 2.5cm^2, while the visualised fields were only 1mm^2, leaving large areas of the chamber not assessed.

Furthermore, all fields photographed were along the midline of the chamber, again in accordance with the McGetterick, et al. (2010) protocol. As shear stress calculations used with this system apply to the midline (ibidi Application Note 11), the edges were not assessed. The shear rate in these locations could not be guaranteed; shear stress within a chamber demonstrates parabolic flow profiles, with the degree of shear stress lower at the edges of the chamber, and the calculated shear stress applicable to the centre of the chamber (Lawrence and Springer, 1991; ibidi Application Note 11). Alternatively, it is possible that the results obtained when neutrophils were flowed over TNF-α-treated monolayers represent the maximum level of adhesion achievable using this number of neutrophils, or that the functional effect of BLM is comparable to that of TNF-α, at least in this system.

These results are not similar to those of previously published works assessing neutrophil adherence in response to stimulation with cytokines including TNF-α, which routinely report greater numbers of adherent cells, between 350-700 cells/mm^2/10^6 cells perfused (Luu, et al., 2010; Luu, et al., 2000; Sheikh, et al., 2005). However, these reports use more cells (1 x 10^6/ml) and a different protocol, whereby neutrophils are delivered into the chamber as a bolus and then washed out using PBS. It is after this wash-out stage that neutrophil behaviour was assessed (Sheikh, et al., 2005; Luu, et al., 2000; Luu, et al., 2010; Burton, et al., 2011). Using such a protocol, more neutrophils enter the chamber before analysis occurs, though it may be questioned how rolling behaviour can be assessed using this method. When neutrophil behaviour was assessed during perfusion and not after wash-out, the results reported are more similar to that of this work (Rainger, et al., 1995; Sheikh, et al., 2002).

Though both methods were used in this series of experiments initially, and data was collected and analysed from both during the neutrophil perfusion and after the wash-out step for the 6- and 24-hour BLM treatment experiments, it was decided that measuring

neutrophil behaviour following bolus infusion and wash-out – when a large number of neutrophils was present in the chamber and all non-adherent neutrophils had been removed from the system – was not physiologically relevant. *In vivo*, neutrophils would be present in circulation at all times, and measuring neutrophil adhesion once a large number of cells has entered the chamber and no more were flowing over the endothelium is artificial. Measuring rolling neutrophils using this model would be a measurement of neutrophil dissociation from the endothelium, rather than of tethering, slowing, and adherence.

When data collected after wash-out was analysed, greater numbers of adherent neutrophils were observed in these experiments than in those where data was collected while neutrophils were being perfused (data not shown). The reason for this is uncertain; this may merely reflect the increased number of cells that have entered the chamber. When assessing neutrophil adhesion during perfusion, recording began when $5x10^5$ neutrophils had been perfused, and ended when $1x10^6$ had been perfused (at speeds slow enough to adhere), while in the wash-out data, $1x10^6$ neutrophils had been perfused before recording started. Alternatively, interactions between flowing cells may have prevented adhesion during perfusion; in some fields, contact between adherent and non-adherent cells under flow resulted in neutrophil detachment. As the wash-out phase introduces neutrophils from the tubing or upstream fields and, decreased cell counts are present in suspension, neutrophils may have had more opportunity to adhere or remain adherent as they are not “knocked off” during wash-out. Lastly, it is possible that by switching between neutrophil suspension and washing buffer, a disturbance in the shear flow rate allows neutrophils to adhere more, as the flow rate decreases. Such cells may not then be dislodged as the shear stress returns to set levels.

The use of a different recording protocol may explain the discrepancies noted between this work and that of others, and this may be compounded by the differences in the numbers of neutrophils used. While this means the results of this work are not directly comparable to those of other groups, the method used here represents a more physiologically relevant model, and it was decided that this method would be used in future experiments.

6.4.5 Identification of Adhesion Molecules Mediating Increased Adhesion

Treatment of isolated neutrophils with anti-CD18 blocking antibody was observed to decrease the binding of neutrophils to TNF-α-treated endothelial monolayers by approximately 30%, in line with previous literature (van Epps, et al., 1989; Smith, et al., 1988; Meerschaert and Furuie, 1993; Lopez-Farré, et al., 1993), suggesting that neutrophil adhesion to TNF-α treated monolayers was at least in part ICAM-1 dependent. However, neutrophil adhesion to BLM-treated monolayers was not prevented by the addition of anti-CD18 antibody to neutrophil suspensions. Therefore, ICAM-1 is perhaps not involved in neutrophil adhesion to BLM-treated endothelial cells. This was somewhat surprising, as ICAM-1 was the adhesion molecule most upregulated by BLM treatment in previous experiments, and was clearly involved in neutrophil adhesion to TNF-α treated monolayers. Moreover, previous reports (albeit using murine models) have identified strong associations between pulmonary venule and capillary ICAM-1 expression and the accumulation of leukocytes at the vessel wall and in the perviascular space in rodents treated with BLM (Wang, et al., 2011; Sato, et al., 2000). However, the results of this work suggest that, in human cells, ICAM-1 is not involved in neutrophil adhesion to endothelial cells in response to BLM treatment.

As neutrophil adhesion did not appear to be modulated by ICAM-1 expression, blockade of E-selectin was assessed to determine whether this molecule was reponsible for the increased adhesion noted. Again, there was a decrease in the adhesion of neutrophils to TNF-α treated monolayers, with around 60% of adhesion blocked. This was of a smaller magnitude than that reported by Ploppa, et al. (2010) and Martin-Satué, et al. (1998), but was still substantial. However, once again, the blockade of E-selectin did not diminish neutrophil adhesion to BLM-treated monolayers; there was a slight decrease in neutrophil adhesion, but this was not statistically significant. Based on these observations, it appears that one or more alternative adhesion molecules must be involved in, and responsible for, the increased adhesion of neutrophils to BLM-treated monolayers.

Previous reports have implicated VCAM-1 in neutrophil adhesion to pulmonary vessels following BLM treatment in mice (Wang, et al., 2011), though the mechanisms by which

neutrophils utilise VLA-4 to adhere to endothelial VCAM-1 are poorly resolved. VCAM-1 may be responsible for the increased adhesion, but as VCAM-1 upregulation in response to BLM was shown to be small, it is equally feasible that an adhesion molecule not previously analysed is responsible.

In light of these results, future would would ideally seek to identify the adhesion molecule responsible for the increased neutrophil binding to BLM treated monolayers. As VCAM-1 was the adhesion molecule upregulated by BLM that was not blocked in these experiments, further work to block VCAM-1 on BLM and TNF-α treated monolayers, to determine whether this molecule is responsible for increased adhesion, is a logical next step. Alternatively, a molecule not previously assessed may be involved in neutrophil adhesion to monolayers, and so it may be of interest to assess the expression of other adhesion molecules in response to BLM.

This could include ICAM-2, implicated in leukocyte crawling along the endothelium (Schenkel, et al., 2004; Phillipson, et al., 2006), or the sialomucin-like GlyCAM-1, which like PSGL-1, binds neutrophil L-selectin, but appears more involved in lymphocyte than neutrophil tethering (Dwir, et al., 1998), though the potential role of this molecule in extravasation is very poorly resolved. Further, CD34, a sulfated sialomucin which also binds to neutrophil L-selectin (Wagner and Roth, 2000) may support neutrophil adhesion in this model, or proteins such as fibronectin may be involved; neutrophils express several ligands for fibronectin including VLA-4, -5, and CD18/CD11b (Williams and Solomkin, 1999; van den Berg, et al., 2001), endothelial cells synthesise and express fibronectin (Peters, et al., 1990; Jaffe and Mosher, 1978) and fibronectin may bind endothelial cells via interactions with integrins such as αVβ3 and α4β1 (Johansson, et al., 1997). It is feasible that, much like that observed with monocytes (van Gils, et al., 2009), fibronectin attached to endothelial ligands may support bringing interactions between endothelial cells and neutrophils. Alternatively, a previously undescribed molecule may play a role in neutrophil adhesion under these circumstances.

6.4.6 Technical Difficulties Encountered in Adhesion Molecule Blocking Experiments

This particular work was fraught with technical difficulties. Primarily, that treatment with anti-CD18 antibody and isotype control antibody often resulted in the activation of isolated neutrophils, leaving no cells available to run the assay (6.3.3). There was no obvious reason for this; while treatment with antibodies added an extra 30 minutes to the experiment, neutrophils were still viable after treatment on three occasions.

It was thought that CD18 ligation may have resulted in cell loss initially, though, while CD18 is implicated in a host of neutrophil responses including phagocytosis and spreading on the endothelial monolayer (Tan, 2010.; El Kebir and Filep, 2013; Petersen, et al., 1994; Suzuki, et al.2006), and the degranulation of endothelium-bound and TNF-α stimulated neutrophils (Schleiffenbaum, et al., 1987; Richter, et al., 1990), there are no reports of CD18 ligation activating suspended neutrophils, or causing neutrophil apoptosis. In fact, CD18 ligation appears more related to apoptosis inhibition in neutrophils (El Kabir and Filep, 2013). Therefore, it is as likely that the prolonged experimental time and increased agitation of isolated neutrophils resulted in activation, rather than this being a product of CD18 ligation. That the isotype control also induced such activation supports this notion.

6.4.7 Non-Specific Binding of Isotype Control Antibody to Endothelial Monolayer

Interestingly, there was a decrease in neutrophil adhesion to endothelial monolayers when endothelial cells were pre-treated with the isotype control antibody, compared to when neutrophils were treated with the isotype control. This decrease was statistically significant when TNF-α treated monolayers were compared. The reason for this is unknown, though the isotype control may have bound to one or more endothelial cell adhesion molecules involved in neutrophil adhesion in a non-specific manner, but not to neutrophil ligands involved in neutrophil adhesion to the endothelium.

The endothelial cell molecule(s) to which the istoype control antibody binds is unknown. Earlier experiments identified increased levels of non-specific isotype control binding to

both TNF-α and BLM-treated cells, which could not be attributed to Fc receptor expression, and so it is unlikely this non-specific expression could be attributed to Fc receptors in this work; in fact, these results suggest that a molecule involved in neutrophil adhesion to the endothelial monolayer (expressed by the endothelial cells) may have been a target for isotype control binding, at least to a small degree. Further work to determine the molecule(s) to which the isotype control is binding is required before any strong conclusions may be drawn, however.

6.4.8 Overall Conclusions

In all, BLM treatment of endothelial cells for 6 and 24 hours increases neutrophil adhesion to endothelial monolayers, but this work failed to identify the adhesion molecule(s) responsible for this, as the blockade of neither the ICAM-1 ligand CD18, nor endothelial E-selectin, dimished this binding. However, this is the first work to report that, using human cells, BLM increases neutrophil adhesiveness to endothelial cells, and this may contribute to the inflammatory cell influx seen within the lungs during BPF development.

7 Other Chemotherapeutic Agents and their Effects on HUVEC Adhesion Molecule and Cytokine Expression and Release

7.1 Introduction

BLM is not unique in its ability to induce pulmonary fibrosis; many other chemotherapeutic agents, such as mitomycin, carmustine, busulfan, methotrexate, cyclophosphamide, fludarabine, and chlorambucil are also associated with the condition (Barton-Burke, et al., 1996). Based on the hypothesis that the effect of BLM on the endothelium contributes to BPF by inducing adhesion molecule upregulation, it would be interesting to determine whether the upregulation of adhesion molecules is a unique feature of BLM treatment. If so, this would bolster the idea that endothelial adhesion molecule upregulation is a contributory feature to the unique fibrotic response observed.

Drugs were selected that induce cell death via similar mechanisms to BLM, as this would allow the determination of whether drugs which cause DNA-scission mediated death also cause adhesion molecule upregulation. As BLM has a unique mechanism of action (Dorr, 1992), three drugs which cause cytotoxicity due to strand scission and apoptosis were selected; etoposide, doxorubicin, and carboplatin. The expression of adhesion molecules and release of cytokines by endothelial cells treated with these agents will be assessed. In this case the same panel of adhesion molecules as previously assessed using BLM, and IL-8, increased by treatment with BLM, will be tested.

Using pulmonary microvascular endothelial cells would be more physiologically relevant; however, as the current work has previously shown that HUVECs, at least in response to BLM, are a suitable surrogate for this cell type, they will be used for these experiments. A literature review was conducted to determine suitable, pharmacologically revelant concentrations of each drug to use.

7.1.1 Etoposide Mechanism of Action, Pharmacokinetics, and Use

Etoposide, used in the treatment of testicular cancer and lymphomas (Ando, et al., 1996), has a similar mechanism of action to BLM, effecting cytotoxicity by inducing both single- and double-strand DNA cleavage (Sinha, et al., 1988). Though a topoisomerase II inhibitor, etoposide does not prevent the action of topoisomerases, but "poisons" the topoisomerase II enzyme by increasing the concentration of cleavage complexes. Topoisomerase II then generates excessive DNA breaks which may cause apoptosis (Hande, 1998). Both p53-mediated apoptosis and autophagic cell death have been reported to occur due to etoposide treatment (Mizumoto, et al., 1994; Karpinich, et al., 2002; Yoo, et al., 2012), and though the generally accepted mechanism of action involves typical intrinsic apoptosis (Grandela, et al., 2007), caspase 8 may also be involved (Liu, et al., 2011).

Etoposide pharmacokinetics depend on whether the drug is given orally or intravenously, with the former resulting in variable pharmacokinetic profiles (de Jong, et al., 1997) – i.e., if given orally, a dose of 100-150 mg/m^2 results in C_{max} values of 2.8-4.4 µg/ml; if I.V., between 9 and 32 µg/ml (Simon, et al., 2006; Kato, et al., 2003). Moreover, a range of doses are used in man dependent on the target disease, which will also impact the pharmacokinetics of the drug. A review of etoposide pharmacokinetics in a variety of doses and patient groups is shown in Table 7.1.

Although pulmonary fibrosis is not strongly associated with etoposide, there have been documented cases. These include three patients with lung cancer, one of whom received 50mg etoposide orally, and suffered diffuse interstitial fibrosis with evidence of atypical AECs and leukocyte infiltration before succumbing five days after presentation (Dajczman, et al., 1995); another who was given 100mg/m^2 etoposide (I.V.) and later 50mg/day etoposide (oral) and developed interstitial fibrosis and AEC hyperplasia; and a third treated with three doses of etoposide (80mg/m^2) who developed similar diffuse alveolar fibrosis with bilateral interstitial infiltrates and hyperplasic AEC, which also proved fatal (Gurjal, et al., 1999). While the pattern of fibrosis following etoposide delivery is similar to that of BLM, the development and time until fatality is faster, and immune cell infiltration is not fully described. However, that fibrosis occurs in a similar way suggests this could be of interest.

Table 7.1: Etoposide pharmacokinetics for up to 24 hours post-dose.

Study	Dose and Dosing Route	Treatment Group	C_{max} values post-dose	C_{max} values 3H post-dose	C_{max} values 6H post-dose	C_{max} values 24H post-dose
Köhl, et al. (1992)	720mg/m^2 ; short I.V. infusion	Adults	130 µg/ml	30µg/ml	Not assessed	5µg /ml
Sinkule, et al., (1984)	200mg/m^2 ; 30 min. I.V. infusion	Children	40 µg/ml	Not assessed	9µg/ml	1-2µg/ml
Schroeder, et al., (2004)	500mg/m^2 ; I.V. bolus	Children prior to marrow transplant	100µg/ml	Not assessed	Not assessed	Up to 15 µg/ml
Chrzanowska, et al. (2011)	60mg/kg;I.V. bolus	Children prior to marrow transplant	100-500µg/ml	Not assessed	10-100µg/ml	1-20µg/ml
Toffoli, et al. (2001)	100mg; oral dosing	Adults	4 µg/ml	Not assessed	2 µg/ml	1 µg/ml

A definitive list of studies that have assessed the pharmacokinetics of etoposide in a range of patient groups for up to 24-hours post-dosing via various routes, using various total doses of etoposide.

HUVECs will be incubated with etoposide for 24 hours to assess adhesion molecule expression and cytokine release, C_{max} values achievable around 24-hours post dose were chosen. must be used. Based on the above data, these will be 3 µg/ml, 10 µg/ml, and 30 µg/ml (5.1µM, 17µM, and 51µM, respectively).

7.1.2 Doxorubicin Mechanism of Action, Pharmacokinetics, and Use

Doxorubicin (DOX) is a cytotoxic anthracycline antibiotic (Benjamin, et al., 1973) and has a range of cytotoxic effects including DNA synthesis inhibition and cross-linking, interference with DNA unwinding via helicase retardation, and both free radical generation and topoisomerase II inhibition leading to DNA cleavage and apoptosis; however, these effects and are not fully understood (Gewirtz, 1999). It is used in the treatment of breast cancer, Kaposi's sarcoma, and small-cell lung cancer, with a recommended effective dose of 60-75mg/m^2 (Chan, et al., 2004). Side-effects include irreversible cardiotoxicity, dependent on cumulative dose, although children and adolescents are very susceptible (Zhang, et al. 2009). There have been reports of pulmonary fibrosis following DOX therapy when combined with mitomycin C (Zappa, et al., 2009) and paclitaxel (Nevandunsky, et al., 2013), although this may be due to the latter drug in both cases (Verweij, et al., 1987; Nevandunsky, et al., 2013).

DOX exhibits rapid distribution but slow clearance (Barpe, et al., 2010), and the pharmacokinetics of the drug vary widely (Frost, et al., 2002), most noticable immediately after dosing - Callies et al. (2002) saw a broad range of C_{max} values in patients given 75mg/m^2 by IV bolus over 30 minutes, falling between 700ng/ml and 1400 ng/ml. Pharmacokinetics also depends on dosing route, weight, and age. Frost, et al., (2002), for example, noted that while patients under the age of 2 and over the age of six has similar plasma concentrations of doxorubicin immediately after a dose of 40mg/m^2 by 24-hour I.V. infusion (around 50ng/ml), that seen in children aged 2-6 years was far higher - up to 78ng/ml - though no ill effects were seen in this group.

Table 7.2: Doxorubicin pharmacokinetics for up to 24 hours post-dose.

Study	Patient Group	Dose and Route	Plasma conc. immediately after dose	Plasma conc. 6H after dose	Plasma conc. 8H after dose	Plasma conc. 24H after dose
Barpe, et al. (2010)	Normal-weight females	60mg/m^2 intravenous	630ng/ ml	105ng/ml	Not assessed	40ng/ml
	Overweight females	60mg/m^2 intravenous	370ng/ml	100ng/ml	Not assessed	40ng/ml
Speth, et al. (1987)	Adults	30mg/m^2 by IV bolus	1170ng/ml - 2110ng /ml	Not assessed	30ng/ml	9ng/ml - 11ng/ml
		30mg/m^2 by 8 hour I.V. infusion	35ng/ml - 135ng/ml	Not assessed	10ng/ml	Not assessable
Callies, et al. (2002)	Adults	75mg/m^2 30-minute IV infusion	700ng/ml - 1400 ng/ml	30-60ng/ml	Not assessed	5-30ng/ml
Bronchud, et al. (1990)	Adult females	100mg/m^2 10 minute IV infusion	1100 – 3000ng/ml	70ng/ml	~60ng/ml	30ng/ml
Twelves, et al. (1991)	Adult females	75mg/m^2 bolus doses	Around 1200ng/ml	Around 30ng/ml	Not assessed	Around 15-20ng/ml
		25mg/m^2 bolus doses	Around 200ng/ml	Around 20ng/ml	Not assessed	Around 15-20ng/ml

A definitive list of studies that have investigated the pharmacokinetics of DOX for up to 24 hours after dosing in a variety of patients at a variety of doses.

As DOX pharmacokinetics vary so widely, this work will investigate only C_{max} values 24 hours after dosing. It appears that, over long periods, the dosing type and the patient characteristics are less determinant of the plasma DOX concentration; 24 hours after dosing, the plasma concentration is between 5 and 50ng/ml. Therefore, concentrations within this range will be used.

7.1.3 Carboplatin Mechanism of Action, Pharmacokinetics, and Use

Carboplatin is a non-classical ankylating-like agent that induces cell death (Lokich and Anderson, 1998) via the formation of DNA intrastrand adducts, a form of cross-linking involving adjacent bases, leading to cell death via apoptosis as pro-apoptotic proteins detect damage (Siddik, 2003). Adducts may also prevent DNA replication and transcription, resulting in cell-cycle disruption (Kelland, 2007), and, as with BLM (where the number of DSBs determines cytotoxicity) a linear relationship between platin-DNA binding and cell death has been noted (Fraval and Roberts, 1979). However, unlike DOX and BLM, which both have severe side-effects, and the related drug oxaliplatin, associated with the development of lung fibrosis (Ryu, et al., 2011; Mundt, et al., 2007), carboplatin is relatively side-effect free, with only myelotoxicity a known issue (Kelland, et al., 2007).

Carboplatin requires activation to exert its effects. While cisplatin is activated by the loss of chloride groups, leaving reactive metabolites, carboplatin lacks these groups (St Germain, et al., 2010; Cepeda, et al., 2007), instead having a less reactive cyclobutanedicarboxylate group (Fichtinger-Schepman, et al., 1995) which makes the drug more stable. It is thought that reaction with carbonate results in an "open-ring", reactive form of the drug. This has been suggested both *in vivo* and in experimental models, and sufficient carbonate to induce activation is thought to be present in blood and culture media (Di Pasqua, et al., 2006; Ciancetta, et al., 2012).

To assess carboplatin pharmacokinetics, free platinum in plasma ultrafiltrate is generally measured, as this is the therapeutically active form. Total platinum is also often measured, but this represents free and protein-bound platinum (Alberts and Dorr, 1997), and may overestimate concentrations. Though some suggest that free carboplatin is not detectable after 10 hours, while free platinum is (Korst, et al., 1997), others found that both free platinum and carboplatin are present in the plasma at comparable levels for around 9 to 16 hours following dosing (Elferink, et al., 1987; Mulder, et al., 1990). As carboplatin cannot be activated in this work prior to cell treatment, though carboplatin activation appears possible in culture medium (Di Pasqua, et al., 2006), studies that have assessed carboplatin levels will be assessed (Table 7.3). Using these concentrations, HUVECs will be exposed to the same level of carboplatin as endothelial cells would be in

vivo. A range of concentrations between 0.1 and 8µM appear appropriate; therefore, concentrations of 0.1, 1, and 10µM will be used.

Table 7.3: Carboplatin pharmacokinetics for up to 24 hours post-dose.

Study	Patient Population	Dose and Route	Plasma conc. immediately after dosing.	Plasma conc. 6 H after dosing.	Plasma conc. 12 H after dosing.	Plasma conc. 24 H after dosing.
Zandvliet, et al. (2008)	Adults with solid tumours (*n=111*).	30 minute IV infusion – sufficient carboplatin to achieve an AUC of 4-6mg min^{-1} ml^{-1}	Around 100µM	Around 6 and 20µM	Not assessed.	Between 0.3 and 8µM
Riccardi, et al. (1994).	Children	400, 500, 600 mg/m^2;1-hour IV fusion (AUC between 4 and 8mg min^{-1} ml^{-1})	30 - 80µg/ml (81-216µM)	1 - 2 µg/ml (2.7-5.2µM)	0.2 - 0.8 µg/ml (0.52-3µM),	0.09 - 0.3µg /ml (0.27-0.81µM
Mulder, et al. (1990)	Adults given carboplatin over several cycles.	250 mg/m^2 dose 1	Around 20-40µg/ ml (55-110µM).	Around 3µg /ml (8µM)	Around 0.4 – 0.5 µg/ml (1.1 – 1.35µM)	0.1 – 0.5µg/ml (0.27-1.35 µM)
		250 mg/m^2 dose 2	Around 20-40µg/ ml (55-110µM).	Around 3µg /ml (8µM)	Around 1-2µg/ml (2.7 - 5.4µM).	0.1-1 µg/ml (0.27-2.7 µM)
		250 mg/m^2 dose 3	Around 20-50µg/ ml (55-128µM).	Around 3µg /ml (8µM)	Around 1-2µg/ml (2.7 - 5.4µM).	0.1-2 µg/ml (0.27-5.4 µM)

A definitive list of studies investigating carboplatin pharmacokinetics for up to 24 hours after dosing in a variety of patients, using a variety of total doses and dosing regimens.

Note that Zandvliet, et al. (2008) used doses tailored to achieve an AUC (area under the curve) value, representative of the total amount of carboplatin available in circulation from dosing to total clearance, based on the now widely used Calvert formula (Calvert, et al., 1989). Further, Mulder, et al. (1990) used multiple dosing - like many other drugs, carboplatin is often not given only as a single dose. However, it appears free carboplatin accumulates in the plasma with repeated dosing, while DOX and etoposide do not (Speth, et al., 1987; Kohl, et al., 1992).

7.2 Materials and Methods

7.2.1 Etoposide, Doxorubicin, and Carboplatin Preparation

Etoposide (>98% purity) and doxorubicin hydrochloride were purchased from Sigma Aldrich. Etoposide was dissolved in 100% dimethyl sulfoxide (DMSO) (Sigma Aldrich) to a concentration of 50mM in line with the provided product information sheet. Dissolved etoposide was stored at -20°C for up to one month. Doxorubicin hydrochloride was dissolved in PBS to a stock concentration of 1mg/ml. This was then stored at -20°C in darkness for up to one month in accordance with work by Hoffman, et al., (1979) and Wood, et al., (1990). Carboplatin was purchased from Tocris (Tocris Biosciences, Bristol, United Kingdom). Carboplatin was dissolved in PBS to a stock concentration of 10mM and frozen at -20^{o}C according to the manufacturer's instructions. All chemotherapeutic agents were dissolved inendothelial cell media to required concentrations prior to use.

7.2.2 Treatment of HUVECs with Etoposide, Doxorubicin, and Carboplatin

Cells were cultured to confluence as outlined in 2.1. Stock solutions of etoposide, doxorubicin, and carboplatin were made as outlined in 2.8. When confluent, cells were treated with etoposide, doxorubicin, or carboplatin dissolved in serum-containing endothelial cell basal medium. The volume of medium was dependent on the experimental protocol being followed (ELISA or FACS analysis). Cells were treated with 3, 10, and 30µg/ml etoposide (or 5.1µM, 17 µM, and 51µM etoposide, with resulting DMSO concentrations of 0.01%, 0.03%, and 0.1% in etoposide-contaning cell culture media); 3, 10, and 30ng/ml doxorubicin; or 0.1, 1, and 10µM carboplatin for 24 hours. In addition, cells were also treated with DMSO, to act as a vehicle control, as etoposide is not soluble in water, PBS, or culture medium alone. Medium containing each concentration of each drug was generated by dilution of stock concentrations in appropriate volumes of serum-containing endothelial cell basal medium.

7.2.3 HUVEC Adhesion Molecule Expression Determination Following Treatment with Etoposide, Doxorubicin, and Carboplatin.

Cells were cultured as outlined in 2.1. To appropriate flasks, 10ml of serum-contaning endothelial cell basal medium contaning various concentrations of etoposide, doxorubicin, carboplatin, or DMSO – as outlined above - was added. Cells were treated for 24 hours. The negative control was HUVECs incubated in serum-contaning endothelial cell basal medium (10ml) without treatment. The positive control was HUVECs incubated in endothelial cell basal medium contaning 10ng/ml TNF-α (10ml). Both negative and positive control cells were incubated for 24 hours. After treatment, cells were dissociated, counted, resuspended to a concentration of 1 x 10^6 cells/ml in endothelial cell medium, and prepared for flow cytometry and analysed using the same range of antibodies, as described in 2.3, 2.4, and 2.5, respectively. Data were analysed using Mann-Whitney-U tests in SPSS v. 19 statistical analysis software.

7.2.4 HUVEC Cytokine Release Determination in Response to Etoposide, Doxorubicin, and Carboplatin Treatment

Cells were cultured as outlined in 2.1 and replated as outlined in 2.7. When adherent, 3ml of serum-containing endothelial cell basal medium containing aforementioned concentrations of etoposide, doxorubicin, carboplatin, or DMSO was added. Cells were incubated in this treatment for 24 hours only. Negative control supernatants were generated as outlined in 2.7. Positive control supernatants were generated by treating cells with 10ng/ml TNFα.

The supernatants were then collected as outlined in 2.7. ELISA kits were purchased from Biolegend. All preliminary work and supernatant handling was conducted as outlined in 2.7. Plates were read using a plate-reader (Thermo Multiskan FC, Thermo Scientific) at the wavelengths instructed by the instructions provided with the kits. This was an initial reading at 450nm and a subsequent reading at 570nm, the second subtracted from the first to reduce background. Data handling was carried out in accordance with section 2.7. Data were analysed by Mann-Whitney-U test in SPSS v. 19 statistical analysis software.

7.3 Results

7.3.1 Adhesion Molecule and Cytokine Expression and Release in Response to Etoposide, Doxorubicin, and Carboplatin

The expression of ICAM-1 was significantly higher (*p=0.05*) in cells treated with all concentrations of etoposide than noted at baseline (untreated cells). The expression of E-selectin and VCAM-1 was also increased by treatment with 3µg and 30µg, and 30µg etoposide, respectively. The changes in adhesion molecule expression were far less substantial in cells treated with DOX compared to those treated with etoposide. However, there was an increase in the expression of ICAM-1, E-selectin, and VCAM-1 when cells were treated with 30ng/ml DOX (Fig. 7.1 A-D). Carboplatin was not observed to significantly upregulate the expression of any of the previous noted adhesion molecules (data not shown). There was no effect on the expression of any adhesion molecule by the use of DMSO as a vehicle (data not shown).

Treatment with all concentrations of etoposide induced a significant increase in the release of IL-8 by HUVECs. There was an increase in IL-8 release in cells treated with the lowest concentration of DOX, but not any other concentration. There were no increases in the release of IL-8 by HUVECs treated with any concentration of carboplatin or DMSO (data not shown).

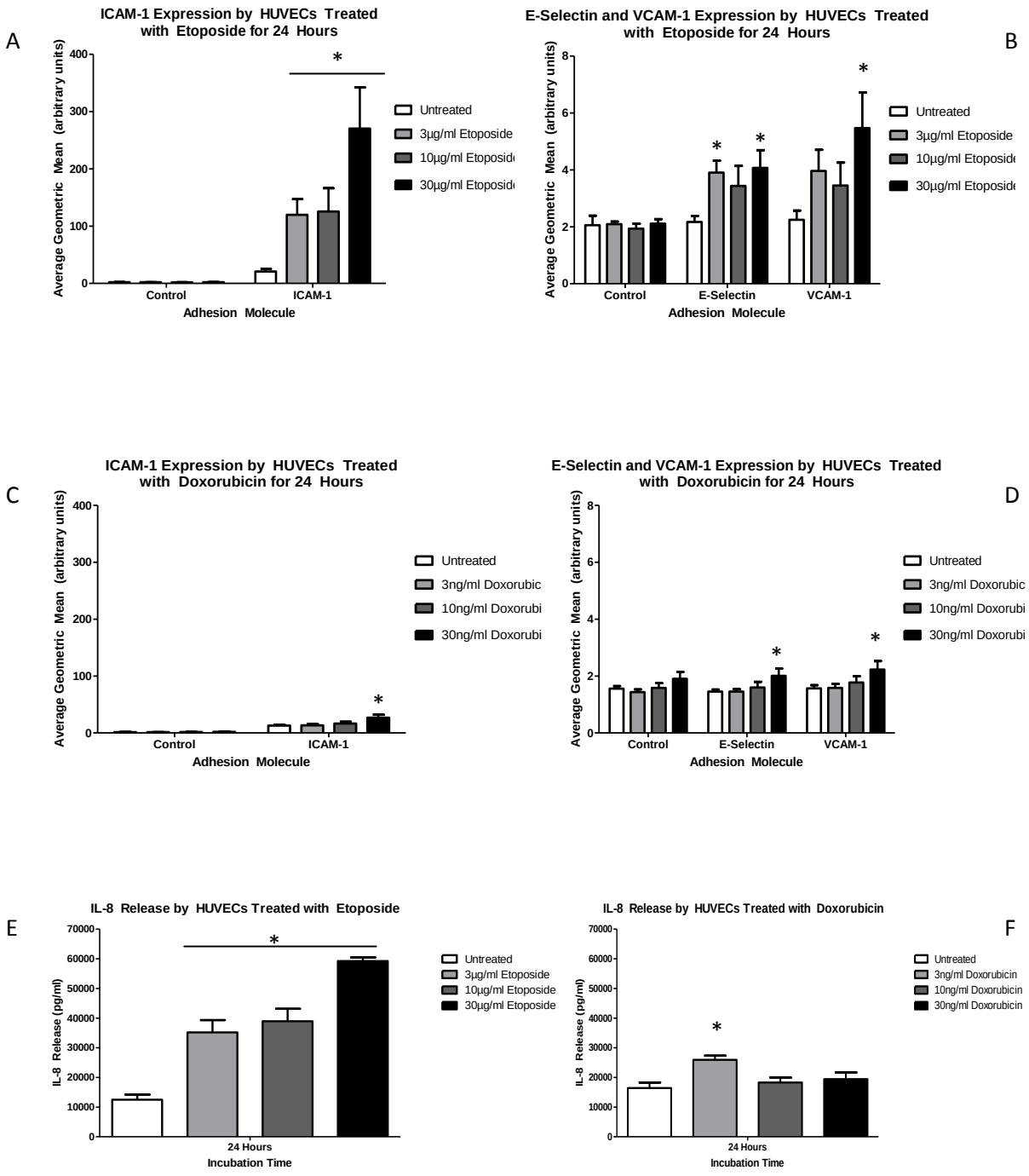

Figure 7.1: Adhesion molecule expression by HUVECs treated with etoposide and doxorubicin.

The expression of ICAM-1 (A), E-selectin and VCAM-1 (B) by HUVECs treated with various concentrations of etoposide, and the expression of ICAM-1 (C),E-Selectin and VCAM-1 (D) by HUVECs treated with various concentrations of doxorubicin, and the release of IL-8 by HUVECs treated with various concentrations of etoposide (E) and doxorubicin (F). Note the different scales of the Y axes. Statistically significant differences in protein expression and release compared to baseline (*p=0.05*) are denoted by an asterisk. *n=3.*

7.3.2 A Comparison of Adhesion Molecule Expression and Cytokine Release Between HUVECs Treated with Etoposide and BLM and Doxorubicin and BLM.

Though it initially appeared that etoposide induced a more substantial increase in ICAM-1 expression than BLM, the upregulation of ICAM-1 in HUVECs was only significantly higher (*p=0.05*) when cells were treated with 30µg/ml etoposide than that seen when HUVECs were treated with BLM at concentrations of 0.1µg/ml and 1µg/ml (Fig 7.2A). The expression of E-selectin between cells treated with all concentrations of BLM was significantly different to those treated with 3 and 30µg/ml etoposide (Fig 7.2B). While VCAM-1 was also increased by treatment with etoposide of various concentrations, this was not significantly different to the increase induced by treatment of HUVECs with BLM (Fig 7.2C).

The changes in adhesion molecule expression were far less substantial in cells treated with DOX compared to those treated with BLM. In all cases, treatment will all concentrations of BLM induced a significantly greater increase in adhesion molecule expression than treatment with all concentrations of DOX (Fig 7.3A-C).

The release of IL-8 was significantly higher by cells treated with all concentrations of etoposide that those treated with all concentrations of BLM (*p=0.05*) (Fig 7.4A). There was a statistically significant difference between the level of IL-8 release induced by treatment with 0.1µg/ml BLM and all concentrations of doxorubicin, but there were no other statistically significant differences between IL-8 release profile (Fig 7.4B).

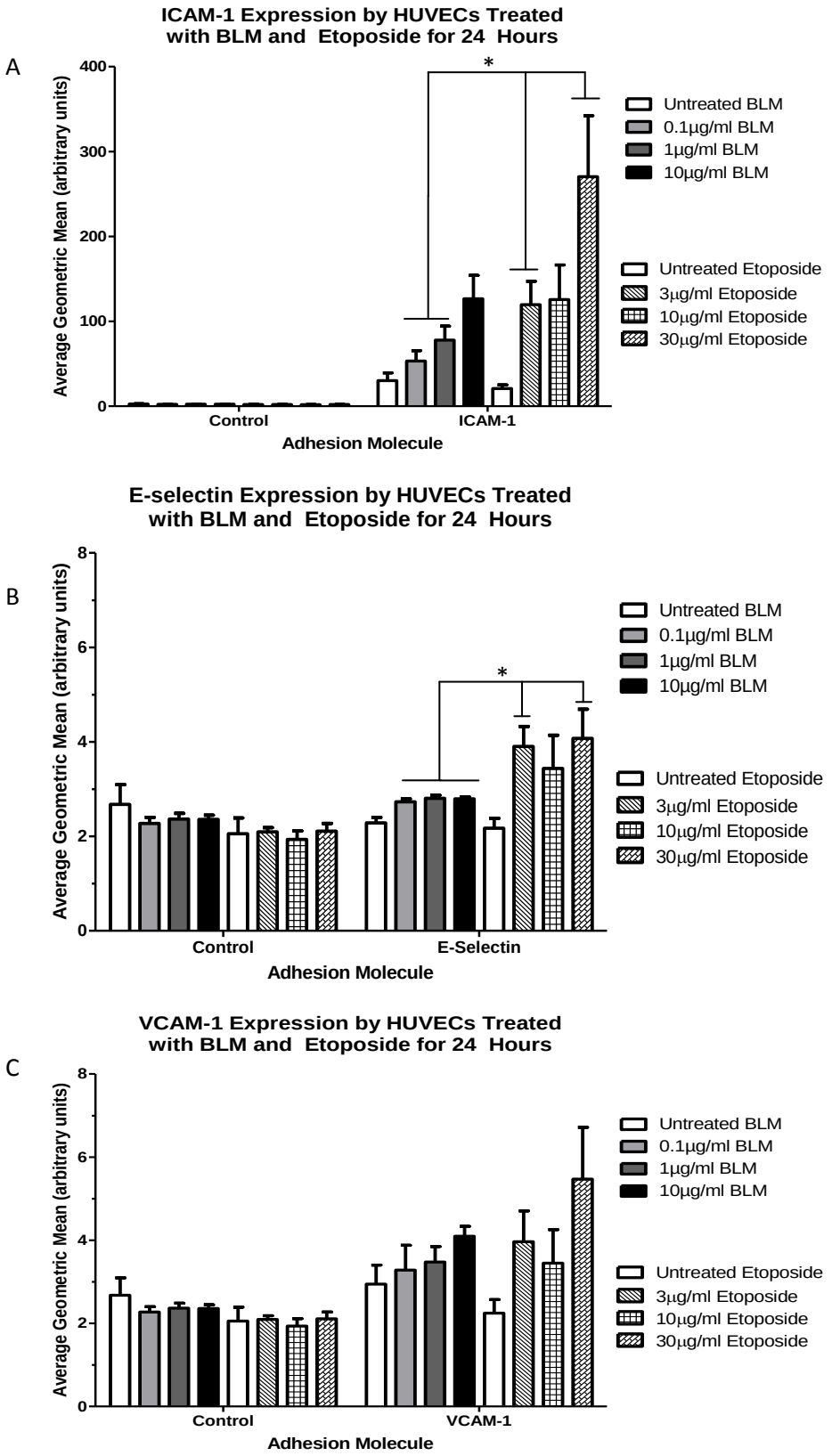

Figure 7.2: Comparisons of adhesion molecule expression by HUVECs treated with BLM and etoposide.

A comparison of the expression of ICAM-1 (A), E-selectin (B) and VCAM-1 (C) by HUVECs treated with etoposide and BLM. Statistically significant differences in protein expression by treated cells (*p=0.05*) are denoted by an asterisk. *n=3.*

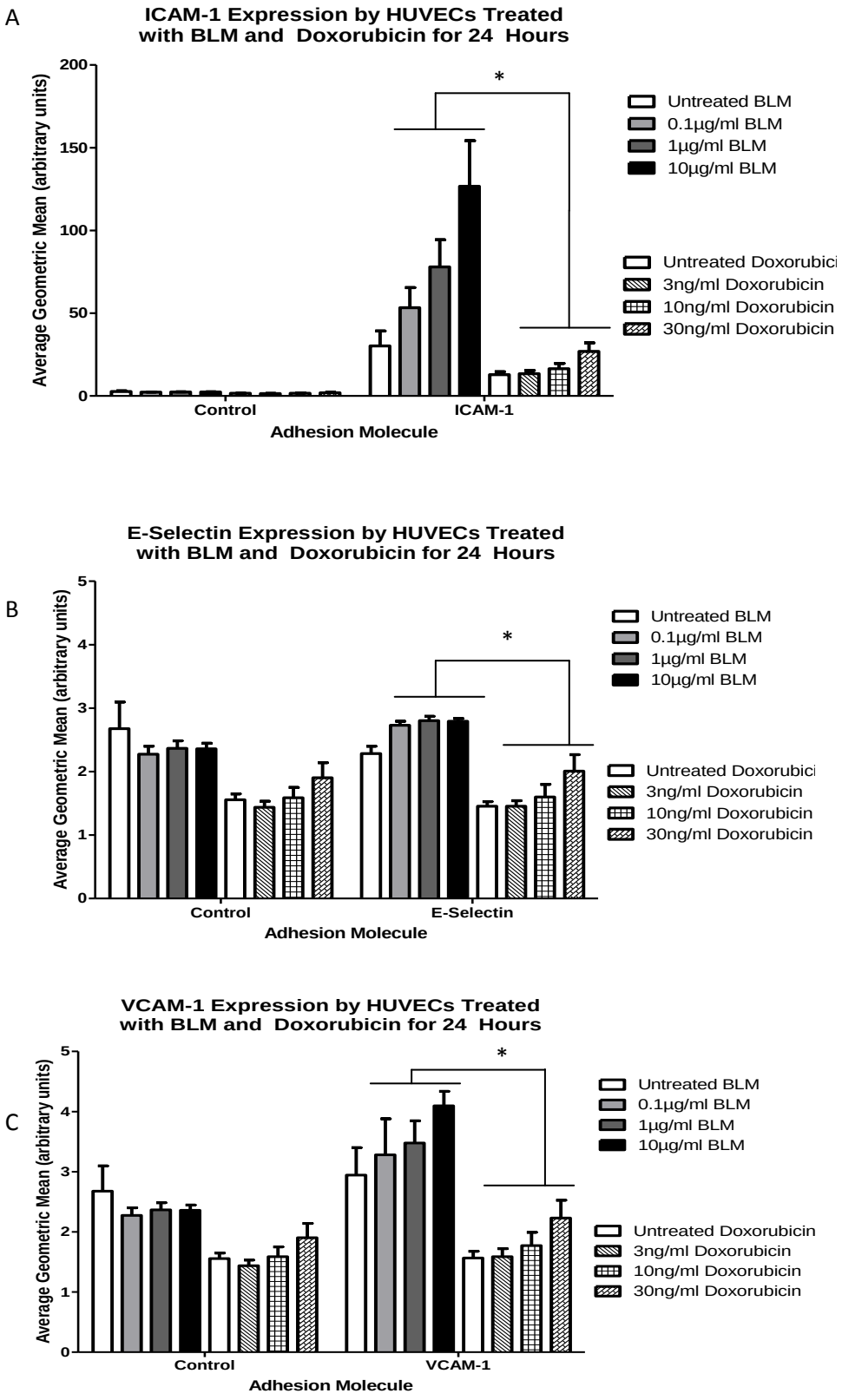

Figure 7.3: Comparisons of adhesion molecule expression by HUVECs treated with BLM and doxorubicin.

A comparison of the expression of ICAM-1 (A), E-selectin (B) and VCAM-1 (C) by HUVECs treated with doxorubicin and BLM. Statistically significant differences in protein expression by treated cells (*p=0.05*) are denoted by an asterisk. *n=3.*

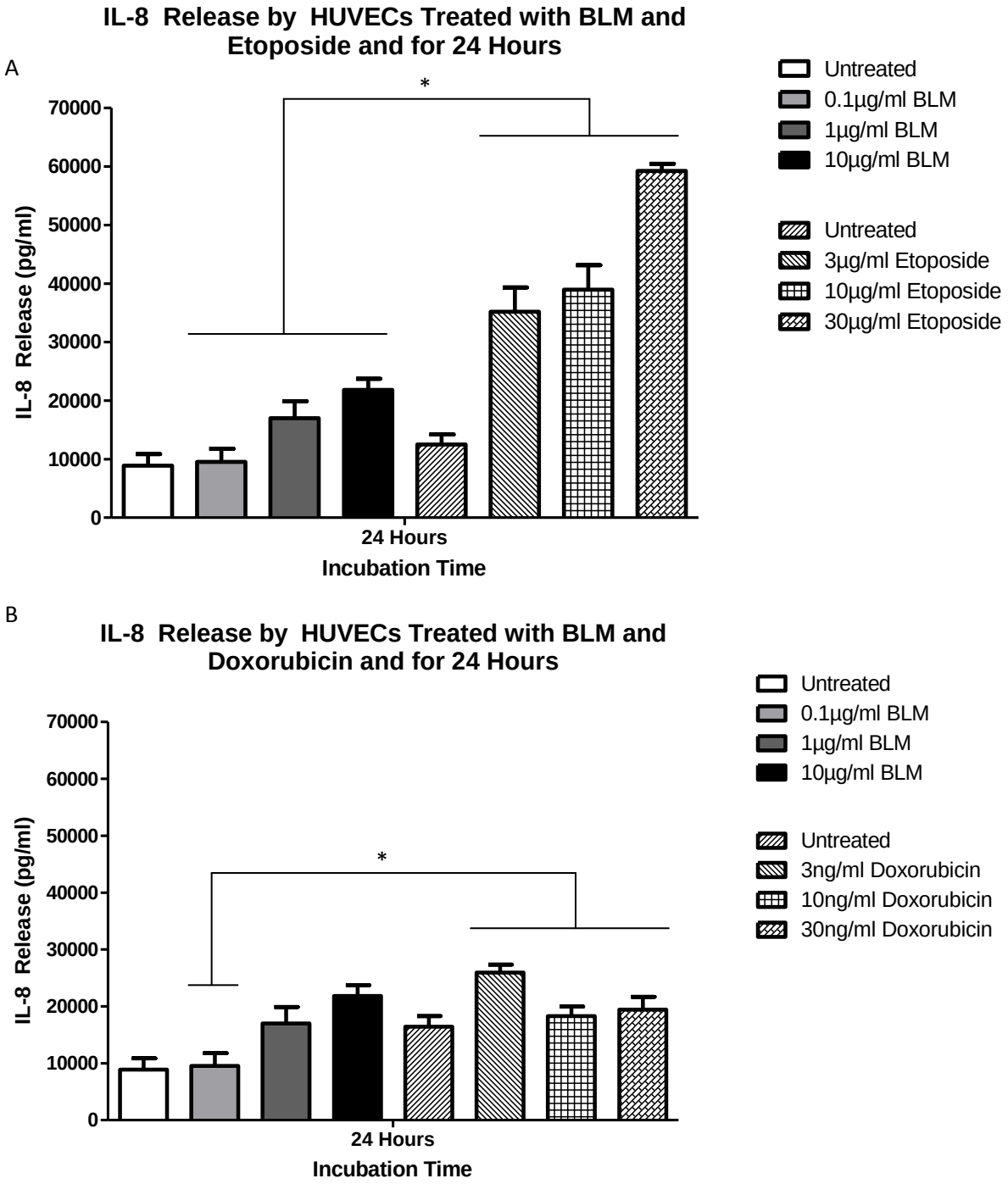

Figure 7.4: Comparisons of IL-8 release by HUVECs treated with BLM, etoposide, and doxorubicin.

A comparison of the expression the release of IL-8 by HUVECs treated with etoposide and BLM (A), and doxorubicin and BLM (B). Statistically significant differences in protein release by treated cells (*p=0.05*) are denoted by an asterisk. *n=3.*

7.4 Discussion and Conclusions

This work was carried out to determine whether other agents which induce cell death in similar ways to BLM induced adhesion molecule expression. These results obtained suggest that the increase in adhesion molecule expression and cytokine release induced by BLM treatment are not unique to BLM, and that other chemotherapeutic agents induce a similar effect. However, not all treatments assessed induce this increase in expression.

Etoposide increased the expression and release of several adhesion molecules and cytokines by HUVECs, which has not previously been reported. While the increase in ICAM-1 expression and IL-8 release was far greater than that induced by BLM, the increases in E-selectin and VCAM-1 expression were broadly similar. Therefore, it appears the effects of etoposide on HUVECs are numerous, although there is currently no known mechanism by which etoposide induced the upregulation of cytokines and adhesion molecules, although as all of the adhesion molecules are regulated at a transcriptional level by NF-κB activation pathways, it is feasible that etoposide is able to induce NF-κB activation and signalling in endothelial cells, as it appears to do in K562 leukaemia blast crisis cells (Morotti, et al., 2006). This would potentially be of interest to other groups.

Increases in ICAM-1, E-selectin, and VCAM-1 expression when cells are treated with DOX has also not been reported. There was also an increase in the expression of IL-8 by HUVECs treated with the lowest concentration of the drug used, which has also not previously been identified. However, this increase was potentially anomalous, and further repeats of this experiment may provide a more conclusive picture. However, in all but one case, the increase in adhesion molecule expression and cytokine release was lower in magnitude than that induced by treatment with BLM.

Treatment of HUVECs with various concentrations of carboplatin had no discernable effect on the expression of adhesion molecules or release of cytokines, though as it is thought that carboplatin requires carbonate to induce activation, it is possible that this activation did not occur under cell culture conditions. However, previous reports suggest that sufficient carbonate is present in culture medium of a physiologically relevant pH (Di Pasqua, et al., 2006) to activate the drug, and so this may not be the case. As previously

stated, oxaliplatin is associated with fibrosis, and cisplatin is known to induce ICAM-1 expression by HUVECs (Yu, et al., 2011). However, there are no reports of adhesion molecule or cytokine expression, or lung fibrosis following carboplatin therapy, though there is a single report of pulmonary fibrosis following a combined chemotherapy regimen including carboplatin and vinorelbine (Kirkbride, et al., 2002). This thesis is the first report to suggest that carboplatin has no effect on adhesion molecule or cytokine expression by HUVECs.

That BLM is not unique in inducing the increased expression of adhesion molecule and release of cytokines initially appears to call into question the idea that this is potentially a causative factor for the side-effect of BLM. If several chemotherapy agents induce adhesion molecule expression and cytokine release, then why does only BLM result in lung fibrosis with such frequency?

However, the only chemotherapeutic agent that induced comparable or greater adhesion molecule expression than BLM is the only other agent which is known to induce pulmonary fibrosis. Though etoposide-induced pulmonary fibrosis is poorly described, it does appear to be quite similar to BPF, albeit with a more rapid progression rate. Though there has been no report of immune cell infiltration in etoposide-induced fibrosis, this may be due to the low number of studies describing this condition, and more data are required before any conclusions can be drawn as to the nature of etoposide-induced pulmonary fibrosis.

Further, it is possible that while etoposide increases adhesion molecule upregulation, this may not be the case in pulmonary microvascular endothelial cells, or that this upregulation may not be localised to the lung. It was reported that ICAM-1 upregulation in rodents following BLM dosing occurs in the lung within 4 hours of administration, occurring only later in the liver and spleen (Weiner, et al., 1998). Perhaps BLM is lung-specific, but etoposide is not. This would require further work to elucidate.

In conclusion, while this work suggests BLM is not unique in its ability to induce adhesion molecule expression, that both BLM and etoposide cause lung fibrosis and induce adhesion molecule upregulation suggests that adhesion molecules and cytokines expressed and released by endothelial cells may contribute to lung fibrosis, potentially via

inducing immune cell infiltration. This work may be furthered by future experiments assessing the expression of adhesion molecules and the release of cytokines by PMVECs treated with etoposide, and by determining the signalling pathways that result in this expression by endothelial cells treated with both BLM and etoposide. It would also be interesting to better assess the temporal and spatial localisation of adhesion molecule expression *in vivo* when rodents are treated with these agents. If it were found that only BLM induced PMVEC adhesion molecule expression, that only BLM-induced adhesion molecule upregulation was localised to the lung, or that the increased expression occurred more quickly in the lung following dosing with BLM than etoposide, this may suggest why fibrosis is more commonly observed in response to BLM than etoposide.

8 General Discussion

Bleomycin (BLM) is an effective chemotherapeutic agent used in the treatment of a range of cancers, but has the unfortunate side effect of inducing potentially fatal pulmonary fibrosis in some patients (Sleijfer, et al., 2001). While the drug is often used to model fibrotic lung disease in animals, little is known about the development of the human form of the disease. Moreover, human BPF results from I.V. delivery of the drug, while the majority of animal modelling studies today utilise the I.T. delivery system. When I.T. delivery is used, the initial injury is alveolar epithelial cell damage. However, studies in animals using I.V. BLM delivery noted that the initial injury was to the vascular endothelium, suggesting this may also be the site of initial injury in man.

In BPF induced by I.V. and I.T. delivery in rodents, and I.V. delivery in man, infiltration of the lung by leukocytes is a known feature of the disease. As leukocyte extravasation from the vasculature into the lung is dependent on endothelial adhesion molecule expression and on the presentation of cytokines on the endothelium, this work sought to determine whether exposure to relevant concentrations of BLM induced the expression of these molecules, and whether the expression observed had a functional relevance in leukocyte adhesion to the endothelium.

8.1 Findings of the Work

This work reported that the treatment of endothelial cells with BLM resulted in increased adhesion molecule expression by both HUVECs and PMVECs. In addition to previously reported E-selectin expression in HUVECs (Ishii and Takada, 2000; Miyamoto, et al., 2001) and ICAM-1 in PMVECs (Fichtner, et al., 2004), this work found, for the first time, that BLM increases ICAM-1 and VCAM-1 expression by HUVECs and VCAM-1 expression by PMVECs. This work also identified that BLM alters the release of endothelial cytokines in both HUVECs and PMVECs. While increased IL-8 release in response to BLM has previously been observed (Fichtner, et al., 2004; Miyamoto, et al., 2001), we report for the first time that BLM treatment increases MCP-1 release and modifies Endothelin-1 release in both cell types. The alterations in expression and release of all of these proteins by HUVECs were observed to be regulated at a transcriptional level, as determined by

qPCR, suggesting that BLM treatment results in regulation of both the synthesis and expression/release of these proteins, albeit via a currently unknown mechanism.

This work then went on to compare the expression and release of adhesion molecules and cytokines by HUVECs and PMVECs treated with BLM. It was found that, while HUVECs express more ICAM-1 in total, the magnitude increase from baseline in both cell types was roughly similar. However, PMVECs expressed more VCAM-1 than HUVECs, and the level of expression of E-selectin was greater by HUVECs than PMVECs in response to BLM. While BLM increased the release of both IL-8 and MCP-1 by HUVECs and PMVECs, HUVECs expressed more IL-8 and MCP-1 in response to BLM than PMVECs, though the fold-change increase from baseline was higher in PMVECs.

The only clear difference in expression patterns arose when Endothelin-1 was assessed. In PMVECs, Endothelin-1 release declined in response to BLM. This was quite different from the results obtained from HUVECs, in which Endothelin-1 increased when cells were treated with 0.1 and 1μg/ml BLM, and decreased when treated with 10μg/ml BLM. The cause of this of this disparity – and its relevance to disease - is uncertain, however.

Having found the molecular changes described above it was decided to investigate whether the increased adhesion molecule expression had any functional relevance. Increased neutrophil rolling and adhesion in rodent vessels following BLM administration has been reported by Wang, et al. (2011) and Sato, et al. (2000), and this correlated with both increased ICAM-1 and VCAM-1 expression in rodent lung venules and capillaries and with increased leukocyte infiltration of the perivascular space and the peribronchiolar regions. However, this phenomenon has never been reported in man, nor using human cells *in vitro.* This thesis reported, for the first time, that the adhesion of neutrophils to human endothelial monolayers treated with BLM is increased compared to baseline. However, this did not appear to be related to endothelial ICAM-1 or E-selectin expression, and so an as-yet unidentified molecule may be responsible for this.

Lastly, additional work was conducted to determine whether BLM is unique in inducing this adhesion molecule expression. It was observed in this work that, as well as BLM, etoposide and doxorubicin also have an impact on the release of IL-8 and the expression of adhesion molecules on endothelial cells. While the expression levels in response to

doxorubicin were generally lower than those observed when cells were treated with BLM, the adhesion molecule expression and cytokine release observed when endothelial cells were treated with etoposide was of a similar level to, or greater than, that observed when cells were treated with BLM. This thesis represents the first time that the effect of etoposide on endothelial adhesion molecule expression has been assessed.

8.2 Implications of the Work

The observations of this study represent the first step to developing a better understanding of the pathogenic process of BPF in man. As it stands, little is known, with studies assessing the lungs of patients with the disease usually being conducted at autopsy (Simpson, et al., 1998) and most models of disease development being derived from rodent work, in which BLM is delivered I.T. and pulmonary immune cell infiltration may result from the pulmonary cytokine storm that follows alveolar epithelial cell injury.

When I.V. dosing is used, as it is in man, the pulmonary vascular endothelium is the first lung tissue to encounter the drug. This work shows that BLM impacts the endothelium in a variety of ways, including increased adhesion molecule expression and proinflammatory cytokine release, and that BLM-treated endothelial cells are able to support increased neutrophil adhesion. Based on these observations, it appears possible that an early step of the process of human BPF development involves aberrant adhesion molecule expression by pulmonary vascular endothelial cells which leads to lung immune cell infiltration, as leukocytes adhere to, and migrate through, the endothelium at an increased rate, thus leading to the AEC injury which results in fibrosis development. With this in mind, further work to determine the contribution of the endothelium to the development of this disease may unravel an as-yet unrecognised “crucial step” in the pathogenesis of the disease, which may increase our knowledge of how human BPF develops.

As the effect of BLM on the vascular endothelium may contribute to the development of BPF by permitting increased lung infiltration by leukocytes, the author also suggests that a move away from the I.T. dosing route to model BPF in rodents would be advantageous.

The authors strongly believe that, if the intravenous BLM dosing route was re-instated in animal modelling – as was used in earlier studies such as that of Fleischer, et al. (1978) - a more accurate model of the pathogenic processes involved in human BPF than what is currently available may be developed whilst still utilising *in vivo* studies in animals.

If a better understanding of the pathogenesis of human BPF can be developed based on the results shown here, then potential interventional or preventative therapies for the condition may be investigated. Currently, there is no available proven treatment for this disease, and there is little strong supporting data for the use of corticosteroids to treat BPF, though they are often given to patients with the condition. In fact, the only step shown to reduce BPF development once it has started is to cease dosing and wait (Sleijfer, et al., 2000; Reinert, et al., 2013). If endothelial cells respond to BLM, and their response to BLM is shown to contribute to the development of the disease, then preventing the expression of adhesion molecules or the release of pro-inflammatory cytokines using methods other than steroid therapy may be of interest.

The results of this work may also have important implications for other fibrotic diseases, for example, IPF. Though generally not associated with immune cell infiltration due to the work of Selman and Pardo (2000), IPF may well have an inflammatory component early on in its development (as recently reviewed by Williamson, et al., (2015)). It may be worth investigating whether the observation made in this work are also seen in pulmonary vascular endothelial cells isolated from patients with IPF; if so, then the aberrant expression of adhesion molecules in IPF may contribute to the development of the disease. If not, then we still have a slightly improved understanding of the pathogenesis of the condition, as the potential role of endothelial adhesion molecules in IPF development is excluded.

Lastly, though BLM is not unique in upregulating adhesion molecule expression in endothelial cells, that etoposide also causes pulmonary fibrosis may suggest that the upregulation of adhesion molecules and cytokines in the vasculature is a critical factor for the development of not only BPF, but also other fibrotic diseases, such as etoposide-induced pulmonary fibrosis. Further investigation of this possibility would allow us to

begin to unravel the causes of these conditions, and potentially work to prevent them occuring in patients given such chemotherapeutic regimens.

8.3 Limitations of the Work

Despite the best efforts of the author, this work of course has several limitations, brought about by the experimental techniques used and both financial and time constraints within this setting. As such, further work would be required to address these limitations.

Firstly, while the expression of a panel of 13 adhesion molecules and the release of six cytokines was assessed in this work, this does not offer a complete picture of the adhesion molecule expression and cytokine release profiles of BLM-treated endothelial cells. This is a clear limitation, as of course it is impossible to assess the contribution of un-assessed adhesion molecules and cytokines to disease development. Moreover, while 13 adhesion molecules were assessed in PMVECs, only three cytokines were tested due to resource constraints, and so the picture of PMVEC adhesion molecule expression and cytokine release when stimulated with BLM is yet more limited. Further work would ideally seek to better characterise and compare the response of both HUVECs and PMVECs to BLM treatment.

Moreover, while the regulation of this increased expression and release was visualised using qPCR in HUVECs, such work was not carried out for PMVECs due to both financial and time constraints. Therefore, while it may be inferred that, as BLM appears to regulate adhesion molecule expression and cytokine release at a transcriptional level in HUVECs, this is likely to also be the case in PMVECs, this cannot be proven at this time, and further work to confirm this using cDNA isolated from BLM-treated PMVECs would be favourable.

Additionally, though BLM appears to regulate adhesion molecule expression and cytokine release at a transcriptional level, this work was unable to identify the pathways responsible for this (e.g., the NF-κB pathway) or how BLM induces this (e.g., receptor binding), and so the author cannot report on the mechanisms responsible for adhesion molecule expression and cytokine release. This limits the results to a report of increased

protein expression and release, and increased transcript synthesis, with only conjecture regarding the cell signalling pathways that induce this; however, time constraints meant that this work was not possible.

A further limitation of this work is the low number of repeats; when assessing cytokine release and adhesion molecule expression using ELISA and FACS analysis, only three repeats of each experiment were conducted. This is both due to time constraints – HUVECs and PMVECs are slow-growing *in vitro* – and financial constraints including the cost of ELISA kits, antibodies, cells, and medium. Therefore, $n = 3$, a minimum required for publication, was conducted only.

This may affect the reliability of results, as low numbers of repeats garner mean values impacted strongly (and potentially skewed) by outlying results and can result in a large degree of standard error such as that seen when assessing Endothelin-1 release by BLM-treated HUVECs. The use of $n = 3$ also meant that normal distribution could not be assumed, and so poorly-powered non-parametric statistical analyses (Mann-Whitney-U tests) were used, which may underestimate the significance of differences observed. However, the author felt that with $n=3$, the use of this test was unavoidable. The use of a greater number of repeats would have not only allowed the use of more powerful statistical analyses, but also would have generated results less impacted by outliers with a smaller degree of standard error, which would have improved the reliability of the results and given mean values likely more representative of the true protein expression and release profiles of BLM-treated endothelial cells.

The observation that etoposide, like BLM, induces adhesion molecule expression and cytokine release by HUVECs, suffers similar limitations. Again, 13 adhesion molecules were assessed, but only IL-8 release was examined, and thus a full expression and release profile of etoposide-treated endothelial cells cannot be presented. Further, only 3 repeats were conducted, and qPCR was not carried out, so this is again a superficial report. However, as this work was conducted to assess the uniqueness of BLM in inducing adhesion molecule expression and cytokine release, this series of works has achieved its objective.

While the release of IL-8 and MCP-1 – and to a lesser extent, Endothelin-1 – is reported to be modulated by BLM treatment in this work, no functional relevance of this was assessed. This limits these observations to proteomic and transcriptomic reports, with no allusion to the impact that this altered release may have. Thus, while this altered release remains an interesting observation, its role in the disease state studied cannot be confirmed from the results of this thesis.

However, a greater limitation of this work lies in the report that, while neutrophils adhere more to BLM-treated endothelial monolayers, the adhesion molecule(s) responsible for this could not be identified. In this respect, this thesis has not been able to address the research question – the role of endothelial adhesins in immune cell adhesion to BLM-treated endothelial monolayers remains incompletely resolved. That this work was only conducted using HUVECs, and not PMVECs, may also call into the question of the physiological relevance of these results, as a surrogate cell type was used. However, if this phenomenon was also observed when PMVECs were used, and were the adhesion molecule(s) responsible for this increased adhesion identified, then this would greatly augment the impact that the novel observation of this work - that neutrophils adhere more to BLM-treated monolayers – has among existing literature. This, therefore, is the most important avenue for future *in vitro* work.

A limitation inherent to each section of this report is that all work is *in vitro* and so no data demonstrate that the increased adhesion molecule expression and neutrophil adhesion to the endothelium observed occurs in human BPF. It seem feasible that increased adhesion molecule expression has functional relevance *in vivo* - work by Wang, et al. (2010) and Sato, et al. (2000) showed that ICAM-1 and VCAM-1 expression correlates with immune cell rolling and adhesion to the endothelium and immune cell infiltration of the lung in I.T.-BLM treated rodents - but it cannot be inferred that these processes occur in human BPF patients – or in I.V. BLM-treated rodents - from either the current work, or that of Wang and Sato.

Thus, a great deal of additional work - some *in vitro* and much *in vivo* (and perhaps *ex vivo*) - is required to delineate whether increased adhesion molecule expression and increased neutrophil adhesion to the BLM-treated endothelium contribute to the

inflammation that precedes human BPF; whether this is also the case in murine BPF stemming from I.V. dosing; and how this immune cell adhesion to the endothelium and potential infiltration of the lung contributes to fibrosis development in both I.V. BLM-treated man and mouse. Such work using rodents, and more importantly a population of BPF patients, was sadly not available at the Trust in which this work occurred, but would have been most interesting to conduct.

8.4 Further Work

There are several aspects of the project in which work may be carried out to not only further our understanding of the role of endothelial cells in fibrotic lung disease, but also to address some of the limitations of the thesis identified in the previous section. Firstly, further work could be carried out to further assess and characterise the adhesion molecules and cytokines expressed and released by HUVECs and PMVECs treated with BLM, to build a better picture of the exact response of these cell types to BLM. Molecules such as L-Selectin, MAdCAM-1, and GlyCam-1, and cytokines such as MIP-1α, TNF-α, and IL-1β would be logical choices, and once a better understanding of the repertoire of proteins expressed and released by these cells types in response to BLM is gained – and further comparisons between adhesion molecule and cytokine expression and release between the two cell types has been conducted - further research may be carried out in the vein of this thesis.

This work also identified that the increased expression of adhesion molecules and the release of proinflammatory cytokines was regulated at a transcriptional level, at least in HUVECs. Further work may carry on in this vein and assess whether BLM also regulates the increased expression and release of adhesion molecules and cytokines by PMVECs at a transcriptional level, if only to confirm that this process in analogous in the two cell types.

However, while it appears that BLM alters adhesion molecule and cytokine expression and release by modulating transcription, it is unclear how this transcription modulation is mediated. Further work to delineate this would be of great use. BLM may interact with an

as-yet unidentified surface receptor on endothelial cells, resulting in signalling events which result in increased transcription and expression of adhesion molecules and cytokines. This may be assessed using a similar technique to Pron, et al. (1999), via the isolation of endothelial cell membranes and co-incubation of these with radioactive BLM prior to visualisation on a semi-denaturing gel using Coomassie Blue. Alternatively, BLM may induce the endothelial expression of proinflammatory factors such as TNF-α and IL-1β, which may act in an autocrine fashion to increase adhesion molecule expression and cytokine release. Whether this is the case may be assessed by ELISA for these cytokines using supernatant from BLM-treated cells.

Having determined the mechanism by which this occurs, it would be advantageous to determine the signalling pathways by which the transcription of these proteins is altered, as the opportunity to conduct these experiments in this thesis was not available. With the exception of Endothelin-1, all of the proteins seen to be expressed or released at increased levels in this work are regulated by NF-κB signalling (as discussed in 1.6.3 and 4.1), and so while this work did not attempt to identify the signalling pathways involved in the observed increase in transcript and protein levels, it seems feasible that NF-κB may be involved, though signalling pathways such as JNK, P38 MAPK, ERK1/2 or PI3K may contribute. Further work using Western Blot to detect protein phosphorylation, or EMSA to assess protein binding to DNA, in response to BLM may be of assistance in unravelling the pathways involved.

In this work, the functional relevance of increased cytokine release was not investigated, and so this would also be a logical progression of the results presented here. Increased IL-8 and MCP-1 expression may logically result in increased leukocyte movement to the site of expression or presentation. *In vitro* assessment of the role of these chemoattractant cytokines - using Transwell inserts and endothelial cell / leukocyte co-cultures - to assess whether the migration of leukocytes to BLM-treated endothelial cells is increased, would confirm whether increased proinflammatory cytokine release resulted in the predicted increase in leukocyte migration to the site of expression, and may hint at a role for endothelial IL-8, MCP-1, and other cytokines in the development of BPF.

The role of Endothelin-1, the only protein differentially regulated by BLM treatment in HUVECs and PMVECs, would also be interesting to investigate. This is a potent pro-fibrotic cytokine (Fonseca, et al., 2009) associated with fibrotic development in the rodent BPF model (Mutsaers, et al., 1998; Park, et al., 1998), and while increased HUVEC Endothelin-1 release may point towards a role in pro-fibrotic processes, the decreased release of Endothelin-1 by PMVECs confounds this idea. Work to determine whether endothelial Endothelin-1 expression plays a part in the development of human BPF would be of great value; the role of Endothelin-1 in the pathogenesis of other fibrotic lung diseases is, after all, unresolved (Williamson, et al., 2015).

Further characterisation of the molecule(s) involved in neutrophil adhesion to BLM-treated monolayers would also be desirable. This work reported that neutrophil adhesion to BLM-treated monolayers was increased compared to baseline, but was not able to identify the adhesion molecule responsible for this, and this is perhaps the greatest limitation of this body of work. ICAM-1 and E-Selectin binding blockade, while decreasing TNF-α mediated adhesion, did not block BLM-mediated adhesion. Experimental work blocking VCAM-1 would be a logical next step, to see if this is the molecule responsible for increased binding. If this were not the adhesion molecule responsible for increased adhesion, further molecules would need to be assessed, perhaps based on any finding from earlier supplemental work to identify other adhesion molecules expressed at increased levels by BLM-treated monolayers, in order to determine the protein(s) responsible for the increased neutrophil adhesion reported in this research.

Of course, adhesion molecules may not be the only protein involved in this process; it is feasible that cytokines also play a role. IL-8, for example, increases neutrophil adhesion to ICAM-1 (Lomakina and Waugh, 2006), as does Endothelin-1 (Lopez Farré, et al., 1993; Fernandez-Patron, et al., 2001; Zouki, et al., 1999). However, the increased adhesion of neutrophils induced by both cytokines is related to increased CD18 ligand expression, and this may be blocked by anti-CD18 antibodies such as TS1/18 (Lopez Farré, et al., 1993; Lomakina and Waugh, 2006). This work did not observe decreased adhesion of CD18-antibody-treated neutrophils to BLM-treated endothelial monolayers, and so it does not appear that increased IL-8 and Endothelin-1 release impacted neutrophil adhesion.

To confirm this, the blockade of cytokines (using blocking antibodies) may be utilised, to determine whether cytokines expressed by BLM-treated endothelial cells are increasing neutrophil adhesion. This may be conducted concurrently with adhesion molecule blockade, in an attempt to identify which (if any) cytokines are increasing neutrophil adhesion to which (if any) adhesion molecules.

Additionally, other as yet unidentified endothelial cell-released cytokines may contribute to increased neutrophil adhesion in this model, so the identification of further endothelial cytokines released in response to BLM, and an investigation of their roles in neutrophil adhesion as outlined above, would be beneficial.

The neutrophil adhesion work may of course be built upon using PMVECs, to see if increased neutrophil binding is observed using both cell types. Again,this work was not able to identify the molecule(s) responsible for neutrophil adhesion in this model, and while the expression profiles of HUVECs and PMVECs was seen to be similar in this work, it is possible that an as-yet unidentified adhesion molecules – which may be differentially expressed between the cell types - may mediate adhesion in this model. Therefore, assessing whether the adhesion supported by HUVECs is also supported by PMVECs will not only bring a further degree of physiological relevance to the work, but also confirm that HUVECs are a suitable surrogate for PMVECs *in vitro*.

All in all, by carrying out further work and identifying the adhesion molecule(s) or other proteins (potentially cytokines) responsible for the increased neutrophil adhesion to HUVECs observed, and assessing whether this increased neutrophil adhesion is also observed on BLM-treated PMVECs and identifying the protein(s) responsible for this, we would be closer to addressing the primary research objective - and thus the primary limitation - of this thesis; unravelling the role of endothelial adhesins in leukocyte adhesion in response to pharmaceutical agents that induce pulmonary fibrosis. However, we would not answer the question with just this information; yet more work would be needed.

The next step would be to assess whether the *in vitro* findings of this work apply to *in vivo* models. To determine how the observations of the neutrophil adhesion work reported here could apply to human disease, and the role of adhesins in the process, there are

several steps which may be taken, some of which involve the modelling of BPF in rodents, and others, the recruitment of human volunteers suffering from BPF. Initially, the focus of this *in vivo* research would be in determining whether observations from previous publications using I.T. BLM dosing apply to I.V.BLM dosing models, and to carry these results - as well as those of this thesis - forward, to investigate how I.V. BLM impacts the human pulmonary vascular endothelium, and whether this is contributory to disease.

Sato, et al. (2000) and Wang, et al. (2011) both reported increased leukocyte rolling and adhesion in the lung venules and capillaries of BLM-dosed mice, correlating with increased leukocyte infiltration of the interstitium and associated with ICAM-1 and VCAM-1 expression, but both used I.T. dosing and so it is uncertain whether the behaviour of the rodent pulmonary endothelium was due to a response to BLM, or a response to the BLM-induced cytokine storm ongoing within the lung, caused by direct BLM administration to the alveoli. TNF-α expression in the lung, for example, may lead to endothelial adhesion molecule expression and cytokine release as the pro-inflammatory mediator diffuses out of the lung.

In vivo studies using I.V. BLM dosing in rodents would combat this; if similar neutrophil rolling and adhesion is seen after I.V. BLM administration then it can be said that the impact of BLM on the pulmonary vascular endothelium may contribute to BPF development in rodents (as the pulmonary vascular endothelium would be the first point of contact within and around the lung for the circulating blood-borne drug). This may also go some way to explain why immune cell infiltration into the lung is observed when no direct intra-pulmonary injury has occurred in man following treatment with I.V. BLM. Therefore, the first *in vivo* step would be to carry out analyses analogous of those carried out by Sato and Wang, and to determine the adhesion molecules responsible for any increased neutrophil adhesion reported in rodents treated with I.V. BLM. From here, information gathered could be used to direct future *in vivo* work in human participants.

Next, assessing vascular permeability following BLM dosing would also be of interest. It has been reported that endothelial tight junctions in the pulmonary vasculature are held in an open configuration after I.T. BLM dosing (Yin, et al., 2012), and so whether this is also the case after I.V. dosing would be of interest. The “holding open” of tight junctions

in man would not only increase the access of immune cells to the lung, but may also allow the formation of the reported pulmonary oedema in BPF, and potentially the movement of blood-borne BLM into the lung, where further damage can be caused. This, if possible to conduct on *ex vivo* samples, or *in vivo* in human patients using fluorochrome or radioactive tracer-tagged antibodies against human zona occludens proteins, would definitely represent an interesting avenue for research, though would perhaps fall outside the remit of work which may represent a continuation of this thesis.

Lastly, in rodents, BLM induces ICAM-1 expression in the lung vasculature before it occurs in any other locations, and the upregulation in the lung is seen to be more severe than in other organs (Weiner, et al., 1994). It would be interesting to fully characterise the expression of adhesion molecules in the rodent pulmonary vasculature following I.V. dosing, and to assess the spatial and temporal localisation of these molecules. Using the information collected from these series of experiments, it would then be possible to go forward and assess such features in the lungs of BLM-treated human patients.

While it would be challenging to conduct *in vivo* assessments on human patients, there are steps which may be taken to characterise the vascular endothelial response to BLM in man, and to determine whether the observations made in this thesis truly have a functional relevance *in vivo*. Should it not be possible to conduct the type of *in vivo* studies conducted in mice in humans, assessment of *ex vivo* tissue samples by immunohistochemistry, to determine adhesion molecule expression profiles in the vasculature – taken from the lung, and other organs - from patients suffering the disease, would be useful to assess the temporal and spatial arrangement of adhesion molecule expression in BLM-treated human patients. Alternatively, the use of adhesion-molecule specific, intravenously delivered, ^{111}Indium-tagged antibodies to patients with the condition (as pioneered in rodents by John, et al., (2013)) which may then be visualised using SPECT/CT, would allow the identification and localisation of upregulated adhesion molecules in the vasculature of a variety of human organs following BLM dosing and during the process of BPF development.

This would enable the identification of areas in man in which the vasculature is particularly affected by BLM, to see if the observations by Weiner, et al. (1994) may be

translated to human disease. If, in humans, the upregulation of adhesion molecules following BLM dosing was localised to the lungs, as it appears to be in rodents, and this upregulation is more rapid and more severe than in any other organs, then this may suggest why BLM induces fibrosis in the lungs preferentially, and would contribute to what is already known about BPF development in humans.

Should it be possible, then it would also be interesting to directly assess the role of upregulated endothelial adhesion molecules in the development of human BPF; again, utilising non-blocking fluorochrome- or radioactive tracer-tagged antibodies to bind to both the adhesion molecules of the pulmonary vasculature, and also to neutrophil markers (for example, CD15 or CD16), would allow any neutrophil adhesion to the pulmonary vascular endothelium in man following BLM dosing and the behaviour of neutrophils and potentially their migration through into the lung, to be recorded and visualised, either by SPECT/CT (John, et al., 2013), or potentially via fluorescent or confocal microscopy (though notably, when this was used in rodents, sacrifice was required (Sato, et al., 2000)). This could then potentially demonstrate the exact role of BLM-induced adhesins in neutrophil adhesion to the endothelium and inflammation in human BPF.

In doing so, one would need to take extreme care to localise anti-adhesion molecule antibodies only to the lung vasculature and to avoid inducing mass neutrophilic degranulation, whilst also limiting the exposure of patients to undue levels of radiation if visualising using SPECT/CT. However, this work would provide the best evidence to date of the role of the endothelium and endothelial adhesion molecule expression in response to BLM, and their role in the development of the disease, and would represent a breakthrough in our knowledge of the formation of this disease whilst also signposting potential treatment modalities.

If it is found that the behaviour of the endothelium and its expression and release of adhesion molecules and cytokines contributes to the development of BPF in man, then the results of the current and future work may be carried forward and applied to patients with other fibrotic diseases. For example, the use of immunohistochemistry to identify adhesion molecule expression in explanted lung tissue from patients with IPF may be

used to determine whether increased adhesion molecule expression in the vessels of the lung is also seen in this disease. Similarly, fluorochrome- or radioactive tracer-tagged antibodies against endothelial adhesion molecules and immune cells could be used to visualise both the temporal and spatial expression of adhesion molecules and their role in the recruitment of immune cells to the lung in this disease, if any. This would allow the results of this work to be translated into investigations for a much more common, but equally devastating, disease. It may also be possible to isolate vascular endothelial cells from the vasculature of IPF patients and to assess and use these cells in a similar way – characterising the adhesion molecules expressed and the cytokines released by these cells, and assessing whether IPF patient endothelial cells are able to support neutrophil adhesion under flow at an increased level compared to normal endothelial cells. The opportunities to apply this research to other fibrotic diseases are numerous, as it is entirely possible that IPF, like BPF, is an inflammatory disease (Williamson, et al., 2015).

If this work is able to identify and localise the expression and release of adhesion molecules and cytokines by BLM-exposed endothelial cells *in vivo*; determine the contribution of this to the leukocyte tethering and inflammatory cell influx seen in BPF; identify which protein(s) are responsible for any increased immune cell tethering and influx; assess whether this contributes to fibrotic lung disease, and identify the signalling pathways and associated cellular receptors responsible for this BLM-induced adhesion molecule expression, it may then be possible to develop treatments. Such treatment modalities may potentially involve novel targets, such as the involved adhesion molecules, or may work to block signalling pathways and receptor binding leading to the expression of these adhesion molecules, and could replace the somewhat ineffective corticosteroids used today; should this be acheived, and the finding of this work discovered to be applicable to other fibrotic diseases such as IPF, then perhaps treatments for this disease may also be developed.

The novel observation made by this work, that etoposide also induces increased adhesion molecule expression and cytokine release, may represent the first step in a wide avenue of research into this poorly characterised disease. Little is known about etoposide-induced fibrosis, including whether it has an inflammatory component. However, if it is an inflammatory condition characterised by immune cell infiltration of the lungs, there

may be clinical value in carrying out further work, including assessing whether other adhesion molecules and cytokines are expressed and released at a greater level when endothelial cells are treated with etoposide; confirming whether this is regulated at a transcriptional level by qPCR; and determining the pathways by which etoposide mediates this increase. Of course, assessing whether this response is also seen in in PMVECs, and assessing the temporal and spatial expression of adhesion molecules by endothelial cells in response to etoposide would also be valuable, and may be achieved in both man and rodents using the techniques outlined previously.

This may identify a potential cause for etoposide induced pulmonary fibrosis: if etoposide induced pulmonary fibrosis does indeed have an inflammatory component, and if adhesion molecule expression occurs in PMVECs in response to etoposide when assessed *in vitro*; then this may feasibly be contributory to fibrosis development, and further *in vivo* work may be carried out, as outlined above. From this, it may also be concluded that increased pulmonary vessel endothelium adhesion molecule expression is a characteristic side-effect of pulmonary fibrosis-inducing chemotherapies - though this would not explain why fibrosis occurs so commonly in response to BLM, it would add to our understanding of chemotherapy-induced pulmonary fibrosis. Conversely, this investigation may provide an explanation of why BLM causes pulmonary fibrosis more often than etoposide; BLM induces adhesion molecule upregulation in pulmonary vascular endothelial cells *in vitro*, and this is observed in the lungs before anywhere else *in vivo*, with ICAM-1 expression only occurring later in the liver and spleen (Weiner, et al., 1994). If etoposide induces a lower level of adhesion molecule expression by PMVECs *in vitro and in vivo,* compared to BLM, or induces increased adhesion molecule expression preferentially in other vascular beds, e.g., the liver, this may be why BLM-induced lung fibrosis is so common compared to that caused by other drugs.

8.5 Concluding Statement

In all, this work has widened our understanding of the impact of BLM treatment on endothelial cells, and has demonstrated how these effects may contribute to the inflammation that characterises the disease. Further work may expand on this and help

develop a better model of BPF in humans which may aid in the alleviation of this disease, and potentially other fibrotic conditions.

9 References

Adamson, I.Y. (1976). Pulmonary toxicity of bleomycin. *Environ Health Perspect.* 16:119-26.

Adamson, I.Y. (1984). Drug-induced pulmonary fibrosis. *Environ Health Perspect*. 55:25-36.

Adamson, I.Y., Bowden, D.H. (1974). The pathogenesis of bleomycin-induced pulmonary fibrosis in mice. *Am J Pathol.* 77 (2):185-97.

Adamson, I.Y., Bowden, D.H. (1977). Origin of ciliated alveolar epithelial cells in bleomycin-induced lung injury. *Am J Pathol*. 87 (3) :569-80.

Adamson, I.Y., Bowden, D.H. (1979). Bleomycin-induced injury and metaplasia of alveolar type 2 cells Relationship of cellular responses to drug presence in the lung. *Am J Pathol*. 96 (2) :531-44

Adamson, I.Y., King, G.M., Bowden, D.H. (1988). Collagen breakdown during acute lung injury. *Thorax*. 43 (7) :562-8

Ahmad, M., Theofanidis, P., Medford, R.M. (1998). Role of activating protein-1 in the regulation of the vascular cell adhesion molecule-1 gene expression by tumor necrosis factor-alpha. *J Biol Chem.* 273(8):4616-21

Ahmed, R.A., Murao, K., Imachi, H., Yoshida, K., Dobashi, H., Hosomi, N., Ishida, T. (2009). c-Jun N-terminal kinases inhibitor suppresses the TNF-alpha induced MCP-1 expression in human umbilical vein endothelial cells. *Endocrine*. 35(2):184-8.

Ahmedat, A.S., Warnken, M., Seemann, W.K., Mohr, K., Kostenis, E., Juergens, U.R., Racké, K. (2013). Pro-fibrotic processes in human lung fibroblasts are driven by an autocrine/paracrine endothelinergic system. *Br J Pharmacol*. 168(2):471-87

Aird, W.C. (2007). Phenotypic heterogeneity of the endothelium: I. Structure, function, and mechanisms. *Circ Res*. 100(2):158-73

Aird, W.C. (2012). Endothelial cell heterogeneity. Cold Spring Harb Perspect Med. 2012 Jan;2(1):a006429

Albelda, S.M., Elias, J.A., Levine, E.M., Kern, J.A. (1989). Endotoxin stimulates platelet-derived growth factor production from cultured human pulmonary endothelial cells. *Am J Physiol*. 257(2 Pt 1):L65-70.

Albelda, S.M., Muller, W.A., Buck, C.A., Newman, P.J. (1991). Molecular and cellular properties of PECAM-1 (endoCAM/CD31): a novel vascular cell-cell adhesion molecule. *J Cell Biol*. 114(5):1059-68

Alberts, D.S., Chen, H.S., Liu, R., Himmelstein, K.J., Mayersohn, M., Perrier, D., Gross, J., Moon, T., Broughton, A., Salmon, S.E. (1978). Bleomycin pharmacokinetics in man I Intravenous administration. *Cancer Chemother Pharmacol*. 1(3) :177-81.

Alberts, D.S., Dorr, R.T. (1998). New Perspectives on an Old Friend: Optimizing Carboplatin for the Treatment of Solid Tumors. *Oncologist*. 3(1):15-34

Alon, R., Kassner, P.D., Carr, M.W., Finger, E.B., Hemler, M.E., Springer, T.A. (1995). The integrin VLA-4 supports tethering and rolling in flow on VCAM-1. *J Cell Biol*. 128 (6) :1243-53

Allen, J., Cooper, D. Jr. (2000). Pulmonary Fibrosis. Pathways are slowly coming into light. *Am J Respir Cell Mol Biol.* 22: 520-523.

Ando, Y., Minami, H., Saka, H., Ando, M., Sakai, S., Shimokata, K. (1996). Therapeutic drug monitoring in 21-day oral etoposide treatment for lung cancer. *Jpn J Cancer Res*. 87(8):856-61.

Annes, J.P., Chen, Y., Munger, J.S., Rifkin, D.B. (2004). Integrin alphaVbeta6-mediated activation of latent TGF-beta requires the latent TGF-beta binding protein-1. *J Cell Biol*. 165 (5) :723-34.

Antoniades, H.N., Bravo, M.A., Avila, R.E., Galanopoulos, T., Neville-Golden, J., Maxwell, M., Selman, M. (1990). Platelet-derived growth factor in idiopathic pulmonary fibrosis. *J Clin Invest*. 86(4):1055-64

Anwar, K.N., Fazal, F., Malik, A.B., Rahman, A. (2004). RhoA/Rho-associated kinase pathway selectively regulates thrombin-induced intercellular adhesion molecule-1

expression in endothelial cells via activation of I kappa B kinase beta and phosphorylation of RelA/p65. *J Immunol*. 173(11):6965-72

Aoshiba, K., Tsuji, T., Nagai, A. (2003). Bleomycin induces cellular senescence in alveolar epithelial cells. *Eur Respir J*. 22 (3) :436-43

Aoshiba, K., Yasui, S., Tamaoki, J., Nagai, A. (2000). The Fas/Fas-ligand system is not required for bleomycin-induced pulmonary fibrosis in mice. *Am J Respir Crit Care Med.* 162 (2 Pt 1):695-700.

Aouida, M., Poulin, R., Ramotar, D. (2010). The human carnitine transporter SLC22A16 mediates high affinity uptake of the anticancer polyamine analogue bleomycin-A5. *J Biol Chem.* 285 (9) :6275-84.

Arribillaga, L., Dotor, J., Basagoiti, M., Riezu-Boj, J.I., Borrás-Cuesta, F., Lasarte, J.J., Sarobe, P., Cornet, M.E., Feijoó, E. (2011). Therapeutic effect of a peptide inhibitor of TGF-β on pulmonary fibrosis. *Cytokine.* 53 (3) :327-33.

Asai, T., Ohno, Y., Minatoguchi, S., Funaguchi, N., Yuhgetsu, H., Sawada, M., Takemura, G., Komada, A., Fujiwara, T., Fujiwara, H. (2007). The specific free radical scavenger edaravone suppresses bleomycin-induced acute pulmonary injury in rabbits. *Clin Exp Pharmacol Physiol.* 34 (1-2):22-6

Asimakopoulos, G., Lidington, E.A., Mason, J., Haskard, D.O., Taylor, K.M., Landis, R.C. (2001). Effect of aprotinin on endothelial cell activation. *J Thorac Cardiovasc Surg*. 122 (1) :123-8.

Ashida, N., Arai, H., Yamasaki, M., Kita, T. (2001). Distinct signaling pathways for MCP-1-dependent integrin activation and chemotaxis. *J Biol Chem.* 276(19):16555-60.

Atzori, L., Chua, F., Dunsmore, S.E., Willis, D., Barbarisi, M., McAnulty, R.J., Laurent, G.J. (2004). Attenuation of bleomycin induced pulmonary fibrosis in mice using the heme oxygenase inhibitor Zn-deuteroporphyrin IX-2,4-bisethylene glycol. *Thorax*. 59 (3) :217-23.

Aumiller, V., Balsara, N., Wilhelm, J., Günther, A., Königshoff, M. (2013). WNT/β-catenin signaling induces IL-1β expression by alveolar epithelial cells in pulmonary fibrosis. *Am J Respir Cell Mol Biol*. 49(1):96-104

Azambuja, E., Fleck, J.F., Batista, R.G., Menna Barreto, S.S. (2005). Bleomycin lung toxicity: who are the patients with increased risk? *Pulm Pharmacol Ther.* 18(5):363-6.

Azuma, A., Furuta, T., Enomoto, T., Hashimoto, Y., Uematsu, K., Nukariya, N., Murata, A., Kudoh, S. (1998). Preventive effect of erythromycin on experimental bleomycin-induced acute lung injury in rats. *Thorax*. 53(3):186-9

Azuma, A., Li, Y.J., Abe, S., Usuki, J., Matsuda, K., Henmi, S., Miyauchi, Y., Ueda, K., Izawa, A., Sone, S., Hashimoto, S., Kudoh, S. (2005). Interferon-{beta} inhibits bleomycin-induced lung fibrosis by decreasing transforming growth factor-{beta} and thrombospondin. *Am J Respir Cell Mol Biol.* 32(2):93-8.

Azuma, A., Takahashi, S., Nose, M., Araki, K., Araki, M., Takahash,i T., Hirose, M., Kawashima, H., Miyasaka, M., Kudoh, S. (2000). Role of E-selectin in bleomycin induced lung fibrosis in mice. *Thorax.* 55 (2):147-52.

Baer, M., Dillner, A., Schwartz, R.C., Sedon, C., Nedospasov, S., Johnson, P.F. (1998). Tumor necrosis factor alpha transcription in macrophages is attenuated by an autocrine factor that preferentially induces NF-kappaB p50. *Mol Cell Biol.* 18(10):5678-89

Bahra, P., Rainger, G.E., Wautier, J.L., Nguyet-Thin, L., Nash, G.B. (1998). Each step during transendothelial migration of flowing neutrophils is regulated by the stimulatory concentration of tumour necrosis factor-alpha. *Cell Adhes Commun*. 6(6):491-501.

Barkauskas, C.E., Cronce, M.J., Rackley, C.R., Bowie, E.J., Keene, D.R., Stripp, B.R., Randell, S.H., Noble, P.W., Hogan, B.L. (2013). Type 2 alveolar cells are stem cells in adult lung. *J Clin Invest*. 123(7):3025-36.

Barpe, D.R., Rosa, D.D., Froehlich, P.E. (2010). Pharmacokinetic evaluation of doxorubicin plasma levels in normal and overweight patients with breast cancer and simulation of dose adjustment by different indexes of body mass. *Eur J Pharm Sci*. 41(3-4):458-63.

Barton-Burke, M., Wilkes, G.M., Ingwersen, K. (1996). Potential toxicities and nursing management. In M. Barton-Burke, G.M. Wilkes, & K. Ingwersen (Eds) "*Cancer Chemotherapy: A Nursing Process Approach",* pp. 159. Subdury, Massachusetts. Jones and Bartlett.

Barreiro, O., Yañez-Mó, M., Serrador, J.M., Montoya, M.C., Vicente-Manzanares, M., Tejedor, R., Furthmayr, H., Sanchez-Madrid, F. (2002). Dynamic interaction of VCAM-1 and ICAM-1 with moesin and ezrin in a novel endothelial docking structure for adherent leukocytes*. J Cell Biol*. 157(7):1233-45

Beck, G.C., Yard, B.A., Breedijk, A.J., Van Ackern, K., Van Der Woude, F.J. (1999). Release of CXC-chemokines by human lung microvascular endothelial cells (LMVEC) compared with macrovascular umbilical vein endothelial cells. *Clin Exp Immunol*. 118(2):298-303.

Bedrossian, C.W., Luna, M.A., Mackay, B., Lichtiger, B. (1973). Ultrastructure of pulmonary bleomycin toxicity. *Cancer.* 32 (1):44-51.

Bedrossian, C.W., Miller, W.C., Luna, M.A. (1979). Methotrexate-induced diffuse interstitial pulmonary fibrosis. *South Med J*. 72 (3) :313-8

Benjamin, R.S., Riggs, C.E. Jr., Bachur, N.R. (1973). Pharmacokinetics and metabolism of adriamycin in man. *Clin Pharmacol Ther*. 14(4):592-600.

Bergmann, M., Tiroke, A., Schäfer, H., Barth, J., Haverich, A. (1998). Gene expression of profibrotic mediators in bronchiolitis obliterans syndrome after lung transplantation. *Scand Cardiovasc J*. 32(2):97-103.

Berman, M.E., Muller, W.A. (1995). Ligation of platelet/endothelial cell adhesion molecule 1 (PECAM-1/CD31) on monocytes and neutrophils increases binding capacity of leukocyte CR3 (CD11b/CD18). *J Immunol*. 154(1):299-307

Bevilacqua, M.P., Pober, J.S., Mendrick, D.L., Cotran, R.S., Gimbrone, M.A. Jr. (1987). Identification of an inducible endothelial-leukocyte adhesion molecule. Proc Natl Acad Sci U S A. 84 (24) :9238-42.

Bevilacqua, M.P., Stengelin, S., Gimbrone, M.A. Jr., Seed, B. (1989). Endothelial leukocyte adhesion molecule 1: an inducible receptor for neutrophils related to complement regulatory proteins and lectins. *Science*. 243(4895):1160-5.

Biffl, W.L., Moore, E.E., Moore, F.A., Barnett, C. (1996). Nitric oxide reduces endothelial expression of intercellular adhesion molecule (ICAM)-1. *J Surg Res*. 63(1):328-32.

Bilsel, A.S., Moini, H., Tetik, E., Aksungar, F., Kaynak, B., Özer, A. (2000). 17Beta-estradiol modulates endothelin-1 expression and release in human endothelial cells. *Cardiovasc Res*. 46(3):579-84.

Binion, D.G., Heidemann, J., Li, M.S., Nelson, V.M., Otterson, M.F., Rafiee, P. (2009). Vascular cell adhesion molecule-1 expression in human intestinal microvascular endothelial cells is regulated by PI 3-kinase/Akt/MAPK/NF-kappaB: inhibitory role of curcumin. *Am J Physiol Gastrointest Liver Physiol*. 297(2):G259-68

Blanks, J.E., Moll, T., Eytner, R., Vestweber, D. (1998). Stimulation of P-selectin glycoprotein ligand-1 on mouse neutrophils activates beta 2-integrin mediated cell attachment to ICAM-1. *Eur J Immunol*.28(2):433-43.

Blum, R.H., Carter, S.K., Agre, K. (1973). A clinical review of bleomycin--a new antineoplastic agent. *Cancer.* 31 (4):903-14.

Bonner, J.C. (2004). Regulation of PDGF and its receptors in fibrotic diseases. *Cytokine Growth Factor Rev*. 15(4):255-73.

Bonniaud, P., Margetts, P.J., Kolb, M., Haberberger, T., Kelly, M., Robertson, J., Gauldie, J. (2003). Adenoviral gene transfer of connective tissue growth factor in the lung induces transient fibrosis. *Am J Respir Crit Care Med*. 168 (7) :770-8.

Borges, E., Pendl, G., Eytner, R., Steegmaier, M., Zöllner, O., Vestweber, D. (1997). The binding of T cell-expressed P-selectin glycoprotein ligand-1 to E- and P-selectin is differentially regulated. *J Biol Chem*. 272 (45) :28786-92.

Borish, L., Rosenbaum, R., Albury, L., Clark, S. (1989). Activation of neutrophils by recombinant interleukin 6. *Cell Immunol*. 121(2):280-9

Borzone, G., Moreno, R., Urrea, R., Meneses, M., Oyarzún, M., Lisboa, C. (2001). Bleomycin-induced chronic lung damage does not resemble human idiopathic pulmonary fibrosis. *Am J Respir Crit Care Med*. 163 (7) :1648-53

Bowen-Pope, D.F., Hart, C.E., Seifert, R.A. (1989). Sera and conditioned media contain different isoforms of platelet-derived growth factor (PDGF) which bind to different classes of PDGF receptor. *J Biol Chem.* 264(5):2502-8.

Brasier, A.R. (2010). The nuclear factor-kappaB-interleukin-6 signalling pathway mediating vascular inflammation. *Cardiovasc Res.* 86 (2) :211-8

Breen, E., Shull, S., Burne, S., Absher, M., Kelley, J., Phan, S., Cutroneo, K.R. (1992). Bleomycin regulation of transforming growth factor-beta mRNA in rat lung fibroblasts. *Am J Respir Cell Mol Biol*. 6 (2) :146-52

Brömme, D., Rossi, A.B., Smeekens, S.P., Anderson, D.C., Payan, D.G. (1996). Human bleomycin hydrolase: molecular cloning, sequencing, functional expression, and enzymatic characterization. *Biochemistry.* 35 (21) :6706-14.

Bronchud, M.H., Margison, J.M., Howell, A., Lind, M., Lucas, S.B., Wilkinson, P.M. (1990). Comparative pharmacokinetics of escalating doses of doxorubicin in patients with metastatic breast cancer. *Cancer Chemother Pharmacol*. 25(6):435-9.

Broughton, A., Strong, J.E., Holoye, P.Y., Bedrossian, C.W. (1977). Clinical pharmacology of bleomycin following intravenous infusion as determined by radioimmunoassay. *Cancer*. 40 (6) :2772-8.

Brown, R.F., Drawbaugh, R.B., Marrs, T.C. (1988). An investigation of possible models for the production of progressive pulmonary fibrosis in the rat. The effects of repeated intratracheal instillation of bleomycin. *Toxicology.* 51 (1) :101-10.

Brown, Z., Gerritsen, M.E., Carley, W.W., Strieter, R.M., Kunkel, S.L., Westwick, J. (1994). Chemokine gene expression and secretion by cytokine-activated human microvascular endothelial cells. Differential regulation of monocyte chemoattractant protein-1 and interleukin-8 in response to interferon-gamma. *Am J Pathol*. 145(4):913-21

Burger, R.M. (1998). Cleavage of Nucleic Acids by Bleomycin. *Chem Rev*. 98 (3):1153-1170.

Burger, R.M., Horwitz, S.B., Peisach, J., Wittenberg, J.B. (1979). Oxygenated iron bleomycin A short-lived intermediate in the reaction of ferrous bleomycin with O2. *J Biol Chem.* 254 (24):12999-302.

Burton, V.J., Butler, L.M., McGettrick, H.M., Stone, P.C., Jeffery, H.C., Savage, C.O., Rainger, G.E., Nash, G.B. (2011). Delay of migrating leukocytes by the basement membrane deposited by endothelial cells in long-term culture. Exp Cell Res. 317(3):276-92

Bustin, S.A., Benes, V., Garson, J.A., Hellemans, J., Huggett, J., Kubista, M., Mueller, R., Nolan, T., Pfaffl, M.W., Shipley, G.L., Vandesompele, J., Wittwer, C.T. (2009). The MIQE guidelines: minimum information for publication of quantitative real-time PCR experiments. *Clin Chem*. 55(4):611-22.

Calvert, A.H., Newell, D.R., Gumbrell, L.A., O'Reilly, S., Burnell, M., Boxall, F.E., Siddik, Z.H., Judson, I.R., Gore, M.E., Wiltshaw, E. (1989). Carboplatin dosage: prospective evaluation of a simple formula based on renal function. *J Clin Oncol*. 7(11):1748-56

Callies, S., de Alwis, D.P., Wright, J.G., Sandler, A., Burgess, M., Aarons, L. (2003). A population pharmacokinetic model for doxorubicin and doxorubicinol in the presence of a novel MDR modulator, zosuquidar trihydrochloride (LY335979). *Cancer Chemother Pharmacol*. 51(2):107-18

Carlos, T., Kovach, N., Schwartz, B., Rosa, M., Newman, B., Wayner, E., Benjamin, C., Osborn, L., Lobb, R., Harlan, J. (1991). Human monocytes bind to two cytokine-induced adhesive ligands on cultured human endothelial cells: endothelial-leukocyte adhesion molecule-1 and vascular cell adhesion molecule-1. *Blood*. 77 (10) :2266-71.

Carlos, T.M., Schwartz, B.R., Kovach, N.L., Yee, E., Rosa, M., Osborn, L., Chi-Rosso, G., Newman, B., Lobb, R. (1990). Vascular cell adhesion molecule-1 mediates lymphocyte adherence to cytokine-activated cultured human endothelial cells. *Blood*. 76 (5) :965-70.

Carman, C.V., Jun, C.D., Salas, A., Springer, T.A. (2003). Endothelial cells proactively form microvilli-like membrane projections upon intercellular adhesion molecule 1 engagement of leukocyte LFA-1. *J Immunol*. 171(11):6135-44.

Carman, C.V., Springer, T.A. (2004). A transmigratory cup in leukocyte diapedesis both through individual vascular endothelial cells and between them. *J Cell Biol*. 167(2):377-88

Carmona, G., Chavakis, E., Koehl, U., Zeiher, A.M., Dimmeler, S. (2008). Activation of Epac stimulates integrin-dependent homing of progenitor cells. *Blood*. 111(5):2640-6.

Cavarra, E., Carraro, F., Fineschi, S., Naldini, A., Bartalesi, B., Pucci, A., Lungarella, G. (2004). Early response to bleomycin is characterized by different cytokine and cytokine receptor profiles in lungs. *Am J Physiol Lung Cell Mol Physiol*. 287 (6) :L1186-92.

Cepeda, V., Fuertes, M.A., Castilla, J., Alonso, C., Quevedo, C., Pérez, J.M. (2007). Biochemical mechanisms of cisplatin cytotoxicity. *Anticancer Agents Med Chem*. 7(1):3-18.

Chan, S., Davidson, N., Juozaityte, E., Erdkamp, F., Pluzanska, A., Azarnia, N., Lee, L.W. (2004). Phase III trial of liposomal doxorubicin and cyclophosphamide compared with epirubicin and cyclophosphamide as first-line therapy for metastatic breast cancer. *Ann Oncol*. 15(10):1527-34

Chappey, O., Wautier, M.P., Boval, B., Wautier, J.L. (1996). Endothelial cells in culture: an experimental model for the study of vascular dysfunctions. *Cell Biol Toxicol*. 12(4-6):199-205.

Chen, B., Jiang, I., Zhao, H. (1996). [Consecutive study on alveolar macrophage release of tumor necrosis factor-alpha and platelet-derived growth factor in bleomycin-induced pulmonary fibrosis in rats]. *Zhonghua Jie He He Hu Xi Za* Zhi. 19 (4) :209-11.

Chesnutt, B.C., Smith, D.F., Raffler, N.A., Smith, M.L., White, E.J., Ley, K. (2006). Induction of LFA-1-dependent neutrophil rolling on ICAM-1 by engagement of E-selectin. *Microcirculation*. 13(2):99-109

Chien, M., Grollman, A.P., Horwitz, S.B. (1977). Bleomycin-DNA interactions: fluorescence and proton magnetic resonance studies. *Biochemistry.*16 (16):2641-7.

Choe, J.Y., Park, K.Y., Lee, S.J., Park, S.H., Kim, S.K. (2010). Rebamipide inhibits tumor necrosis factor-α-induced interleukin-8 expression by suppressing the NF-κB signal pathway in human umbilical vein endothelial cells. *Inflamm Res*. 59(12):1019-26.

Choi ,Y.W., Kim, H.J., Park, S.S., Chung, J.H., Lee, H.W., Oh, S.O., Kim, B.S., Kim, J.B., Chung, H.Y., Yu, B.P., Kim, C.D., Yoon, S. (2009). Inhibition of endothelial cell adhesion by the new anti-inflammatory agent alpha-iso-cubebene. *Vascul Pharmacol*. 51(4):215-24

Chow, M.S., Liu, L.V., Solomon, E.I. (2008). Further insights into the mechanism of the reaction of activated bleomycin with DNA. *Proc Natl Acad Sci USA.* 105(36):13241-5.

Chrzanowska, M., Sobiak, J., Grund, G., Wachowiak, J. (2011). Pharmacokinetics of high-dose etoposide administered in combination with fractionated total-body irradiation as conditioning for allogeneic hematopoietic stem cell transplantation in children with acute lymphoblastic leukemia. *Pediatr Transplant.* 15(1):96-102

Chua, F., Dunsmore, S.E., Clingen, P.H., Mutsaers, S.E., Shapiro, S.D., Segal, A.W., Roes, J., Laurent, G.J. (2007). Mice lacking neutrophil elastase are resistant to bleomycin-induced pulmonary fibrosis. *Am J Pathol.* 170 (1) :65-74

Chua, F., Gauldie, J., Laurent, G.J. (2005). Pulmonary fibrosis: searching for model answers. *Am J Respir Cell Mol Biol.* 33 (1):9-13.

Chuluyan, H.E., Osborn, L., Lobb, R., Issekutz, A.C. (1995). Domains 1 and 4 of vascular cell adhesion molecule-1 (CD106) both support very late activation antigen-4 (CD49d/CD29)-dependent monocyte transendothelial migration. *J Immunol*. 155(6):3135-4

Ciancetta, A., Coletti, C., Marrone, A., Re, N. (2012). Activation of carboplatin by carbonate: a theoretical investigation. *Dalton Trans*. 41(41):12960-9

Clark, J.G., Starcher, B.C., Uitto, J. (1980). Bleomycin-induced synthesis of type I procollagen by human lung and skin fibroblasts in culture. *Biochim Biophys Acta.* 631 (2) :359-70.

Clark, P.I., Slevin, M.L., Joel, S.P., Osborne, R.J., Talbot, D.I., Johnson, P.W., Reznek, R., Masud, T., Gregory, W., Wrigley, P.F. (1994). A randomized trial of two etoposide schedules in small-cell lung cancer: the influence of pharmacokinetics on efficacy and toxicity. *J Clin Oncol*. 12(7):1427-35.

Clinical Screening Co-operative Group of the European Organization for Research on the Treatment of Cancer. (1970). Study of the clinical efficiency of bleomycin in human cancer. *Br Med J.* 2(5710):643-5.

Coker, R.K., Laurent, G.J., Shahzeidi, S., Lympany, P.A., du Bois, R.M., Jeffery, P.K., McAnulty, R.J. (1997). Transforming growth factors-beta 1, -beta 2, and -beta 3 stimulate fibroblast procollagen production in vitro but are differentially expressed during bleomycin-induced lung fibrosis. *Am J Pathol*. 150 (3) :981-91.

Collins, T., Pober, J.S., Gimbrone, M.A. Jr, Hammacher, A., Betsholtz, C., Westermark, B., Heldin, C.H. (1987). Cultured human endothelial cells express platelet-derived growth factor A chain. *Am J Pathol.* 126(1):7-12.

Collins, T., Read, M.A., Neish, A.S., Whitley, M.Z., Thanos, D., Maniatis, T. (1995). Transcriptional regulation of endothelial cell adhesion molecules: NF-kappa B and cytokine-inducible enhancers. *FASEB J*. 9(10):899-909

Cooke, B.M., Usami, S., Perry, I., Nash, G.B. (1993). A simplified method for culture of endothelial cells and analysis of adhesion of blood cells under conditions of flow. *Microvasc Res*. 45(1):33-45

Cook-Mills, J.M. (2002). VCAM-1 signals during lymphocyte migration: role of reactive oxygen species. *Mol Immunol.* 39(9):499-508.

Corbel, M., Belleguic, C., Boichot, E., Lagente, V. (2002). Involvement of gelatinases (MMP-2 and MMP-9) in the development of airway inflammation and pulmonary fibrosis. *Cell Biol Toxicol*. 18(1):51-61

Cornish, R. J. (1928). Flow in a Pipe of Rectangular Cross-Section. *Proc. R. Soc*. A **12o**(786): 691-700.

Cortijo, J., Cerdá-Nicolás, M., Serrano, A., Bioque, G., Estrela, J.M., Santangelo, F., Esteras, A., Llombart-Bosch, A., Morcillo, E.J (2001). Attenuation by oral N-acetylcysteine of bleomycin-induced lung injury in rats. *Eur Respir J*. 17(6):1228-35.

Cutroneo, K.R., White, S.L., Phan, S.H., Ehrlich, H.P. (2007). Therapies for bleomycin induced lung fibrosis through regulation of TGF-beta1 induced collagen gene expression. *J Cell Physiol.* 211 (3):585-9

da Costa Martins, P., García-Vallejo, J.J., van Thienen, J.V., Fernandez-Borja, M., van Gils, J.M., Beckers, C., Horrevoets, A.J., Hordijk, P.L., Zwaginga, J.J. (2007). P-selectin glycoprotein ligand-1 is expressed on endothelial cells and mediates monocyte adhesion to activated endothelium. *Arterioscler Thromb Vasc Biol*. 27 (5) :1023-9.

Dajczman, E., Srolovitz, H., Kreisman, H., Frank, H. (1995). Fatal pulmonary toxicity following oral etoposide therapy. *Lung Cancer.* 12(1-2):81-6.

D'Andrea, A.D., Haseltine, W.A. (1978). Sequence specific cleavage of DNA by the antitumor antibiotics neocarzinostatin and bleomycin. *Proc Natl Acad Sci U S A*. 75 (8) :3608-12

Dangerfield, J., Larbi, K.Y., Huang, M.T., Dewar, A., Nourshargh, S. (2002) PECAM-1 (CD31) homophilic interaction up-regulates alpha6beta1 on transmigrated neutrophils in vivo and plays a functional role in the ability of alpha6 integrins to mediate leukocyte migration through the perivascular basement membrane. *J Exp Med*. 196(9):1201-11

Daniels, R.H., Finnen, M.J., Hill, M.E., Lackie, J.M. (1992). Recombinant human monocyte IL-8 primes NADPH-oxidase and phospholipase A2 activation in human neutrophils. *Immunology*. 75 (1) :157-63

Datta, A., Scotton, C.J., Chambers, R.C. (2011). Novel therapeutic approaches for pulmonary fibrosis. *Br J Pharmacol.* 163 (1):141-72.

Davies, D., Hughes, C. (2000). Dead Cell Discrimination. In Diamond, R.A., DeMaggio, S. (Eds) "*In Living Colour - Protocols in Flow Cytometry and Cell Sorting*", pp 372-376. Berlin, Germany. Springer-Verlag Berlin Heidelberg.

de Jong, R.S., Mulder, N.H., Uges, D.R., Kaul, S., Winograd, B., Sleijfer, D. Th., Groen, H.J., Willemse, P.H., van der Graaf, W.T., de Vries, E.G. (1997). Randomized comparison of etoposide pharmacokinetics after oral etoposide phosphate and oral etoposide. *Br J Cancer*. 75(11):1660-6.

de Jonge, H.J., Fehrmann, R.S., de Bont, E.S., Hofstra, R.M., Gerbens, F., Kamps, W.A., de Vries, E.G., van der Zee, A.G., te Meerman, G.J., ter Elst, A. (2007). Evidence based selection of housekeeping genes. *PLoS One*. 2(9):e898.

de Oliveira, S., Saldanha, C. (2010) An overview about erythrocyte membrane. *Clin Hemorheol Microcirc*. 44(1):63-74.

Decker, A., Chow, M.S., Kemsley, J.N., Lehnert, N., Solomon, E.I. (2006). Direct hydrogen-atom abstraction by activated bleomycin: an experimental and computational study. *J Am Chem Soc.* 128(14):4719-33.

Degryse, A.L., Tanjore, H., Xu, X.C., Polosukhin, V.V., Jones, B.R., Boomershine, C.S., Ortiz, C., Sherrill, T.P., McMahon, F.B., Gleaves, L.A., Blackwell, T.S., Lawson, W.E. (2011). TGFβ signaling in lung epithelium regulates bleomycin-induced alveolar injury and fibroblast recruitment. *Am J Physiol Lung Cell Mol Physiol.* 300(6):L887-97.

Dempsey, O.J., Kerr, K.M., Gomersall, L., Remmen, H., Currie, G.P. (2006). Idiopathic pulmonary fibrosis: an update. *QJM*. 99 (10):643-54.

Desmoulière, A., Geinoz, A., Gabbiani, F., Gabbiani, G. (1993). Transforming growth factor-beta 1 induces alpha-smooth muscle actin expression in granulation tissue myofibroblasts and in quiescent and growing cultured fibroblasts. *J Cell Biol.* 122 (1) :103-11

Deshmane, S.L., Kremlev, S., Amini, S., Sawaya, B.E. (2009). Monocyte chemoattractant protein-1 (MCP-1): an overview. *J Interferon Cytokine Res*. 29(6):313-26.

Detmers, P.A., Lo, S.K., Olsen-Egbert, E., Walz, A., Baggiolini, M., Cohn, Z.A. (1990). Neutrophil-activating protein 1/interleukin 8 stimulates the binding activity of the

leukocyte adhesion receptor CD11b/CD18 on human neutrophils. *J Exp Med.* 171(4):1155-62.

Di Pasqua, A.J., Goodisman, J., Kerwood, D.J., Toms, B.B., Dubowy, R.L., Dabrowiak, J.C. (2006). Activation of carboplatin by carbonate. *Chem Res Toxicol*.19(1):139-49.

Ding, Z.M., Babensee, J.E., Simon, S.I., Lu, H., Perrard, J.L., Bullard, D.C., Dai, X.Y., Bromley, S.K., Dustin, M.L., Entman, M.L., Smith, C.W., Ballantyne, C.M. (1999). Relative contribution of LFA-1 and Mac-1 to neutrophil adhesion and migration. *J Immunol*. 163(9):5029-38

Doerschuk, C.M. (2000). Leukocyte trafficking in alveoli and airway passages. *Respir Res*. 1(3):136-40.

Doerschuk, C.M. (2001). Mechanisms of leukocyte sequestration in inflamed lungs. *Microcirculation*. 8(2):71-88

Dorr, R.T. (1992). Bleomycin pharmacology: mechanism of action and resistance, and clinical pharmacokinetics. Semin Oncol. 19(2 Suppl 5):3-8.

Duncan, G.S., Andrew, D.P., Takimoto, H., Kaufman, S.A., Yoshida, H., Spellberg, J., de la Pompa, J.L., Elia, A., Wakeham, A., Karan-Tamir, B., Muller, W.A., Senaldi, G., Zukowski, M.M., Mak, T.W. (1999). Genetic evidence for functional redundancy of Platelet/Endothelial cell adhesion molecule-1 (PECAM-1): CD31-deficient mice reveal PECAM-1-dependent and PECAM-1-independent functions. *J Immunol*. 162(5):3022-30.

Duncan, M.R., Frazier, K.S., Abramson, S., Williams, S., Klapper, H., Huang, X., Grotendorst, G.R. (1999). Connective tissue growth factor mediates transforming growth factor beta-induced collagen synthesis: down-regulation by cAMP. *FASEB J*. 13 (13) :1774-86

Dunne, J.L., Ballantyne, C.M., Beaudet, A.L., Ley, K. (2002). Control of leukocyte rolling velocity in TNF-alpha-induced inflammation by LFA-1 and Mac-1. *Blood*. 99(1):336-41.

Dunne, J.L., Collins, R.G., Beaudet, A.L., Ballantyne, C.M., Ley, K. (2003). Mac-1, but not LFA-1, uses intercellular adhesion molecule-1 to mediate slow leukocyte rolling in TNF-alpha-induced inflammation. *J Immunol*. 171(11):6105-11.

Dwir, O., Shimron, F., Chen, C., Singer, M.S., Rosen, S.D., Alon, R. (1998). GlyCAM-1 supports leukocyte rolling in flow: evidence for a greater dynamic stability of L-selectin rolling of lymphocytes than of neutrophils. Cell Adhes Commun. 6(4):349-70.

Ekimoto, H., Takahashi, K., Matsuda, A., Takita, T., Umezawa, H. (1985). Lipid peroxidation by bleomycin-iron complexes in vitro. *J Antibiot (Tokyo)*. 38 (8) :1077-82.

El Kebir, D., Filep, J.G. (2013). Modulation of Neutrophil Apoptosis and the Resolution of Inflammation through β2 Integrins. Front Immunol. 4:60

Elferink, F., van der Vijgh, W.J., Klein, I., Vermorken, J.B., Gall, H.E., Pinedo, H.M. (1987). Pharmacokinetics of carboplatin after i.v. administration. *Cancer Treat Rep*. 71(12):1231-7

Eom, Y.W., Kim, M.A., Park, S.S., Goo, M.J., Kwon, H.J., Sohn, S., Kim, W.H., Yoon, G., Choi, K.S. (2005). Two distinct modes of cell death induced by doxorubicin: apoptosis and cell death through mitotic catastrophe accompanied by senescence-like phenotype. *Oncogene*. 24(30):4765-77

Etienne-Manneville, S., Manneville, J.B., Adamson, P., Wilbourn, B., Greenwood, J., Couraud, P.O. (2000). ICAM-1-coupled cytoskeletal rearrangements and transendothelial lymphocyte migration involve intracellular calcium signaling in brain endothelial cell lines. *J Immunol*. 165(6):3375-83

Everson, M.P., Chandler, D.B. (1992). Changes in distribution, morphology, and tumor necrosis factor-alpha secretion of alveolar macrophage subpopulations during the development of bleomycin-induced pulmonary fibrosis. *Am J Pathol*. 140 (2) :503-12.

Fagan, K.A., McMurtry, I.F., Rodman, D.M. (2001). Role of endothelin-1 in lung disease. *Respir Res*. 2(2):90-101.

Fan, K., Bell, R., Eudy, S., Fullenwider, J. (1987). Amiodarone-associated pulmonary fibrosis: Evidence of an immunologically mediated mechanism. *Chest*. 92 (4) :625-30.

Fattman, C.L., Gambelli, F., Hoyle, G., Pitt, B.R., Ortiz, L.A. (2008). Epithelial expression of TIMP-1 does not alter sensitivity to bleomycin-induced lung injury in C57BL/6 mice. *Am J Physiol Lung Cell Mol Physiol*. 294(3):L572-81

Fernandez-Patron, C., Zouki, C., Whittal, R., Chan, J.S., Davidge, S.T., Filep, J.G. (2001) Matrix metalloproteinases regulate neutrophil-endothelial cell adhesion through generation of endothelin-1[1-32]. *FASEB J*. 15(12):2230-40.

Ferrando, A.A., Velasco, G., Campo, E., Lopez-Otin, C. (1996). Cloning and expression analysis of human bleomycin hydrolase, a cysteine proteinase involved in chemotherapy resistance. *Cancer Res.* 56 (8) :1746-50.

Ferrante, A., Hauptmann, B., Seckinger, P., Dayer, J.M. (1991). Inhibition of tumour necrosis factor alpha (TNF-alpha)-induced neutrophil respiratory burst by a TNF inhibitor. *Immunology.* 72 (3) :440-2

Feuerhake, F., Füchsl, G., Bals, R., Welsch, U. (1998). Expression of inducible cell adhesion molecules in the normal human lung: immunohistochemical study of their distribution in pulmonary blood vessels. *Histochem Cell Biol*. 110 (4) :387-94

Fichtinger-Schepman, A.M., van Dijk-Knijnenburg, H.C., van der Velde-Visser, S.D., Berends, F., Baan, R.A. (1995). Cisplatin- and carboplatin-DNA adducts: is PT-AG the cytotoxic lesion? *Carcinogenesis*.16(10):2447-53.

Fichtner, F., Koslowski, R., Augstein, A., Hempel, U., Röhlecke, C., Kasper, M. (2004). Bleomycin induces IL-8 and ICAM-1 expression in microvascular pulmonary endothelial cells. *Exp Toxicol Pathol.* 55(6):497-503.

Fine, A., Goldstein, R.H. (1987). The effect of transforming growth factor-beta on cell proliferation and collagen formation by lung fibroblasts. *J Biol Chem*. 262 (8) :3897-902

Fleischman, R.W., Baker, J.R., Thompson, G.R., Schaeppi, U.H., Illievski, V.R., Cooney, D.A., Davis, R.D. (1971). Bleomycin-induced interstitial pneumonia in dogs*. Thorax.* 26 (6):675-82.

Fonseca, C., Abraham, D., Renzoni, E.A. (2011). Endothelin in pulmonary fibrosis. *Am J Respir Cell Mol Biol*. 44(1):1-10.

Fontana, L., Chen, Y., Prijatelj, P., Sakai, T., Fässler, R., Sakai, L.Y., Rifkin, D.B. (2005). Fibronectin is required for integrin alphavbeta6-mediated activation of latent TGF-beta complexes containing LTBP-1. *FASEB J*. 19 (13) :1798-808.

Foxall, C., Watson, S.R., Dowbenko, D., Fennie, C., Lasky, L.A., Kiso, M., Hasegawa, A., Asa, D., Brandley, B.K. (1992). The three members of the selectin receptor family recognize a common carbohydrate epitope, the sialyl Lewis(x) oligosaccharide. *J Cell Biol*. 117(4):895-902

Fraval, H.N., Roberts, J.J. (1979). Excision repair of cis-diamminedichloroplatinum(II)-induced damage to DNA of Chinese hamster cells. *Cancer Res*. 39(5):1793-7

Frenette, P.S., Johnson, R.C., Hynes, R.O., Wagner, D.D. (1995). Platelets roll on stimulated endothelium in vivo: an interaction mediated by endothelial P-selectin. *Proc Natl Acad Sci U S A*. 92 (16) :7450-4

Frey,T. (1995). Nucleic acid dyes for detection of apoptosis in live cells. *Cytometry*. 21(3):265-74.

Fridlender, Z.G., Cohen, P.Y., Golan, O., Arish, N., Wallach-Dayan, S., Breuer, R. (2007). Telomerase activity in bleomycin-induced epithelial cell apoptosis and lung fibrosis. *Eur Respir J*. 30(2):205-13.

Frost, B.M., Eksborg, S., Björk, O., Abrahamsson, J., Behrendtz, M., Castor, A., Forestier, E., Lönnerholm, G. (2002). Pharmacokinetics of doxorubicin in children with acute lymphoblastic leukemia: multi-institutional collaborative study. *Med Pediatr Oncol*. 38(5):329-37

Gane, J., Stockley, R. (2012). Mechanisms of neutrophil transmigration across the vascular endothelium in COPD. *Thorax*. 67(6):553-61

Garantziotis, S., Steele, M.P., Schwartz, D.A. (2004). Pulmonary fibrosis: thinking outside of the lung. *J Clin Invest*.114 (3) :319-21

Gasse, P., Mary, C., Guenon, I., Noulin, N., Charron, S., Schnyder-Candrian, S., Schnyder, B., Akira, S., Quesniaux, V.F., Lagente, V., Ryffel, B., Couillin, I. (2007). IL-1R1/MyD88 signaling and the inflammasome are essential in pulmonary inflammation and fibrosis in mice*. J Clin Invest.* 117 (12) :3786-99

Gasse, P., Riteau, N., Charron, S., Girre, S., Fick, L., Pétrilli, V., Tschopp, J., Lagente, V., Quesniaux, V.F., Ryffel, B., Couillin, I. (2009). Uric acid is a danger signal activating NALP3 inflammasome in lung injury inflammation and fibrosis. *Am J Respir Crit Care Med.* 179 (10) :903-13.

Gee, B.E., Platt, O.S. (1995). Sickle reticulocytes adhere to VCAM-1. *Blood*. 85(1):268-74

Gerszten, R.E., Garcia-Zepeda, E.A., Lim, Y.C., Yoshida, M., Ding, H.A., Gimbrone, M.A. Jr., Luster, A.D., Luscinskas, F.W., Rosenzweig, A. (1999). MCP-1 and IL-8 trigger firm adhesion of monocytes to vascular endothelium under flow conditions. *Nature*. 398(6729):718-23.

Gewirtz, D.A. (1999). A critical evaluation of the mechanisms of action proposed for the antitumor effects of the anthracycline antibiotics adriamycin and daunorubicin. *Biochem Pharmacol*. 57(7):727-41

Gharaee-Kermani, M., Denholm, E.M., Phan, S.H. (1996). Costimulation of fibroblast collagen and transforming growth factor beta1 gene expression by monocyte chemoattractant protein-1 via specific receptors. *J Biol Chem*. 271(30):17779-84

Gharaee-Kermani, M., McGarry, B., Lukacs, N., Huffnagle, G., Egan, R.W., Phan, S.H. (1998). The role of IL-5 in bleomycin-induced pulmonary fibrosis. *J Leukoc Biol.* 64 (5):657-66.

Gharaee-Kermani, M., Nozaki, Y., Hatano, K., Phan, S.H. (2001). Lung interleukin-4 gene expression in a murine model of bleomycin-induced pulmonary fibrosis. *Cytokine*. 15(3):138-47.

Giagulli, C., Ottoboni, L., Caveggion, E., Rossi, B., Lowell, C., Constantin, G., Laudanna, C., Berton, G. (2006). The Src family kinases Hck and Fgr are dispensable for inside-out, chemoattractant-induced signaling regulating beta 2 integrin affinity and valency in

neutrophils, but are required for beta 2 integrin-mediated outside-in signaling involved in sustained adhesion. *J Immunol*. 177(1):604-11

Giaid, A., Michel, R.P., Stewart, D.J., Sheppard, M., Corrin, B., Hamid, Q. (1993). Expression of endothelin-1 in lungs of patients with cryptogenic fibrosing alveolitis. *Lancet*. 341(8860):1550-4.

Gimbrone, M.A. Jr., Obin, M.S., Brock, A.F., Luis, E.A., Hass, P.E., Hébert, C.A., Yip, Y.K., Leung, D.W., Lowe, D.G., Kohr, W.J.. (1989). Endothelial interleukin-8: a novel inhibitor of leukocyte-endothelial interactions. *Science*. 246(4937):1601-3.

Giri, S.N., Hyde, D.M., Nakashima, J.M. (1986). Analysis of bronchoalveolar lavage fluid from bleomycin-induced pulmonary fibrosis in hamsters. *Toxicol Pathol.* 14(2):149-57.

Godaly, G., Hang, L., Frendéus, B., Svanborg, C. (2000). Transepithelial neutrophil migration is CXCR1 dependent in vitro and is defective in IL-8 receptor knockout mice. *J Immunol.* 165(9):5287-94.

Göksel, T., Soyer, S., Tąsbakan, S., Şanlı, U.A., Ateş, M., Göker, E. (2002). Single-agent oral etoposide in patients with relapsed or refractory extensive small-cell lung cancer. *Turkish Respiratory Journal.* 3(1):15-18

Golden, C.L., Nick, H.S., Visner, G.A. (1998). Thrombin regulation of endothelin-1 gene in isolated human pulmonary endothelial cells. *Am J Physiol*. 274(5 Pt 1):L854-63.

Goodwin, K.D., Lewis, M.A., Long, E.C., Georgiadis, M.M. (2008). Crystal structure of DNA-bound Co(III) bleomycin B2: Insights on intercalation and minor groove binding. *Proc Natl Acad Sci U S A.* 105 (13):5052-6.

Grandela, C., Pera, M.F., Grimmond, S.M., Kolle, G., Wolvetang, E.J. (2007). p53 is required for etoposide-induced apoptosis of human embryonic stem cells. Stem Cell Res. 1(2):116-28

Green, C.E., Pearson, D.N., Camphausen, R.T., Staunton, D.E., Simon, S.I. (2004). Shear-dependent capping of L-selectin and P-selectin glycoprotein ligand 1 by E-selectin signals activation of high-avidity beta2-integrin on neutrophils. *J Immunol*. 172(12):7780-90

Green, C.E., Schaff, U.Y., Sarantos, M.R., Lum, A.F., Staunton, D.E., Simon, S.I. (2006). Dynamic shifts in LFA-1 affinity regulate neutrophil rolling, arrest, and transmigration on inflamed endothelium. *Blood*. 107(5):2101-11.

Grotendorst, G.R., Duncan, M.R. (2005). Individual domains of connective tissue growth factor regulate fibroblast proliferation and myofibroblast differentiation. *FASEB J.* 19 (7) :729-38.

Grotendorst, G.R., Rahmanie, H., Duncan, M.R. (2004). Combinatorial signaling pathways determine fibroblast proliferation and myofibroblast differentiation. *FASEB J.* 18 (3) :469-79

Guo, F., Zhou, Z., Dou, Y., Tang, J., Gao, C., Huan, J. (2012). GEF-H1/RhoA signalling pathway mediates lipopolysaccharide-induced intercellular adhesion molecular-1 expression in endothelial cells via activation of p38 and NF-κB. *Cytokine*. 57(3):417-28

Gurjal, A., An, T., Valdivieso, M., Kalemkerian, G.P. (1999). Etoposide-induced pulmonary toxicity. *Lung Cancer.* 26(2):109-12.

Gurujeyalakshmi, G., Giri, S.N. (1995). Molecular mechanisms of antifibrotic effect of interferon gamma in bleomycin-mouse model of lung fibrosis: downregulation of TGF-beta and procollagen I and III gene expression. *Exp Lung Res.* 21 (5) :791-808

Gurujeyalakshmi, G., Hollinger, M.A., Giri, S.N. (1999). Pirfenidone inhibits PDGF isoforms in bleomycin hamster model of lung fibrosis at the translational level. *Am J Physiol*. 276 (2 Pt 1) :L311-8.

Haas, C.D., Coltman, C.A. Jr., Gottlieb, J.A., Haut, A., Luce, J.K., Talley, R.W., Samal, B., Wilson, H.E., Hoogstraten, B. (1976). Phase II evaluation of bleomycin A Southwest oncology Group study. *Cancer*. 38 (1) :8-12.

Hagimoto, N., Kuwano, K., Inoshima, I., Yoshimi, M., Nakamura, N., Fujita, M., Maeyama, T., Hara, N. (2002). TGF-beta 1 as an enhancer of Fas-mediated apoptosis of lung epithelial cells. *J Immunol*. 168 (12) :6470-8.

Hagimoto, N., Kuwano, K., Miyazaki, H., Kunitake, R., Fujita, M., Kawasaki, M., Kaneko, Y., Hara, N. (1997b). Induction of apoptosis and pulmonary fibrosis in mice in response to ligation of Fas antigen. *Am J Respir Cell Mol Biol.* 17 (3):272-8.

Hagimoto, N., Kuwano, K., Nomoto, Y., Kunitake, R., Hara, N. (1997). Apoptosis and expression of Fas/Fas ligand mRNA in bleomycin-induced pulmonary fibrosis in mice. *Am J Respir Cell Mol Biol.* 16 (1) :91-101.

Hagiwara, S., Iwasaka, H., Matsumoto, S., Noguchi, T. (2007). Antisense oligonucleotide inhibition of heat shock protein (HSP) 47 improves bleomycin-induced pulmonary fibrosis in rats. *Respir Res*. 8:37.

Hagiwara, S.I., Ishii, Y., Kitamura, S. (2000). Aerosolized administration of N-acetylcysteine attenuates lung fibrosis induced by bleomycin in mice. *Am J Respir Crit Care Med*. 162(1):225-31

Halnan, K.E., Bleehen, N.M., Brewin, T.B., Deeley, T.J., Harrison, D.F., Howland, C., Kunkler, P.B., Ritchie, G.L., Wiltshaw, E., Todd, I.D. (1972). Early clinical experience with bleomycin in the United Kingdom in series of 105 patients. *Br Med J.* 4(5841):635-8.

Hall, S.W., Strong, J.E., Broughton, A., Frazier, M.L., Benjamin, R.S. (1982). Bleomycin clinical pharmacology by radioimmunoassay. *Cancer Chemother Pharmacol*. 9 (1) :22-5.

Hamaguchi, Y., Nishizawa, Y., Yasui, M., Hasegawa, M., Kaburagi, Y., Komura, K., Nagaoka, T., Saito, E., Shimada, Y., Takehara, K., Kadono, T., Steeber, D.A., Tedder, T.F., Sato, S. (2002). Intercellular adhesion molecule-1 and L-selectin regulate bleomycin-induced lung fibrosis*. Am J Pathol.* 161 (5):1607-18

Hande, K.R. (1998). Etoposide: four decades of development of a topoisomerase II inhibitor. *Eur J Cancer*. 34(10):1514-21

Hao, H., Cohen, D.A., Jennings, C.D., Bryson, J.S., Kaplan, A.M. (2000). Bleomycin-induced pulmonary fibrosis is independent of eosinophils*. J Leukoc Biol.* 68 (4):515-21.

Harada, A., Sekido, N., Akahoshi, T., Wada, T., Mukaida, N., Matsushima, K. (1994). Essential involvement of interleukin-8 (IL-8) in acute inflammation. *J Leukoc Biol*. 56(5):559-64.

Haraldsen, G., Kvale, D., Lien, B., Farstad, I.N., Brandtzaeg, P. (1996). Cytokine-regulated expression of E-selectin, intercellular adhesion molecule-1 (ICAM-1), and vascular cell adhesion molecule-1 (VCAM-1) in human microvascular endothelial cells. *J Immunol*. 156(7):2558-65

Hardie, W.D., Hagood, J.S., Dave, V., Perl, A.K., Whitsett, J.A., Korfhagen, T.R., Glasser, S. (2010). Signaling pathways in the epithelial origins of pulmonary fibrosis. *Cell Cycle*. 9 (14):2769-76

Hardy, L.A., Booth, T.A., Lau, E.K., Handel, T.M., Ali, S., Kirby, J.A. (2004). Examination of MCP-1 (CCL2) partitioning and presentation during transendothelial leukocyte migration. *Lab Invest*. 84(1):81-90.

Harlan, J.M., Thompson, P.J., Ross, R.R., Bowen-Pope, D.F. (1986). Alpha-thrombin induces release of platelet-derived growth factor-like molecule(s) by cultured human endothelial cells. *J Cell Biol*. 103(3):1129-33

Hart, S.P., Alexander, K.M., Dransfield, I. (2004). Immune complexes bind preferentially to Fc gamma RIIA (CD32) on apoptotic neutrophils, leading to augmented phagocytosis by macrophages and release of proinflammatory cytokines. *J Immunol*. 172(3):1882-7.

Hashimoto, N., Jin, H., Liu, T., Chensue, S.W., Phan, S.H. (2004). Bone marrow-derived progenitor cells in pulmonary fibrosis*. J Clin Invest.* 113(2):243-52.

Hashimoto, S., Gon, Y., Matsumoto, K., Takeshita, I., Horie, T. (2001). N-acetylcysteine attenuates TNF-alpha-induced p38 MAP kinase activation and p38 MAP kinase-mediated IL-8 production by human pulmonary vascular endothelial cells. *Br J Pharmacol*.132(1):270-6.

Hattori, R., Hamilton, K.K., Fugate, R.D., McEver, R.P., Sims, P.J. (1989). Stimulated secretion of endothelial von Willebrand factor is accompanied by rapid redistribution to

the cell surface of the intracellular granule membrane protein GMP-140. *J Biol Chem*. 264 (14) :7768-71

Hecht, S.M. (2000). Bleomycin: new perspectives on the mechanism of action*. J Nat Prod.* 63 (1):158-68.

Helene, M., Lake-Bullock, V., Zhu, J., Hao, H., Cohen, D.A., Kaplan, A.M. (1999). T cell independence of bleomycin-induced pulmonary fibrosis*. J Leukoc Biol.* 65 (2):187-95

Hentzen, E.R., Neelamegham, S., Kansas, G.S., Benanti, J.A., McIntire, L.V., Smith, C.W., Simon, S.I. (2000). Sequential binding of CD11a/CD18 and CD11b/CD18 defines neutrophil capture and stable adhesion to intercellular adhesion molecule-1. *Blood*. 95(3):911-20

Hoffman, D.M., Grossano, D.D., Damin, L., Woodcock, T.M. (1979). Stability of refrigerated and frozen solutions of doxorubicin hydrochloride. *Am J Hosp Pharm*. 36(11):1536-8.

Hol, J., Otterdal, K., Breland, U.M., Stang, E., Pedersen, T.M., Hagelsteen, K., Ranheim, T., Kasprzycka, M., Halvorsen, B., Haraldsen, G., Aukrust, P. (2012). Statins affect the presentation of endothelial chemokines by targeting to multivesicular bodies. *PLoS One*. 7(7):e40673.

Homeister, J.W., Zhang, M., Frenette, P.S., Hynes, R.O., Wagner, D.D., Lowe, J.B., Marks, R.M. (1998). Overlapping functions of E- and P-selectin in neutrophil recruitment during acute inflammation. *Blood*. 92(7):2345-52

Hopkins, A.M., Baird, A.W., Nusrat, A. (2004). ICAM-1: targeted docking for exogenous as well as endogenous ligands. *Adv Drug Deliv Rev*. 56 (6) :763-78

Horikawa, M., Fujimoto, M., Hasegawa, M., Matsushita, T., Hamaguchi, Y., Kawasuji, A., Matsushita, Y., Fujita, T., Ogawa, F., Takehara, K., Steeber, D.A., Sato, S. (2006). E- and P-selectins synergistically inhibit bleomycin-induced pulmonary fibrosis*. Am J Pathol.* 169 (3):740-9

Horowitz, J.C., Thannickal, V.J. (2006). Epithelial-mesenchymal interactions in pulmonary fibrosis. *Semin Respir Crit Care Med*. 27 (6) :600-12.

Hoshino, T., Okamoto, M., Sakazaki, Y., Kato, S., Young, H.A., Aizawa, H. (2009). Role of proinflammatory cytokines IL-18 and IL-1beta in bleomycin-induced lung injury in humans and mice. *Am J Respir Cell Mol Biol.* 41 (6) :661-70.

Hoyle, G.W., Li, J., Finkelstein, J.B., Eisenberg, T., Liu, J.Y., Lasky, J.A., Athas, G., Morris, G.F., Brody, A.R. (1999). Emphysematous lesions, inflammation, and fibrosis in the lungs of transgenic mice overexpressing platelet-derived growth factor. *Am J Pathol*. 154(6):1763-75.

Hu, B., Wu, Z., Phan, S.H. (2003). Smad3 mediates transforming growth factor-beta-induced alpha-smooth muscle actin expression. *Am J Respir Cell Mol Biol*. 29 (3 Pt 1) :397-404

Hu, C.J., Lee, Y.L., Shih, N.Y., Yang, Y.Y., Charoenfuprasert, S., Dai, Y.S., Chang, S.M., Tsai, Y.H., Tseng, H., Liu, C.Y., Leu, S.J. (2009). Reduction of monocyte chemoattractant protein-1 and interleukin-8 levels by ticlopidine in TNF-alpha stimulated human umbilical vein endothelial cells. *J Biomed Biotechnol*. 2009:917837.

Huang, A.J., Manning, J.E., Bandak, T.M., Ratau, M.C., Hanser, K.R., Silverstein, S.C. (1993). Endothelial cell cytosolic free calcium regulates neutrophil migration across monolayers of endothelial cells. *J Cell Biol*. 120(6):1371-80.

Huang, C.H., Mirabelli, C.K., Jan, Y., Crooke, S.T. (1981). Single-strand and double-strand deoxyribonucleic acid breaks produced by several bleomycin analogues. *Biochemistry.* 20 (2):233-8.

Huaux, F., Liu, T., McGarry, B., Ullenbruch, M., Xing, Z., Phan, S.H. (2003) Eosinophils and T lymphocytes possess distinct roles in bleomycin-induced lung injury and fibrosis. *J Immunol.* 171(10):5470-81.

Huber, A.R., Kunkel, S.L., Todd, R.F. 3rd, Weiss, S.J. (1991). Regulation of transendothelial neutrophil migration by endogenous interleukin-8. *Science*. 254(5028):99-102.

Hulspas, R., O'Gorman, M.R., Wood, B.L., Gratama, J.W., Sutherland, D.R. (2009) Considerations for the control of background fluorescence in clinical flow cytometry. *Cytometry B Clin Cytom*. 76(6):355-64.

Hyduk, S.J., Chan, J.R., Duffy, S.T., Chen, M., Peterson, M.D., Waddell, T.K., Digby, G.C., Szaszi, K., Kapus, A., Cybulsky, M.I. (2007). Phospholipase C, calcium, and calmodulin are critical for alpha4beta1 integrin affinity up-regulation and monocyte arrest triggered by chemoattractants. *Blood*. 109(1):176-84.

Iademarco, M.F., McQuillan, J.J., Rosen, G.D., Dean, D.C. (1992). Characterization of the promoter for vascular cell adhesion molecule-1 (VCAM-1). *J Biol Chem*. 267(23):16323-9.

ibidi GmbH (17th September 2012). Application Note 13 version 3.1 [online]. Available: http://ibidi.com/fileadmin/support/application_notes/AN13_HUVECs_under_perfusion.pdf [Accessed 1 May 2014].

ibidi GmbH (4th November 2014). Application Note 11 version 4 [online]. Available: http://ibidi.com/fileadmin/support/application_notes/AN11_Shear_stress.pdf [Accessed 1 May 2014].

Iop, A., Cartei, G., Isaia, A. (1998). Vinorelbine, bleomycin and methotrexate as a salvage therapy for patients with head and neck squamous carcinoma in relapse after cisplatin/fluorouracil. *Ann Oncol.* 9 (2) :225-7.

Ishii, H., Takada, K. (2002). Bleomycin induces E-selectin expression in cultured umbilical vein endothelial cells by increasing its mRNA levels through activation of NF-kappaB/Rel. *Toxicol Appl Pharmacol.* 184 (2) :88-97.

Iyer, S.N., Hyde, D.M., Giri, S.N. (2000). Anti-inflammatory effect of pirfenidone in the bleomycin-hamster model of lung inflammation. *Inflammation.* 24 (5):477-91.

Izbicki, G., Segel, M.J., Christensen, T.G., Conner, M.W., Breuer, R. (2002). Time course of bleomycin-induced lung fibrosis. *Int J Exp Pathol*. 83 (3) :111-9.

Izumo, T., Kondo, M., Nagai, A. (2009). Effects of a leukotriene B4 receptor antagonist on bleomycin-induced pulmonary fibrosis. *Eur Respir J*. 34 (6):1444-51.

Jaffe, E.A., Mosher, D.F. (1978). Synthesis of fibronectin by cultured human endothelial cells. *J Exp Med*. 147(6):1779-91.

Jagels, M.A., Daffern, P.J., Hugli, T.E. (2000). C3a and C5a enhance granulocyte adhesion to endothelial and epithelial cell monolayers: epithelial and endothelial priming is required for C3a-induced eosinophil adhesion. *Immunopharmacology*. 46(3):209-22.

Jia, G.Q., Gonzalo, J.A., Hidalgo, A., Wagner, D., Cybulsky, M., Gutierrez-Ramos, J.C. (1999). Selective eosinophil transendothelial migration triggered by eotaxin via modulation of Mac-1/ICAM-1 and VLA-4/VCAM-1 interactions. *Int Immunol*. 11 (1) :1-10

Jiang, M.Z., Tsukahara, H., Hayakawa, K., Todoroki, Y., Tamura, S., Ohshima, Y., Hiraoka, M., Mayumi, M. (2005). Effects of antioxidants and NO on TNF-alpha-induced adhesion molecule expression in human pulmonary microvascular endothelial cells. *Respir Med*. 99(5):580-91.

Joerger, M., Huitema, A.D., Richel, D.J., Dittrich, C., Pavlidis, N., Briasoulis, E., Vermorken, J.B., Strocchi, E., Martoni, A., Sorio, R., Sleeboom, H.P., Izquierdo, M.A., Jodrell, D.I., Féty, R., de Bruijn, E., Hempel, G., Karlsson, M., Tranchand, B., Schrijvers, A.H., Twelves, C., Beijnen, J.H., Schellens, J.H.; EORTC-PAMM-NDDG. (2007). Population pharmacokinetics and pharmacodynamics of doxorubicin and cyclophosphamide in breast cancer patients: a study by the EORTC-PAMM-NDDG. *Clin Pharmacokinet*. 46(12):1051-68

Johansson, S., Svineng, G., Wennerberg, K., Armulik, A., Lohikangas, L. (1997). Fibronectin-integrin interactions. *Front Biosci*. 2:d126-46.

John, A.E., Luckett, J.C., Tatler, A.L., Awais, R.O., Desai, A., Habgood, A., Ludbrook, S., Blanchard, A.D., Perkins, A.C., Jenkins, R.G., Marshall, J.F. (2013). Preclinical SPECT/CT imaging of αvβ6 integrins for molecular stratification of idiopathic pulmonary fibrosis. *J Nucl Med*. 54(12):2146-52.

Johnson, G.L., Bibby, D.F., Wong, S., Agrawal, S.G., Bustin, S.A. (2012). A MIQE-compliant real-time PCR assay for Aspergillus detection. *PLoS One*. 7(7):e40022

Jones, A.W. (1978). Bleomycin lung damage: the pathology and nature of the lesion. *Br J Dis Chest*. 72 (4):321-6

Kalayarasan, S., Sriram, N., Sudhandiran, G. (2008). Diallyl sulfide attenuates bleomycin-induced pulmonary fibrosis: critical role of iNOS, NF-kappaB, TNF-alpha and IL-1beta. *Life Sci*. 6; 82 (23-24) :1142-53

Karam, H., Hurbain-Kosmath, I., Housset, B. (1998). Antioxidant activity in alveolar epithelial type 2 cells of rats during the development of bleomycin injury. *Cell Biol Toxicol*. 14 (1):13-22

Karmiol, S., Remick, D.G., Kunkel, S.L., Phan, S.H. (1993). Regulation of rat pulmonary endothelial cell interleukin-6 production by bleomycin: effects of cellular fatty acid composition. *Am J Respir Cell Mol Biol*. 9 (6):628-36

Karmouty-Quintana, H., Cannet, C., Zurbruegg, S., Blé, F.X., Fozard, J.R., Page, C.P., Beckmann, N. (2007). Bleomycin-induced lung injury assessed noninvasively and in spontaneously breathing rats by proton MRI. *J Magn Reson Imaging*. 26(4):941-9.

Karpinich, N.O., Tafani, M., Rothman, R.J., Russo, M.A., Farber, J.L. (2002). The course of etoposide-induced apoptosis from damage to DNA and p53 activation to mitochondrial release of cytochrome c. *J Biol Chem*. 277(19):16547-52

Kato, Y., Nishimura, S., Sakura, N., Ueda, K. (2003). Pharmacokinetics of etoposide with intravenous drug administration in children and adolescents. *Pediatr Int*. 45(1):74-9.

Kavanaugh, W.M., Harsh, G.R. 4th, Starksen, N.F., Rocco, C.M., Williams, L.T. (1988). Transcriptional regulation of the A and B chain genes of platelet-derived growth factor in microvascular endothelial cells. *J Biol Chem*. 263(17):8470-2

Kawamoto, M., Fukuda, Y. (1990). Cell proliferation during the process of bleomycin-induced pulmonary fibrosis in rats. *Acta Pathol Jpn*. 40 (4) :227-38.

Keck, M.V., Manderville, R.A., Hecht, S.M. (2001). Chemical and structural characterization of the interaction of bleomycin A2 with d(CGCGAATTCGCG)2 efficient, double-strand DNA cleavage accessible without structural reorganization. *J Am Chem Soc*. 123 (36) :8690-700

Keeney, M., Gratama, J.W., Chin-Yee, I.H., Sutherland, D.R. (1998). Isotype controls in the analysis of lymphocytes and CD34+ stem and progenitor cells by flow cytometry--time to let go! *Cytometry*. 34(6):280-3.

Kelland, L. (2007). The resurgence of platinum-based cancer chemotherapy. *Nat Rev Cancer*. 7(8):573-84.

Khalil, N., Bereznay, O., Sporn, M., Greenberg, A.H. (1989). Macrophage production of transforming growth factor beta and fibroblast collagen synthesis in chronic pulmonary inflammation. *J Exp Med*. 170 (3) :727-37.

Khalil, N., Corne, S., Whitman, C., Yacyshyn, H. (1996). Plasmin regulates the activation of cell-associated latent TGF-beta 1 secreted by rat alveolar macrophages after in vivo bleomycin injury. *Am J Respir Cell Mol Biol*. 15 (2) :252-9.

Khalil, N., O'Connor, R.N., Flanders, K.C., Shing, W., Whitman, C.I. (1994). Regulation of type II alveolar epithelial cell proliferation by TGF-beta during bleomycin-induced lung injury in rats. *Am J Physiol*. 267(5 Pt 1):L498-507

Khalil, N., Whitman, C., Zuo, L., Danielpour, D., Greenberg, A. (1993). Regulation of alveolar macrophage transforming growth factor-beta secretion by corticosteroids in bleomycin-induced pulmonary inflammation in the rat. *J Clin Invest*. 92 (4) :1812-8

Khew-Goodall, Y., Butcher, C.M., Litwin, M.S., Newlands, S., Korpelainen, E.I., Noack, L.M., Berndt, M.C., Lopez, A.F., Gamble, J.R., Vadas, M.A. (1996). Chronic expression of P-selectin on endothelial cells stimulated by the T-cell cytokine, interleukin-3. *Blood*. 87(4):1432-8.

Kiely, J.M., Hu, Y., García-Cardeña, G., Gimbrone, M.A. Jr. (2003). Lipid raft localization of cell surface E-selectin is required for ligation-induced activation of phospholipase C gamma. *J Immunol*. 171(6):3216-24.

Kim, I., Moon, S.O., Kim, S.H., Kim, H.J., Koh, Y.S., Koh, G.Y. (2001). Vascular endothelial growth factor expression of intercellular adhesion molecule 1 (ICAM-1), vascular cell adhesion molecule 1 (VCAM-1), and E-selectin through nuclear factor-kappa B activation in endothelial cells. *J Biol Chem*. 276(10):7614-20

Kim, J.Y., Choeng, H.C., Ahn, C., Cho, S.H. (2009). Early and late changes of MMP-2 and MMP-9 in bleomycin-induced pulmonary fibrosis. *Yonsei Med J*. 50 (1) :68-77

Kirkbride, P., Hatton, M., Lorigan, P., Joyce, P., Fisher, P. (2002). Fatal pulmonary fibrosis associated with induction chemotherapy with carboplatin and vinorelbine followed by CHART radiotherapy for locally advanced non-small cell lung cancer. *Clin Oncol (R Coll Radiol)*.14(5):361-6.

Köhl, P., Köppler, H., Schmidt, L., Fritsch, H.W., Holz, J., Pflüger, K.H., Jungclas, H. (1992). Pharmacokinetics of high-dose etoposide after short-term infusion. *Cancer Chemother Pharmacol*. 29(4):316-20

Kolaczkowska, E., Kubes, P. (2013). Neutrophil recruitment and function in health and inflammation. *Nat Rev Immunol*. 13(3):159-75.

Kolb, M., Margetts, P.J., Anthony, D.C., Pitossi, F., Gauldie, J. (2001). Transient expression of IL-1beta induces acute lung injury and chronic repair leading to pulmonary fibrosis. *J Clin Invest*. 107(12):1529-36.

Konstantopoulos, K., Kukreti, S., Smith, C.W., McIntire, L.V. (1997). Endothelial P-selectin and VCAM-1 each can function as primary adhesive mechanisms for T cells under conditions of flow. *J Leukoc Biol*. 61(2):179-87.

Korst, A.E., van der Sterre, M.L., Eeltink, C.M., Fichtinger-Schepman, A.M., Vermorken, J.B., van der Vijgh, W.J. (1997). Pharmacokinetics of carboplatin with and without amifostine in patients with solid tumors. *Clin Cancer Res*. 3(5):697-703

Koslowski, R., Morgner, J., Seidel, D., Knoch, K.P., Kasper, M. (2004). Postmitotic differentiation of rat lung fibroblasts: induction by bleomycin and effect on prolyl 4-hydroxylase. *Exp Toxicol Pathol*. 55 (6) :481-7.

Kothapalli, D., Frazier, K.S., Welply, A., Segarini, P.R., Grotendorst, G.R. (1997). Transforming growth factor beta induces anchorage-independent growth of NRK fibroblasts via a connective tissue growth factor-dependent signaling pathway. *Cell Growth Differ*. 8 (1) :61-8.

Kourembanas, S., Faller, D.V. (1989). Platelet-derived growth factor production by human umbilical vein endothelial cells is regulated by basic fibroblast growth factor. *J Biol Chem*. 264(8):4456-9

Kozera, B., Rapacz, M. (2013). Reference genes in real-time PCR. *J Appl Genet*. 54(4):391-406.

Kroll, M.H., Afshar-Kharghan, V. (2012). Platelets in pulmonary vascular physiology and pathology. *Pulm Circ*. 2(3):291-308

Krump-Konvalinkova, V., Bittinger, F., Unger, R.E., Peters, K., Lehr, H.A., Kirkpatrick, C.J. (2001). Generation of human pulmonary microvascular endothelial cell lines. *Lab Invest*. 81(12):1717-27.

Kuebler, W.M. (2009). Effects of Pressure and Flow on the Pulmonary Endothelium. In N.F. Voelkel & S. Rounds (Eds) "*The Pulmonary Endothelium: Function in Health and Disease",* pp. 309-311. Chichester, United Kingdom. John Wiley & Sons Ltd.

Kuijpers, T.W., Hakkert, B.C., Hart, M.H., Roos, D. (1992). Neutrophil migration across monolayers of cytokine-prestimulated endothelial cells: a role for platelet-activating factor and IL-8. *J Cell Biol*. 117 (3) :565-72.

Kulasekaran, P., Scavone, C.A., Rogers, D.S., Arenberg, D.A., Thannickal, V.J., Horowitz, J.C. (2009). Endothelin-1 and transforming growth factor-beta1 independently induce fibroblast resistance to apoptosis via AKT activation. *Am J Respir Cell Mol Biol.* 41 (4):484-93

Kumar, R.K., O'Grady, R., Maronese, S.E., Wilson, M.R. (1996). Epithelial cell-derived transforming growth factor-beta in bleomycin-induced pulmonary injury. *Int J Exp Pathol*. 77 (3):99-107

Kumar, R.K., Watkins, S.G., Lykke, A.W. (1985). Pulmonary responses to bleomycin-induced injury: an immunomorphologic and electron microscopic study. *Exp Pathol*. 28 (1) :33-43.

Kuramochi, H., Takahashi, K., Takita, T., Umezawa, H. (1981). An active intermediate formed in the reaction of bleomycin-Fe(II) complex with oxygen. *J Antibiot (Tokyo)*. 34 (5) :576-82.

Kurihara, H., Yoshizumi, M., Sugiyama, T., Takaku, F., Yanagisawa, M., Masaki, T., Hamaoki, M., Kato, H., Yazaki, Y. (1989). Transforming growth factor-beta stimulates the expression of endothelin mRNA by vascular endothelial cells. *Biochem Biophys Res Commun*. 159(3):1435-40.

Kurotani, R., Okumura, S., Matsubara, T., Yokoyama, U., Buckley, J.R., Tomita, T., Kezuka, K., Nagano, T., Esposito, D., Taylor, T.E., Gillette, W.K., Ishikawa, Y., Abe, H., Ward, J.M., Kimura, S. (2011). Secretoglobin 3A2 suppresses bleomycin-induced pulmonary fibrosis by transforming growth factor beta signaling down-regulation. *J Biol Chem*. 286 (22) :19682-92.

Kuschert, G.S., Coulin, F., Power, C.A., Proudfoot, A.E., Hubbard, R.E., Hoogewerf, A.J., Wells, T.N. (1999). Glycosaminoglycans interact selectively with chemokines and modulate receptor binding and cellular responses. *Biochemistry.* 38(39):12959-68.

Kuwano, K., Hagimoto, N., Kawasaki, M., Yatomi, T., Nakamura, N., Nagata, S., Suda, T., Kunitake, R., Maeyama, T., Miyazaki, H., Hara, N. (1999). Essential roles of the Fas-Fas ligand pathway in the development of pulmonary fibrosis. *J Clin Invest*. 104(1):13-9.

Kuwano, Y., Spelten, O., Zhang, H., Ley, K., Zarbock, A. (2010). Rolling on E- or P-selectin induces the extended but not high-affinity conformation of LFA-1 in neutrophils. *Blood*. 116(4):617-24

Lai, K.K., Cook, L., Krantz, E.M., Corey, L., Jerome, K.R. (2005). Calibration curves for real-time PCR. *Clin Chem*. 51(7):1132-6

Lakshminarayanan, V., Drab-Weiss, E.A., Roebuck, K.A. (1998). H2O2 and tumor necrosis factor-alpha induce differential binding of the redox-responsive transcription factors AP-1 and NF-kappaB to the interleukin-8 promoter in endothelial and epithelial cells. *J Biol Chem*. 273(49):32670-8.

Lappalainen, U., Whitsett, J.A., Wert, S.E., Tichelaar, J.W., Bry, K. (2005). Interleukin-1beta causes pulmonary inflammation, emphysema, and airway remodeling in the adult murine lung. *Am J Respir Cell Mol Biol*. 32 (4) :311-8.

Lasky, J.A., Ortiz, L.A., Tonthat, B., Hoyle, G.W., Corti, M., Athas, G., Lungarella, G., Brody, A., Friedman, M. (1998). Connective tissue growth factor mRNA expression is upregulated in bleomycin-induced lung fibrosis. *Am J Physiol*. 275 (2 Pt 1) :L365-71.

Lau, E.K., Paavola, C.D., Johnson, Z., Gaudry, J.P., Geretti, E., Borlat, F., Kungl, A.J., Proudfoot, A.E., Handel, T.M. (2004). Identification of the glycosaminoglycan binding site of the CC chemokine, MCP-1: implications for structure and function in vivo. *J Biol Chem.* 279(21):22294-305.

Laurell, H., Iacovoni, J.S., Abot, A., Svec, D., Maoret, J.J., Arnal, J.F., Kubista, M. (2012). Correction of RT-qPCR data for genomic DNA-derived signals with ValidPrime. *Nucleic Acids Res*. 40(7):e51

Lawrence, M.B., Springer, T.A. (1991). Leukocytes roll on a selectin at physiologic flow rates: distinction from and prerequisite for adhesion through integrins. *Cell*. 65(5):859-73.

Lazo, J.S., Humphreys, C.J. (1983). Lack of metabolism as the biochemical basis of bleomycin-induced pulmonary toxicity. *Proc Natl Acad Sci U S A*. 80 (10) :3064-8.

Ledebur, H.C., Parks, T.P. (1995). Transcriptional regulation of the intercellular adhesion molecule-1 gene by inflammatory cytokines in human endothelial cells. Essential roles of a variant NF-kappa B site and p65 homodimers. *J Biol Chem*. 270(2):933-43

Lefort, C.T., Ley, K. (2012). Neutrophil arrest by LFA-1 activation. *Front Immunol*. 3:157

Lefterov, I.M., Koldamova, R.P., King, J., Lazo, J.S. (1998). The C-terminus of human bleomycin hydrolase is required for protection against bleomycin-induced chromosomal damage. *Mutat Res*. 421 (1) :1-7.

Lewis, H., Kaszubska, W., DeLamarter, J.F., Whelan, J. (1994). Cooperativity between two NF-kappa B complexes, mediated by high-mobility-group protein I(Y), is essential for cytokine-induced expression of the E-selectin promoter. *Mol Cell Biol*. 14(9):5701-9.

Ley, K. (2003). The role of selectins in inflammation and disease. *Trends Mol Med*. 9(6):263-8

Ley, K., Laudanna, C., Cybulsky, M.I., Nourshargh, S. (2007). Getting to the site of inflammation: the leukocyte adhesion cascade updated. *Nat Rev Immunol*. 7 (9) :678-89.

Li, N., Mao, D., Lü, S., Tong, C., Zhang, Y., Long, M. (2013). Distinct binding affinities of Mac-1 and LFA-1 in neutrophil activation. *J Immunol*. 190(8):4371-81.

Li, X., Zhang, H., Soledad-Conrad, V., Zhuang, J., Uhal, B.D. (2003). Bleomycin-induced apoptosis of alveolar epithelial cells requires angiotensin synthesis de novo. *Am J Physiol Lung Cell Mol Physiol*. 284 (3):L501-7.

Li, Y., Azuma, A., Takahashi, S., Usuki, J., Matsuda, K., Aoyama, A., Kudoh, S. (2002). Fourteen-membered ring macrolides inhibit vascular cell adhesion molecule 1 messenger RNA induction and leukocyte migration: role in preventing lung injury and fibrosis in bleomycin-challenged mice. *Chest*. 122 (6) :2137-45.

Liao, F., Huynh, H.K., Eiroa, A., Greene, T., Polizzi, E., Muller, W.A. (1995). Migration of monocytes across endothelium and passage through extracellular matrix involve separate molecular domains of PECAM-1. *J Exp Med*. 182(5):1337-43

Lin, C.F., Chen, C.L., Chang, W.T., Jan, M.S., Hsu, L.J., Wu, R.H., Tang, M.J., Chang, W.C., Lin, Y.S. (2004). Sequential caspase-2 and caspase-8 activation upstream of mitochondria during ceramideand etoposide-induced apoptosis. *J Biol Chem*. 279(39):40755-61.

Liu, J., Uematsu, H., Tsuchida, N., Ikeda, M.A. (2011). Essential role of caspase-8 in p53/p73-dependent apoptosis induced by etoposide in head and neck carcinoma cells. Mol Cancer. 10:95

Liu, L.V., Bell, C.B. 3rd, Wong, S.D., Wilson, S.A., Kwak, Y., Chow, M.S., Zhao, J., Hodgson, K.O., Hedman, B., Solomon, E.I. (2010). Definition of the intermediates and mechanism of the anticancer drug bleomycin using nuclear resonance vibrational spectroscopy and related methods. *Proc Natl Acad Sci USA*. 107(52):22419-24.

Liu, X., Das, A.M., Seideman, J., Griswold, D., Afuh, C.N., Kobayashi, T., Abe, S., Fang, Q., Hashimoto, M., Kim, H., Wang, X., Shen, L., Kawasaki, S., Rennard, S.I. (2007). The CC

chemokine ligand 2 (CCL2) mediates fibroblast survival through IL-6. *Am J Respir Cell Mol Biol*. 37(1):121-8.

Liu, Z., Miner, J.J., Yago, T., Yao, L., Lupu, F., Xia, L., McEver, R.P. (2010b). Differential regulation of human and murine P-selectin expression and function in vivo. *J Exp Med.* 207(13):2975-87.

Lo Re, S., Lecocq, M., Uwambayinema, F., Yakoub, Y., Delos, M., Demoulin, J.B., Lucas, S., Sparwasser, T., Renauld, J.C., Lison, D., Huaux, F. (2011). Platelet-derived growth factor-producing CD4+ Foxp3+ regulatory T lymphocytes promote lung fibrosis. *Am J Respir Crit Care Med*. 184(11):1270-81

Lokich, J., Anderson, N. (1998). Carboplatin versus cisplatin in solid tumors: an analysis of the literature. *Ann Oncol*. 9(1):13-21.

Lomakina, E.B., Waugh, R.E. (2009). Adhesion between human neutrophils and immobilized endothelial ligand vascular cell adhesion molecule 1: divalent ion effects. *Biophys J*. 96 (1) :276-84.

Lomakina, E.B., Waugh, R.E. (2010). Signaling and Dynamics of Activation of LFA-1 and Mac-1 by Immobilized IL-8. *Cell Mol Bioeng*. 3(2):106-116

López Farré, A., Riesco, A., Espinosa, G., Digiuni, E., Cernadas, M.R., Alvarez, V., Montón, M., Rivas, F., Gallego, M.J., Egido, J., Casado, S., Caramelo, C. (1993). Effect of endothelin-1 on neutrophil adhesion to endothelial cells and perfused heart. *Circulation*. 88(3):1166-71.

Lorenzon, P., Vecile, E., Nardon, E., Ferrero, E., Harlan, J.M., Tedesco, F., Dobrina, A. (1998). Endothelial cell E- and P-selectin and vascular cell adhesion molecule-1 function as signaling receptors. *J Cell Biol*. 142(5):1381-91.

Lou, O., Alcaide, P., Luscinskas, F.W., Muller, W.A. (2007). CD99 is a key mediator of the transendothelial migration of neutrophils. *J Immunol*. 178 (2) :1136-43.

Lu, Y., Azad, N., Wang, L., Iyer, A.K., Castranova, V., Jiang, B.H., Rojanasakul, Y. (2010). Phosphatidylinositol-3-kinase /akt regulates bleomycin-induced fibroblast proliferation and collagen production. *Am J Respir Cell Mol Biol*. 42 (4) :432-41.

Lum, A.F., Green, C.E., Lee, G.R., Staunton, D.E., Simon, S.I. (2002). Dynamic regulation of LFA-1 activation and neutrophil arrest on intercellular adhesion molecule 1 (ICAM-1) in shear flow. *J Biol Chem*. 277(23):20660-70.

Lutty, G.A., Taomoto, M., Cao, J., McLeod, D.S., Vanderslice, P., McIntyre, B.W., Fabry, M.E., Nagel, R.L. (2001). Inhibition of TNF-alpha-induced sickle RBC retention in retina by a VLA-4 antagonist. *Invest Ophthalmol Vis Sci*. 42(6):1349-55.

Luu, N.T., Rahman, M., Stone, P.C., Rainger, G.E., Nash, G.B. (2010). Responses of endothelial cells from different vessels to inflammatory cytokines and shear stress: evidence for the pliability of endothelial phenotype. J Vasc Res. 47(5):451-61.

Luu, N.T., Rainger, G.E., Nash, G.B. (2000). Differential ability of exogenous chemotactic agents to disrupt transendothelial migration of flowing neutrophils. *J Immunol*. 164(11):5961-9

Ma, Y.Q., Plow, E.F., Geng, J.G. (2004). P-selectin binding to P-selectin glycoprotein ligand-1 induces an intermediate state of alphaMbeta2 activation and acts cooperatively with extracellular stimuli to support maximal adhesion of human neutrophils. *Blood*. 104(8):2549-56.

Madan, B., Batra, S., Ghosh, B. (2000). 2'-hydroxychalcone inhibits nuclear factor-kappaB and blocks tumor necrosis factor-alpha- and lipopolysaccharide-induced adhesion of neutrophils to human umbilical vein endothelial cells. *Mol Pharmacol.* 58 (3):526-34

Male, D. (2006). Mechanisms of innate immunity. In D. Male, J. Brostoff, D.B. Roth, & I. Roitt (Eds) *Immunology.* pp. 130-138. Philadelphia. Mosby Elsevier.

Makó, V., Czúcz, J., Weiszhár, Z., Herczenik, E., Matkó, J., Prohászka, Z., Cervenak, L. (2010). Proinflammatory activation pattern of human umbilical vein endothelial cells induced by IL-1β, TNF-α, and LPS. *Cytometry A*. 77(10):962-70.

Mamdouh, Z., Chen, X., Pierini, L.M., Maxfield, F.R., Muller, W.A. (2003). Targeted recycling of PECAM from endothelial surface-connected compartments during diapedesis. *Nature*. 421(6924):748-53

Mamdouh, Z., Mikhailov, A., Muller, W.A. (2009). Transcellular migration of leukocytes is mediated by the endothelial lateral border recycling compartment. *J Exp Med*. 206(12):2795-808.

Manderville, R.A., Ellena, J.F, Hecht, S.M., (1994). Solution structure of a Zn(II)-Bleomycin A_5-d(CGCTAGCG)$_2$ complex. *J Am Chem Soc.* 116:10851-10852.

Manoury, B., Nenan, S., Leclerc, O., Guenon, I., Boichot, E., Planquois, J.M., Bertrand, C.P., Lagente, V. (2005). The absence of reactive oxygen species production protects mice against bleomycin-induced pulmonary fibrosis. *Respir Res.* 6:11.

Marsen, T.A., Simonson, M.S., Dunn, M.J. (1995). Thrombin induces the preproendothelin-1 gene in endothelial cells by a protein tyrosine kinase-linked mechanism. *Circ Res*. 76(6):987-95.

Marshall, B.T., Long, M., Piper, J.W., Yago, T., McEver, R.P., Zhu, C. (2003b). Direct observation of catch bonds involving cell-adhesion molecules. *Nature*. 423(6936):190-3

Marshall, L.J., Ramdin, L.S., Brooks, T., Charlton, P., Shute, J.K. (2003). Plasminogen activator inhibitor-1 supports IL-8-mediated neutrophil transendothelial migration by inhibition of the constitutive shedding of endothelial IL-8/heparan sulfate/syndecan-1 complexes. *J Immunol*. 171(4):2057-65.

Martinet, Y., Rom, W.N., Grotendorst, G.R., Martin, G.R., Crystal, R.G. (1987). Exaggerated spontaneous release of platelet-derived growth factor by alveolar macrophages from patients with idiopathic pulmonary fibrosis. *N Engl J Med*. 317(4):202-9

Martín-Satué, M., Marrugat, R., Cancelas, J.A., Blanco, J. (1998). Enhanced expression of alpha(1,3)-fucosyltransferase genes correlates with E-selectin-mediated adhesion and metastatic potential of human lung adenocarcinoma cells. *Cancer Res*. 58(7):1544-50

Marui, N., Offermann, M.K., Swerlick, R., Kunsch, C., Rosen, C.A., Ahmad, M., Alexander, R.W., Medford, R.M. (1993). Vascular cell adhesion molecule-1 (VCAM-1) gene transcription and expression are regulated through an antioxidant-sensitive mechanism in human vascular endothelial cells. *J Clin Invest*. 92(4):1866-74.

Matsui, N.M., Borsig, L., Rosen, S.D., Yaghmai, M., Varki, A., Embury, S.H. (2001). P-selectin mediates the adhesion of sickle erythrocytes to the endothelium. Blood. 98(6):1955-62

Matsuoka, H., Arai, T., Mori, M., Goya, S., Kida, H., Morishita, H., Fujiwara, H., Tachibana, I., Osaki, T., Hayashi, S. (2002). A p38 MAPK inhibitor, FR-167653, ameliorates murine bleomycin-induced pulmonary fibrosis. *Am J Physiol Lung Cell Mol Physiol*. 283 (1):L103-12.

Matsuse, T., Teramoto, S., Katayama, H., Sudo, E., Ekimoto, H., Mitsuhashi, H., Uejima, Y., Fukuchi, Y., Ouchi, Y. (1999). ICAM-1 mediates lung leukocyte recruitment but not pulmonary fibrosis in a murine model of bleomycin-induced lung injury. *Eur Respir J*. 13 (1):71-7.

Matsushima, K., Larsen, C.G., DuBois, G.C., Oppenheim, J.J. (1989). Purification and characterization of a novel monocyte chemotactic and activating factor produced by a human myelomonocytic cell line. *J Exp Med*. 169 (4):1485-90.

Matute-Bello, G., Frevert, C.W., Martin, T.R. (2008). Animal models of acute lung injury. *Am J Physiol Lung Cell Mol Physiol*. 295 (3) :L379-99.

Matheny, H.E., Deem, T.L., Cook-Mills, J.M. (2000). Lymphocyte migration through monolayers of endothelial cell lines involves VCAM-1 signaling via endothelial cell NADPH oxidase. *J Immunol*. 164(12):6550-9.

McCormick, C.J., Craig, A., Roberts, D., Newbold, C.I., Berendt, A.R. (1997). Intercellular adhesion molecule-1 and CD36 synergize to mediate adherence of Plasmodium falciparum-infected erythrocytes to cultured human microvascular endothelial cells. J Clin Invest. 100(10):2521-9.

McEver, R.P. (1997). Regulation of the Selectins. In D. Vesweber (Ed) *The Selectins - Initiators of Leukocyte Endothelial Adhesion.* Pp. 31. Amsterdam. Harwood Academic Publishers.

McEver, R.P., Beckstead, J.H., Moore, K.L., Marshall-Carlson, L., Bainton, D.F. (1989). GMP-140, a platelet alpha-granule membrane protein, is also synthesized by vascular endothelial cells and is localized in Weibel-Palade bodies*. J Clin Invest*. 84 (1):92-9

McEver, R.P., Zhu, C. (2010). Rolling cell adhesion. *Annu Rev Cell Dev Biol*. 26:363-96

McGettrick, H.M., Buckley, C.D., Ed Rainger, G., Nash, G.B. (2010). Influence of stromal cells on lymphocyte adhesion and migration on endothelial cells. *Methods Mol Biol.* 616:49-68

McGettrick, H.M., Smith, E., Filer, A., Kissane, S., Salmon, M., Buckley, C.D., Rainger, G.E., Nash, G.B. (2009). Fibroblasts from different sites may promote or inhibit recruitment of flowing lymphocytes by endothelial cells. *Eur J Immunol*. 39(1):113-25.

Meerschaert, J., Furie, M.B. (1994). Monocytes use either CD11/CD18 or VLA-4 to migrate across human endothelium in vitro. *J Immunol*. 152(4):1915-26.

Mekid, H., Tounekti, O., Spatz, A., Cemazar, M., El Kebir, F.Z., Mir, L.M. (2003). In vivo evolution of tumour cells after the generation of double-strand DNA breaks. *Br J Cancer*. 88 (11) :1763-71.

Melgarejo, E., Medina, M.A., Sánchez-Jiménez, F., Urdiales, J.L. (2009). Monocyte chemoattractant protein-1: a key mediator in inflammatory processes. *Int J Biochem Cell Biol.* 41(5):998-1001.

Melrose, J., Tsurushita, N., Liu, G., Berg, E.L. (1998). IFN-gamma inhibits activation-induced expression of E- and P-selectin on endothelial cells. *J Immunol*. 161 (5) :2457-64.

Meltzer, E.B., Noble, P.W. (2008). Idiopathic pulmonary fibrosis. *Orphanet J Rare Dis*. 3:8

Metcalf, D.J., Nightingale, T.D., Zenner, H.L., Lui-Roberts, W.W., Cutler, D.F. (2008). Formation and function of Weibel-Palade bodies. *J Cell Sci*. 121(Pt 1):19-27

Millán, J., Hewlett, L., Glyn, M., Toomre, D., Clark, P., Ridley, A.J. (2006). Lymphocyte transcellular migration occurs through recruitment of endothelial ICAM-1 to caveola- and F-actin-rich domains. *Nat Cell Biol*. 8(2):113-23.

Min, W., Pober, J.S. (1997). TNF initiates E-selectin transcription in human endothelial cells through parallel TRAF-NF-kappa B and TRAF-RAC/CDC42-JNK-c-Jun/ATF2 pathways. *J Immunol*. 159(7):3508-18.

Miyamoto, H., Sugawara, I., Azuma, A., Saito, Y., Kohno, N., Kudoh S. (2002). Differential secretion of cytokines and adhesion molecules by HUVEC stimulated with low concentrations of bleomycin. *Cell Immunol*. 219 (2):73-81.

Mizumoto, K., Rothman, R.J., Farber, J.L. (1994). Programmed cell death (apoptosis) of mouse fibroblasts is induced by the topoisomerase II inhibitor etoposide. *Mol Pharmacol*. 46(5):890-5.

Molestina, R.E., Miller, R.D., Lentsch, A.B., Ramirez, J.A., Summersgill, J.T. (2000). Requirement for NF-kappaB in transcriptional activation of monocyte chemotactic protein 1 by Chlamydia pneumoniae in human endothelial cells. *Infect Immun*. 68 (7) :4282-8

Montgomery, K.F., Osborn, L., Hession, C., Tizard, R., Goff, D., Vassallo, C., Tarr, P.I., Bomsztyk, K., Lobb, R., Harlan, J.M., Pohlman, T.H. (1991). Activation of endothelial-leukocyte adhesion molecule 1 (ELAM-1) gene transcription. *Proc Natl Acad Sci U S A*. 88(15):6523-7.

Moodley, Y.P., Misso, N.L., Scaffidi, A.K., Fogel-Petrovic, M., McAnulty, R.J., Laurent, G.J., Thompson, P.J., Knight, D.A. (2003). Inverse effects of interleukin-6 on apoptosis of fibroblasts from pulmonary fibrosis and normal lungs. *Am J Respir Cell Mol Biol.* 29(4):490-8.

Moore, B.B., Hogaboam, C.M. (2008). Murine models of pulmonary fibrosis. *Am J Physiol Lung Cell Mol* Physiol. 294 (2) :L152-60

Moore, B.B., Peters-Golden, M., Christensen, P.J., Lama, V., Kuziel, W.A., Paine, R. 3rd, Toews, G.B. (2003). Alveolar epithelial cell inhibition of fibroblast proliferation is

regulated by MCP-1/CCR2 and mediated by PGE2. *Am J Physiol Lung Cell Mol Physiol*. 284(2):L342-9

Morotti, A., Cilloni, D., Pautasso, M., Messa, F., Arruga, F., Defilippi, I., Carturan, S., Catalano, R., Rosso, V., Chiarenza, A., Taulli, R., Bracco, E., Rege-Cambrin, G., Gottardi, E., Saglio, G. (2006). NF-kB inhibition as a strategy to enhance etoposide-induced apoptosis in K562 cell line. *Am J Hematol*. 81(12):938-45

Moseley, P.L., Hemken, C., Hunninghake, G.W. 1986. Augmentation of fibroblast proliferation by bleomycin. *J Clin Invest*. 78 (5):1150-4.

Mukaida, N., Harada, A., Matsushima, K. (1998). Interleukin-8 (IL-8) and monocyte chemotactic and activating factor (MCAF/MCP-1), chemokines essentially involved in inflammatory and immune reactions. *Cytokine Growth Factor Rev*. 9 (1) :9-23

Mulder, P.O., de Vries, E.G., Uges, D.R., Scaf, A.H., Sleijfer, D.T., Mulder, N.H. (1990). Pharmacokinetics of carboplatin at a dose of 750 mg m-2 divided over three consecutive days. *Br J Cancer*. 61(3):460-4

Muller, W.A., Weigl, S.A., Deng, X., Phillips, D.M. (1993). PECAM-1 is required for transendothelial migration of leukocytes. *J Exp Med*. 178 (2):449-60

Mundt, P., Mochmann, H.C., Ebhardt, H., Zeitz, M., Duchmann, R., Pauschinger, M. (2007). Pulmonary fibrosis after chemotherapy with oxaliplatin and 5-fluorouracil for colorectal cancer. *Oncology.* 73(3-4):270-2.

Mungunsukh, O., Griffin, A.J., Lee, Y.H., Day, R.M. (2010). Bleomycin induces the extrinsic apoptotic pathway in pulmonary endothelial cells. *Am J Physiol Lung Cell Mol Physiol*. 298(5):L696-703.

Murao, K., Imachi, H., Momoi, A., Sayo, Y., Hosokawa, H., Sato, M., Ishida, T., Takahara, J. (1999). Thiazolidinedione inhibits the production of monocyte chemoattractant protein-1 in cytokine-treated human vascular endothelial cells. *FEBS Lett*. 454(1-2):27-30.

Mutin, M., George, F., Lesaule, G., Sampol, J. (1996). Reevaluation of trypsin EDTA for endothelial cell detachment before flow cytometry analysis. *Endothelium*. 4(4):289-295.

Mutsaers, S.E., Foster, M.L., Chambers, R.C., Laurent, G.J., McAnulty, R.J. (1998). Increased endothelin-1 and its localization during the development of bleomycin-induced pulmonary fibrosis in rats. *Am J Respir Cell Mol Biol*. 18 (5):611-9

Nagaoka, I., Trapnell, B.C., Crystal, R.G. (1990). Upregulation of platelet-derived growth factor-A and -B gene expression in alveolar macrophages of individuals with idiopathic pulmonary fibrosis. *J Clin Invest*. 85(6):2023-7.

Nakagome K, Dohi M, Okunishi K, Tanaka R, Miyazaki J, Yamamoto K. (2006). In vivo IL-10 gene delivery attenuates bleomycin induced pulmonary fibrosis by inhibiting the production and activation of TGF-beta in the lung. Thorax. 61 (10) :886-94.

Nalysnyk, L., Cid-Ruzafa, J., Rotella, P., Esser, D. (2012). Incidence and prevalence of idiopathic pulmonary fibrosis: review of the literature. *Eur Respir Rev*. 21(126):355-61

Navaratnam, V., Fleming, K.M., West, J., Smith, C.J., Jenkins, R.G., Fogarty, A., Hubbard, R.B. (2011). The rising incidence of idiopathic pulmonary fibrosis in the U.K. *Thorax*. 66(6):462-7

Nevadunsky, N.S., Mbagwu, C., Mizrahi, N., Burton, E., Goldberg, G.L. (2013). Pulmonary fibrosis after pegylated liposomal Doxorubicin in a patient with uterine papillary serous carcinoma. *J Clin Oncol*. 31(10):e167-9.

Newman, P.J. (1994). The role of PECAM-1 in vascular cell biology. *Ann N Y Acad Sci*. 714:165-74.

Newman, P.J., Newman, D.K. (2003). Signal transduction pathways mediated by PECAM-1: new roles for an old molecule in platelet and vascular cell biology. *Arterioscler Thromb Vasc Biol*. 23(6):953-64. Review

Nicholson, A.G., Fulford, L.G., Colby, T.V., du Bois, R.M., Hansell, D.M., Wells, A.U. (2002). The relationship between individual histologic features and disease progression in idiopathic pulmonary fibrosis. *Am J Respir Crit Care Med*. 166(2):173-7.

Nilsen, E.M., Johansen, F.E., Jahnsen, F.L., Lundin, K.E., Scholz, T., Brandtzaeg, P., Haraldsen, G. (1988). Cytokine profiles of cultured microvascular endothelial cells from the human intestine. *Gut.* 42(5):635-42.

Nishio, K., Suzuki, Y., Aoki, T., Suzuki, K., Miyata, A., Sato, N., Naoki, K., Kudo, H., Tsumura, H., Serizawa, H., Morooka, S., Ishimura, Y., Suematsu, M., Yamaguchi, K. (1998). Differential contribution of various adhesion molecules to leukocyte kinetics in pulmonary microvessels of hyperoxia-exposed rat lungs. *Am J Respir Crit Care Med*. 157(2):599-609.

Noble, R.T., Blackwood, A.D., Griffith, J.F., McGee, C.D., Weisberg, S.B. (2010). Comparison of rapid quantitative PCR-based and conventional culture-based methods for enumeration of Enterococcus spp. and Escherichia coli in recreational waters. *Appl Environ Microbiol*. 76(22):7437-43.

O'Brien, C.D., Ji, G., Wang, Y.X., Sun, J., Krymskaya, V.P., Ruberg, F.L., Kotlikoff, M.I., Albelda, S.M. (2001). PECAM-1 (CD31) engagement activates a phosphoinositide-independent, nonspecific cation channel in endothelial cells. *FASEB* J. 15(7):1257-60.

Ockenhouse, C.F., Tegoshi, T., Maeno, Y., Benjamin, C., Ho, M., Kan, K.E., Thway, Y., Win, K., Aikawa, M., Lobb, R.R. (1992). Human vascular endothelial cell adhesion receptors for Plasmodium falciparum-infected erythrocytes: roles for endothelial leukocyte adhesion molecule 1 and vascular cell adhesion molecule 1. *J Exp Med*. 176(4):1183-9.

Oken, M.M., Crooke, S.T., Elson, M.K., Strong, J.E., Shafer, R.B. (1981). Pharmacokinetics of bleomycin after im administration in man. *Cancer Treat Rep*. 65 (5-6) :485-9

Okuma, T., Terasaki, Y., Kaikita, K., Kobayashi, H., Kuziel, W.A., Kawasuji, M., Takeya, M. (2004). C-C chemokine receptor 2 (CCR2) deficiency improves bleomycin-induced pulmonary fibrosis by attenuation of both macrophage infiltration and production of macrophage-derived matrix metalloproteinases. *J Pathol*. 204(5):594-604.

Ortiz, L.A., Lasky, J., Hamilton, R.F. Jr., Holian, A., Hoyle, G.W., Banks, W., Peschon, J.J., Brody, A.R., Lungarella, G., Friedman, M. (1998). Expression of TNF and the necessity of TNF receptors in bleomycin-induced lung injury in mice. *Exp Lung Res*. 24(6):721-43..

Ortiz, L.A., Lasky, J., Lungarella, G., Cavarra, E., Martorana, P., Banks, W.A., Peschon, J.J., Schmidts, H.L., Brody, A.R., Friedman, M. (1999). Upregulation of the p75 but not the p55 TNF-alpha receptor mRNA after silica and bleomycin exposure and protection from lung injury in double receptor knockout mice. *Am J Respir Cell Mol Biol*. 20(4):825-33

Ortiz, L.A., Moroz, K., Liu, J.Y., Hoyle, G.W., Hammond, T., Hamilton, R.F., Holian, A., Banks, W., Brody, A.R., Friedman, M. (1998b). Alveolar macrophage apoptosis and TNF-alpha, but not p53, expression correlate with murine response to bleomycin. *Am J Physiol.* 275(6 Pt 1):L1208-18.

Osborn, L., Hession, C., Tizard, R., Vassallo, C., Luhowskyj, S., Chi-Rosso, G., Lobb, R. (1989). Direct expression cloning of vascular cell adhesion molecule 1, a cytokine-induced endothelial protein that binds to lymphocytes. *Cell.* 59(6):1203-11

Ostermann, G., Weber, K.S., Zernecke, A., Schröder, A., Weber, C. (2002). JAM-1 is a ligand of the beta(2) integrin LFA-1 involved in transendothelial migration of leukocytes. *Nat Immunol*. 3 (2) :151-8.

O'Sullivan, J.M., Huddart, R.A., Norman, A.R., Nicholls, J., Dearnaley, D.P., Horwich, A. (2003). Predicting the risk of bleomycin lung toxicity in patients with germ-cell tumours. *Ann Oncol*. 14 (1):91-6.

Øynebråten, I., Barois, N., Hagelsteen, K., Johansen, F.E., Bakke, O., Haraldsen, G. (2005). Characterization of a novel chemokine-containing storage granule in endothelial cells: evidence for preferential exocytosis mediated by protein kinase A and diacylglycerol. *J Immunol.* 175(8):5358-69.

Pan, L., Kreisle, R.A., Shi, Y. (1999). Expression of endothelial cell IgG Fc receptors and markers on various cultures. *Chin Med J (Engl)*. 112(2):157-61.

Pan, L.L., Liu, X.H., Gong, Q.H., Wu, D., Zhu, Y.Z. (2011). Hydrogen sulfide attenuated tumor necrosis factor-α-induced inflammatory signaling and dysfunction in vascular endothelial cells. *PLoS One*. 6 (5) :e19766.

Papaioannou, T.G., Stefanadis, C. (2005). Vascular wall shear stress: basic principles and methods. *Hellenic J Cardiol*. 46(1):9-15

Park, S.H., Saleh, D., Giaid, A., Michel, R.P. (1997). Increased endothelin-1 in bleomycin-induced pulmonary fibrosis and the effect of an endothelin receptor antagonist. *Am J Respir Crit Care Med*. 156 (2 Pt 1) :600-8.

Park, S.K., Yang, W.S., Han, N.J., Lee, S.K., Ahn, H., Lee, I.K., Park, J.Y., Lee, K.U., Lee, J.D. (2004). Dexamethasone regulates AP-1 to repress TNF-alpha induced MCP-1 production in human glomerular endothelial cells. *Nephrol Dial Transplant*. 19(2):312-9.

Parry, G.C., Martin, T., Felts, K.A., Cobb, R.R. (1998). IL-1beta-induced monocyte chemoattractant protein-1 gene expression in endothelial cells is blocked by proteasome inhibitors. *Arterioscler Thromb Vasc Biol*. 18(6):934-40.

Peacock, A.J., Dawes, K.E., Shock, A., Gray, A.J., Reeves, J.T., Laurent, G.J. (1992). Endothelin-1 and endothelin-3 induce chemotaxis and replication of pulmonary artery fibroblasts. *Am J Respir Cell Mol Biol*. 7(5):492-9.

Peng, R., Sridhar, S., Tyagi, G., Phillips, J.E., Garrido, R., Harris, P., Burns, L., Renteria, L., Woods, J., Chen, L., Allard, J., Ravindran, P., Bitter, H., Liang, Z., Hogaboam, C.M., Kitson, C., Budd, D.C., Fine, J.S., Bauer, C.M., Stevenson, C.S. (2013) Bleomycin induces molecular changes directly relevant to idiopathic pulmonary fibrosis: a model for "active" disease. *PLoS One*. 8(4):e59348.

Peters, J.H., Sporn, L.A., Ginsberg, M.H., Wagner, D.D. (1990). Human endothelial cells synthesize, process, and secrete fibronectin molecules bearing an alternatively spliced type III homology (ED1). *Blood*. 75(9):1801-8.

Petersen, M.M., Steadman, R., Williams, J.D. (1994). Human neutrophils are selectively activated by independent ligation of the subunits of the CD11b/CD18 integrin. J Leukoc Biol. 56(6):708-13.

Petruzzelli, L., Maduzia, L., Springer, T.A. (1998). Differential requirements for LFA-1 binding to ICAM-1 and LFA-1-mediated cell aggregation. *J Immunol*. 160(9):4208-16.

Pfaffl, M.W. (2001). A new mathematical model for relative quantification in real-time RT-PCR. *Nucleic Acids Res*. 1;29(9):e45.

Phan, S.H. (2002). The myofibroblast in pulmonary fibrosis. *Chest*. 122 (6 Suppl):286S-289S.

Phan, S.H., Gharaee-Kermani, M., McGarry, B., Kunkel, S.L., Wolber, F.W. (1992). Regulation of rat pulmonary artery endothelial cell transforming growth factor-beta production by IL-1 beta and tumor necrosis factor-alpha. *J Immunol*. 149(1):103-6.

Phan, S.H., Gharaee-Kermani, M., Wolber, F., Ryan, U.S. (1991). Bleomycin stimulates production of transforming growth factor-beta by rat pulmonary artery endothelial cells. *Chest*. 99 (3 Suppl):66S.

Phillipson, M., Heit, B., Colarusso, P., Liu, L., Ballantyne, C.M., Kubes, P. (2006). Intraluminal crawling of neutrophils to emigration sites: a molecularly distinct process from adhesion in the recruitment cascade. *J Exp Med*. 203 (12) :2569-75

Piguet, P.F., Collart, M.A., Grau, G.E., Kapanci, Y., Vassalli, P. (1989). Tumor necrosis factor/cachectin plays a key role in bleomycin-induced pneumopathy and fibrosis. *J Exp Med*. 170 (3) :655-63.

Piguet, P.F., Vesin, C. (1994). Treatment by human recombinant soluble TNF receptor of pulmonary fibrosis induced by bleomycin or silica in mice. *Eur Respir J*. 7(3):515-8

Piguet, P.F., Vesin, C., Grau, G.E., Thompson, R.C. (1993). Interleukin 1 receptor antagonist (IL-1ra) prevents or cures pulmonary fibrosis elicited in mice by bleomycin or silica. *Cytokine*. 5 (1) :57-61.

Ping, D., Boekhoudt, G., Zhang, F., Morris, A., Philipsen, S., Warren, S.T., Boss, J.M. (2000). Sp1 binding is critical for promoter assembly and activation of the MCP-1 gene by tumor necrosis factor. *J Biol Chem.* 275(3):1708-14.

Pintavorn, P., Ballermann, B.J. (1997). TGF-beta and the endothelium during immune injury. *Kidney Int.* 51(5):1401-12

Ploppa, A., Kampmann, M., Johannes, T., Haeberle, H.A., Nohé, B. (2012). Effects of different leukocyte subpopulations and flow conditions on leukocyte accumulation during reperfusion. *J Vasc Res*. 49(2):169-80

Pober, J.S., Gimbrone, M.A. Jr., Lapierre, L.A., Mendrick, D.L., Fiers, W., Rothlein, R., Springer, T.A. (1986). Overlapping patterns of activation of human endothelial cells by interleukin 1, tumor necrosis factor, and immune interferon. *J Immunol*. 137 (6) :1893-6

Pogozelski, W.K., Tullius, T.D. (1998). Oxidative Strand Scission of Nucleic Acids: Routes Initiated by Hydrogen Abstraction from the Sugar Moiety. *Chem Rev*. 98 (3) :1089-1108.

Ponticos, M., Holmes, A.M., Shi-wen, X., Leoni, P., Khan, K., Rajkumar, V.S., Hoyles, R.K., Bou-Gharios, G., Black, C.M., Denton, C.P., Abraham, D.J., Leask, A., Lindahl, G.E. (2009). Pivotal role of connective tissue growth factor in lung fibrosis: MAPK-dependent transcriptional activation of type I collagen. *Arthritis Rheum*. 60 (7) :2142-55

Privratsky, J.R., Newman, D.K., Newman, P.J. (2010). PECAM-1: conflicts of interest in inflammation. *Life Sci*. 87(3-4):69-82. doi: 10.1016/j.lfs.2010.06.001. Review.

Pron, G., Belehradek, J. Jr., Mir, L.M. (1993). Identification of a plasma membrane protein that specifically binds bleomycin. *Biochem Biophys Res Commun*. 194 (1):333-7.

Pron, G., Mahrour, N., Orlowsk,i S., Tounekti, O., Poddevin, B., Belehradek, J. Jr., Mir, L.M. (1999). Internalisation of the bleomycin molecules responsible for bleomycin toxicity: a receptor-mediated endocytosis mechanism. *Biochem Pharmacol*. 57 (1):45-56.

Raghu, G., Collard, H.R., Egan, J.J., Martinez, F.J., Behr, J., Brown, K.K., Colby, T.V., Cordier, J.F., Flaherty, K.R., Lasky, J.A., Lynch, D.A., Ryu, J.H., Swigris, J.J., Wells, A.U., Ancochea, J., Bouros, D., Carvalho, C., Costabel, U., Ebina, M., Hansell, D.M., Johkoh, T., Kim, D.S., King, T.E. Jr., Kondoh, Y., Myers, J., Müller, N.L., Nicholson, A.G., Richeldi, L., Selman, M., Dudden, R.F., Griss, B.S., Protzko, S.L., Schünemann, H.J.; ATS/ERS/JRS/ALAT Committee on Idiopathic Pulmonary Fibrosis. (2011). An official ATS/ERS/JRS/ALAT statement: idiopathic pulmonary fibrosis: evidence-based guidelines for diagnosis and management. *Am J Respir Crit Care Med*. 183(6):788-824

Rahman, A., Anwar, K.N., True, A.L., Malik, A.B. (1999). Thrombin-induced p65 homodimer binding to downstream NF-kappa B site of the promoter mediates endothelial ICAM-1 expression and neutrophil adhesion. *J Immunol*. 162(9):5466-76

Rahman, A., Fazal, F. (2009). Hug tightly and say goodbye: role of endothelial ICAM-1 in leukocyte transmigration. *Antioxid Redox Signal*. Apr;11(4):823-39. doi: 10.1089/ARS.2008.2204. Review

Rahman, A., Kefer, J., Bando, M., Niles, W.D., Malik, A.B. (1998). E-selectin expression in human endothelial cells by TNF-alpha-induced oxidant generation and NF-kappaB activation. *Am J Physiol*. 275 (3 Pt 1) :L533-44.

Rainger, G.E., Fisher, A., Shearman, C., Nash, G.B. (1995). Adhesion of flowing neutrophils to cultured endothelial cells after hypoxia and reoxygenation in vitro. *Am J Physiol*. 269(4 Pt 2):H1398-406

Rajeevan, M.S., Ranamukhaarachchi, D.G., Vernon, S.D., Unger, E.R. (2001) Use of real-time quantitative PCR to validate the results of cDNA array and differential display PCR technologies. *Methods*. 25(4):443-51

Ramotar, D., Wang, H. (2003). Protective mechanisms against the antitumor agent bleomycin: lessons from Saccharomyces cerevisiae. *Curr Genet*. 43 (4) :213-24

Read, M.A., Whitley, M.Z., Gupta, S., Pierce, J.W., Best, J., Davis, R.J., Collins, T. (1997). Tumor necrosis factor alpha-induced E-selectin expression is activated by the nuclear factor-kappaB and c-JUN N-terminal kinase/p38 mitogen-activated protein kinase pathways. *J Biol Chem*. 272(5):2753-61

Read, M.A., Whitley, M.Z., Williams, A.J., Collins, T. (1994). NF-kappa B and I kappa B alpha: an inducible regulatory system in endothelial activation. *J Exp Med*. 179(2):503-12

Reibman, J., Meixler, S., Lee, T.C., Gold, L.I., Cronstein, B.N., Haines, K.A., Kolasinski, S.L., Weissmann, G. (1991). Transforming growth factor beta 1, a potent chemoattractant for human neutrophils, bypasses classic signal-transduction pathways. *Proc Natl Acad Sci U S A*. 88 (15) :6805-9.

Reichenberger, F., Schauer, J., Kellner, K., Sack, U., Stiehl, P., Winkler, J. (2001). Different expression of endothelin in the bronchoalveolar lavage in patients with pulmonary diseases. *Lung*. 179(3):163-74.

Reinert, T., Serodio da Rocha Baldotto, C., Pereira Nunes, F.A., Alves de Souza Scheliga, A. (2013). Bleomycin-Induced Lung Injury. *J Cancer Res*. 2013:9

Riccardi, R., Riccardi, A., Lasorella, A., Di Rocco, C., Carelli, G., Tornesello, A., Servidei, T., Iavarone, A., Mastrangelo, R. (1994). Clinical pharmacokinetics of carboplatin in children. *Cancer Chemother Pharmacol*. 33(6):477-83.

Richter, J., Ng-Sikorski, J., Olsson, I., Andersson, T. (1990). Tumor necrosis factor-induced degranulation in adherent human neutrophils is dependent on CD11b/CD18-integrin-triggered oscillations of cytosolic free Ca2+. Proc Natl Acad Sci U S A. 87(23):9472-6.

Rinne, M., Caldwell, D., Kelley, M.R. (2004). Transient adenoviral N-methylpurine DNA glycosylase overexpression imparts chemotherapeutic sensitivity to human breast cancer cells. *Mol Cancer Ther*. 3(8):955-67.

Rock, J.R., Barkauskas, C.E., Cronce, M.J., Xue, Y., Harris, J.R., Liang, J., Noble, P.W., Hogan, B.L. (2011). Multiple stromal populations contribute to pulmonary fibrosis without evidence for epithelial to mesenchymal transition. *Proc Natl Acad Sci U S A*. 108(52):E1475-83.

Romer, L.H., McLean, N.V., Yan, H.C., Daise, M., Sun, J., DeLisser, H.M. (1995). IFN-gamma and TNF-alpha induce redistribution of PECAM-1 (CD31) on human endothelial cells. *J Immunol*. 154(12):6582-92

Ronald, J.A., Ionescu, C.V., Rogers, K.A., Sandig, M. (2001). Differential regulation of transendothelial migration of THP-1 cells by ICAM-1/LFA-1 and VCAM-1/VLA-4. *J Leukoc Biol*. 70(4):601-9.

Rosenbloom, J., Feldman, G., Freundlich, B., Jimenez, S.A. (1984). Transcriptional control of human diploid fibroblast collagen synthesis by gamma-interferon. *Biochem Biophys Res Commun*. 123 (1) :365-72.

Ross, B., D'Orléans-Juste, P., Giaid, A. (2010). Potential role of endothelin-1 in pulmonary fibrosis: from the bench to the clinic. *Am J Respir Cell Mol Biol*. 42 (1) :16-20

Rot, A., Hub, E., Middleton, J., Pons, F., Rabeck, C., Thierer, K., Wintle, J., Wolff, B., Zsak, M., Dukor, P. (1996). Some aspects of IL-8 pathophysiology. III: Chemokine interaction with endothelial cells. *J Leukoc Biol.* 59(1):39-44.

Russell, F.D., Davenport, A.P. (1999). Secretory pathways in endothelin synthesis. *Br J Pharmacol*. 126(2):391-8.

Russo, R.C., Guabiraba, R., Garcia, C.C., Barcelos, L.S., Roffê, E., Souza, A.L., Amaral, F.A., Cisalpino, D., Cassali, G.D., Doni, A., Bertini, R., Teixeira, M.M. (2009). Role of the chemokine receptor CXCR2 in bleomycin-induced pulmonary inflammation and fibrosis. *Am J Respir Cell Mol Biol*. 40 (4) :410-21

Rydell-Törmänen, K., Andréasson, K., Hesselstrand, R., Risteli, J., Heinegård, D., Saxne, T., Westergren-Thorsson, G. (2012). Extracellular matrix alterations and acute inflammation; developing in parallel during early induction of pulmonary fibrosis. *Lab Invest*. 92(6):917-25.

Ryu, C.G., Jung, E.J., Kim, G., Kim, S.R., Hwang, D.Y. (2011). Oxaliplatin-induced Pulmonary Fibrosis: Two Case Reports. *J Korean Soc Coloproctol*. 27(5):266-9

Saito, F., Tasaka, S., Inoue, K., Miyamoto, K., Nakano, Y., Ogawa, Y., Yamada, W., Shiraishi, Y., Hasegawa, N., Fujishima, S., Takano, H., Ishizaka, A. (2008). Role of interleukin-6 in bleomycin-induced lung inflammatory changes in mice. *Am J Respir Cell Mol Biol*. 38(5):566-71.

Sakanashi, Y., Takeya, M., Yoshimura, T., Feng, L., Morioka, T., Takahashi, K. (1994). Kinetics of macrophage subpopulations and expression of monocyte chemoattractant protein-1 (MCP-1) in bleomycin-induced lung injury of rats studied by a novel monoclonal antibody against rat MCP-1. J Leukoc Biol. 56(6):741-50.

Saleh, D., Furukawa, K., Tsao, M.S., Maghazachi, A., Corrin, B., Yanagisawa, M., Barnes, P.J., Giaid, A. (1997). Elevated expression of endothelin-1 and endothelin-converting enzyme-1 in idiopathic pulmonary fibrosis: possible involvement of proinflammatory cytokines. *Am J Respir Cell Mol Biol*. 16(2):187-93.

Samuels, M.L., Johnson, D.E., Holoye, P.Y. (1975). Continuous intravenous bleomycin (NSC-125066) therapy with vinblastine (NSC-49842) in stage III testicular neoplasia. *Cancer Chemother Rep*. 59 (3) :563-70.

Samuels, M.L., Johnson, D.E., Holoye, P.Y., Lanzotti, V.J. (1976). Large-dose bleomycin therapy and pulmonary toxicity A possible role of prior radiotherapy. *JAMA*. 235 (11) :1117-20.

Santana, A., Saxena, B., Noble, N.A., Gold, L.I., Marshall, B.C. (1995). Increased expression of transforming growth factor beta isoforms (beta 1, beta 2, beta 3) in bleomycin-induced pulmonary fibrosis. *Am J Respir Cell Mol Biol*. 13(1):34-44.

Sato, E., Koyama, S., Masubuchi, T., Takamizawa, A., Kubo, K., Nagai, S., Izumi, T. (1999). Bleomycin stimulates lung epithelial cells to release neutrophil and monocyte chemotactic activities. *Am J Physiol*. 276 (6 Pt 1):L941-50.

Sato, K., Tashiro, Y., Chibana, S., Yamashita, A., Karakawa, T., Kohrogi, H. (2008). Role of lipid-derived free radical in bleomycin-induced lung injury in mice: availability for ESR spin trap method with organic phase extraction. *Biol Pharm Bull*. 31 (10) :1855-9.

Sato, N., Suzuki, Y., Nishio, K., Suzuki, K., Naoki, K., Takeshita, K., Kudo, H., Miyao, N., Tsumura, H., Serizawa, H., Suematsu, M., Yamaguchi, K. (2000). Roles of ICAM-1 for abnormal leukocyte recruitment in the microcirculation of bleomycin-induced fibrotic lung injury. *Am J Respir Crit Care Med*. 161(5):1681-8.

Sausville, E.A., Peisach, J., Horwitz, S.B. (1978). Effect of chelating agents and metal ions on the degradation of DNA by bleomycin. *Biochemistry*. 17 (14) :2740-6

Sawa, Y., Sugimoto, Y., Ueki, T., Ishikawa, H., Sato, A., Nagato, T., Yoshida, S. (2007). Effects of TNF-alpha on leukocyte adhesion molecule expressions in cultured human lymphatic endothelium. *J Histochem Cytochem*. 55(7):721-33.

Schaff, U.Y., Yamayoshi, I., Tse, T., Griffin, D., Kibathi, L., Simon, S.I. (2008). Calcium flux in neutrophils synchronizes beta2 integrin adhesive and signaling events that guide inflammatory recruitment. *Ann Biomed Eng*. 36(4):632-46.

Schein, P.S., DeVita, V.T. Jr, Hubbard, S., Chabner, B.A., Canellos, G.P., Berard, C., Young, R.C. (1976). Bleomycin, adriamycin, cyclophosphamide, vincristine, and prednisone (BACOP) combination chemotherapy in the treatment of advanced diffuse histiocytic lymphoma. *Ann Intern Med*. 85 (4) :417-22.

Schenkel, A.R., Mamdouh, Z., Muller, W.A. (2004). Locomotion of monocytes on endothelium is a critical step during extravasation. *Nat Immunol*. 5 (4) :393-400.

Schindler, U., Baichwal, V.R. (1994). Three NF-kappa B binding sites in the human E-selectin gene required for maximal tumor necrosis factor alpha-induced expression. *Mol Cell Biol*. 14(9):5820-31

Schleiffenbaum, B., Moser, R., Patarroyo, M., Fehr, J. (1989). The cell surface glycoprotein Mac-1 (CD11b/CD18) mediates neutrophil adhesion and modulates degranulation independently of its quantitative cell surface expression. J Immunol. 142(10):3537-45.

Scholz, D., Devaux, B., Hirche, A., Pötzsch, B., Kropp, B., Schaper, W., Schaper, J. (1996). Expression of adhesion molecules is specific and time-dependent in cytokine-stimulated endothelial cells in culture. *Cell Tissue Res*. 284(3):415-23.

Schrier, D.J., Phan, S.H., McGarry, B.M. (1983). The effects of the nude (nu/nu) mutation on bleomycin-induced pulmonary fibrosis A biochemical evaluation. *Am Rev Respir Dis*. 127 (5) :614-7.

Schroeder, P.E., Hofland, K.F., Jensen, P.B., Sehested, M., Langer, S.W., Hasinoff, B.B. (2004). Pharmacokinetics of etoposide in cancer patients treated with high-dose etoposide and with dexrazoxane (ICRF-187) as a rescue agent. *Cancer Chemother Pharmacol*. 53(1):91-3.

Schultz-Cherry, S., Murphy-Ullrich, J.E. (1993). Thrombospondin causes activation of latent transforming growth factor-beta secreted by endothelial cells by a novel mechanism. *J Cell Biol*. 122 (4):923-32.

Schumann, R.R., Pfeil, D., Lamping, N., Kirschning, C., Scherzinger, G., Schlag, P., Karawajew, L., Herrmann, F. (1996). Lipopolysaccharide induces the rapid tyrosine phosphorylation of the mitogen-activated protein kinases erk-1 and p38 in cultured

human vascular endothelial cells requiring the presence of soluble CD14. *Blood*. 87(7):2805-14

Schwanhäusser, B., Busse, D., Li, N., Dittmar, G., Schuchhardt, J., Wolf, J., Chen, W., Selbach, M. (2011) Global quantification of mammalian gene expression control. *Nature*. 473(7347):337-42.

Schwartsmann, G., Sprinz, E., Kromfield, M., Kalakun, L., Sander, E., Prolla, G., Di Leone, L., Gerhardt, L., Mans, D.R. (1997). Clinical and pharmacokinetic study of oral etoposide in patients with AIDS-related Kaposi's sarcoma with no prior exposure to cytotoxic therapy. *J Clin Oncol*. 15(5):2118-24.

Schwartz, D.R., Homanics, G.E., Hoyt, D.G., Klein, E., Abernethy, J., Lazo, J.S. (1999). The neutral cysteine protease bleomycin hydrolase is essential for epidermal integrity and bleomycin resistance. *Proc Natl Acad Sci U S A*. 13; 96 (8) :4680-5

Scott, D.W., Vallejo, M.O., Patel, R.P. (2013). Heterogenic endothelial responses to inflammation: role for differential N-glycosylation and vascular bed of origin. *J Am Heart Assoc*. 2(4):e000263

Segel, G.B., Halterman, M.W., Lichtman, M.A. (2011). The paradox of the neutrophil's role in tissue injury. *J Leukoc Biol*. 89(3):359-72

Selman, M., Pardo, A. (2002). Idiopathic pulmonary fibrosis: an epithelial/fibroblastic cross-talk disorder. *Respir Res*. 3:3.

Seo, S.M., McIntire, L.V., Smith, C.W. (2001). Effects of IL-8, Gro-alpha, and LTB(4) on the adhesive kinetics of LFA-1 and Mac-1 on human neutrophils. *Am J Physiol Cell Physiol.* 281(5):C1568-78.

Serrano-Mollar, A., Closa, D., Cortijo, J., Morcillo, E.J., Prats, N., Gironella, M., Panés, J., Roselló-Catafau, J., Bulbena, O. (2002). P-selectin upregulation in bleomycin induced lung injury in rats: effect of N-acetyl-L-cysteine. *Thorax*. 57(7):629-34.

Serrano-Mollar, A., Nacher, M., Gay-Jordi, G., Closa, D., Xaubet, A., Bulbena, O. (2007). Intratracheal transplantation of alveolar type II cells reverses bleomycin-induced lung fibrosis. *Am J Respir Crit Care Med*. 176 (12):1261-8

Shahar, I., Fireman, E., Topilsky, M., Grief, J., Schwarz, Y., Kivity, S., Ben-Efraim, S., Spirer, Z. (1999). Effect of endothelin-1 on alpha-smooth muscle actin expression and on alveolar fibroblasts proliferation in interstitial lung diseases. I*nt J Immunopharmacol*. 21(11):759-75.

Sheikh, S., Parhar, R., Al-Mohanna, F. (2002). Rapid static adhesion of human naïve neutrophil to naïve xenoendothelium under physiologic flow is independent of Galalpha1,3-gal structures. J Leukoc Biol. 71(6):932-40

Sheikh, S., Rahman, M., Gale, Z., Luu, N.T., Stone, P.C., Matharu, N.M., Rainger, G.E., Nash, G.B. (2005). Differing mechanisms of leukocyte recruitment and sensitivity to conditioning by shear stress for endothelial cells treated with tumour necrosis factor-alpha or interleukin-1beta. *Br J Pharmacol*. 145(8):1052-61

Shen, J., Ham, R.G., Karmiol, S. (1995). Expression of adhesion molecules in cultured human pulmonary microvascular endothelial cells. *Microvasc Res*. 50 (3) :360-72.

Shi-wen, X., Kennedy, L., Renzoni, E.A., Bou-Gharios, G., du Bois, R.M., Black, C.M., Denton, C.P., Abraham, D.J., Leask, A. (2007). Endothelin is a downstream mediator of profibrotic responses to transforming growth factor beta in human lung fibroblasts. *Arthritis Rheum*. 56(12):4189-94.

Siddik, Z.H. (2003). Cisplatin: mode of cytotoxic action and molecular basis of resistance. *Oncogene.* 22(47):7265-79.

Sime, P.J., Marr, R.A., Gauldie, D., Xing, Z., Hewlett, B.R., Graham, F.L., Gauldie, J. (1998). Transfer of tumor necrosis factor-alpha to rat lung induces severe pulmonary inflammation and patchy interstitial fibrogenesis with induction of transforming growth factor-beta1 and myofibroblasts. *Am J Pathol*. 153(3):825-32.

Simon, G.R., Lush, R.M., Gump, J., Tetteh, L., Williams, C., Cantor, A., Antonia, S., Garrett, C., Rocha-Lima, C., Fishman, M., Sullivan, D.M., Munster, P.N. (2006). Sequential oral 9-

nitrocamptothecin and etoposide: a pharmacodynamic- and pharmacokinetic-based phase I trial. *Mol Cancer Ther*. 5(8):2130-7.

Simon, S.I., Hu, Y., Vestweber, D., Smith, C.W. (2000). Neutrophil tethering on E-selectin activates beta 2 integrin binding to ICAM-1 through a mitogen-activated protein kinase signal transduction pathway. *J Immunol*. 164(8):4348-58.

Simpson, A.B., Paul, J., Graham, J., Kaye, S.B. (1998). Fatal bleomycin pulmonary toxicity in the west of Scotland 1991-95: a review of patients with germ cell tumours. *Br J Cancer*. 78 (8):1061-6.

Sinha, B.K., Haim, N., Dusre, L., Kerrigan, D., Pommier, Y. (1988). DNA strand breaks produced by etoposide (VP-16,213) in sensitive and resistant human breast tumor cells: implications for the mechanism of action. *Cancer Res*. 48(18):5096-100.

Sinkule, J.A., Hutson, P., Hayes, F.A., Etcubanas, E., Evans, W. (1984). Pharmacokinetics of etoposide (VP16) in children and adolescents with refractory solid tumors. *Cancer Res*. 44(7):3109-13

Skehan, P., Storeng, R., Scudiero, D., Monks, A., McMahon, J., Vistica, D., Warren, J.T., Bokesch, H., Kenney, S., Boyd, M.R. (1990). New colorimetric cytotoxicity assay for anticancer-drug screening. J *Natl Cancer Inst*. 82(13):1107-12.

Sleijfer, S. (2001). Bleomycin-induced pneumonitis. *Chest*. 120 (2):617-24

Smith, C.W., Marlin, S.D., Rothlein, R., Toman, C., Anderson, D.C. (1989). Cooperative interactions of LFA-1 and Mac-1 with intercellular adhesion molecule-1 in facilitating adherence and transendothelial migration of human neutrophils in vitro. *J Clin Invest*. 83(6):2008-17

Smith, R.E., Strieter, R.M., Phan, S.H., Lukacs, N., Kunkel, S.L. (1998). TNF and IL-6 mediate MIP-1alpha expression in bleomycin-induced lung injury. *J Leukoc Biol*. 64 (4) :528-36.

Smith, R.E., Strieter, R.M., Phan, S.H., Lukacs, N.W., Huffnagle, G.B., Wilke, C.A., Burdick, M.D., Lincoln, P., Evanoff, H., Kunkel, S.L. (1994). Production and function of murine

macrophage inflammatory protein-1 alpha in bleomycin-induced lung injury. *J Immunol*. 153 (10) :4704-12.

Smith, W.B., Gamble, J.R., Clark-Lewis, I., Vadas, M.A. (1991). Interleukin-8 induces neutrophil transendothelial migration. *Immunology*. 72(1):65-72.

Solis-Herruzo, J.A., Brenner, D.A., Chojkier, M. (1988). Tumor necrosis factor alpha inhibits collagen gene transcription and collagen synthesis in cultured human fibroblasts. *J Biol Chem*. 263(12):5841-5.

Song, M., He, B., Qiu, Z. (1998). [Expressions of TNF alpha, PDGF in alveolar type II epithelial cells of rats with bleomycin-induced pulmonary fibrosis]. *Zhonghua Jie He He Hu Xi Za Zhi*. 21 (4):221-3.

Sperandio, M., Smith, M.L., Forlow, S.B., Olson, T.S., Xia, L., McEver, R.P., Ley, K. (2003). P-selectin glycoprotein ligand-1 mediates L-selectin-dependent leukocyte rolling in venules. *J Exp Med*. 197 (10) :1355-63.

Spertini, O., Cordey, A.S., Monai, N., Giuffrè, L., Schapira, M. (1996). P-selectin glycoprotein ligand 1 is a ligand for L-selectin on neutrophils, monocytes, and CD34+ hematopoietic progenitor cells. *J Cell Biol*. 135(2):523-31.

Speth, P.A., Linssen, P.C., Boezeman, J.B., Wessels, H.M., Haanen, C. (1987). Cellular and plasma adriamycin concentrations in long-term infusion therapy of leukemia patients. *Cancer Chemother Pharmacol*. 20(4):305-10.

Sprinz, E., Caldas, A.P., Mans, D.R., Cancela, A., DiLeone, L., Dalla Costa, T., Schwartsmann, G. (2001). Fractionated doses of oral etoposide in the treatment of patients with aids-related kaposi sarcoma: a clinical and pharmacologic study to improve therapeutic index. *Am J Clin Oncol*. 24(2):177-84

St Germain, C., Niknejad, N., Ma, L., Garbuio, K., Hai, T., Dimitroulakos, J. (2010). Cisplatin induces cytotoxicity through the mitogen-activated protein kinase pathways and activating transcription factor 3. *Neoplasia. 12(7):527-38.*

Star, G.P., Giovinazzo, M., Langleben, D. (2009). Effects of bone morphogenic proteins and transforming growth factor-beta on In-vitro production of endothelin-1 by human pulmonary microvascular endothelial cells. *Vascul Pharmacol*. 50(1-2):45-50.

Starksen, N.F., Harsh, G.R. 4th, Gibbs, V.C., Williams, L.T. (1987). Regulated expression of the platelet-derived growth factor A chain gene in microvascular endothelial cells. *J Biol Chem*. 262(30):14381-4.

Steighner RJ, Povirk LF. (1990). Bleomycin-induced DNA lesions at mutational hot spots: implications for the mechanism of double-strand cleavage. *Proc Natl Acad Sci U S A*. 87 (21) :8350-4.

Stewart, R.J., Kashour, T.S., Marsden, P.A. (1996). Vascular endothelial platelet endothelial adhesion molecule-1 (PECAM-1) expression is decreased by TNF-alpha and IFN-gamma. Evidence for cytokine-induced destabilization of messenger ribonucleic acid transcripts in bovine endothelial cells. *J Immunol*. 156(3):1221-8

Stow, L.R., Jacobs, M.E., Wingo, C.S., Cain, B.D. (2011). Endothelin-1 gene regulation. *FASEB J*. 25(1):16-28

Strieter, R.M. (2002). Interleukin-8: a very important chemokine of the human airway epithelium. *Am J Physiol Lung Cell Mol Physiol*. 283(4):L688-9

Strober, W. (2001) Trypan blue exclusion test of cell viability. *Curr Protoc Immunol*. May;Appendix 3:Appendix 3B.

Su, W.H., Chen, H.I., Huang, J.P., Jen, C.J. (2000). Endothelial [Ca(2+)](i) signaling during transmigration of polymorphonuclear leukocytes. *Blood*. 96(12):3816-22

Subramaniam, M., Saffaripour, S., Van De Water, L., Frenette, P.S., Mayadas, T.N., Hynes, R.O., Wagner, D.D. (1997). Role of endothelial selectins in wound repair. *Am J Pathol*. 150(5):1701-9.

Sugama, Y., Tiruppathi, C., Offakidevi, K., Andersen, T.T., Fenton, J.W. 2nd, Malik, A.B. (1992). Thrombin-induced expression of endothelial P-selectin and intercellular adhesion molecule-1: a mechanism for stabilizing neutrophil adhesion. *J Cell Biol*. 119 (4) :935-44

Sugiura, Y., Kikuchi, T. (1978). Formation of superoxide and hydroxy radicals in iron(II)-bleomycin-oxygen system: electron spin resonance detection by spin trapping. *J Antibiot (Tokyo).* 31 (12) :1310-2.

Sullivan, D.E., Ferris, M., Nguyen, H., Abboud, E., Brody, A.R. (2009). TNF-alpha induces TGF-beta1 expression in lung fibroblasts at the transcriptional level via AP-1 activation. *J Cell Mol Med*. 13(8B):1866-76.

Sun, Y., Li, Y., Luo, D., Liao, D.J. (2012). Pseudogenes as weaknesses of ACTB (Actb) and GAPDH (Gapdh) used as reference genes in reverse transcription and polymerase chain reactions. *PLoS One*. 7(8):e41659

Suzuki, H., Nagai, K., Akutsu, E., Yamaki, H., Tanaka, N. (1970). On the mechanism of action of bleomycin Strand scission of DNA caused by bleomycin and its binding to DNA in vitro. *J Antibiot (Tokyo*). 23(10):473-80

Suzuki, T., Yanai, M., Kubo, H., Kanda, A., Sasaki, H., Butler, J.P. (2006). Interaction of non-adherent suspended neutrophils to complement opsonized pathogens: a new assay using optical traps. Cell Res. 16(11):887-94.

Suzuki, Y., Miyake, H., Sakai, M., Inuyama, Y., Matsukawa, J. (1969). Bleomycin in malignant tumors of head and neck. *Keio J Med*. 18 (3):153-62..

Swerlick, R.A., Garcia-Gonzalez, E., Kubota, Y., Xu, Y.L., Lawley, T.J. (1991). Studies of the modulation of MHC antigen and cell adhesion molecule expression on human dermal microvascular endothelial cells. *J Invest Dermatol*. 97(2):190-6.

Takami, M., Terry, V., Petruzzelli, L. (2002). Signaling pathways involved in IL-8-dependent activation of adhesion through Mac-1. *J Immunol.* 168(9):4559-66.

Takeshita, M., Grollman, A.P., Ohtsubo, E., Ohtsubo, H. (1978). Interaction of bleomycin with DNA. *Proc Natl Acad Sci U S A*. 75 (12) :5983-7.

Tanjore, H., Xu X.C., Polosukhin, V.V., Degryse, A.L., Li B., Han, W., Sherrill, T.P., Plieth, D., Neilson, E.G., Blackwell, T.S., Lawson, W.E. (2009). Contribution of epithelial-derived fibroblasts to bleomycin-induced lung fibrosis. *Am J Respir Crit Care Med*. 180(7):657-65.

Tan, S.M. (2012). The leucocyte β2 (CD18) integrins: the structure, functional regulation and signalling properties. Biosci Rep. 32(3):241-69.

Tanaka, Y., Albelda, S.M., Horgan, K.J., van Seventer, G.A., Shimizu, Y., Newman, W., Hallam, J., Newman, P.J., Buck, C.A., Shaw, S. (1992). CD31 expressed on distinctive T cell subsets is a preferential amplifier of beta 1 integrin-mediated adhesion. *J Exp Med*. 176(1):245-53

Tang, D., Lahti, J.M., Kidd, V.J. (2000). Caspase-8 activation and bid cleavage contribute to MCF7 cellular execution in a caspase-3-dependent manner during staurosporine-mediated apoptosis. *J Biol Chem*. 275(13):9303-7.

Tanner, J.E. (2004). Nucleosomes activate NF-kappaB in endothelial cells for induction of the proangiogenic cytokine IL-8. Int J Cancer. 112 (1) :155-60.

Taooka, Y., Maeda, A., Hiyama, K., Ishioka, S., Yamakido, M. (1997). Effects of neutrophil elastase inhibitor on bleomycin-induced pulmonary fibrosis in mice. *Am J Respir Crit Care Med*. 156 (1) :260-5.

Todorovic, V., Sersa, G., Flisar, K., Cemazar, M. (2009). Enhanced cytotoxicity of bleomycin and cisplatin after electroporation in murine colorectal carcinoma cells. *Radiol Oncol*. 43(4):264-273.

Toffoli, G., Corona, G., Sorio, R., Robieux, I., Basso, B., Colussi, A.M., Boiocchi, M. (2001). Population pharmacokinetics and pharmacodynamics of oral etoposide. *Br J Clin Pharmacol*. 52(5):511-9.

Tounekti, O., Kenani, A., Foray, N., Orlowski, S., Mir, L.M. (2001). The ratio of single- to double-strand DNA breaks and their absolute values determine cell death pathway. *Br J Cancer*. 84 (9):1272-9.

Tounekti, O., Pron, G., Belehradek, J. Jr., Mir, L.M. (1993). Bleomycin, an apoptosis-mimetic drug that induces two types of cell death depending on the number of molecules internalized. *Cancer Res*. 53 (22) :5462-9.

Tufvesson, E., Westergren-Thorsson, G. (2000). Alteration of proteoglycan synthesis in human lung fibroblasts induced by interleukin-1beta and tumor necrosis factor-alpha. *J Cell Biochem*. 77(2):298-309.

Twelves, C.J., Dobbs, N.A., Aldhous, M., Harper, P.G., Rubens, R.D., Richards, M.A. (1991). Comparative pharmacokinetics of doxorubicin given by three different schedules with equal dose intensity in patients with breast cancer. *Cancer Chemother Pharmacol*. 28(4):302-7.

Thompson, P.W., Randi, A.M., Ridley, A.J. (2002). Intercellular adhesion molecule (ICAM)-1, but not ICAM-2, activates RhoA and stimulates c-fos and rhoA transcription in endothelial cells. *J Immunol*. Jul 15;169(2):1007-13.

Thompson, R.D., Noble, K.E., Larbi, K.Y., Dewar, A., Duncan, G.S., Mak, T.W., Nourshargh, S. (2001). Platelet-endothelial cell adhesion molecule-1 (PECAM-1)-deficient mice demonstrate a transient and cytokine-specific role for PECAM-1 in leukocyte migration through the perivascular basement membrane. *Blood*. 97(6):1854-60.

Thrall, R.S., Barton, R.W., D'Amato, D.A., Sulavik, S.B. (1982). Differential cellular analysis of bronchoalveolar lavage fluid obtained at various stages during the development of bleomycin-induced pulmonary fibrosis in the rat. *Am Rev Respir Dis*. 126 (3) :488-92.

Thrall, R.S., McCormick, J.R., Jack, R.M., McReynolds, R.A., Ward ,P.A. (1979). Bleomycin-induced pulmonary fibrosis in the rat: inhibition by indomethacin. *Am J Pathol.* 95 (1) :117-30.

Umezawa, H. (1971). Natural and artificial bleomycins: chemistry and antitumor activities. *Pure Appl Chem*. 28 (4) :665-80.

Umezawa, H., Ishizuka, M., Maeda, K., Takeuchi, T. (1967). Studies on bleomycin. *Cancer*. 20 (5) :891-5.

Umezawa, H., Maeda, K., Takeuchi, T., Okami, Y. (1966). New antibiotics, bleomycin A and B. *J Antibiot (Tokyo).* 19 (5):200-9.

Umezawa, H., Takeuchi, T., Hori, S., Sawa, T., Ishizuka, M. (1972). Studies on the mechanism of antitumor effect of bleomycin of squamous cell carcinoma. *J Antibiot (Tokyo)*. 25 (7) :409-20.

Utgaard, J.O., Jahnsen, F.L., Bakka, A., Brandtzaeg, P., Haraldsen, G. (1998). Rapid secretion of prestored interleukin 8 from Weibel-Palade bodies of microvascular endothelial cells. *J Exp Med*. 188(9):1751-6.

Uzel, I., Ozguroglu, M., Uzel, B., Kaynak, K., Demirhan, O., Akman, C., Oz, F., Yaman, M. (2005). Delayed onset bleomycin-induced pneumonitis. *Urology*. 66(1):195

van Buul, J.D., van Rijssel, J., van Alphen, F.P., van Stalborch, A.M., Mul, E.P., Hordijk, P.L. (2010). ICAM-1 clustering on endothelial cells recruits VCAM-1. *J Biomed Biotechnol*. 2010;2010:120328.

van den Berg, J.M., Mul, F.P., Schippers, E., Weening, J.J., Roos, D., Kuijpers, T.W. (2001).. Beta1 integrin activation on human neutrophils promotes beta2 integrin-mediated adhesion to fibronectin. *Eur J Immunol*. 31(1):276-84

van den Berg, T.A. (2008). Iron catalyzed oxidation chemistry from C-H bond activation to DNA cleavage. Ph.D. diss., Rijksuniversiteit Groningen (University of Groningen), Netherlands.

van Gils, J.M., Zwaginga, J.J., Hordijk, P.L. (2009). Molecular and functional interactions among monocytes, platelets, and endothelial cells and their relevance for cardiovascular diseases. *J Leukoc Biol*. 85 (2) :195-204.

Van Epps, D.E., Potter, J., Vachula, M., Smith, C.W., Anderson, D.C. (1989). Suppression of human lymphocyte chemotaxis and transendothelial migration by anti-LFA-1 antibody. *J Immunol*. 143(10):3207-10.

van Wetering, S., van den Berk, N., van Buul, J.D., Mul, F.P., Lommerse, I., Mous, R., ten Klooster, J.P., Zwaginga, J.J., Hordijk, P.L. (2003). VCAM-1-mediated Rac signaling controls endothelial cell-cell contacts and leukocyte transmigration. *Am J Physiol Cell Physiol*. 285(2):C343-52

Vanderwall, D.E., Lui, S.M., Wu, W., Turner, C.J., Kozarich, J.W., Stubbe, J. (1997). A model of the structure of HOO-Cobleomycin bound to d(CCAGTACTGG): recognition at the d(GpT) site and implications for double-stranded DNA cleavage. *Chem Biol*. 4(5):373-87.

Vandesompele, J., De Preter, K., Pattyn, F., Poppe, B., Van Roy, N., De Paepe, A., Speleman, F. (2002) Accurate normalization of real-time quantitative RT-PCR data by geometric averaging of multiple internal control genes. *Genome Biol*. 3(7):RESEARCH0034.

Verweij, J., van Zanten, T., Souren, T., Golding, R., Pinedo, H.M. (1987). Prospective study on the dose relationship of mitomycin C-induced interstitial pneumonitis. *Cancer*. 60(4):756-61.

Vogel, C., Marcotte, E.M. (2012). Insights into the regulation of protein abundance from proteomic and transcriptomic analyses. *Nat Rev Genet*. 13(4):227-32

Vyalov, S.L., Gabbiani, G., Kapanci, Y. (1993). Rat alveolar myofibroblasts acquire alpha-smooth muscle actin expression during bleomycin-induced pulmonary fibrosis. *Am J Pathol*. 143 (6) :1754-65.

Wagner, J.G., Roth, R.A. (2000). Neutrophil migration mechanisms, with an emphasis on the pulmonary vasculature. *Pharmacol Rev*. 52(3):349-74

Wakelin, M.W., Sanz, M.J., Dewar, A., Albelda, S.M., Larkin, S.W., Boughton-Smith, N., Williams, T.J., Nourshargh, S. (1996). An anti-platelet-endothelial cell adhesion molecule-1 antibody inhibits leukocyte extravasation from mesenteric microvessels in vivo by blocking the passage through the basement membrane. *J Exp Med*. 184(1):229-39

Wallach-Dayan, S.B., Izbicki, G., Cohen, P.Y., Gerstl-Golan, R., Fine, A., Breuer, R. (2006). Bleomycin initiates apoptosis of lung epithelial cells by ROS but not by Fas/FasL pathway. *Am J Physiol Lung Cell Mol Physiol*. 290(4):L790-L796.

Wang, D.L., Tang, C.C., Wung, B.S., Chen, H.H., Hung, M.S., Wang, J.J. (1993). Cyclical strain increases endothelin-1 secretion and gene expression in human endothelial cells. *Biochem Biophys Res Commun.* 195(2):1050-6

Wang, P.M., Kachel, D.L., Cesta, M.F., Martin, W.J. 2nd. (2011). Direct leukocyte migration across pulmonary arterioles and venules into the perivascular interstitium of murine lungs during bleomycin injury and repair. *Am J Pathol*. 178(6):2560-72

Wang, Q., Wang, Y., Hyde, D.M., Gotwals, P.J., Koteliansky, V.E., Ryan, S.T., Giri, S.N. (1999d). Reduction of bleomycin induced lung fibrosis by transforming growth factor beta soluble receptor in hamsters. *Thorax*. 54 (9) :805-12.

Wang, R., Alam, G., Zagariya, A., Gidea, C., Pinillos, H., Lalude, O., Choudhary, G., Oezatalay, D., Uhal, B.D. (2000b). Apoptosis of lung epithelial cells in response to TNF-alpha requires angiotensin II generation de novo. *J Cell Physiol*. 185(2):253-9.

Wang, R., Ibarra-Sunga, O., Verlinski, L., Pick, R., Uhal, B.D. (2000). Abrogation of bleomycin-induced epithelial apoptosis and lung fibrosis by captopril or by a caspase inhibitor. *Am J Physiol Lung Cell Mol Physiol*. 279 (1) :L143-51

Wang, R., Ramos, C., Joshi, I., Zagariya, A., Pardo, A., Selman, M., Uhal, B.D. (1999). Human lung myofibroblast-derived inducers of alveolar epithelial apoptosis identified as angiotensin peptides. *Am J Physiol*. 277 (6 Pt 1):L1158-64.

Wang, R., Zagariya, A., Ang, E., Ibarra-Sunga, O., Uhal, B.D. (1999c). Fas-induced apoptosis of alveolar epithelial cells requires ANG II generation and receptor interaction. *Am J Physiol*. 277(6 Pt 1):L1245-50

Wang, R., Zagariya, A., Ibarra-Sunga, O., Gidea, C., Ang, E., Deshmukh, S., Chaudhary, G., Baraboutis, J., Filippatos, G., Uhal, B.D. (1999b). Angiotensin II induces apoptosis in human and rat alveolar epithelial cells. *Am J Physiol*. 276(5 Pt 1):L885-9

Ward, H.E., Nicholas, T.E. (1984). Alveolar type I and type II cells. *Aust N Z J Med*. 14(5 Suppl 3):731-4.

Wayman, A.M., Chen, W., McEver, R.P., Zhu, C. (2010). Triphasic force dependence of E-selectin/ligand dissociation governs cell rolling under flow. *Biophys J*. 99(4):1166-74

Webb, L.M., Ehrengruber, M.U., Clark-Lewis, I., Baggiolini, M., Rot, A. (1993). Binding to heparan sulfate or heparin enhances neutrophil responses to interleukin 8. *Proc Natl Acad Sci U S A.* 90(15):7158-62.

Weber, C., Alon, R., Moser, B., Springer, T.A. (1996). Sequential regulation of alpha 4 beta 1 and alpha 5 beta 1 integrin avidity by CC chemokines in monocytes: implications for transendothelial chemotaxis. *J Cell Biol.* 134(4):1063-73.

Weber, C., Erl, W., Pietsch, A., Danesch, U., Weber, P.C. (1995). Docosahexaenoic acid selectively attenuates induction of vascular cell adhesion molecule-1 and subsequent monocytic cell adhesion to human endothelial cells stimulated by tumor necrosis factor-alpha. *Arterioscler Thromb Vasc Biol*. 15(5):622-8

Weber, C., Springer, T.A. (1998). Interaction of very late antigen-4 with VCAM-1 supports transendothelial chemotaxis of monocytes by facilitating lateral migration. *J Immunol*. 161(12):6825-34

Weber, K.S., von Hundelshausen, P., Clark-Lewis, I., Weber, P.C., Weber, C. (1999). Differential immobilization and hierarchical involvement of chemokines in monocyte arrest and transmigration on inflamed endothelium in shear flow. *Eur J Immunol.* 29(2):700-12.

Weibel, E.R., Palade, G.E. (1964). New cytoplasmic components in arterial endothelia. *J Cell Biol*. 23:101-12.

Weiner, R.E., Sasso, D.E., Gionfriddo, M.A., Syrbu, S.I., Smilowitz, H.M., Vento, J., Thrall, R.S. (1998). Early detection of bleomycin-induced lung injury in rat using indium-111-labeled antibody directed against intercellular adhesion molecule-1. *J Nucl Med*. 39(4):723-8. Erratum in: J Nucl Med. 39(5):869.

White, D.A., Stover, D.E. (1984). Severe bleomycin-induced pneumonitis. Clinical features and response to corticosteroids. Chest. 86(5):723-8.

Whitley, M.Z., Thanos, D., Read, M.A., Maniatis, T., Collins, T. (1994). A striking similarity in the organization of the E-selectin and beta interferon gene promoters. *Mol Cell Biol*. 14(10):6464-75.

Wilson, M.S., Wynn, T.A. (2009). Pulmonary fibrosis: pathogenesis, etiology and regulation. *Mucosal Immunol*. 2 (2):103-21.

Willam, C., Schindler, R., Frei, U., Eckardt, K.U. (1999). Increases in oxygen tension stimulate expression of ICAM-1 and VCAM-1 on human endothelial cells. *Am J Physiol*. 276(6 Pt 2):H2044-52

Williams, M.A., Solomkin, J.S. (1999). Integrin-mediated signaling in human neutrophil functioning. *J Leukoc Biol*. 65(6):725-36. Erratum in: *J Leukoc Biol* 66(1):194

Williamson, J.D., Sadofsky, L.R., Hart, S.P. (2015). The pathogenesis of bleomycin-induced lung injury in animals and its applicability to human idiopathic pulmonary fibrosis. *Exp Lung Res*. 41(2):57-73.

Wójciak-Stothard, B., Williams, L., Ridley, A.J. (1999). Monocyte adhesion and spreading on human endothelial cells is dependent on Rho-regulated receptor clustering. *J Cell Biol*. Jun 14;145(6):1293-307

Wolff, B., Burns, A.R., Middleton, J., Rot, A. (1998). Endothelial cell "memory" of inflammatory stimulation: human venular endothelial cells store interleukin 8 in Weibel-Palade bodies. *J Exp Med.* 188(9):1757-62.

Woltmann, G., McNulty, C.A., Dewson, G., Symon, F.A., Wardlaw, A.J. (2000). Interleukin-13 induces PSGL-1/P-selectin-dependent adhesion of eosinophils, but not neutrophils, to human umbilical vein endothelial cells under flow. *Blood*. 95 (10) :3146-52

Wood, M.J., Irwin, W.J., Scott, D.K. (1990). Photodegradation of doxorubicin, daunorubicin and epirubicin measured by high-performance liquid chromatography. *J Clin Pharm Ther*. 15(4):291-300.

Wung, B.S., Ni, C.W., Wang, D.L. (2005). ICAM-1 induction by TNFalpha and IL-6 is mediated by distinct pathways via Rac in endothelial cells. *J Biomed Sci*. 12(1):91-101.

Wynn, T.A. (2011). Integrating mechanisms of pulmonary fibrosis. *J Exp Med*. 208 (7) :1339-50.

Xu, T., Liu, W., Luo, J., Li, C., Ba, X., Ampah, K.K., Wang, X., Jiang, Y., Zeng, X. (2013). Lipid Raft is required for PSGL-1 ligation induced HL-60 cell adhesion on ICAM-1. *PLoS One*. 8(12):e81807

Yago, T., Shao, B., Miner, J.J., Yao, L., Klopocki, A.G., Maeda, K., Coggeshall, K.M., McEver, R.P. (2010). E-selectin engages PSGL-1 and CD44 through a common signaling pathway to induce integrin alphaLbeta2-mediated slow leukocyte rolling. *Blood*. 116(3):485-94

Yago, T., Zarnitsyna, V.I., Klopocki, A.G., McEver, R.P., Zhu, C. (2007). Transport governs flow-enhanced cell tethering through L-selectin at threshold shear. *Biophys J*. 92(1):330-42.

Yamada, M., Kuwano, K., Maeyama, T., Hamada, N., Yoshimi, M., Nakanishi, Y., Kasper, M. (2008). Dual-immunohistochemistry provides little evidence for epithelial-mesenchymal transition in pulmonary fibrosis. *Histochem Cell Biol*. 129 (4):453-62.

Yan, W., Zhao, K., Jiang, Y., Huang, Q., Wang, J., Kan, W., Wang, S. (2002). Role of p38 MAPK in ICAM-1 expression of vascular endothelial cells induced by lipopolysaccharide. *Shock*. 17(5):433-8.

Yanagisawa, M., Kurihara, H., Kimura, S., Tomobe, Y., Kobayashi, M., Mitsui, Y., Yazaki, Y., Goto, K., Masaki, T. (1988). A novel potent vasoconstrictor peptide produced by vascular endothelial cells. *Nature*. 332(6163):411-5.

Yang, J., Velikoff, M., Canalis, E., Horowitz, J.C., Kim, K.K. (2014). Activated Alveolar Epithelial Cells Initiate Fibrosis Through Autocrine and Paracrine Secretion of Connective Tissue Growth Factor. *Am J Physiol Lung Cell Mol Physiol*. 306(8):L786-96

Yang, Y., Cardarelli, P.M., Lehnert, K., Rowland, S., Krissansen, G.W. (1998). LPAM-1 (integrin alpha 4 beta 7)-ligand binding: overlapping binding sites recognizing VCAM-1, MAdCAM-1 and CS-1 are blocked by fibrinogen, a fibronectin-like polymer and RGD-like cyclic peptides. *Eur J Immunol*. 28 (3) :995-1004

Yang, Y., Koo, S., Lin, C.S., Neu, B. (2010). Specific binding of red blood cells to endothelial cells is regulated by nonadsorbing macromolecules. *J Biol Chem*. 285(52):40489-95.

Yang, Y.Y., Hu, C.J., Chang, S.M., Tai, T.Y., Leu, S.J. (2004). Aspirin inhibits monocyte chemoattractant protein-1 and interleukin-8 expression in TNF-alpha stimulated human umbilical vein endothelial cells. *Atherosclerosi*s. 174(2):207-13.

Yao, L., Pan, J., Setiadi, H., Patel, K.D., McEver, R.P. (1996). Interleukin 4 or oncostatin M induces a prolonged increase in P-selectin mRNA and protein in human endothelial cells. *J Exp Med*. 184(1):81-92

Yehualaeshet, T., O'Connor, R., Green-Johnson, J., Mai, S., Silverstein, R., Murphy-Ullrich, J.E., Khalil, N. (1999). Activation of rat alveolar macrophage-derived latent transforming growth factor beta-1 by plasmin requires interaction with thrombospondin-1 and its cell surface receptor, CD36. *Am J Pathol*. 155 (3) :841-51.

Yen, H., Zhang, Y., Penfold, S., Rollins, B.J. (1997). MCP-1-mediated chemotaxis requires activation of non-overlapping signal transduction pathways. *J Leukoc Biol*. 61(4):529-32.

Yin, Q., Nan, H., Yan, L., Huang, X., Wang, W., Cui, G., Wei, J. (2012). Alteration of tight junctions in pulmonary microvascular endothelial cells in bleomycin-treated rats. *Exp Toxicol Pathol*. 64 (1-2) :81-91

Yin, Q., Nan, H.Y., Zhang, W.H., Yan, L.F., Cui, G.B., Huang, X.F., Wei, J.G. (2011). Pulmonary microvascular endothelial cells from bleomycin-induced rats promote the transformation and collagen synthesis of fibroblasts. *J Cell Physiol.* 226 (8):2091-102.

Yoo, S.H., Yoon, Y.G., Lee, J.S., Song, Y.S., Oh, J.S., Park, B.S., Kwon, T.K., Park, C., Choi, Y.H., Yoo, Y.H. (2012). Etoposide induces a mixed type of programmed cell death and overcomes the resistance conferred by Bcl-2 in Hep3B hepatoma cells. *Int J Oncol*. 41(4):1443-54.

Yoshida, M., Sakuma, J., Hayashi, S., Abe, K., Saito, I., Harada, S., Sakatani, M., Yamamoto, S., Matsumoto, N., Kaneda, Y. (1995). A histologically distinctive interstitial pneumonia induced by overexpression of the interleukin 6, transforming growth factor beta 1, or platelet-derived growth factor B gene. *Proc Natl Acad Sci U S A*. 92(21):9570-4.

Young, L., Adamson, I.Y. (1993). Epithelial-fibroblast interactions in bleomycin-induced lung injury and repair. *Environ Health Perspect*. 101 (1) :56-61.

Yu, M., Han, J., Cui, P., Dai, M., Li, H., Zhang, J., Xiu, R. (2008). Cisplatin up-regulates ICAM-1 expression in endothelial cell via a NF-kappaB dependent pathway. *Cancer Sci*. 99(2):391-7

Yu, Q., Stamenkovic, I. (2000). Cell surface-localized matrix metalloproteinase-9 proteolytically activates TGF-beta and promotes tumor invasion and angiogenesis. *Genes Dev*. 14 (2) :163-76

Yue, J., Mulder, K.M. (2001). Transforming growth factor-beta signal transduction in epithelial cells. *Pharmacol Ther*. 91(1):1-34

Yusuf-Makagiansar, H., Anderson, M.E., Yakovleva, T.V., Murray, J.S., Siahaan, T.J. (2002). Inhibition of LFA-1/ICAM-1 and VLA-4/VCAM-1 as a therapeutic approach to inflammation and autoimmune diseases. *Med Res Rev*. 22 (2) :146-67.

Zandvliet, A.S., Schellens, J.H., Dittrich, C., Wanders, J., Beijnen, J.H., Huitema, A.D. (2008). Population pharmacokinetic and pharmacodynamic analysis to support treatment optimization of combination chemotherapy with indisulam and carboplatin. *Br J Clin Pharmacol*. 66(4):485-97.

Zappa, L., Savady, R., Humphries, G.N., Sugarbaker, P.H. (2009). Interstitial pneumonitis following intrapleural chemotherapy. *World J Surg Oncol.* 7:17.

Zarbock, A., Abram, C.L., Hundt, M., Altman, A., Lowell, C.A., Ley, K. (2008). PSGL-1 engagement by E-selectin signals through Src kinase Fgr and ITAM adapters DAP12 and FcR gamma to induce slow leukocyte rolling. *J Exp Med*. 205(10):2339-47

Zarbock, A., Ley, K., McEver, R.P., Hidalgo, A. (2011). Leukocyte ligands for endothelial selectins: specialized glycoconjugates that mediate rolling and signaling under flow. *Blood*. 118 (26) :6743-51.

Zarbock, A., Müller, H., Kuwano, Y., Ley, K. (2009). PSGL-1-dependent myeloid leukocyte activation. *J Leukoc Biol*. 86 (5) :1119-24.

Zeilhofer, H.U., Schorr, W. (2000). Role of interleukin-8 in neutrophil signaling. *Curr Opin Hematol*. 7(3):178-82.

Zen, K., Cui, L.B., Zhang, C.Y., Liu, Y. (2007). Critical role of mac-1 sialyl lewis x moieties in regulating neutrophil degranulation and transmigration. *J Mol Biol*. 374 (1) :54-63

Zimmerman, G.A. (2001). Two by two: the pairings of P-selectin and P-selectin glycoprotein ligand 1. *Proc Natl Acad Sci U S A*. 98 (18) :10023-4

Zhan, D.Y., Zhang, Y., Long, M. (2012). Spreading of human neutrophils on an ICAM-1-immobilized substrate under shear flow. *Chin Sci Bull*. 57(7):769-775

Zhang, F., Nielsen, L.D., Lucas, J.J., Mason, R.J. (2004). Transforming growth factor-beta antagonizes alveolar type II cell proliferation induced by keratinocyte growth factor. *Am J Respir Cell Mol Biol*. 31(6):679-86.

Zhang, H., Issekutz, A.C. (2001). Growth factor regulation of neutrophil-endothelial cell interactions. *J Leukoc Biol*. 70(2):225-32

Zhang, H.Y., Gharaee-Kermani, M., Zhang, K., Karmiol, S., Phan, S.H. (1996). Lung fibroblast alpha-smooth muscle actin expression and contractile phenotype in bleomycin-induced pulmonary fibrosis. *Am J Pathol*. 148 (2) :527-37.

Zhang, K., Flanders, K.C., Phan, S.H. (1995). Cellular localization of transforming growth factor-beta expression in bleomycin-induced pulmonary fibrosis. *Am J Pathol*. 147(2):352-61.

Zhang, K., Gharaee-Kermani, M., Jones, M.L., Warren, J.S., Phan, S.H. (1994). Lung monocyte chemoattractant protein-1 gene expression in bleomycin-induced pulmonary fibrosis. *J Immunol*. 153 (10):4733-41

Zhang, K., Rekhter, M.D., Gordon, D., Phan, S.H. (1994b). Myofibroblasts and their role in lung collagen gene expression during pulmonary fibrosis A combined immunohistochemical and in situ hybridization study. *Am J Pathol*. 145 (1) :114-25.

Zhang, Y., Hayenga, H.N., Sarantos, M.R., Simon, S.I., Neelamegham, S. (2008). Differential regulation of neutrophil CD18 integrin function by di- and tri-valent cations: manganese vs. gadolinium. *Ann Biomed Eng*. 36(4):647-60.

Zhang, Y.W., Shi, J., Li, Y.J., Wei, L. (2009). Cardiomyocyte death in doxorubicin-induced cardiotoxicity. *Arch Immunol Ther Exp (Warsz).* 57(6):435-45

Zhao, Y., Liu, Y., Chen, Z., Korteweg, C., Gu, J. (2011). Immunoglobulin g (IgG) expression in human umbilical cord endothelial cells. *J Histochem Cytochem*. 59(5):474-88.

Zhou, C., Chen, H., King, J.A., Sellak, H., Kuebler, W.M., Yin, J., Townsley, M.I., Shin, H.S., Wu, S. (2010). Alpha1G T-type calcium channel selectively regulates P-selectin surface expression in pulmonary capillary endothelium. *Am J Physiol Lung Cell Mol Physiol*. 299 (1) :L86-97

Zhou, Y., Koli, K., Hagood, J.S., Miao, M., Mavalli, M., Rifkin, D.B., Murphy-Ullrich, J.E. (2009). Latent transforming growth factor-beta-binding protein-4 regulates transforming growth factor-beta1 bioavailability for activation by fibrogenic lung fibroblasts in response to bleomycin. *Am J Pathol*. 174 (1) :21-33.

Zhu, J., Cohen, D.A., Goud, S.N., Kaplan, A.M. (1996). Contribution of T lymphocytes to the development of bleomycin-induced pulmonary fibrosis. *Ann N Y Acad Sci*. 796:194-202

Zouki, C., Baron, C., Fournier, A., Filep, J.G. (1999) Endothelin-1 enhances neutrophil adhesion to human coronary artery endothelial cells: role of ET(A) receptors and platelet-activating factor. *Br J Pharmacol*. 127(4):969-79.

Appendix A Supplementary Material

A I Additional Materials and Methods

A.I.I Generation of DEPC-treated water.

DEPC-treated water was generated by combining diethylpyrocarbonate (Sigma Aldrich) with distilled H_2O (0.1% v/v). This was agitated and autoclaved prior to storage at room temperature.

A.I.II Generation of the IV.3 Antibody.

IV.3 antibody was generated in house from supernatant collected from a murine hybridoma cell line (K562). In brief, K652 cells were thawed at room temperature and incubated in 75cm^2 flasks in DMEM medium (Lonza) supplemented with FCS (10%) (Gibco), penicillin (100µg/ml)-streptomycin (100U/ml) (PAA, Pasching, Austria), and L-glutamine (2nM) (Lonza). Cells were then incubated in an atmosphere containing 5% CO_2 at 37°C until confluent. The IV.3-containing supernatant was aspirated from the flasks as required and stored at 4°C until required.

A.I.III HEK-293 RNA Isolation for use as a Positive Control for PCR

HEK-293 cells were cultured in 75cm^2 flasks in DMEM medium (Lonza) supplemented with FCS (10%) (Gibco), penicillin (100µg/ml)-streptomycin (100U/ml) (PAA, Pasching, Austria), and L-glutamine (2nM) (Lonza). Cells were dissociated from culture flasks by agitation, and the RNA extracted and reverse transcribed to generate cDNA as outlined in section 2.9. Preparation for PCR and PCR itself was carried out as outlined in section 3.2.6.

A.I.IV Generation of 1mM EDTA in PBS.

Anhydrous ethylenediamineteraacetic acid (Sigma Aldrich) (292mg) was added to PBS (1L) and dissolved by agitation. This was left overnight and autoclaved prior to storage at room temperature.

A.I.V **Generation of 1 x TAE solution**

1 x TAE solution was generated by diluting 50 x TAE solution 1:49 with distilled H_2O. 50 x TAE solution was made by combining 242g Tris base (Fisher) with 600ml distilled H_2O and dissolving this by agitation. To this, 57.1ml acetic (Sigma Aldrich) and 100ml 0.5M EDTA (generated by combining 146.1g anhydrous EDTA (Sigma Aldrich) in 1L distilled H_2O) was added, and the volume adjusted to 1L with distilled H_2O. This was stored at room temperature.

A.II Standard Curves Generated for ELISA and qPCR Experiments

Standard curves were generated for all ELISA and qPCR experiments carried out throughout this thesis. These are shown in Fig A.1-A.7. The specifications of each standard curve are outlined below each figure. All standard curves were generated using data collected from experimental work and GraphPad v.5.0.4. All standard curves met the defined criteria for succesful ELISA experiments and specific primer activity in qPCR.

Note that on all graphs, cDNA quantity is expressed using logarithmic scale. Therefore, “1” on the x-axis in fact represents 10ng/well, while “-1” represents 0.1ng/well. Logarithmic scales were used to assist in the determination of primer efficiency calculations.

Treatment	Isotype Control Binding (Geometric Mean)	Treatment	Isotype Control Binding (Geometric Mean)	Treatment	Isotype Control Binding (Geometric Mean)
Untreated	**5.56**				
Untreated	**5.04**				
Untreated	**7.50**				
TNF-α 1ng/ml	**10.27**	LPS 100ng/ml	**8.48**	IFN-γ 100u/ml	**6.02**
TNF-α 1ng/ml	**9.79**	LPS 100ng/ml	**6.78**	IFN-γ 100u/ml	**5.01**
TNF-α 1ng/ml	**15.31**	LPS 100ng/ml	**10.58**	IFN-γ 100u/ml	**7.35**
TNF-α 3ng/ml	**11.26**	LPS 300ng/ml	**7.05**	IFN-γ 300U/ml	**7.24**
TNF-α 3ng/ml	**13.42**	LPS 300ng/ml	**8.52**	IFN-γ 300U/ml	**6.63**
TNF-α 3ng/ml	**14.6**	LPS 300ng/ml	**10.83**	IFN-γ 300U/ml	**7.54**
TNF-α 10ng/ml	**9.17**	LPS 1µg/ml	**6.67**	IFN-γ 1000U/ml	**6.56**
TNF-α 10ng/ml	**8.73**	LPS 1µg/ml	**17.22**	IFN-γ 1000U/ml	**6.83**
TNF-α 10ng/ml	**12.66**	LPS 1µg/ml	**10.04**	IFN-γ 1000U/ml	**8.81**
TNF-α 30ng/ml	**9.22**	LPS 3µg/ml	**7.87**	IFN-γ 3000U/ml	**7.69**
TNF-α 30ng/ml	**11.59**	LPS 3µg/ml	**7.68**	IFN-γ 3000U/ml	**5.62**
TNF-α 30ng/ml	**11.65**	LPS 3µg/ml	**12.08**	IFN-γ 3000U/ml	**9.13**

Table A.1: Tabulated isotype control binding to inflammatory mediator treated HUVECs.

The binding of the isotype control antibody to HUVECs treated with inflammatory mediators as part of optimisation experiments (expressed as the obtained geometric mean). Treatment with all mediators increased the binding of the isotype control to HUVECs. As all experiments were conducted simultaneously, only one set of results is available from “untreated” cells.

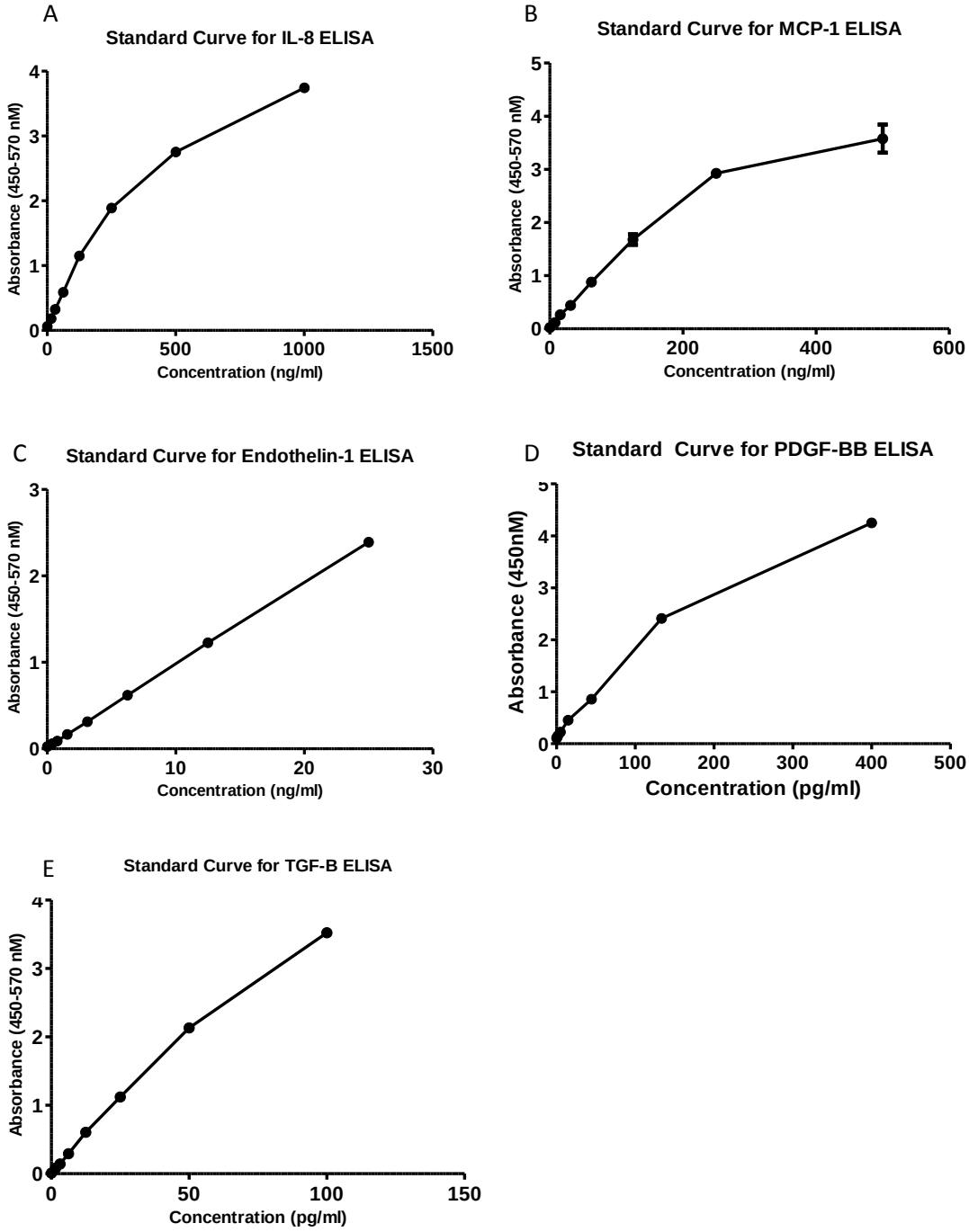

Figure A.1: Standard curves for HUVEC cytokine ELISAs

Standard curves achieved based on standards in cytokine ELISAs used to determine cytokine expression in HUVEC treated with various concentrations of BLM. All standard curves were generated using Prism GraphPad version 5.04. All standard curves are representative of ideal standard curves supplied with ELISA kit instructions.

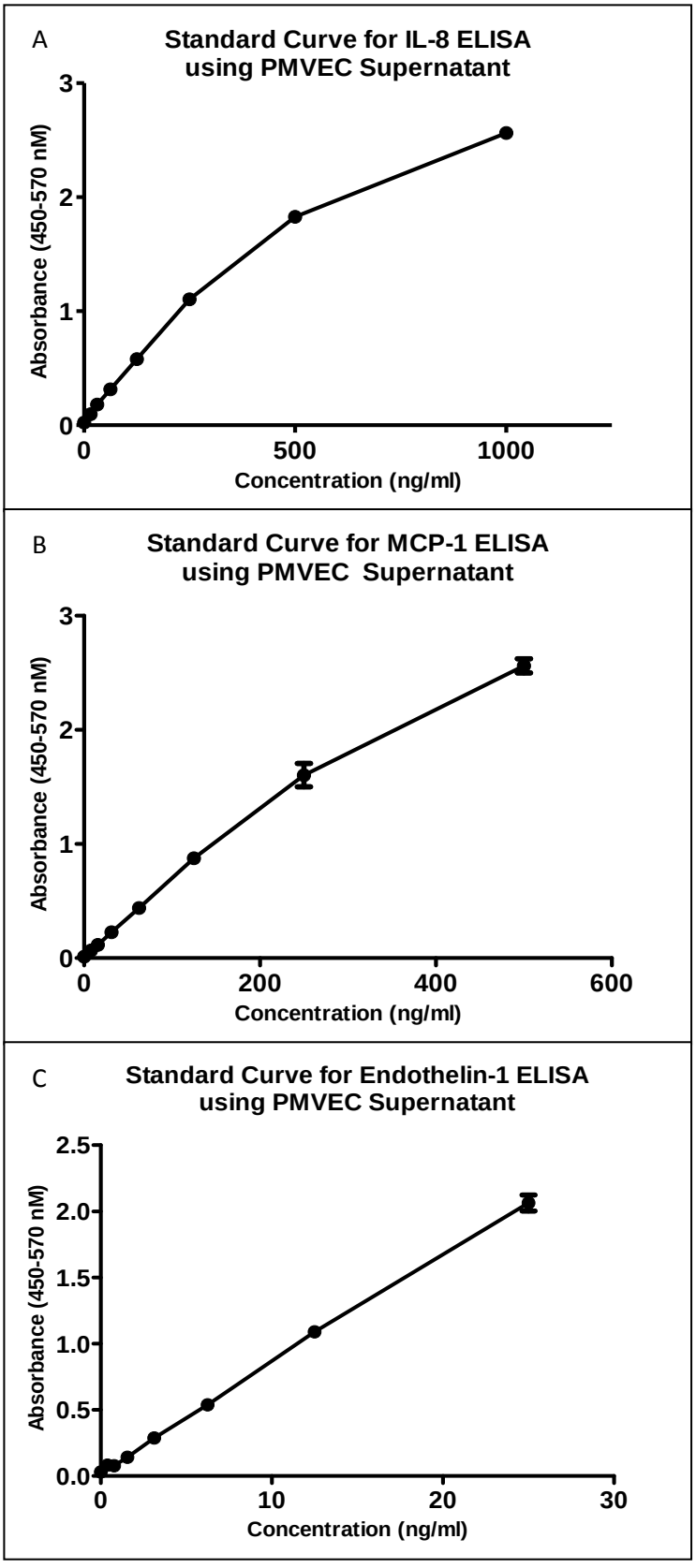

Figure A.2: Standard curves for PMVEC cytokine ELISAs

Standard curves achieved based on standards in cytokine ELISAs used to determine cytokine expression in PMVECs treated with various concentrations of BLM. All standard curves were generated using Prism GraphPad version 5.04. All standard curves are representative of ideal standard curves supplied with ELISA kit instructions.

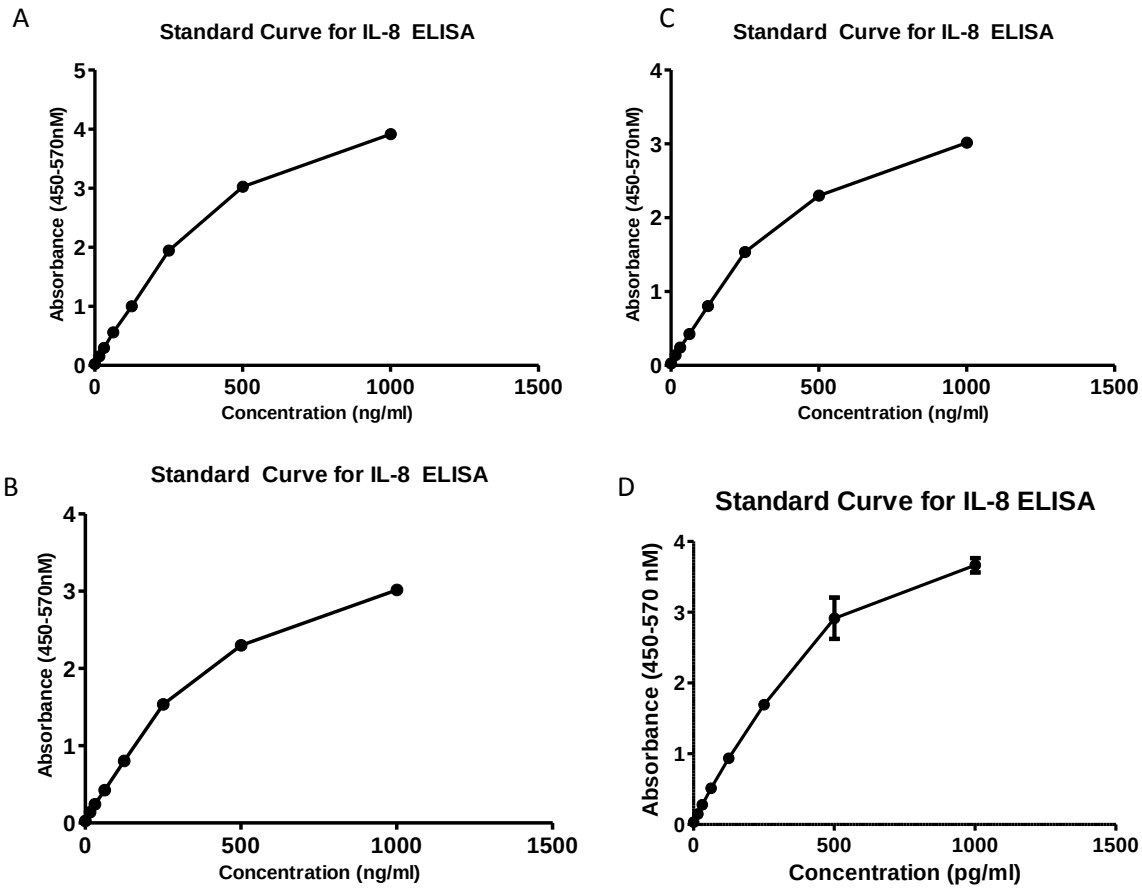

Figure A.3: Standard curves for cytokine ELISAs using HUVECs treated with other chemotherapeutic agents

Standard curves achieved based on standards in interleukin-8 ELISAs used to determine expression in cells treated with A) etoposide, B) doxorubicin, C) carboplatin, and D) the vehicle control, dimethyl sulfoxide. All curves are representative of ideal standard curves supplied with ELISA kit instructions.

A

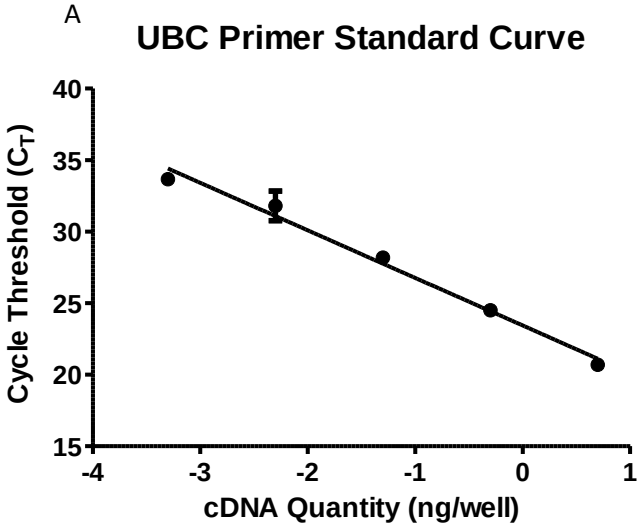

Slope	-3.324
Y Intercept	23.44
R^2 value	0.9766
P value	< 0.0001
Efficiency	99.91%

B

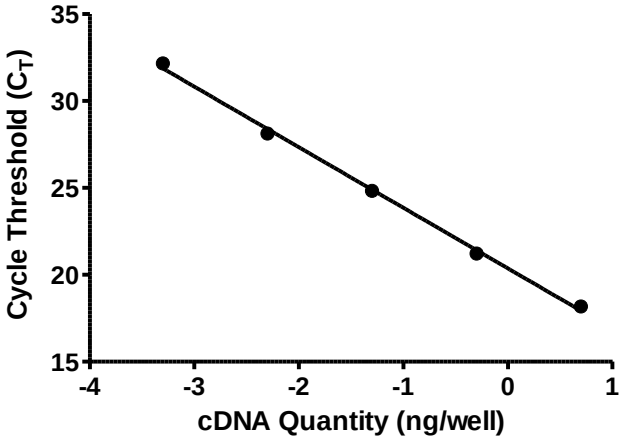

Slope	-3.486
Y Intercept	20.37
R^2 value	0.997
P value	< 0.0001
Efficiency	93.58%

C

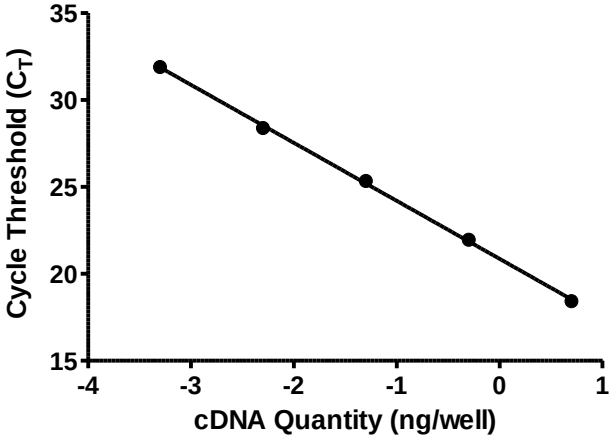

Slope	-3.337
Y Intercept	20.86
R^2 value	0.9986
P value	< 0.0001
Efficiency	99.37%

D

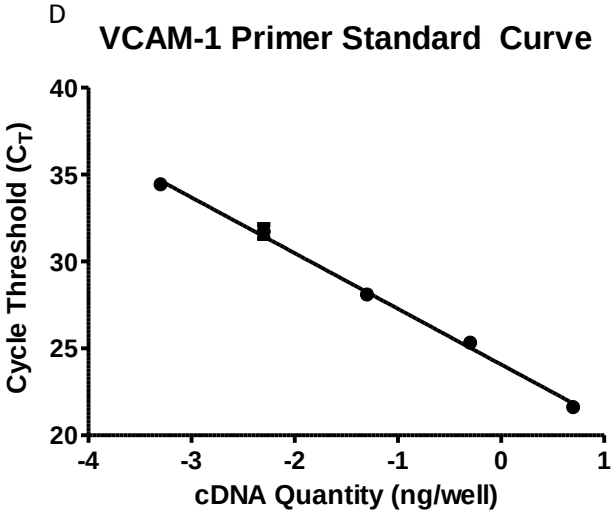

Slope	-3.203
Y Intercept	24.07
R^2 value	0.9944
P value	< 0.0001
Efficiency	105.21%

E

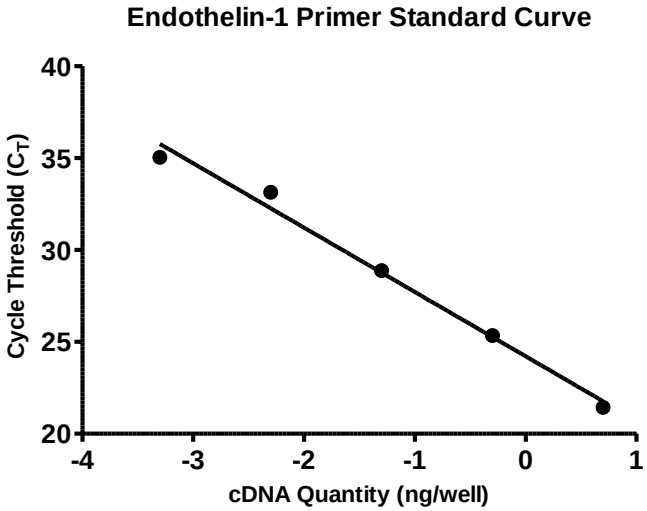

Slope	-3.501
Y Intercept	24.21
R^2 value	0.9872
P value	< 0.0001
Efficiency	93.03%

Figure A.4: qPCR standard curves (five-point)

Standard curves generated based on a series of five serial dilutions of samples used for qPCR. Each standard curve was conducted simultaneously, in duplicate, on cDNA obtained from HUVECs treated with 10ng TNF-α (UBC (A), IL-8 (B), MCP-1 (C), and VCAM-1 (D)), or 4U/ml thrombin (Endothelin-1 (E)) to induce gene expression. Relevant data from each standard curve is shown in the table accompanying each curve. The *P* value refers to the significance of the slope value from zero. All primers showed efficiencies within the acceptable 90-110% range and data will not need correcting.

Note that on all graphs, cDNA quantity is expressed using logarithmic scale.

A

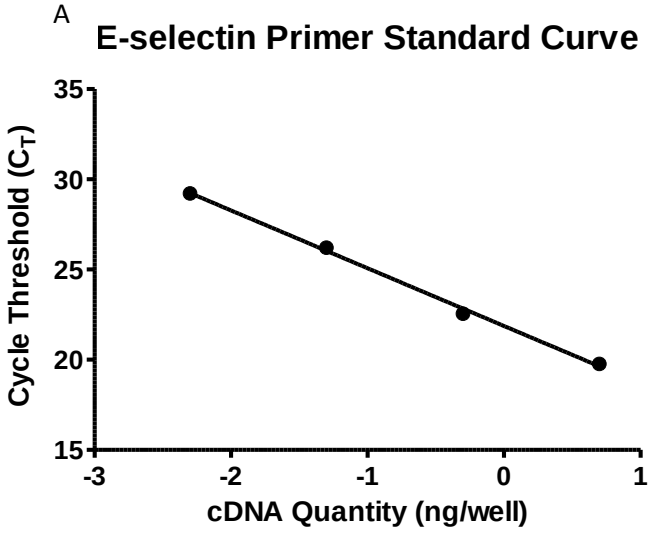

Slope	-3.202
Y Intercept	21.84
R^2 value	0.9952
P value	< 0.0001
Efficiency	105.26%

B

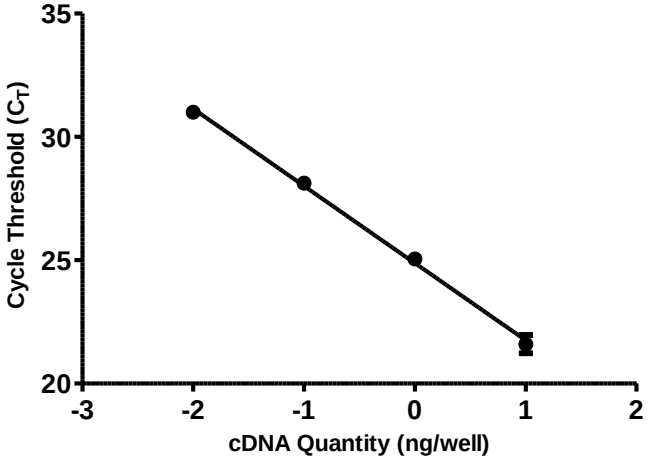

Slope	-3.129
Y Intercept	24.88
R^2 value	0.9941
P value	< 0.0001
Efficiency	108.73%

Figure A.5: qPCR standard curves (four-point).

Standard curves generated based on a series of five serial dilutions of samples used for qPCR. Each standard curve was conducted simultaneously, in duplicate, on cDNA obtained from HUVECs treated with 10ng TNF-α (E-selectin) (A), or 3U/ml thrombin (PDGF-BB) (B) to induce gene expression. Relevant data from each standard curve is shown in the table accompanying each curve. The *P* value refers to the significance of the slope value from zero. All primers showed efficiencies within the acceptable 90-110% range and data will not need correcting. In both cases, reliable data was not obtainable for the lowest dilution (0.0001ng/well) in repeated experiments, so a standard curve was made using four sets of results.

Note that on all graphs, cDNA quantity is expressed using logarithmic scale.

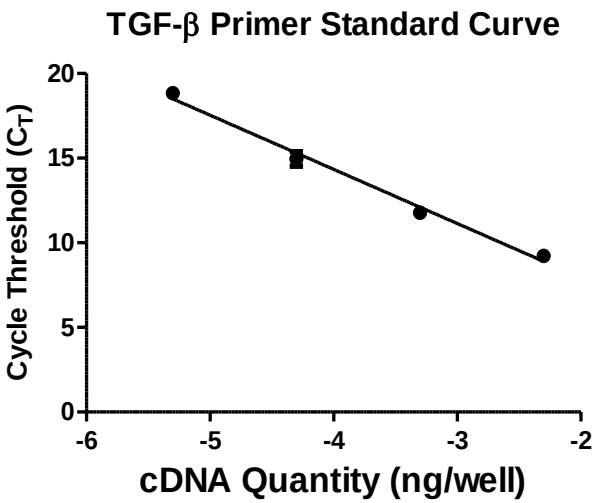

Slope	-3.200
Y Intercept	1.537
R^2 value	0.9877
P value	< 0.0001
Efficiency	105.35%

Figure A.6: qPCR standard curve for TGF-β (four point).

Standard curve generated based on a series of five serial dilutions of purified samples used for qPCR. The standard curve was conducted simultaneously, in duplicate, on cDNA obtained from HUVECs and purified to ensure sufficient cDNA. The *P* value refers to the significance of the slope value from zero. The primer showed efficiency within the acceptable 90-110% range and data will not need correcting. Reliable data was not obtainable for the lowest dilution (0.0001ng/µl of purified cDNA at a concentration of 2ng/ml) in repeated experiments, so a standard curve was made using four sets of results.

Note that on all graphs, cDNA quantity is expressed using logarithmic scale.

Slope	-3.428
Y Intercept	27.49
R^2 value	0.996
P value	< 0.0001
Efficiency	95.75%

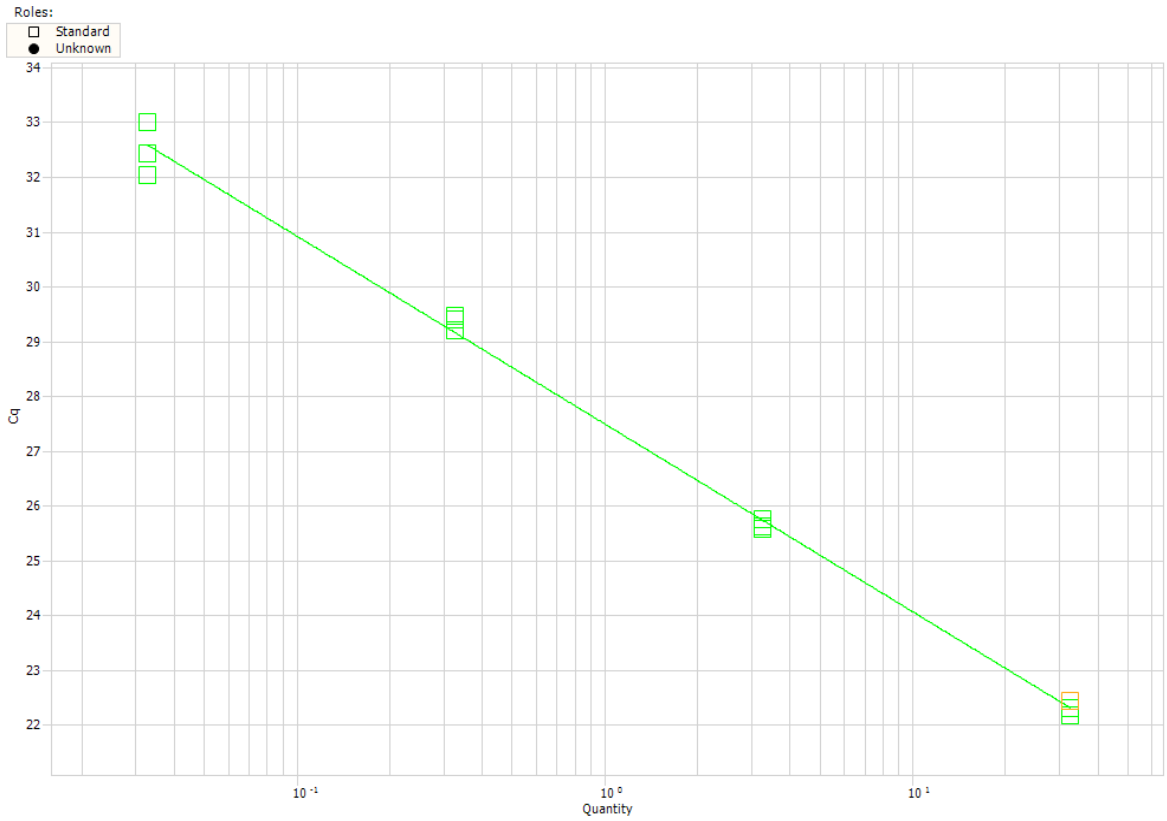

Figure A.7: qPCR standard curve for ICAM-1 (four point).

Standard curve generated based on a series of five serial dilutions of lung cDNA, generated graciously by Rebecca Gover of PrimerDesign. The standard curve was conducted simultaneously, in triplicate. The *P* value refers to the significance of the slope value from zero. The primer showed efficiency within the acceptable 90-110% range and data will not need correcting. Reliable data was not obtainable for the lowest dilution (0.003ng/µl of cDNA) in repeated experiments, so a standard curve was made using four sets of results.

Note that on all graphs, cDNA quantity is expressed using logarithmic scale.

A.III Neutrophil Adhesion Raw Data Analysis

Shown in Figure A.8 and A.9 are examples of neutrophil adhesion raw data assessment. Raw data was inputted into Microsoft Word and a grid placed above each image. Adherent neutrophils were identified and their movement under flow tracked. The number of neutrophils seen to be adherent at the beginning of the field which did not become un-adherent, the number which adhered as a new adhesion event and did not become un-adherent, and the number which adhered and then rolled along the endothelium were identified. The following were regarded a neutrophil adhesion events.

- Cells that were adherent from the beginning of visualisation and did not un-adhere
- Cells that were adherent and un-adhered (but remained adherent for at least two frames)
- Cells that adhered during flow and remained adherent throughout visualisation
- Cells that adhered during flow, remained adhered for at least two frames, and then un-adhered
- Rolling and slow rolling cells that met the two-frame adherence criteria outlined above. “Slow rolling” cell events were those seen to be moving at ≤10µm/second (outlined in 6.2.6.1). If cells were observed to be moving at speeds above 10µm/second but were clearly visible and slower than non-adherent neutrophils, cells were deemed to be “rolling”.

Cells that became adherent or rolled for only one frame were not counted.

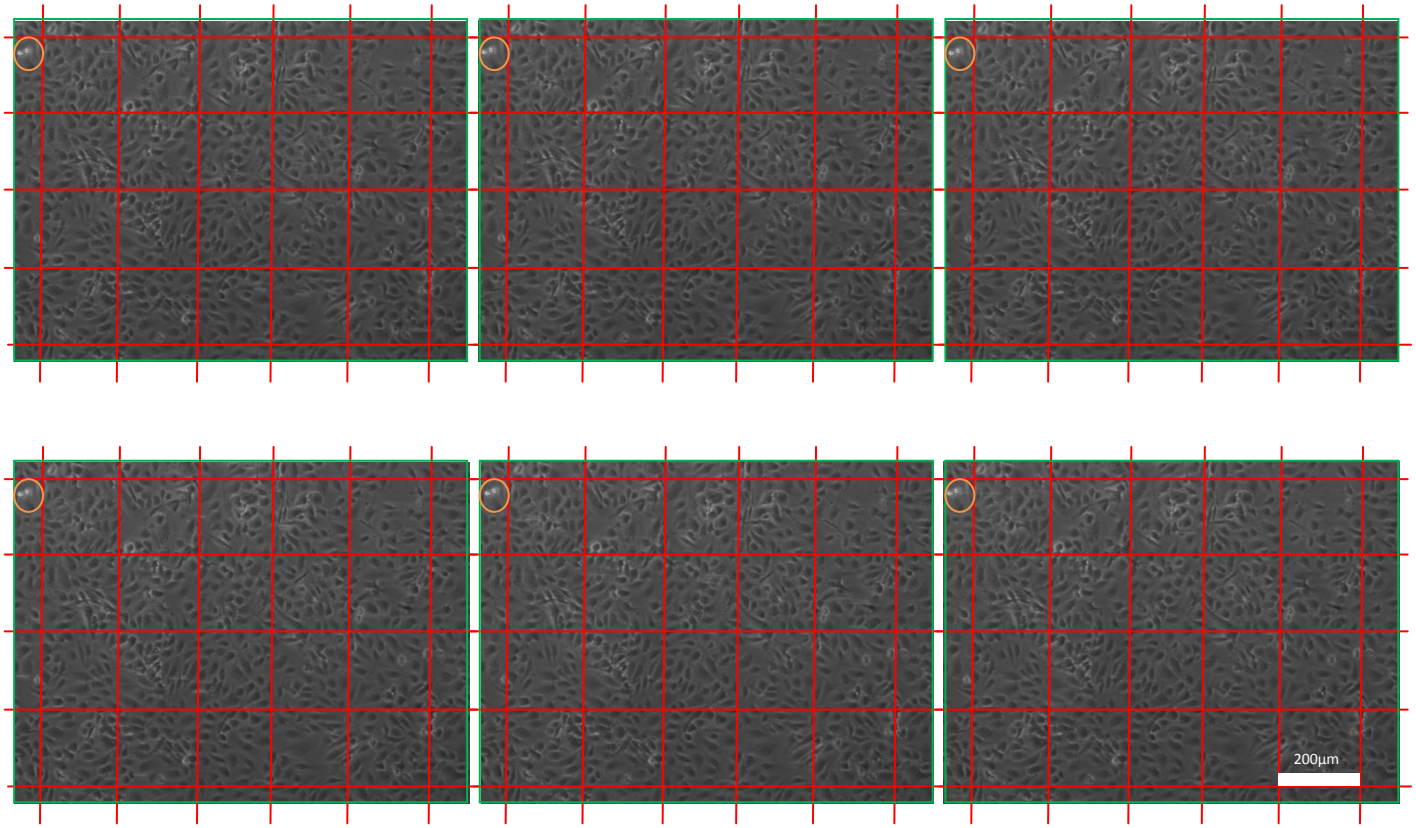

Figure A.8: Neutrophil adhesion assessment (negative control - untreated endothelial cells)

An example of neutrophil adhesion assessment. Neutrophils that were adherent from the first frame and remained adherent are denoted by orange circles. These cells remained adherent throughout the analysis and represent two neutrophil adhesion events observed in this experiment. Six frames are shown only.

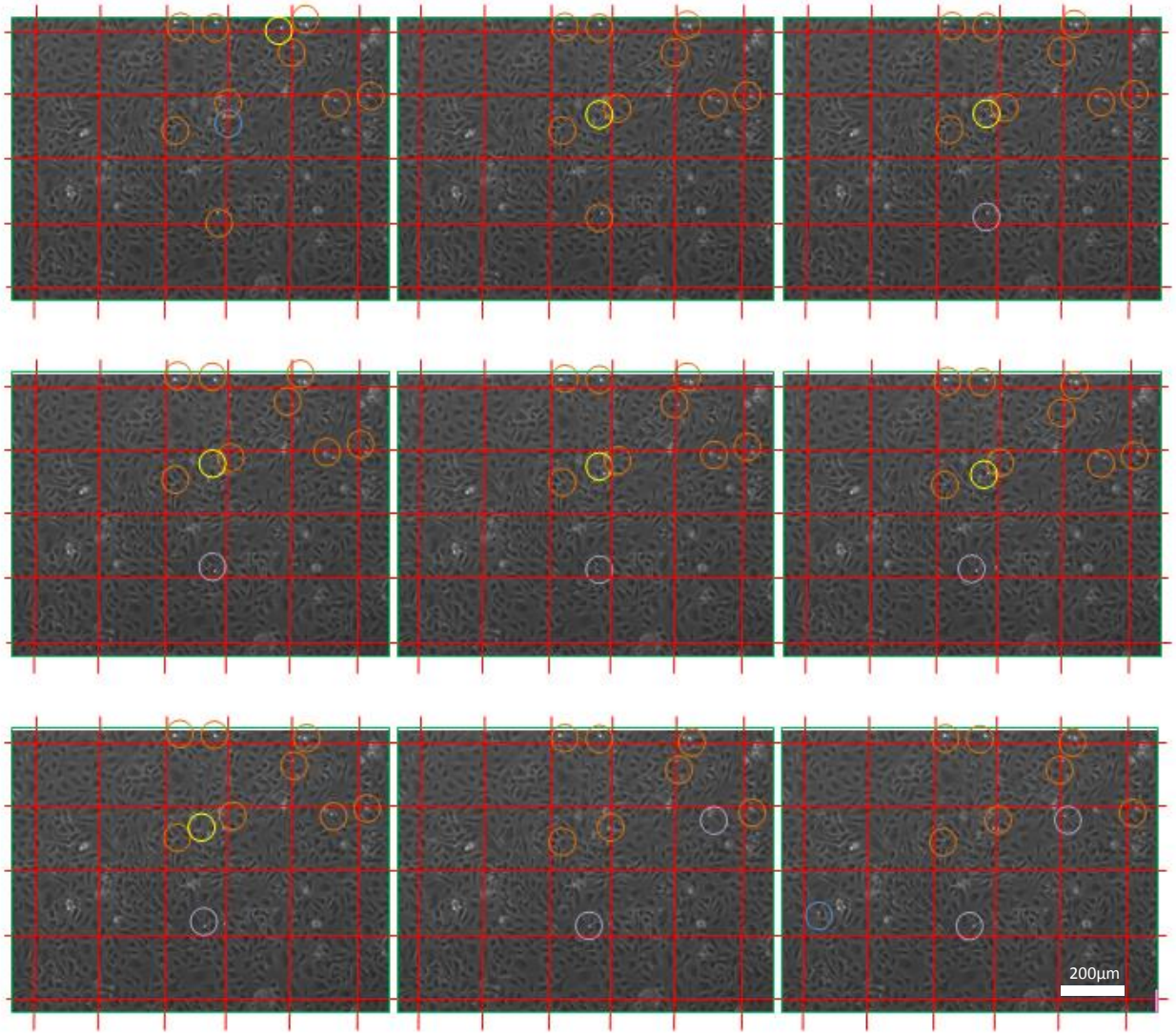

Figure A.9: Neutrophil adhesion assessment (TNF-α treated endothelial cells.)

An example of neutrophil adhesion assessment. New cel adhesion events are marked in blue circles. New adhesion events that results in rolling are denoted by yellow circles. Static cells (adherent from the first frame and remained adherent) are denoted by orange circles. Cells that were originally adherent and began to roll under shear are denoted by purple circles.

Many cells met adherence criteria in this analysis and represent a snap-shot of the adhesion events seen in this analysis. Nine frames are shown only.

A.IV Movies of Neutrophil Adhesion to Endothelial Cells Under Flow

Movies of neutrophil adhesion to endothelial cells treated with 10ng/ml TNF-α under flow can be found in the accompanying material (Disc A). Twenty individual movies have been submitted with this thesis. The movies depict an experiment conducted explicity for the purpose of making moving images of this process and were not used as data for the results depicted in chapter 6. In these movies, neutrophil suspensions of a higher neutrophil concentration ($1x10^6$/ml) were used by way of demonstration. In standard experiments, concentrations of $5x10^5$/ml neutrophils in suspension were used. In half of the movies submitted, neutrophils were treated with isotype control antibody as used in the blocking experiments, and the endothelial monolayer remained untreated. In the other half of the movies, the endothelial monolayer was treated with the isotype control antibody, and the neutrophils remained untreated.

Appendix B Ethical Approval for Blood Collection from Volunteer Donors

H·Y·M·S
THE HULL YORK MEDICAL SCHOOL

Tel 0870 1245500

HULL
The University of Hull
Hull
HU6 7RX
Fax 01482 464705

YORK
The University of York
Heslington
York
YO10 5DD
Fax 01904 321696

www.hyms.ac.uk

13 February 2014

Dr Simon Hart/Mr James Williamson
2nd Floor Daisy Building
Castle Hill Hospital
Castle Road
Cottingham
HU15 5JQ

Dear Dr Hart and Mr Williamson

13 09 – The immunology of Bleomycin-induced Pulmonary Fibrosis

Thank you Mr Williamson for attending the HYMS on Friday 7 February to discuss your proposed study.

The application was clear and considered possible ethical implications carefully. The Committee did not identify any areas for concern and the only recommendation following discussion is that you state explicitly on participant information sheet that consent is given to use blood for the in vitro experiments described and not for other purposes. Therefore on behalf of the HYMS Ethics Committee, I am pleased to inform you that your project was given **ethical approval.**

Please ensure that the documents used in the study are equivalent to the attached referenced versions which you should retain for your records. If during the course of the project you need to deviate significantly from the above-approved document please inform me since written approval will be required. Please also inform me should you decide to terminate the project prematurely.

Yours sincerely

Professor William McGuire
Chair
HYMS Ethics Committee

University of Hull
The University of York
In association with the NHS

Fig. B.1: Ethical approval for blood sample collection from volunteer donors.

Ethical approval granted by the HYMS Ethics Board for the collection of blood samples from volunteer donors for use in the neutrophil adhesion assays carried out in Chapter 6 of this thesis.